Topics in Stereochemistry, Volume 13

Editors
Norman L. Allinger
Ernest L. Eliel
Samuel H. Wilen

JOHN WILEY & SONS

TOPICS IN STEREOCHEMISTRY

VOLUME 13

ADVISORY BOARD

STEPHEN J. ANGYAL, *University of New South Wales, Sydney, Australia*

ALAN R. BATTERSBY, *Cambridge University, Cambridge, England*

GIANCARLO BERTI, *University of Pisa, Pisa, Italy*

F. ALBERT COTTON, *Texas A&M University, College Station, Texas*

JOHANNES DALE, *University of Oslo, Oslo, Norway*

DAVID GINSBURG, *Technion, Israel Institute of Technology, Haifa, Israel*

JAN MICHALSKI, *Centre of Molecular and Macromolecular Studies, Polish Academy of Sciences, Lodz, Poland*

KURT MISLOW, *Princeton University, Princeton, New Jersey*

SAN-ICHIRO MIZUSHIMA, *Japan Academy, Tokyo, Japan*

GUY OURISSON, *University of Strasbourg, Strasbourg, France*

VLADIMIR PRELOG, *Eidgenössische Technische Hochschule, Zurich, Switzerland*

GÜNTHER SNATZKE, *Ruhruniversität, Bochum, Federal Republic of Germany*

HANS WYNBERG, *University of Groningen, Groningen, The Netherlands*

TOPICS IN

STEREOCHEMISTRY

EDITORS

NORMAN L. ALLINGER
Professor of Chemistry
University of Georgia
Athens, Georgia

ERNEST L. ELIEL
Professor of Chemistry
University of North Carolina
Chapel Hill, North Carolina

SAMUEL H. WILEN
Professor of Chemistry
City College, City University of New York
New York, New York

VOLUME 13



AN INTERSCIENCE ® PUBLICATION
JOHN WILEY & SONS
New York • Chichester • Brisbane • Toronto • Singapore

An Interscience® Publication
Copyright © 1982 by John Wiley & Sons, Inc.

All rights reserved. Published simultaneously in Canada.

Reproduction or translation of any part of this work beyond that permitted by Section 107 or 108 of the 1976 United States Copyright Act without the permission of the copyright owner is unlawful. Requests for permission or further information should be addressed to the Permissions Department, John Wiley & Sons, Inc.

Library of Congress Catalog Card Number: 67–13943

ISBN 0–471–05680–4

Printed in the United States of America

10 9 8 7 6 5 4 3 2 1

INTRODUCTION TO THE SERIES

During the past two decades several texts in the areas of stereochemistry and conformational analysis have been published, including *Stereochemistry of Carbon Compounds* (Eliel, McGraw-Hill, 1962) and *Conformational Analysis* (Eliel, Allinger, Angyal, and Morrison, Interscience, 1965). While the writing of these books was stimulated by the high level of research activity in the area of stereochemistry, it has, in turn, spurred further activity. As a result, many of the details found in these texts are already inadequate or out of date, although the student in stereochemistry and conformational analysis may still learn the basic concepts of the subject from them.

For both human and economic reasons, standard textbooks can be revised only at infrequent intervals. Yet the spate of periodical publications in the field of stereochemistry is such that it is an almost hopeless task for anyone to update himself by reading all the original literature. The present series is designed to bridge the resulting gap.

If that were its only purpose, this series would have been called "Advances (or "Recent Advances") in Stereochemistry." It must be remembered, however, that the above-mentioned texts were themselves not treatises and did not aim at an exhaustive treatment of the field. Thus the present series has a second purpose, namely, to deal in greater detail with some of the topics summarized in the standard texts. It is for this reason that we have selected the title *Topics in Stereochemistry*.

The series is intended for the advanced student, the teacher, and the active researcher. A background for the basic knowledge in the field of stereochemistry is assumed. Each chapter is written by an expert in the field and, hopefully, covers its subject in depth. We have tried to choose topics of fundamental import aimed primarily at an audience of inorganic and organic chemists but involved frequently with fundamental principles of physical chemistry and molecular physics, and dealing also with certain stereochemical aspects of biochemistry.

It is our intention to bring out future volumes at intervals of one to two years. The editors will welcome suggestions as to suitable topics.

We are fortunate in having been able to secure the help of an international board of editorial advisers who have been of great assistance by suggesting topics and authors for several chapters and by helping us avoid duplication of topics appearing in other, related monograph series. We are grateful to the editorial advisers for this assistance, but the editors and authors alone must assume the responsibility for any shortcomings of *Topics in Stereochemistry*.

N. L. ALLINGER
E. L. ELIEL
S. H. WILEN

PREFACE

Following publication of an entire volume (Volume 12) devoted to inorganic and organometallic stereochemistry it would be tempting to say that, with Volume 13, *Topics in Stereochemistry* returns to its more familiar format, namely, that devoted to organic stereochemistry. We wish to signal, however, that we expect to continue to present, at regular intervals, articles on stereochemical topics of interest to inorganic chemists and biochemists, as well as others. At the same time, we call attention to the fact that with this volume Professor Samuel H. Wilen of the City College, City University of New York, has become a regular co-editor of the series.

The first chapter in this volume is a particularly timely one given the recent surge of activity in natural product synthesis based upon stereocontrolled Aldol Condensations. D. A. Evans, one of the principal protagonists in this effort, and his associates, J. V. Nelson and T. R. Taber, have surveyed the several modern variants of the Aldol Condensation and discuss models to rationalize the experimental results, particularly with respect to stereochemistry, in a chapter entitled "Stereoselective Aldol Condensations." The authors examine Aldol diastereoselection under thermodynamic and kinetic control as well as enantioselection in Aldol Condensations involving chiral reactants.

The second chapter, by E. Ōsawa and H. Musso, is entitled "Application of Molecular Mechanics Calculations to Organic Chemistry." It describes the force field models presently in use as well as their scope and limitations. The authors survey the applications of these models to conformational analysis, to reaction mechanisms, to the analysis of NMR spectra, and to the design of medicinal agents.

M. V. Stewart and E. M. Arnett are the authors of the third chapter, "Chiral Monolayers at the Air–Water Interface." The chapter brings together the disciplines of surface chemistry and stereochemistry to demonstrate that the properties of stereoisomers may be useful in extending our understanding of the weak yet important intermolecular forces that operate in surface monolayers. The authors demonstrate that, in a complementary way, the techniques of surface chemistry make possible novel experiments that yield clear and

convincing evidence of intermolecular interaction that is stereochemically pertinent.

Because this area is not too well known, the authors have taken pains to describe, in some detail, experimental monolayer chemistry. The centerpiece of the chapter is enantiomer and diastereomer discrimination in monolayers. It concludes with a discussion of surface properties, in particular energetics, which are quite sensitive to stereochemistry. We call attention to the fact that this chapter is of potential interest to biochemists, notably those concerned with lipids and with cell membrane organization.

Configurational assignments and the determination of enantiomeric purity by NMR spectroscopy are techniques that are in frequent use by contemporary experimentalists. One of these techniques, involving Chiral Lanthanide Shift Reagents (CLSR) was surveyed in Volume 10 of this series. A complementary technique of earlier provenance applies "NMR Chiral Solvating Agents" (CSA) to these problems. The authors of this fourth chapter, W. H. Pirkle and D. J. Hoover, examine the nature of CSA-induced nonequivalence and survey the correlation of absolute configuration with a wide range of solvents. The limitations and exceptions to the models applied to the configurational assignments are carefully delineated. In addition, self-induced nonequivalence is described and a comparison is made between the CSA and CLSR techniques.

Organosulfur chemistry is presently a particularly dynamic subject area. The stereochemical aspects of this field are surveyed by M. Mikołajczyk and J. Drabowicz in the fifth chapter, entitled "Chiral Organosulfur Compounds." The synthesis, resolution, and application of a wide range of chiral sulfur compounds are described as are the determination of absolute configuration and of enantiomeric purity of these substances. A discussion of the dynamic stereochemistry of chiral sulfur compounds including racemization processes follows. Finally, nucleophilic substitution on and reaction of such compounds with electrophiles, their use in asymmetric synthesis, and asymmetric induction in the transfer of chirality from sulfur to other centers is discussed in a chapter that should be of interest to chemists in several disciplines, in particular synthetic and natural product chemistry.

NORMAN L. ALLINGER
ERNEST L. ELIEL
SAMUEL H. WILEN

Athens, Georgia
Chapel Hill, North Carolina
New York, New York
January 1982

CONTENTS

STEREOSELECTIVE ALDOL CONDENSATIONS 1
by D. A. Evans, J. V. Nelson, and T. R. Taber,
Division of Chemistry and Chemical Engineering,
California Institute of Technology,
Pasadena, California

APPLICATION OF MOLECULAR MECHANICS CALCULATIONS TO ORGANIC CHEMISTRY 117
by Eiji Ōsawa, Department of Chemistry,
Faculty of Science, Hokkaido University, Sapporo, Japan;
and Hans Musso, Institut für Organische Chemie,
Universität Karlsruhe, Federal Republic of Germany

CHIRAL MONOLAYERS AT THE AIR-WATER INTERFACE 195
by Martin V. Stewart,
Department of Chemistry and Physics,
Middle Tennessee State University,
Murfreesboro, Tennessee;
and Edward M. Arnett,
Department of Chemistry, Gross Laboratory,
Duke University, Durham, North Carolina

NMR CHIRAL SOLVATING AGENTS 263
by Marian Mikołajczyk and Józef Drabowicz,
The Roger Adams Laboratory,
School of Chemical Sciences,
University of Illinois, Urbana, Illinois

CHIRAL ORGANOSULFUR COMPOUNDS 333
by Marian Mikołajczyk and Józef Drabowicz,
Centre of Molecular and Macromolecular Studies,
Polish Academy of Sciences,
Department of Organic Sulfur Compounds, Lodz, Poland

SUBJECT INDEX 471

CUMULATIVE INDEX, VOLUMES 1–13 487

TOPICS IN STEREOCHEMISTRY

VOLUME 13

Stereoselective Aldol Condensations*

D. A. EVANS, J. V. NELSON, and T. R. TABER

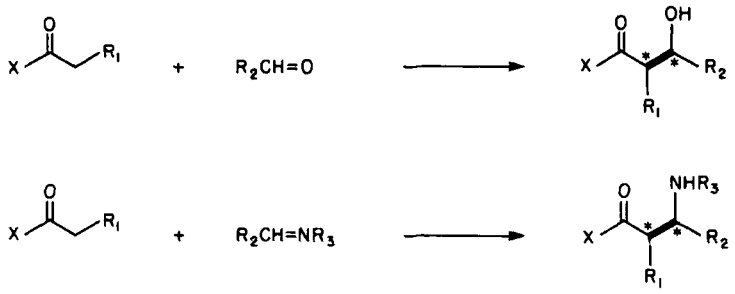
Division of Chemistry and Chemical Engineering
California Institute of Technology,
Pasadena, California

I. Prologue 2
II. Introduction 4
III. Aldol Stereochemical Assignments 5
IV. Thermodynamically Controlled Aldol Diastereoselection 7
V. Kinetically Controlled Aldol Diastereoselection: Achiral Reaction Partners 13
A. Diastereoselectivity as a Function of Enolate Geometry 13
B. Group I and II Metal Ketone Enolates 22
C. Group I and II Metal Ester and Amide Enolates 26
D. Boron Enolates 37
E. Zirconium and Other Metal Enolates 50
F. Enolsilanes 55
G. Azomethine-Enolate Condensations 59
VI. The Question of Asymmetric Induction 66
A. Chiral Aldehydes and Achiral Enolates 66
B. Chiral Enolates and Aldehydes 76
1. Chiral Ester Enolates 79
2. Chiral Ketone Enolates 80
3. Chiral Amide and Imide Enolates 88
4. Metal-Localized Chirality Transfer 101
VII. Conclusions 108
Acknowledgments 109
References 109

*Contribution No. 6437 from the Laboratories of Chemistry, California Institute of Technology.

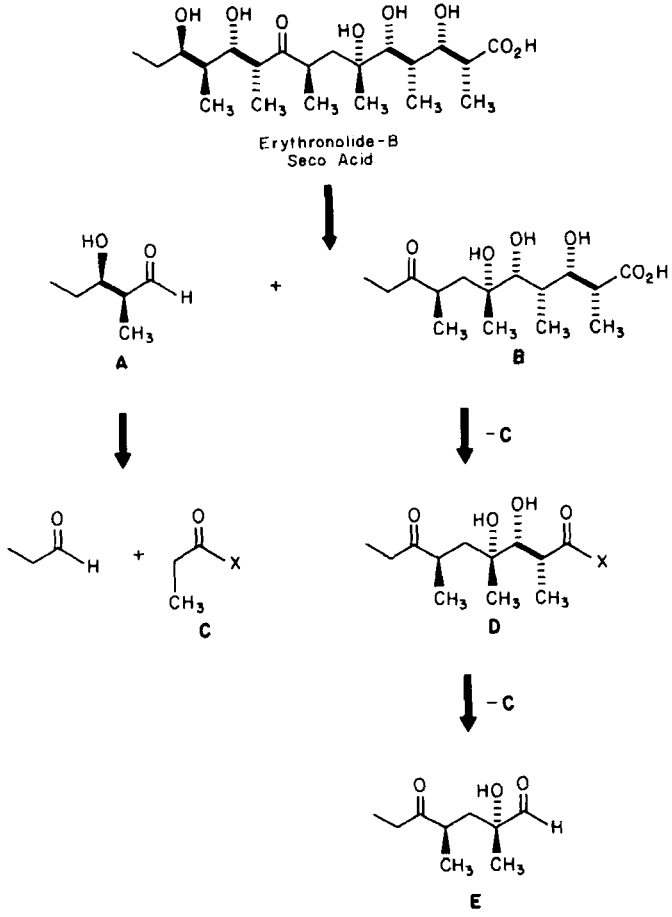
I. PROLOGUE

The aldol process constitutes one of the fundamental bond constructions in biosynthesis. This reaction, along with related variants involving Schiff bases, is among the oldest classes of reactions in organic chemistry and is well recognized as the most obvious bond

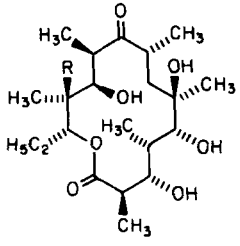


construction for the creation of 1,3-*O,O* and 1,3-*N,O* heteroatom-heteroatom relationships in organic molecules. In recent years the macrolide and ionophore antibiotics have been generally recognized as viable targets for total synthesis. Because the aldol process is intimately involved in the biosynthesis of these classes of molecules, there has been a renewed interest in the development of stereoregulated aldol condensations that might be applied to the efficient synthesis of such target structures. The erythromycin aglycones, erythronolide A (R = OH) and erythronolide B (R = H) illustrate the prominence of the aldol process in the biosynthesis of these structures. An examination of the erythronolide B seco acid (Scheme 1) reveals the four obvious aldol disconnections illustrated wherein the propionate subunit C might be perceived to be involved in three of the four condensations with the possible generation of eight of the ten required asymmetric centers.

The major obstacle confronting the implementation of such "biomimetic" syntheses has been associated with the stereochemical aspects of the aldol process. Over the past few years considerable progress has been made in the development of stereoregulated aldol condensations. This chapter attempts to survey this aspect of the topic. For a more general treatment of the subject the reader is referred to several other excellent reviews (1).

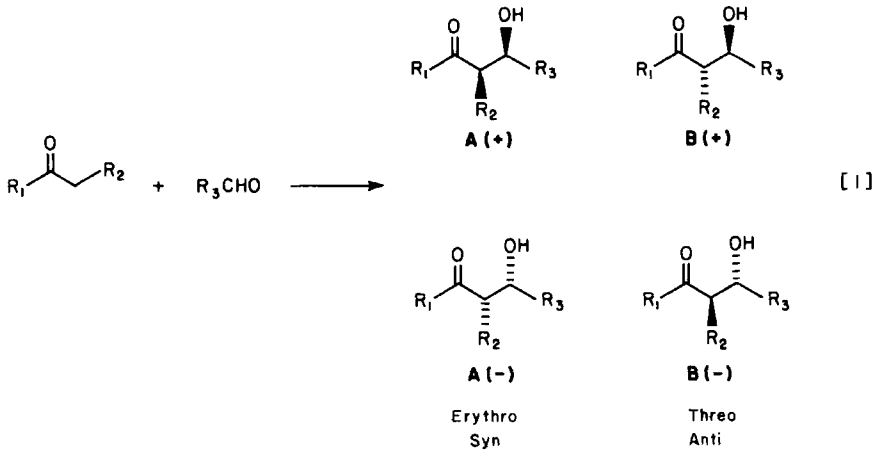

Erythronolide-B
Seco Acid
A
B
C
D
E
-C
-C

Scheme 1


R = OH, Erythronolide A
R = H, Erythronolide B

II. INTRODUCTION

In the crossed aldol condensation between carbonyl partners there are four possible product stereoisomers (eq. [1]). Consequently, there are two stereochemical aspects associated with the reaction: The first deals with internal stereochemical control or *diastereoselection* [A(±) vs. B(±)], and the second deals with absolute stereochemi-

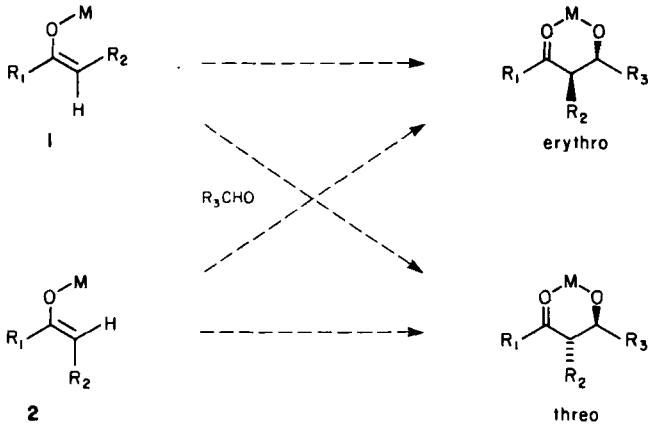


[1]

cal control for a given diastereomer or *enantioselection* [A(+) vs. A(−) or B(+) vs. B(−)]. With regard to the diastereomer nomenclature, two conventions are now in existence. The widespread practice of referring to **A** and **B** as the erythro and threo diastereomers, respectively, is not rigorously correct for *all* possible structural permutations of R_2 and R_3 and has caused some confusion. This issue has recently been addressed by both Heathcock (2) and Masamune (3) within the context of the aldol problem. Given the extended or "zigzag" conformation of the carbon backbone containing the relevant functions (=O, OH) as illustrated, that diastereomer, **A**, disposing the substituents R_2 and OH in a gauche relationship, has been defined as either the erythro (2) or the syn diastereomer (3). In an analogous fashion, isomer **B** has been defined as either the threo or the anti diastereomer. Because of the popularity of the erythro-threo convention, its usage is continued in this discussion in the context of the foregoing definition.

In principle, stereoselective aldol condensations can be carried out under two distinct sets of conditions. Under the influence of acid catalysis, stabilized enol derivatives of defined geometry (M = $SiMe_3$,

alkyl) can be induced to condense with aldehydes and acetals in a stereoselective fashion (4). However, data accumulated on the acid-catalyzed aldol variants to date have been insufficient to permit detailed speculation on the possible transition state control elements responsible for kinetic aldol diastereoselection. Alternatively, the same process can be carried out directly with aldehydes (R_3CHO) and preformed metal enolates (M = Li, MgL, ZnL, AlL_2, BL_2, etc.) of defined geometry (eq. [2]). In kinetically controlled condensations there now exists an abundant body of data that correlates aldol product stereochemistry to enolate geometry (2,5,6). This aspect of the topic is treated in detail. With regard to enolate stereochemical nomenclature, the structures 1 possessing a syn stereochemical relationship between the enolate ligand R_2 and oxygen substituent (OM) will be referred to as (*Z*)-enolates. In a similar fashion the anti stereochemical relationship between R_2 and OM as in 2 will be designated as the (*E*)-enolate.



[2]

III. ALDOL STEREOCHEMICAL ASSIGNMENTS

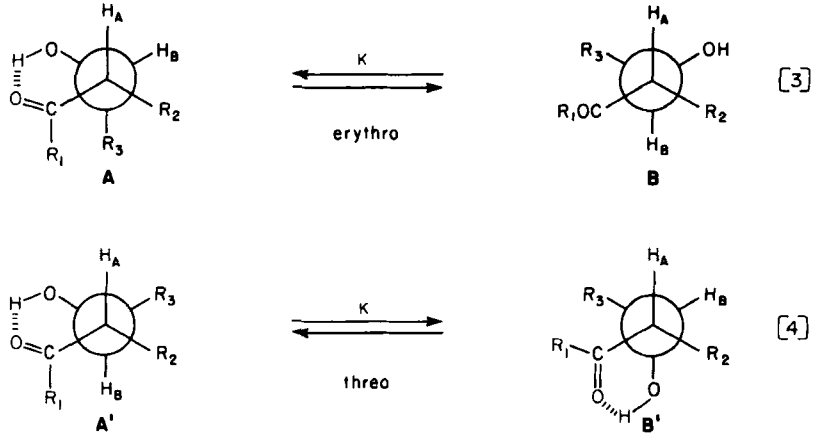
One of the most popular spectroscopic methods for the assignment of aldol stereochemistry is proton (nuclear) magnetic resonance (^{1}H NMR) spectroscopy (7). In many instances erythro-threo stereochemical assignments may be conveniently made from the magnitude of the vicinal coupling constant J_{AB}. When intramolecular hydrogen bonding provides the dominant conformational bias ($K < 1$) J_{AB} (erythro) falls in the approximate range of 3 to 6 Hz, and J_{AB} (threo)

is about 7 to 9 Hz (eqs. [3] and [4]). Nonetheless, the gauche interactions between R_2 and R_3 in the hydrogen-bonded conformations A and A′ can become dominant in dictating conformations B and B′ where both R_2 and R_3 are sterically demanding. From the examples provided in Table 1 it is clear that in many instances this method of assigning stereochemistry is reliable; however, when the accumulated steric effects of R_2 and R_3 become severe (entries D–F, L), the method fails for the reasons stated. It also appears that when the central R_2 substituent becomes sterically demanding (R_2 = t-C_4H_9) the combined nonbonded $R_2 \leftrightarrow R_1$ and $R_2 \leftrightarrow R_3$ interactions are sufficient to disrupt the hydrogen-bonded ketol solution conformations A and A′ even when R_1 and R_3 = Me (Table 1, entry M) (12).

In numerous complex aldol adducts it is not always possible to extract the relevant vicinal proton coupling constants. Heathcock and co-workers have recently noted that for the β-hydroxy ketones and esters that exist in the preferred hydrogen-bonded conformations A and A′, ^{13}C NMR spectroscopy may be conveniently employed to assign stereochemistry (13).

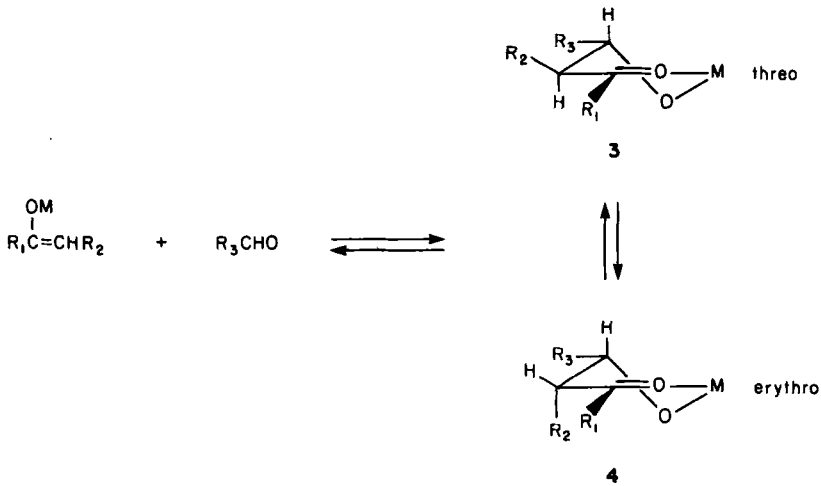
Table 1
Vicinal Coupling Constants J_{AB} for Diastereomeric Aldol Adducts Versus Ligand Variables R_1, R_2, and R_3 ($CDCl_3$)

				J_{AB} (Hz)		
Entry	R_1	R_2	R_3	Erythro	Threo	Ref.
A	OMe	Me	Ph	4.7	8.6	8
B	OMe	Et	Ph	6.2	8.4	8
C	OMe	Ph	Ph	7.6	9.2	8
D	OMe	i-C_3H_7	Ph	8.2	6.4	8
E	OMe	t-C_4H_9	Ph	10.1	4.5	8
F	OMe	Ph	t-C_4H_9	7.7	4.6	9
G	S-t-C_4H_9	Me	Ph	4.0	8.0	6
H	S-t-C_4H_9	Me	i-C_3H_7	3.0	7.0	6
I	Ph	Me	Ph	3.0	9.0	2
J	Ph	Ph	Ph	4.5	9.0	10
K	t-C_4H_9	Me	Ph	5.0	7.0	2
L	Me	t-C_4H_9	Ph	10.0	3.5	2,11
M	Me	t-C_4H_9	Me	7.5	3.0	12

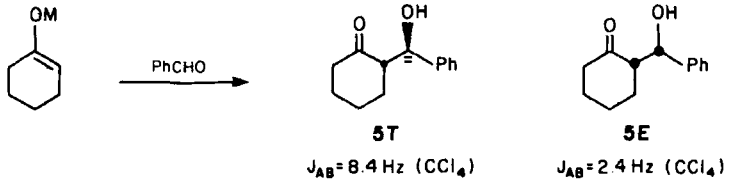


IV. THERMODYNAMICALLY CONTROLLED ALDOL DIASTEREOSELECTION

It has been well established that either kinetic or thermodynamic principles can be employed in the aldol process to define product stereochemistry. When conditions are chosen such that the condensation process is rendered reversible, the more stable threo metal aldolate complex 3 with diequatorial substituents R_2 and R_3 is usually the dominant diastereomer observed (2,5,14).



In a frequently cited investigation, House studied the condensations of a variety of metal enolates with aldehydes under conditions of thermodynamic control (14). In the cyclohexanone enolate-benzaldehyde condensation (eq. [5]), it was observed that the zinc enolate (14°C, 5 min) afforded a 5:1 ratio of aldol adducts **5T** and



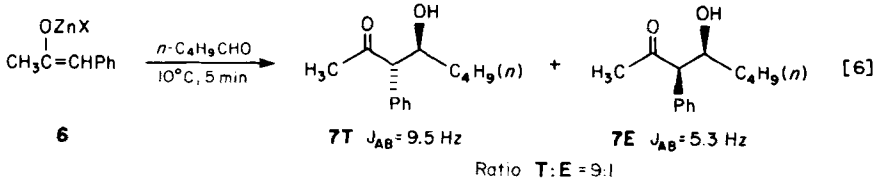
[5]

5T J_{AB} = 8.4 Hz (CCl_4) **5E** J_{AB} = 2.4 Hz (CCl_4)

5E, whereas the corresponding lithium enolate (+5°C, 5 min) afforded a 2:1 mixture of **5T** and **5E**. The diastereomer ratios obtained under these conditions are to be contrasted to those obtained under *kinetic* conditions (-78°C, 5 sec) where virtually no diastereoselection was observed for the lithium enolate (Table 2). The related condensations illustrated below (eq. [6]-[8]) are informative. While the zinc enolate **6** (*E*) afforded largely the threo adduct **7T** (threo/erythro = 9:1) upon condensation with *n*-butyraldehyde, the related zinc enolate **8** (*E*/*Z* = 1) afforded nearly a 1:1 mixture of adducts **9T** and **9E**, which appear to have been fully equilibrated (14). For the two sets of ketols illustrated above (eqs. [6] and [7]), the interchange of phenyl and *n*-butyl substituents between the 2- and 3-positions results in a marked change in the observed stability of the threo and erythro zinc chelates. The condensation of the (*Z*)-enolate **10** under both kinetic (-78°C) and equilibrating conditions (eq. [8]) provides a further example of the experimental options that might be exploited in the aldol process for zinc enolates (15).

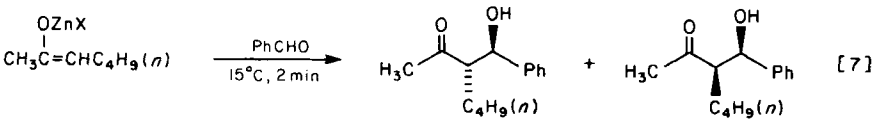
Table 2
Cyclohexanone Enolate Condensation
with Benzaldehyde (eq. [5])

Metal	Solvent	*T* (°C)	Time	Product Ratio 5T:5E	Ref.
ZnCl	DME-Et_2O	+14	5 min	83:17	14
Li	DME	+5	5 min	67:33	14
Li	DME	-72	5 sec	52:48	2



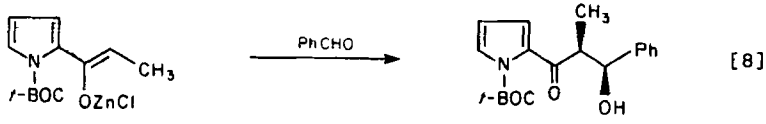
6 7T J_{AB} = 9.5 Hz 7E J_{AB} = 5.3 Hz

Ratio T:E = 9:1



8 9T J_{AB} = 8.7 Hz 9E J_{AB} = 6.6 Hz

Ratio T:E ~ 1:1

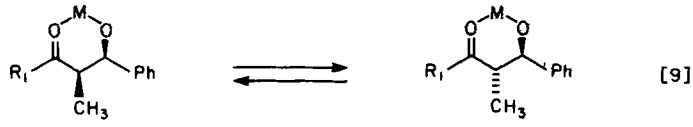


10 11E J_{AB} = 1.5 Hz

Temp, T°C	Ratio, T:E
-78°	1:3
+ 4°	3:1

11T J_{AB} = 7.8 Hz

Recent investigations have provided additional data on erythro-threo metal aldolate equilibration as a function of metal ion M and carbonyl ligand R_1 (eq. [9]) (2). Representative results are included in Table 3. It is apparent from these cases that no conclusions can be drawn concerning the relative rates of equilibration of lithium versus zinc aldolates. It is noteworthy that these data as well as other literature precedents suggest that under equilibrating conditions, the threo diastereomer population may be enhanced in progressing to better chelating metals such as zinc.

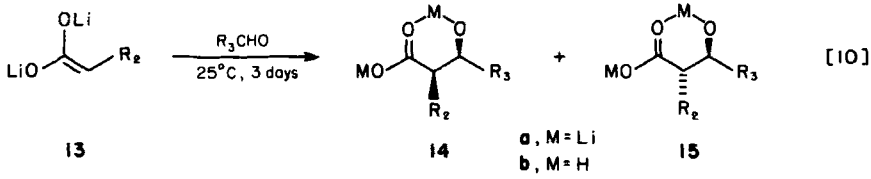


12E 12T

Table 3
Equilibration of Metal Aldolates **12E** and **12T** (eq. [9]) (2)

Entry	R_1	Metal	Half-Life [at T(°C)]	Product Ratio **12E**: **12T** [at T(°C)]
A	Ph	Li	1 min (-60)	48:52 (-15)
B	Ph	ZnX	4 min (-10)	25:75 (-10)
C	Mesityl	Li	5 min (0)	23:77 (0)
D	Mesityl	ZnX	30 sec (-78)	9:91 (-78)
E	Et	Li	–	44:56 (0)
F	$CHMe_2$	Li	–	44:56 (0)

Other studies have provided additional data on the relative stabilities of the lithium aldolates **14** and **15** derived from the condensation of dilithium enediolates **13** (R_2 = alkyl, aryl) with representative aldehydes (eq. [10]) (16). Kinetic aldol ratios were also obtained for comparison in this and related studies (16,17). As summarized in Table 4, the diastereomeric aldol chelates **14a** and **15a**, derived from the enolate of phenylacetic acid **13** (R_2 = Ph), reach equilibrium after 3 days at 25°C (entries A–D). The percentage of threo diastereomer **15** increases with the increasing steric bulk of the aldehyde ligand R_3 as expected. It is noteworthy that the diastereomeric aldol chelates **14a** and **15a** (R_2 = CH_3, C_2H_5, i-C_3H_7) do not equilibrate at room temperature over the 3 day period (16). In a related study directed at delineating the stereochemical control elements of the Reformatsky reaction, Kurtev examined the equilibration of *both*



13 **14** **15**

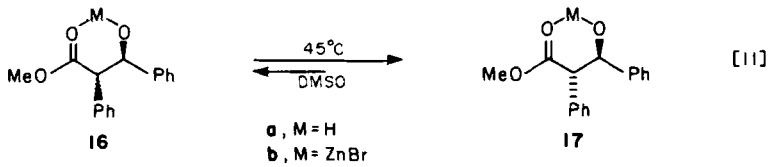
the erythro and threo hydroxy esters **16** and **17** as a function of both counterion and solvent (eq. [11]) (17). The zinc chelates **16a** and **16b** were found to be stable in nonpolar solvents (C_6H_6, 45°C, 1 hr), but complete equilibration was realized from either diastereomer in dimethyl sulfoxide (DMSO) (45°C, 1 hr). The equilibrium ratio obtained in this study, **16**:**17** = 35:65, differs significantly from that observed by Mulzer in the related system, **14**:**15** (R_2, R_3 = Ph) = 8:92 (Table 4, entry D).

Table 4
Thermodynamically Controlled Aldol Condensations
of Enediolate **13** (eq. [10]) (16)

Entry	R_2	R_3	Product Ratio **14**:**15**
A	Ph	CH_3	36:64
B	Ph	C_2H_5	36:64
C	Ph	i-C_3H_7	20:80
D	Ph	Ph	8:92
E	Ph	t-C_4H_9	2:98
F	t-C_4H_9	Ph	2:98
G[a]	t-C_4H_9	t-C_4H_9	2:98

[a]Equilibrium reached at 45°C, 3 days.

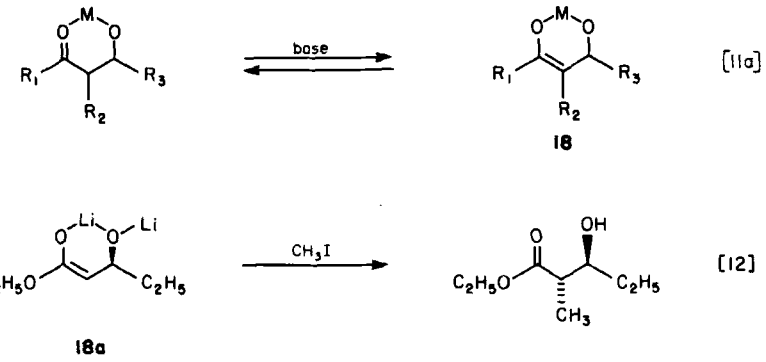
In the equilibration studies previously cited, two mechanisms for the interconversion of aldol diastereoisomers are possible, the most obvious being via the retroaldol process (28). In some instances, however, base-catalyzed equilibration via the aldolate enolate **18** is certainly possible (eq. [11a]), and such enolates are well documented as useful intermediates in synthesis (19). For example, Fráter has demonstrated that aldolate enolate **18a** may be generated from



16 **17** [11]

the corresponding β-hydroxy ester, without competing retroaldolization, and that subsequent alkylations occur with excellent threo diastereoselection (≥95%) (19a). Related observations have been noted by Seebach and Kraus (19b, 19c).

It would be highly desirable to be able to correlate metal ion structure as well as the individual steric requirements of the specific substituents R_1, R_2, and R_3 with the equilibration studies cited above. Because of the numerous uncertainties associated with the data, however, only qualitative generalizations can be made. The higher-valent metal aldolate complexes (M = ZnL, MgL, AlL_2), upon equilibration, appear to favor the threo diastereomer to a greater extent than the monovalent metal aldolates (M = Li, Na). With regard to



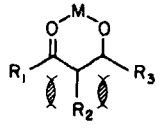
[11a]

18

18a

[12]

substituent steric effects, it is tempting to conclude that the increased steric requirements of the R_2-aldolate ligand for a given permutation of substituents R_1, R_2, and R_3 should play the dominant role in the perturbation of the erythro-threo-aldolate equilibrium. An increase in the size of R_2 will increase both the

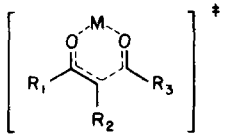


$R_3 \leftrightarrow R_2$ and $R_2 \leftrightarrow R_1$ gauche interactions; however, for the same set of substituents, an increase in the steric requirements of either R_1 or R_3 will influence only one set of vicinal steric interactions ($R_1 \leftrightarrow R_2$ or $R_3 \leftrightarrow R_2$). Some support for these conclusions has been cited (eqs. [6] and [7]). These qualitative arguments may also be relevant to the observed populations of hydrogen- and nonhydrogen-bonded populations of the aldol adducts as well (see Table 1, entries K, L). Unfortunately, little detailed information exists on the solution geometries of these metal chelates. Furthermore, in many studies it is impossible to ascertain whether the aldol condensations between metal enolates and aldehydes were carried out under kinetic or thermodynamic conditions. Consequently, the importance of metal structure and enolate geometry in the definition of product stereochemistry remains ill defined. This is particularly true in the numerous studies reported on the Reformatsky reaction (20) and related variants (21).

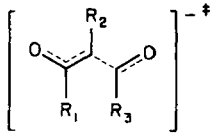
V. KINETICALLY CONTROLLED ALDOL DIASTEREOSELECTION: ACHIRAL REACTION PARTNERS

The ultimate goal of designing highly enantioselective aldol condensations demands that all stereochemical aspects of the bond construction process be kinetically controlled. Over the past 5 years, this objective has stimulated a great deal of research, and a wealth of new information is now becoming available on the important kinetic stereochemical control elements and possible transition state geometries for this reaction.

For reactions involving metal enolates (M = Li, MgL, ZnL, BL_2, AlL_2, etc.), the pericyclic transition state **I**, first proposed by Zimmerman in 1957 (22), has gained widespread acceptance, and a considerable amount of experimental data supports this general transition state geometry (see below). On the other hand, considerably less information is available for the preferred transition state geometries for reactions between aldehydes and "naked" or ion-pair dissociated enolates. It has been proposed that, in the absence of the organization features of Lewis acidic metals, such enolates may prefer to react via an "open" or acyclic transition state such as **II** (4). Similar, but positively charged, acyclic transition states may also be important in the Lewis acid-catalyzed condensations of aldehydes or acetals with enol ethers (4).



I

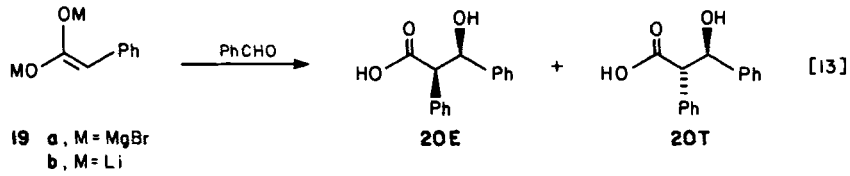


II

A. Diastereoselectivity as a Function of Enolate Geometry

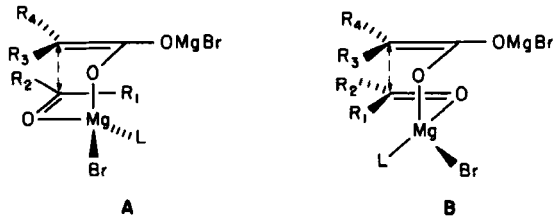
From a historical standpoint, the Zimmerman-Traxler study on the stereochemical aspects of the Ivanov reaction is of considerable significance (22). Their investigation revealed that the magnesium enediolate **19a**, upon condensation with benzaldehyde (Et_2O, reflux 5 hr), afforded the erythro and threo acids **20E** and **20T**, respectively, in a 24:76 ratio (eq. [13]). In the analysis of plausible transition states, both chair **A** and boat **B** geometries were considered. Zimmerman and Traxler concluded that the major diastereomer **20T** could

be rationalized as having arisen from the chair-preferred transition state A (R_2,R_3 = Ph; R_1,R_4 = H). It is worth noting that the control experiments demonstrating *kinetic* diastereoselection were not



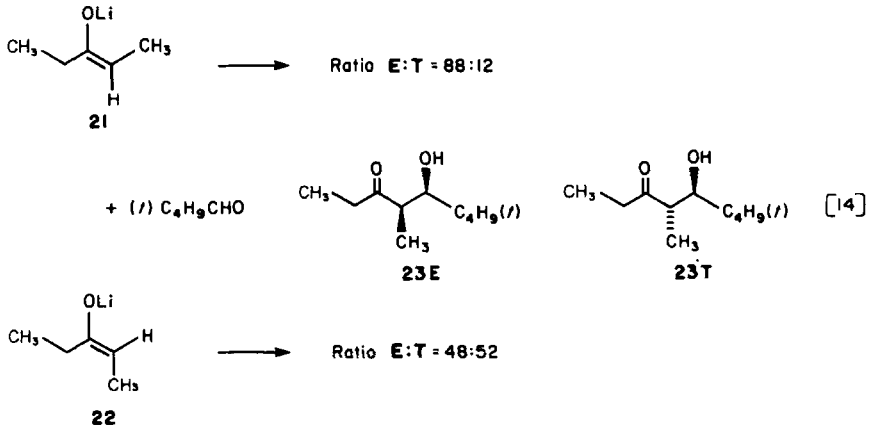
19 a, M = MgBr
b, M = Li

20E **20T**



carried out; nonetheless, subsequent studies by Mulzer (16) on the condensation of the analogous lithium enolate **19b** (THF, -50°C, 10 min) under kinetically controlled conditions afforded similar results (**20E**:**20T** = 29:71) (23).

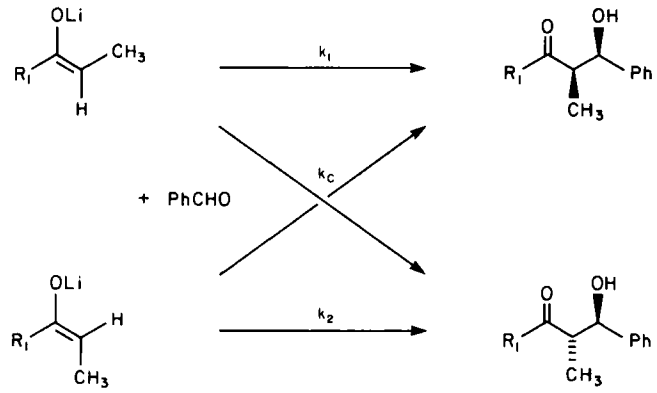
One of the first important studies to address the implications of enolate geometry on aldol product stereochemistry was reported by Dubois and Fellmann (eq. [14]) (5c). The condensation of the (*Z*)-



and (*E*)-lithium enolates **21** and **22** with pivaldehyde (Et_2O, -10°C). afforded the diastereomeric aldol adducts **23E** and **23T** in the ratios indicated. The interesting observation that the (*Z*)-enolate **21** exhibited good erythro diastereoselection (**E**:**T** = 88:12) whereas the (*E*)-enolate **22** was virtually stereorandom, has been substantiated in more recent studies on related lithium enolates (cf. Table 5) (2). The additional observation that **21** undergoes aldol condensation five to seven times more rapidly than **22** could have a bearing on the respective transition state geometries; however, an interpretation of such rate differences is seriously complicated by solution aggregation phenomena, which also must be addressed (24).

The observed aldol stereoselection as a function of both enolate geometry and enolate ligand R_1 is summarized in Table 5. It is clear from these results that the increasing steric requirements of the substituent R_1 appear to confer greater kinetic stereoselection from the (*Z*)- as opposed to the (*E*)-enolate geometry (Scheme 2).

An additional important observation that (*Z*)-enolates exhibit erythro diastereoselection was made by Dubois and Fellmann (5b). Their investigation demonstrated that the magnesium enolate **24a** (20°C, Et_2O) condensed with benzaldehyde under "kinetic conditions" to give exclusively the erythro diastereomer **25E** (R_3 = Ph, **E**:**T** > 95:5), and upon prolonged equilibration afforded the isomeric threo adduct (**T**:**E** > 95:5) (eq. [15]). Heathcock has reported



Scheme 2

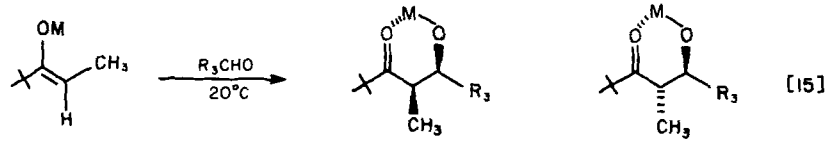
analogous results with benzaldehyde and the lithum enolate **24b**, and has also noted that the half-life for erythro → threo equilibration is approximately 8 hr (25°C). Control experiments have revealed that

Table 5
Kinetic Diastereoselection as a Function of Enolate Structure (2)[a]

Enolate Ligand R_1	(*Z*)-Enolates, k_1/k_c	(*E*)-Enolates, k_2/k_c
CH_3O	–	1.5
t-C_4H_9O	–	1.0
H	1	1.5
C_2H_5	9 (7.3)[b]	1.0 (1.08)[b]
i-C_3H_7	9	1.0
C_6H_5	7	–
t-C_4H_9	>50	–
1-Adamantyl	>50	–
2,4,6-$(CH_3)_3C_6H_2$	>50	>50

[a]Condensation carried out at -72°C for 5 sec, except as noted.
[b]Condensation carried out at -10°C (Et_2O), ref. 5c.

the retroaldol process associated with **25E** (M = Li, R_3 = Ar) is *rapid* ($T_{1/2} \approx 15$ min) at 0°C and that the slow diastereomer equilibration is related to the exceptional levels of erythro diastereoselection exhibited by enolate **24b** ($k_{erythro}:k_{threo} \approx 80$) (2). The French group subsequently demonstrated the uniformly high kinetic erythro diastereoselection for enolate **24a** for a range of aldehydes (R_3 = CH_3, C_2H_5, i-C_3H_7, t-C_4H_9) (5d).



24 a, M = MgBr
b, M = Li

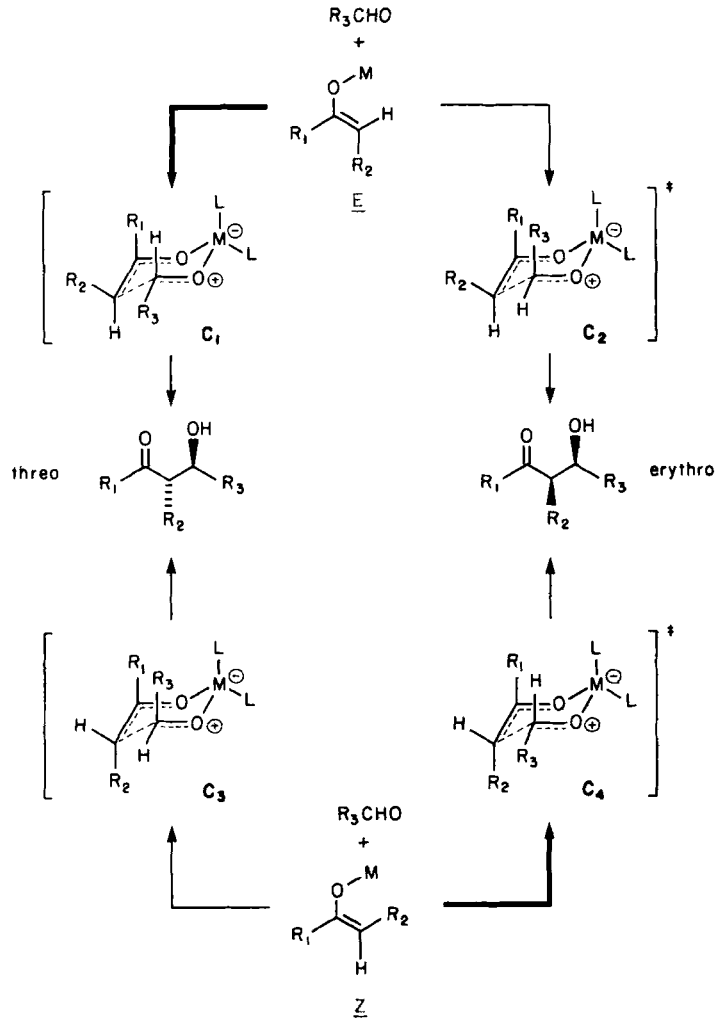
25E

25T

95:5 (kinetic)
<5:95 (thermodynamic)

[15]

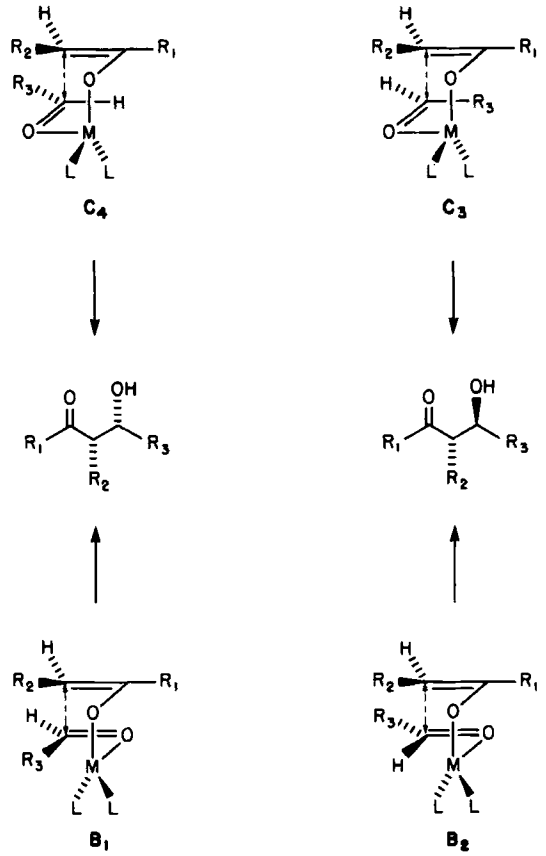
The correlation of metal enolate geometry and aldol product stereochemistry via diastereomeric chair-preferred transition states has been widely accepted (2,5,6,16). The observations that the steric bulk of the enolate ligand R_1 and attendant aldol diastereoselection are directly coupled are consistent with the elaborated Zimmerman model illustrated in Scheme 3 for chair-preferred transition states. For example, for (*E*)-enolates, transition state C_2 is predicted to be destabilized relative to C_1 because of the $R_1 \leftrightarrow R_3$ variable steric



Scheme 3

parameter. In a similar fashion, transition state C_3 is destabilized relative to C_4 for (*Z*)-enolates (6). It is somewhat less obvious why (*E*)-lithium enolates are generally less stereoselective (cf Table 5) than the isomeric (*Z*)-enolates. It has been argued that transition state gauche interactions between R_2 and R_3 must also be considered (2), but detailed arguments to support this contention, taking into consideration $R_2 \leftrightarrow R_3$ gauche effects for *both* transition states C_1 and C_2, were not provided.

The basic assumption of the chair-preferred transition state (for tetrahedral metal centers) is clearly tenuous, and diastereomeric boat transition state geometries should not be discounted. For example, the diastereomeric chair and boat transition states for (*Z*)-enolates are illustrated in Scheme 4. For this enolate geometry it is entirely reasonable to consider that the heat of formation of boat transition state $\mathbf{B_2}$ might actually be *less* than chair transition state $\mathbf{C_4}$ for certain combinations of substituents R_1, R_2, and R_3. For example, boat transition state $\mathbf{B_2}$ not only disposes substituents R_2 and R_3 in a staggered conformation as in chair transition states $\mathbf{C_3}$ and $\mathbf{C_4}$, but also minimizes $R_1 \leftrightarrow R_3$ eclipsing, which must be significant in chair transition state $\mathbf{C_3}$. The change in kinetic aldol diastereoselection of



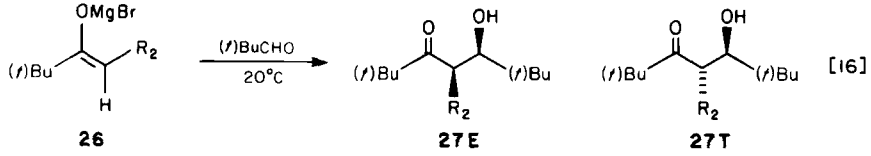
Scheme 4

Table 6
Kinetic Diastereoselection as a Function
of the Enolate Ligand R_2 (eq. [16]) (5d)

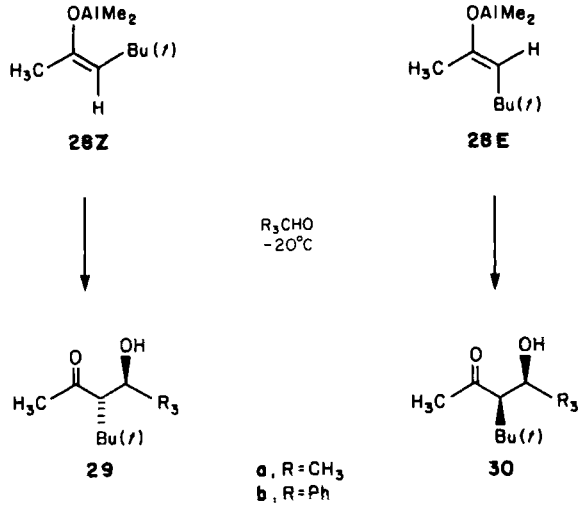
Enolate Ligand R_2	Product Ratio[a] 27E:27T	J_{AB} (Hz)[b] 27E	27T
CH_3	100:0	1.1	4.5
C_2H_5	100:0	1.2	3.0
n-C_3H_7	98:2	0	2.1
i-C_4H_9	97:3	0	2.0
i-C_3H_7	29:71	–	1.1
t-C_4H_9	0:100	–	0.8

[a]Condensations carried out at 20°C (Et_2O) and times ranging from 5 to 45 min.
[b]Determined in CCl_4.

(*Z*)-enolate **26** as a function of the steric requirements of the enolate ligand R_2 (eq. [16]) is summarized in Table 6. The continuous change from high levels of erythro diastereoselection for $R_2 = CH_3$ (**E**:**T** = 100:0) to threo diastereoselection for $R_2 = t$-C_4H_9 (**T**:**E** = 100:0) could be ascribed to a crossover from a chair-preferred (transition state C_4) to a boat-preferred (transition state B_2) process. By inspection, it appears that the boat transition state B_2 (R_1, R_2, R_3 = t-C_4H_9) may be no more sterically congested than the alternate chair transition state C_3 leading to the threo aldol product manifold. The results obtained in the investigation above are in accord with a related study reported by Jeffery (12), in which the individually purified (*Z*)- and (*E*)-aluminum enolates **28Z** and **28E** were condensed with both acetaldehyde and benzaldehyde under conditions of apparent kinetic control (Scheme 5). With acetaldehyde, the aldol process proceeded with complete threo stereoselection to give **29a** in good yield with the (*Z*)-enolate **28Z** while the (*E*)-enolate **28E** afforded largely the erythro adduct **30a** (**30a**:**29a** = 93:7). In the analogous study with benzaldehyde, both enolates afforded the threo adduct **29b**. The lack of complete stereochemical correspondence for



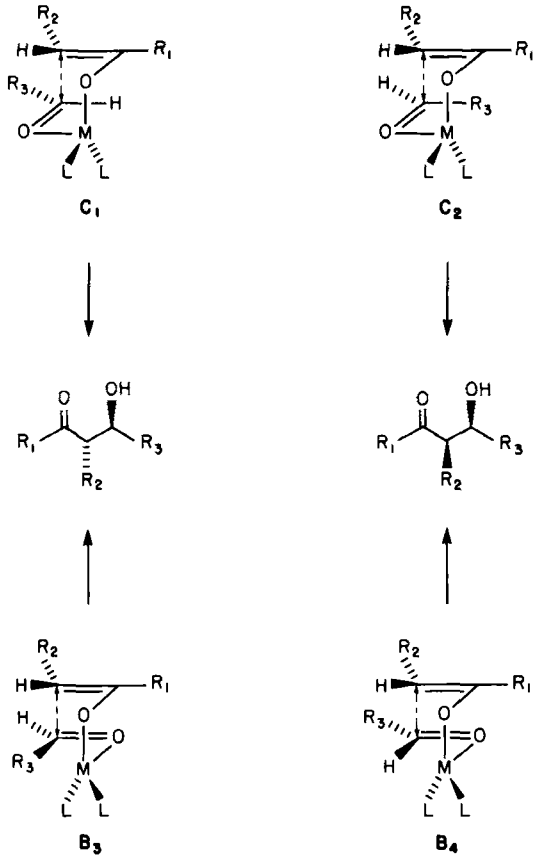
26 **27E** **27T** [16]



Vicinal Coupling Constants J_{AB} (CCl_4) : 29a, 3.0 Hz ; 30a, 7.5 Hz
29b, 3.2 Hz

Scheme 5

the two aldehydes could be ascribed to a property of the aldolate complexes derived from benzaldehyde, which appear to exhibit a greater tendency to undergo retroaldolization than the analogous aldolate complexes derived from aliphatic aldehydes (25). The stereochemical consequences of the aldol condensations of aluminum enolate **28Z** and magnesium enolate **26Z** (R_2 = *t*-C_4H_9) (Table 6) are identical (100% threo diastereoselection) and apparently independent of the enolate ligand R_1 (CH_3 vs. *t*-C_4H_9). The observance of an erythro selective condensation from the (*E*)-aluminum enolate is of considerable significance from a mechanistic standpoint. If the diastereomeric chair and boat transition states are considered for (*E*)-enolates (Scheme 6), erythro product stereoselection must arise from either the chair transition state C_2 or the highest energy boat transition state B_4 wherein substituents R_2 and R_3 are eclipsed. These observations, taken with the generally lower levels of threo diastereoselection observed for (*E*)-enolates (Table 5), suggest that the magnitude of the transition state $R_2 \leftrightarrow R_3$ gauche interactions in the diastereomeric chair transition states C_1 and C_2 may be *different*. If the $R_2 \leftrightarrow R_3$ interaction is assumed to be *greater* in C_1 than in C_2, the lower levels of threo diastereoselection and the predominant erythro diastereoselection observed for enolate 28E and acetaldehyde



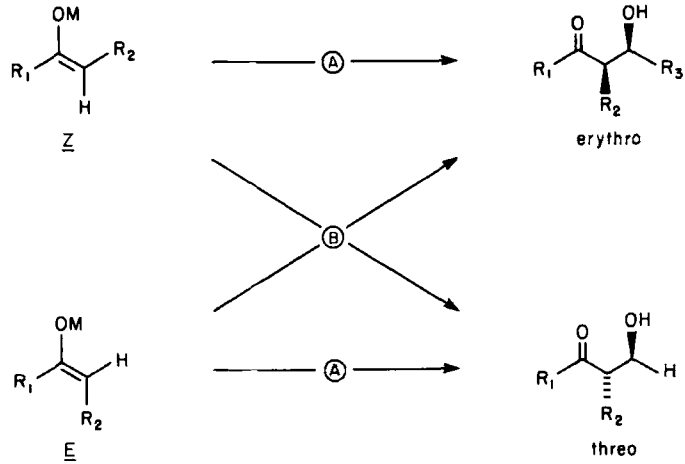
Scheme 6

are adequately accounted for by a consideration of the diastereomeric chair transition states C_1 and C_2. From an editorial standpoint it should be pointed out that a rigorous stereochemical assignment of the isomeric enolates **28Z** and **28E** has not been made (12). In this context it is rather surprising that thermal equilibration of **28Z** affords **28E**.

The studies just cited demonstrate several important design features pertaining to the objective of achieving highly stereoselective aldol condensations with Group I–II metal enolates.

1. Enolate geometry is an important stereochemical aspect of the problem.

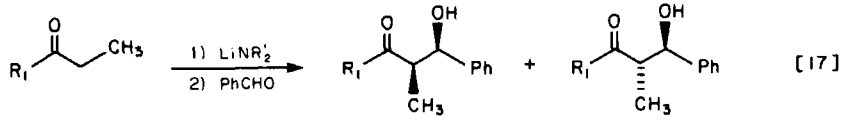
2. Lithium, magnesium, and aluminum enolates appear to afford comparable levels of kinetic aldol diastereoselection for a given enolate of defined structure.
3. The steric influence of the enolate substituents R_1 and R_2 plays a dominant role in the alteration of kinetic stereoselectivity, whereas the aldehyde ligand appears to contribute to a minor extent. Good correlation between enolate geometry and aldol stereochemistry is possible when R_1 is sterically demanding and R_2 is sterically subordinate (R_2 = methyl or *n*-alkyl). In this case dominant path A stereoselection is observed. When R_2 becomes sterically demanding (R_2 = *t*-Bu) path B stereoselection is observed and becomes dominant.



4. The Zimmerman (22) cyclic transition state model involving either the chair or the boat geometry adequately correlates existing data.

B. Group I and II Metal Ketone Enolates

The tables that follow provide additional examples not cited in the foregoing discussion and further amplify the conclusions drawn above. Table 7 summarizes the influence of the ketone substituent R_1 on



[17]

Table 7
Kinetic Aldol Condensations of Acyclic Lithium Ketone Enolates with Benzaldehyde (eq. [17]) (2, 26)

Enolate Ligand R_1	Base[a]	Enolate Ratio $Z:E$[b]	Erythro-Threo Product Ratio[c]
H	Via Silyl ether	100:00	50:50
H	Via Silyl ether	0:100	65:35
C_2H_5	LDA	30:70	64:36
C_2H_5	LCPA	35:65	62:38
C_2H_5	LHMDS	66:34	77:23
C_2H_5	LTMP	20:80	66:34
i-C_3H_7	LDA	60:40	82:18
i-C_3H_7	LCPA	59:41	75:25
i-C_3H_7	LHMDS	>98:2	90:10
i-C_3H_7	LTMP	32:68	58:42
i-C_3H_7	Via Silyl ether	0:100	45:55
t-C_4H_9	LDA	>98:2	>98:2
C(OTMS)Me_2	LDA	NA	>98:2
1-Adamantyl	LDA	>98:2	>98:2
TMS	LDA	38:62	58:42
C_6H_5	LDA	>98:2	88:12
C_6H_5	LCPA	>98:2	87:13
C_6H_5	LHMDS	>98:2	88:12
C_6H_5	LTMP	>98:2	83:17
Mesityl	LDA	5:95	8:92
Mesityl	LCPA	4:96	9:91
Mesityl	LHMDS	87:13	88:12
Mesityl	LTMP	NA	4:96

[a]LDA, lithium diisopropylamide; LCPA, lithium cyclohexylisopropylamide; LHMDs, lithium hexamethyldisilylamide; LTMP, lithium 2,2,6,6-tetramethylpiperidide.
[b]NA, not analyzed.
[c]Condensations carried out at -72°C, 5 sec.

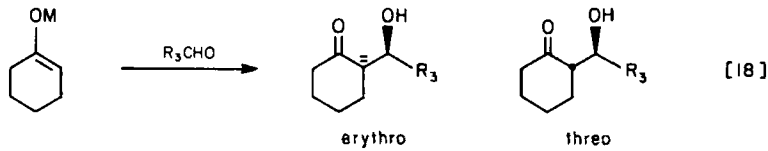
both the enolization process and the resultant aldol condensation of the lithium enolates derived from ethyl ketones (eq. [17]).

A large number of studies have addressed the condensation of cyclic ketones with both aliphatic and aromatic aldehydes under conditions that reflect both thermodynamic (cf. Table 2) and kinetic control of stereochemistry. The data for cyclohexanone enolates are summarized in Table 8. Except for the boryl enolates cited (6), the outcome of the kinetic aldol process for these enolates

Table 8
Kinetic Aldol Condensations of
Cyclohexanone Enolates with Aromatic Aldehydes (eq. [18])

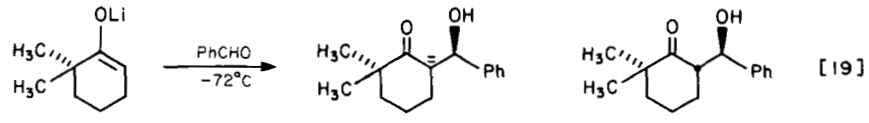
Aldehyde Ligand R_3	Metal	Solvent [at T(°C)]	Erythro-Threo Product Ratio	Ref.
Ph	Li	THF (-72)	48:52	2
Ph	$AlMe_2$	THF (-20)	50:50	21a
Ph	$B(c\text{-}C_5H_9)_2$	Et_2O (-78)	32:68	6
Ph	$B(c\text{-}C_5H_9)_2$	Pentane (-78)	15:85	6
Ph	$B(c\text{-}C_5H_9,C_6H_{13})$	THF (-78)	4:96	6
$p\text{-}NO_2C_6H_4$	Na	H_2O (0)	36:64	10

is uniformly nonstereoselective. With regard to the importance of the steric effects at the enolate center, it is not surprising that the condensation of enolate 31 is more stereoselective (eq. [19]) than the unsubstituted cyclohexanone lithium enolate (Table 8) (2) and that α-substitution provides little enhancement in kinetic product diastereoselection with the aluminum enolate 32 (eq. [20]) (21a). Related

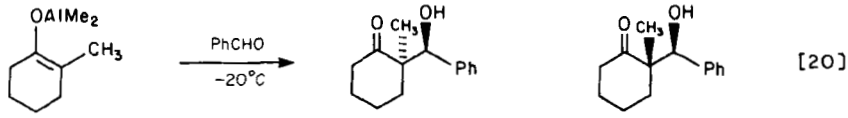


[18]

studies that address the issues of both kinetic and thermodynamic aldol diastereoselection with cyclopentanone and a range of aldehydes have been reported by Dubois (27,28). In this investigation the condensations were carried out with hydroxide bases at various temperatures. Good levels of kinetic threo diastereoselection were noted in several instances. The consequences of added enolate steric effects and the relationship between kinetic aldol diastereoselection in the cyclopentanone system have also been reported by Fellmann and Dubois (eq. [21]) (5d). This study complements the stereochemical observations cited earlier for magnesium enolate 26 (eq. [16], Table 6). The results summarized in Table 9 are consistent with the conclusions drawn earlier on the relative importance of enolate substituents R_1 and R_2 on aldol diastereoselection. As noted earlier, when R_2 is not sterically demanding ($R_2 = CH_3$, C_2H_5), good levels of threo diastereoselection (via a chair-preferred transi-

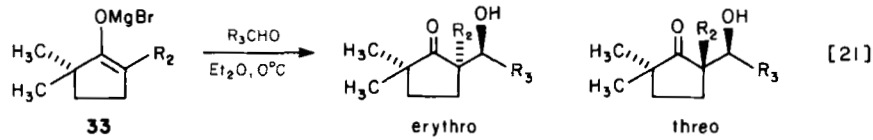


31 [19]



32 [20]

tion state?) would be expected and are observed. The importance of enolate geminal-dimethyl substitution (large R_1) is no doubt responsible for the good stereoselectivity (cf. eqs. [15] and [16]) in this system. With the increasing steric requirements of the enolate ligand R_2, aldol diastereoselection is observed to shift to the erythro manifold, via either a boat or a chair transition state geometry.



33 [21]

Table 9
Kinetic Aldol Condensation of Enolate 33 (eq. [21]) (5d)

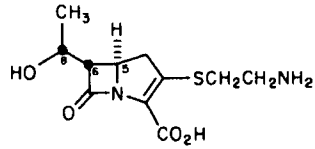
R_2^a	R_3	Erythro-Threo Ratio
CH_3	CH_3	6.5:93.5
CH_3	C_2H_5	6.0:94.0
CH_3	i-C_3H_7	3.0:97.0
CH_3	t-C_4H_9	1:99
C_2H_5	CH_3	12.5:87.5
i-C_3H_7	CH_3	54:46
t-C_4H_9	CH_3	71:29

[a]Condensations carried out at either -20 or 0°C (Et_2O); times from 1 to 30 min.

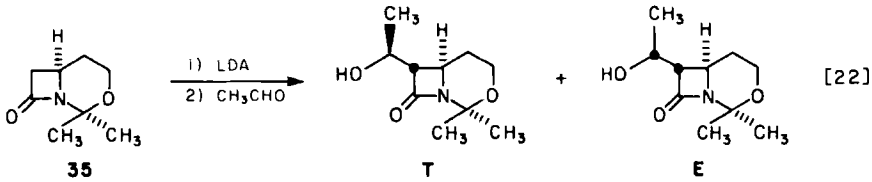
C. Group I and II Metal Ester and Amide Enolates

The medicinally important β-lactam antibiotic thienamycin (**34**) has stimulated several investigations into the application of the aldol reaction for the introduction of the hydroxyethyl moiety with the indicated C_6 and C_8 stereochemistry (29,30). Low-temperature enolization (LDA, THF) of either **35** (29a,b) or **36** (30) and subsequent condensation with excess acetaldehyde afforded the illustrated kinetic aldol adducts (eqs. [22] and [23]). In both examples the modest levels of threo diastereoselection are comparable to related data for unhindered cyclic ketone lithium enolates. Related condensations on the penam nucleus have also been reported (31).

The kinetic enolization of esters with amide bases such as lithium diisopropylamide (LDA) and the resultant aldol condensations with representative aldehydes have been investigated by several groups (2,32,33). The enolate stereochemical assignments were determined by silylation in direct analogy to studies reported by Ireland (34). The preponderance of (*E*)-enolate observed with LDA (THF) in these

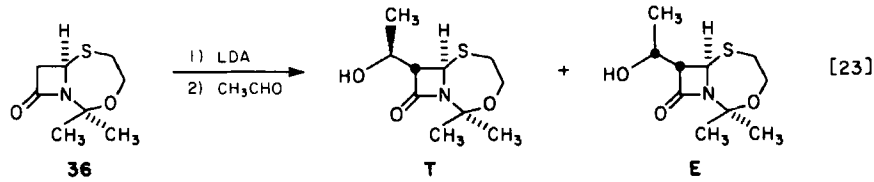


34



35 **T** **E**

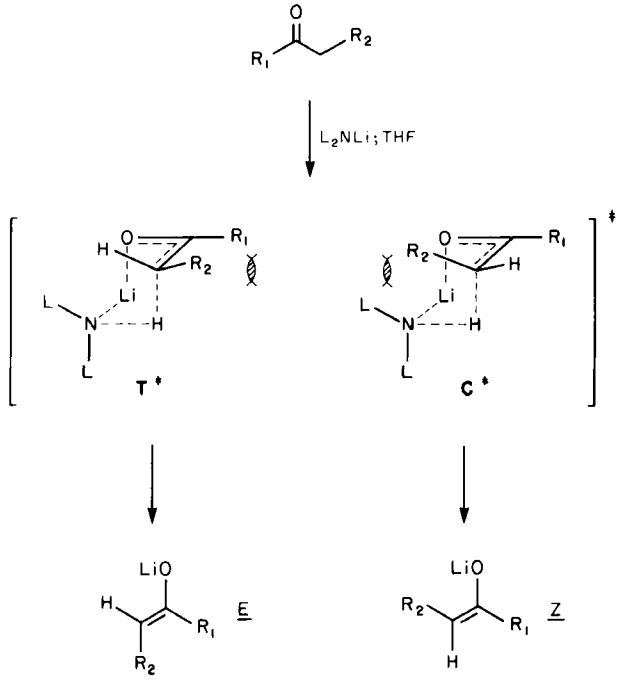
Ratio, **T**:**E** = 60:40



36 **T** **E**

Ratio, **T**:**E** = 67:33

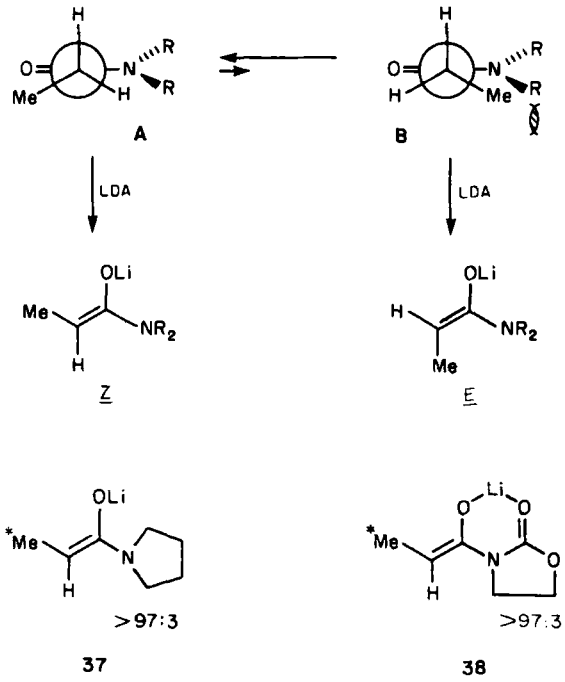
and related studies with ketonic substrates can be rationalized by a consideration of the nonbonding interactions in the pericyclic transitions states $T^{\ddagger}$ and $C^{\ddagger}$, respectively, illustrated in Scheme 7 (34).



Scheme 7

Dominant $R_1 \leftrightarrow R_2$ steric control elements are predicted to disfavor transition state $T^{\ddagger}$ and promote enolization to give the (*Z*)-geometry, whereas dominant $R_2 \leftrightarrow L$ nonbonded interactions should disfavor transition state $C^{\ddagger}$ and promote enolization to afford the (*E*)-enolate geometry. As summarized below in Table 10, under conditions of "apparent" kinetic control, esters and thioesters afford largely (*E*)-enolates (transition state $T^{\ddagger}$), and the dialkylamides exhibit predominant to exclusive (*Z*)-enolization (transition state $C^{\ddagger}$).

In conjunction with our studies on the synthetic utility of amide enolates (35,36), we have postulated that the high (*Z*)-stereoselection observed in the deprotonation of dialkylamides is a consequence of ground state allylic strain considerations (37), which strongly disfavor amide conformation **B** (Scheme 8), and consequently the associated transition state $T^{\ddagger}$ (Scheme 7) for deprotonation, to give (*E*)-enolates.



Scheme 8

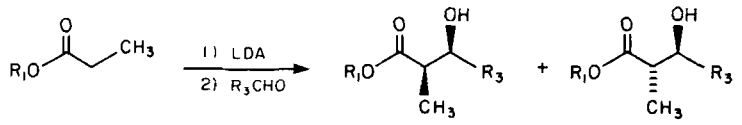
Detailed investigations indicate that the enolization process (LDA, THF) affords enolates 37 and 38 with *at least* 97% (*Z*)-stereoselection. Related observations have recently been reported on the stereoselective enolization of dialkylthioamides (38). In this latter study, the Ireland-Claisen strategy (34) was employed to assign enolate geometry. Table 10 summarizes the enolization stereoselection that has been observed for both esters and amides with LDA. Complementary kinetic enolization ratios for ketonic substrates are included in Table 7. Recent studies on the role of base structure and solvent are now beginning to appear in the literature (39,40), and the Ireland enolization model for lithium amide bases has been widely accepted. A tabular survey of the influence of the ester moiety (OR_1) on a range of aldol condensations via the lithium enolates is provided in Table 11 (eq. [24]). Enolate ratios for some of the condensations illustrated may be found in Table 10. It is apparent from these data that (*E*)-enolates derived from alkyl propionates (R_1 = CH_3, t-C_4H_9) exhibit low aldol stereoselectivity. In contrast, the enolates derived from alkoxyalkyl esters (R_1 = CH_2OR') exhibit ~ 10:1 threo diastereo-

Table 10
Kinetic Enolization of Carboxylic
Acid Esters and Amides (Scheme 7)

R_1	R_2	Base[a]	Enolate Ratio $E:Z$	Ref.
OCH_3	CH_3	LDA	95:5	2
OCH_3	C_2H_5	LDA	91:9	34
OCH_3	Ph	LDA	29:71	34
OCH_3	t-C_4H_9	LDA	97:3	34
Ot-C_4H_9	CH_3	LDA	95:5	2
Ot-C_4H_9	C_2H_5	LDA	95:5	34
St-C_4H_9	CH_3	LDA	90:10	35
$N(C_2H_5)_2$	CH_3	LDA	<3:97	36b
$N(CH_2)_4$	CH_3	LDA	<3:97	36a
$N(i$-$C_3H_7)_2$	CH_3	LDA	19:81	2

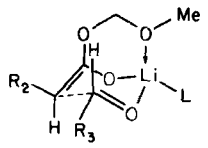
[a] All reactions were carried out at about -70°C in tetrahydrofuran.

selection (32). The enhanced aldol diastereoselection resulting from the inclusion of potential chelating centers is a noteworthy observation, and chelated bicyclic transition states such as **39** and **40** could be responsible for the enhanced threo diastereoselection. However,

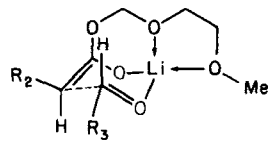


[24]

the generality of Meyers' observations has recently been called into question by the observation that ester **41** (LDA) afforded only a 1:1 ratio of diastereomeric aldol adducts **42** with benzaldehyde (eq. [25]) (2). The lower level of aldol diastereoselection observed in this case is fully consistent with the earlier discussion on $R_2 \leftrightarrow$

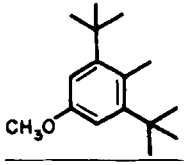


39



40

Table 11
Kinetic Aldol Condensations of Ester Lithium Enolates[a] (eq. [24])

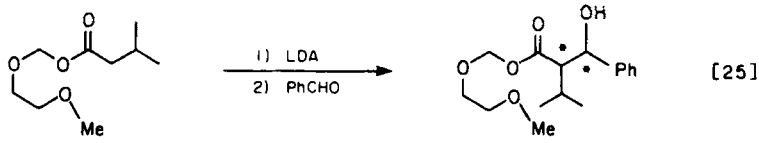
R_1	R_3	Erythro-Threo Ratio	Ref.
CH_3	i-C_3H_7	45:55	32
CH_3	CH_3	43:57	32
CH_3	C_6H_5	45:55	32
CH_3	C_6H_5	62:38	2
t-C_4H_9	C_6H_5	49:51	2
t-C_4H_9	C_6H_5	35:65[b]	2
CH_3OCH_2	i-C_3H_7	10:90	32
CH_3OCH_2	CH_3	33:67	32
$CH_3OCH_2CH_2OCH_2$	i-C_3H_7	9:91	32
$CH_3OCH_2CH_2OCH_2$	C_6H_5	25:75	2, 32
$C_2H_5OCH(CH_3)$	i-C_3H_7	9:91	32
2,6-$(CH_3)_2C_6H_3$	C_6H_5	12:88	33
2,6-$(CH_3)_2C_6H_3$	n-C_5H_{11}	14:86	33
2,6-$(CH_3)_2C_6H_3$	i-C_3H_7	<2:98	33
2,6-$(CH_3)_2C_6H_3$	t-C_4H_9	<2:98	33
	n-C_5H_{11}	<2:98	33

[a]Except where noted lithium diisopropylamide (LDA) was employed as the enolization base.
[b]Lithium 2,2,6,6-tetramethylpiperidide used instead of LDA.

R_3 transition state gauche effects (cf. Scheme 6), which appear to be greater in transition state C_1 than in C_2.

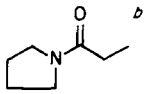
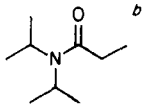
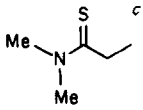
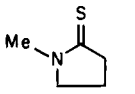
The enolates derived from 2,6-disubstituted phenyl propionates appear to exhibit the highest levels of threo aldol diastereoselection yet reported for lithium-mediated condensations (33). These substrates should enjoy widespread use in stereoselective synthesis.

The kinetic aldol diastereoselection observed for a range of amide lithium enolates is reported in Table 12. It is significant that the



41 42 T:E = 1:1 [25]

Table 12
Stereoselective Aldol Condensations of Dialkylamide Lithium Enolates

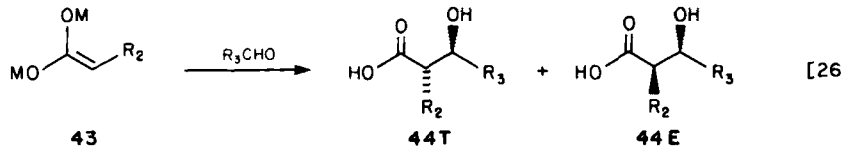
Amide	Aldehyde	Conditions[a]	Erythro-Threo Ratio	Ref.
 [b]	PhCHO	-70°C (5 sec)	60:40	35
 [b]	PhCHO	-70°C (5 sec)	61:39 63:37	35 2
 [c]	PhCHO	-78°C (2 min)	87:13	38
	C_2H_5CHO	-78°C (10 min)	90:10	38
 [c]	i-C_3H_7CHO	-78°C (10 min)	19:81	38

[a] All reactions carried out in THF.
[b] Enolization with LDA.
[c] Enolization with n-C_4H_9Li.

illustrated acyclic thioamides exhibit somewhat higher erythro diastereoselection than the corresponding amide systems (38). Related amide zinc enolates, generated via the Reformatsky procedure, exhibit comparable levels of diastereoselection (41).

Extensive studies have been carried out on the metal enediolates of carboxylic acids and the influence of substrate structure on kinetic aldol diastereoselection (eq. [26]). For all but the most sterically demanding substituents (R_2 = t-C_4H_9, mesityl, 1-adamantyl) the condensations exhibit only modest threo diastereoselection (Table 13). The reader is referred to Table 4 for the analogous thermodynamically controlled aldol data.

A study aimed at gaining further insight into possible transition state stereochemical control elements examined the effect of added



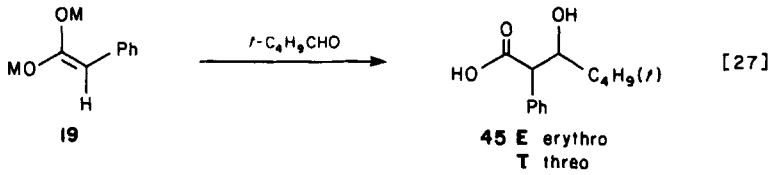
43 44T 44E [26]

Table 13
Kinetic Aldol Condensations of Enediolate 43 as a Function of M, R_2, and R_3 (eq. [26])

R_2	R_3	M[a]	Product Ratio 44*T*:44*E*	Ref.
CH_3	Ph	Li	55:45	16
CH_3	t-C_4H_9	Li	50:50	16
C_2H_5	Ph	Li	52:48	16
i-C_3H_7	Ph	Li	55:45	16
Ph	Ph	Li	71:29	16
Ph	Ph	MgBr	76:24	22
Ph	t-C_4H_9	Li	70:30	17
t-C_4H_9	i-C_3H_7	Li	79:21	16
t-C_4H_9	t-C_4H_9	Li	80:20	16
Mesityl	Mesityl	Li	>98:2	17
1-Adamantyl	1-Adamantyl	Li	>98:2	17
1-Adamantyl	t-C_4H_9	Li	>98:2	17

[a]Enolization was carried out with 2 equiv LDA in THF. Condensations were run between -70 and 0°C.

metal chelating agents on the specific aldol condensation illustrated in eq. [27] (17). In the absence of chelating agents, enolate 19 (M = Li, Na, K) exhibited 70 to 79% kinetic threo diastereoselection. The dramatic influence of chelating agents becomes apparent with the



19

45 E erythro
T threo

[27]

most ionic potassium enediolate, where greater than 97% threo diastereoselection was observed (Table 14). Suitable control experiments were carried out to ensure that kinetic rather than thermodynamic stereochemical control (45E ⇌ 45T = 2:98; cf. Table 4) was operational. In the *presumed* absence of metal ion-mediated pericyclic transition states, the four transition state geometries illustrated in Scheme 9 were considered. Based on the steric requirements of enolate and aldehyde substituents chosen (R_3 = t-C_4H_9), transition states $B^{\ddagger}$ and $C^{\ddagger}$, with gauche and eclipsed substituents, were excluded.

Table 14
Kinetic Aldol Condensations of Enediolate 19 (eq. [27]).
Influence of Chelating Addends (17)

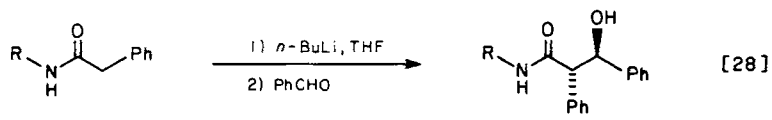
Entry	Metal	Chelate Addend[a]	Product Ratio 45*T*:45*E*
A	Li	None	70:30
B	Li	Cryptofix (2.1.1)	70:30
C	Na[b]	None	79:21
D	Na[b]	Cryptofix (2.1.1)	82:18
E	K[b]	None	79:21
F	K[b]	Cryptofix (2.2.2)	90:10
G	K[b]	18-Crown-6	>97:3

[a]Condensations carried out in THF (-50°C, 10 min) in the presence of 2 equiv of chelating agent.

[b]Enolate prepared from the metal naphthalenide.

It was concluded by Mulzer that the observed high levels of threo diastereoselection imply that there is an intrinsic preference for the syn-carbonyl-enolate transition state orientation (e.g., **A**‡ or **C**‡), with transition state **A** being preferred on steric grounds. Mulzer has raised the interesting suggestion that highest occupied and lowest unoccupied molecular orbital interactions may be responsible for this preference (17). In the context of this discussion it is noteworthy that Hauser has reported the highly threo selective kinetic aldol condensation of the bis-metalated phenylacetamides **46a** to **46c** with benzaldehyde to give exclusively the threo adducts **47** (eq. [28]) (42).

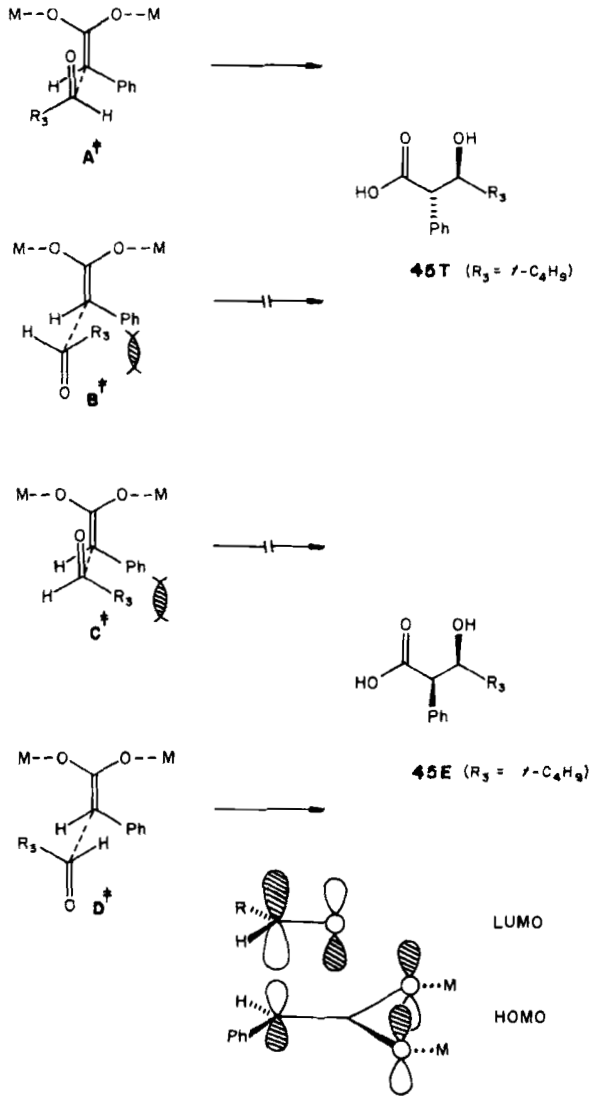
Only limited precedent exists for the stereoselective enolization and subsequent condensation of α-heteroatom-substituted esters **48a** and **48b** (eq. [29]). Ireland has examined the enolization process for α-amino ester derivatives where the Claisen rearrangement (chair-preferred transition states) was employed to ascertain enolate geometry (Scheme 10) (43). These results imply that **48a** [X = $N(CH_2Ph)_2$] exhibits only modest selectivity for (*E*)-enolate formation under the



46 **a**, R = H
b, R = CH_3
c, R = Ph

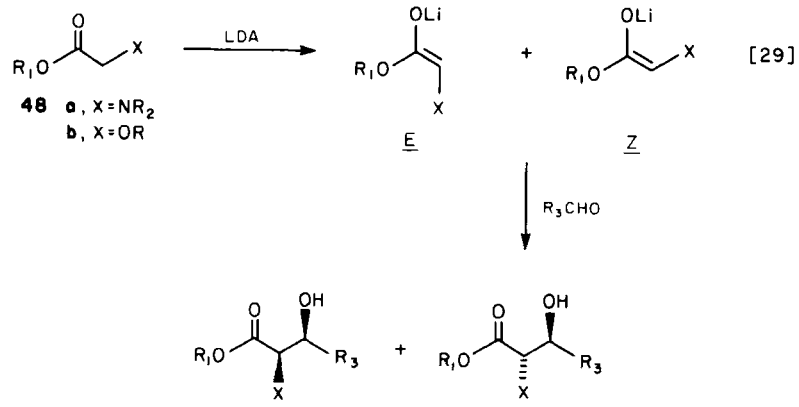
47

[28]



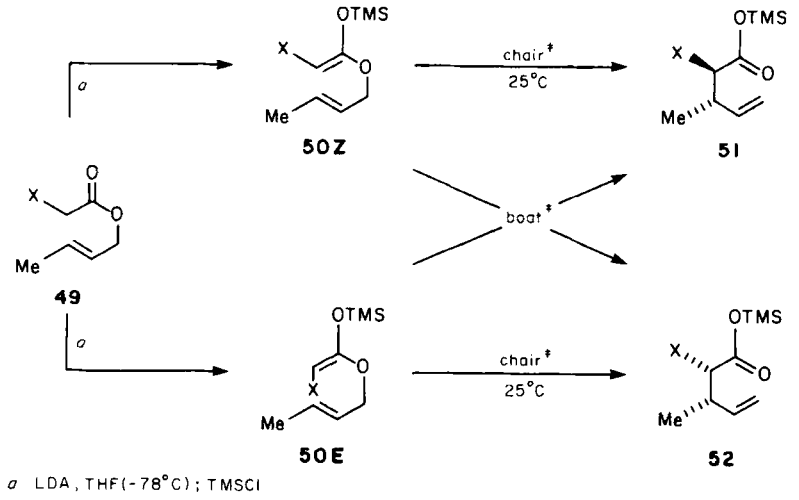
Scheme 9

usual enolization conditions (Table 15, entry A) with LDA (THF). On the other hand, the corresponding urethane **49** (X = $NHCO_2t$-Bu) afforded the (*Z*)-enolate with *at least* 90% stereoselectivity. Apparently the presence of a charged chelating ligand is sufficient to promote the (*Z*)-enolization process. Other evidence for this type of



directivity has been cited earlier (cf. enolate **18a**, eq. [12]). A recently reported study (44) (eqs. [30, 31]) is in complete accord with the observations above.

The enolization (LDA, THF) and subsequent condensation of α-amino ester **53a** under kinetic conditions affords low levels of kinetic aldol diastereoselection. From the preceding discussion it is probable that the major enolate derived from **53a** possesses the (*E*)-geometry. The observation that moderate levels of erythro diastereoselection are observed with benzaldehyde (Table 16) are consistent



Scheme 10

Table 15
Ester Enolate Claisen Rearrangement **49** (Scheme 10) (43)

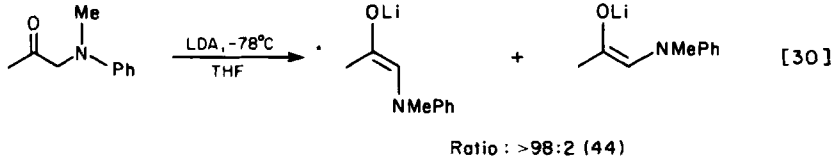
Entry	X	Conditions[a,b]	Product Ratio **51**:**52** (**50***Z*:**50***E*)
A	$-N(CH_2Ph)_2$	LDA, THF	1:1.4
B	$-N(CH_2Ph)_2$	LDA, THF-HMPA	2.18:1
C	$-NHCO_2t$-Bu	2 LDA, THF	>9.5:1[c]
D	$-NHCO_2t$-Bu	2 LDA, THF-HMPA	>9.5:1[c]

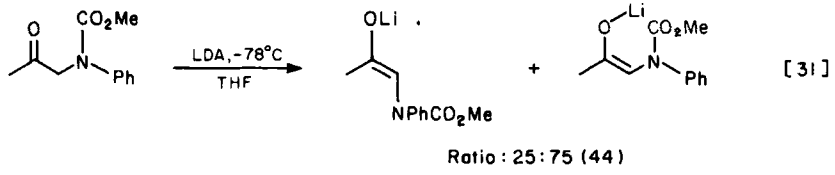
[a]Enolization carried out at -78°C.

[b]Rearranged as the trimethylsilyl ketene acetal (25°C).

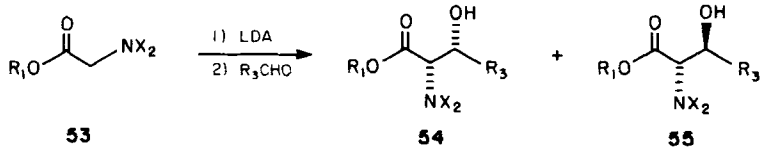
[c]Minor diastereomer **52** not detectable by ^{1}H NMR.

with studies previously cited (Table 6, eq. [16]; cf. Scheme 5), where sterically demanding enolate substituents at the 2-position (R_2) appear to induce a crossover in erythro-threo diastereoselection from a geometrically defined enolate. In complementary studies, the con-





densations of amide **53b** were executed under conditions of *apparent* thermodynamic control where excellent levels of diastereoselection were noted (46). Related condensations have also been reported by others (47). The reader is referred to a study by Marchand for ^{1}H NMR studies relevant to the assignment of stereochemistry for this class of aldol adducts. (48).

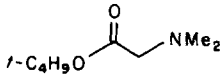
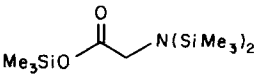


53 54 55 [32]

D. Boron Enolates

The major deficiency associated with the utilization of Group I and II metals in kinetically controlled condensations is apparent from the preceding discussion: the diastereoselection observed for a given enolate is strongly influenced by the enolate substituents, in most cases principally R_1. In addition to the $R_1 \leftrightarrow R_3$ transition state steric parameter, which raises the heat of formation of transition state C_2 relative to C_1, variable metal ligand effects $R_3 \leftrightarrow L$ can also serve as a powerful stereochemical control element to destabilize one of the diastereomeric chair transition states (6). For the chair transition state geometries, it is predicted that $R_3 \leftrightarrow R_1$ and $R_3 \leftrightarrow L$ control elements will be cooperative (Scheme 3), but for boat transition states these two control elements are antagonistic (Schemes 4 and 6). In addition, it should be noted that the magnitude of the $R_3 \leftrightarrow L$ interaction might be expected to be inversely proportional to *both*

Table 16
Condensation of the Lithium Enolate Derived from **53** with Representative Aldehydes (eq. [32])

Ester	Aldehyde	Product Ratio **54**:**55**	Ref.
 **53a**	CH_3CHO	50:50[a]	45
	PhCHO	75:25[a]	45
 **53b**	CH_3CHO	Only **55**[b]	46
	PhCHO	Only **55**[b]	46

[a]Condensation carried out in THF, (-78°C, 5 min).
[b]Condensation carried out in THF (-78°C, 1 hr, followed by 0.5 hr at 0°C).



C_1 C_2

metal-ligand and metal-oxygen bond lengths (cf. Table 17), as well as directly proportional to the steric requirements of the metal ligand (6). As the data in Table 17 suggest, boryl enolates should generally enhance levels of aldol diastereoselection if the relevant transition states possess the chair geometry.

The methods of generating boryl enolates can be divided into two classes: those involving the indirect formation of the enolate by the insertion of an enolate precursor into the carbon-boron or heteroatom-boron bond of an organoborane (eqs. [33-36]) and those involving the direct enolization of the substrate with a dialkyl boron enolization reagent. The general applicability of the indirect methods is limited by the requirement to incorporate a group from the organoborane into the enolate; however, for some applications this may not be a problem.

Table 17
Metal-Oxygen and Metal-Ligand Bond Lengths for Metals Commonly Used in the Aldol Condensation[a]

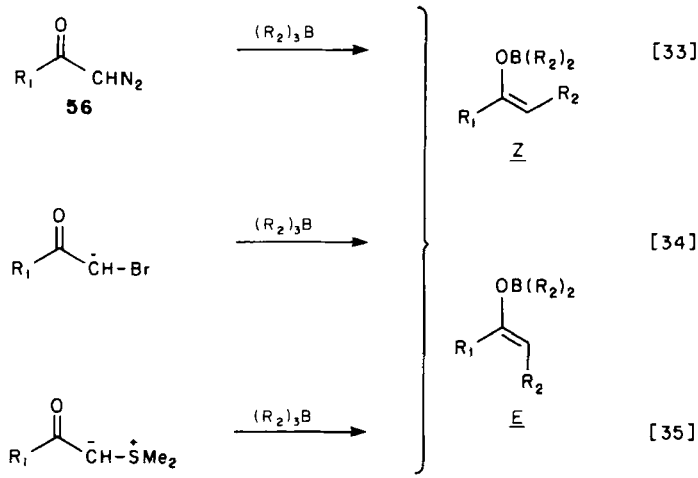
Metal	M–O Bond Length (Å)	L	M–L Bond Length (Å)
Li	1.92-2.00	OR_2	1.92-2.00[b]
Mg	2.01-2.13	Br	2.43
		Cl	2.18
		OR_2	2.01-2.13[b]
Zn	1.92-2.16	Cl	2.18-2.25
		I	2.42
		OR_2	1.92-2.16[b]
Al	1.92	CR_3	2.00-2.24
B	1.36-1.47	CR_3	1.51-1.58
Ti	1.62-1.73	Cl	2.18-2.21
Zr	2.15	C_5H_5	2.21

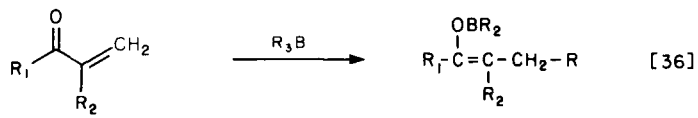
[a]Data taken from ref. 49.

[b]Value cited is for covalently bound alkoxide or acid and should be interpreted as a minimum bond length.

In the late 1960s, methods were developed for the synthesis of alkylated ketones, esters, and amides via the reaction of trialkylboranes with α-diazocarbonyl compounds (50,51), halogen-substituted enolates (52), and sulfur ylids (53) (eqs. [33]–[35]). Only one study has addressed the stereochemical aspects of these reactions in detail. Masamune (54) reported that diazoketones **56** ($R_1 = CH_3$, CH_2Ph, Ph), upon reaction with tributylborane, afford "almost exclusively" the (*E*)-enolate, in qualitative agreement with an earlier report by Pasto (55). It was also found that (*E*) → (*Z*)-enolate isomerization could be accomplished with a catalytic amount of lithium phenoxide (C_6H_6, 16 hr, 22°C) (54).

Brown and co-workers have established the feasibility of the "conjugate addition" of trialkylboranes to α,β-unsaturated ketones (eq. [36]) (56), and one investigation has addressed the question of





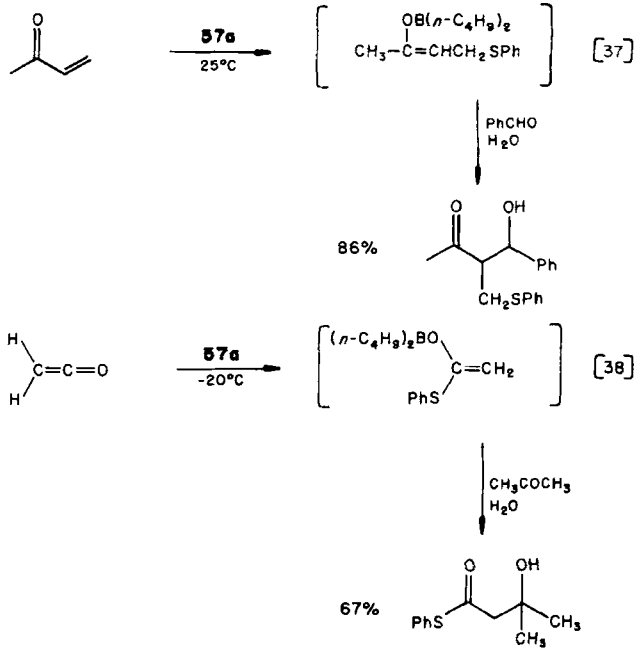
enolate geometry in this reaction (57). In this study the enolate stereochemistry was found to be markedly dependent on the enone substituents, and no clear trends in predictive stereochemical control were revealed. Mukaiyama (51a) has employed this reaction for the

generation of boryl enolates for subsequent condensation studies; however, neither enolate ratios nor aldol diastereomer ratios were addressed. Related addition reactions can be carried out with thioboronite esters **57a** and **57b**. It has been demonstrated that **57a** readily adds to methyl vinyl ketone at room temperature and that the resultant boryl enolate will condense with aldehydes (eq. [37]) (51a). Mukaiyama has also demonstrated that thioester enolates can

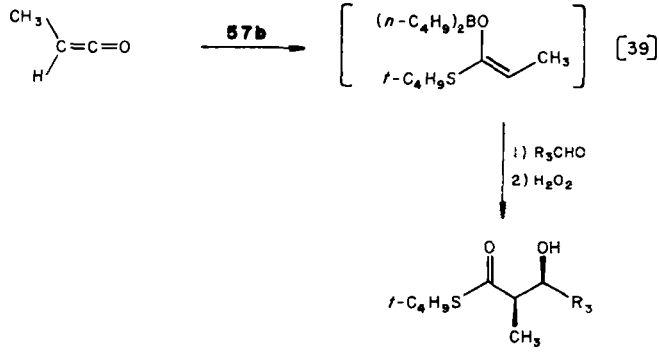
$(n\text{-}C_4H_9)_2B\text{—}SPh$ $(n\text{-}C_4H_9)_2B\text{—}St\text{-}C_4H_9$

57a **57b**

be prepared from ketene (eq. [38]) (51a,59). Masamune subsequently carried out analogous studies with methyl ketene (eq. [39]) (58), noting that the resultant aldol condensation, which proceeded with more than 93% erythro diastereoselection, implicated the

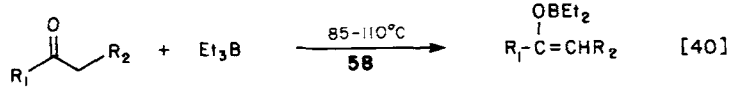


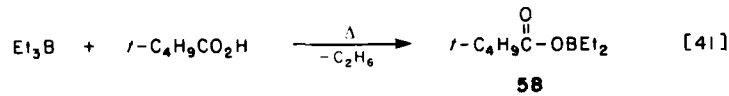
illustrated (*Z*)-enolate geometry. The reactions of ketene with heteroatom-substituted boranes appear to possess considerable generality. Paetzold and co-workers have demonstrated that boryl enolates derived from acid halides may be prepared via the addition of haloboranes to ketene (60).



Several investigations have addressed the synthesis of boryl enolates by carbonyl enolization. Köster has examined in detail the thermal reaction of triethylborane with substituted ethyl ketones catalyzed by diethylboryl pivalate (58) (eq. [40]) (61). The boryl pivalate 58 is undoubtedly the active reagent in this system, and it is regenerated by the illustrated protonolysis (eq. [41]) (62). The vigorous conditions employed in this procedure probably result in the generation of the equilibrated boryl enolates. The enolate ratios obtained by way of this procedure are summarized in Table 18.

Enolization of ketonic substrates can be carried out under far milder conditions if the dialkylboryl trifluoromethanesulfonate esters 59 (eq. [24]) are employed in the presence of hindered tertiary amines (eq. [43]) (6,63). At low temperatures (−78 → 0°C), enolization is completely kinetically controlled (6). A systematic study of this reaction has revealed that the structural features of the ketone, tertiary amine, and boryl triflate individually contribute to





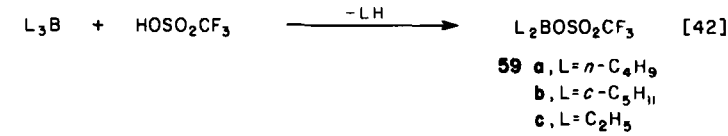
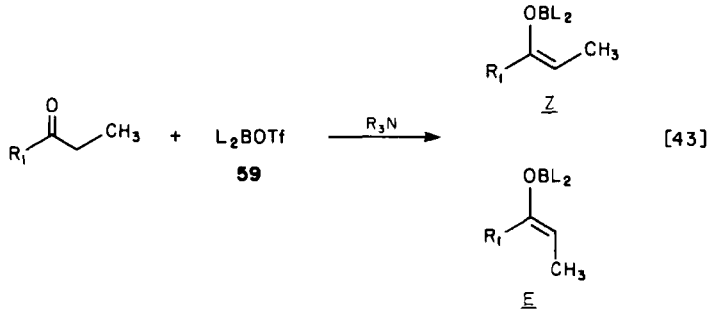


Table 18
Stereochemistry of the Enolates Generated by the Reaction of Ketones and Diethylboryl Pivalate-Et_3B (eq. [40]) (61)

R_1	R_2	Enolate Ratio Z:E
C_2H_5	CH_3	90:10
i-C_3H_7	CH_3	90:10
C_6H_{11}	CH_3	95:5
Ph	CH_3	100:0
Ph	n-C_3H_7	100:0
Ph	Ph	100:0

the observed enolate stereoselection (6). A summary of these reaction variables on the observed kinetic enolate ratios is provided in Table 19. A rationalization of the observed kinetic enolate ratios as a function of the reaction variables has been presented (6a).

The first indication that high levels of kinetic aldol diastereoselection were possible came from the investigation by Köster (eqs. [44–46]) (61). Subsequent stability studies on the boron aldolates have been carried out, and these adducts exhibit remarkable stability even at elevated temperatures (6). The results indicated that the boryl enolates exhibit exceptionally high levels of aldol diastereoselection. Recent investigations have fully substantiated that these observations are quite general (6,64,65). Table 20 presents a representative summary of condensations between substituted ethyl ketones and benzaldehyde. In all cases where enolate geometry was determined, the correspondence between enolate geometry and product stereo-



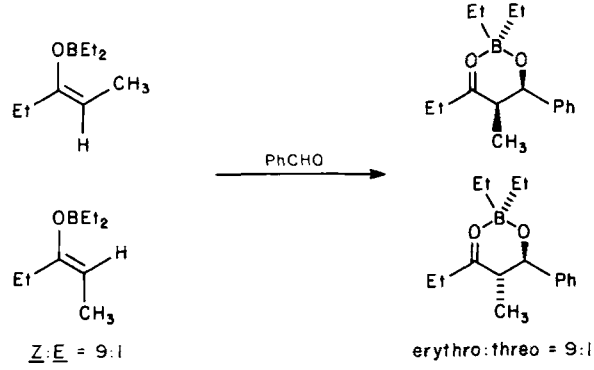
[43]

Table 19
Kinetic Enolate Formation with Triflates **59a** and **59b** (eq. [43]) (6)

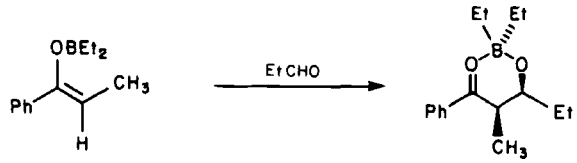
R_1	**59** (L)	Base[a]	Conditions[b]	Enolate Ratio **Z:E**[c]
Et	L = *n*-C_4H_9	DPEA	-78°C, 30 min	97:3
Et	L = *n*-C_4H_9	Lut	-78°C, 30 min	69:31
Et	L = *n*-C_4H_9	Lut	+77°C, 3 hr	(86:14)
Et	L = *c*-C_5H_9	DPEA	0°C, 30 min	82:18
Me_2CH	L = *n*-C_4H_9	DPEA	-78°C, 30 min	45:55
Me_2CH	L = *n*-C_4H_9	Lut	-78°C, 30 min	56:44
Me_2CH	L = *n*-C_4H_9	Lut	+77°C, 30 min	(73:27)
Me_2CH	L = *c*-C_5H_9	Lut	0°C, 30 min	42:58
Me_2CH	L = *c*-C_5H_9	DPEA	0°C, 30 min	19:81
Me_3C	L = *n*-C_4H_9	DPEA	0°C, 30 min	25:75
Me_3C	L = *n*-C_4H_9	DPEA	+35°C, 2 hr	(>97:3)
Me_2CHCH_2	L = *n*-C_4H_9	DPEA	-78°C, 30 min	>97:3
C_6H_5	L = *n*-C_4H_9	DPEA	25°C, 1 hr	>97:3
Me_3CS	L = *n*-C_4H_9	DPEA	0°C, 30 min	≤5:95

[a]DPEA, diisopropylethylamine; Lut, 2,6-lutidine.
[b]Except where noted, all reactions carried out in ether.
[c]Ratios reported in parentheses constitute equilibrium values.

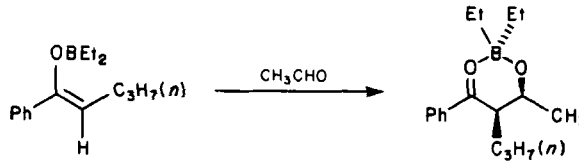
chemistry was exceptional. For (*E*)-boryl enolates the observed threo diastereoselection was found to be somewhat less than the isomeric (*Z*)-enolates (eq. [48]), but still considerably better than the corresponding lithium enolates (54).



[44]

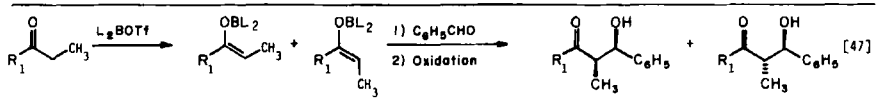


[45]



[46]

Table 20
Aldol Condensations of Acyclic Ketone Boryl Enolates (6)

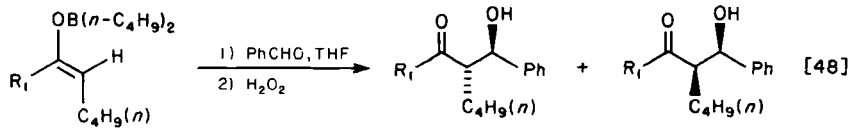


[47]

Z E

R_1	L	Enolization[a] Temperature (°C)	Enolate Ratio *Z*:*E*	Adduct Ratio Erythro-Threo	Yield[b]	Ref.
C_2H_5	*n*-C_4H_9	-78	>97:3	>97:3	77	6b
C_2H_5	*n*-C_4H_9	0	–	89:11	(80)	6b
C_2H_5	*c*-C_5H_9	0	82:18	84:16	(86)	6b
i-C_4H_9	*n*-C_4H_9	-78	>99:1	>97:3	82	6b
i-C_4H_9	*c*-C_5H_9	0	–	84:16	(85)	6b
i-C_3H_7	*n*-C_4H_9	-78	45:55	44:56	65	6b
i-C_3H_7	*c*-C_5H_9	0	19:81	18:82	(87)	6b
t-C_4H_9	*n*-C_4H_9	35	>99:1	>97:3	65	6b
c-C_6H_{11}	*c*-C_5H_9	-78–0	12:88	14:86	88	65
c-C_6H_{11}	9-BBN[c]	-78–0	>99:1	>97:3	79	65
C_6H_5	*n*-C_4H_9	25	>99:1	>97:3	82	6b
TMS	*n*-C_4H_9	-78	–	19:81	53	6b
TMS	*c*-C_5H_9	0	–	35:65	(68)	6b
 t-BOC	*n*-C_4H_9	-78	–	>97:3	(95)	6b

[a]Diisopropylethylamine employed in the enolization process.
[b]Isolated yields except those in parentheses, which are yields of unpurified product.
[c]9-Borabicyclo[3.3.1]nonane.



R_1	Ratio
Ph-	75:25
$PhCH_2$-	80:20
CH_3-	75:25

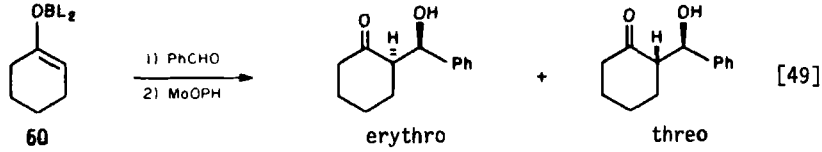
The interplay between solvent polarity and boron ligand structure in the enhancement of aldol stereoselection has been examined in several systems (6). The representative trends that have been noted for the boryl enolates derived from both cyclohexanone and *tert*-butyl thiopropionate (eqs. [49] and [50]) are summarized in Table 21.

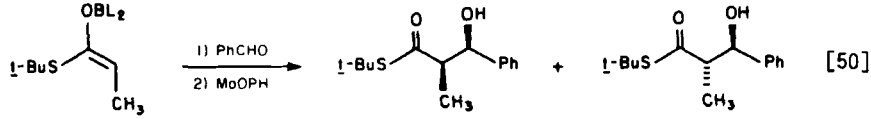
As noted in Table 21, for a given boron ligand there is a small but consistent improvement in aldol diastereoselection when the less polar solvents are employed. This trend is observed for both enolates **60** and **61**. In subsequent studies it has been noted that aldol diastereoselection in methylene chloride is comparable to that observed

Table 21
Aldol Condensation of **60** and **61** with Benzaldehyde (eq. [49,50]): Solvent and Ligand Effects (6)

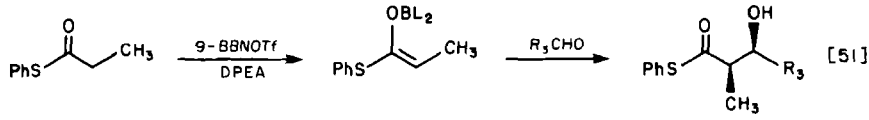
Enolate	L_1, L_2BOTf[a]	Solvent	Erythro-Threo Ratio
60	$L_1, L_2 = n\text{-}C_4H_9$	Ether	33:67
60	$L_1, L_2 = n\text{-}C_4H_9$	Pentane	17:83
60	$L_1, L_2 = c\text{-}C_5H_9$	Ether	32:68
60	$L_1, L_2 = c\text{-}C_5H_9$	Pentane	15:85
60	$L_1 = c\text{-}C_5H_9$, $L_2 = C_6H_{13}$[b]	CH_2Cl_2	6:94
60	$L_1 = c\text{-}C_5H_9$, $L_2 = C_6H_{13}$[b]	THF	<4:96
61	$L_1, L_2 = n\text{-}C_4H_9$	Ether	10:90
61	$L_1, L_2 = n\text{-}C_4H_9$	Pentane	5:95
61	$L_1, L_2 = c\text{-}C_5H_9$	Ether	5:95
61	$L_1, L_2 = c\text{-}C_5H_9$	Pentane	≤5:95

[a] All reactions employed diisopropylethylamine as the amine base.
[b] 2,3-Dimethyl-2-butyl (thexyl).

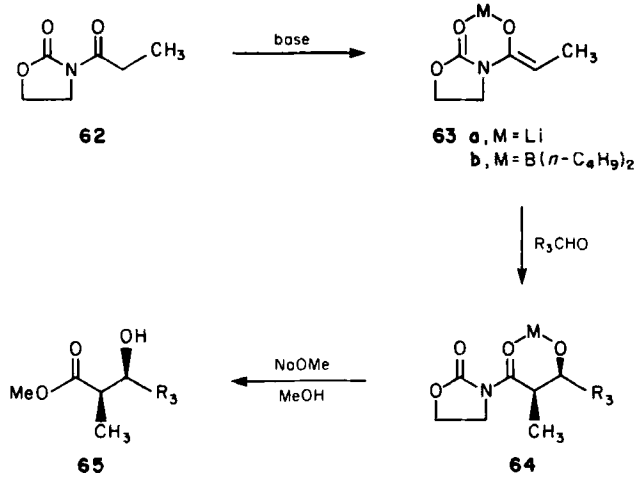




in pentane, and the former is frequently the solvent of choice (6). Assuming that these reactions proceed via the pericyclic aldol mechanism, the less polar solvents could well result in "transition state compression," thereby enhancing the steric parameters that appear to regulate diastereoselection. The effect of boron ligand structure on aldol diastereoselection is of the same magnitude as the solvent effects noted, and both reaction parameters appear to be cumulative. Masamune (65) has studied the enolization of thiopropionates with the 9-BBN-triflate **63b** and has noted that phenyl thiopropionate affords the (*Z*)-enolate, which exhibits excellent erythro diastereoselection with a range of aldehydes (eq. [51]). The (*Z*)-enolate formed in this reaction could well have arisen via equilibration of the kinetic (*E*)-enolate. Mukaiyama has noted that the 9-BBN-enolates are subject to facile isomerization (63b).



In studies not yet published (66), the *N*-acyl-oxazolidine-2-one **62** has been found to exhibit exceptionally high levels of (*Z*)-enolization stereoselection with either amide bases (LDA, THF, -78°C) or boryl triflates [$(n\text{-}C_4H_9)_2BOTf$, CH_2Cl_2, -78°C] in the presence of diisopropylethylamine (DPEA). Upon aldol condensation, the enolates **63a** and **63b** afford the aldolates **64** (Scheme 11), which react readily with nucleophiles at the carbonyl function (Table 22). As discussed earlier, the large preference for (*Z*)-enolate formation in this system can be attributed to allylic strain considerations (37)



Scheme 11

(Scheme 8), which also control the enolate stereochemistry in amide systems. The influence of metal ion structure on the stereochemical outcome of the aldol process again underscores the importance of metal ligand effects in the enhancement of aldol stereoselection.

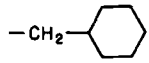
Although simple alkyl esters (ethyl propionate) fail to enolize with the boryl triflate reagents under normal conditions, the more acidic acyloxyboranes **66** readily form the diboryl enediolates **67** (eq. [52]) (6a,66). Several interesting trends are noted in the data included in Table 23. Since previous studies have demonstrated that enolate geometry *strongly* correlates with product stereochemistry, enediolate **67** has been employed to directly compare the reactivities

Table 22
Aldol Condensation of Enolates **63a** and **63b**
and Subsequent Methanolysis to **65** (Scheme 11) (66)

Enolate (M)	R_3CHO	Erythro-Threo Ratio[a]	Yield (% **65**)
63a (Li)	PhCHO	45:55	72
63b (B)	PhCHO	98:2	58
63b (B)	i-C_3H_7CHO	97:3	57
63b (B)	TMSC≡C–CHO	98:2	61

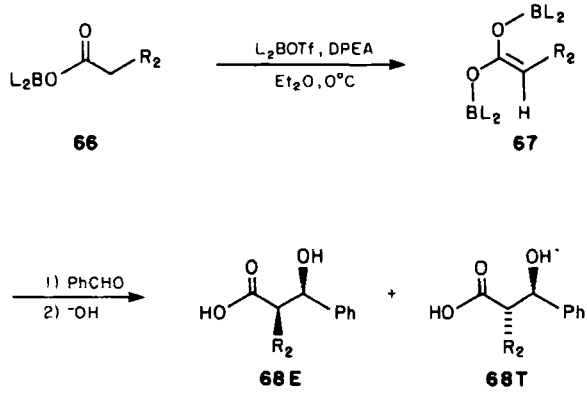
[a]Ratios determined by gas liquid chromatography (GLC).

Table 23
Influence of R_2 on Aldol Diastereoselection of Enediolate **67**, L = *n*-C_4H_9 (eq. [52]) (6,66)

Entry	R_2	Erythro-Threo Ratio **68E:68T**	Yield (%)
A	$-CH_3$	35:65	87
B	$-CH_3$[a]	20:80	85
C	$-CH_2-$ 	40:60	93
D	$-CH{=}CH_2$[b]	<5:95[b,c]	94
E		80:20	86
F	$-Cl$	9:91	98
G	$-OCH_2Ph$	<5:95[c]	85

[a]Derived from enediolate **67** (L = cyclopentyl).
[b]Enolate prepared from crotonic acid.
[c]Erythro adduct undetected by ^1H NMR.

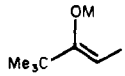
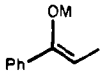
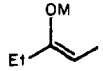
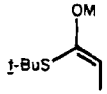
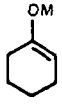
of (*Z*)- and (*E*)-boryl enolates by internal competition ($k_Z : k_E \cong$ **68E:68T**). Except for the case of entry E, the condensations exhibit varying levels of threo diastereoselection. These experiments imply that (*E*)-boryl enolates exhibit somewhat greater reactivity than the isomeric (*Z*)-enolates. These conclusions are in contrast to those noted by Dubois for the isomeric lithium enolates derived from 3-pentanone (5c), where enolate aggregation phenomena may com-



plicate the kinetic analysis. The high levels of threo diastereoselection found for the heteroatom-substituted enolates **67** (R_2 = Cl, OCH_2Ph) could be attributed to internal chelation between R_2 and the syn boron substituent. The stereochemical crossover noted for the enediolate derived from cyclohexylacetic acid (**67**, R_2 = cyclohexyl) parallels a now familiar trend that has been noted throughout this chapter (cf. eq. [16], Table 6; **28T** → **30**, Scheme 5; **53a**, Table 16), where sterically demanding R_2 substituents induce a crossover in aldol stereoselection with the potential intervention of nonchair transition states. In this case one may be observing yet an additional example that illustrates this point.

A summary of representative stereochemically defined metal enolates and their respective kinetic aldol condensations with benzaldehyde is provided in Table 24. Both the metal center and the enolate substituent R_1 for the substituted carbonyl derivatives

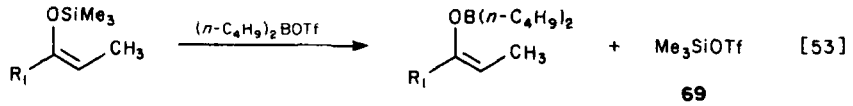
Table 24
Influence of Metal Center on Kinetic Aldol Reactions with Benzaldehyde

Enolate	Metal (M)	Erythro-Threo Ratio	Ref.
	Li	>98:2	2
	MgBr	>97:3	5b
	$B(C_4H_9)_2$	>97:3	6
	Li	88:12	2
	$B(C_4H_9)_2$	>97:3	6
	Li	88:12	5c
	$B(C_4H_9)_2$	>97:3	6
	Li	60:40	35
	$B(C_4H_9)_2$[a]	5:95	6
	Li	48:52	2
	$Al(Et)_2$	50:50	21a
	$B(C_5H_9)C_6H_{13}$[b]	4:96	6

[a] Reaction carried out in pentane. All other boryl enolates were run in ether except where noted.
[b] Reactions carried out in THF.

R_1COEt appear to have a cooperative influence. *As noted earlier these trends are fully consistent with the predictions made by a consideration of diastereomeric chair transition states (Scheme 3) involving boron and not the alternate boat geometries (Schemes 4 and 6).*

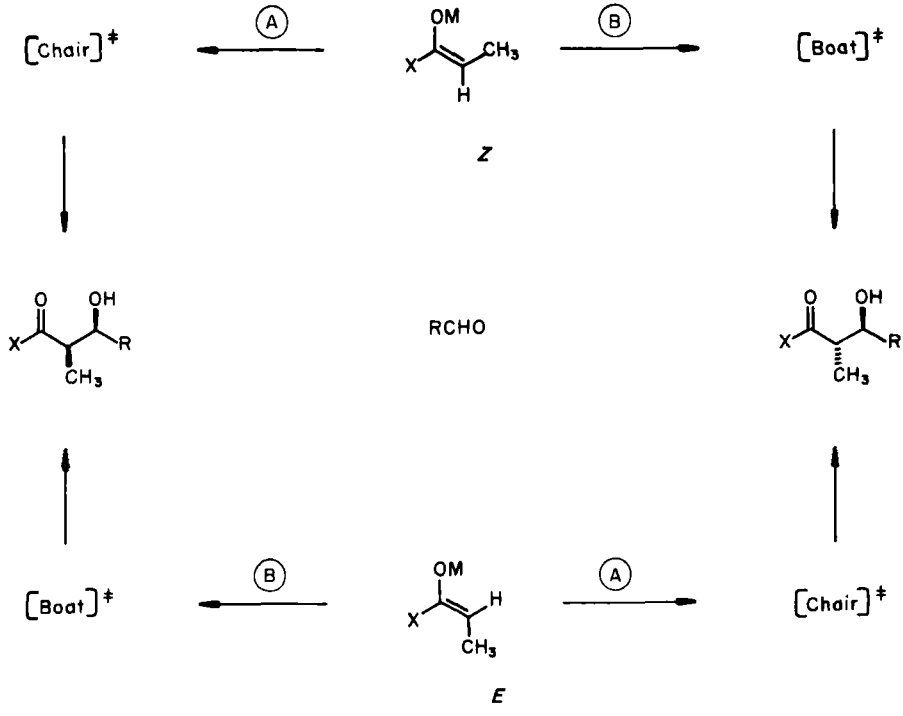
In large measure, the problem associated with the execution of a stereoselective aldol condensation has been reduced to the generation of a specific enolate geometry. The recent results of Kuwajima (66a), which demonstrate that enolsilanes may be transformed into boryl enolates without apparent loss of stereochemistry (eq. [53]), should enhance the utility of vinyloxyboranes in stereoselective synthesis. The only current drawback to this procedure is associated with the presence of trimethylsilyl triflate (**69**), which must be removed from the reaction medium before the aldol condensation. It has recently been established that **69** is an effective catalyst for the aldol process (4).



[53]

E. Zirconium and Other Metal Enolates

For the vast majority of aldol condensations involving metal enolates that have been investigated, the presumed pericyclic transition states have involved tetrahedral metal centers (M = Li, MgX, ZnX, AlX_2, BX_2). Before the initiation of studies in these laboratories (35), the relationship between the transition state oxygen-metal-oxygen bond angle and the resultant kinetic aldol diastereoselection for a given enolate geometry had not been systematically investigated. Such studies were initiated with the intention of defining the metal enolates that might undergo either erythro or threo selective aldol condensations *independently* of enolate geometry. In principle, such an objective could be realized if greater control over transition state geometry (boat vs chair) could be realized for a given enolate geometry (Scheme 12). For example, complementary path A stereoselection for (*Z*)-enolates and path B stereoselection for (*E*)-enolates would result in an erythro selective process that was independent of enolate geometry. Investigations in this laboratory have demonstrated that the sterically hindered zirconium enolates [M = $ZrCl(C_5H_5)_2$] afford such unprecedented erythro diastereoselection from either (*Z*)-



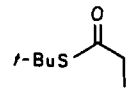
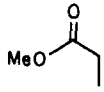
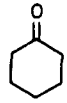
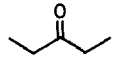
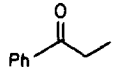
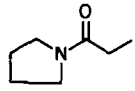
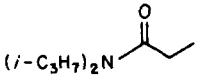
Scheme 12

or (*E*)-enolates (35). Parallel studies have recently been reported by Yamamoto (67).

Earlier studies had demonstrated that such enolates would participate in aldol condensations with aldehydes; however, the stereochemical aspects of the reaction were not investigated (68). For the cases summarized in Table 25, the zirconium enolates were prepared from the corresponding lithium enolates (eq. [54]). Control experiments indicated that no alteration in enolate geometry accompanies this ligand exchange process, and that the product ratio is kinetically controlled (35). From the cases illustrated, both (*E*)-enolates (entries A-E) and (*Z*)-enolates (entries F-H) exhibit predominant kinetic erythro diastereoselection. Although a detailed explanation of these observations is clearly speculative, certain aspects of a probable

$$X\text{–}\underset{\displaystyle OLi}{\underset{|}{C}}\text{=}CHCH_3 + Cp_2ZrCl_2 \xrightarrow{THF} X\text{–}\underset{\displaystyle OZrClCp_2}{\underset{|}{C}}\text{=}CHCH_3 \qquad [54]$$

Table 25
Kinetically Controlled Aldol Condensations
of Zirconium Enolates with Benzaldehyde

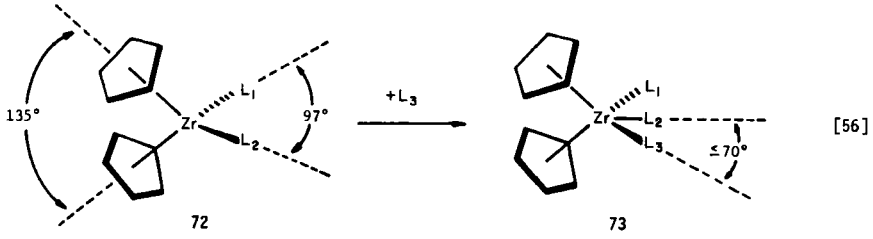
Entry	Substrate	Enolate Ratio *Z:E*	Erythro-Threo Product Ratio[a]	Yield (%, Zr case)	Ref.
A		10:90	93:7 (Zr) 63:37 (Li)	70	35
B		5:95	87:13 (Zr) 62:38 (Li)[b]	80	35
C		–	64:36 (Zr) 52:48 (Li)[b]	75	67
D		–	74:26 (Zr)	82	67
E		14:86	88:12 (Zr) 30:70 (Li)	70	67
F		>98:2[b]	90:10 (Zr) 88:12 (Li)[b]	62	35 35
G		>95:5	95:5 (Zr) 60:40 (Li)	80	35
H		81:19[b]	98:2 (Zr) 63:37 (Li)[b]	87	35

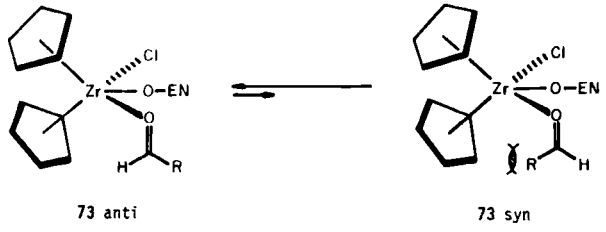
[a] Condensations carried out in THF, -78°C, 30 to 60 min.
[b] See ref. 2.

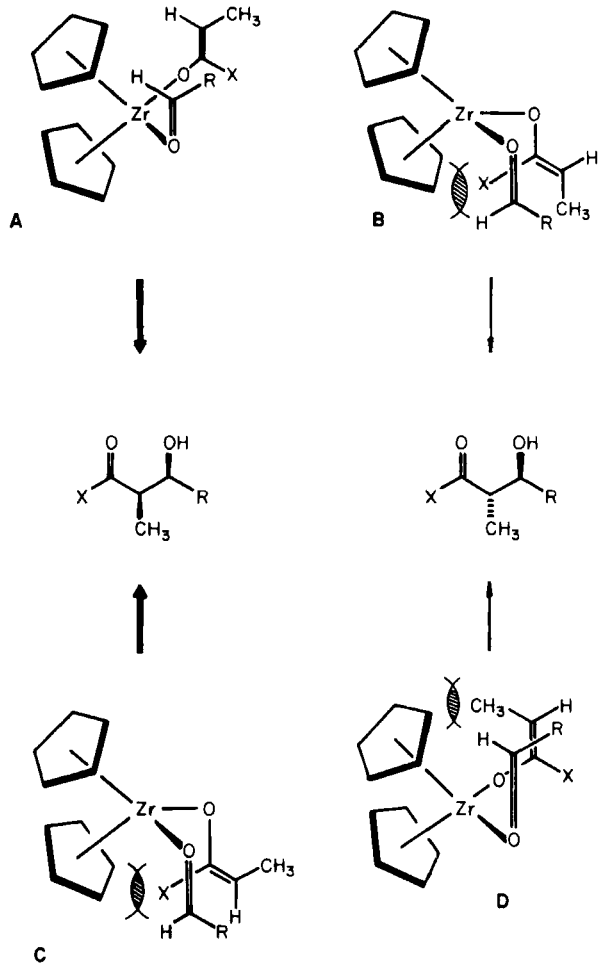
mechanism may be addressed. The issue pertaining to the intervention of pericyclic versus acyclic transition states is of greatest importance. One might anticipate added steric hindrance at the metal center to exert a significantly greater perturbation on the former rather than the latter process. In this regard, the preparation of more hindered bent-sandwich metal enolate complexes (cf. **71a**, **71b**) are currently being evaluated (eq. [55]) (69).



Based on the premise that pericyclic transition states are involved in these condensations, one can speculate on aspects of the reaction. Theory predicts that the 16-electron zirconocenes have a vacant ligation site that lies in the L_1–Zr–L_2 plane (eq. [56]) (70). Since the bond angles in 72 (L_1, L_2 = Cl) are known to be 97° (71), it is probable that the corresponding relevant 18-electron complexes **73** possesses metal-ligand bond angles considerably less than this angle (cf. ref. 72). It also seems reasonable that the anti aldehyde complex might be strongly preferred on steric grounds. Some of the transition state steric considerations for the aldol condensations of (*Z*)- and (*E*)-enolates are illustrated in Scheme 13. The observed erythro-aldol



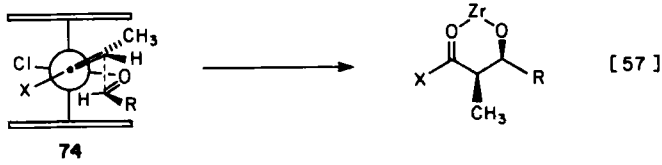




Scheme 13. Note that the chlorine ligand has been deleted to simplify drawings.

diastereoselection for (*E*)-enolates could arise via conformation **A**, where the competing conformation **B** is destabilized by nonbonded Cp ↔ X interactions. The origin of the erythro diastereoselection for (*Z*)-enolates is less obvious, since both conformations **C** and **D** are destabilized via interactions between the enolate substituents X and CH_3 and the metal center. It is possible that these steric effects could be minimized by rotation. A Newman projection such as **74** most clearly depicts another transition state geometry that must be

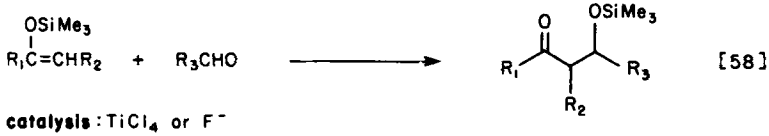
seriously considered. Additional studies that more rigorously define the origin of the diastereoselection in these and related systems are warranted.



74 [57]

F. Enolsilanes

A number of methods that utilize enolsilanes directly in the aldol process with either aldehydes or acetals have been developed recently. These reactions may be catalyzed with either Lewis acids such as titanium tetrachloride (73) or with fluoride ion (74).

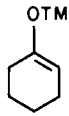
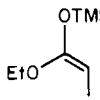
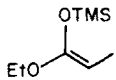


[58]

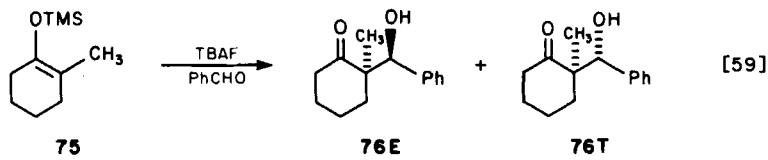
In the titanium tetrachloride-promoted aldol condensations of stereochemically defined enolsilanes (eq. [58]) variable levels of aldol diastereoselection have been noted (Table 26) (73). A detailed analysis of this reaction in terms of probable intermediates and transition state awaits further studies; however, some experimental observations suggest that titanium enolates may not be involved (73b).

Related reactions, catalyzed by tetra-*n*-butylammonium fluoride (TBAF), have been reported (74). Under the influence of 5 to 10 mol % of TBAF (THF, -78°C), enolsilane **75** afforded the erythro and threo adducts **76E** and **76T** whose ratios were time dependent (5 min, E:T = 1:2; 10.5 hr, E:T = 1:3) (74). The reaction of enolsilane **77** at various temperatures has also been reported (2). At -78°C (1 hr) complete kinetic erythro diastereoselection was observed under the conditions reported by Noyori (74), but at higher temperatures product equilibration was noted (2). It is significant that the kinetic aldol condensation of this tetraalkylammonium enolate exhibits complete erythro selection as noted for the analogous lithium derivative.

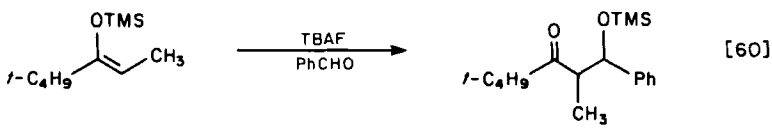
Table 26
Condensations of Enolsilanes and Aldehydes
Promoted by Titanium Tetrachloride (73)

Enolsilane	Aldehyde [at T (°C)][a]	Erythro-Threo Ratio	Yield (%)
	PhCHO (-78)	1:3	92
	PhCHO (0)	1:2.5	81
	PhCHO (-78)	1:1	68
	PhCHO (0)	1:1	74
	$PhCH_2CHO$ (-78)	1:1	95
	PhCHO (-78)	1:3[c]	79
	n-$C_5H_{11}CHO$ (-78)	4:96[c]	77
	i-C_3H_7CHO (-78)	0:100[c]	75
	PhCHO (-78)	33:67	78
	n-$C_5H_{11}CHO$ (-78)	47:53	77
	i-C_3H_7CHO (-78)	48:52	77

[a] Reactions carried out at indicated temperatures (CH_2Cl_2) in the presence of 1.0 equiv of $TiCl_4$.
[b] Contains 15% of the isomeric (*Z*)-enolate.
[c] Product ratios corrected for (*Z*)-enolate contaminant (73b).

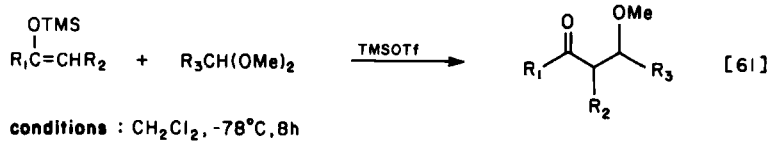


75 76E 76T [59]



77 78 E = erythro T = threo [60]

Noyori (4) has recently disclosed the mechanistically intriguing condensation of enolsilanes and acetals, which is catalyzed by trimethylsilyl triflate (**69**) (eq. [61]). The results of a set of representative condensations between stereochemically defined enolates and

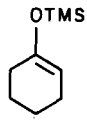
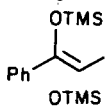
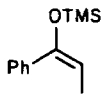
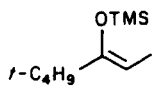


[61]

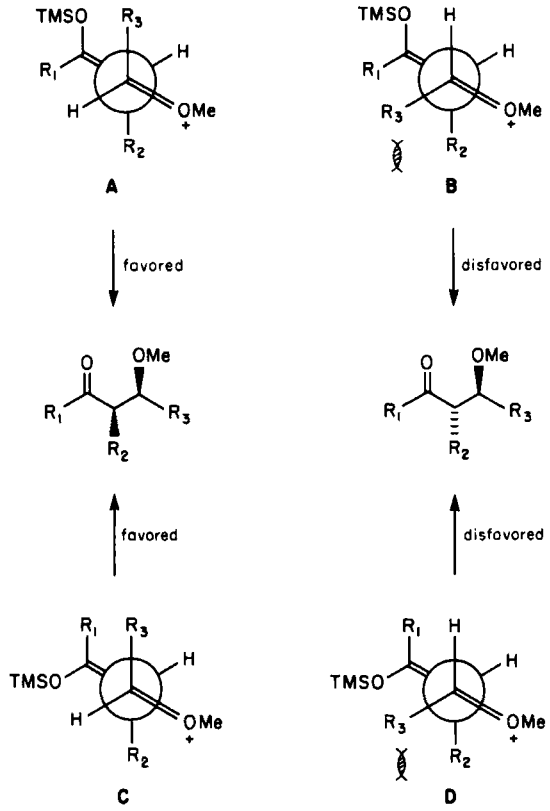
aldehyde acetals are included in Table 27. The kinetic erythro diastereoselection that has been observed from either (*Z*)- or (*E*)-enolsilanes has been explained by a consideration of the diastereomeric acyclic transition states illustrated in Scheme 14.

It was postulated that the role of the triflate reagent **69** is to activate the acetal, with the possible intervention of either **79** or **80** as the putative electrophilic species, which undergoes reaction with the enolsilanes via the extended acyclic transition state **81** (4). Based on the assumption that transition state $R_2 \leftrightarrow R_3$ interactions from either enolate geometry dictate the stereochemical course of

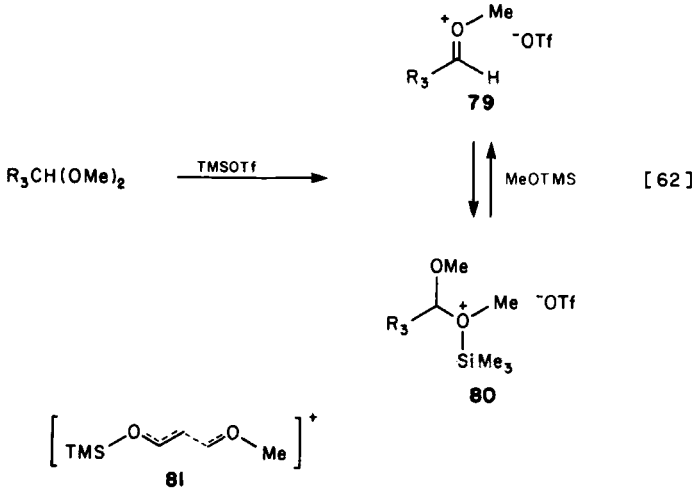
Table 27
Trimethylsilyl Triflate-Catalyzed Condensation of Enolsilanes and Acetals (eq. [61]) (4)

Enolsilane	Acetal	Erythro-Threo Ratio[a]	Yield (%)
	$PhCH(OMe)_2$	93:7	89
	$i\text{-}C_3H_7CH(OMe)_2$	86:14	95
	$n\text{-}C_3H_7CH(OMe)_2$	89:11	91
	$PhCH(OMe)_2$	84:16	97
	$PhCH(OMe)_2$	71:29	83
	$PhCH(OMe)_2$	95:5	94

[a]Condensations carried out with 1 to 5 mol % **69** at -78°C (CH_2Cl_2), 4 to 12 hr.


TMSO
R3
R1
H
H
OMe
R2
A
B
favored
disfavored
O
OMe
C
D

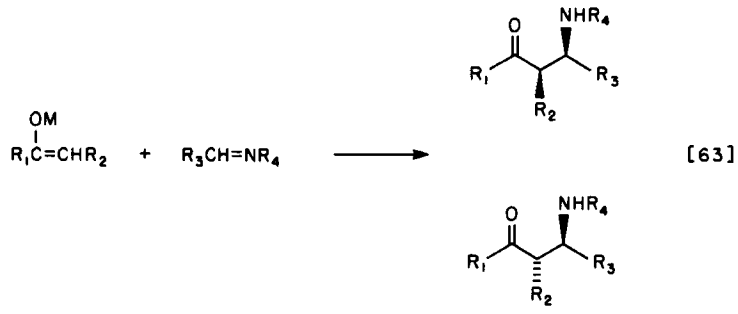
Scheme 14


R3CH(OMe)2
TMSOTf
Me
OTf
79
MeOTMS
[62]
OMe
SiMe3
80
TMS
81

the reaction, it was postulated that transition state **A** is favored for (*Z*)-enolsilanes and transition state **C** is favored for (*E*)-enolsilanes. These projections appear to be reasonable and could be generally applicable to other related condensations.

G. Azomethine-Enolate Condensations

In contrast to the extensive studies that have been directed at the elucidation of the stereochemical control elements of the aldol process, parallel investigations on the condensations of metal enolates with imines (eq. [63]) have been far less extensive. A review of the

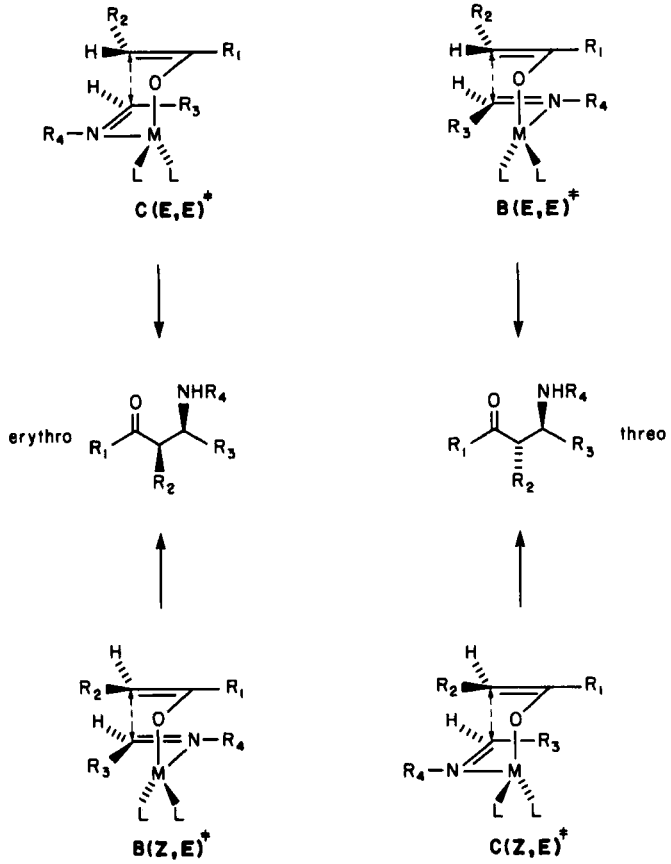


[63]

Geometrical Control Elements : a) enolate geometry
b) imine geometry

Reformatsky reaction has covered aspects of this topic (20b). If analogous pericyclic transition states are involved in these condensations, the added stereochemical control element imposed on the condensation by the *imine geometry* should provide a more well-defined set of transition states than for the analogous aldehyde condensations. The four diastereomeric chair and boat transition states for (*E*)- and (*Z*)-enolates with (*E*)-imines are illustrated in Scheme 15.

An analogous set of four transition states for the (*Z*)-imine geometry could also be constructed. The transition state descriptors, such as **B(Z,E)** and **C(Z,E)**, may be employed to denote boat (B) or chair (C) transition states respectively, possessing (*Z*)-enolate and (*E*)-imine geometries. The interrelationships between the stereochemical features of reactants, transition states, and products are summarized in Table 28. Unfortunately, the kinetic diastereoselection in such condensations as a function of either enolate or imine geometry has not been systematically studied. In all the early work in this field



Scheme 15

stereochemically undefined zinc ester enolates, generated under Reformatsky conditions, were condensed with (*E*)-imines (20b).

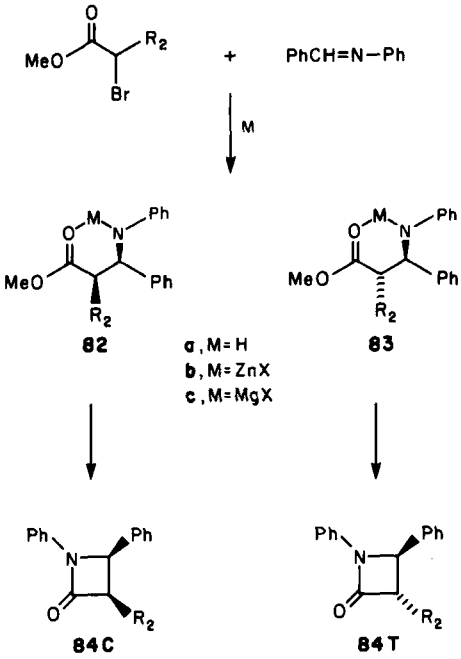
Early investigations by Gilman (75) demonstrated the viability of applying the Reformatsky reaction to imines. The products from this reaction (carried out in toluene at reflux) were β-lactams (Scheme 16). Subsequent studies that have extended these original observations have revealed that the ratios of diastereomeric lactams **84C** and **84T** were markedly influenced by the reaction solvent (Table 29). Control experiments confirmed that the diastereomeric lactams **84C** and **84T**, once formed, were stable to the reaction conditions (76c). Both zinc and magnesium enolates were reported to give comparable ratios of β-lactam isomers. Generation of **83c** (R_2 = *i*-C_3H_7) from the cor-

Table 28
Correlation Between Reactant and Product Stereochemistry

Enolate Geometry	Imine Geometry	Transition State	Product Stereochemistry
E	*E*	Chair	Erythro
E	*E*	Boat	Threo
Z	*E*	Chair	Threo
Z	*E*	Boat	Erythro
E	*Z*	Chair	Threo
E	*Z*	Boat	Erythro
Z	*Z*	Chair	Erythro
Z	*Z*	Boat	Threo

responding β-amino ester (EtMgBr) was followed by cyclization to **84T** (R_2 = *i*-C_3H_7) without loss of stereochemistry.

The influence of temperature on aldol diastereoselection has been noted in several instances. The condensation of zinc enolates **85a** to



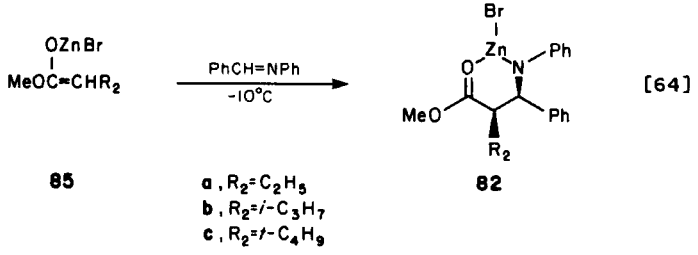
Scheme 16

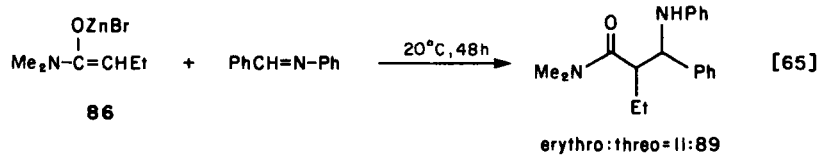
Table 29
Aldol Condensation of Zinc Ester Enolates
with Benzaldehyde Anil: Solvent Effects (Scheme 16) (76)

$MeO_2CCHBrR_2$	Ratio[a] 84C:84T	
	Solvent A	Solvent B
CH_3	73:27	80:20
C_2H_5	64:36	74:26
i-C_3H_7	55:45	100:0
c-C_6H_{11}	45:55	100:0
t-C_4H_9	25:75	100:0
$-C_6H_5$	0:100	0:100

[a] Condensations carried out for 2 hr. at reflux in either toluene (solvent A) or THF (solvent B).

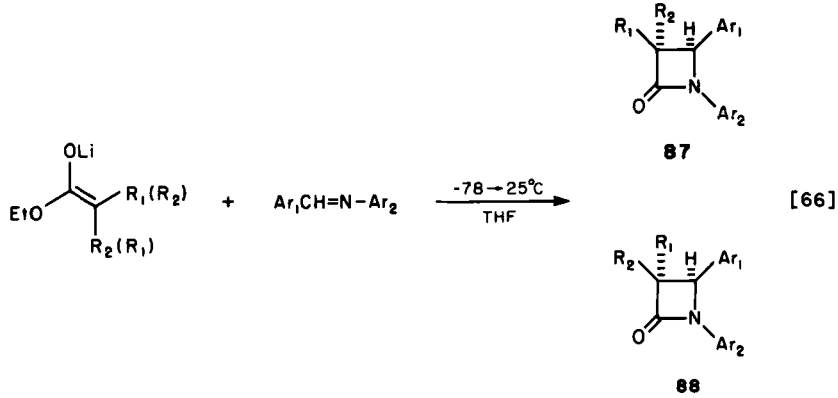
85c (stereochemistry undefined) at lower temperatures (−10 to −18°C) with benzaldehyde anil (eq. [64]) has been reported to afford exclusively the erythro adducts 82a to 82c (76c,77); however, upon warming, the zinc aldolates afford cis-trans mixtures of β-lactams. Crossover experiments demonstrated that the loss in stereochemistry during the attempted cyclization of 82 was due to retroaldolization. The analogous condensations of amide enolates have also been examined in detail by Gaudemar (78), who has noted that the zinc enolate 86 (stereochemistry undefined) exhibits good levels of kinetic threo diastereoselection upon condensation (20°C, 48 hr) with the illustrated imine (eq. [65]). The exclusive erythro diastereoselection noted for ester enolate 85 (eq. [64]) and the complementary threo diastereoselection found for amide enolate 86 (eq. [65]) could be consequences of differing enolate geometries in the two systems. If ester enolate 85 possessed the (*E*)-geometry, chair transition state C(E,E) (Scheme 15) could explain the observed erythro diastereo-





[65]

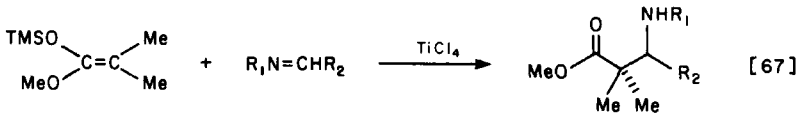
selection. In a complementary fashion, the (*Z*)-amide enolate **86** might be expected to exhibit threo diastereoselection via chair transition state C(Z,E). The previously noted propensity for the formation of (*Z*)-enolates in amide systems has ample precedent (Table 10) (2,35,36).



[66]

More recently, a study pertaining to the condensation of lithium ester enolates with substituted imines has appeared (eq. [66]) (79). Although monosubstituted enolates [R_1 = H; R_2 = Ph, N=C(OLi)Ph] afforded moderate yields (35–45%) of *trans*-lactam **87**, disubstituted enolates (R_1 = OLi, CH_3; R_2 = Ph, CH_3) afforded good yields (66–91%) of lactam products. The authors concluded from their study that the condensation step was probably reversible.

An exceptionally mild procedure for the cross-condensation of aldimines and enolsilanes has been described (eq. [67]) (80). This titanium tetrachloride-mediated reaction is predicated on the previous analogies provided by Mukaiyama for related aldol condensations (73a). Depending on aldimine structure and reaction time, either β-lactams or their penultimate β-amino esters may be isolated from the reaction. The authors postulate that these reactions are proceeding via titanium enolates derived from ligand exchange by



[67]

R_1	R_2	% Yield
Ph	Ph	95
Ph	CH_2Ph	77
Ph	CH_3	72
i-C_3H_7	CH_2Ph	43
C_2H_5	CHMePh	54

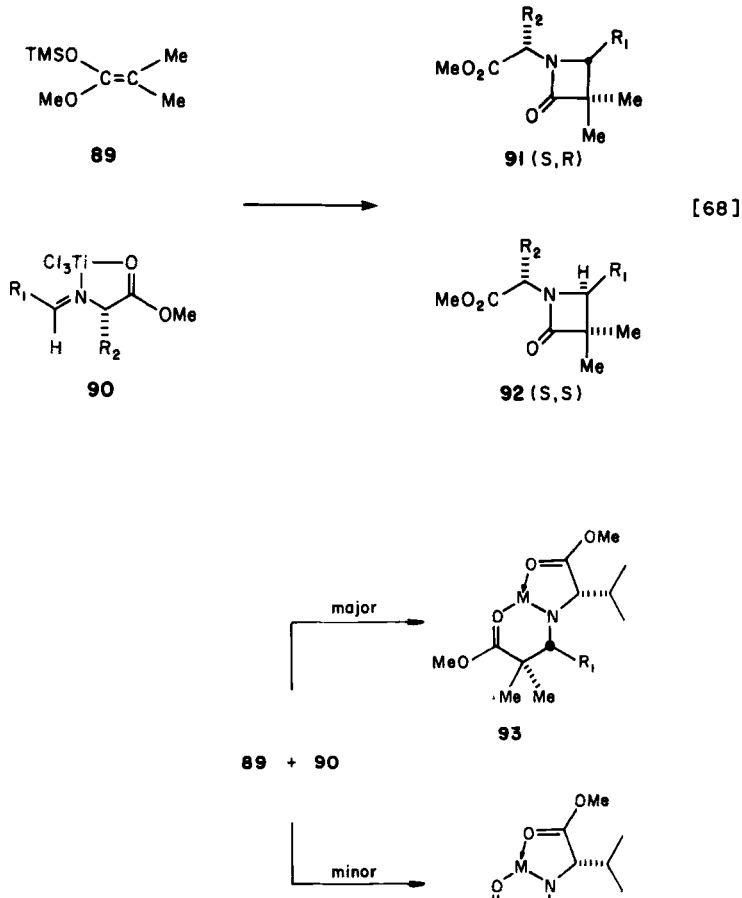
conditions : $TiCl_4$, CH_2Cl_2, 25°C, 1h

$TiCl_4$ on the silyl ketene acetal; however, other data suggest that metal enolates may not be involved (73b). In subsequent studies, this reaction has been extended to chiral imines (81,82).

Some impressive levels of asymmetric induction were noted in the following examples (eq. [68], Table 30). From the cases studied, it is readily apparent that the steric requirements of the R_2 ligand at the resident asymmetric center in aldimine chelate **90** exerts a profound effect on the degree of asymmetric induction. Earlier studies (80) offer a precedent for the suggestion that the aldolate complexes **93** and **94** are the penultimate precursors to the major and minor diastereomeric β-lactams **91** and **92**, respectively (Scheme 17). The pericyclic transition state **95** (M = TiL_n) could well explain the sense of chirality transfer (82).

Table 30
Diastereoselective Condensations of Imine **90** with Ketene Acetal **89** (eq. [68]) (82)

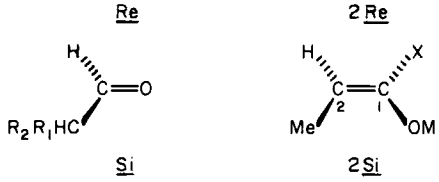
R_1	R_2	Yield (%)	Product Ratio **91**:**92**
C_2H_5	i-C_3H_7	73	97:3
n-C_4H_9	i-C_3H_7	77	95:5
i-C_4H_9	i-C_3H_7	81	99:1
C_2H_5	CH_3	28	73:27
C_2H_5	i-C_4H_9	49	70:30
C_2H_5	CH_2Ph	45	79:21


TMSO
Me
C=C
MeO
Me
89
R2
R1
MeO2C
N
Me
O
Me
91 (S,R)
[68]
Cl3Ti
O
R1
N
OMe
H
R2
90
H
92 (S,S)
OMe
major
M
MeO
Me Me
93
89 + 90
minor
H
94
95
93
91

Scheme 17

VI. THE QUESTION OF ASYMMETRIC INDUCTION

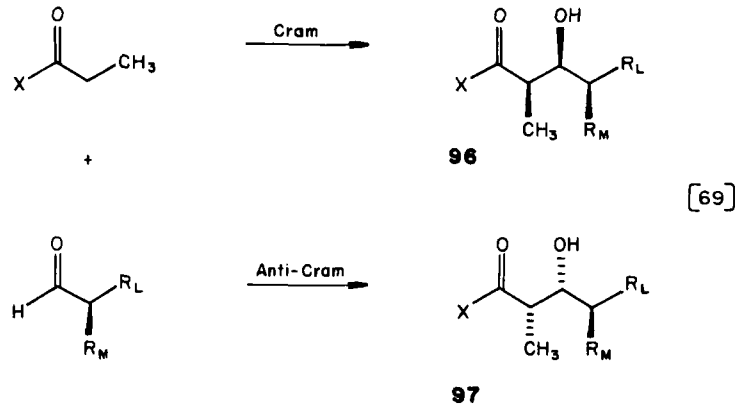
Section V summarized a number of methods for achieving good levels of kinetic diastereoselection for a given aldol bond construction. For the synthesis of complex structures, both the *relative stereochemistry and the absolute stereochemistry* of the newly generated centers of asymmetry must be defined. A detailed understanding of the influence of resident chirality in either or both condensation partners on the sense of asymmetric induction is essential to rational synthesis design involving this reaction. In dealing with this topic the Izumi-Tai nomenclature for asymmetric reactions is employed (83a). For example, in the condensation partners illustrated below, the trigonal carbons directly involved in the bond construction may be attacked by the complementary reagent from either the *Re* or the *Si* face (83b). When both the aldehyde and the enolate are



achiral, the trigonal faces of each are *enantiotopic*; however, if there is resident chirality in the molecule these faces become *diastereotopic*. For example, the *diastereoface selection* that is observed in the addition of organometallic reagents to chiral α-substituted aldehydes has been well studied and is highly predictable (84–89). In the two subsections that follow three classes of chiral aldol process are surveyed: diastereoface selection between chiral aldehydes and achiral enolates, diastereoface selection between achiral aldehydes and chiral enolates, and double diastereoface selection between chiral reactant pairs. In the last category the mutual involvement of chirality may either be cooperative (consonant) or antagonistic (dissonant).

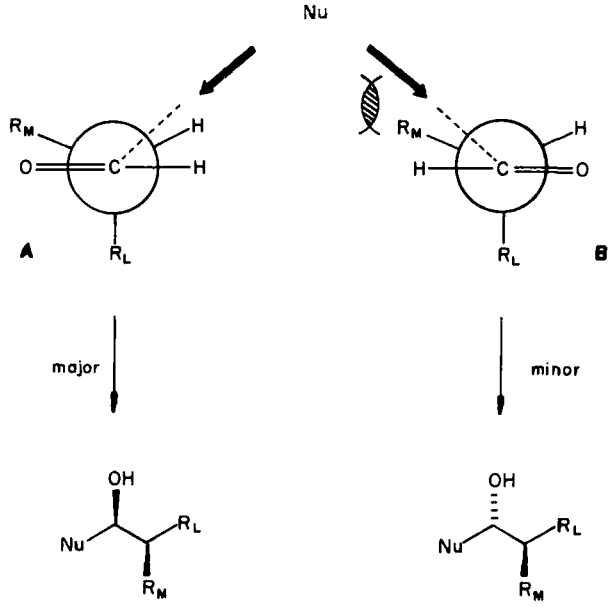
A. Chiral Aldehydes and Achiral Enolates

For purposes of illustration, consider the erythro selective reaction illustrated in eq. [69]. For aldehydes containing an adjacent asymmetric center (R_M, R_L = medium and large alkyl substituents), the bias for nucleophilic addition from a given diastereotopic face of the aldehyde is predicted empirically by Cram's rule (the "open-chain



[69]

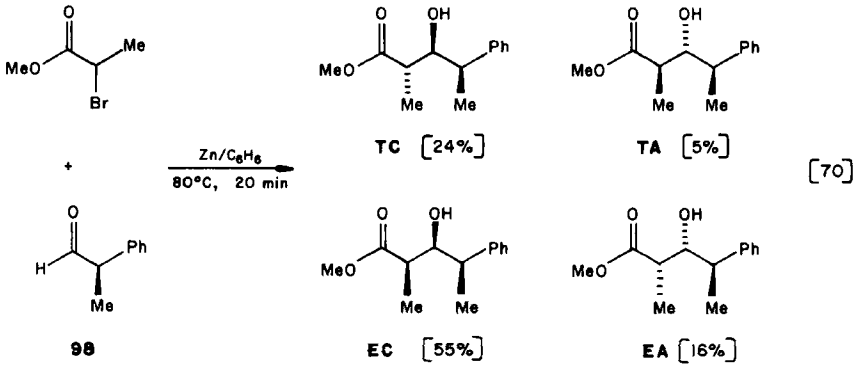
model") (84). Other transition state models for polar and chelating substituents have provided a measure of predictability for aldehyde diastereoface selection (86–88). Recent *ab initio* calculations (89) plus the inclusion of the Dunitz-Bürgi trajectory for carbonyl addition (90) have refined the earlier Felkin model (88) and provide a more rational explanation (89) for the experimental observations (Scheme 18). The Anh transition state model states that the large



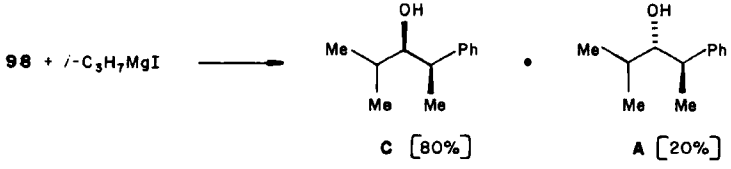
Scheme 18

ligand (R_L) is oriented perpendicular to the carbonyl plane and that $R_M \leftrightarrow$ Nu transition state steric effects favor transition state **A** over **B** (89). Superimposed on the conformational bias created by steric considerations (R_M, R_L = carbon substituents) are transition state $\pi^*_{C=O}$-$\sigma^*_{C_2-R}$ stabilizing interactions that are *larger* for the anti periplanar orientation than for the alternative syn periplanar conformation. Consequently, the C_2-substituent (R_M or R_L) having the lowest energy $\sigma^*_{C_2-R}$ orbital should be considered to be the "large" substituent (R_L) and oriented perpendicular to the σ-carbonyl plane. Thus, when considering α-halo and α-alkoxy-substituted carbonyl derivatives, the lowest energy $\sigma^*_{C_2-X}$ bonds will be carbon-halogen and carbon-oxygen respectively, and these substituents are assigned the largest "effective size" (R_L) as in transition state **A** (Scheme 18). These and related models predict that aldol adduct **96** (Cram) is favored over **97** (anti-Cram).

One of the earliest studies to address the issue of aldehyde diastereoface selection in enolate condensation was performed by Matsumoto and coworkers (91). The Reformatsky reaction of methyl 2-bromopropionate and 2-phenylpropanal (**98**) afforded the four aldol adducts illustrated in eq. [70]. Although the aldol diastereo-

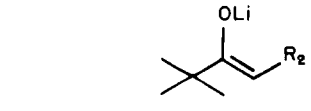


[70]

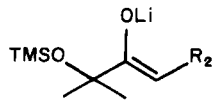


selection was low ($\Sigma_{erythro}:\Sigma_{threo}$ = EC + EA:TC + TA = 2.4:1), the aldehyde diastereoface selection (TC + EC:TA + EA = 3.8:1) favored the adducts (TC + EC) as predicted by "Cram's rule." For comparison purposes, the ratio of Cram to anti-Cram diastereoface selection (C:A) in the addition of isopropylmagnesium iodide to **98** was also found to be 4:1.

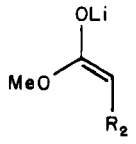
Recently, the issue of aldehyde diastereoface selection has been examined for the enolates **99** to **103** (2,26,33,64). For these substituted enolates, aldol diastereoselection has been demonstrated to



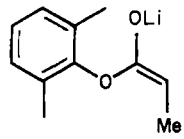
99 a, R_2 = H; b, R_2 = Me



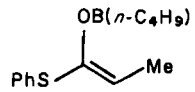
100



101



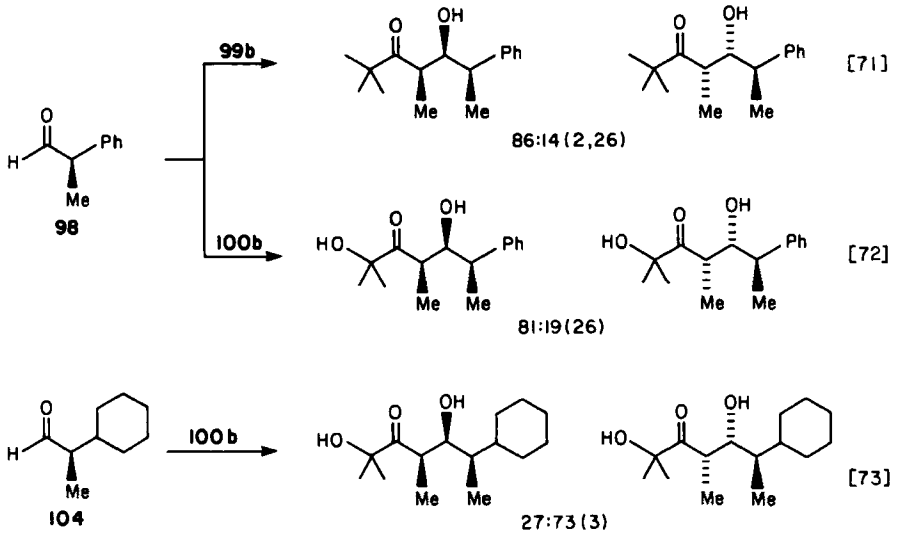
102



103

be good. For aldehyde **98** and enolates **99b** (2,26), **100b** (26), and **102** (33), Cram-predicted diastereoface selection was observed in all cases with a 3–4:1 bias (eqs. [71, 72, 74]). In addition, the threo selective enolate **102** also exhibited analogous 4:1 diastereoface selection with the structurally complex aldehyde **105** (eq. [75]) (94). In view of these results, it is striking that aldehyde **104** has been reported to exhibit predominantly the anti-Cram diastereoface selection with enolate **100b** (eq. [73]) (3).

Remote steric effects have also been noted to play an unanticipated role in the sense of asymmetric induction. This is apparent from related condensations carried out on aldehydes **106** (26) and **107** (eqs. [76]-[78]) (26,92). Other examples illustrating the influence of remote structural perturbations on the carbonyl addition process have been observed in these laboratories. The addition of the lithio benzoxazole **110** to aldehyde **108** proceeded with good Cram diastereoface selection (95a), whereas the same nucleophilic addition to aldehyde **109** was stereorandom (95b).

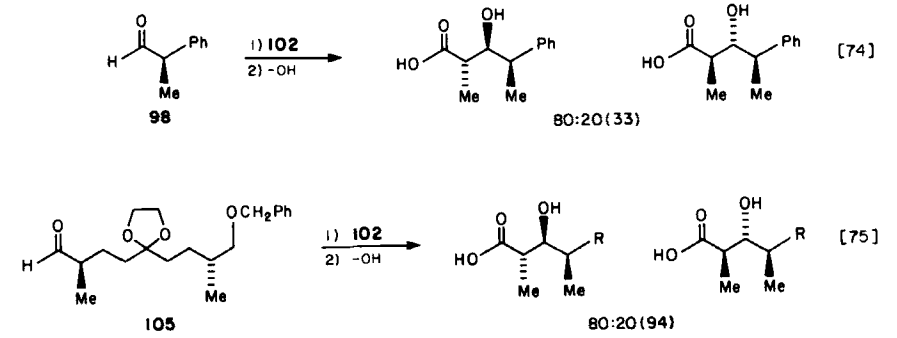


[71]

[72]

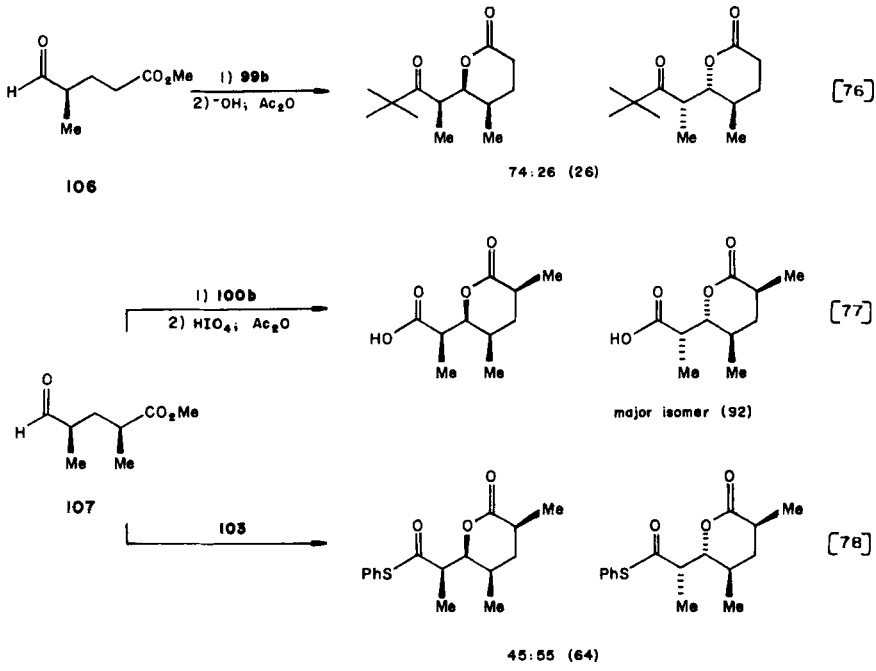
[73]

The degree of substitution on the enolate moiety does not appear to significantly alter the Cram-preferred selectivity for chiral aldehydes. For example, the addition of the lithium enolate derived from ethyl dithioacetate has been reported to undergo selective aldol condensation with the illustrated epoxyaldehyde (eq. [79]) to give a 3:1 ratio of aldol diastereomers, with the major diastereomer C having the stereochemistry predicted by Cram's rule (96). In two independent approaches to the synthesis of the ionophore monensin, the disposition of the C_7-hydroxyl function relative to the masked C_9-carbonyl and C_6-methyl-bearing stereocenters was recognized as being complementary to the aldol transform illustrated in eq. [80]



[74]

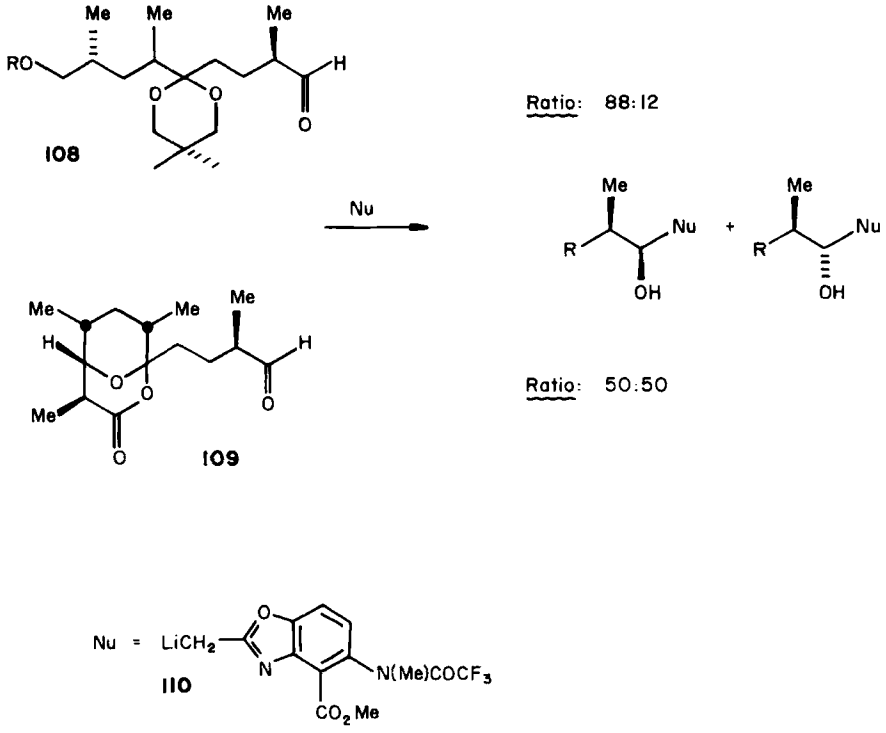
[75]



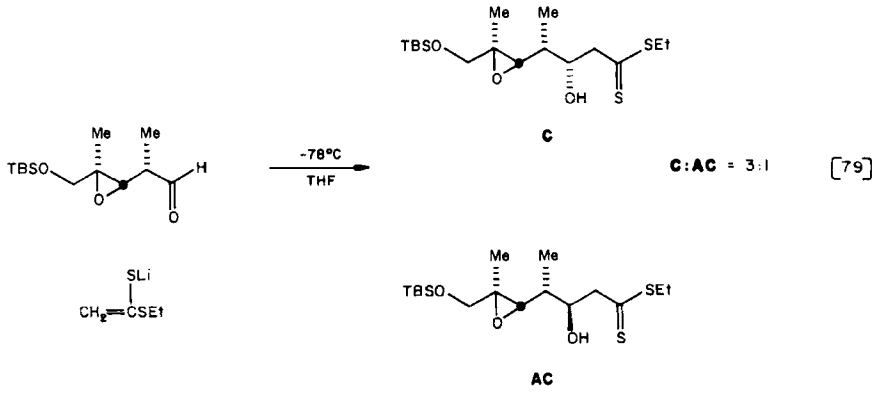
(97). This aldol bond construction, carried out under kinetic conditions with the magnesium enolate, has been reported to give the expected C_7-diastereomer C with selectivities (C:AC) ranging from 3:1 for X = $SiMe_3$ (97b) to >8:1 for X = benzyl (97a).

Diastereoface selection has been investigated in the addition of enolates to α-alkoxy aldehydes (93). In the absence of chelation phenomena, transition states A and B (Scheme 19), with the OR substituent aligned perpendicular to the carbonyl σ plane (R_L = OR), are considered ($\sigma^*_{C-OR} < \sigma^*_{C-R_2}$), and transition state $R_2 \leftrightarrow$ Nu steric parameters dictate that predominant diastereoface selection from A will occur. In the presence of strongly chelating metals, the cyclic transition states C and D can be invoked (85), and the same $R_2 \leftrightarrow$ Nu control element predicts the opposite diastereoface selection via transition state D (98). The aldol diastereoface selection that has been observed for aldehydes **111** and **112** with lithium enolates **99**, **100**, and **101** (eqs. [81-84]) (93) can generally be rationalized by a consideration of the Felkin transition states A and B (88) illustrated in Scheme 19, where A is preferred on steric grounds.

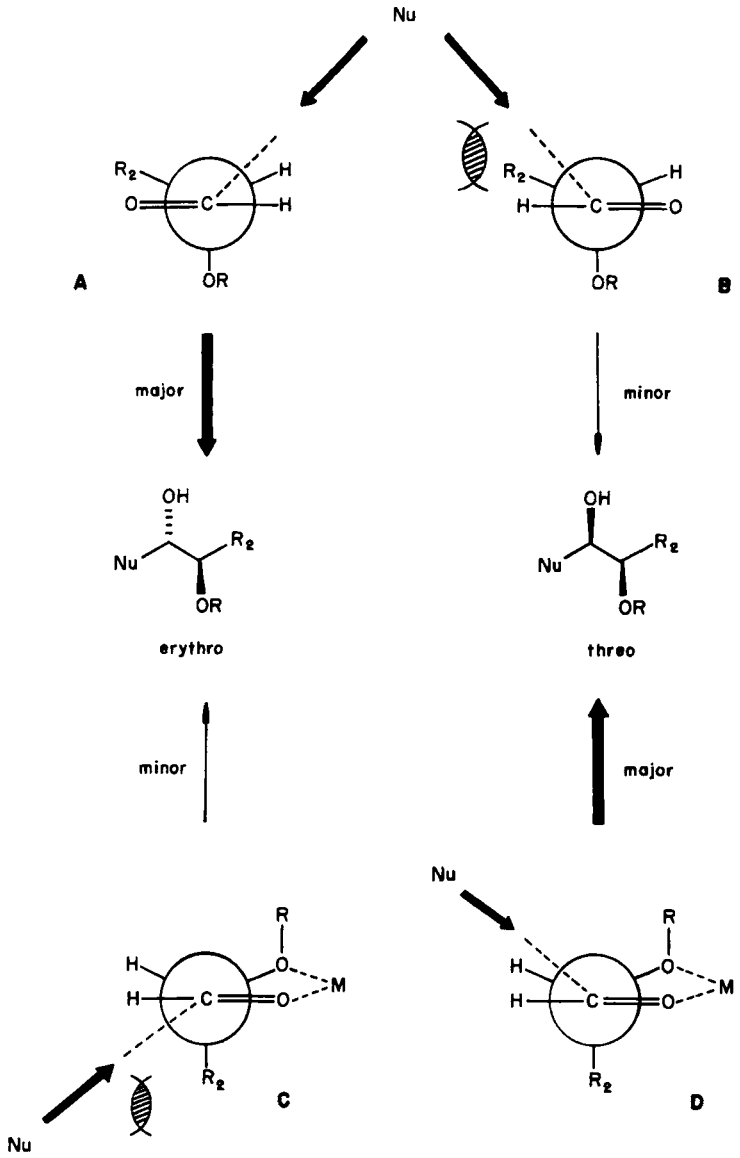
To date, detailed studies of the influence of metal ion on related aldol condensations have not appeared. One might project from



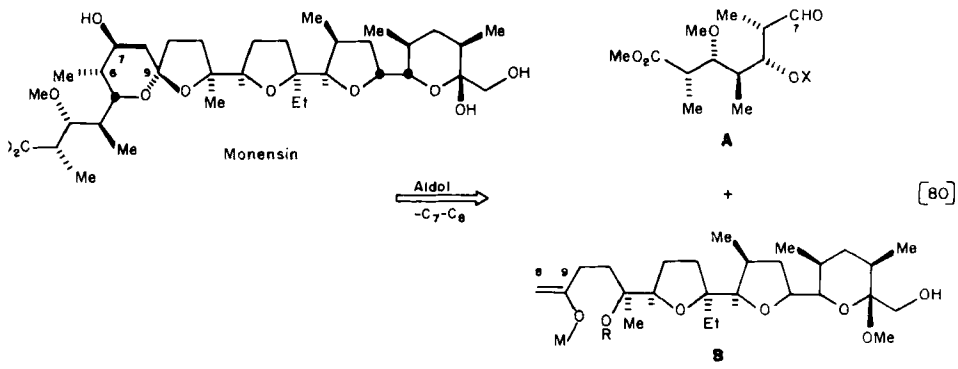
analogies established by Still (99) that the more Lewis acidic magnesium enolates might be induced to exhibit the *opposite* sense of diastereoface selection via chelation-controlled transition states (Scheme 19). An example of such metal ion-dependent diastereoface selection is illustrated in eq. [85] (99).

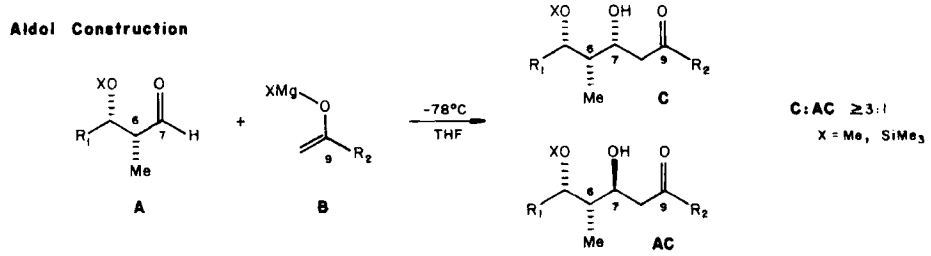


An example of a chelation-controlled titanium tetrachloride-catalyzed aldol condensation has been featured in a recent synthesis of pestalotin (eq. [86]) (100). The condensation illustrated afforded

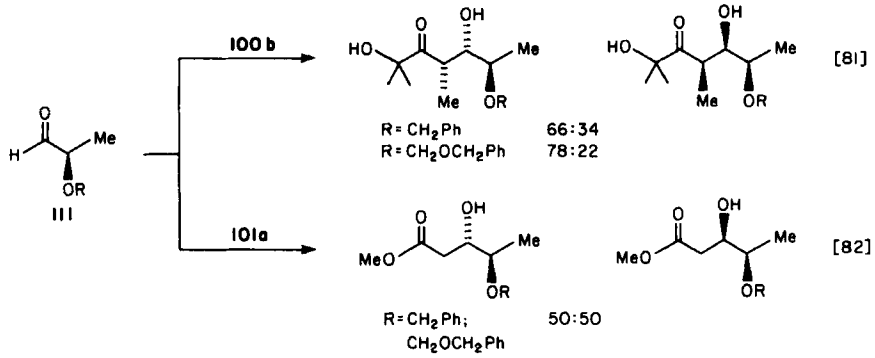


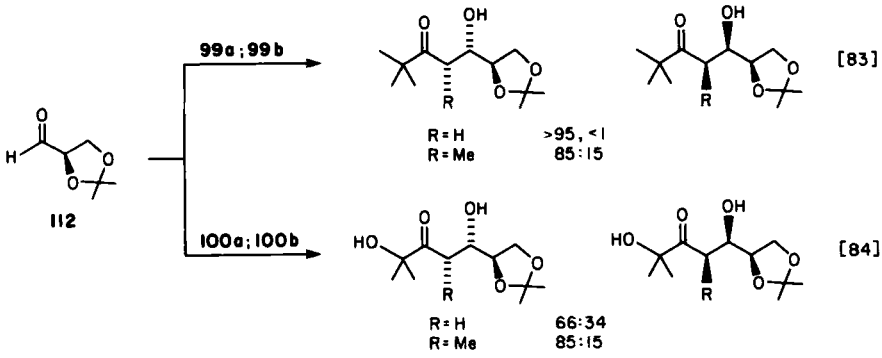
Scheme 19





the adduct **113b** with 85% diastereoface selection (**113a**:**113b** = 15:85). Two excellent examples of metal ion-dependent diastereoface selection have been illustrated in Still's recent synthesis of monensin (101). The addition of the magnesium enolate **100b** to the aldehyde illustrated afforded a 5:1 ratio of **114** and **115** (eq. [87]), where aldehyde diastereoface selection via the chelated transition state **120** must be invoked. To achieve the opposite stereochemical result, metal nucleophiles *incapable* of bis-ligation may be employed. The

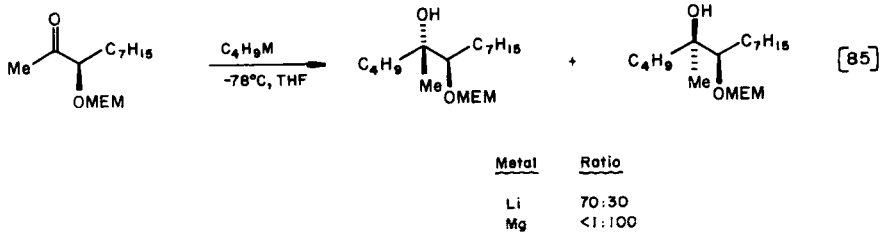




[83]

[84]

addition of (*Z*)-2-butenyldiethylalane (**117**) to aldehyde **116** (eq. [88]) afforded predominantly the diastereomer **118a** (**118a**:**119a** = 3:1) in accord with this speculation. In this case the major diastereomer **119** presumably arises via the normal Felkin transition state

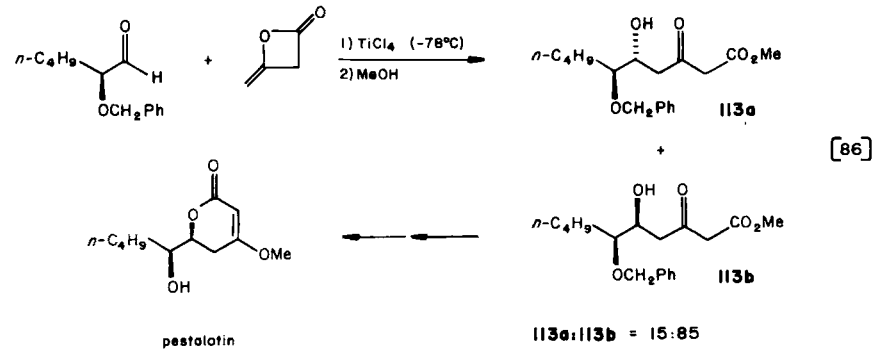


[85]

Metal	Ratio
Li	70:30
Mg	<1:100

[A, R_L = CH(R)OMe, R_M = Me, Scheme 18].

In general, a good level of predictability is now associated with the sense of asymmetric induction in aldol condensations of achiral enolates and chiral α-substituted aldehydes. At present, the perturba-



[86]

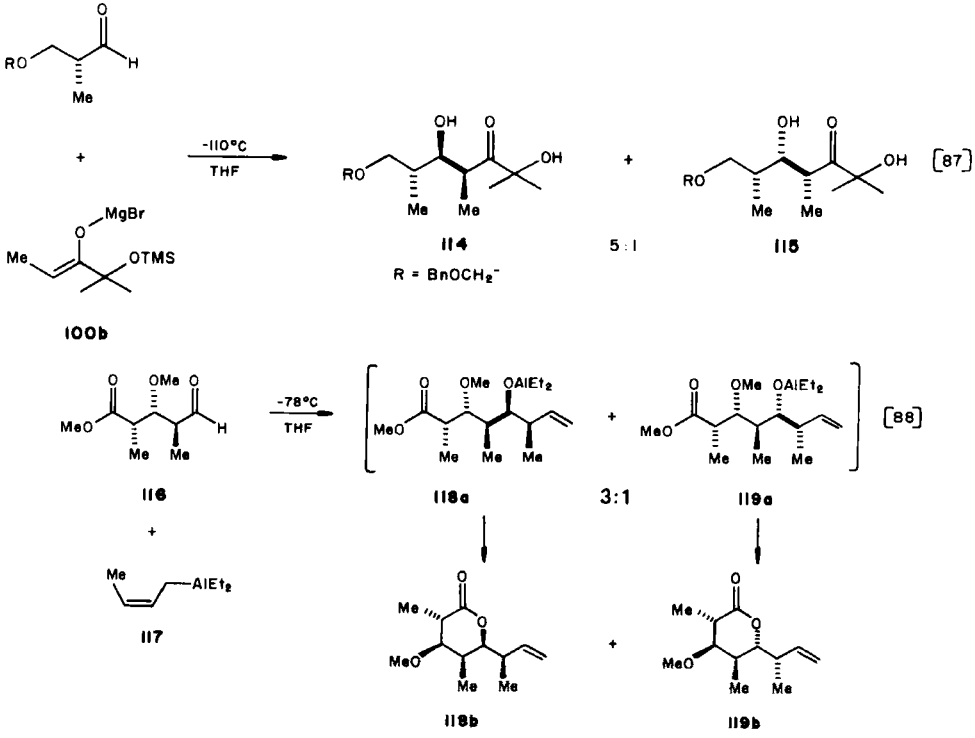


120 R = CH_2OCH_2Ph

tion of remote substituents on the extent of aldehyde diastereoface selection interjects a measure of uncertainty into synthesis design incorporating this chiral control element in the aldol bond construction.

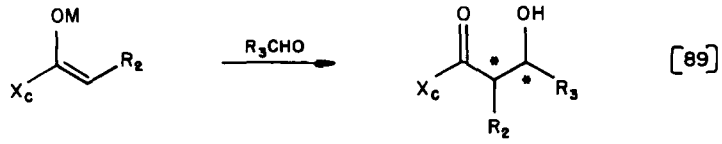
B. Chiral Enolates and Aldehydes

The application of asymmetric synthesis through reaction of chiral enolates with aldehydes is commanding a great deal of current interest, and aspects of this topic have been the subject of a number of recent

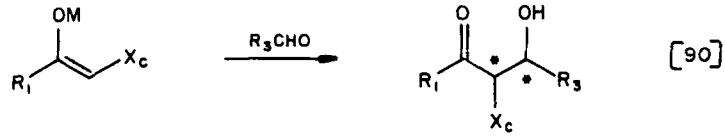


excellent reviews (102–107) and monographs (83,98). In discussing the recent advances that have been made in the development of chiral enolates and their respective aldol condensations, emphasis is placed on control of stereochemistry in acyclic systems (108). An excellent treatment of chirality transfer in the construction of rings via aldol processes has recently appeared (103); consequently, this area is not addressed.

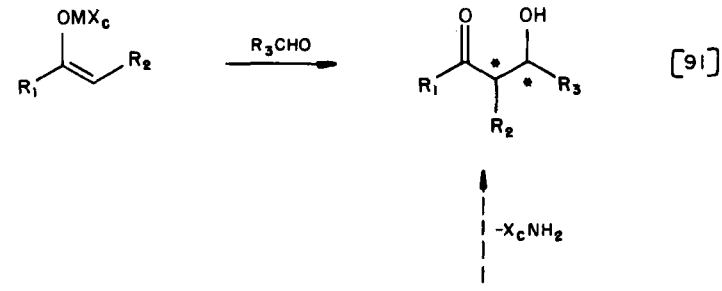
Given the chiral moiety X_c, there are a limited number of positional permutations for the substitution of this ligand on the enolate system (eqs. [89]-[92]). When X_c is attached to the carbon framework



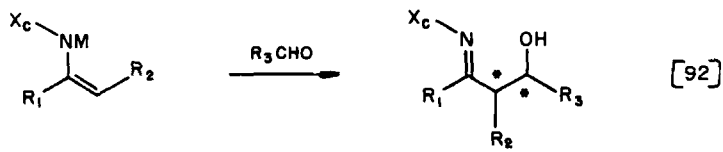
[89]



[90]



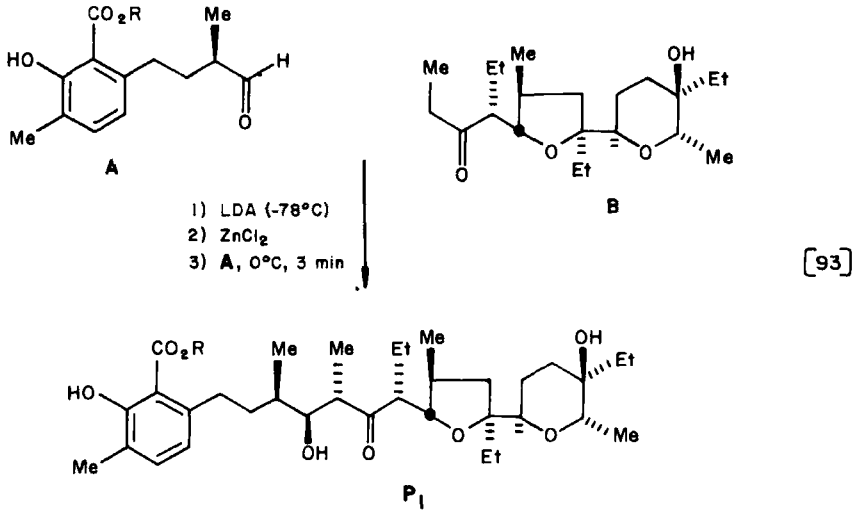
[91]



[92]

(eqs. [89], and [90]), there are two strategic subsets of chiral nucleophiles: in one set the chiral moiety is an integral part of the molecule being constructed; in the other set the chiral ligand is "pruned out" after the desired chirality transfer has been achieved. Two additional options for the emplacement of chirality in the enolate moiety are illustrated in eqs. [91] and [92]. The first case illustrates the option of designing chiral (prochiral) metal centers and the second points to the utility of chiral metalated enamines as enolate synthons. Examples illustrating all four general strategies for chiral enolate design may be found in the literature.

As a corollary to the cases above, the aldehyde may also contain a proximal center of asymmetry. In these cases the resident chirality in *both* the enolate and the aldehyde can influence the generation of new asymmetry in either a mutually cooperative (consonant) or an antagonistic (dissonant) fashion. The consonant or dissonant diastereoface selection imparted to *both* condensation partners has been referred to as double stereodifferentiation (83,109). This issue becomes important in the lasalocid A aldol bond construction illustrated in eq. [93]. This pivotal aldol condensation has been examined in detail



Lasalocid A (R = H)

Aldol Diastereomer Ratios:	$P_1 : P_2 : P_3 : P_4$
Kishi (110a)	54 : 31 : 7 : 5
Ireland (110d)	67 : 17 : 11 : 5

in two independent syntheses of this ionophore (110). Condensation of the zinc enolate derived from the illustrated resolved ethyl ketone B with the (*R*)-aldehyde A under equilibrating conditions (14) afforded the four expected aldol diastereomers of benzyl lasalocid A (R = benzyl) from which the major diastereomer (P_1) was isolated. Subsequent studies (110c) have revealed that the initial aldol condensations reported in this area (110a) were actually carried out on nearly racemic aldehyde.

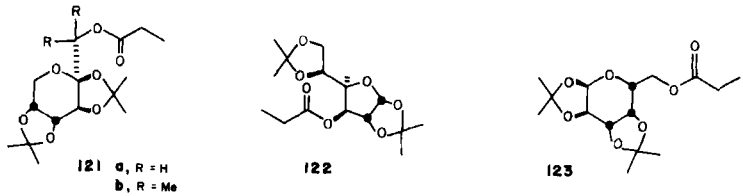
1. Chiral Ester Enolates

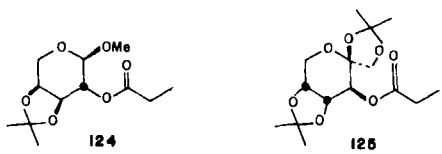
Extensive investigations have been directed toward the development of chiral ester enolates that might exhibit practical levels of aldol asymmetric induction. Much of the early work in this area has been reviewed (111). In general, metal enolates derived from chiral acetate and propionate esters exhibit low levels of aldol asymmetric induction that rarely exceed 50% enantiomeric excess. The added problems associated with the low levels of aldol diastereoselection found with most substituted ester enolates (cf. Table 11) further detract from their utility as effective chiral enolates for the aldol process. Recent studies have examined the potential applications of the chiral propionates **121** to **125** in the aldol condensation (eq. [94]), and the observed erythro-threo diastereoselection and diastereoface selection for these enolates are summarized in Table 31. For the six lithium enolates the threo diastereoselection was found to be

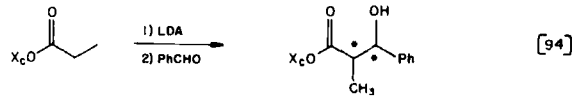
Table 31
Condensation of the Lithium Enolates Derived from Esters **121** to **125** with Benzaldehyde (eq. [94]) (112)

Ester	Erythro-Threo Ratio	Diastereoface Selection[a]
121a	1:3	4.0
121b	1:2.3	1.3-1.7
122	1:1	1.3-1.9
123	1:23	1.1-1.2
124	1:5	1.0-1.3
125	1:6	2.4

[a]Expressed as the ratio of the total reaction at the two diastereotopic faces of the enolate.







[94]

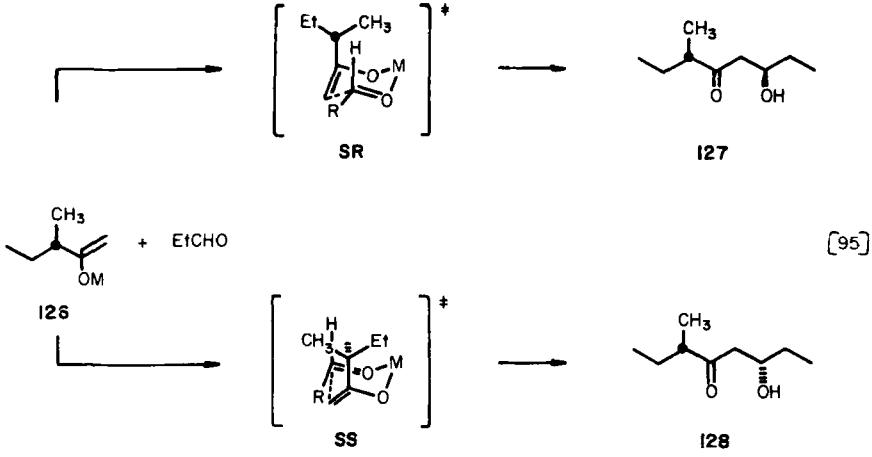
modest, ranging from 1 to 6, whereas the diastereoface selection fell in the range of 1 to 4. The absolute stereostructures of the aldol adducts were not determined in all cases (112).

2. *Chiral Ketone Enolates*

One of the first careful studies of the influence of chirality proximal to ketone enolates is illustrated in eq. [95] (113). Condensation of the enolate **126** (M = Li) with propanal (THF, -100°C) afforded a modest bias for the (*S,R*)-diastereomeric aldol adduct **127** (**127**:**128** = 57:43). The influence of the metal center in this condensation has recently been examined. The boryl enolate **126** [M = $B(n\text{-}C_4H_9)_2$] afforded a ratio **127**:**128** = 64:36 in pentane (-78°C) (6a, 113). Similar studies designed to probe the dependence of diastereoface selection on metal enolate structure have been carried out with metal enolates **129** (eq. [96], Table 32).

Several trends in these comparative condensations were noted. For both substituted lithium and boron enolates **129a** and **129b** (M = Li, BBu_2), greater diastereoface selection was observed for **129b** than with the analogous unsubstituted methyl ketone enolates **129a**. This observation now appears to be generally applicable (see below). Second, the boryl enolates show significantly higher levels of aldol diastereoface selection than the analogous lithium enolates.

The aldol condensations of the chiral lithium enolate **132** have been demonstrated to exhibit excellent erythro diastereoselection as

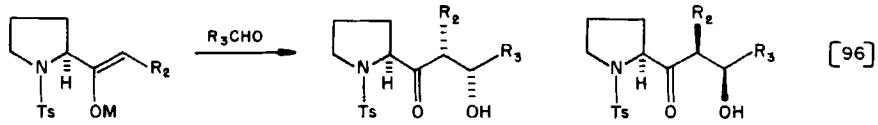


well as diastereoface selection (115). Representative cases are summarized in Table 33. Consonant double diastereodifferentiation has also been demonstrated in the condensation of (±)-**132** with both (±)-**98** and (±)-**112** (eq. [98]). In both instances double asymmetric induction results in diastereoselection ratios of 45:1 (115). To date, only tentative assignments for the stereostructures **135** and **136** have been made. It has been proposed that the diastereoface selection in enolate **132** is defined by ground state lithium chelation (eq. [99]). The chelated transition state **138**, which disposes the smallest ligand (H) on the chiral center *endocyclic*, predicts the sense of asymmetric induction. The interplay between steric and polar effects is difficult

Table 32
Metal-Dependent Condensations of Enolates
129 with Representative Aldehydes (eq. [96]) (114)

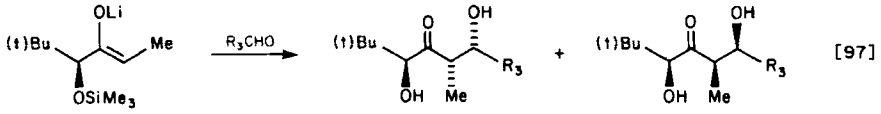
R_2	Metal	R_3CHO	Solvent	Product Ratio **130**:**131**
H	Li[a]	PhCHO	Et_2O	45:55
H	BBu_2[b]	PhCHO	CH_2Cl_2	83:17
H	Li[a]	*i*-C_3H_7CHO	Et_2O	54:46
H	BBu_2[b]	*i*-C_3H_7CHO	CH_2Cl_2	74:26
Me	Li[a]	*i*-C_3H_7CHO	THF	70:30
Me	BBu_2[b]	*i*-C_3H_7CHO	CH_2Cl_2	>97:3

[a]Carried out under kinetic conditions (-78°C, 5 sec).
[b]Condensations carried out at -78 to 0°C.



[96]

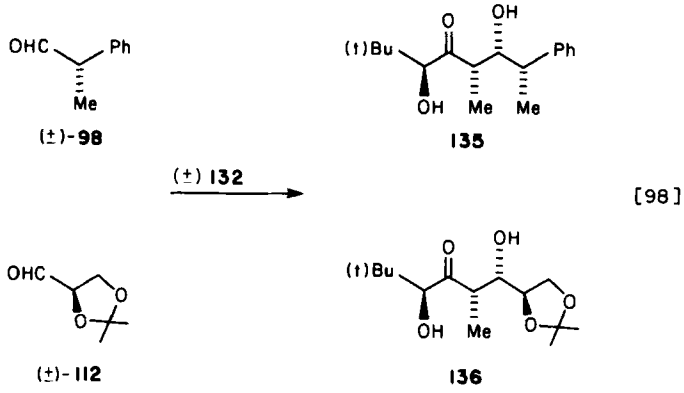
129 a, R_2 = H; b, R_2 = Me **130** **131**



[97]

(±)**132** **133** **134**

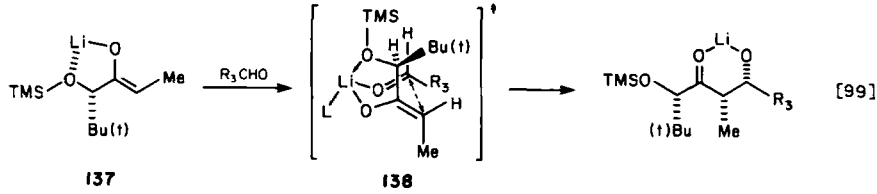
to assess at present because only a limited number of studies have addressed this issue. A steric model that correlates aldol diastereoface selection has also been proposed (Scheme 20) (6a, 114). For the



[98]

Table 33
Stereoselective Condensations of **132** with Representative Aldehydes (eq. [97]) (115)

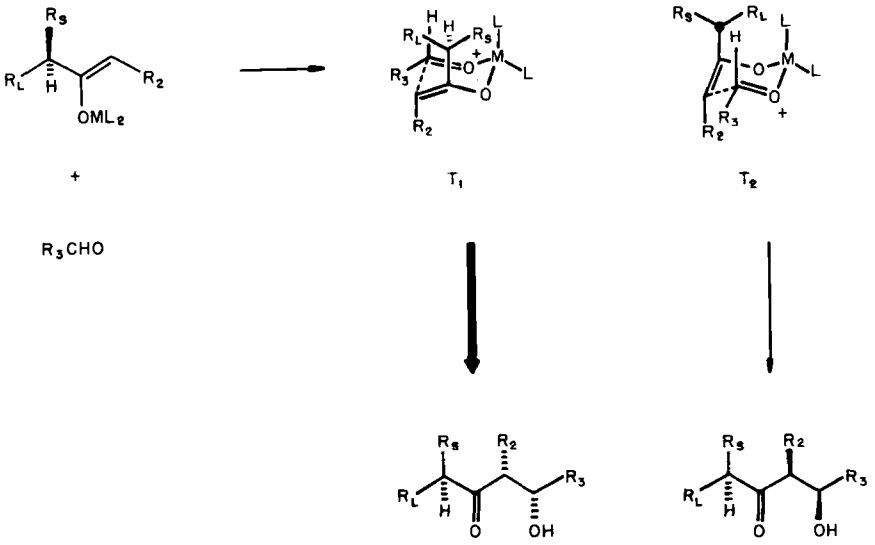
Entry	R_3CHO	Product Ratio **133**:**134**	Yield of **133**+**134** (%)
A	Ph_2CHCHO	⩾90:10	69
B	$PhCH_2CHO$	87:13	75
C	*i*-C_3H_7CHO	75:25	93
D	*t*-C_4H_9CHO	⩾95:5	47
E	PhCHO	67:33	75



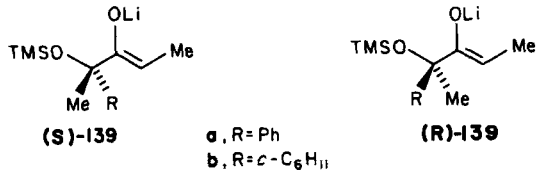
[99]

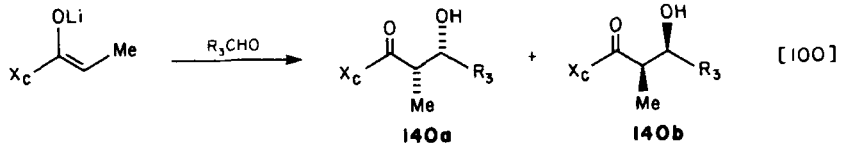
related condensations of boryl enolates **126**, **129a**, and **129b**, the preferred diastereoface selection can be correlated with the preferential formation of transition state T_1 ($ML_2 = BBu_2$) where R_L and R_S are the "large" and "small" substituents on the chiral center (6a). It is possible that the influence of transition state metal center steric effects $R_S \leftrightarrow L$ and $R_L \leftrightarrow L$ is important in the preferential formation of transition state T_1. It is worth noting that steric considerations could also be applied to enolate **132** (115), where the preferred transition state T_1 (R_L = *t*-Bu, R_S = OTMS) is the same as that predicted by chelation (cf. **138**).

Other related chiral erythro selective ketone enolates (*S*)-**139** and (*R*)-**139**, readily prepared from (*S*)- and (*R*)-atrolactic acid, also exhibit good aldol diastereoface selection (3). From the data summarized in Table 34a, the influence of asymmetry in both condensation partners (entries C–F) has been amply demonstrated. The



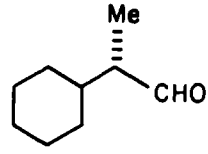
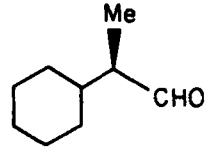
Scheme 20

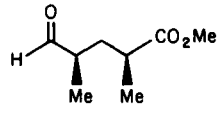




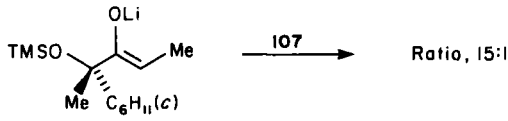
complementary condensations of the (*S*)- and (*R*)-enolates **139b** with the optically pure aldehyde **107** were examined in conjunction with the development of a Prelog-Djerassi lactonic acid synthesis (3). The enhanced diastereoface selection noted with enolate **139b** is consistent with earlier observations that **107** exhibits a preference for "anti-Cram" aldehyde diastereoface selection (cf. eq. [77]) (92).

Table 34*a*
Aldol Condensation of (*S*)-**139** and (*R*)-**139** with Representative Aldehydes (eq. [100]) (3)

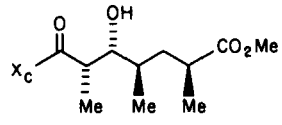
Entry	Enolate	R_3CHO	Product Ratio **140a**:**140b**
A	(*S*)-**139a**	PhCHO	3.5:1
B	(*S*)-**139a**	$PhCH_2CHO$	6:1
C	(*S*)-**139a**		8:1
D	(*R*)-**139a**		1:1.5
E	(*S*)-**139a**		1.5:1
F	(*R*)-**139a**		1:8



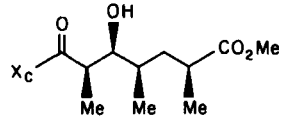
107



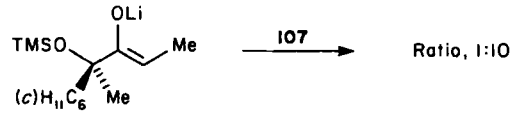
(S)-139b



140a

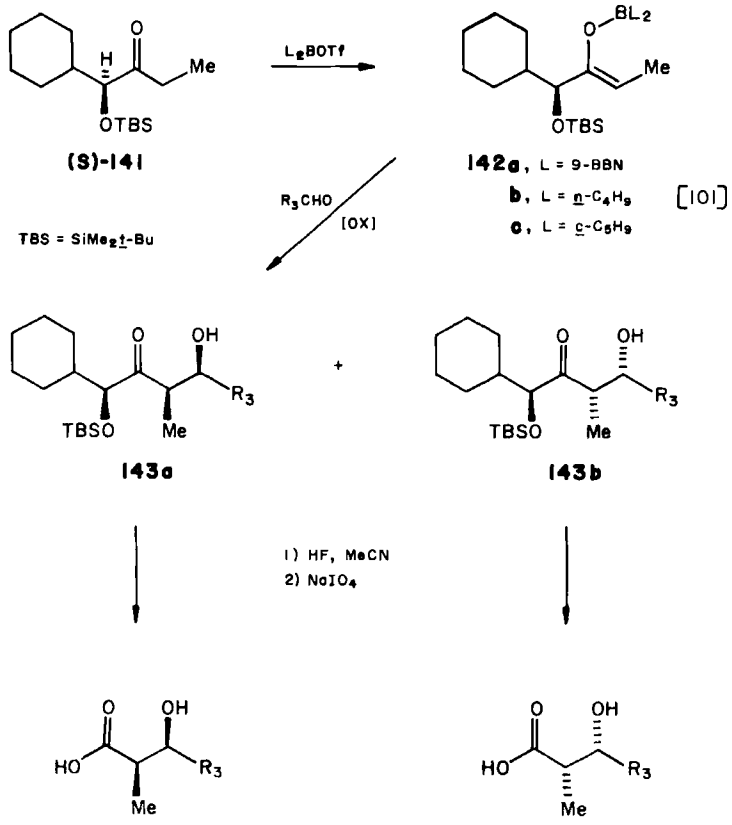


140b



(R)-139b

Recently, the improved chiral ethyl ketone (*S*)-141, derived in three steps from (*S*)-mandelic acid, has been evaluated in the aldol process (115). Representative condensations of the derived (*Z*)-boron enolates (*S*)-142 with aldehydes are summarized in Table 34b. It is evident from the data that the nature of the boron ligand L plays a significant role in enolate diastereoface selection in this system. It is also noteworthy that the sense of asymmetric induction noted for the boron enolate (*S*)-142 is *opposite* to that observed for the lithium enolate (*S*)-139a and (*S*)-139b derived from (*S*)-atrolactic acid (3) and the related lithium enolate 139. A detailed interpretation of these observations in terms of transition state steric effects (cf. Scheme 20) and chelation phenomena appears to be premature at this time. Further applications of (*S*)-141 and (*R*)-141 as chiral propionate enolate synthons for the aldol process have appeared in a 6-deoxyerythronolide B synthesis recently disclosed by Masamune (115b).

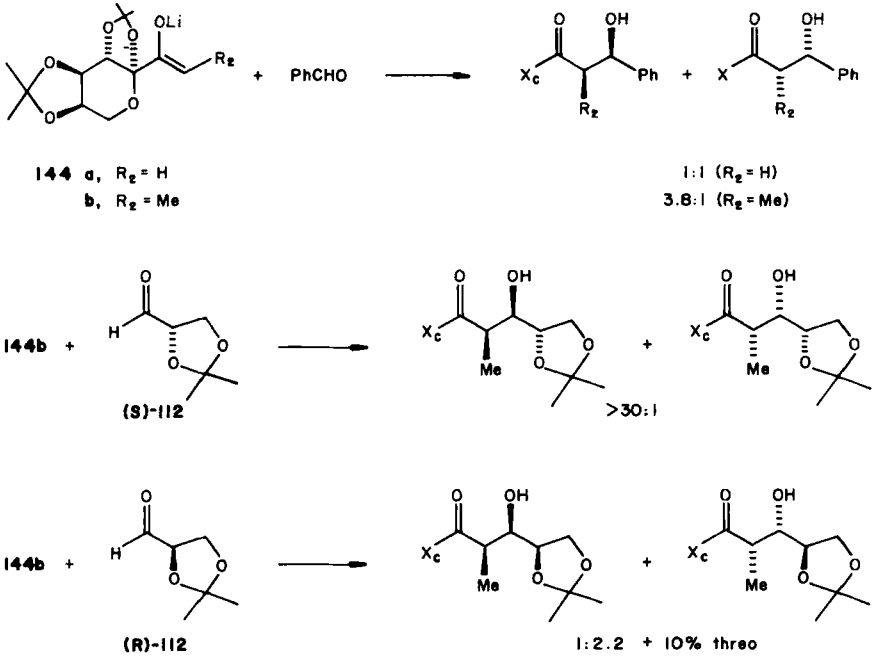


Other chiral ethyl ketone enolates derived from carbohydrates have recently been evaluated (109,112). The aldol condensations of one of the more promising systems is illustrated in Scheme 21. The aldol condensation of the (*Z*)-enolate **144b** with benzaldehyde proceeded with good erythro selection and a 3:1 diastereoface selection. The stereochemistry of the major aldol adduct was unambiguously determined by X-ray crystallography. In marked contrast, the unsubstituted enolate **144a** exhibited *no* diastereoface selection, in analogy with related observations cited earlier (cf. enolate 129, Table 32). In condensations with the (*R*)- and (*S*)-glyceraldehyde acetonides 112, (*S*)-112 exhibited a consonant erythro diastereodifferentiation exceeding 30:1, whereas (*R*)-112 afforded only a 2.2:1 ratio of erythro diastereomers (112,116).

Table 34b
Aldol Condensations of Boron Enolate **142**
with Representative Aldehydes (eq. [101]) (115a)

Boron Enolate (L)[a]	Aldehyde	Product Ratio[b] **143a:143b**
143a (9-BBN)		14:1
143b (n-C_4H_9)	PhCHO	40:1
143c (c-C_5H_9)		75:1
143a (9-BBN)		17:1
143b (n-C_4H_9)	EtCHO	50:1
143c (c-C_5H_9)		100:1
143a (9-BBN)		100:1
143b (n-C_4H_9)	i-C_3H_7CHO	100:1
143c (c-C_5H_9)		No reaction

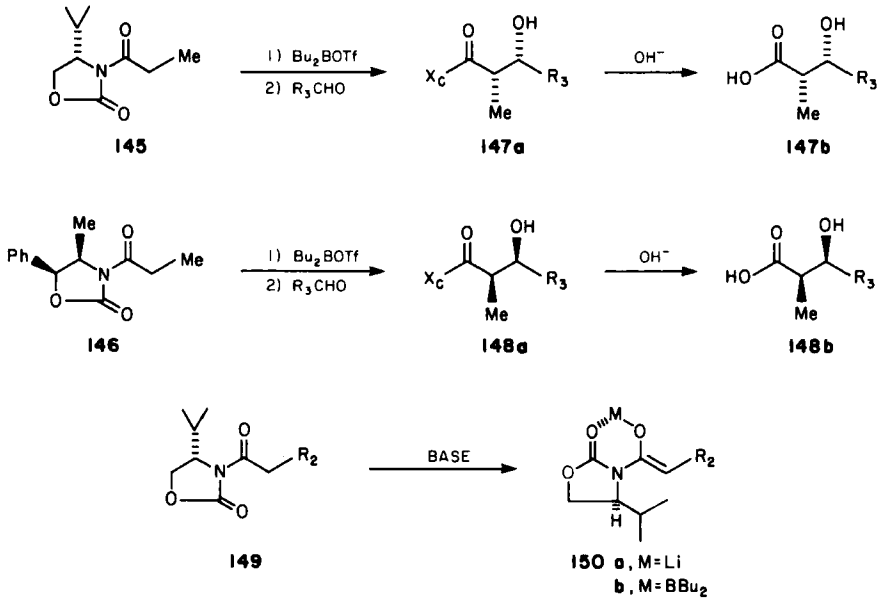
[a]Two equivalents of enolate employed per equivalent of R_3CHO at 0°C in CH_2Cl_2.
[b]Determined by ^1H NMR.



Scheme 21

3. *Chiral Amide and Imide Enolates*

Recent investigations from this laboratory (117) have defined the utility of propionyl imides **145** and **146** in achieving high levels of erythro diastereoface selection in aldol condensations of the derived boryl enolates (Scheme 22). The chiral auxiliaries were readily prepared from either (*S*)-valinol or the commercially available (1*S*,2*R*)-norephedrine. Enolization of imides **145** or **146** with either LDA or dibutylboryl triflate afforded a single (*Z*)-enolate (cf. **150**), in direct analogy with the enolization stereoselection observed for amides (cf. Scheme 8). Although the lithium enolates exhibited low levels of stereoselection, the boryl enolates exhibited remarkably good stereochemical control. The erythro diastereoselection was found to be ⩾99:1; the diastereoface selection was ⩾100:1 for the representative aldehydes shown in Table 35. The resultant aldol adducts may be conveniently hydrolyzed to the respective β-hydroxy acids with aqueous base, and the oxazolidone chiral auxiliaries are readily recovered. It is mechanistically significant that the boryl enolate derived from the *N*-acetyl oxazolidone **149a** exhibited *low* levels of asymmetric induction with representative aldehydes (Table



145 **147a** **147b**

146 **148a** **148b**

149 **150 a**, M=Li
b, M=BBu$_2$

Scheme 22

Table 35
Aldol Condensations of **145** and **146** with
Representative Aldehydes (Scheme 22) (117)

Imide	R_3CHO	Product Ratio[a] **147a:148a**	Yield of **147b (148b)** (%)[b]
145	*i*-C_3H_7CHO	497:1	69
146	*i*-C_3H_7CHO	<1:500	78
145	*n*-C_4H_9CHO	141:1	68
146	*n*-C_4H_9CHO	<1:500	71
145	PhCHO	>500:1	82
146	PhCHO	<1:500	60

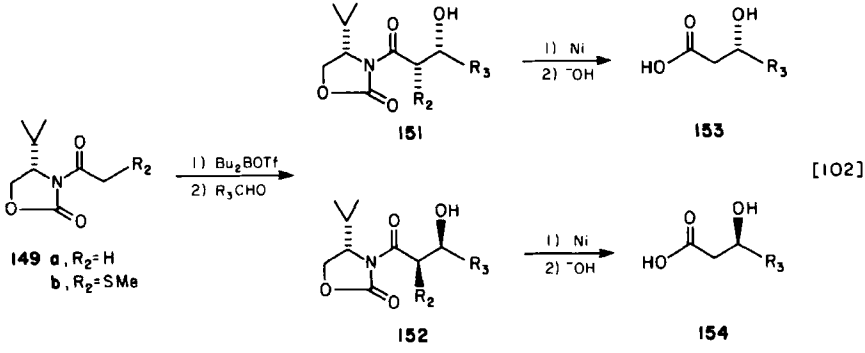
[a] Determined by capillary GLC.
[b] Values reported are for the overall conversion of **145 (146)** → **147b (148b)**.

36). The importance of the (*Z*)-enolate substitution has been noted elsewhere in this chapter (see Table 32). A practical solution to the generation of a useful chiral acetate enolate synthon has been to employ a substituted enolate where the ligand R_2 may be removed after the aldol condensation. Enolate **149b** (R_2 = SMe) serves this purpose adequately (eq. [102]). The resultant aldol adducts **151b**

Table 36
Aldol Condensations of **149a** and **149b** with
Representative Aldehydes (eq. [102]) (117)

Imide	R_3CHO	Product Ratio **151:152**[a]	Product Ratio **153:154**[b]
149a	*i*-C_3H_7CHO	52:48	
149b	*i*-C_3H_7CHO	98.4:1.6	97.8:2.2
149a	*n*-C_3H_7CHO	63:37	
149b	*n*-C_3H_7CHO	98.9:1.1	99.4:0.6
149a	CH_3CHO	72:28	
149b	CH_3CHO	99.6:0.4	>99.9:<0.1
149a	PhCHO	62:38	
149b	PhCHO	92.4:7.6	92.4:7.6

[a] Determined by capillary GLC before purification for enolate **149a** and after desulfurization for enolate **149b**.
[b] Inferred from the ratios **151:152** after chromatographic purification and resultant hydrolysis.



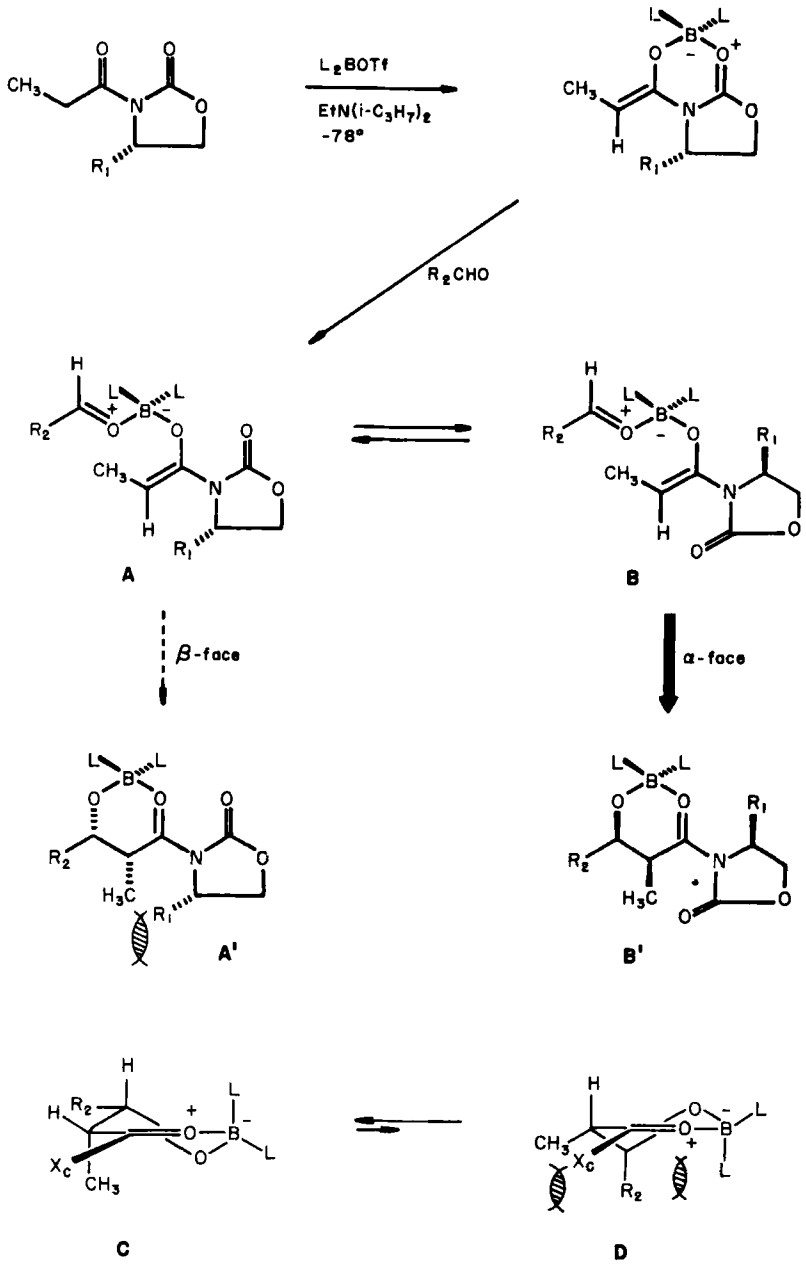
[102]

(152b) are readily desulfurized and hydrolyzed to the β-hydroxy acids 153 (154) in good yields. The results are summarized in Table 36.

One possible explanation for the diastereoface selection ($\Delta\Delta G^{\ddagger}$ -78°C ~ 3 kcal/mol) observed for these chiral enolates is illustrated in Scheme 23. In the respective aldol transition states derived from conformers A and B leading to erythro diastereomers A′ and B′, it may be assumed that developing imide resonance (118) will lock the chiral auxiliary in one of the in-plane conformations illustrated in products A′ or B′. Based on an examination of models, it is projected that developing $CH_3 \leftrightarrow R_1$ allylic strain steric interaction (37) disfavors that transition state leading to A′. These steric considerations are largely attenuated in the transition state leading to the observed erythro adduct B′.

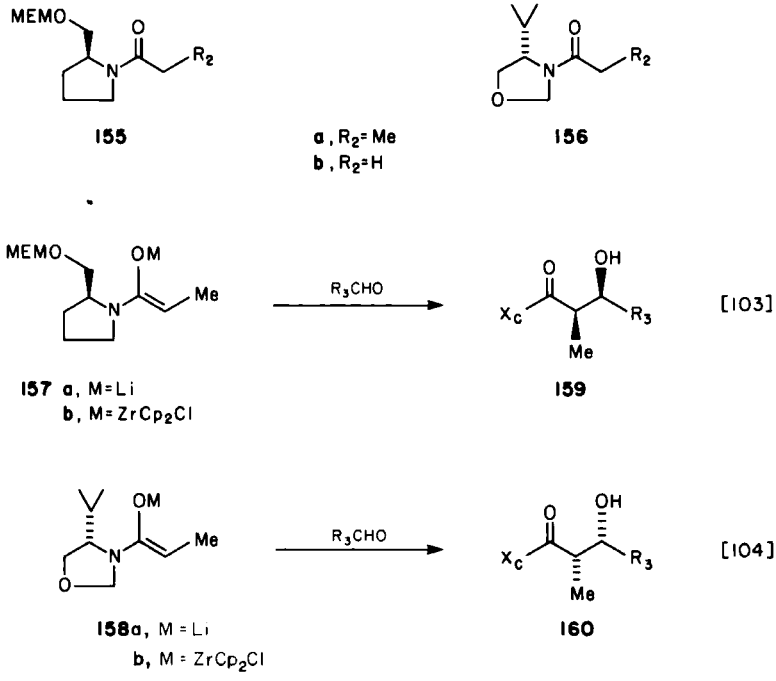
It should also be noted that there is a strong conformational bias for only *one* of the product chelate conformers. For example, erythro chelate D should be strongly disfavored by both 1,3-diaxial $R_2 \leftrightarrow L$ and $CH_3 \leftrightarrow X_C$ steric control elements. Consequently, it is assumed that the transition states leading to *either* adduct will reflect this conformational bias. Further support for these projections stems from the observations that the chiral acetate enolates derived from **149a** exhibit only poor diastereoface selection. In these cases the developing $R_1 \leftrightarrow CH_3$ interaction leading to diastereomer A′ is absent. Similar transition state allylic strain considerations also appear to be important with the zirconium enolates, which are discussed below.

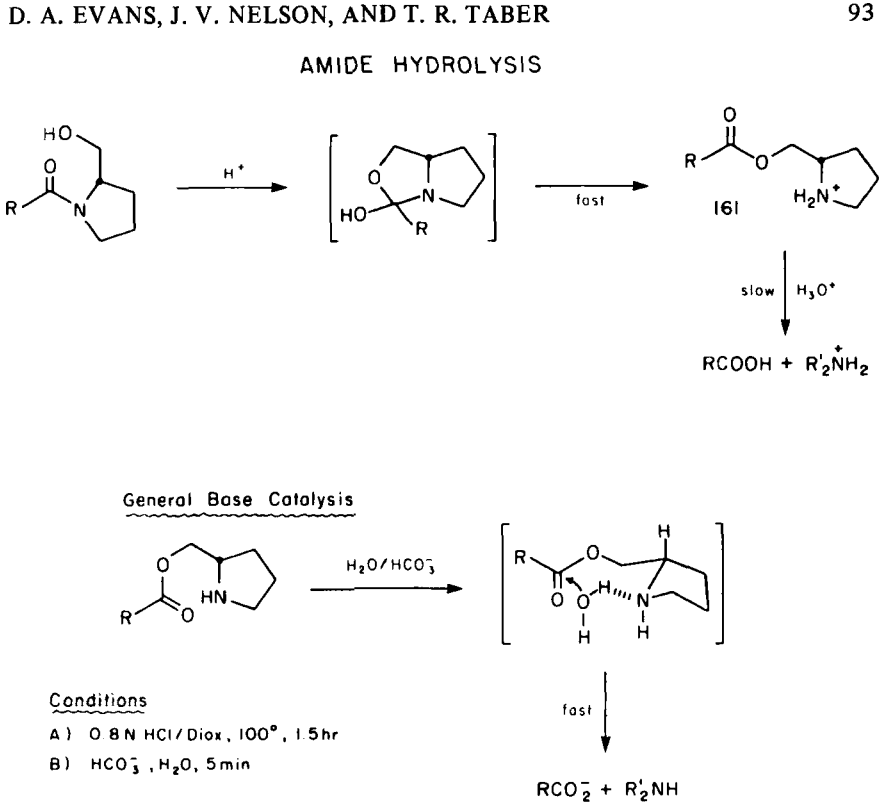
The preceding discussion clearly demonstrates the important role that metal-centered steric effects can exert on enolate diastereoface selection in the aldol process. A recent publication from this laboratory provides an additional example of the importance of this



Scheme 23

stereochemical control element (119). It has been demonstrated that the lithium enolates derived from prolinol amides exhibit diastereoface selection ratios of 15 to 30 in alkylation reactions (36). In view of this level of stereoselectivity it is somewhat surprising that the aldol condensations of these and related derivatives (cf. **157a**, **158a**) are nearly stereorandom. However, excellent aldol stereoregulation may be restored to these systems via the zirconium enolates **157b** and **158b**. With this sterically demanding metal center, erythro diastereoselection is achieved (erythro/threo $\approx$ 50), and enolate diastereoface selection ratios in the range of 50 to 200 may be achieved. Chiral enolate **157b**, derived from (*S*)-prolinol, afforded predominantly erythro stereoisomer **159** (eq. [103]), whereas enolate **158b**, derived from (*S*)-valinol, resulted in the complementary adduct **160** with representative aldehydes (eq. [104]) (119). In the design of these chiral auxiliaries, a latent hydroxyl function has been incorporated to facilitate amide hydrolysis under mild conditions. For example, under acidic conditions N → O acyl transfer has been demonstrated to occur followed by a slower acid-catalyzed hydrolysis of the resultant ester (Scheme 24) (36). If the ammonium ester **161**, once

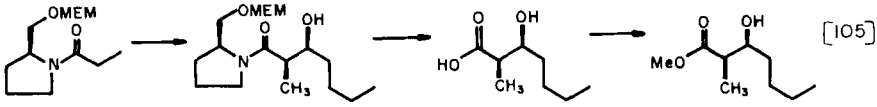




Scheme 24

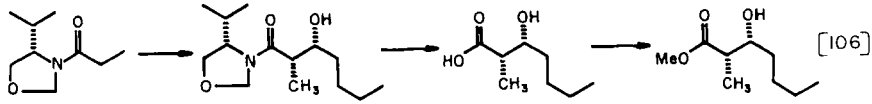
formed, is subsequently basified, general base catalysis exerts a strong catalytic role in the final liberation of the aldol adduct without loss of stereochemistry. Typical results of the aldol condensations of **155a** and **156a** with *n*-pentanal and the subsequent acid-catalyzed hydrolyses are illustrated in eqs. [105] and [106]. The comparative lithium and zirconium aldol condensations are summarized in Table 37. The condensation of zirconium enolate **158b** with the (*R*)- and (*S*)-enantiomers of aldehyde **162** have also been examined to assess the influence of resident chirality in the aldehyde condensation partner on aldol stereoselection (Scheme 25). From the data presented it is clear that the perturbation of this added chiral element is minor.

It is significant to note that the sense of asymmetric induction noted for amide enolates **157** and **158** is the same as that found for the boryl enolates derived from the chiral oxazolidone imides **146** and **145**, respectively (cf. Scheme 22). The arguments presented



[105]

155a $E_1:E_2$ = 98:2 2R,3S $[\alpha]_D$ - 14.2° 80% yield



[106]

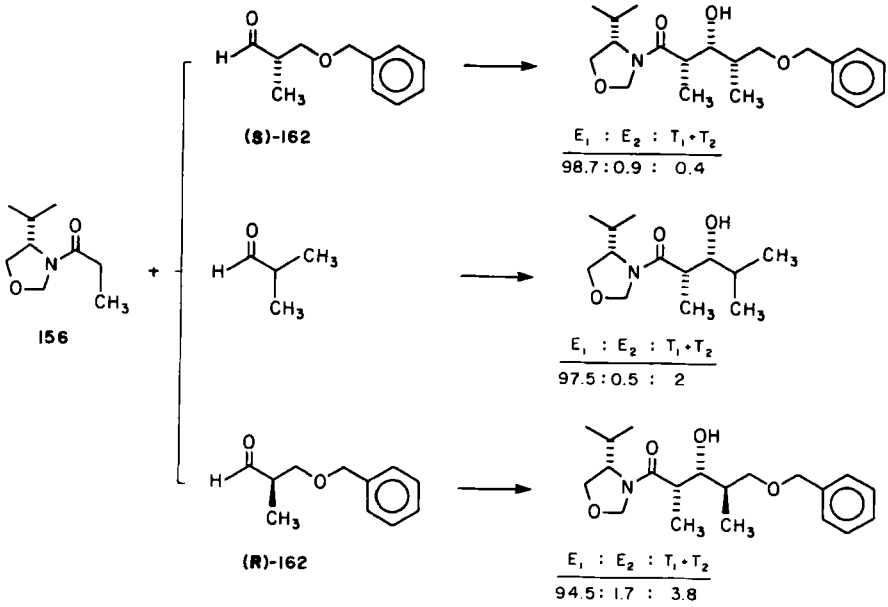
156a $E_1:E_2$ = 1:99 2S,3R $[\alpha]_D$ + 14.8° 82% yield

earlier for the sense of asymmetric induction in these systems (cf. Scheme 23) may also apply to the zirconium enolate systems. A rationalization of the chirality transfer in these condensations is

Table 37
Comparative Aldol Condensations of the Lithium and Zirconium Enolates **157** and **158** (eqs. [103, 104]) (119)

Enolate	Metal[a]	R_3CHO	Product Distribution[b] $E_1:E_2$[c]	$T_1:T_2$
157b	Zr	*n*-C_4H_9CHO	96:2	1:1
157a	Li		39:29	15:17
158b	Zr		1:97	1:1
158a	Li		35:42	6:17
157b	Zr	*i*-C_3H_7CHO	96:2	1.5:0.5
157a	Li		43:36	9:12
158b	Zr		0.5:98.3	0.8:0.4
158a	Li		42:41	13:4
157b	Zr	PhCHO	96:1	2:1
157a	Li		31:33	23:13
158b	Zr		1.3:95.2	1.2:2.2
158a	Li		41:29	24:6

[a] Zr refers to $ZrCp_2Cl$.
[b] Determined by capillary GLC.
[c] The absolute stereochemical assignments associated with E_1 and E_2 are as illustrated in structures **159** and **160**, respectively.



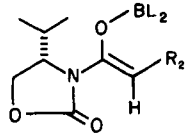
Scheme 25

illustrated with the aid of a Newman projection at the metal center in Scheme 26. In these enolate systems, the importance of enolate substitution on enolate diastereoface selection has again been noted. The previously cited examples documenting this observation for a range of chiral auxiliaries and metals are summarized in Table 38. These trends are clearly important considerations, which must be addressed in the design of chiral acetate enolates.

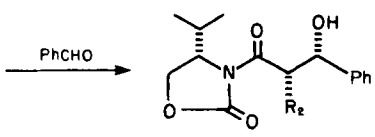
The utility of chiral oxazoline enolates in asymmetric synthesis has elegantly been demonstrated by Myers (106,120). The stereoselective aldol condensations of these enolates have been examined in a limited number of cases (eq. [107]) (32,121). Assuming that the enolate formed has the geometry indicated in **164** (120b), the diastereoselection observed for *both* the aldol condensation and the previously reported alkylations favors electrophile attack on the *Re* face as indicated. In contrast, the unsubstituted enolate **163b** exhibits significantly poorer diastereoface selection with a range of aldehydes (eq. [108]) (121).

An excellent chiral acetate enolate synthon has recently been reported by Solladie (eq. [109]) (122). The (*R*)-α-sulfinylacetate enolate **165** was found to undergo aldol condensation (-78°C, THF)

Table 38
The Importance of Enolate Substitution in Aldol Diastereoface Selection[a]

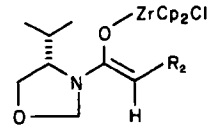


150b

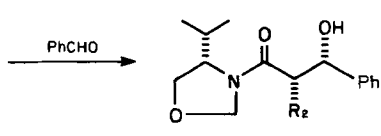


R_2 = Me, >500:1
R_2 = H, 1.6:1

Ref. 117

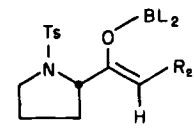


158b

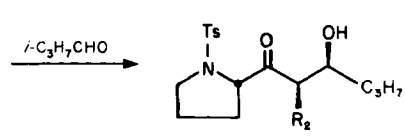


R_2 = Me, 63:1
R_2 = H, 1.5:1

Ref. 119

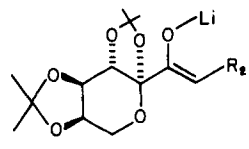


129

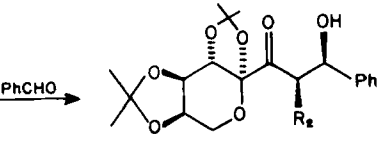


R_2 = Me, >32:1
R_2 = H, 5:1

Ref. 6a, 114

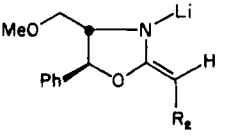


143

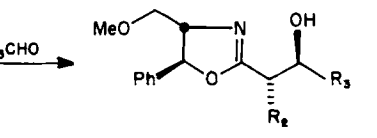


R_2 = Me, 3.8:1
R_2 = H, 1:1

Ref. 116



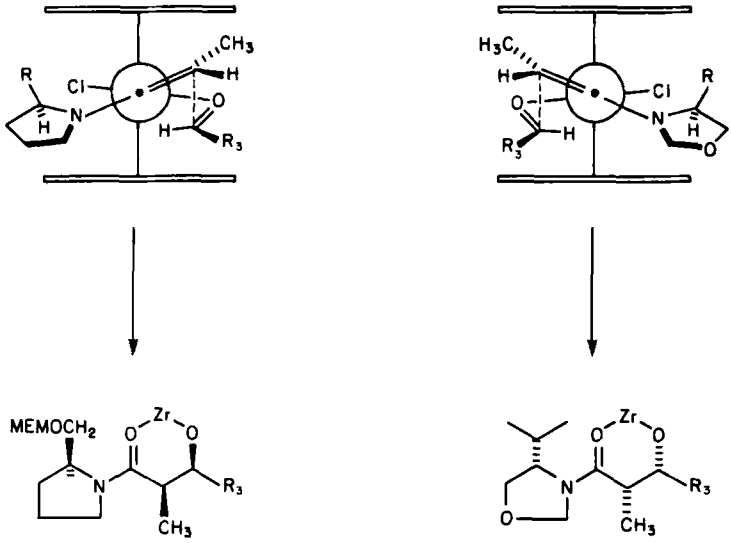
163



R_2 = Me, R_3 = *i*-C_3H_7; 18:1
R_2 = H, R_3 = Et; 1.4:1

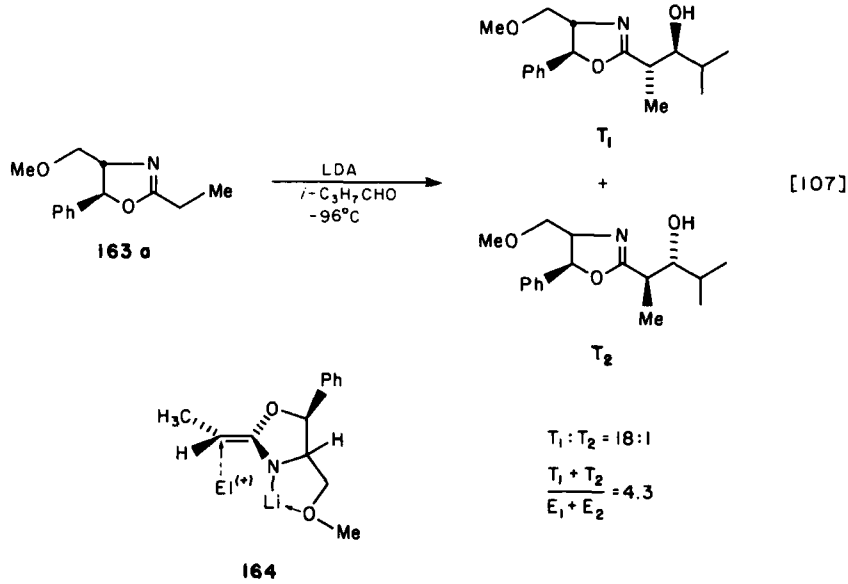
Ref. 32, 121

[a]The ratios noted are for the two erythro diastereomers for **150b**, **158b**, and **129** (R_2 = Me) and the two threo diastereomers for **163** (R_2 = Me).



Scheme 26

with a variety of carbonyl compounds that after desulfurization (Al/Hg), afforded the adducts **166/167** in good overall yields (75–90%). The efficiency of asymmetric induction directly correlates with the differential steric requirements of the carbonyl derivative



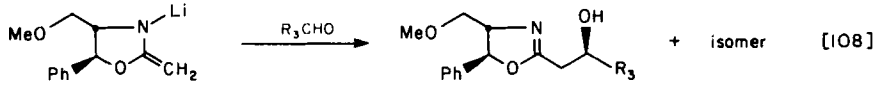
163 a

164

$T_1 : T_2 = 18:1$

$\frac{T_1 + T_2}{E_1 + E_2} = 4.3$

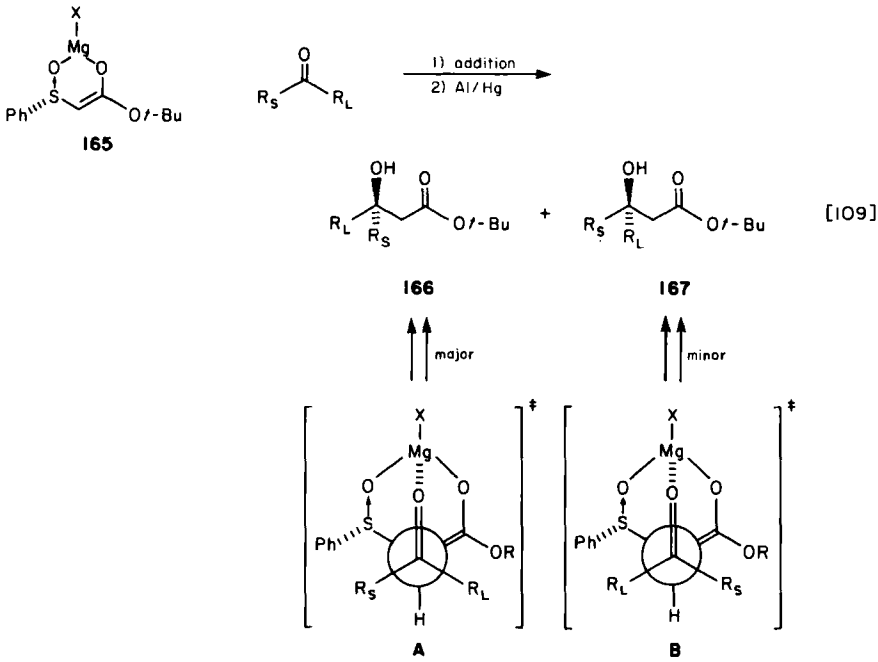
[107]



163 b

Diastereoface Selection ~ 1.5:1

(R_L = large, R_S = small substituent). From the data summarized in Table 39, it is apparent that the asymmetric induction observed is excellent for aldehydes, and that stereoselection generally increases as the aldehyde ligand becomes more sterically demanding. The major aldol adduct, **166**, has been rationalized as evolving from transition state A. A priori it is difficult to evaluate the relative



importance of the various gauche interactions that are present in the two transition states. Corey, who recently employed this chiral enolate strategy in a maytansine synthesis (eq. [110]) (124), chose the related enolate **168** because of the sensitivity of this system to the acidic conditions usually employed for the removal of *tert*-butyl esters. A less successful application of the α-sulfinyl ester enolate **165** to a synthesis of (*R*)-mevalonolactone has also been reported (eq. [111]) (125). The low levels of asymmetric induction probably

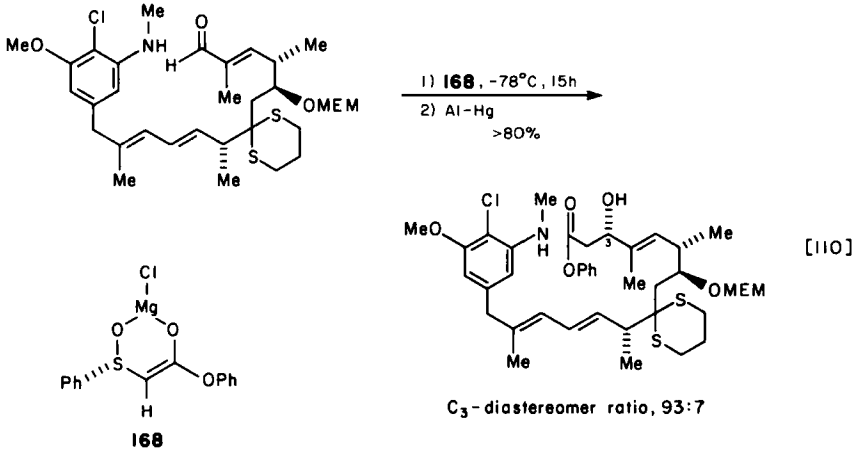
Table 39
Aldol Condensation of Enolate **165** with
Representative Carbonyl Compounds, $R_SR_LC=O$ (eq. [109]) (122)

R_S	R_L	Product Ratio **166:167**	Yield (%)
H	n-C_7H_{15}	93:7	80
H	–Ph	95:5	85
H	i-C_3H_7[a]	99:1	71
H	–C(Me)=CHMe (E)[a,b]	89:11	80
Me	Ph	84:16	75
Me	c-C_6H_{11}	>97:3	88

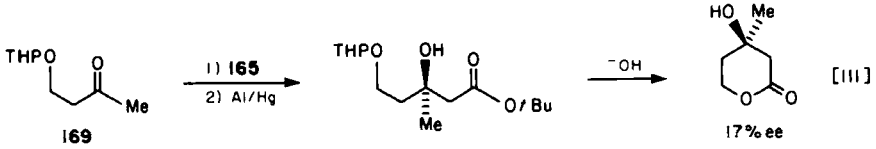
[a] Ref. 123.
[b] Absolute configuration not determined.

reflect the relatively small size differentiation between the carbonyl substituents [R_S = Me, R_L = $(CH_2)_2OTHP$] in **169**.

One highly successful strategy for the construction of chiral enolate synthons has been to employ the analogous imine substrate derived from readily available chiral amines (eq. [112]). A basic structural requirement for these chiral auxiliaries appears to be that the auxiliary contain a proximal chelating ligand to provide a structurally organized metalloenamine with a well-defined facial bias (cf. 173a–173c). Considerable effort has been devoted to the enantio-

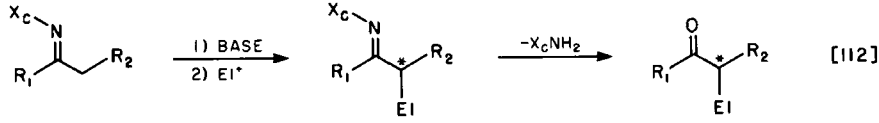


[110]

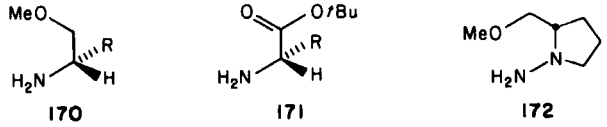


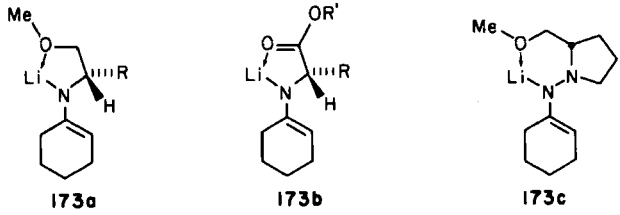
[111]

selective alkylations of the metalated enamines derived from **170** (126), **171** (127), and **172** (128), and the weight of evidence supports the enolate structures illustrated (126–129). In enolates for which olefin geometry is not an issue (e.g., **173**) alkylation diastereoface selection is quite high (10–100) for all three chiral auxiliaries. Although the potential of these chiral enolate systems in the aldol process has yet to be delineated, one study has addressed the utility of the prolinol-derived hydrazones illustrated in eq. [113] (130).

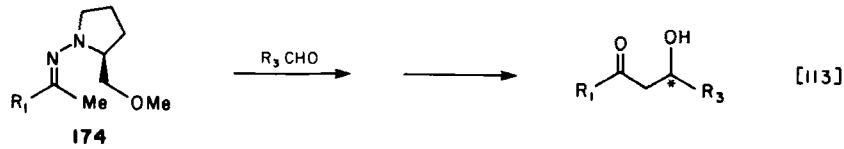


[112]





The resultant aldol adducts derived from **174** (R_1 = Me, Et, *i*-C_3H_7, *t*-C_4H_9) and representative aldehydes (four cases) were formed with optical purities ranging from 17 to 62% e.e. In view of the profound

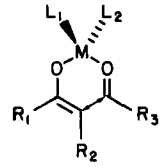


[113]

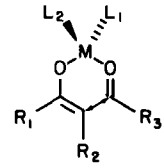
influence of enolate substituents on diastereoface selection (cf. Table 38), the relatively low levels of asymmetric induction in this system are not surprising.

4. *Metal-Localized Chirality Transfer*

In principle, one general strategy for the design of enantioselective aldol condensations is to construct Zimmerman pericyclic transition states where chirality is transferred from the metal center to the stereocenter being constructed. Given either transition state A or B, where $L_1 \neq L_2$, metal center chirality transfer to the developing centers of asymmetry could be highly efficient, in direct analogy with related Cope and Claisen transition states. For an enolate of defined geometry, two design requirements must be met for chirality transfer of this type. First, the chiral ligands L_1 and L_2 on the



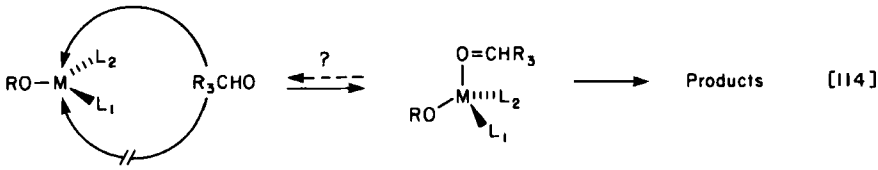
A



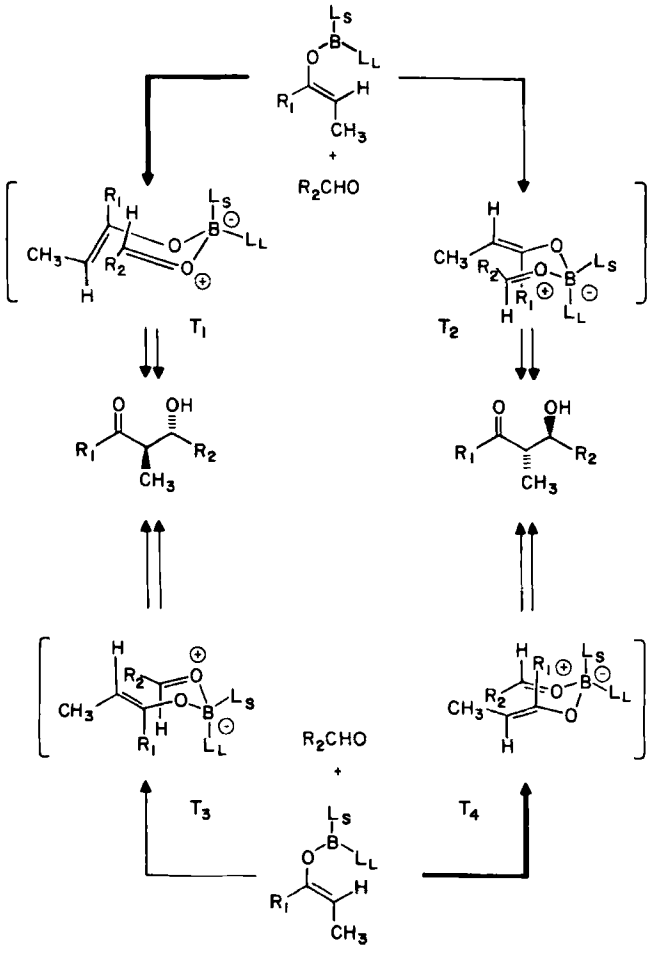
B

metal enolate must strongly bias one of the prochiral faces of the metal center (eq. [114]). Second, the chiral ligand L_1 and/or L_2 must have *significantly* different steric requirements proximal to the metal center (e.g., L_1 large, L_2 small). This second feature is illustrated in Scheme 27 for boryl enolates where L_S and L_L are the small and large ligands, respectively. Assuming that only transition states T_1 and T_2 are formed (condition I), racemic product will be obtained if the steric requirements of $L_S = L_L$. If $L_L > L_S$ (condition II), transition state T_1 will be preferred for the obvious reasons ($R_1 \leftrightarrow L_L > R_1 \leftrightarrow L_S$).

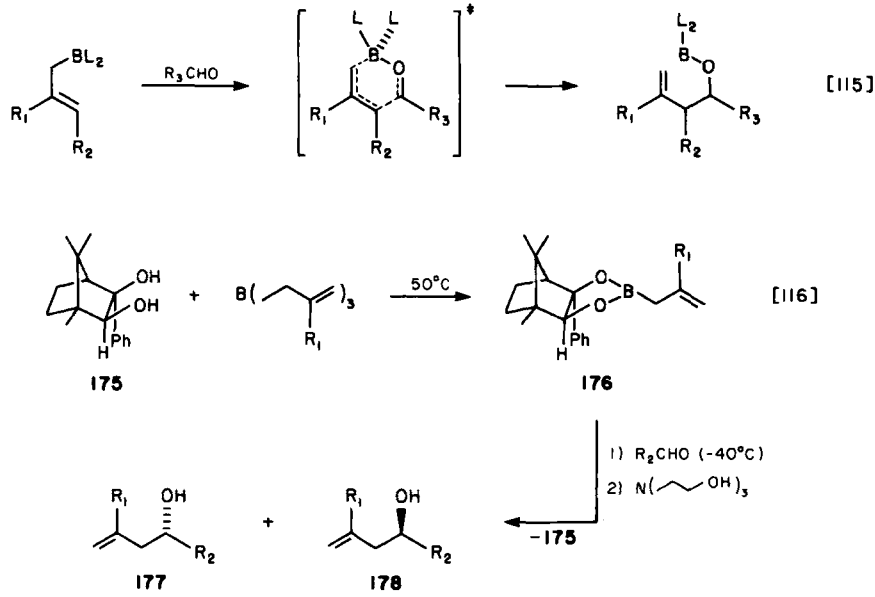
Although this general principle of asymmetric induction has not been demonstrated for boron enolates, the related addition reactions of allylboranes to aldehydes (eq. [115]) (131) have been examined in this context. The reaction of chiral diol 175 with either triallylborane or tri-β-methallylborane afforded the boronic esters 176 (R_1 = H, Me) in yields exceeding 95% (132a). The addition reactions of 176 to representative aldehydes are summarized in Table 40. In all cases reported, the sense of asymmetric induction from the chiral



auxiliary 175 favored enantiomeric alcohol 177 with only minor perturbations imposed on the levels of asymmetric induction by the substituent variables R_1 and R_2. The two relevant chairlike transition state structures, which correlate reactant and product stereochemistry



Scheme 27



(major product enantiomer), are illustrated in Scheme 28. Transition states T_1 and T_3 correlate with the aldol transition states T_1 and T_3 illustrated in Scheme 27. From the experimental observations it is not possible to unequivocally determine whether aldehyde complexation occurs from the *Re* or *Si* face of the boron. However, it might be speculated that 177 arises from *Si* face coordination via transition state T_1, based on the assumption that the phenyl group defines its adjacent oxygen ligand as the *larger* of the two oxygen substituents.

Erythro diastereoselection has also been examined in these addition reactions. The addition of the (*Z*)-2-butenylboronate ester 179 [>95% (*Z*)-isomer] to representative aldehydes (Me, C_2H_5, i-C_3H_7, Ph) was found to exhibit excellent erythro selection (eq. [117]) (132c), in direct analogy with the similar stereoselection observed with boryl enolates (6).

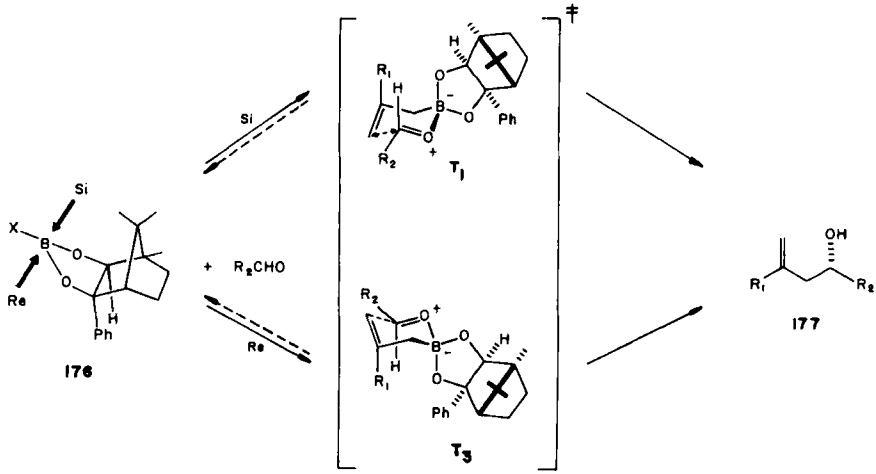
The condensations of chiral (*E*)- and (*Z*)-2-butenylboronate esters **180a** and **180b** with chiral aldehyde **181** have also been examined (132b). The reaction of (–)-**180a** with racemic aldehyde (±)-**181** afforded a 3:1 ratio of Cram and anti-Cram threo adducts **182C** and **182A**, respectively, (eq. [118]). In contrast, the analogous reaction with the (*Z*)-boronate (–)-**180b** afforded predominantly the anti-Cram erythro diastereomer **183A** (**183C**:**183A** = 30:70) as illustrated in eq. [119].

Table 40
Addition of Allylboronate Ester **176** to
Representative Aldehydes (eq. [116]) (132a)

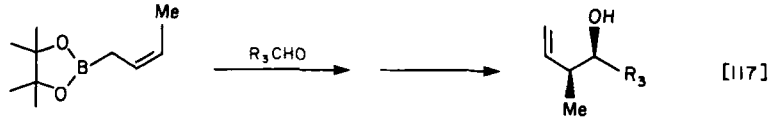
R_1	R_2[a]	Product Ratio **177:178**	Yield (%)
H	Me	82:18	92
H	C_2H_5	89:11	91
H	*n*-C_3H_7	86:14	93
H	*i*-C_3H_7	85:15	88
H	*t*-C_4H_9	73:27	85
Me	Me	87:13	82
Me	C_2H_5	85:15	85
Me	*n*-C_3H_7	82:18	84
Me	*i*-C_3H_7	88:12	87
Me	*t*-C_4H_9	85:15	92

[a]The addition reaction was carried out at -40°C (1 hr) followed by 12 hr at 25°C.

The observation that aldehyde diastereoface selection is interrelated with allylborane geometry has important implications for the related aldol processes. The reactions of (–)-**180a** and (–)-**180b** with both enantiomers of aldehyde **181** revealed both consonant and dissonant double stereodifferentiation. For the Cram-selective (*E*)-crotyl



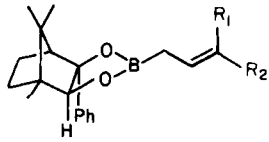
Scheme 28



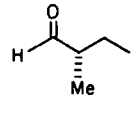
179 erythro:threo ≥ 94:6 [117]

boronic ester (–)-**180a**, consonant double stereodifferentiation was observed with (*S*)-**181** (**182C**:**182A** = 92:8). In an analogous fashion, enhanced double stereodifferentiation was also noted for the anti-Cram-selective (*E*)-crotyl boronic ester (–)-**180b** with (*R*)-**181** (**184C**:**184A** = 5:95, eq. [120]).

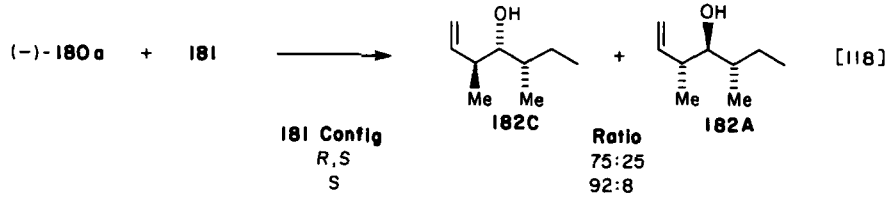
The correlation between allylboronic ester stereochemistry and aldehyde diastereoface selection stands in contrast to the behavior of stereochemically defined lithium enolates, which generally exhibit a preference for the Cram mode of addition to chiral aldehydes from *either* enolate geometry (cf. eqs. [72]–[77]). The stereochemical



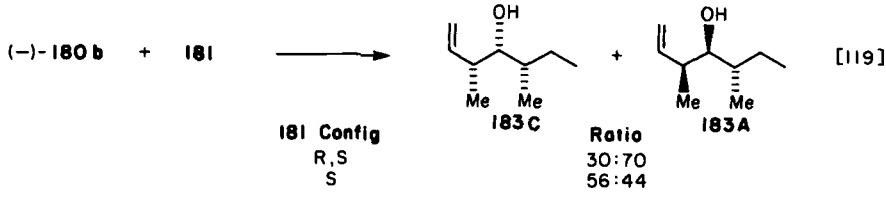
(–)-**180a**, R_1 = H, R_2 = Me
b, R_1 = Me, R_2 = H



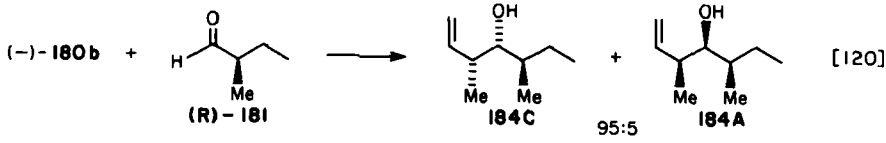
181



[118]



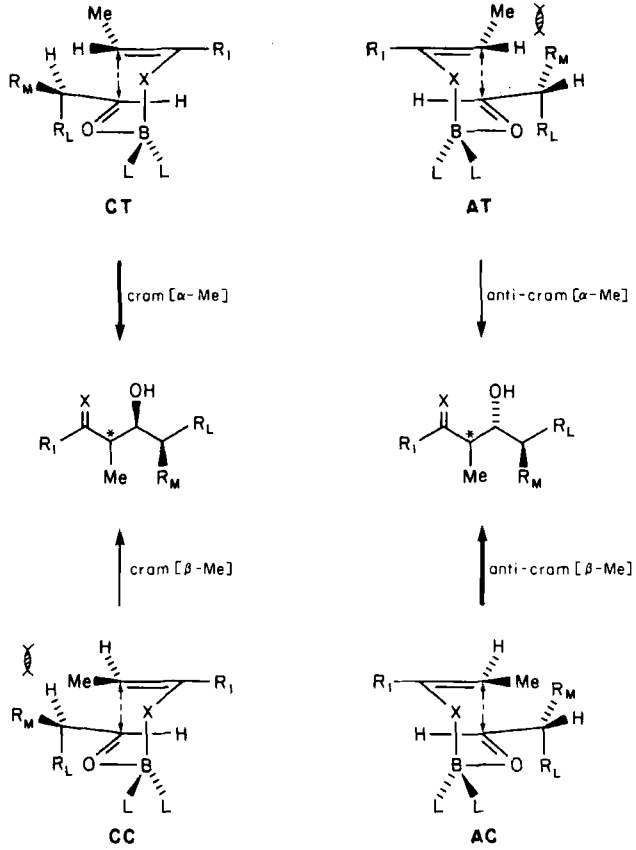
[119]



[120]

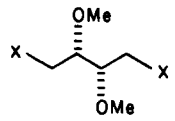
control elements that may be important are illustrated in Scheme 29. The important transition state steric parameter, Me ↔ R_M, appears to disfavor the anti-Cram mode for the trans-substituted crotylborane (e.g., transition state **AT**, X = CH_2). Related arguments appear to disfavor the Cram mode of addition for cis-substituted crotylborane as illustrated in transition **CC** (X = CH_2). Similar trends for the related boryl enolates have not yet been examined.

The use of chiral chelating agents in reactions of organometallic reagents with carbonyl compounds has been intensively investigated (134–138). However, the influence of such chiral addends in the aldol process has not met with much success. In the presence of the

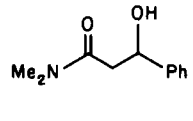


Scheme 29

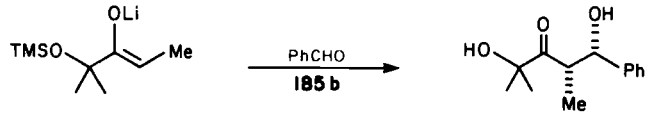
tartrate-derived chelating agent **185a**, the lithium enolate of dimethylacetamide afforded the benzaldehyde adduct **186** with only marginal asymmetric induction (15% e.e.) (135). Similar results were obtained in the condensation of enolate **100b** in the presence of chiral addent **185b** (110). The major erythro enantiomer **187** (7% e.e.) was shown



185 a, X=NMe_2
b, X=OMe



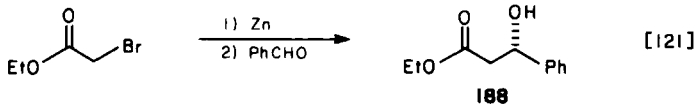
186
15% ee



100b

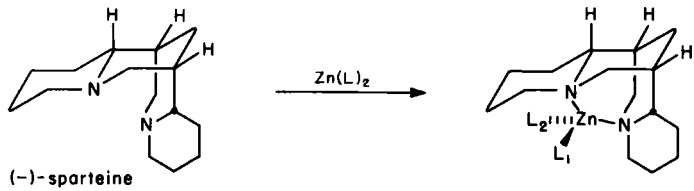
187
7% ee

to have the illustrated absolute configuration by degradation. Considerably higher levels of asymmetric induction have been obtained in the Reformatsky condensation where (-)-sparteine **189** has been used as the chiral chelating agent (eq. [121]) (136,137). The adduct **188** possessed the (*S*)-configuration in 95 ± 3% optical purity. The major detraction in these reactions appear to be the rather low chemical yields. Asymmetric induction in this reaction has been interpreted in terms of both *O*- and *C*-metalated enolate tautomeric



188

[121]



(-)-sparteine
189

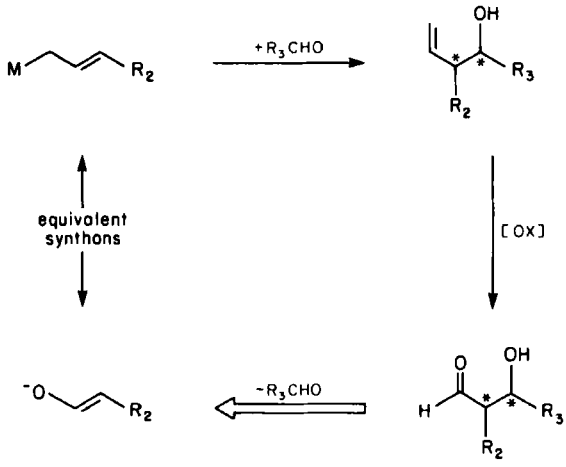
190

structures (137). Inspection of models indicates that the L_1 ligand position in the zinc chelate **190** is decidedly less sterically congested.

VII. CONCLUSIONS

The challenges associated with the regulation of stereochemistry during bond construction integrate all aspects of organic chemistry, and the development of highly stereoselective processes invariably results in significant benefits to the investigators of synthesis and mechanism. The progress that has been made in the area of the aldol problem has been truly impressive. It is clear from the preceding discussion that absolute stereochemical control in erythro selective aldol condensations has been achieved with levels of asymmetric induction unparalleled in any other bond construction to date. Given the current level of interest in this area, one can predict with certainty that equally impressive advances are on the horizon.

One parallel research area that is currently developing as a direct outgrowth of the aldol studies is illustrated in Scheme 30. Allylic



Scheme 30

organometallic reagents are well recognized as enolate synthons, and an examination of the stereoregulated carbonyl addition reactions has already begun to reveal a number of mechanistic parallels with the aldol process. The reader is referred to several significant new studies that address this stereochemical issue (132,138).

ACKNOWLEDGMENTS

We express our warm gratitude to Mrs. Dorothy Lloyd and Mrs. Heather Marr for their technical assistance. We also thank Prof. Clayton Heathcock for providing us with research results before publication. Partial support for this contribution was provided by the National Science Foundation (CHE-7950006) and the National Institutes of Health.

REFERENCES

1. (a) Nielsen, A. T.; Houlihan, W. J. *Org. React.* **1968**, *16*, 1–438. (b) Reiff, H. *Newer Methods, Prep. Org. Chem.* **1971**, *6*, 48–66. (c) Hajos, Z. G. In "Carbon-Carbon Bond Formation," Vol. 1; Augustine, R. L. Ed.; Dekker: New York, 1979; pp. 1–84. (d) Mukaiyama, T. *Org. React.* **1981**, in press.
2. Heathcock, C. H.; Buse, C. T.; Kleschick, W. A.; Pirrung, M. C.; Sohn, J. E.; Lampe, J. *J. Org. Chem.* **1980**, *45*, 1066–1081, and citations to earlier work.
3. Masamune, S.; Ali, S. A.; Snitman, D. L.; Garvey, D. S. *Angew. Chem.* **1980**, *92*, 573–575; *Angew. Chem. Int. Ed. Engl.* **1980**, *19*, 557–558.
4. Murata, S.; Suzuki, M.; Noyori, R. *J. Am. Chem. Soc.* **1980**, *102*, 3248–3249, and references cited therein.
5. (a) Dubois, J. E.; Fort, J. F. *Tetrahedron* **1972**, *28*, 1653–1663, 1665–1675, and references cited therein. (b) Dubois, J. E.; Fellmann, P. *C. R. Acad. Sci.* **1972**, *274*, 1307–1309. (c) Dubois, J. E.; Fellmann, P. *Tetrahedron Lett.* **1975**, 1225–1228. (d) Fellmann, P.; Dubois, J. E. *Tetrahedron* **1978**, *34*, 1349–1357.
6. (a) Evans, D. A.; Nelson, J. V.; Vogel, E.; Taber, T. R. *J. Am. Chem. Soc.* **1981**, *103*, 3099–3111. (b) Evans, D. A.; Vogel, E.; Nelson, J. V. *ibid.* **1979**, *101*, 6120–6123.
7. Gaudemer, A., "Determination of Configurations by Spectrometric Methods." In "Stereochemistry, Fundamentals and Methods," Kagan, H. B., Ed.; Thieme: Stuttgart, 1977; Vol. I, pp. 69–71.
8. (a) Canceill, J.; Basselier, J. J.; Jacques, J. *Bull. Soc. Chim. Fr.* **1967**, 1024–1030. (b) Canceill, J.; Jacques, J. *ibid.* **1970**, 2180–2187.
9. (a) Auerback, R. A.; Kingsbury, C. A. *Tetrahedron* **1971**, *27*, 2069–2077.
10. Stiles, M.; Winkler, R. R.; Chang, Y.-l.; Traynor, L. *J. Am. Chem. Soc.* **1964**, *86*, 3337–3342.
11. Smith, R. A. J.; Heng, K. *Tetrahedron* **1979**, *34*, 425–435. These authors originally assigned the diastereomers incorrectly. Later work has corrected this error; see ref. 2. See also ref. 12 for related studies.
12. Jeffery, E. A.; Meisters, A.; Mole, T. *J. Organomet. Chem.* **1974**, *74*, 365–372, 373–384.
13. Heathcock, C. H.; Pirrung, M. C.; Sohn, J. E. *J. Org. Chem.* **1979**, *44*, 4294–4299.

14. House, H. O.; Crumrine, D. S.; Teranishi, A. Y.; Olmstead, H. D. *J. Am. Chem. Soc.* **1973**, *95*, 3310-3324, and references cited therein.
15. Sacks, C. E. Ph.D. Thesis, California Institute of Technology, Pasadena, 1980.
16. Mulzer, J.; Segner, J.; Brüntrup, G. *Tetrahedron Lett.* **1977**, 4651-4654.
17. Mulzer, J.; Brüntrup, G.; Finke, J.; Zippel, M. *J. Am. Chem. Soc.* **1979**, *101*, 7723-7725.
18. Mladenova, M.; Blagoev, B.; Kurtev, B. *Bull. Soc. Chim. Fr.* **1974**, 1464-1468.
19. (a) Fráter, G. *Helv. Chim. Acta* **1979**, *62*, 2828-2828, 2829-2832. (b) Seebach, D.; Wasmuth, D. *ibid.* **1980**, *63*, 197-200. (c) Kraus, G. A.; Taschner, M. J. *Tetrahedron Lett.* **1977**, 4575-4578.
20. (a) For a recent review see: Rathke, M. W. *Org. React.* **1975**, *22*, 423-460. (b) Gaudemar, M. *Organomet. Chem. Rev. A* **1972**, *8*, 183-233. (c) Shriner, R. L. *Org. React.* **1942**, *1*, 1-37.
21. (a) Maruoka, K.; Hashimoto, S.; Kitagawa, Y.; Yamamoto, H.; Nazaki, H. *J. Am. Chem. Soc.* **1977**, *99*, 7705-7707. (b) Nozaki, H.; Oshima, K.; Takai, K.; Ozawa, S. *Chem. Lett.* **1979**, 379-380.
22. Zimmerman, H. E.; Traxler, M. D. *J. Am. Chem. Soc.* **1957**, *79*, 1920-1923.
23. See Table 4, entry D, for the analogous thermodynamically controlled aldol condensation.
24. Jackman, L. M.; Lange, B. C. *Tetrahedron* **1977**, *33*, 2737-2769.
25. Evans, D. A., unpublished observations.
26. Buse, C. T.; Heathcock, C. H. *J. Am. Chem. Soc.* **1977**, *99*, 8109-8110.
27. Dubois, J. E.; Dubois, M. *Tetrahedron Lett.* **1967**, 4215-4219.
28. Dubois, J. E.; Dubois, M. *Bull. Soc. Chim. Fr.* **1969**, 3553-3561.
29. (a) Johnston, D. B. R.; Schmitt, S. M.; Bouffard, F. A.; Christensen, B. G. *J. Am. Chem. Soc.* **1978**, *100*, 313-315. (b) Bouffard, F. A.; Johnston, D. B. R.; Christensen, B. G. *J. Org. Chem.* **1980**, *45*, 1130-1135. (c) Salzmann, T. N.; Ratcliffe, R. W.; Christensen, B. G.; Bouffard, F. A. *J. Am. Chem. Soc.* **1980**, *102*, 6161-6163.
30. Pfaendler, H. R.; Gosteli, J.; Woodward, R. B. *J. Am. Chem. Soc.* **1980**, *102*, 2039-2043.
31. (a) DiNinno, F.; Beattie, T. R.; Christensen, B. G. *J. Org. Chem.* **1977**, *42*, 2960-2965. (b) Aimetti, J. A.; Kellogg, M. S. *Tetrahedron Lett.* **1979**, 3805-3808.
32. Meyers, A. I.; Reider, P. J. *J. Am. Chem. Soc.* **1979**, *101*, 2501-2502.
33. Pirrung, M. C.; Heathcock, C. H. *J. Org. Chem.* **1980**, *45*, 1727-1728.
34. Ireland, R. E.; Mueller, R. H.; Willard, A. K. *J. Am. Chem. Soc.* **1976**, *98*, 2868-2877.
35. Evans, D. A.; McGee, L. R. *Tetrahedron Lett.* **1980**, 3975-3978.
36. (a) Evans, D. A.; Takacs, J. M. *Tetrahedron Lett.* **1980**, 4233-4236. (b) Takacs, J. M. Ph.D. Thesis, California Institute of Technology, Pasadena, 1981.
37. (a) For a general review see: Johnson, F. *Chem. Rev.* **1968**, *68*, 375-413. (b) Chow, Y. L.; Colón, C. J.; Tam, J. N. S. *Can. J. Chem.* **1968**, *46*,

2821–2825. (c) Paulsen, H.; Todt, K. *Angew. Chem.* **1966**, *78*, 943–944; *Angew. Chem. Int. Ed. Engl.* **1966**, *5*, 899–890. (d) Quick, J.; Mondello, C.; Humora, M.; Brenan, T. *J. Org. Chem.* **1978**, *43*, 2705–2708.

38. Tamaru, Y.; Harada, T.; Nishi, S.; Mitsutani, M.; Hioki, T.; Yoshida, Z. *J. Am. Chem. Soc.* **1980**, *102*, 7806–7808.
39. Fataftah, Z. A.; Kopka, I. E.; Rathke, M. W. *J. Am. Chem. Soc.* **1980**, *102*, 3959–3960.
40. Nakamura, E.; Hashimoto, K.; Kuwajima, I. *Tetrahedron Lett.* **1978**, 2079–2082.
41. Curé, J.; Gaudemar, M. *Bull. Soc. Chim. Fr.* **1973**, 2418–2421.
42. von Schriltz, D. M.; Kaiser, E. M.; Hauser, C. R. *J. Org. Chem.* **1967**, *32*, 2610–2615.
43. Ireland, R. E.; Anderson, R. C., unpublished results.
44. Garst, M. E.; Bonfiglio, J. N.; Grudoski, D. A.; Marks, J. *J. Org. Chem.* **1980**, *45*, 2307–2315. In the cases cited the primary enolization path was via methyl deprotonation.
45. Touzin, A. M. *Tetrahedron Lett.* **1975**, 1477–1480.
46. Shanzer, A.; Somekh, L.; Butina, D. *J. Org. Chem.* **1979**, *44*, 3967–3969.
47. Ruehlmann, K.; Kaufmann, K. D.; Ickert, K. *Z. Chem.* **1970**, *10*, 393–394.
48. Marchand, J.; Pais, M.; Jarreau, F.-X. *Bull. Soc. Chim. Fr.* **1971**, 3742–3746.
49. Sutton, L. E., Ed. "Tables of Interatomic Distances and Configuration in Molecules and Ions"; The Chemical Society: London, 1958. Sutton, L. E., Ed. "Supplement 1956–1959"; The Chemical Society: London, 1965. Kennard O.; Watson, D. G.; Allen, F. H.; Isaacs, N. W.; Motherwell, W. D. S.; Pettersen, R. C.; Town, W. G., Eds. "Molecular Structures and Dimensions"; A. Oosthoek: Utrecht, 1972; Vol. A1, "Interatomic Distances 1960–1965, Organic and Organometallic Crystal Structures."
50. Hooz, J.; Linke, S. *J. Am. Chem. Soc.* **1968**, *90*, 5936–5937. Hooz, J.; Linke, S. *ibid.* **1968**, *90*, 6891–6892. Hooz, J.; Morrison, G. F. *Can. J. Chem.* **1970**, *48*, 868–870.
51. (a) Mukaiyama, T.; Inomata, K.; Muraki, M. *J. Am. Chem. Soc.* **1973**, *95*, 967–968. (b) Daniewski, A. R. *J. Org. Chem.* **1975**, *40*, 3135–3136.
52. Brown, H. C.; Rogic, M. M.; Rathke, M. W.; Kabalka, G. W. *J. Am. Chem. Soc.* **1968**, *90*, 818–820. Brown, H. C.; Rogic, M. M.; Rathke, M. W. *ibid.* **1968**, *90*, 6218–6219.
53. Tufariello, J. J.; Lee, L. T. C.; Wojtkowski, P. *J. Am. Chem. Soc.* **1967**, *89*, 6804–6805.
54. Masamune, S.; Mori, S.; Van Horn, D.; Brooks, D. W. *Tetrahedron Lett.* **1979**, 1665–1668.
55. Pasto, D. J.; Wojtkowski, P. W. *Tetrahedron Lett.* **1970**, 215–218.
56. Suzuki, A.; Arase, A.; Matsumoto, H.; Itoh, M.; Brown, H. C.; Rogic, M. M.; Rathke, M. W. *J. Am. Chem. Soc.* **1967**, *89*, 5708–5709.
57. Fenzl, W.; Köster, R.; Zimmerman, H.-J. *Justus Liebigs Ann. Chem.* **1975**, 2201–2210.
58. Hirama, M.; Masamune, S. *Tetrahedron Lett.* **1979**, 2225–2228.
59. Inomata, K.; Muraki, M.; Mukaiyama, T. *Bull. Chem. Soc. Jpn.* **1973**, *46*, 1807–1810.

60. (a) Paetzold, P.; Biermann, H. *Chem. Ber.* **1977**, *110*, 3678-3688. (b) Paetzold, P.; Kosma, S. *ibid.* **1979**, *112*, 654-662. (c) Paetzold, P.; Lasch, M. *ibid.* **1979**, *112*, 663-667.

61. (a) Fenzl, W.; Köster, R. *Justus Liebigs Ann. Chem.* **1975**, 1322-1338. (b) Fenzl, W.; Kosfeld, H.; Köster, R. *ibid.* **1976**, 1370-1379.

62. For studies relating to the protonolysis of organoboranes see: (a) Toporcer, L. H.; Dessey, R. E.; Green, S. I. E. *J. Am. Chem. Soc.* **1965**, *87*, 1236-1240. (b) Trofimenko, S. *ibid.* **1969**, *91*, 2139-2140.

63. (a) Mukaiyama, T.; Inoue, T. *Chem. Lett.* **1976**, 559-562. (b) Inoue, T.; Uchimaru, T.; Mukaiyama, T. *ibid.* **1977**, 153-154. (c) Inoue, T.; Mukaiyama, T. *Bull. Chem. Soc. Jpn.* **1980**, *53*, 174-178.

64. Hirama, M.; Garvey, D. S.; Lu, L. D.-L.; Masamune, S. *Tetrahedron Lett.* **1979**, 3937-3940.

65. Van Horn, D. E.; Masamune, S. *Tetrahedron Lett.* **1979**, 2229-2232.

66. Evans, D. A.; Cherpeck, R. E.; Tanis, S., unpublished results.

66a. Kuwajima, I.; Kato, M.; Mori, A. *Tetrahedron Lett.* **1980**, 4291-4294. See also Wada, M. *Chem. Lett.* **1981**, 153-156.

67. Yamamoto, Y.; Maruyama, K. *Tetrahedron Lett.* **1980**, 4607-4610.

68. Schwartz, J.; Loots, M. J.; Kosugi, H. *J. Am. Chem. Soc.* **1980**, *102*, 1333-1340, and earlier cited references.

69. Evans, D. A.; McGee, L. R., unpublished results.

70. Lauher, J. W.; Hoffmann, R. *J. Am. Chem. Soc.* **1976**, *98*, 1729-1742.

71. Prout, K.; Cameron, T. S.; Forder, R. A.; Critchley, S. R.; Denton, B.; Rees, G. V. *Acta Crystallogr., Sect. B* **1974**, *30*, 2290-2304.

72. Fachinetti, G.; Floriani, C.; Marchetti, F.; Merlino, S. *J. Chem. Soc., Chem. Commun.* **1976**, 522-523.

73. (a) Mukaiyama, T.; Banno, K.; Narasaka, K. *J. Am. Chem. Soc.* **1974**, *96*, 7503-7509. (b) Chan, T. H.; Aida, T.; Lau, P. W. K.; Gorys, V.; Harpp, D. N. *Tetrahedron Lett.* **1979**, 4029-4032.

74. Noyori, R.; Yokoyama, K.; Sakata, J.; Kuwajima, I.; Nakamura, E.; Shimizu, M. *J. Am. Chem. Soc.* **1977**, *99*, 1265-1267.

75. Gilman, H.; Speeter, M. *J. Am. Chem. Soc.* **1943**, *65*, 2255-2256.

76. (a) Luche, J. L.; Kagan, H. B. *Bull. Soc. Chim. Fr.* **1969**, 3500-3505. (b) Kagan, H. B.; Basselier, J. J.; Luche, J. L. *Tetrahedron Lett.* **1964**, 941-948. (c) Luche, J. L.; Kagan, H. B. *Bull Soc. Chim. Fr.* **1971**, 2260-2261.

77. (a) Dardoize, F.; Moreau, J. L; Gaudemar, M. *C. R. Acad. Sci. Ser. C* **1970**, *270*, 233-236. (b) Dardoize, F.; Moreau, J. L; Gaudemar, M. *Bull. Soc. Chim. Fr.* **1973**, 1668-1672.

78. (a) Dardoize, F.; Gaudemar, M. *Bull. Soc. Chim. Fr.* **1976**, 1561-1566. (b) Dardoize, F.; Gaudemar, M. *ibid.* **1974**, 939-942.

79. Gluchowski, C.; Cooper, L.; Bergbreiter, D. E.; Newcomb, M. *J. Org. Chem.* **1980**, *45*, 3413-3416.

80. Ojima, I.; Inaba, S.; Yoshida, K. *Tetrahedron Lett.* **1977**, 3643-3646.

81. Ojima, I.; Inaba, S. *Tetrahedron Lett.* **1980**, 2077-2080.

82. Ojima, I.; Inaba, S. *Tetrahedron Lett.* **1980**, 2081-2084.

83. (a) Izumi, Y.; Tai, A. "Stereodifferentiating Reactions"; Kodanshar Ltd.: Tokyo; Academic Press: New York, 1977. (b) Hanson, K. R. *J. Am. Chem. Soc.* **1966**, *88*, 2731–2742.
84. (a) Cram, D. J.; Abd Elhafez, F. A. *J. Am. Chem. Soc.* **1952**, *74*, 5828–5835. (b) Cram, D. J.; Kopecky, K. R. *ibid.* **1959**, *81*, 2748–2755.
85. Cram, D. J.; Wilson, D. R. *J. Am. Chem. Soc.* **1963**, *85*, 1245–1249.
86. Cornforth, J. W.; Cornforth, R. H.; Mathew, K. K. *J. Chem. Soc.* **1959**, 112–127.
87. Karabatsos, G. J. *J. Am. Chem. Soc.* **1967**, *89*, 1367–1371.
88. Chérest, M.; Felkin, H.; Prudent, N. *Tetrahedron Lett.* 1968, 2199–2204.
89. Anh, N. T.; Eisenstein, O. *Nouv. J. Chim.* **1977**, *1*, 61–70.
90. Bürgi, H. B.; Lehn, J. M.; Wipff, G. *J. Am. Chem. Soc.* **1974**, *96*, 1956–1957. Bürgi, H. B.; Dunitz, J. D.; Lehn, J. M.; Wipff, G. *Tetrahedron* **1974**, *30*, 1563–1572.
91. Matsumoto, T.; Hosoda, Y.; Mori, K.; Fukui, K. *Bull. Chem. Soc. Jpn.* **1972**, *45*, 3156–3160.
92. Masamune, S. *Aldrichim Acta* **1978**, *11*, 23–32.
93. Heathcock, C. H.; Young, S. D.; Hagen, J. P.; Pirrung, M. C.; White, C. T.; van Derveer, D. *J. Org. Chem.* **1980**, *45*, 3846–3856.
94. Evans, D. A.; Crimmins, M. T., unpublished results.
95. (a) Evans, D. A.; Sacks, C. E.; Kleschick, W. A.; Taber, T. R. *J. Am. Chem. Soc.* **1979**, *101*, 6789–6791. (b) Taber, T. R. Ph.D. Thesis, California Institute of Technology, Pasadena, 1981.
96. Meyers, A. I.; Comins, D. L.; Roland, D. M.; Henning, R.; Shimizu, K. *J. Am. Chem. Soc.* **1979**, *101*, 7104–7105.
97. (a) Fukuyama, T.; Akasaka, K.; Karanewsky, D. S.; Wang, C.-L. J.; Schmid, G.; Kishi, Y. *J. Am. Chem. Soc.* **1979**, *101*, 262–263 and references cited therein. (b) Collum, D. B.; McDonald, III, J. H.; Still, W. C. *J. Am. Chem. Soc.* **1980**, *102*, 2120–2121, and references cited therein.
98. Morrison, J. D.; Mosher, H. S. "Asymmetric Organic Reactions"; Prentice-Hall: Englewood Cliffs, NJ, 1971; pp. 84–133.
99. (a) Still, W. C.; McDonald, III, J. H.; *Tetrahedron Lett.* **1980**, 1031–1034. (b) Still, W. C.; Schneider, J. A. *ibid.* **1980**, 1035–1038.
100. Izawa, T.; Mukaiyama, T. *Chem. Lett.* **1978**, 409–412.
101. Collum, D. B.; McDonald, III, J. H.; Still, W. C. *J. Am. Chem. Soc.* **1980**, *102*, 2118–2120.
102. Scott, J. W.; Valentine, Jr., D. *Science* **1974**, *184*, 943–952.
103. Cohen, N. *Acc. Chem. Res.* **1976**, *9*, 412–417.
104. Kagan, H. B.; Fiaud, J. C. *Top. Stereochem.* **1978**, *10*, 175–285.
105. Valentine, Jr., D.; Scott, J. W. *Synthesis* **1978**, 329–356.
106. Meyers, A. I. *Pure Appl. Chem.* **1979**, *51*, 1255–1268.
107. ApSimon, J. W.; Seguin, R. P. *Tetrahedron* **1979**, *35*, 2797–2842.
108. For an excellent general review of stereochemical control in acyclic systems see: Bartlett, P. A. *Tetrahedron* **1980**, *36*, 3–72.
109. Heathcock, C. H.; White, C. T. *J. Am. Chem. Soc.* **1979**, *101*, 7076–7077.

110. (a) Nakata, T.; Schmid, G.; Vranesic, B.; Okigawa, M. Smith-Palmer, T.; Kishi, Y. *J. Am. Chem. Soc.* **1978**, *100*, 2933-2935. (b) Ireland, R. E.; Thaisrivongs, S.; Wilcox, C. S. *ibid.* **1980**, *102*, 1155-1157. (c) Ireland, R. E.; McGarvey, G. J.; Anderson, R. C.; Badoud, R.; Fitzsimmons, B.; Thaisrivongs, S. *ibid.* **1980**, *102*, 6178-6180. (d) Ireland, R. E.; Badoud, R., unpublished observations.

111. (a) See ref. 98, pp. 142-150. (b) For more recent examples see: Dongala, E. B.; Dull, D. L.; Mioskowski, C.; Solladie, G. *Tetrahedron Lett.* **1973**, 4983-4986.

112. Heathcock, C. H.; White, C. T.; Morrison, J. J.; van Derveer, D. *J. Org. Chem.* **1981**, *46*, 1296-1309.

113. Seebach, D.; Ehrig, V.; Teschner M. *Justus Liebigs Ann. Chim.* **1976**, 1357-1369.

114. Evans, D. A.; Taber, T. R. *Tetrahedron Lett.* **1980**, 4675-4678.

115. (a) Masamune, S.; Choy, W.; Kerdesky, A. J. Imperiali, B. *J. Am. Chem. Soc.* **1981**, *103*, 1566-1568. (b) Masamune, S.; Hirama, M.; Mori, S.; Ali, S. A.; Garvey, D. S. *ibid.* **1981**, *103*, 1568-1571.

116. Heathcock, C. H.; Pirrung, M. C.; Buse, C. T.; Hagen, J. P.; Young, S. D.; Sohn, J. E. *J. Am. Chem. Soc.* **1979**, *101*, 7077-7079.

117. Evans D. A.; Bartroli, J.; Shih, T. L. *J. Am. Chem. Soc.* **1981**, *103*, 2127-2129.

118. Noe, E. A.; Raban, M. *J. Am. Chem. Soc.* **1975**, *97*, 5811-5820.

119. Evans, D. A.; McGee, L. R. *J. Am. Chem. Soc.* **1981**, *103*, 2876-2878.

120. (a) Meyers, A. I.; Mihelich, E. D. *Angew. Chem.* **1976**, *88*, 321-332; *Angew. Chem. Int. Ed. Engl.* **1976**, *15*, 270-281. (b) Meyers, A. I.; Snyder, E. S.; Ackerman, J. J. H. *J. Am. Chem. Soc.* **1978**, *100*, 8186-8189, and references therein.

121. Meyers, A. I.; Knaus, G. *Tetrahedron Lett.* **1974**, 1333-1336.

122. (a) Mioskowski, C.; Solladie, G. *Tetrahedron* **1980**, *36*, 227-236. (b) Mioskowski, C.; Solladie, G. *J. Chem. Soc., Chem. Commun.* **1977**, 162-163.

123. Evans, D. A.; Shih, T. L., unpublished results.

124. Corey, E. J.; Weigel, L. O.; Chamberlin, A. R.; Cho, H.; Hua, D. H. *J. Am. Chem. Soc.* **1980**, *102*, 6613-6615.

125. Abushanab, E.; Reed, D.; Suzuki, F.; Sih, C. J. *Tetrahedron Lett.* **1978**, 3415-3418.

126. (a) Meyers, A. I.; Williams, D. R.; Druelinger, M. *J. Am. Chem. Soc.* **1976**, *98*, 3032-3033. (b) Whitesell, J. K.; Whitesell, M. A. *J. Org. Chem.* **1977**, *42*, 377-378. (c) Worster, P. M.; McArthur, C. R.; Leznoff, C. C. *Angew. Chem.* **1979**, *91*, 225; *Angew. Chem. Int. Ed. Engl.* **1979**, *18*, 221-222. (d) Meyers, A. I.; Williams, D. R. *J. Org. Chem.* **1978**, *43*, 3245-3247. (e) Meyers, A. I.; Poindexter, G. S.; Brich, Z. *ibid.* **1978**, *43*, 892-898.

127. (a) Hashimoto, S. I.; Koga, K. *Chem. Pharm. Bull.* **1979**, *27*, 2760-2766. (b) Hashimoto, S. I.; Koga, K. *Tetrahedron Lett.* **1978**, 573-576.

128. (a) Enders, D.; Eichenauer, H. *Angew. Chem.* **1979**, *91*, 425-426; *Angew. Chem. Int. Ed. Engl.* **1979**, *18*, 397-399. (b) Enders, D.; Eichenauer, H. *Angew. Chem.* **1976**, *88*, 579-581; *Angew. Chem. Int. Ed. Engl.* **1976**,

15, 549-551. (c) Enders, D.; Eichenauer, H. *Chem. Ber.* **1979**, *112*, 2933-2960. (d) Enders, D.; Eichenauer, H. *Tetrahedron Lett.* **1977**, 191-194. (e) Davenport, K. G.; Eichenauer, H.; Enders, D.; Newcomb, M.; Bergbreiter, D. E. *J. Am. Chem. Soc.* **1979**, *101*, 5654-5659.

129. (a) Fraser, R. R.; Banville, J.; Dhawan, K. L. *J. Am. Chem. Soc.* **1978**, *100*, 7999-8001. (b) Fraser, R. R.; Banville, J. *J. Chem. Soc., Chem. Commun.* **1979**, 47-48. (c) Fraser, R. R.; Akiyama, F.; Banville, J. *Tetrahedron Lett.* **1979**, 3929-3932.

130. Eichenauer, H.; Friedrich, E.; Lutz, W.; Enders, D. *Angew. Chem.* **1978**, *90*, 219-220; *Angew. Chem. Int. Ed. Engl.* **1978**, *17*, 206-208.

131. For relevant literature on these reactions see: (a) Mikhailov, B. M. *Organomet. Chem. Rev., Sect. A* **1972**, *8*, 1-65. (b) Kramer, G. W.; Brown, H. C. *J. Org. Chem.* **1977**, *42*, 2292-2299.

132. (a) Herold, T.; Hoffmann, R. W. *Angew Chem.* **1978**, *90*, 822-823; *Angew. Chem. Int. Ed. Engl.* **1978**, *17*, 768-769. (b) Hoffmann, R. W.; Zeiss, H. J. *Angew. Chem.* **1980**, *92*, 218-223; *Angew. Chem. Int. Ed. Engl.* **1980**, *19*, 218-219. (c) Hoffmann, R. W.; Zeiss, H. J. *Angew. Chem.*, **1979**, *91*, 329; *Angew. Chem. Int. Ed. Engl.*, **1979**, *18*, 306-307.

133. For a general review see ref. 96, Chapter 10.

134. Seebach, D.; Kalinowski, H. O.; Bastani, B.; Crass, G.; Daum, H.; Dörr, H.; DuPreez, N. P.; Ehrig, V.; Langer, W.; Nüssler, C.; Oei, H. A.; Schmidt, M. *Helv. Chim. Acta* **1977**, *60*, 301-325, and references cited therein.

135. Seebach, D. "Schriftenreike des Fonds der chemische Industrie"; 1975, S. B.

136 Guetté, M.; Guetté, J.-P; Capillon, J. *Tetrahedron Lett.* **1971**, 2863-2866.

137. Guetté, M.; Capillon, J.; Guetté, J.-P. *Tetrahedron* **1973**, *29*, 3659-3667.

138. (a) Hiyama, T.; Kimura, K.; Nozaki, H. *Tetrahedron Lett.* **1981**, 1037-1040. (b) Sato, F.; Iijima, Sato, M. *ibid.* **1981**, 243-246. (c) Yamamoto, Y.; Yatagai, H.; Naruta, Y.; Marugama, K. *J. Am. Chem. Soc.* **1980**, *102*, 7109-7110, and references cited therein. (d) Yamamoto, Y.; Yatagai, H.; Marugama, K. *J. Chem. Soc., Chem. Commun.* **1980**, 1072-1073.

Application of Molecular Mechanics Calculations to Organic Chemistry*

EIJI ŌSAWA

Department of Chemistry, Faculty of Science, Hokkaido University, Sapporo, Japan

HANS MUSSO

Institut für Organische Chemie, Universität Karlsruhe, Karlsruhe, Federal Republic of Germany

I. Introduction 118
II. Scope and Limitations of Molecular Mechanics 120
III. Current Force Field Models 121
IV. Conformational Analysis 125
A. Simple Acyclic Alkanes 125
B. Overcrowded Methanes and Ethanes. 126
C. Monocyclic Alkanes and Alkenes 129
D. Polycyclic Hydrocarbons 131
1. Bicyclo[3.1.1]heptane 131
2. Bicyclo[2.2.1]heptane 132
3. Bicyclo[4.2.0]octane 132
4. Bicyclo[3.3.1]nonane 133
5. Bicyclo[4.4.0]decane. 134
6. Bicyclo[4.4.1]undecane 135
7. Bicyclo[3.3.3]undecane 135
8. Tetrahedrane 135
9. Perhydrotriptycene 136
E. Olefins 137
F. Aromatic Molecules 138
G. Heteroatom Systems 146
1. Ethers and Alcohols. 147
2. Carbonyl Compounds and Carbonium Ions. 148
3. Nitrogen-Containing Molecules. 150
4. Silanes. 150
5. Halides 151
6. Sulfur-Containing Molecules 151
7. Phosphorus-Containing Molecules. 152

*Part 13 of a series, "Application of Potential Energy Calculations to Organic Chemistry," from Hokkaido (1).

H. Metal Chelates 153
I. Natural Products and Molecules of Biological Interest 153
J. Heats of Formation 158
V. Reaction Mechanisms 158
A. Simulated Transition States 159
1. Hydrolysis and Esterification 159
2. Nucleophilic Substitutions 161
3. Nucleophilic Additions 161
4. Carbonium Ion Reactions 163
5. Product-like Transition States 164
6. Reactant-like Transition States 164
B. Conformational Control 166
C. Thermolysis of the Carbon-Carbon Bond 168
D. Product Distribution 168
VI. Special Applications 170
A. Separation of Electronic and Steric Effects 170
B. Bredt's Rule 171
C. Analysis of NMR Spectra 171
D. Molecular Modeling and Drug Design 173
E. Crystals 174
VII. Calculations of Unknown Molecules 175
VIII. Perspectives and Conclusions 177
Acknowledgements 178
References 179

I. INTRODUCTION

The majority of experimental chemists are looking for theoretical calculations to interpret their results, to guide their future plans, or even to gain information that cannot be obtained by any existing experimental approaches. Computational chemistry has now reached a state where it can usually respond to the needs of experimentalists and give them more or less useful information. With ready access to fast computers and to well-tested programs,* more and more people do calculations by themselves rather than consulting theoreticians (2).

In principle there are three methods of calculation: the *ab initio* molecular orbital (MO) method, the semiempirical MO method, and molecular mechanics. The choice depends on a number of factors such as the size of the molecule, the type of information required, and the budget. Whereas the *ab initio* method is the most basic and reliable quantum mechanical method,† the time requirement is so

*The major source for programs is: Quantum Chemistry Program Exchange (QCPE), Department of Chemistry, Indiana University, Bloomington, IN 47405.

†The program package GAUSSIAN is one of the best known (3). The latest version is GAUSSIAN 80 (4).

large, especially when full geometry optimization is included, that molecules containing more than 10 heavy (nonhydrogen) atoms are practically impossible to handle at present, and more than five or six heavy atoms usually require a small basis set, and reduced accuracy. Semiempirical MO calculations can be used for larger molecules. For example, two of the most respected semi-empirical methods, PRDDO (5) and MNDO (6) are claimed to perform roughly 16 and 100 times faster, respectively, than the *ab initio* method with a minimal basis set (STO-3G). Nevertheless, semiempirical MO calculations are still too slow to handle many molecules of interest to experimentalists, in addition to limitations due to approximations introduced (6-8).

On the other hand, the molecular mechanics method is purely empirical and pragmatic. The principle was conceived by experimentalists (9), and the technique has been perfected (10). The molecules are represented as though constructed from balls and springs with a series of potential energy functions to express the molecular force field as a sum of these functions. The parameters of the potential energy functions are so adjusted that the final set reproduces the desired properties of molecules, (e.g., molecular geometry, heat of formation, strain energy, dipole moment, or vibrational frequencies). Parameterization is usually carried out against a set of observed values of these properties. Since the molecular mechanics concept assumes the transferability of parameters among molecules of different types, the number of experimental data available for calibration is generally much larger than the number of parameters to be optimmized. Therefore, the accuracy can, in principle, be as high as that of the experimental values on which the optimization is based.

This computation involves of course all possible atom-atom interaction pairs—a relatively small population compared to the vast number of interorbital integrals that must be computed during MO calculations. As a consequence of these features, the molecular mechanics calculations far exceed in accuracy and speed the two other methods mentioned above.

For many purposes and for medium to large molecules, molecular mechanics is clearly the method of choice. Actually, the molecular mechanics programs are current "best-sellers" of QCPE, and a surprisingly larger number of applications have been published in every field of chemistry, especially in stereochemistry.

In view of the expected increase in interest in this useful technique, we present here a practical guide to the literature for potential as well as for current users. First, the scope and limitation of the principles are discussed, then available programs and past applications to organic chemistry are critically reviewed.

The molecular mechanics technique has been called by many different names, including Westheimer method, strain-energy method, conformational energy calculations, empirical potential energy calculations, atom-atom pair potential method, and force field calculations.* "Empirical force field" is widely used, but somewhat long, and many authors omit "empirical," leading to confusion with spectroscopic force field calculations. "Molecular mechanics" (11) now appears to be favored (10a) and is used (abbreviated as MM) throughout this chapter.

The subject was reviewed several times from various standpoints in the mid-1970s (10,11). This chapter covers the period after these reviews up to the first quarter of 1980.

Calculations of the MM type have long been popular in the fields of polymers (12) and biochemistry (proteins) (13), where the huge size of the molecules demands drastic simplification of potential energy functions. These applications are not discussed here.

II. SCOPE AND LIMITATIONS OF MOLECULAR MECHANICS

Let us first discuss some limitations inherent in the MM concept. No current molecular force field is yet complete. The present expression in terms of Hook's law for bond stretching or contraction and valence angle deformation, and a high-order exponential function of internuclear distance for nonbonded repulsion, might be almost adequate for describing the internuclear forces in a molecule, but not for the still enigmatic behavior of electrons in molecular orbitals. Torsional and nonbonded attractive terms have been added to make up for the electronic effects on the molecular properties such as structures and energy. The problem is that these corrections are not enough. Whenever some peculiar aspects originally arising from molecular orbital properties are to be subjected to the MM method, a new device must be added to the existing force field forms. The anomeric effect, hydrogen bonding, half-broken bonds in the transition state of an S_N2 reaction, and internal rotation are cases that demanded more or less special treatments (see below). In other

*Some authors use the terms "valence force field" and "Urey-Bradley force field" in the sense of molecular mechanics. The former refers to the force field taking no explicit account of 1,3-interactions, which are inlcuded in the latter.

words, the MM method cannot deductively solve unsolved problems; rather, it treats problems inductively by interpolation.

An important, implicit assumption is that the potential energy function holds only if the nuclear displacement from a position of equilibrium is not too large. Hence, highly strained molecules are not the best targets. Whereas the MM calculations give the steric energy distribution within a molecule, which no other computational method can provide, one must be aware that this distribution is correct for the *model* of the molecule, not necessarily for the molecule itself (11f).

Advantages of the MM method are numerous. The greatest is the high speed with which geometrical optimization is accomplished. With a fast computer, crude coordinates of cholesterol, for example, can be refined within a few minutes! The structure relaxation methods are so efficient and accurate that theoreticians often use the MM-optimized geometry as the fixed input for MO calculations. The computation time for MM increases roughly with square of the number of atoms in the molecule, whereas in sophisticated MO calculations the time increases with the fourth power of the number of basis orbitals (10d). This advantage of MM combines favorably with rapidly increasing computer memory capacity. One of the authors' programs processes molecules containing up to a maximum of 400 atoms.

III. CURRENT FORCE FIELD MODELS

Allinger's review (10d) contains a table of various force fields including performances with various functional groups. This section discusses characteristics of several MM programs based on our own experience.

Three versions of Allinger's program are widely used:

Name	Year	QCPE	Ref.
–	1971	(348)	14
MMI/MMPI	1973	318	15
MM2	1977	395	16

MMI/MMPI incorporates a modified Newton-Raphson energy minimization algorithm that moves atoms one by one and is quite efficient. The force field is parameterized not only for saturated hydrocarbons including cyclopropane, but also for nonconjugated olefins (17c),

alkynes (17b), and various heteroatoms including oxygen (17c–17e), nitrogen (17f), sulfur (17g–17j), halogens (17k), silicon (171), and phosphorus (17m). These heteroatom parameters are essentially intended for molecules containing only one kind of heteroatom or group. It is generally dangerous to devise ad hoc parameters of multi-heteroatom systems by combining the single heteroatom parameters. A modification of MMI (GEOP) is reported (18).

MMPI (15b) is designed for molecules containing a conjugated π-electron system such as aromatics, polyolefins and α,β-unsaturated ketones. The program includes variable electronegativity self-consistent field (VESCF) π-MO calculation capability (19) and performs π-MO and MM alternately until self-consistency is attained. This is virtually the only practical way of calculating structures for large, deformed, π systems such as cyclophanes (20), nonplanar polyolefins (21), and unsaturated ketones (22). The available (QCPE) version of MMPI is not designed to give heats of formation, and one should use only the structure and steric energy from the results (23). MMPI requires a much longer computation time than MMI. Therefore it is recommended that MMI (or MM2) be used for benzene derivatives whenever the aromatic ring is planar by changing the bond length and the stretching parameters of C_{sp^2}–C_{sp^2} bonds (15c).

MM2 is the result of several significant improvements in MMI (24). The recently released QCPE version (16b) contains revised parameters for many of the heteroatoms included in MMI and MMPI.

Previously used force fields listed in Table 1 reproduce the heat of formation for hydrocarbons with about 50% greater standard deviation than is found in the errors of experimental values. The Wertz-Allinger force field is close to an "experimental error-limited force

Table 1
Standard Deviations in Heats of Formation for Hydrocarbons for a Standard Set of Compounds

Approach	Standard Deviation (kcal/mol)
Experimental combustion	0.40
1971 Allinger force field (14)	0.69
1973 Engler-Schleyer force field (26a)	0.83
MMI/MMPI (15)	0.61
MM2 (16)	0.42
Wertz-Allinger experimental error limit force field (25)	0.38

field" (25), of the Urey-Bradley type, including the evaluation of zero-point energies and the effects of vibrational thermal excitation. The resultant standard deviation is in fact equal to the average error of combustion measurements used in the parameterization. The added terms are significantly large. For example, in adamantane, steric, zero-point, and thermal vibration energies are 4.94, 139.12, and 5.92 kcal/mol, respectively. However, the calculation of the vibrational frequencies needs time and this version is not of practical value, especially since the accuracy of MM2 for energy calculations is not significantly lower than that of the Wertz force field (Table 1).

The Schleyer-Mislow program BIGSTRN (26b) likewise is extensively used. This program incorporates the so-called Engler-Schleyer force field (26a) as well as Allinger's 1971 force field as standard options and is unique in that it uses pattern-search methods of energy minimization. This method is effective at the outset but slows down as the geometry approaches a minimum (Table 2).

A small data base of energy and structure for various types of hydrocarbon has been compiled and provides one of the most valuable applications of the Schleyer-Mislow program (26).

Several modifications of the Engler-Schleyer force field have appeared. White (27) added olefin parameters and used an efficient two-stage Newton-Raphson minimization modification. The accuracy of the White force field regarding heat of formation calculations is

Table 2
CPU Time Comparison Between Two Minimization Techniques on a FACOM 230-75 System

Molecule	Starting coordinates	Time (sec.) Pattern Search (BIGSTRN)	Time (sec.) Modified Newton-Raphson (MMI)
2,2,3,3,4,4-Hexamethylpentane, staggered	Molecular model	616	23
Humulene	X-Ray coordinates of Ag^+ complex[a]	342	87

[a] McPhail, A. T.; Sim, G. A. *J. Chem. Soc., B* **1966**, 112.

expressed in terms of *average* deviation, and this should not be confused with *standard* deviation. Mislow tried to improve the accuracy of energy calculations by performing a single extended Hückel MO (EHMO) calculation at fixed geometry after completing the minimization with Engler-Schleyer force field (28). This hybrid approach appears to be promising, although EHMO turned out to underestimate steric effects. A search of other combinations of MM and MO may be worthwhile trying. The Engler-Schleyer force field is built into DeTar's extensive molecular calculation system MOLMEC (29).

A word of caution on the use of the Schleyer-Mislow program BIGSTRN as obtained from QCPE may be appropriate. The default criteria for termination of the energy minimization loop, namely, 0.01 kcal/mol regardless of the size of molecule, is too loose. One can strengthen the criteria 100-fold with one of the options, with the inevitable consequence of prolonged computation time (29a).

QCFF/PI+MCA is a superbly written program consisting of the well-known consistent force field (CFF) (10c), its quantum chemical extension, and molecular crystal packing analysis (30). Programs from the Lifson school generally have a philosophy considerably different from those of other major force fields. Emphasis is placed on the calculation of vibrational frequencies as well as structure and energy, a feature important in the identification of conformational stationary points (31). The default parameters in the program have been tested on only a small body of standards and unsatisfactory results may be obtained from calculations relying on them. CFF is best suited for those who wish to develop optimized parameter sets by themselves for individual purposes. For example, Rasmussen (10c) developed his own version of CFF particularly for calculating carbohydrates (32) and metal complexes (33). Rasmussen's latest version, PE400 (34) for carbohydrates is characterized by almost complete neglect of torsional terms.*

The authors have no experience with the following programs:

CONFI. Simple force field program released by QCPE (35).

MUB-2. Bartell's latest version of his modified Urey-Bradley force field model (36).

MOLECULAR BUILDER. One of the earliest successful MM programs by Boyd (37) has been used as a prototype of several other force field programs. For example, a modified version is in-

*See ref. 54 for more modifications of CFF.

corporated into Altona's molecular properties calculation system UTAH-5 (10f,38). Another modification has been reported (39).

In addition to these, ENERMOL (40), GEMO (41), WMIN (42), and MODELS (43) are mentioned in the literature. WMIN calculates intermolecular nonbonded forces in crystals and is often used by crystallographers.

IV. CONFORMATIONAL ANALYSIS

The ability of the MM method to calculate accurately potential energies and geometries of molecules is best suited for quantitative conformational analysis (44). Numerical values can readily be given to such terms as "strain" and "stability" (45). The topic is extensively covered in Allinger's review (10d), therefore only some recent developments are mentioned.

A. Simple Acyclic Alkanes

The MM method works best for the simple acyclic alkanes because a large body of standard physical properties is available for calibration and because the molecules in this class are nonpolar. Recent debates (36,46–48) on the gauche hydrogen hypothesis (15a) stimulated improvements in the force field model. Inclusion of lower-order torsional potential terms (24,49) now appears to have been well-accepted and has taken place in MM2 (16) and MUB-2 (36). This has led to a significant reduction in the "hardness" of C and H van der Waals interactions, as White (47) has insisted. It may appear strange that MM2 failed to reproduce very well the large rotational barriers of overcrowded hydrocarbons such as hexamethylethane (50).* Therefore the reported high performance of Rasmussen's new force field in which torsional terms are virtually neglected (34) is perhaps more astonishing and interesting.

A trend in the gas phase electron diffraction (ED) analyses is to supplement by MM calculations such inherent disadvantages as the scarcity of information, weak signal due to randomness, disorder, and conformational mobility of gaseous molecules. Hydrocarbons naturally provide the best material for such studies. Some recent

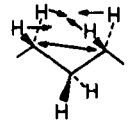
*Crucial experimental data that were needed here became available after the parameterization was completed.

examples are given in Table 3. Some more examples with polycyclic systems and haloalkanes are mentioned later.

Hexamethylethane suffers a twist of 5° from D_{3d} symmetry around its central C–C bond. This twist was reproduced, albeit in somewhat exaggerated form, by MM calculations (56)* and ascribed to nonbonded H–H interactions across the central bond (56). In contrast, the global minimum energy conformation of hexamethyldisilane (1) is predicted to have D_{3d} symmetry, since the Si–Si bond is longer (2.34 Å) (61).

$(CH_3)_3Si-Si(CH_3)_3$

1



2

The average C–C bond length of *n*-hexadecane (1.542 ± 0.004 Å) observed by ED analysis is 0.01 Å longer than those of small alkanes and was interpreted by MUB-2 calculations as having arisen from repulsion between internal geminal CH_2 groups (2) (59). An alternative explanation of the analogous effect in propane invokes attractive H–H and repulsive 1,3-C–C interactions (62). Furthermore, the ED measurements of *n*-hexadecane were carried out at 150°C, where both the anharmonicity of the vibrations and the population of gauche conformations must be relatively high. Hence, a large bond length (and large C–C–C angle; obs. 114.06 ± 0.6°) would be expected to result (62). An algorithm was announced for calculating approximate conformational energy populations of methyl-substituted alkanes (63).

B. Overcrowded Methanes and Ethanes

Mislow, who discussed MM in some detail in his textbook (64), has performed excellent systematic studies of overcrowded methanes (3) (molecular propellers) and ethanes (4) and their metal analogs by the combination of dynamic NMR with MM calculations. Since his own reviews have been published (65,66), only very recent results are mentioned.

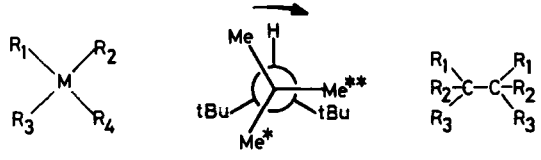
Tri-*tert*-butylmethane (3, M = C, R_1–R_3 = *t*Bu, R_4 = H) is intriguing not only as one of the standard examples of strong nonbonded inter-

*See also footnote 39 of ref. (60).

Table 3
Recent Examples of Complementary Use of MM Calculations
in Electron Diffraction Analyses of Simple Acyclic Hydrocarbons

Compound	References	
	ED	MM
n-Butane	51	50,52
Isobutane	53	46,54
Neopentane	55	55
2,3-Dimethylbutane	56	46,48
Hexamethylethane	56	56
di-*tert*-Butylmethane	55	55
tri-*tert*-Butylmethane	57	54,58
n-Hexadecane	59	59

actions (54,57,58), but also as a material for dynamic study. Intramolecular crowding leads to twisting deformations around the C_m–C_q bond, hence the molecular symmetry is C_3. Indeed, magnetically different methyl groups (Me, Me*, Me** in 3′) were observed in the



3 3′ 4

^{1}H NMR spectrum at −127°C. According to MM calculations, the best mechanism for the topomerization of three methyl groups is the rotation of C_t–C_q bond in the direction shown by the arrow in 3′. The observed barrier agrees with that calculated (67). Similar correlated movements of *tert*-butyl groups were also detected and analyzed with tri-*tert*-butylsilane (3, M = Si, R_1–R_3 = *t*Bu, R_4 = H) (68).

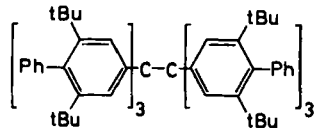
Dynamic ^{1}H NMR experiments at 270 MHz of dimesityl-2,4,6-trimethoxyphenylmethane [3, M = C; R_1, R_2 = $C_6H_2(CH_3)_3$-2,4,6; R_3 = $C_6H_2(OCH_3)_3$-2,4,6; R_4 = H) confirmed the advantage of the "two-ring flip" mechanism previously proposed by Mislow (66) for the racemization of triarylmethanes (69). In tris (dialkylamino)borane (3, M = B, R_1–R_4 = NRR′), however, the one-ring flip mechanism is preferred. In this case, the B–N π-bonding contribution must domin-

ate over steric compression in the torsional transition state (70). The calculated activation energy for the racemization of optically active trimesitylamine (25–27 kcal/mol) was found to be in satisfactory agreement with the experimental value (28 kcal/mol) for perchlorotriphenylamine (70a).

In accordance with the overwhelming tendency of type 3 molecules to take on an S_4 ground state symmetry, tetracyclohexylsilane (3, M = Si, R's = cyclo-C_6H_{11}) was confirmed by X-ray analysis as belonging to this point group. MM calculations of other conformers are available (71).

The stereochemistry of crowded ethanes (4) is no less intriguing than that of 3 (72). One of the well-known problems with 4 is the contrast in the favored ground state conformations for 1,1,2,2-tetraalkylethanes (gauche) (73,74) and 1,1,2,2-tetraarylethanes (anti) (75,76). Repulsion between geminal substituents has been demonstrated as a key factor by careful dynamic NMR and X-ray analysis as well as by MM calculations. This repulsion increases the R–C–R angles and leads to severe interactions among vicinal substituents in the anti form, whereas the gauche form somehow can manage to release this repulsion by twisting around the central bond and by similar means. In tetraarylethanes, the vicinal interactions in the anti form can be reduced by stacking orientations of aryl groups, whereas the equilibrium stacking in the gauche form is less effective in reducing overcrowding. These steric effects are more important than the polar effects (75).

Rieker's report (77) on the isolation and X-ray structure characterization of the hexaphenylethane derivative 5 aroused a lot of interest, since the observed central bond length was abnormally short (1.47 ± 0.02 Å), in sharp contradiction to the MM prediction (1.635 Å) for the parent hydrocarbon (78). However, the X-ray data need to be further refined before a final conclusion can be reached, and MM calculations of 5 itself confirm the long C–C bond (79).



5

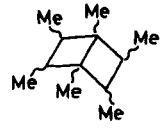
C. Monocyclic Alkanes and Alkenes

Carbocyclic molecules occupy a special position in stereochemistry. While Barton's proposal (80) triggered explosive developments in the conformational analysis of six-membered ring compounds (80a), the inability of the qualitative theory to interpret the behavior of rings other than six membered prompted Hendrickson to utilize the MM method (9b). Further developments in this area have been well summarized (10, 81). Some of the more recent topics are mentioned below.

Three-membered rings are out of the range of the Engler-Schleyer force field because the deviation of the valence angle from the alkane equilibrium value for sp^3-hybridized carbon is too large (26a). Therefore, the reported agreements between the observed and calculated heats of formation by this force field for the *cis*- and *trans*-bicyclo[6.1.0]nonanes **6** are surprising (82). Now, the three- as well as four-membered ring carbons are given special parameters in MMI and MM2 (16,92). Steric energy calculations of seven configurational isomers of 1,2,3,4,5,6-hexamethylbicyclo[2.2.0]hexane (7) with MMI helped to explain novel skeletal inversion from "four or three endo-7" to "four or three exo-7" (83).



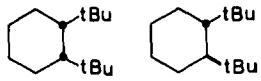
6



7

The calculations above did not give satisfactory results concerning the structure of even the parent hydrocarbons (cyclobutane and bicyclo[2.2.0]hexane), but highly strained cyclobutene, methylenecyclobutene, Dewar benzene, and so on, were shown to be handled well by MM2 (83a).

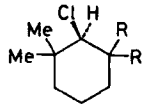
Experimental results indicate that for the cis isomer of 1,2-di-*tert*-butylcyclohexane (**8a**), either the chair (84) or the boat (85) conformation is the most stable, whereas for the trans isomer (**8b**) the diaxial chair and the twist (86) or boat (87) forms are supposed to be in equilibrium. According to MM calculations of the cis isomer, a boat form is preferred when Bartell's force field (36) is used, whereas with Lifson's force field (30) the chair form is predicted (87). Schäfer performed *ab initio* calculations with the STO-3G, basis set on the final structures resulting from these MM calculations and found the boat conformer to be consistently more stable than the chair (87). For the trans isomer (**8b**), MM calculations again are inconsistent, but *ab initio* calculations on the final MM geometries result in almost



8a 8b

equal stabilities for the diaxial chair and the boat conformations (87). We will return to Schäfer's strategy shortly.

In 1-X-2,2,4,4-tetramethylcyclohexane (e.g., **9a**), the reflex effect between two 1,3-diaxial methyl groups brings about inward displacements of the equatorial methyl groups, which interact severely with the axial chlorine atom. For this reason, the conformational energy in **9a** increases as much as 3 kcal/mol according to MMI calculations (17k). Similar deformation-induced interactions were observed with the 2,2-dimethyl derivative (**9b**) as well, for which the calculated and observed conformational energies agreed particularly well (87a). In these instances, the conformational energies were determined by the low-temperature ^{13}C NMR technique (see also ref. 87b).



9 a: R=Me
b: R=H

Larger cycloalkanes have attracted much interest from the time of the "diamond lattice theory" (81). As far as the stable conformations are concerned, Dale's analysis (88) of the relative energies of a large number of ring systems by an approach based on the torsional potential curve of *n*-butane is unique for its simplicity and usefulness. More sophisticated MM treatments of large carbocyclic systems are clearly desirable, and the first such attempt was recently reported by Allinger (89). In this study cyclohexadecane, and its 1,9-dione and ketals, were calculated and the conformational population predictions checked by dipole moment measurements. Allinger's conclusion that cyclohexadecane exists to a large extent in a "square diamondoid" conformation (D_{2d}) agrees with Dale's prediction (88).

The dynamic behavior of ring systems is one of the most active areas of MM applications, since the energy hypersurface of a large molecule that does not involve bond formation or breaking can be adequately explored only by this technique. Here again, Dale sum-

marizes basic problems (90). Exploratory work has been reported in a series of papers by Anet, who clearly demonstrated the power of the dynamic NMR-MM combination (81,91,92); examples are compiled in Table 4. Anet uses a modified version of Boyd's program (37) that affords calculations of vibrational frequencies. The agreement between the observed and the lowest calculated barriers is generally excellent. A key feature of a potential surface search is the technique of driving one or more bonds to simulate the ring deformation processes. Several algorithms suitable for such purposes have been described (39,105–108). A combination of the Lagrangian multiplier method with the Newton-Raphson minimization scheme appears to be the most promising (39,105,108).

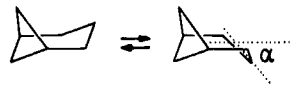
D. Polycyclic Hydrocarbons

1. Bicyclo[3.1.1]heptane

For bicyclic and polycyclic systems, fewer conformations and interconversion pathways need to be considered than is the usual case for monocyclic systems. For example, placing a CH_2 bridge on a

Table 4
Cycloalkanes and Cycloalkenes Whose Dynamic Behavior Has Been Studied by the Dynamic NMR and Molecular Mechanics Techniques

Cyclo Compound	Ref.
cis,cis-1,3-Cyclooctadiene	93
cis,cis-1,4-Cyclooctadiene	94
cis,cis-1,5-Cyclooctadiene	95
anti-3,7-Dimethyl-*cis,cis*-1,5-cyclooctadiene	96
1,3,5- and 1,3,6-Cyclooctatriene	96a
1,2-Cyclononadiene	97
cis,cis-1,5-Cyclononadiene	98
1,2,6-Cyclononatriene	97
1,4,7-Cyclononatriene	99
1,2,6,7-Cyclodecatetraene	97
Cycloundecane	100
Cyclododecane	101
cis-Cyclododecene	102
Cyclododecyne	103
trans,trans,trans-1,5,9-Cyclododecatriene	104
Cyclotridecane	100
Cyclopentadecane	100

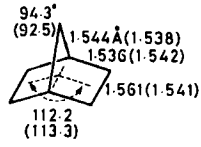


10

cyclohexane ring to give bicyclo[3.1.1]heptane(norpinane) (**10**) leads to only one simple mechanism for ring inversion. The inversion is much more rapid than in cyclohexane, for which the chair-chair interconversion barrier is 10 to 11 kcal/mol (81). NMR experiments in solution provide only the upper limit value of 4 kcal/mol (110) for norpinane, but three independent MM calculations (111–113) unanimously suggest 0.7 to 1.1 kcal/mol for this barrier height. The calculated value of $\alpha = 25°$ is much smaller than the value 37° deduced from gas electron diffraction analysis (114). Reexamination of the experimental data is indicated.

2. *Bicyclo[2.2.1]heptane*

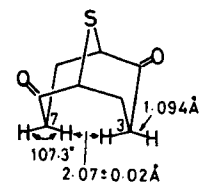
Those who attempt to parameterize empirical force field potential functions are embarrassed by serious inconsistencies in the structure of bicyclo[2.2.1]heptane, an important molecule as determined by various physical measurements. A structure (**11**) was "synthesized"



11



12a



12b

based on one X-ray and two electron diffraction results (115); figures in parentheses are calculated by MM2 (16). The disagreement in the C_2–C_3 bond length is more than one would expect.

3. *Bicyclo[4.2.0]octane*

Both the cis and trans isomers of bicyclo[4.2.0]octane are other examples of the auxiliary use of the MM method in precise structure determinations by vapor phase electron diffraction (115a).

4. *Bicyclo[3.3.1]nonane* (12a)

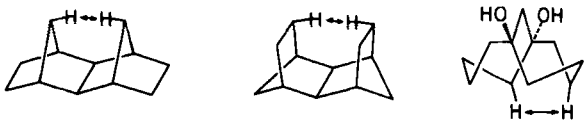
The conformations of bicyclo[3.3.1]nonane and related molecules have been intensively studied during the past few years (116). A major concern of the MM method is how well the calculations reproduce the close H3 · · · H7 distance. One problem here has been the lack of reliable experimental data. Recently, combined X-ray and neutron diffraction analyses of **12b** determined the exact geometry of the 3-methylene group (116). Although **12b** turned out to have a slightly skewed structure, fitting the 3-methylene geometry to the carbon skeletons from previous X-ray data of double chair bicyclo [3.3.1]nonanes gave C_{2v} geometries with an average H3 · · · H7 distance of 1.86 Å for **12a** (116). In an independent study of an ester of bicyclo[3.3.1]nonan-9-ol, Sim concluded with corrections for the influence of the bulky 9-substituent by MM calculations and for the observed C–H bond lengths (which were too short), that the H3 · · · H7 distance in **12a** is 1.85 Å (117). Table 5 gives these and additional examples of short intramolecular H · · · H distances. Clearly, the three force fields used in this table, all of which are characterized by "soft" hydrogen atoms, still overestimate such close nonbonded distances by about 0.1 Å.

Introduction of α-substituents into the 3- or 7-position of **12a** leads to a shift of the prevailing conformation from chair-chair (cc) to boat-chair (bc), and finally to twist double boat (**16**) as judged by ^{1}H NMR spectra (121). The changes in the H:H coupling constants in these derivatives can be interpreted with skewed cc conformations as well. MM calculations, however, ruled out the latter possibility (121). The results of acetolysis of exo- and endobicyclo[3.3.1]nonan-3-yl tosylates were also interpreted with the aid of MM calculations (122).

Table 5
Short Intramolecular Nonbonded H . . . H Distances (Å)

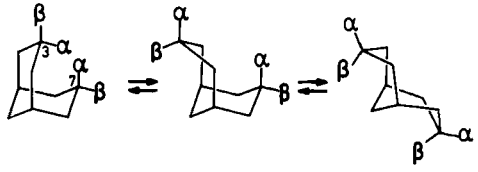
Compound	Observed	Ref.	Calculated	MM Technique	Ref.
12a	1.86	116	1.97	WB[a]	27,47
	1.85	117	2.03	MM2	120
13	1.82	118	1.90	CFF	118
14	1.85	118	1.96	CFF	118
15	2.15	119	2.21	WB[a]	119

[a]White-Bovill force field (27).



13 14 15

Probably an attempt should be made to replicate the one-bond drive results reported in this paper by the multibond drive technique (108,120).



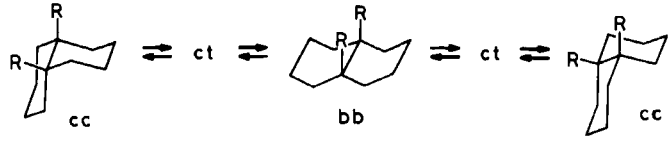
cc bc t-bb

16

5. Bicyclo[4.4.0]decane

The success of the gas phase electron diffraction analysis of *cis*- and *trans*-decalin (123) is another example of the use of MM calculations as an auxiliary technique. Minimum energy conformations and vibrational amplitudes were calculated by both the Lifson and Boyd force fields (30,31) and were used as the starting values for refinement of the geometrical and vibrational parameters for the least-squares analysis. The results revealed no appreciable strain in *cis*-decalin (123) other than that expected from gauche interactions.

Conformational inversion barriers of 5,10-substituted decalins (17) were determined by ^{13}C NMR, and MMI calculations were carried out to see whether the twist-chair (ct) or the boat-boat (bb), correspond to the higher barrier. The ct was found to be higher in *cis*-decalin (17, R = H), but the introduction of substituents at the ring junction is expected to raise the energy of the bb. The observed $\Delta G^{\ddagger}$ agreed with the calculated value for ct, which is about 5 kcal/mol higher than that of bb when R = CH_3 or OH (124).



cc bb cc

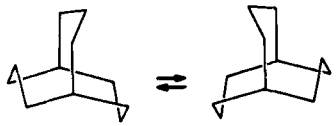
17

6. *Bicyclo[4.4.1]undecane*

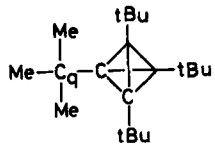
X-ray analysis of the 1,6-diol derivative (15) of the bicyclo[4.4.1]-undecane ring system revealed the often calculated (9a,81) but rarely observed twist-chair cycloheptane ring. MM calculations confirmed that the observed conformation of **15** is the global minimum conformation (119).

7. *Bicyclo[3.3.3]undecane*

The observed low barrier of conformational interconversion in manxane (18, 12 ± 2 kcal/mol) was satisfactorily reproduced by the Schleyer force field (125). This molecule also involves a number of close intramolecular nonbonded H · · · H contacts (126). The flipping of one methylene bridge is transmitted readily through space to the



18



19

other bridges, and the conformational interconversion must be more or less concerted (125). For additional examples of "correlated" intramolecular movements in molecules having polymethylene bridges, see ref. 127.

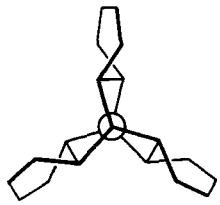
8. *Tetrahedrane (128)*

Since the structure of tetra-*tert*-butyltetrahedrane (**19**) has not been experimentally determined (128), one needs some courage to make predictions about it. Nevertheless, it seems likely that C–C_q bond will be twisted from a gauche value (ϕ(CCC$_q$Me) = 60°, T_d point group) because of severe crowding among the *tert*-butyl groups at the tetrahedrane nucleus.* MM calculations predict a structure with a ϕ value near 45° (T symmetry) to be 4 kcal/mol more stable than the gauche conformation (130).

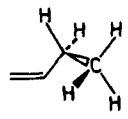
*See the cover photograph of a molecular model of **19** in the issue of *Angewandte Chemie* containing Maier's synthetic report (129).

9. *Perhydrotriptycene*

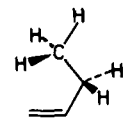
Exhaustive catalytic hydrogenation of triptycene affords an equilibrium mixture of perhydrotriptycene isomers. As expected, Boyd's force field (37) calculations, with a modified torsional constant, reproduced the observed composition fairly well (Table 6). All important conformations were taken into account for each isomer. The most stable conformations agree with the results of the X-ray analysis (131) and have the characteristic that the cyclohexane rings are invariably either boat or deformed chair. The most stable conformation of all is **20** (ttt). The predominant conformation of ccc, in which all cyclohexane rings are boat, has an enthalpy only 2.56 kcal/mol above that of **20**. The difference is virtually all due to angle and torsional terms.



20



Me-skew



Me-syn

21

Table 6
Observed and Calculated Equilibrium Composition of Perhydrotriptycene Mixture at 172°C (131)

Configuration[a]	Composition (%)		X-Ray Ref.
	Observed	Calculated	
ttt (**20**)	61.2	64.3	131d
ttc	27.0	20.6	131e
tcc	7.3	6.6	131c
ccc	3.4	6.4	131d
tc'c	1.1	0.8	–
cc'c	<0.1	2×10^{-5}	131a

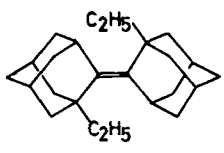
[a]The notation refers to the configuration at the junction of three cyclohexane rings with the bicyclo[2.2.2]octane skeleton. A prime indicates that the cyclohexane ring is oriented counterclockwise when viewed along the C_3-axis of bicyclooctane part; otherwise the orientation is clockwise.

E. Olefins

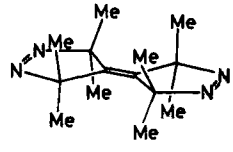
1-Butene exists as an equilibrium mixture of two conformations, Me-skew and Me-syn (21). The most reliable composition to date is 83:17% according to combined ED, microwave (MW), and *ab initio* MO analysis (133). This study includes the MM (CFF)-ED-MW analysis of this molecule for comparison, which gave a final skew/syn ratio of 80:20. The molecular orbital constrained electron diffraction (MOCED) results appear to agree better with the observed data than does the MM constrained analysis, the R value of the least-squares analysis of the latter being 20% higher than that of MOCED. However, one may ask whether such a small difference in R values justifies the enormous difference in computer time between the *ab initio* (about 200 hr on an IBM 370/155) and MM (less than a minute) methods used in this work.

Crowded olefins continue to attract chemists. This subject has recently been reviewed with special reference to MM analysis (134). The double bond in crowded ethylenes is highly resistant to elongation: the longest recorded lengths are 1.358 ± 0.004 Å (calculated by MMI; 1.364 Å) for 22 (135) and 1.356 ± 0.002 Å for 23 (136). The opening of the C=C–C angle takes place more readily: the record is 138.7° (calculated by CFF, 138.9°) for 24 (137). Another way of relieving strain is to twist the double bond. One of the highest recorded twist angles is 24° for 25 (138). For the still elusive tetra-*tert*-butylethylene (26), a twist of 75° is predicted (CFF, ref. 139).

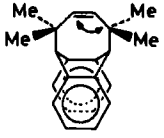
Butadiene exists as an equilibrium mixture of *s*-trans and *s*-cis conformations (140). Although MM calculation had indicated the preference of gauche over *s*-cis (141), a recent recalculation with GEOM



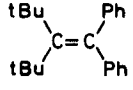
22



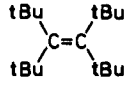
23



24



25



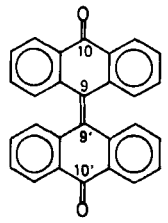
26

(18) correctly reproduced the experimental conformational energy and the barrier to the *s*-trans *s*-cis interconversion (18). The success of MM calculations of butadiene indirectly supports Bartell's "nonbonded interaction theory" on the shortening of sp^2—sp^2 bond (142).

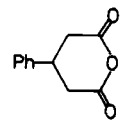
We mentioned briefly in Sect. III that the combination of MM with MO methods is the only reasonable way of handling nonplanar conjugated π systems. A collection of 37 conjugated dienes and trienes and their homologs have been calculated by MMPI and the geometries of the most stable conformers were presented (21b). For some of these, and for several additional nonplanar polyenes, electronic spectra (frequency and intensity) were calculated by the VESCF MO configuration interaction (CI) method. The agreement with observed spectra is satisfactory (21a). Heats of formation of nonplanar polyenes now can be calculated by computing the contribution of the C_{sp^2}—C_{sp^2} double bond energy with the aid of a fast SCF calculation. Allinger's method afforded an average deviation of 1.34 kcal/mol from experiment for a very large set of conjugated molecules that included both polyenes and aromatics (23).

F. Aromatic Molecules

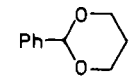
The term "aromatic" applies here to molecules containing benzenoid fragments. Prior to the quantum mechanical extension [as in MMPI (156) and QCFF (30)], aromatic molecules were given a "mechanical" treatment (Sect. III). This approach gives satisfactory results when the substrate contains planar benzene rings, and it is still recommended for economic reasons. Studies (143) of the isomerism of bianthrone 27 have been particularly illuminating in view of the good agreement with experimental observations. A colored isomer of 27 (B form) is suggested to have the central bond twisted by 57° on the basis of NMR data and MM and MO calculations. The MM calculations indicate that the "step" conformation



27



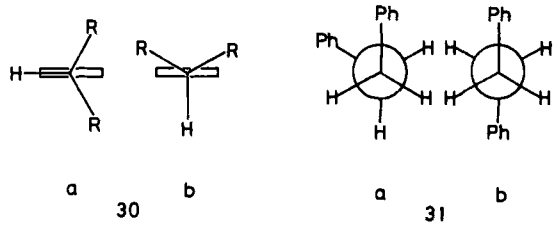
28



29

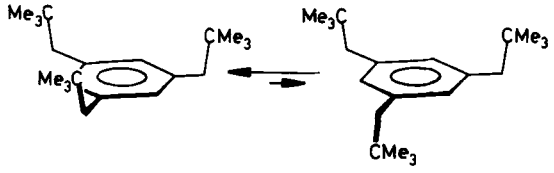
with the two planar anthrone moieties is a distinct local energy minimum second in stability only to the twisted conformation (A form). Here the central double bond is not twisted, but the two anthrone rings are folded about the 9-10 (and 9'-10') axis and displaced in opposite directions from one another. The calculated activation energy for the interconversion B → A (20 kcal/mol) agrees with the observed energy (13–15 kcal/mol).

The favored orientation of phenyl rings attached to cyclohexane (144) in glutaric acid anhydride **28** (145) and 1,3-dioxane **29** (146) rings has also been successfully worked out without invoking the π-MO system: **30a** is favored over **30b**.



The tendency of polyphenylethanes to take up anti conformations was mentioned above (Sect. IV-B). Some confusion arose, however, when Ivanov (MMI, ref. 147) and Jacob (BIGSTRN, ref. 148) independently reported that MM calculations gave lower energies for the gauche-1,2-diphenylethane **31a** than for the anti conformer **31b**, while the reverse was actually observed in crystals. Ivanov even reasoned that the calculated higher stability of **31a** in the vapor state arose from attractive nonbonded $C_{ar} \cdots C_{ar}$ interactions. MM2 calculations (62) as well as the hybrid EFF-EHMO approach (28) gave results consistent with experimental observations, however. For "mechanical" benzene ring calculations with other crowded polyphenylethanes, see ref. 149.

In view of these results, the "attractive" explanation (150) of the greater stability observed for the more crowded conformer of 1,3,5-trineopentylbenzene (**32a**) over the less hindered one (**32b**) must be received with due care. The proposal cites attractive nonbonded forces between $H \cdots C_{sp^3}$ as a contributing factor of the observed equilibrium. Our reservation stems from the inherent danger of assigning a particular observation to one of the potential terms, in this case to the attractive term of nonbonded potential (10f). Nonetheless, suggestions concerning the importance of attractive van der Waals forces involving aromatic rings are not rare. 2,4,6-Tribromo-



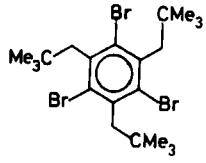
a b

32

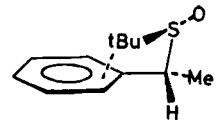
ΔH^{Calc} - 0.91 kcal/mol(150)
ΔG^{Obs} - 1.04 kcal/mol(151)

1,3,5-trineopentylbenzene (**33**) was found to exist as a 1:1 mixture of the conformer types **32a** and **32b** in the crystal (152). A number of gauche- or syn-folded conformations have been reported for two types of compounds represented by **34** (153) and **35** (154). It is claimed (153) that an attractive interaction of the H · · · π type is responsible for conformations resembling **34**. Based on WMIN (42) calculations for compounds resembling **35** (154), the donor-acceptor interaction is excluded, and an unspecified nonbonded attraction is said to be responsible.

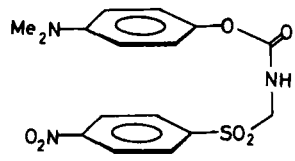
As the final example of the simplified treatment of an aromatic ring, a novel potential energy calculation of a naphthoquinone derivative (**36**) with a program called EENY will be briefly mentioned (155). This program seems to resemble WMIN in that it calculates only van der Waals energy. The rotation around the cyclopropylquinonoid bonds is calculated to have a barrier of about 10 kcal/mol. In this and another case (156), the results could be considerably improved by full relaxation MM calculations.



33

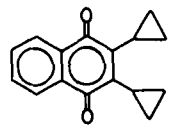


34

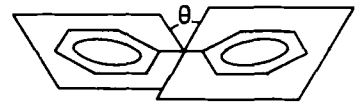


35

The quantum mechanical extention of the MM method covers an enormous potential range of applications. Complete relaxation calculations of biphenyl (37) in the S_1 excited state were carried out for the first time using QCFF (30) and the S_1 conformation was con-

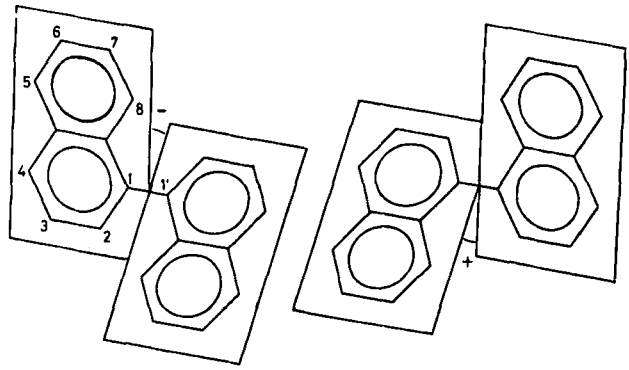


36



37

firmed as being planar ($\Theta = 0$). The spectroscopic behavior of S_1-biphenyl is now fully explained (157). 1,1'-Binaphthyl (38) was subjected to a similar treatment (158). Interest in 1,1'-binaphthyl has largely centered around its chirality, especially the mechanism of inversion. Extensive MMPI (15b) calculations involving forced driving of the 1,1'-bond revealed that the lowest transition state occurs along the anti inversion path involving only one close H · · · H con-



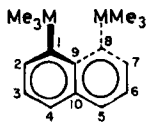
38

tact, among several other possibilities. The calculated barrier for this mechanism (20.2 kcal/mol) agrees well with the experimental barrier (159a). The optical stability of 38 does not significantly change upon introduction of a substituent at the 8-position but increases greatly upon substitution at the 2-position. According to MMPI calculations on 8-substituted 38, the energy minimum conformations are destabilized as much as the torsional transition states are de-

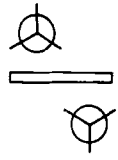
stabilized, whereas the transition state of 2-substituted **38** is extremely crowded (159b).

In the inversion transition state of **38**, the nonbonded repulsions among hydrogen atoms at the 2, 2′, 8, and 8′ positions are so strong that the MMPI-calculated structure of the naphthalene nucleus shows considerable deviation from planarity. Such a deformed naphthalene ring has been difficult to observe in the ground state (except in cyclophanes, see below), despite the "flexible aromatic ring" proposal (160). Recently, however, introduction of two bulky groups at the peri positions (**39**) led to this type of deformation. Three examples (**39**, M = C, Ge, Sn) were analyzed by X-ray and MM methods (161, 162). In each of these, planes $C_1-C_9-C_8$ and $C_4-C_{10}-C_5$ are twisted about the C_9-C_{10} bond in opposite directions, imparting a near-C_2 symmetry to the molecule. The peri $M(CH_3)_3$ groups are further deflected to opposite sides of the molecular plane. Thus, C_1 and C_8 approach a pyramidal configuration. When M = C, other structures having C_{2v} and C_s symmetries were calculated to be much less stable than the C_2 structure (161). Skeletal deformations decrease in the order C $\gg$ Ge $>$ Sn, that is, in the inverse order of the covalent radius of M.

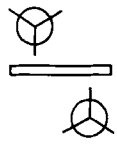
An interesting feature in this series is a characteristic transition of the conformation of $M(CH_3)_3$ groups. When M = C, the preferred conformation is as shown in **40**, whereas a conformation such as **41**



39



40

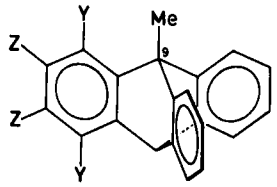


41

is observed when M = Ge and Sn. This contrast persists not only in the gas phase and solution, but also in the solid state (163). Calculations with M = Ge and Sn were carried out using BIGSTRN, namely, by the "mechanical" aromatic ring approach (163). Free energies of activation in the rotation about the C–M bond are 4 to 7 kcal/mol, decreasing in the order C $>$ Ge $>$ Sn. The low barriers are surprising in view of the steric compression between the peri groups that brought about such unusual deformations of the naphthalene ring. The foregoing trend in $\Delta G^{\ddagger}$ of C–M rotation is the reverse of the order calculated by the MM method (164), but the accuracy of such calculations

is questionable in view of the apparently inadequate parameterization, neglecting polar interactions around the metal atom.

It may be pertinent to mention here a recent criticism of the gear effect by methyl groups, since most of the known examples used in the study of the gear effect are in aromatic molecules. Based on dynamic NMR data on the internal rotation of the 9-methyl group in 42, which indicated a far lower barrier for 42a than for 42b, Ōki

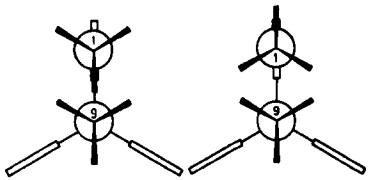


	Y	Z
a:	CH_3	H
b:	Cl	Cl

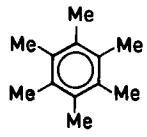
42

(166) presented a gearing scheme (43) to interpret the unexpectedly "small" size of the methyl groups. As opposed to this, Mislow's (165) BIGSTRN calculations on these systems concluded that the global minimum energy conformation of 42a looked like 44 rather than like 43, and that the forced rotation of the 9-methyl group did not induce "correlated rotation" but only effected "concerted libration" of the 1-methyl group. The calculated barrier agreed with the experimental one. Mislow presented an alternative interpretation involving the ability of the methyl group to reduce its effective internal size by changing the H–C–H and H–C–C angles. These calculations may suffer from the inadequacies in the nonbonded H · · · H potential function in BIGSTRN (47). Nevertheless, the conclusion seems safe, since this force field, with its "hard" H:H potential, should have overestimated the gear effect if it were present. Gear effects involving the *tert*-butyl groups in 39 appear real. MMI and MMPI proved to be unsatisfactory in the calculations of rotational barriers in 9-methyltriptycene (167).

A rate process was observed for the methyl rotation in solid hexamethylbenzene (45) and this was interpreted as a sure case of



43 44



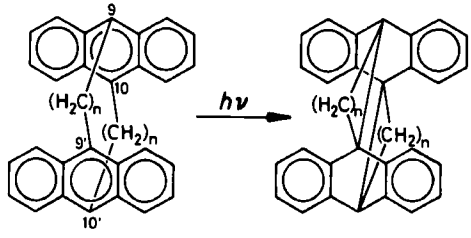
45

disrotatory cogwheeling involving all of the methyl groups (168). In the case of 1,8-bis(trimethylelement)naphthalene (39) mentioned above, however, MM calculations suggest no gearing but only the forced libration between the peri substituents (164).

Cyclophanes are naturally suited for MMPI (15b) calculations. The results of such calculations regarding the structures and electronic spectra of the [*n*]paracyclophanes (n = 5–10) agreed well with the experimental data (169). Attempted X-ray analyses of [2.4]- and [2.5](9,10)-anthracenophanes (46) encountered serious disorder in the aliphatic bridges. MMPI calculations of all possible conformers of these molecules revealed four and six energy minima for **46a** and **46b**, respectively. Comparison of the calculated C10···C10′ distances and bridge conformations with X-ray information unambiguously identified two conformations each for **46a** and **46b** as the final solutions. These and the calculated structures of photoisomer 47 were highly useful in the interpretation of fluorescence spectra and photoisomerization processes of **46** (170).

Lindner (171) developed his own π-SCF MO force field that is similar to MMPI in construction. This program was applied to simulate racemization of metacyclophane (48) and hexahelicene (50). In metacyclophane the *m*-phenylene ring flips readily at room temperature. Two mechanisms can be conceived: one operates by way of a high steric energy conformation (**48b**); the other involves a biradical intermediate (**49**). The calculated activation energies are 17 and 32 kcal/mol, respectively. The experimental value is 17.7 kcal/mol, in accord with the first mechanism (172). The structures and energies of seven types of cyclophane have been calculated (172).

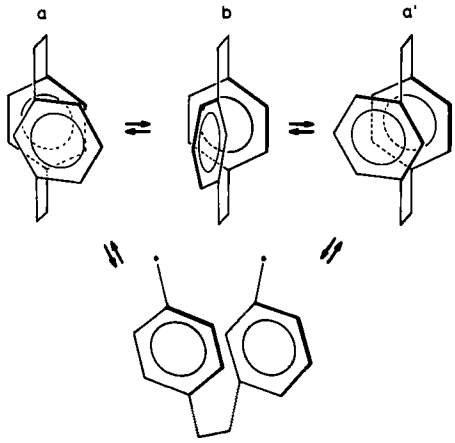
The same argument was applied to hexahelicene (173) in which the possibility of bond rupture and recombination had been excluded



a: n = 4, b: n = 5 — n = 4

46 — 47

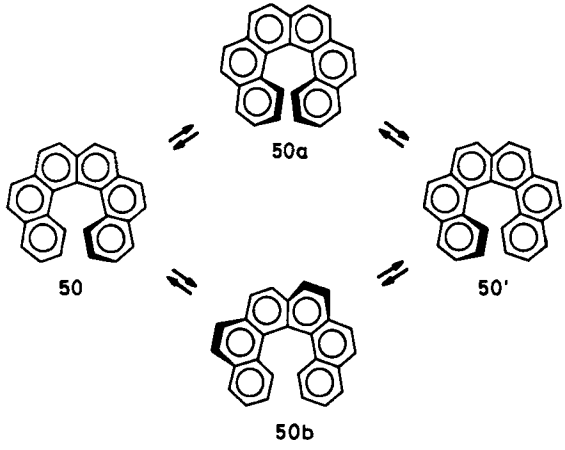
48



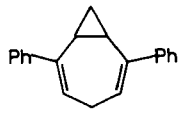
49

by experiment. Of the two conformational possibilities illustrated, the activation energy calculated for the transition state **50a** having opposed spiral ends (C_s symmetry) compares better with the observed value than that of the alternative with bent shape **50b**.

$\Delta H^{\ddagger}$ (kcal/mol)	
Calculated	Observed
41.0 (through **50a**)	36.0
70.1 (through **50b**)	–



The same π-SCF force field was used for calculations on 2,6-diphenylhomotropilidene (51). In the crystal, this molecule exists in the chair form, which proved to be the global energy minimum. The MM calculations of nonbenzonoid aromatic hydrocarbons have been reviewed elsewhere (10d).



51

G. Heteroatom Systems

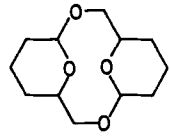
Several current MM programs are parameterized for various functional groups. Parameterizing for monoheterofunctional groups is basically possible as an addition to the existing hydrocarbon force field, if the necessary reference data are available for optimization. The accuracy of such calculations is generally lower than that of hydrocarbons (fewer and less accurate data are available for the parameterization); nonetheless the results are good enough to warrant widespread application.

Polyfunctional organic molecules present serious problems. Charge interactions among polar groups are not additive because of induced polarization. Furthermore, the medium in which the electrostatic interactions occur is not homogeneous but heterogeneous in the intramolecular environment. A promising approach to these problems is being explored within the MM framework. Allinger (175) calculated induced dipole moments based on the Smith-Eyring method, while extending the original method from considering interactions between bonded atoms only to include all nonbonded atoms (thus, this is called modified Smith-Eyring method, MSE). The charge distribution corrected for induction is used to calculate an electrostatic interaction energy, which is then incorporated into the MM scheme. While the heterogeneity of the electrostatic interaction medium is neglected, the MSE approach correctly reproduced the preference of the diaxial over the diequatorial conformation in *trans*-1,2-dichlorocyclohexane (175). The effect of solvent, a highly influential factor for the conformation of polar molecules, was taken into account by considering the solvent as an isotropic continuum having some macroscopic dielectric constant interacting with the molecular dipole and quadrupole (176).

These provisions have not been included in Allinger's QCPE programs, except for simple calculations of dipole-dipole or point charge interactions. We discuss below mainly the results obtained with monofunctional molecules.

1. Ethers and Alcohols

The program MMI treats the lone electron pairs on oxygen and nitrogen as a quasi-atom having a bond length of 0.5 Å and other suitable parameters (17c). Burkert (177) has proposed various modifications including abandoning an explicit account of lone pairs, and improvements in van der Waals and torsional terms. In the calculations of the stable conformers of a tricyclic polyether (52) by ENERMOL (40), the charge interactions were neglected, but the calculated structure agreed with NMR information (178).



52

One of the well-studied areas of conformational analysis of oxygen-containing molecules is the anomeric effect, a special behavior of the anomeric carbon in pyranosides caused by bonding to two oxygen atoms (13a, 179). Although this problem is a classical example of the successful application of *ab initio* MO calculations to a stereochemical problem (13a,180), extention of the calculations to polysaccharides clearly requires the MM technique. Following several preliminary studies to devise a suitable force field (17c,181), Jeffrey was able to reproduce the observed geometries and energies of pyranosides by modifying the equilibrium C–O bond lengths in MMI (182). He states that the hydrocarbon part of MMI is not adequate to reproduce the primary alcohol group conformation in aldohexopyranoses (182).*

Rasmussen's efforts to adopt CFF to saccharides merit special attention (32). His latest version (34), which virtually eliminated the torsional term, awaits critical examination. Tvaroska and Bleha (183) performed partial relaxation MM calculations on dimethoxymethane

*The problem should be rechecked with Allinger's MM2 force field (16,62).

and stressed the importance of atomic dipole moment dependence on hybridization.

Recent calculations on the pseudorotation of 1-aminoribose and 1-aminodeoxyribose with the QCFF/PI program (30) suggest an extreme flexibility of these important rings, with an estimated barrier of only 0.5 kcal/mol (183a). As a consequence, the torsional barrier around the sugar-phosphate backbone bond must be extremely low. This prediction should have an important impact on conformational studies of DNA and RNA (see Sect. VI-D).

2. *Carbonyl Compounds (17d,17e) and Carbonium Ions*

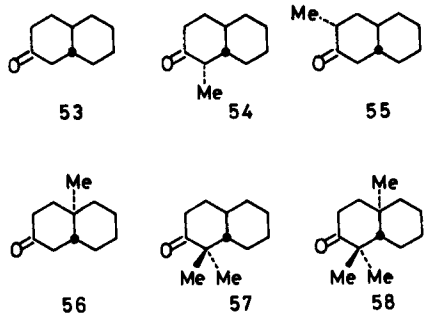
Conformational studies on monocyclic C_8 to C_{11} ketones have been reviewed with reference to the MM method (184; see also ref. 89). Extensive comparisons of the conformational energies of *trans*-2-decalone derivatives (53–58) calculated by MM and *ab initio* MO methods gave inconsistent results (Table 7). In this ambitious project of treating very large molecules by *ab initio* methods, the MM-minimized structures were used for the single geometry MO calculations. The casual introduction of carbonyl parameters into the hydrocarbon force fields [Lifson-Warshel version of CFF (30) and Bartell's old force field (186)] appeared to be primarily responsible for the results. Nevertheless, the use of MM-minimized geometries in MO calculations will be more and more widely adopted.

As a rigorous test, Allinger subjected his MSE treatment of poly-

Table 7
Energy Differences (kcal/mol) Between Chair-Chair and Chair-Boat[a] Conformations of *trans*-2-Decalone Derivatives **53** to **58** (185)

Derivative	CFF	STO-3G[b]
53	8.3	5.1
54	6.5	2.9
55	7.3	0.69
56	7.9	4.0
57	7.3	3.8
58	4.9 (0.6)[c]	0.76 (1.6)[c]

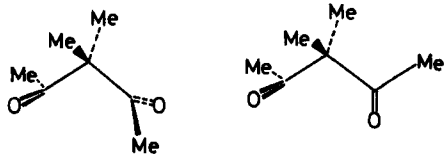
[a] Boat conformation in cyclohexanone ring.
[b] Single determinant *ab initio* MO with STO-3G minimal basis set.
[c] The force field used is Bartell's older version (186).



53 54 55

56 57 58

functional polar molecules to the problem of the conformations of 3,3-dimethyl-2,4-pentanedione (**59**) in solution. In heptane, the most favorable conformation is **59a**; **59b** is the next most stable, and is 0.16 kcal/mol above **59a**. In benzene the order is reversed, with a free energy difference of 0.17 kcal/mol. These calculations gave dipole moments of 3.06 and 3.48 D for the conformer mixture in heptane and benzene, respectively, which compares fairly well with the observed values (2.42, 2.77 D). Without the MSE theory, the usual MMI calculations predicted the shift in the equilibrium between **59a** and **59b** with solvent to be the reverse of that actually found (187).



a b

59

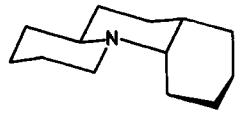
Since carbocations are structurally similar to ketones, they are discussed here. Schleyer's force field incorporates carbocation parameters, and Harris is exploring their application in conformational analysis (188). The calculated angles in a series of rigid polycyclic carbocations correlated well with ketone infrared frequencies (188a). The calculated relative stabilities among various conformers of tertiary cations of methylcyclohexane, methylcycloheptane, and methylcyclooctane do not contradict the limited ^{13}C MNR observations of these species at low temperature (188b).

3. *Nitrogen-Containing Molecules*

Despite considerable development in the experimental conformational analysis of nitrogen-containing molecules (189), MM applications to this class of molecules are rare, primarily because of the lack of good parameters (Table 8). Now that MM2 (and to a lesser extent MMI) includes well-tested (17f) parameters for nitrogen in sp^3, sp^2, and sp configurations, more applications will be seen in the near future.

Table 8
Small Organic Molecules Containing Nitrogen That Have Been Subjected to MM Calculations

Compound	Note	Ref.
Piperidines, etc.	Partial relaxation	190
C_6H_5—CH=N—C_6H_5	MODELS 2, partial relaxation	191
60	MMI, parameters undisclosed	192
$(CH_3)_3N^+CH_2CH_2X$	Partial relaxation	193
R—N=N—R′	MMI, azo parameters reported	194
$(RCO)_2NCH_2CH_2N(CH_3)_2$	MMI, amide parameters reported	195
CH_3CONRR'	MMI, amide parameters reported	196



60

The demand for precise force field parameters of the amide group is high, but only preliminary results have been reported (195,196) (see also Sect. VI-D).

4. *Silanes*

Silicon-containing hydrocarbons have long been the subject of successful MM calculations (197,198). Although the early calculations cannot be easily extended to silanes containing other heteroatoms because of the induced electrostatic interaction problem, polysilanes can be readily handled. Parameters for molecules containing Si—Si

bonds have been added to Mislow's modification of Allinger's force field (199). In tetrasilane ($H_3SiSiH_2SiH_2SiH_3$), unlike its congener *n*-butane, the anti conformation is 0.09 kcal/mol less stable than the gauche. The primary reason is that the nonbonded H_3Si/SiH_3 interaction across the long Si–Si bond (2.3 Å) is not severe. Hexadecamethylbicyclo[3.3.1]nonasilane (**60a**) was found by X-ray analysis to exist in a novel chair-half-chair conformation. MM calculations confirmed that this structure is the global minimum. Thus, the observed conformation of **60a** is not an artifact of crystal packing forces as was first suggested (199).

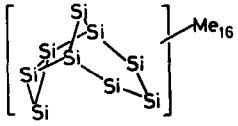
Electron diffraction data on gaseous cyclopentasilane (**61**) fit both the C_2 and C_s models. Rustad's simple MM method calculates virtually equal energies for these conformers, and **61** is likely to undergo pseudorotation, as does cyclopentane (200).

5. *Halides*

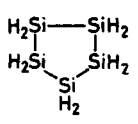
Organic halides have frequently been calculated by partial relaxation force fields including MODELS (43,201), a modified Urey-Bradley type (202), and others (203,204). An MM scheme developed from MODELS is being used in the extensive electron diffraction studies of mono- and polyhaloalkanes by Stolevik (205). MMI parameters for halides (17k) were supplemented for nongeminal dichlorides and fluorides (206). The most important advance has been made, as mentioned above, by Allinger's induced dipole calculations using the MSE approach (175), and by the evaluation of solvent effects (176). The best strategy at the moment for calculating organic halides containing other functional groups will be to use MM2 with some considerations for electrostatic interactions involving induced dipoles.

6. *Sulfur-Containing Molecules*

Whereas the variously catenated modifications of elemental sulfur can be satisfactorily treated by the MM method (207), organic sulfides and other sulfur-containing molecules suffer from the same polarization problem as do oxygen-containing molecules. Thus,



60a

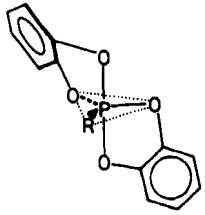


61

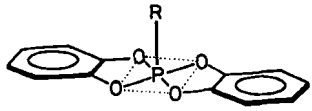
partially relaxing force field treatments of methylvinyl sulfide (208), 1,1-bis(methylthio)ethylene (209), and the 1,3-dioxathiolane ring system (210), as well as Synder's MMI parameters for di- (211) and trisulfides (212), may not be directly applicable to more complicated systems.

7. *Phosphorus-Containing Molecules*

Various hybridization states of the phosphorus atom have been parameterized in various force fields (Table 9). If a force field is to be useful for pentacoordinated phosphoranes, the relative energies of the two basic configurations, trigonal bypyramid (**62**) and square pyramid (**63**), must be differentiated. For this purpose, a 1,3-nonbonded interaction term centered only at the central phosphorus atom was added to MMI. In this modification, account was taken of



62

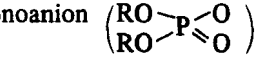


63

the effect of ligand electronegativity, which has the largest influence on the relative stability of these configurations, by giving different equilibrium nonbonded distances for various ligand atoms in this term (213).

The modification of QCFF/PI (Table 9) was intended to evaluate energies of 3′,5′-cyclic adenosine monophosphate (**64**) and related compounds. However, partly because of conventional parameteriza-

Table 9
MM Parameterization of Phosphorus-Containing Organic Molecules

Molecules	Framework Force Field	Ref.
Phosphines (PR_3)	MMI	17m
Phosphoranes (PR_5)	MMI	213
Phosphate monoanion 	QCFF/PI	214
	–	215

tion, the results of calculations were not highly satisfactory (214). Apparently, the charge interactions must be carefully evaluated.

Rigid-geometry *ab initio* MO calculations of 86 torsional isomers of the dimethylphosphate anion $(CH_3O)_2PO_2^-$ led to the determination of parameters for the Lennard-Jones type of nonbonded interaction, two- and three-fold torsional, and electrostatic interaction potential functions (215). Extension of this approach to full relaxation *ab initio* and MM schemes will be extremely useful, not only for phosphorus but also for other heteroatoms.

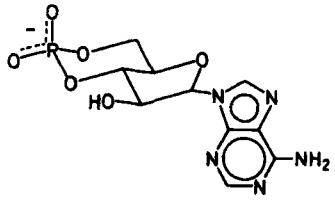
The X-ray structure of 1-dimethylphosphono-1-hydroxycycloheptane (**65**) was compared only with MM calculations of cycloheptane (216), but it should now be possible to include the substituents with one of the force fields in Table 9. Inorganic perhalophosphazenes, $(N{=}PX_2)_n$, have been subjected to MM analysis. Compared to hydrocarbons, the P—N—P bending force constant and the two-fold torsional barrier are small (217).

H. Metal Chelates

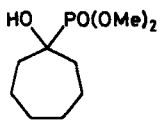
Three MM programs are reported to be able to handle metal chelates (Table 10). Those originating from Boyd's force field do not consider nonbonded interactions beyond 1.2 times the sum of the van der Waals radii (218-221). Rasmussen's version of CFF is much more sophisticated (33,222). However, none of them explicitly considers induced bond dipoles in chelate ions that contain a number of highly polar bonds. This is probably why the previous calculations of metal chelates only compare closely related isomeric structures having the same metal ion.

I. Natural Products and Molecules of Biological Interest

Natural hydrocarbon products such as terpenes and steroids have been subjected successfully to MM calculations. Sesquiterpenes



64



65

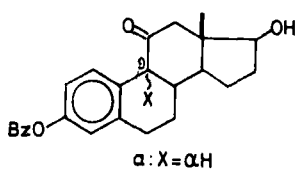
Table 10
MM Programs for Metal Chelates

Original Version	Metal Ion	Ligand Atom	Ref.
Boyd's program (37)	Co^{3+}, Ni^{+}	N	218-221
CFF (30)	Co^{3+}, Cr^{3+}	N, S	33,222

were studied with regard to the conformational control of their cyclization reaction and are discussed in Sect. V. Extensive calculations have been carried out on steroids (10d, 10f, 50). The examples mentioned below, performed by Allinger's earlier force field versions (1971 and MMI) (14,15), unanimously indicate that these versions give reliable structures but not very accurate energies.

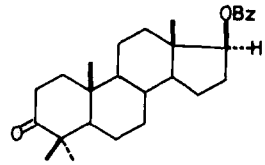
11-Oxoestradiol-3-benzyl ether (**66**) was found to be less stable when the 9-hydrogen is in the normal α-configuration (**66a**) than the 9β-epimer **66b** ($\Delta\Delta G^{\ddagger}$ 1.47 kcal/mol by NMR). MMI calculations on a number of conformations indicate that the most stable conformations of **66a** and **66b** have ring B in the half-chair and ring C in the chair form. However, the calculated enthalpy of the best **66b** conformer was only 0.5 kcal/mol more stable than that of the best **66a** conformer; this is qualitatively correct, but quantitatively disappointing (223).

The A-ring conformation of 4,4-dimethyl-3-keto steroids (e.g. **67**) may not necessarily be a regular chair in view of the flexibility of the ring conferred by the presence of an sp^2 center and the severe steric repulsion between the 4- and 19-methyl groups (224). Indeed, several conformations have been found with the deformed chair dominating (224,224a). Calculations on various conformers of 4,4-dimethyl-3-keto steroids by MMI indicate that the A-ring deformed chair and the twist boat conformations are very close in energy, the difference favoring the chair by about 0.2 kcal/mol (225). It has been found by



a: X=αH
b: X=βH

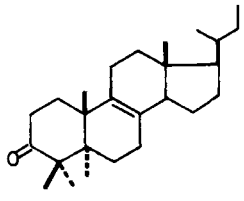
66



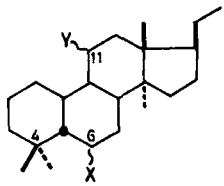
67

X-ray analysis of 4,4-dimethylandrostan-3-on-17β-yl benzoate (**67**) that the A ring is in a deformed chair conformation (225) in the crystal, and NMR and dipole moment measurements show the same to be true in solution.

For lanost-8-en-3-one (**68**), the A-ring boat conformation is 1.00 kcal/mol more stable than the corresponding A-ring chair conformation according to Allinger's 1971 force field. Extended Hückel MO calculation of the final MM geometries (28) reversed the stability order, showing the A-ring chair conformation to be the more stable by 1.14 kcal/mol, which is in accord with NMR observations (224).



68



	OH X	Y
a	α	β
b	β	β
c	β	α
d	α	α

69

More crowded systems are the 4,4,14α-trimethylpregnan-6, 11-diol isomers (**69a–69d**) having a cis B/C ring junction. The α-backside of the molecule is crowded to varying degrees, depending on the orientation of the 6- and 11-OH groups. Unfortunately, X-ray analysis was successful only with **69a**, could not be completed with **69b** and **69c** because of severe disorder, and was totally unsuccessful with **69d**. Hence MMI calculations were performed on various possible conformations to supplement the X-ray results. Table 11 lists the calculated best conformers, along with the results of the X-ray structure analysis. The novel observation of a boat cyclohexane conformation in **69a** as well as in **69b** should be noted. Whereas the agreement between the observed conformations and the best calculated conformers of **69a** and **69c** is gratifying, neither the expected equilibrium CBB ⇌ CCC in **69b**, nor the predicted preference of the nonchair conformation for **69d** could be confirmed by NMR experiments (226).

The C/D ring junction in several derivatives of Δ^8-11-keto steroids (**70**) is preferentially cis, irrespective of the nature of the substituent at C_{17}, which exerts a decisive influence on the C/D cis-trans equilibrium of the saturated 15-keto analogs. MMI calculations suggest that the dihedral angle between the C_{17}-substituent and the angular C_{18}-methyl in **70** is large enough to exclude the possibility of a serious interaction between them, and that the well-known thermody-

Table 11
X-Ray and MM Analysis of 4,4,14α-Trimethylpregnan-6,11-diol Isomers (69) (226)[a]

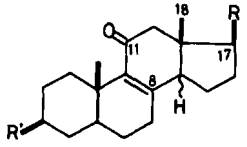
Isomer	X-Ray	MM
69a	CBB	CBB
69b	CBB	CBB ≈ CCC
69c	CCC	CCC
69d	–	CBB

[a]Three-letter notation indicates the chair (C) and boat (B) conformations, respectively, in the A, B, and C rings.

namic stability of *cis*-8-methylhydrindane over the trans form also governs the relative stabilities of cis versus trans isomers of **70** (227).

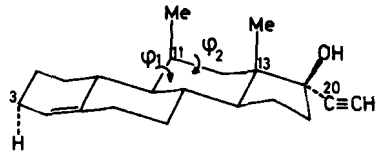
Better agreement with experiments is expected from recalculations on these steroid derivatives with an improved force field.

According to Schneider's MMI calculation (227a) of 11β-methyllynestrenole (**70a**), the calculated minimum energy structure differed considerably from that obtained by X-ray analysis. The disagreement suggests the high flexibility of the molecule. Indeed, the energy surface resulting from the variation of two endocyclic dihedral angles (ϕ_1,ϕ_2) turned out to be flat near the minimum point. Furthermore, a computer experiment was carried out wherein the change in total steric energy was followed during forced bending of the molecule so that its β-side deformed into a convex shape. When the distance between H_3 and C_{20} was decreased from the equilibrium value of 8.4 to 7.2 Å, the total energy increased only 1.7 kcal/mol. This means that the local strain generated by the strong reflex effect between two axial methyl groups at C_{11} and C_{13} must have dissipated over the whole molecule, indicating again the importance of the total relaxation MM treatments in conformational analysis (see Sect. VI-C).



R=H,Et,Pr
R'=H,OH

70

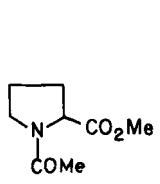


70a

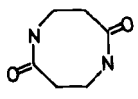
Any attempt to treat biologically interesting molecules such as peptides with one of the popular, full relaxation MM programs will be frustrated by inadequate parameters for amide groups (cf. Table 8). Extensive calculations on *N*-acetylproline methyl ester (71) by DeTar (228) are based on the Schleyer force field with a minimal set of amide parameters added, including a Coulombic charge interaction term; but it is not calibrated against reference molecules. The energy contour map for a pseudorotating ring conformation of 71 thus prepared was, however, similar to those obtained previously by other workers using different methods, and contained 27 out of 40 X-ray geometries in regions whose energies are less than 1.5 kcal/mol above the minimum energy. Thus DeTar concluded that the general features of the molecular energy contour are rather insensitive to the level of the force field model.

White and Guy (229) published a simple valence force field parameterization for the amide group. While this force field does not take induced dipole interactions into account, cyclodi-β-alanyl (72) and cyclotetraglycyl (73) have been well calculated (229,230). The work with the simplest natural protein model 73 illustrates the problems generally associated with polypeptides. The torsion angles ϕ and ψ involve very low barriers, hence a vast number of conformations must be considered to determine the "global minimum energy conformation" (GMEC). For 73, 7776 conformational isomers were processed, first by rational use of chemical constraints (steric requirements for ring closure, etc.) and of a Ramachandran plot, and then by visual screening of the surviving structures with a graphic display system. In this way, the number of GMEC candidates was reduced to 40. MM calculations of these finally gave the structure 73 as the GMEC, which agrees well with NMR observations (230).

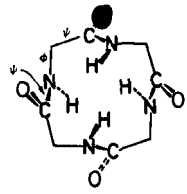
There is considerable activity in the area of MM calculations on small polypeptides. A preliminary amide force field based on the CFF (231,232) and a partial relaxation force field (233) has been reported. Interested readers are referred to review articles cited in ref. 232.



71



72



73

J. Heats of Formation

The final part of this section concerns energy calculations by the MM method. The success of conformational MM calculations depends largely on the accuracy of energy rather than on structure. The problem has been discussed (10d). We mention here only the latest results.

Gas phase enthalpy calculations by various force fields including Allinger's 1971 version (14), MM2 (16), the Schleyer force field (26), and the White-Bovill force field (27) have been compared to assess their accuracy in terms of the careful determination of heats of combustion of polycyclic hydrocarbons (234). For adamantanoid molecules, MM2 predictions agreed with experiments within 0.7 kcal/mol, substantiating the superiority of MM2 over other "first-generation" force fields. Absolute enthalpies may differ from one force field to others and from experimental values in a range of a few kilocalories per mole. Agreement among calculated relative energies of closely related systems is much better, because of cancellation of some of the defects in the force field (234).

Another potential experimental technique that serves as a source of reliable heat data is hydrogenation. The heat of hydrogenation of an unsaturated hydrocarbon gives the difference in enthalpies between the unsaturated and saturated molecules. Sensitive micro devices for precise measurements of heats of hydrogenation have been developed recently (236,237). Based on the heats of hydrogenation of all the linear alkynes containing 6 to 10 carbon atoms, MM2 parameters for alkynes have been determined (237). Conversion of the observed free energy change upon hydrogenation to steric enthalpy requires an estimation of the $T\Delta S$ term. For simple alkynes as studied above, the usual statistical thermodynamic treatment is sufficient (25). For larger molecules, DeTar's program computes partition functions for any methyl-substituted alkane (63).

V. REACTION MECHANISMS

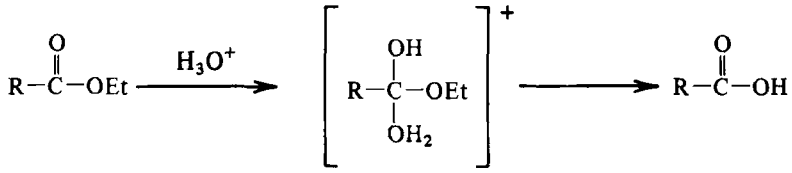
Despite their inherent limitations, MM methods have been intensively exploited as a tool for obtaining information about reaction mechanisms (10a, 10d). If a reaction involves a transition state or a key intermediate with a well-defined geometry, the MM treatment can be applied in a straightforward manner. Even if the mechanism is unknown, a number of ways are available to utilize the MM method

for obtaining mechanistic information by calculating all intermediates as well as all products possible on different pathways to detect those of lowest energy.*

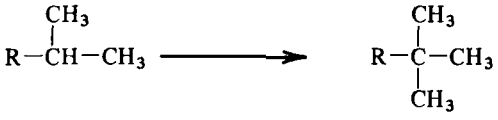
A. Simulated Transition States

1. Hydrolysis and Esterification

The acid-catalyzed ester hydrolysis provides a good target for MM treatments. DeTar first used hydrocarbon models in which an ester was approximated by an isoalkane (74) and the intermediate (75) by a neoalkane (76). He assumed that if the rate of reaction truly is not influenced by polar effects but is governed only by steric effects of R, as has been generally postulated, the rate must be proportional to the energy difference ($\Delta\Delta H_f^\circ$) between 74 and 76. The $\Delta\Delta H_f^\circ$ is mainly determined by the van der Waals strain in these branched alkanes. Nonsteric group increment terms were carefully adjusted, and statistical mechanical corrections for conformer populations



75



74 76

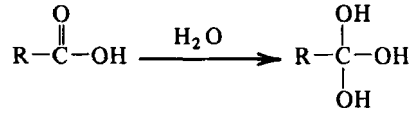
were included. Calculations using the Schleyer force field (26) indeed gave a linear relation:

$$\log\frac{k}{k_0} = -E_s = 4.419 - 0.552\Delta\Delta H_f^\circ$$

*Semi- and nonempirical MO calculations involving complete geometry optimization are now being developed for simulating chemical reactions of small molecules (238,239).

where k is a rate constant, and the subscript zero refers to a standard, ethyl acetate (240).*

Later, DeTar (241) tentatively implemented parameters for alcohols and carboxyl groups in the Schleyer force field to treat esterification, this time using the "orthoacid" model (77):



77

The calculated steric energy difference between 77 and the acid, ΔSE, showed a somewhat closer relation†:

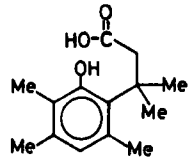
$$\log \frac{k}{k_0} = -E_s = 0.340 - 0.789\Delta SE$$

These studies confirmed that Taft's E_s values are truly a measure of the steric effect of the alkyl group R. DeTar further suggested to use the E_s value as a measure of the van der Waals type of strain in hydrocarbons (242).

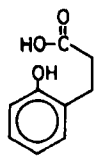
The idea of "stereopopulation control" is an important concept in the study of enzyme reactions, originating from the observation of a 10^{11} increase in the rate of lactonization of polymethylhydrocoumaric acid (78) compared to that of the less crowded model 79. The large rate difference was interpreted as arising from restricted rotation of the sidechain in 78 so that the carboxyl group was effectively frozen into a conformation favorable for the reaction. An alternative interpretation in terms of B-strain relief in 78 is now advanced, based on MM calculations using Boyd's force field (37). The ground state strain of 78 is 8.4 kcal/mol higher than that of the product lactone, whereas the corresponding strain relief in the lactone formation of the unsubstituted 79 is only 1.9 kcal/mol. Consideration of other thermodynamic terms led to a calculated difference in lactonization rates between 78 and 79 of 3×10^{10}, strikingly close to the observed value (243). Secondary isotope effect experiments support the conclusion (244).

*The range of k_{rel} is 10,000 for 24 esters; SD, 0.4; correlation coefficient, -0.95.

†Range of k_{rel}, 4000 for 25 acids; SD, 0.24; correlation coefficient, -0.98.



78



79

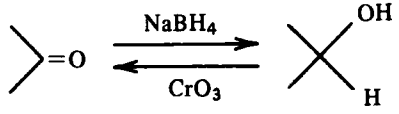
2. *Nucleophilic Substitutions*

Verification of the presumed role of the F-strain in the S_N2 reaction was first attempted by classical hand calculations of the Ingold school on rigid models, then again on rigid models but allowing rotation of groups (245), and finally by the full relaxation MM method (246). In the latter, experimental thermodynamic parameters of standard alkyl series were averaged by Streitwieser's method, and the parameters of a pentacoordinated α-carbon atom and a half-bonded bromine atom (leaving and attacking groups used in this work) for the Schleyer force field were carefully chosen. Agreement between experiment and calculations was satisfactory except for methyl and *t*-butyl bromides (Table 12). Polar effects are suggested to dominate the situation in these two extreme cases (246).

Limited calculations of nonbonded interactions on the presumed transition states of S_E2 (247) and *E*2 (248) reactions have also been reported.

3. *Nucleophilic Additions*

The additions of nucleophiles to ketones have been classified as governed either by "product development control" or by "steric



approach control," depending on whether thermodynamic stability of the product or steric hindrance to the approach of the nucleophile is the prevailing factor. Müller and Perlberger (249) first tried to correlate the observed rates of reduction (k) with complex hydrides by a linear combination of these two factors:

$$\log k_{rel} = A_1 \cdot \Delta_{strain} + A_2 \cdot R + A_3$$

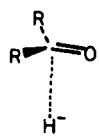
Table 12
Observed and Calculated $\Delta\Delta H^{\ddagger}$ Values in S_N2 Reactions of Alkyl Bromides Relative to Ethyl Bromide (246)

Alkyl Group	$\Delta\Delta H^{\ddagger}$ (kcal/mol)	
	Experimental (Average)	Calculated (MM)
Me	-2.42	-6.20
Et	0.0	0.0
n-Pr	0.28	0.04
i-Bu	1.99	1.87
neo-Pe	6.85	7.03
i-Pr	2.62	4.61
t-Bu	4.01	11.77

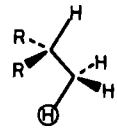
where Δ_{strain} represents the strain difference between the alcohol and the ketone, and R the steric hindrance of the carbonyl group toward an approaching nucleophile from one side; A_1 and A_2 are proportionality constants, and A_3 is a scaling factor. The Δ_{strain} values for a number of ketone-alcohol combinations were calculated using the Allinger 1971 force field (14), but replacing OH with CH_3 because of the lack of OH parameters in this early version. The magnitude of R should correspond to the steric energy of the hydride anion placed close to the carbonyl carbon atom (**80**); it was approximated by summing all the steric interactions of the proton of the methyl group shown in **81**. Regression analysis led to the determination of A_1, A_2, and A_3 with a correlation coefficient of 0.93 and a standard deviation of 0.79 for the equation above.* According to this analysis, the relative rates of ketone reduction can be predicted to within a factor of 6. However, the Δ_{strain} term appears to have been overestimated relative to the R term, since the observed exo-endo ratios could not be reproduced satisfactorily.

To improve the situation, the investigators proceeded to unify Dauben's dual control formalism by postulating a single transition state (**82**), in which the carbonyl carbon is already sp^3-hybridized and the hydride ion partially bound at a distance of 2.30 Å perpendicular to the carbonyl plane. Steric energies of **82** for various ketones were calculated and the differences relative to the steric energies of the starting ketones (Δ_{strain}) were plotted against log k_{rel}. This re-

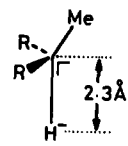
*k_{rel} is the rate constant relative to cyclohexanone under fixed reaction conditions; Δ_{strain} and R are in kilocalories per mole.



80



81



82

fined approach gave a linear relation with a correlation coefficient of 0.85 and a standard deviation of 1.0. For a range of 10^8 in k's, predictions are now possible with an uncertainty of ± 10%, including the correct exo-endo ratios (250).

Wipke and Gund (251) elaborated the idea of steric approach control. They distinguish *steric congestion* in the isolated ketone from *steric hindrance* generated by the approach of a reaction partner. Steric congestion is a ground state property of the ketone. A nucleophile is assumed to attack the carbonyl carbon through a "cone of preferred approach," the axis of which coincides with a line perpendicular to the plane of the carbonyl group. Intersection of the cone with a sphere of the van der Waals radius of the carbonyl carbon represents the accessibility of carbonyl carbon from this side of the carbonyl plane. Congestion is defined as the reciprocal of this cross section and was calculated on the basis of geometries obtained by a simple MM program SYMIN. This treatment satisfactorily reproduced the endo-exo and axial-equatorial ratios of the steric approach-controlled addition of bulky reagents to hindered ketones. Common to both Müller's and Wipke's approach (249–251), the preferred angle between the carbonyl plane and the line of approach of the attacking nucleophile was assumed to be 90°. However, there is strong indication that the angle should be close to the tetrahedral value, based on crystallographic data and MO calculations by Bürgi and Dunitz (252).

4. *Carbonium Ion Reactions*

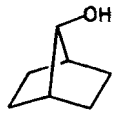
Carbonium ions are well-defined transition states in many reactions. Indeed, one of the earliest applications of MM method to the reactivity problem was concerned with carbonium ions. At present, only the Schleyer force field (26b) and its predecessor (253) are capable of handling carbonium ions, although the parameterization principle used earlier can be readily improved upon to the present standards. Schleyer's measure of steric strain in carbonium ions, Δ_{strain} (the difference in steric energies of free carbonium ion and its

precursor hydrocarbon), correlates well with tertiary (125,253–258) and secondary (260–263) carbonium ion reactivities for a variety of skeletal types.

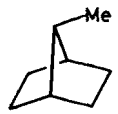
The MM method proved to be remarkably useful for elucidating the complex mechanisms of the famous syntheses of adamantane and diamantane as well as other diamondoid molecules from isomeric polycyclic hydrocarbons under Lewis acid catalysis in Schleyer's laboratory (128,258,264–266).

5. *Product-like Transition States*

If the point of highest energy along the reaction coordinate is close to the product, the activation energy should correlate with the enthalpy difference between reactant and product. The oxidation of secondary alcohols to ketones with chromic acid (reverse of the hydride addition to ketone) appears to fall into this category. Müller and Perlberger applied Allinger's 1971 force field to this problem. Since this version lacked alcohol parameters, they approximated alcohols with the corresponding methyl derivatives (e.g., **83** vs. **84**).



83



84

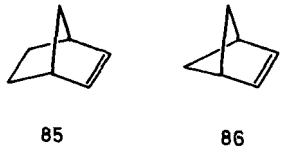
The plot of Δ_{strain} (calculated difference in strain energy between the methyl derivative and the ketone) versus log k_{rel} (observed relative rate of chromic acid oxidation) gave a moderately good linear relation (267,268).

Several additional examples are known wherein late transition states are suggested on the basis of MM calculations (the most stable product tends to form), including dimerization of adamantene (269), ring opening of highly strained cage compounds by catalytic hydrogenation (270) as well as by homoketonization (271), and also transannular ring closure reactions in various cage molecules (272,273).

6. *Reactant-like Transition States*

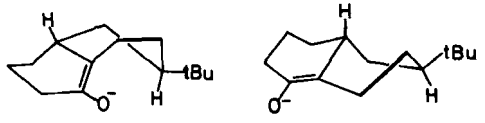
The lactonization of a crowded hydrocoumarin (78), or more generally reactions driven primarily by strain release, can be regarded

as having early transition states. The exceptionally high reactivity of norbornene (85) in addition reactions was studied again by the use of the MM2 force field (16). The olefin strain minus that of the corresponding hydrocarbon (i.e., the Δ_{strain}) of 85 was about half that in bicyclo[2.1.1]hexene (86); thus at least the strain effect can be eliminated as a potential cause for the unusual reactivity of 85 (274).

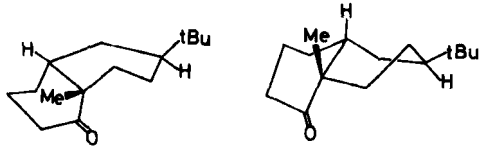


85 86 87

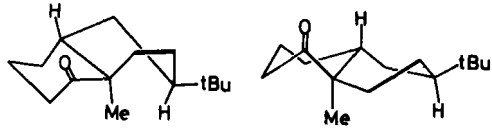
Alkylation of 6-*t*-butyl-decalone-1 enolate (87) was closely followed by X-ray and MM analyses. Based on MMI steric energies of model olefins and X-ray analysis of the *p*-nitrobenzoate of 87, the enolate should have the A ring in a twist-boat conformation as in 87a and 87b. Among all possible initial alkylated products (88–91) obtained from 87a and 87b with the least motion of other atoms, one of the trans products 91 is the most stable according to calculations. However, the final product, as confirmed by X-ray analysis, has a cis ring juncture. Therefore, the transition state of this reaction with the alkylating agent approaching from the less hindered convex



87a 87b



88 89



90 91

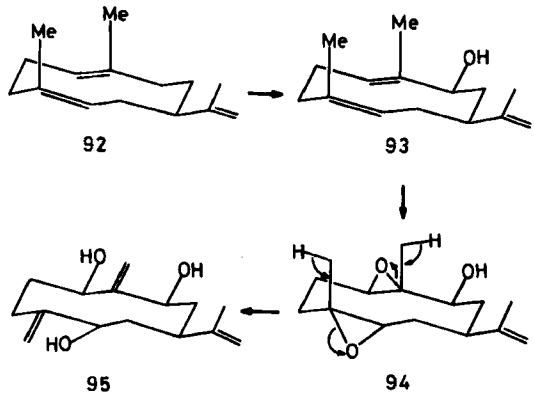
side must lie much earlier on the reaction coordinate than these tentative products indicate (275).

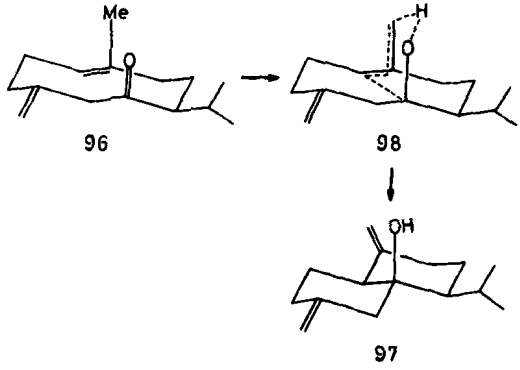
B. Conformational Control

Medium ring compounds are flexible, and a knowledge of their predominant conformations should help to predict the course of reactions in these molecules (276). MM calculations proved to be useful in this respect as well, especially for transannular reactions of sesquiterpenes (10a,277,278).

Germacrene A (**92**), agerol (**93**), agerol diepoxide (**94**), and ageratriol (**95**) are believed to represent a biogenetic series. The indicated conformations have been confirmed by X-ray analysis for **94** and **95** (279) and by an NMR shift reagent study for **93** (280). MM calculations on various conformers by GEMO (279,280) and also by MMI (278b) revealed that the indicated conformations (**92–95**) are GMECs of each compound. Thus, *in vivo* transformations are likely to take place from the most stable ground state conformations.

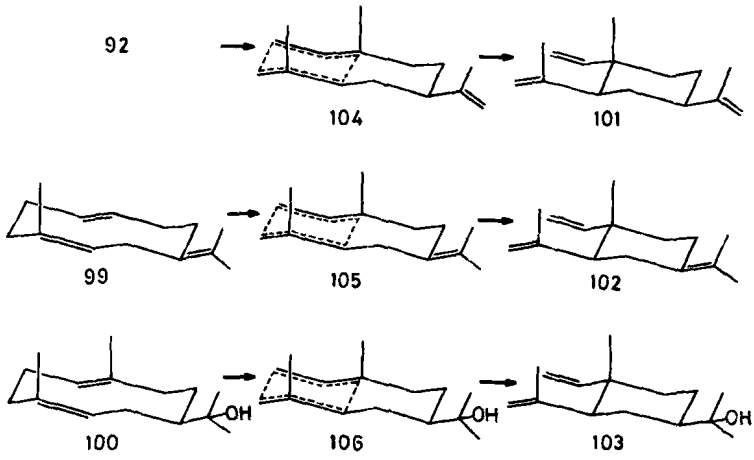
The transannular ring closure reaction of preisocalamendiol (**96**) to dehydroisocalamendiol (**97**) proceeds in a regio- and stereospecific manner even at 180°. The GMEC of **96** (as shown) is only marginally more stable than other conformations of preisocalamendiol, and at the reaction temperature accounts for only 46% of the population, according to MMI (16) calculations. However, the energy difference between GMEC and other conformations increases in a transition state like **98**, which was optimized under some restrictions with appropriate parameters for half-bonds. The product conformation (**97**) agrees with what one would expect from **98**. Hence, in this case too,





the ground state conformational control of **96** over the product conformation surely exists, albeit indirectly (281).

In the Cope rearrangements of germacrene A (**92**), germacrene B (**99**), and hedycaryol (**100**), the indicated conformations of reactants, called "CC" according to the Wharton convention (278a), may seem to control the product conformations (**101–103**), but in the ground state these conformations are occupied to the extent of only 20 to 60%. The CC conformers of **99** and **100** are not even the GMEC according to MMI calculations. However, the assumed transition state conformations **104–106**, which are derived from the CC conformations and optimized as mentioned above, are the overwhelming GMECs among other transition state conformers derived similarly from different ground state conformers (282). It appears desirable that the ad hoc parameters for half-bonds used in these calculations be verified in some independent way.



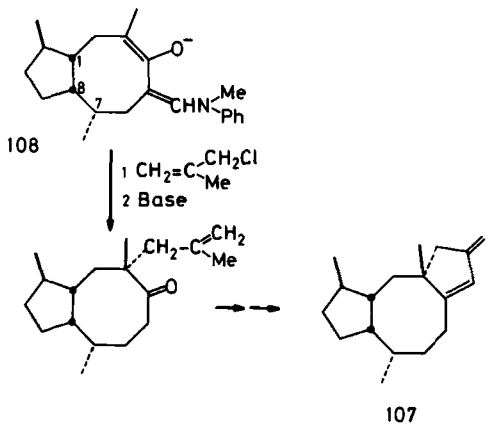
A key feature in the stereochemistry of a novel tricyclo[9.3.0^{3,7}]-tetradecane derivative (**107**) related to the phytotoxic ophiobolins was determined by the MM method. Hydrocarbon models of an intermediate **108** were subjected to MMI calculations and the GMEC thus determined had one side of cyclooctane ring completely blocked by diaxial hydrogen atoms at C_1 and C_7. The alkylating agent (methallyl chloride) then had to approach from the other side of **108**, giving the stereochemistry of the methyl group at the quaternary carbon as shown, agreeing with that of ophiobolin (283).

C. Thermolysis of the Carbon-Carbon Bond

Thermal cleavage of C–C bonds has been studied in cyclopropanes and cyclophanes, and particularly extensively in highly substituted alkanes. Rüchardt and his school discovered a linear correlation between the experimental activation enthalpy for the homolysis of the weakest bond in overcrowded ethanes and the strain in the ground states of these molecules in accordance to MM2 calculations (284).

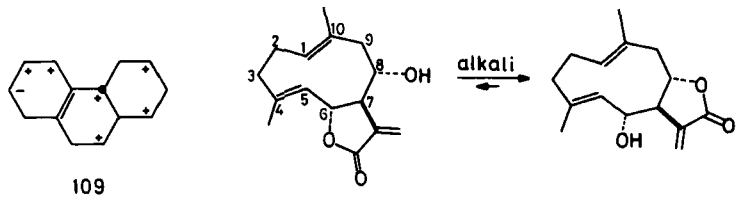
D. Product Distribution

Another area to which the MM method can be advantageously applied is the prediction of product distribution under thermodynamic control, where the errors in energy calculations tend to cancel if structurally related products are compared (120). A remarkable example is the dodecahydrogenation of phenanthrene, in which 25 structural isomer products are possible, each having one to four stable



conformations. No experimental method is available to characterize such a formidable mixture. Exhaustive MMI calculations were performed, and structure **109** was found to be the most stable (285).*

Certain germacranolides containing lactonizable α-oriented oxygen functions at C_6 and C_8 (e.g., **110**) can be relactonized at C_8 to give **111** when treated with strong alkali. MM calculations† of these and related structures confirmed that the steric energy of **111** is 1.4 to 5.9 kcal/mol lower than that of **110**. The greater stability of **111** arises from a smaller calculated dihedral angle along $C_6C_7C_8C_9$ compared to that of $C_5C_6C_7C_8$. The α-methylene-γ-butyrolactone ring prefers a flat structure according to model calculations, and the trans fusion of the α-lactone ring to the cyclodecadiene ring occurs preferentially at the place (in this case at C_8), where the attached lactone ring can occupy a conformation as flat as possible (287).

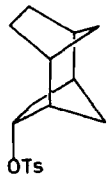


109 110 111

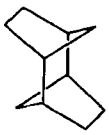
Product distributions in thermodynamically controlled rearrangements of polycyclic hydrocarbons have been extensively studied for a number of neutral C_nH_m families with n up to 20 (288). In these cases, the GMEC is called the "stabilomer," and usually it can be isolated by treating any isomeric hydrocarbon with a strong Lewis acid such $AlBr_3$. Under mild conditions, local minimum energy isomers are sometimes isolated. The local minima are usually important "stations" in the rearrangement pathway between starting structures and stabilomers (255,258,264,288). A "head-to-head" dicyclopentane derivative **112** gave upon acetolysis an acetate-olefin mixture of "head-to-tail" (**113**) as well as "head-to-head" skeletons, with the former predominating. The reverse skeletal transformation, **113** → **112**, does not occur. MM calculations with Schleyer and Allinger 1971 force fields indicate that **113** is about 10 kcal/mol more stable than the carbon skeleton of **112** (289).

*The plus and minus signs indicate, respectively displacements of carbon atoms in the direction above or below the general molecular plane.

† Lactone parameters are introduced into the White-Bovill force field (27) after calibration with experimental data on santonins (286).



112



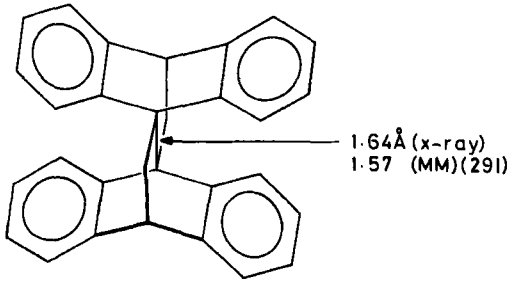
113

VI. SPECIAL APPLICATIONS

This section illustrates several interesting applications of molecular mechanics to problems involving areas other than conformational analysis and reaction mechanisms.

A. Separation of Electronic and Steric Effects

The capacity of the MM method to predict molecular structures with high accuracy can be utilized to identify special electronic effects. Thus, if a MM-calculated structure deviates significantly from the observed in a case where the force constants and potential functions may be presumed to be valid, something not of steric origin is probably responsible. For example, when unusually long C–C bonds are observed in X-ray analyses, crystallographers tend to give steric explanations (290). However, the steric strain may be not large enough to stretch a bond to unusual length. The MM-calculated central bond length of lepidopterene (**114**) is significantly shorter than the observed length. Mislow demonstrated that the observed bond lengthening in these cases are due to "through-bond" coupling between adjacent π systems. The subject has been reviewed (66). Recently, it was recognized that a prestrained σ bond was particularly



114

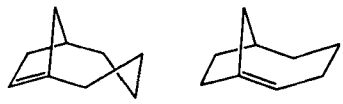
effective as a transmitter of the "through-bond" interactions (291). Other hyperconjugative effects have also been discovered, based on the discrepancy between results calculated by MM and MO methods (253,293).

B. Bredt's Rule

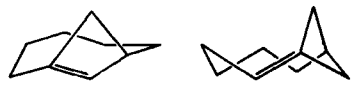
All the amendments to Bredt's rule that have been presented in the past decade have been more or less violated. One reason for these failures is that the past rules ignored the strain in parts of the molecule other than at the bridgehead double bond. Schleyer defines the strain at the bridgehead double bond, or "olefin strain" (OS), as the difference in strain between the olefin and the parent hydrocarbon, analogous to "Δ_{strain}" for carbonium ions (293). He finds that olefins having OS values higher than 21 kcal/mol are too unstable to survive isolation. This rule has so far found no exception. Already Burkert has shown by application of Allinger's 1971 force field (14) that olefins like bicyclo[4.2.1]nonenes (**115**) and bicyclo-[5.1.1]nonenes (**116**) with the double bond located in the smaller ring (**115a**, **116a**) are less strained than the isomers **115b** and **116b**, with the double bond in the larger ring (294). The ingenious use of relative energy differences derived from MM calculations seems appropriate in view of the relatively larger errors in the calculation of the total energies.

C. Analysis of NMR Spectra

There is no doubt that the most powerful tool for studying molecular structures in solution at the present time is NMR. Given the high sensitivity of chemical shifts and coupling constants to conformation and steric environment, an obvious expedient is to use MM-



115a 115b

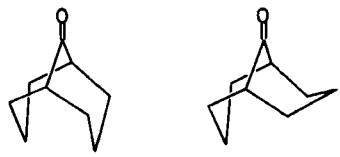


116a 116b

optimized structures for the analysis of NMR spectra. Gas phase conformations of nonpolar molecules are generally very similar to solution conformations, and the importance of using the fully optimized structure is being more fully recognized.

An interesting application of the MM method to the analysis of NMR spectra was the calculation of dihedral angles from vicinal proton coupling constants that took into account electronegativities of substituents at the carbon atoms carrying the protons in question. In this case, dihedral angles calculated by Boyd's force field (37) were used as substitutes for experimental values (295). A recent paper (296) states that $^1J_{C-H}$ values of cyclohexane, cyclopentane, cyclobutane, and cyclopropane correlate with MMI strain energies of these ring compounds (standard deviation 0.2 Hz, correlation coefficient 0.99) better than with bond orders or excitation energies.

In their new approach to the analysis of lanthanide reagent-induced shifts (LIS), in which absolute bond shifts are calculated for lanthanide complexes of well-defined geometries using nonlinear regression analysis, Raber and Johnston (297) often use MMI-optimized geometries of substrates. They find bicyclo[3.3.1]nonan-9-one to exist in CCl_4 as a 78:22 mixture of double chair (**117a**) and chair-boat (**117b**) conformers. The composition corresponds to the point of the best agreement factor (297b).



117a 117b

The most elaborate use of MM calculations in the LIS analysis was described by DeTar and Luthra (298). Their approach was based on the traditional "relative shift" method, wherein lanthanide parameters are adjusted to give optimum agreement with the observed relative LIS values. Based on their previous analysis of proline conformations (228), they determined that *N*-acetylproline methyl ester (71) exists in $CDCl_3$ as a 60:40 mixture of half-chair and envelope conformations by simultaneously adjusting the substrate geometries and the conformer mole fractions, in addition to the lanthanide parameters (298).

The full advantage of using MM-relaxed structures appears in the analysis of ^{13}C NMR spectra (299). Smith and Jurs presented an

empirical method of predicting ^{13}C chemical shifts using an empirical equation containing topological and geometrical descriptors. The parameters in the equation were optimized by multiple linear regression analysis. When structures obtained by the MMI force field were used in the parameterization, the standard deviation in the error of calculated versus observed chemical shifts was only 1.1 ppm (300).

Schneider modified the calculation of the Grant-Cheney force that evaluates shielding by steric perturbations. The force F exerted at the C_i–H bond (C_i being the carbon atom whose chemical shielding is to be computed) is calculated by an equation similar to that for a nonbonded potential:

$$F = k\frac{18\epsilon}{r^*}\left[\left(\frac{r^*}{r}\right)^{10} - \left(\frac{r^*}{r}\right)^{7}\right]\cos\theta$$

where k, ϵ, and r^* are constants, r is the distance between the hydrogen attached to C_i and the interacting H or C, and θ is the angle between the force vector and the C_i–H bond (301). Obviously one may use MM-optimized structures for the calculation of r and θ. With axial methylcyclohexane, for example, the unrelaxed geometry overestimates ΣF for the 1-3 C–H interaction by 500% compared to the fully relaxed structure (227a).

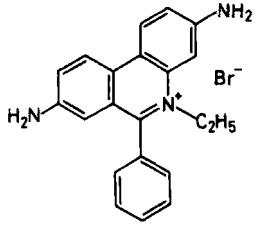
D. Molecular Modeling and Drug Design

As exemplified above, molecular geometries optimized by MM calculations provide the best three-dimensional molecular models available at the lowest possible cost. The relaxed structures are useful for many purposes (303), and an especially active area of research is computer-assisted drug design (304). Several molecular analysis systems designed to assist in developing structure-activity relations are known (304b,305). In such systems, structures are first minimized by the MM technique (304b,305) and then used as inputs for more sophisticated quantum mechanical calculations, for more MM calculations of torsional energy surfaces (306), and for comparison with structures possessing similar biological activities, to look for nonobvious similarities, and so on.

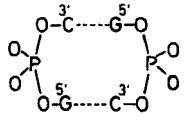
The drug designers often use a graphical display to assess three-dimensional structures, usually in stereo pair projection (307). A technique is being developed to recognize the "pharmacophoric pattern," the geometric arrangement of the key functionality that governs a drug's interaction with its receptor, wherein the MM

technique is useful to optimize particular geometries of the drug molecule in interaction with the receptor (308).

In this regard, recent partial MM relaxation calculation on DNA and RNA intercalation models merit special attention. Kollman (309) performed preliminary studies on the interaction of cationic intercalators like ethidium bromide (118) with two base-paired dinucleoside monophosphates, CpG (119),* and GpC. Their MM scheme minimizes 14 torsional (only for 119) and 12 intermolecular



118



119

(electrostatic and van der Waals interaction) degrees of freedom. The torsional potential is of the Fourier type, consisting of $V2$ and $V3$ terms to simulate the tendency for R–O–P–O groups to have a gauche dihedral angle. Hydrogen bonds were taken care of solely in terms of the Coulombic potential (310). Calculated structures of uncomplexed base pairs and of their complexes with the inserted compound agreed well with those determined by X-ray analysis. Component analysis of calculated interaction energies revealed very strong attractions between the intercalating drug molecule and the sugar-phosphate backbone and the base of the dinucleosides (ca. 80 kcal/mol). These calculations are purely "empirical" in that they were started from crystal coordinates. Otherwise, calculations of such a large molecular assembly would have been impossible because of the enormous number of possible conformations (cf. Sect. VI-I) (311). Further discussion on this topic is beyond the scope of this chapter (13).

E. Crystals

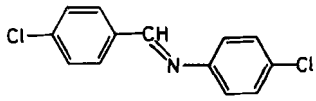
The X-ray analysis of crystals is by far the best experimental method in modern structural chemistry, as judged by the vast amount

*Cytidyl(3′-5′)guanosine monophosphate.

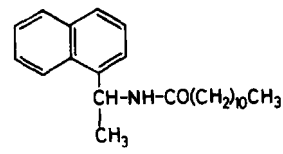
of structural information obtainable from a single determination. For all types of empirical force fields, X-ray results provide an important and rich source of data for parameterization of intra- and intermolecular potential energy functions. Most of the currently available MM schemes concern vapor phase properties, but their parameterization in fact relied heavily on crystal data. The present restriction of the standard MM scheme to the vapor phase is only a consequence of necessity, and future MM programs should encompass the solid and liquid (312) phases as well.

Kitaigorodsky (10b) and a few other groups (13,313–316) have been concerned primarily with molecular potentials in crystals. CFF is now being updated to include parameters for crystalline amides (317) and carboxylic acids (310,318) involving hydrogen bonds. For this purpose, a benchmark data bank consisting of 14 carboxylic acid and 12 amide crystal structures has been presented (318a). The most striking and useful finding in this work is the adequate description of hydrogen bonds by a simple point charge approach without inclusion of a special van der Waals potential function. These results may be transferred to the other force field models. The program MCA (314) calculates crystal energies, equilibrium geometries, and lattice vibrations of molecular crystals (30) and is extremely useful for the analysis of problems that could not be handled by previous rigid body treatments (10c). Recent applications include interpretations of the conformational polymorphism in *N*-(*p*-chlorobenzylidene)-*p*-chloroaniline (120) (319), the large red spectral shift in aggregated chlorophylls (320), as well as the chiral recognition of guest diamides by *N*-R-α-(1-naphthyl)ethylamine (121, R = long acyl chain, e.g., lauroyl) in crystals (321).

Large amplitude motions in molecular crystals such as phase transitions and self-diffusion of solid adamantane have also been treated by a MM method (322). However, the program used in this work is useful only for the calculation of intermolecular interactions.



120



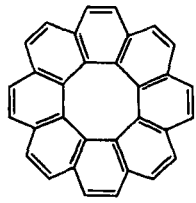
121

VII. CALCULATIONS OF UNKNOWN MOLECULES

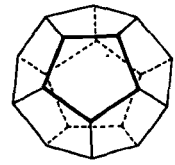
Like other theoretical methods, MM calculations can be used to predict properties of unknown molecules. For example, calculations on a number of unknown Bredt's olefins present a challenging guide to synthetic chemists (293).

The synthetic possibilities of the fascinating [8]circulene 122 may be influenced by MMPI calculations (323). Clearly, such a large circulene cannot have a planar structure. The calculated GMEC is saddle shaped with D_2 symmetry. There is another saddle-shaped isomer with D_{2d} symmetry having a perfect "tub" structure of the inner "cyclooctatetraene" ring, only 1.1 kcal/mol above the D_2 isomer. In these structures, the valence angles are all 120 ± 4°, but the C–C lengths alternate strongly. Hence 122 may be regarded as a constrained cyclooctatetraene. These GMEC structures are predicted to undergo ready bond shifts by passing over a barrier 4 kcal/mol in height.

One of the most talked-about dream targets of synthesis, dodecahedrane (123), has been studied repeatedly by the MM method (128,235). Recent MM2 calculations (234) predict a heat of formation of 22.15 kcal/mol, incidentally equal to the average from the two previous values: 45.28 by the Allinger 1971 force field, and -0.22 kcal/mol by the Schleyer force field (26a). In the I_h structure a very high strain energy is predicted by these two force fields because of the perfect eclipsed orientation of all the C–C as well as C–H bonds. Ermer calculated twisted conformations for this molecule with the CFF and confirmed that the I_h structure was the GMEC (324,324a).



122



123

Calculations of other attractive compounds such as asteranes and catenanes are in progress in the authors' laboratories.

VIII. PERSPECTIVES AND CONCLUSIONS

For MM calculations, the central problem in the future will continue to be the search for improvements in the modeling of molecular force fields. Wiberg (325) and White (326) discuss basic points. The number of potential function types comprising the force field does not appear to increase. The new torsion-bend cross-term was included in MMI (15) but later abandoned in MM2 (16).* In 1972, Allinger (327) began to utilize the results of *ab initio* MO calculations as the initial force constants in the parameterization when experimental values were not available. This technique appears to be a powerful way to obtain constants (62). Bartell studied ethane as the starting point for the *ab initio*-based derivation of quadratic and higher force constants (328). The CFF hydrogen bond parameters have been carefully checked against the results of *ab initio* calculations (318).

With the rapid evolution of the *ab initio* MO technique involving complete geometry optimization, quantum chemists are now seeking analytical expressions of molecular force fields for their expensive results (215). It should be possible, in principle, to construct a complete artificial force field that faithfully describes the Hartee-Fock limit energy surface, but still reflects important properties of the real surface sufficiently to allow useful applications (149).

Two other models of force fields considerably different from the Westheimer type are mentioned here. Scheraga's EPEN (empirical potential using electrons and nuclei) (13) explicitly treats bonding and lone-pair electrons as point charges located in the corresponding orbitals. It evaluates only three types of interactions: overlap repulsion between electrons, Coulombic interactions between all charge centers, and dispersion and other attractive forces. Energy minimization is accomplished by changing only dihedral angles while keeping bond lengths and bond angles at fixed values. EPEN is intended to apply to the calculations of large molecules such as proteins, but it has proved to perform reasonably well even for small molecules.

Wilson's special MM scheme (329) treats bonded and nonbonded

*A stretch-bend cross-term is now widely used in valence force fields but is not needed in the Urey-Bradley force fields.

interactions by the same formalism, namely, by the force functions of the vector positions of several neighboring atoms. This approach has a number of advantages: very fast calculation of forces in terms of vector operations, and rapid energy minimization by the viscous force technique, in which a force proportional to the negative end of each atomic velocity vector is added to bring the atoms in the molecule to an equilibrium arrangement. Wilson's system is also intended to treat large molecules and their chemical dynamics. To save storage space and time, close man-machine symbiosis was introduced and networking of many small computers was devised.

The innovations just mentioned may develop into valuable alternative MM techniques in the future.

The usefulness of a small "data base" consisting of structure drawings, calculated enthalpies, and strain energies (Cartesian coordinates are supplied as supplementary material) in the now classic paper of Engler, Andose, and Schleyer (26a) was mentioned above. Larger collections of geometries and energies of molecules optimized by any of the good MM programs should be as useful as the Cambridge crystallographic data base (303,330), and an architecture for such a large data base has been described (331). Data collections simpler in concept than this already exist in several places. A software data retrieval system especially suited for graphic display is commercially available (332).

In conclusion, we foresee more and more widespread use of MM calculations by chemists of all disciplines. Although we have confined ourselves to organic chemistry and some closely related fields in this chapter, a general calculation method like MM has basically no boundary regarding the extent of its application. The arrival of superminicomputers for personal use will undoubtedly spur the do-it-yourself trend in scientific calculations among experimentalists. It may be noted that a good modern minicomputer is now able to process most of the jobs that had to be done by a supercomputer at a central facility some years ago (333).

ACKNOWLEDGMENTS

This chapter has survived five revisions under the constant encouragement and criticism of Prof. P. v. R. Schleyer, who introduced us into this wonderful art of science. Thanks are due Profs. N. L. Allinger and K. Mislow for many valuable comments, to the Ministry of Education, Culture, and Science (Japan) for Grant-in-Aids for

Scientific Research at Sapporo, and to the Alexander von Humboldt-Stiftung, Bonn, for repeated support of E. O. in Germany, which led to this joint writing project.

REFERENCES

1. Part 12: Ōsawa, E.; Farcasiu, D.; Schleyer, P. v. R.; Engler, E. M.; Sevin, A.; Ledlie, D. B.; Kent, G. J.; Togashi, A.; Tahara, Y.; Iizuka, T.; Tanaka, N.; Kan, T., submitted for publication in *J. Org. Chem.* Part 11: Ōsawa, E.; Furusaki, A.; Hashiba, N.; Matsumoto, T.; Singh, V.; Tahara, Y.; Wiskott, E.; Farcasiu, M.; Iizuka, T.; Tanaka, N.; Kan, T.; Schleyer, P. v. R. *J. Org. Chem.* **1980**, *45*, 2985–2995. Part 10: Ōsawa, E.; Engler, E. M.; Godleski, S. A.; Inamoto, Y.; Kent, G. J.; Kausch, M.; Schleyer, P. v. R. *J. Org. Chem.* **1980**, *45*, 984–991.
2. Richards, G. *Chem. Br.* **1979**, *15*, 68–71.
3. Mallinson, P.; Peters, D. *Chem. Br.* **1978**, *14*, 191–193. Engel, Y. M.; Hagler, A. T. *Isr. J. Chem.* **1977**, *16*, 220–225.
4. Binkley, J. S.; Whiteside, R. A.; Krishnan, R.; Seeger, R.; DeFrees, D. J.; Schlegel, H. B.; Topiol, S.; Kahn, L. R.; Pople, J. A., document circulated by Prof. Pople.
5. Halgren, T. A.; Kleier, D. A.; Hall, J. H., Jr.; Brown, L. D.; Lipscomb, W. N. *J. Am. Chem. Soc.* **1978**, *100*, 6595–6608.
6. Dewar, M. J. S.; Ford, G. P. *J. Am. Chem. Soc.* **1979**, *101*, 5558–5561.
7. McManus, S. P.; Smith, M. R. *Tetrahedron Lett.* **1978**, 1897–1900.
8. Dodziuk, H. *J. Mol. Struct.* **1979**, *55*, 107–111.
9. (a) Westheimer, F. H. in "Steric Effects in Organic Chemistry," Newman, M. S., Ed.; Wiley: New York, 1956; Chapter 12. (b) Hendrickson, J. B. *J. Am. Chem. Soc.* **1961**, *83*, 4537–4547.
10. (a) Hursthouse, M. B.; Moss, G. P.; Sales, K. D. *Annu. Rep. Sect. B. Org. Chem.* **1978**, *75*, 23–35. (b) Kitaigorodsky, A. I. *Chem. Soc. Rev.* **1978**, *7*, 133, (c) Niketić, S. R.; Rasmussen, K. "The Consistent Force Field"; Springer: Berlin; 1977. (d) Allinger, N. L.; *Adv. Phys. Org. Chem.* **1976**, *13*, 1–82. (e) Ermer, O. *Struct. Bonding* **1976**, *27*, 161–211. (f) Altona, C.; Faber, D. H. *Top Curr. Chem.* **1974**, *45*, 1–38.
11. DeTar, D. F. *Comput. Chem.* **1977**, *1*, 139–140, and subsequent papers in "Symposium in Print on Molecular Mechanics."
12. Hopfinger, A. J. "Conformational Properties of Macromolecules"; Academic Press: New York, 1973. Allegra, G.; Calligaris, M.; Randaccio, L. *Macromolecules* **1973**, *9*, 390–396. Yoon, D. Y.; Sundararajan, P. R.; Flory, P. J. *ibid.* **1975**, *8*, 776–783. Suter, U. W. *J. Am. Chem. Soc.* **1979**, *101*, 6481–6496. Abe, A. *Macromolecules* **1977**, *10*, 34–43. Potenzone, R. Jr.; Cavicchi, E.; Weintraub, H. J. R.; Hopfinger, A. J. *Comput. Chem.* **1977**, *1*, 187–194.
13. EPEN: Snir, J.; Nemenoff, R. A.; Scheraga, H. A. *J. Phys. Chem.* **1978**, *82*, 2497–2503, and subsequent papers. ECEPP: Dunfield, L. G.; Burgess, A. W.; Scheraga, H. A. *ibid.* **1978**, *82*, 2609–2616. Zimmerman, S. S.;

Pottle, M. S.; Némethy, G.; Scheraga, H. A.; *Macromolecules* **1977**, *10*, 1-9. Isogai, Y.; Némethy, G.; Scheraga, H. A. *Proc. Natl. Acad. Sci. U. S. A.* **1977**, *74*, 414-418.

13a. Jeffrey, G. A.; Yates, J. H. *J. Am. Chem. Soc.* **1979**, *101*, 820-825.

14. Allinger, N. L.; Tribble, M. T.; Miller, M.A.; Wertz, D. H. *J. Am. Chem. Soc.* **1971**, *93*, 1637-1648.

15. (a) Wertz, D. H.; Allinger, N. L. *Tetrahedron* **1974**, *30*, 1579-1586. (b) Allinger, N. L.; Sprague, J. T. *J. Am. Chem. Soc.* **1973**, *95*, 3893-3907. (c) Allinger, N. L.; Yuh, Y. H. *QCPE* **1980**, *11*, 318.

16. (a) Allinger, N. L. *J. Am. Chem. Soc.* **1977**, *99*, 8127-8134. (b) Allinger, N. L.; Yuh, Y. H. *QCPE* **1980**, *11*, 395.

17. (a) Allinger, N. L.; Sprague, J. T. *J. Am. Chem. Soc.* **1972**, *94*, 5734-5747. (b) Allinger, N. L.; Meyer, A. Y. *Tetrahedron* **1975**, *31*, 1807-1811. (c) Ethers and alcohols: Allinger, N. L.; Chung, D. Y. *J. Am. Chem. Soc.* **1976**, *98*, 6798-6803. (d) Ketones and aldehydes: Allinger, N. L.; Tribble, M. T.; Miller, M. A. *Tetrahedron* **1972**, *28*, 1173-1190. (e) Carboxylic acids and esters: Allinger, N. L.; Chang, S. H. M. *ibid.* **1977**, *33*, 1561-1567. (f) Amino nitrogen: Profeta, S., Jr. Ph. D. Dissertation, The University of Georgia, Athens, 1978. The parameters deduced are included in the QCPE version of MM2. (g) Thioethers and thiol: Allinger, N. L.; Hickey, M. J. *J. Am. Chem. Soc.* **1975**, *97*, 5167-5177. (h) Disulfides: Allinger, N. L.; Hickey, M. J.; Kao, J. *J. Am. Chem. Soc.* **1976**, *98*, 2741-2745; Allinger, N. L.; Kao, J.; Chang, H.-M. Boyd, D. B. *Tetrahedron* **1976**, *32*, 2867-2873. (i) Sulfoxides: Allinger, N. L.; Kao, J. *Tetrahedron*, **1976**, *32*, 529-536. (j) Elemental sulfur: Kao, J.; Allinger, N. L. *J. Inorg. Chem.* **1977**, *16*, 35-41. (k) Halides: Meyer, A. Y.; Allinger, N. L. *Tetrahedron* **1975**, *31*, 1971-1978 (l) Silanes: Tribble, M. T.; Allinger, N. L. *ibid.* **1972**, *28*, 2147-2156. (m) Phosphines: Allinger, N. L.; von Voithenberg, H. *ibid.* **1978**, *34*, 627-633.

18. Pfeffer, H.-U.; Klessinger, M. *Chem. Ber.* **1979**, *112*, 890-898.

19. Allinger, N. L.; Siefert, J. H. *J. Am. Chem. Soc.* **1975**, *97*, 752-760.

20. Allinger, N. L.; Sprague, J. T.; Liljefors, T. *J. Am. Chem. Soc.* **1974**, *96*, 5100-5104.

21. (a) Allinger, N. L.; Tai, J. C. *J. Am. Chem. Soc.* **1977**, *99*, 4256-4259. (b) Tai, J. C.; Allinger, N. L. *ibid.* **1976**, *98*, 7928-7932.

22. Liljefors, T.; Allinger, N. L. *J. Am. Chem. Soc.* **1976**, *98*, 2745-2749.

23. Kao, J.; Allinger, N. L. *J. Am. Chem. Soc.* **1977**, *99*, 975-986.

24. Allinger, N. L.; Hindman, D.; Hönig, H. *J. Am. Chem. Soc.* **1977**, *99*, 3282-3284.

25. Wertz, D. H.; Allinger, N. L. *Tetrahedron* **1979**, *35*, 3-12.

26. (a) Engler, E. M.; Andose, J. D.; Schleyer, P. v. R. *J. Am. Chem. Soc.* **1973**, *95*, 8005-8025. (b) Andose, J. D.; Engler, E. M.; Collins, J. B.; Hummel, J. P.; Mislow, K.; Schleyer, P. v. R. *QCPE*, **1980**, *11*, 348.

27. White, D. N. J.; Bovill, M. J. *J. Chem. Soc., Perkin Trans. II*, **1977**, 1610-1623.

28. Dougherty, D. A.; Mislow, K. *J. Am. Chem. Soc.* **1979**, *101*, 1401-1405.

29. DeTar, D. F. *Comput. Chem.* **1977**, *1*, 141-144.

29a. This deficiency has been eliminated in the much improved, second version of the Schleyer-Mislow program, BIGSTRN-2: Iverson, D. J.; Mislow, K. *QCPE* **1981**, *13*, 410. We thank Prof. Mislow for this information.

30. Warshel, A. *Comput. Chem.* **1977**, *1*, 195–202. Warshel, A. In "Modern Theoretical Chemistry," Segal, G., Ed.; Plenum: New York, 1977; Vol. 7, Chapter 5. Huler, E.; Sharon, R.; Warshel, A. *QCPE* **1980**, *11*, 325.

31. Ermer, O. *Tetrahedron* **1974**, *30*, 3103–3105.

32. (a) Melberg, S.; Rasmussen, K. *Acta Chem. Scand.* **1978**, *A32*, 187–188. (b) Kildeby, K.; Melberg, S.; Rasmussen, K. *ibid.* **1977**, *A31*, 1–13.

33. (a) Niketic, S. R.; Rasmussen, K.; Woldbye, F.; Lifson, S. *Acta Chem. Scand.* **1976**, *A30*, 485–497. (b) Niketić, S. R.; Rasmussen, K. *ibid.* **1978**, *A32*, 391–400. (c) Hald, N. C. P.; Rasmussen, K. *ibid.* **1978**, *A32*, 753–756, (d) Hald, N. C. P.; Rasmussen, K. *ibid.* **1978**, *A32*, 879–886.

34. Rasmussen, K.; Melberg, S. *J. Mol. Struct.* **1979**, *57*, 215–239.

35. Sharafi-Ozeri, S.; Kuszkat, K. A. *QCPE* **1980**, *11*, 334.

36. Fitzwater, S.; Bartell, L. S. *J. Am. Chem. Soc.* **1976**, *98*, 5107–5115.

37. Chang, S.; McNally, D.; Shary-Tehrany, S.; Hickey, M. J.; Boyd, R. H. *J. Am. Chem. Soc.* **1970**, *92*, 3109–3118.

38. Faber, D. H.; Altona, C. *Comput. Chem.* **1977**, *1*, 203–213.

39. Carballeira, L.; Casado, J.; Rios, M. A. *Chem. Phys.* **1976**, *12*, 71–75.

40. Brunel, Y.; Faucher, H.; Gagnaire, D.; Rassat, A. *Tetrahedron* **1975**, *31*, 1075–1091.

41. Cohen, N. C. *Tetrahedron* **1971**, *27*, 789–797.

42. Busing, W. R. *Acta Crystallogr., Sect. A* **1972**, *28*, Suppl. 4, 252.

43. Abraham, R. J.; Parry, K. *J. Chem. Soc., B* **1970**, 539–545. Abraham, R. J.; Loftus, P. *J. Chem. Soc., Chem. Commun.* **1974**, 180–181.

44. Reviews: (a) Eliel, E. L. *J. Chem. Educ.* **1975**, *52*, 762–767. (b) Wilson, E. B. *Chem. Soc. Rev.* **1972**, *1*, 293–318.

45. Greenberg, A.; Liebman, J. F. "Strained Organic Molecules"; Academic Press: New York, 1978.

46. Boyd, R. H. *J. Am. Chem. Soc.* **1975**, *97*, 5353–5357.

47. White, D. N. J.; Bovill, M. J. *J. Mol. Struct.* **1976**, *33*, 273–277.

48. Ōsawa, E.; Collins, J. B.; Schleyer, P. v. R. *Tetrahedron* **1977**, *33*, 2667–2675.

49. Bartell, L. S. *J. Am. Chem. Soc.* **1977**, *99*, 3279–3282.

50. Ōsawa, E.; Shirahama, H.; Matsumoto, T. *J. Am. Chem. Soc.* **1979**, *101*, 4824–4832.

51. Bradford, W. F.; Fitzwater, S.; Bartell, L. S. *J. Mol. Struct.* **1977**, *38*, 185–194.

52. Peterson, M. R.; Csizmadia, I. G. *J. Am. Chem. Soc.* **1978**, *100*, 6911–6916.

53. Hilderbrandt, R. L.; Weiser, J. D. *J. Mol. Struct.* **1973**, *15*, 27–36.

54. Hagler, A. T.; Stern, P. S.; Lifson, S.; Arid, S. *J. Am. Chem. Soc.* **1979**, *101*, 813–819.

55. Bartell, L. S.; Bradford, W. F. *J. Mol. Struct.* **1977**, *37*, 113–126.

56. Bartell, L. S.; Boates, T. L. *J. Mol. Struct.* **1976**, *32*, 379-392.
57. Bürgi, H. B.; Bartell, L. S. *J. Am. Chem. Soc.* **1972**, *94*, 5236-5238.
58. Bartell, L. S.; Bürgi, H. B. *J. Am. Chem. Soc.* **1972**, *94*, 5239-5246.
59. Fitzwater, S.; Bartell, L. S. *J. Am. Chem. Soc.* **1976**, *98*, 8338-8344.
60. Iroff, L. D.; Mislow, K. *J. Am. Chem. Soc.* **1978**, *100*, 2121-2126.
61. Hummel, J. P.; Stackhouse, J.; Mislow, K. *Tetrahedron* **1977**, *30*, 1925-1930.
62. Allinger, N. L., personal communication, University of Georgia, 1979.
63. DeTar, D. F. *Comput. Chem.* **1976**, *1*, 35-43.
64. Mislow, K. "Introduction to Stereochemistry"; Benjamin: New York, 1966; Chapter 1.
65. Mislow, K. *Acc. Chem. Res.* **1976**, *9*, 26-33.
66. Mislow, K.; Dougherty, D. A.; Hounshell, W. D. *Bull. Soc. Chim. Belg.* **1978**, *87*, 555-572.
67. Wroczynski, R. J.; Mislow, K. *J. Am. Chem. Soc.* **1979**, *101*, 3980-3981.
68. Hounshell, W. D.; Iroff, L. D.; Wroczynski, R. J.; Mislow, K. *J. Am. Chem. Soc.* **1978**, *100*, 5212-5213.
69. Willem, R.; Hoogzand, C. *Org. Magn. Reson.* **1979**, *12*, 55-58.
70. Curry, K. K.; Gilje, J. W. *J. Am. Chem. Soc.* **1978**, *100*, 1442-1449.

70a. Hayes, K. S.; Nagumo, M.; Blount, J. F.; Mislow, K. *J. Am. Chem. Soc.* **1980**, *102*, 2773-2776.

71. Karipides, A.; Iroff, L. D.; Mislow, K. *Inorg. Chem.* **1979**, *18*, 907-908.
72. Kingsbury, C. A. *J. Chem. Educ.* **1979**, *56*, 431-437.
73. Baxter, S. G.; Fritz, H.; Hellmann, G.; Kitschke, B.; Lindner, H. J.; Mislow, K.; Rüchardt, C.; Weiner, S. *J. Am. Chem. Soc.* **1979**, *101*, 4493-4497.
74. Beckhaus, H.-D.; Hellmann, G.; Rüchardt, C. *Chem. Ber.* **1978**, *111*, 72-83. Beckhaus, H.-D.; Hellmann, G.; Rüchardt, C.; Kitschke, B.; Lindner, H. J.; Fritz, H. *ibid.* **1978**, *111*, 3764-3779. Beckhaus, H.-D.; Hellmann, G.; Rüchardt, C.; Kitschke, B.; Lindner, H. J. *Chem. Ber.* **1978**, *111*, 3780-3789.
75. Dougherty, D. A.; Llort, F. M.; Mislow, K. *Tetrahedron* **1978**, *34*, 1301-1306.
76. Llort, F. M.; Mislow, K.; Wooten, J. B.; Beyerlein, A. L.; Savitsky, G. B.; Jacobus, J. *J. Am. Chem. Soc.* **1979**, *101*, 292-295.
77. Stein, M.; Winter, W.; Rieker, A. *Angew. Chem.* **1978**, *90*, 737-738; *Angew. Chem. Int. Ed. Engl.* **1978**, *17*, 692-694.
78. Hounshell, W. D.; Dougherty, D. A.; Hummel, J. P.; Mislow, K. *J. Am. Chem. Soc.* **1977**, *99*, 1916-1924.
79. Ōsawa, E.; Onuki, Y.; Mislow, K. *J. Am. Chem. Soc.*, in press.
80. Barton, D. H. R., *Experientia*, **1950**, *6*, 316-329.

80a. Kellie, G. M.; Riddell, F. G. *Top. Stereochem.* **1974**, *8*, 225-269.

81. Anet, F. A. L.; Anet, R. In "Dynamic Nuclear Magnetic Resonance Spectroscopy," Jackman, L. M.; Cotton, F. A., Eds.; Academic Press: New York, 1975; pp. 543-619.

82. Corbally, R. P.; Perkins, M. J.; Carson, A. S.; Laye, P. G.; Steele, W. V. *J. Chem. Soc., Chem. Commun.* **1978**, 778–779.
83. Baas, J. M. A.; van de Graaf, B.; van Rantwijk, F.; van Veen, A. *Tetrahedron* **1979**, *35*, 421–423.
83a. Allinger, N. L.; Yuh, Y. H.; Sprague, J. T. *J. Comput. Chem.* **1980**, *1*, 30–35.
84. van de Graaf, B.; van Bekkum, H.; van Koningsveld, H.; Sinnema, A.; van Veen, A.; Wepster, B. M.; van Wijk, A. M. *Rec. Trav. Chim. Pays-Bas* **1974**, *93*, 135–139.
85. Schubert, W. K.; Southern, J. F.; Schäfer, L. *J. Mol. Struct.* **1973**, *16*, 403–415.
86. van de Graaf, B.; Wepster, B. M. *Tetrahedron Lett.* **1975**, 2943–2944.
87. Askari, M.; Merrifield, D. L.; Schäfer, L. *Tetrahedron Lett.* **1976**, 3497–3498.
87. (a) Schneider, H.-J.; Freitag, W. *Chem. Ber.* **1979**, *112*, 16–27.
(b) Schneider, H.-J.; Hoppen, V. *J. Org. Chem.* **1978**, *43*, 3866–3873.
88. Dale, J. *Acta Chem. Scand.* **1973**, *27*, 1115–1129, 1130–1148, 1149–1158.
89. Allinger, N. L.; Gorden, B.; Profeta, S., Jr. *Tetrahedron* **1980**, *36*, 859–864.
90. Dale, J. *Top. Stereochem.* **1976**, *9*, 199–270.
91. Anet, F. A. L. *Top Curr. Chem.* **1974**, *45*, 169–220.
92. Anet, F. A. L.; Yavari, I. *Tetrahedron* **1978**, *34*, 2879–2886.
93. Anet, F. A. L.; Yavari, I. *J. Am. Chem. Soc.* **1978**, *100*, 7814–7819.
94. Anet, F. A. L.; Yavari, I. *J. Am. Chem. Soc.* **1977**, *99*, 6986–6991.
95. Ermer, O. *J. Am. Chem. Soc.* **1976**, *98*, 3964–3970.
96. Guy, M. H. P.; Heimbach, P.; MacNicol, D. D.; White, D. N. J. *J. Mol. Struct.* **1978**, *48*, 143–146.
96a. Anet, F. A. L.; Yavari, I. *Tetrahedron Lett.* **1975**, 4221–4224.
97. Anet, F. A. L.; Yavari, I. *J. Am. Chem. Soc.* **1977**, *99*, 7640–7649.
98. Anet, F. A. L.; Yavari, I. *J. Am. Chem. Soc.* **1977**, *99*, 6496–6499.
99. Anet, F. A. L.; Ghiaci, M. *J. Am. Chem. Soc.* **1980**, *102*, 2528–2533.
100. Anet, F. A. L.; Rawdah, T. N. *J. Am. Chem. Soc.* **1978**, *100*, 7810–7814.
101. Anet, F. A. L.; Rawdah, T. N. *J. Am. Chem. Soc.* **1978**, *100*, 7166–7171.
102. Anet, F. A. L.; Rawdah, T. N. *Tetrahedron Lett.* **1979**, 1943–1944.
103. Anet, F. A. L.; Rawdah, T. N. *J. Am. Chem. Soc.* **1979**, *101*, 1887–1888.
104. Anet, F. A. L.; Rawdah, T. N. *J. Am. Chem. Soc.* **1978**, *100*, 5003–5007.
105. Thomas, M. W.; Emerson, D. *J. Mol. Struct.* **1973**, *16*, 473–482.
106. Ermer, O. *Tetrahedron* **1975**, *31*, 1849–1854.
107. David. C. W. *Comput. Chem.* **1978**, *2*, 65–69.
108. van de Graaf, B.; Baas, J. M. A.; van Veen, A. *Rec Trav. Chim. Pays-Bas* **1980**, *99*, 175–178.
109. Shirhama, H.; Ōsawa, E.; Matsumoto, T. *J. Am. Chem. Soc.* **1980**, *102*, 3208–3213.
110. Grychtol, K.; Musso, H.; Oth, J. F. M. *Chem. Ber.* **1972**, *105*, 1798–1809.

111. Wiberg, K. B.; Boyd, R. H. *J. Am. Chem. Soc.* **1972**, *94*, 8426–8430.
112. Bürgi, H. B., Swiss Federal Institute of Technology, personal communication, 1977.
113. Stohrer, W. D., University of Frankfurt, Frankfurt/Main, Germany, personal communication, 1977.
114. Dallinga, G.; Toneman, L. H. *Rec. Trav. Chim. Pays-Bas* **1969**, *88*, 185–192.
115. Newton, M. G.; Pantaleo, N. S.; Kirbawy, S.; Allinger, N. L. *J. Am. Chem. Soc.* **1978**, *100*, 2176–2180.
115a. Spelbos, A.; Mijlhoff, F. C.; Bakker, W. H.; Baden, R.; van den Enden, L.; *J. Mol. Struct.* **1977**, *38*, 155–166.
116. Bovill, M. J.; Cox, P. J.; Flitman, H. P.; Guy, M. H. P.; Hardy, A. D. U.; McCabe, P. H.; Macdonald, M. A.; Sim, G. A.; White, D. N. J. *Acta Crystallogr., Sect. B* **1979**, *35*, 669–675.
117. Sim, G. A. *Acta Crystallogr., Sect. B* **1979**, *35*, 2455–2458.
118. Ermer, O. *Angew. Chem.* **1977**, *89*, 833–835; *Angew. Chem. Int. Ed. Engl.* **1977**, *16*, 798–799.
119. White, D. N. J.; Bovill, M. J. *Acta Crystallogr., Sect. B* **1977**, *33*, 3029–3033.
120. Ōsawa, E.; Aigami, K.; Inamoto, Y. *J. Chem. Soc., Perkin Trans. II*, **1979**, 172–180.
121. Peters, J. A.; Baas, J. M. A.; van de Graaf, B.; van der Toorn, J. M.; van Bekkum, H. *Tetrahedron* **1978**, *34*, 3313–3323.
122. Moodie, W. T.; Parker, W.; Watt, I. *J. Chem. Soc., Perkin Trans. II*, **1979**, 664–672.
123. van den Enden, L.; Geise, H. J.; Spelbos, A. *J. Mol. Struct.* **1978**, *44*, 177–185.
124. Browne, L.; Klink, R. E.; Stothers, J. B. *Can. J. Chem.* **1979**, *57*, 803–806.
125. Parker, W.; Tranter, R. L.; Watt, C. I. F.; Chang, L. W. K.; Schleyer, P. v. R. *J. Am. Chem. Soc.* **1974**, *96*, 7121–7122.
126. Wang, A. H.-J.; Missavage, R. J.; Byrn, S. R.; Paul, I. C. *J. Am. Chem. Soc.* **1972**, *94*, 7100–7104.
127. Ōsawa, E. *J. Am. Chem. Soc.* **1979**, *101*, 5523–5529.
128. Eaton, P. E. *Tetrahedron* **1979**, *35*, 2189–2223.
129. Maier, G.; Pfriem, U.; Schäfer, U.; Matusch, R. *Angew. Chem.* **1978**, *90*, 552–553; *Angew. Chem. Int. Ed. Engl.* **1978**, *17*, 520–521.
130. Hounshell, W. D.; Mislow, K. *Tetrahedron Lett.* **1979**, 1205–1208.
131. (a) Brückner, S.; Allegra, G. *Gazz. Chim. Ital.* **1976**, *106*, 1073–1082. (b) Albinati, A.; Brückner, S.; Allegra, G. *Acta Crystallogr.; Sect. B* **1977**, *33*, 229–231; ACC isomer. (c) Albinati, A.; Brückner, S.; Allegra, G. *Acta Crystallogr., Sect. B* **1978**, *34*, 501–504. (d) Brückner, S.; Colombo, A.; Immirzi, A.; Allegra, G. *Gazz. Chim. Ital.* **1978**, *108*, 675–680. (e) Albinati, A.; Brückner, S.; Allegra, G. *J. Appl. Crystallogr.*, in press.
132. Brückner, S.; Allegra, G.; Albinati, A.; Farina, M. *J. Chem. Soc., Perkin Trans. II* **1980**, 523–529.

133. van Hemelrijk, D.; van den Enden, L.; Geise, H. J.; Sellers, H. L.; Schäfer, L. *J. Am. Chem. Soc.* **1980**, *102*, 2189–2195.
134. Lenoir, D. *Nachr. Chem. Tech. Lab.* **1979**, *27*, 762–765.
135. Lenoir, D.; Frank, R. M.; Cordt, F.; Gieren, A.; Lamm. V. *Chem. Ber.* **1980**, *113*, 739–749.
136. Bushby, R. J.; Pollard, M. D.; McDonald. W. S. *Tetrahedron Lett.* **1978**, 3851–3854.
137. Ermer, O. *Angew. Chem.* **1977**, *89*, 665–666; *Angew. Chem. Int. Ed. Engl.* **1977**, *16*, 658–659.
138. Mugnoli, A.; Simonetta, M. *J. Chem. Soc., Perkin Trans. II* **1976**, 1831–1835.
139. Ermer, O.; Lifson, S. *Tetrahedron* **1974**, *30*, 2425–2429.
140. Carreira, L. A. *J. Chem. Phys.* **1975**, *62*, 3851–3854.
141. Braun, H.; Lüttke, W. *J. Mol. Struct.* **1976**, *31*, 97–129.
142. Bartell, L. S. *Tetrahedron* **1978**, *34*, 2891–2892.
143. Korenstein, R.; Muszkat, K. A.; Sharafi-Ozeri, S. *J. Am. Chem. Soc.* **1973**, *95*, 6177–6181.
144. Allinger, N. L.; Tribble, M. T. *Tetrahedron Lett.* **1971**, 3259–3262.
145. (a) Koer, F. J.; Altona, C. *Rec. Trav. Chim. Pays-Bas* **1974**, *93*, 147–151. (b) Koer, F. J.; Faber, D. H.; Altona, C. *ibid.* **1974**, *93*, 307–311.
146. Keller, H.; Langer, E.; Lehner, H. *Monatsh. Chem.* **1976**, *107*, 949–963.
147. Ivanov, P.; Pojarlieff, I.; Tyutyulkov, N. *Tetrahedron Lett.* **1976**, 775–778.
148. Jacobus, J. *Tetrahedron Lett.* **1976**, 2927–2930.
149. Ōsawa, E., manuscript in preparation.
150. Carter, R. E.; Stilbs, P. *J. Am. Chem. Soc.* **1976**, *98*, 7515–7521.
151. Carter, R. E.; Nilsson, B.; Olsson, K. *J. Am. Chem. Soc.* **1975**, *97*, 6155–6159.
152. Aurivillius, B.; Carter, R. E. *J. Chem. Soc., Perkin Trans. II* **1978**, 1033–1037.
153. (a) Kodama, Y.; Nishihata, K.; Nishio, M.; Iitaka, Y. *J. Chem. Soc., Perkin Trans. II* **1976**, 1490–1495. (b) Kodama, Y.; Nishihata, K.; Zushi, S.; Nishio, M.; Uzawa, J.; Sakamoto, K.; Iwamura, H. *Bull. Chem. Soc. Jpn.* **1979**, *52*, 2661–2669.
154 (a) Tel, R. M.; Engberts, J. B. F. N. *J. Chem. Soc., Perkin Trans. II* **1976**, 483–488. (b) Visser, R. J. J.; Vos, A.; Tel. R. M.; Engberts, J. B. F. N. *Rec. Trav. Chim. Pays-Bas* **1978**, *97*, 181–184. (c) Tickle, I.; Hess, J.; Vos, A.; Engberts, J. B. F. N. *J. Chem. Soc., Perkin Trans. II* **1978**, 460–465. (d) Visser, R. J. J.; Vos, A.; Engberts, J. B. F. N. *J. Chem. Soc., Perkin Trans. II* **1978**, 634–639.
155. Nassimbeni, L. R.; Wright, R. W.; Giles, R. G. F.; Mitchell, P. R. K. *S. Afr. J. Chem.* **1979**, *32*, 177–181.
156. Zuccarello, F.; Millefiori, S.; Trovato, S. *Can. J. Chem.* **1976**, *54*, 226–230.
157. Gustav, K.; Sühnel, J.; Wild, U. P. *Helv. Chim. Acta* **1978**, *61*, 2100–2107.

158. Sühnel, J.; Gustav, K. *Z. Chem.* **1978**, *18*, 387-389.
159. (a) Carter, R. E.; Liljefors, T. *Tetrahedron* **1976**, *32*, 2915-2922. (b) Liljefors, T.; Carter, R. E. *ibid.* **1978**, *34*, 1611-1615.
160. Wynberg, H.; Nieuwpoort, W. C.; Jonkman, H. T. *Tetrahedron Lett.* **1973**, 4623-4627.
161. Handal, J.; White, J. G.; Franck, R. W.; Yuh, Y. H.; Allinger, N. L. *J. Am. Chem. Soc.* **1977**, *99*, 3345-3349.
162. Blount, J. F.; Cozzi, F.; Damewood, J. R. Jr.; Iroff, L. D.; Sjöstrand, U.; Mislow, K. *J. Am. Chem. Soc.* **1980**, *102*, 99-103.
163. Anet, F. A. L.; Donovan, D.; Sjöstrand, U.; Cozzi, F.; Mislow, K. *J. Am. Chem. Soc.* **1980**, *102*, 1748-1749.
164. Hutchings, M. G.; Watt, I. *J. Organomet. Chem.* **1979**, *177*, 329-332.
165. Hounshell, W. D.; Iroff, L. D.; Iverson, D. J.; Wroczynski, R. J.; Mislow, K. *Isr. J. Chem.* **1980**, *20*, 65-71.
166. Ōki, M. *Angew. Chem.* **1976**, *88*, 67-74; *Angew. Chem. Int. Ed. Engl.* **1976**, *15*, 87-93.
167. Imashiro, F.; Terao, T.; Saika, A. *J. Am. Chem. Soc.* **1979**, *101*, 3762-3766.
168. Iroff, L. D. *J. Comput. Chem.* **1980**, *1*, 76-80.
169. Allinger, N. L.; Sprague, J. T.; Liljefors, T. *J. Am. Chem. Soc.* **1974**, *96*, 5100-5104.
170. Dunand, A.; Ferguson, J.; Puza, M.; Robertson, G. B. *J. Am. Chem. Soc.* **1980**, *102*, 3524-3530.
171. Lindner, H. J. *Tetrahedron* **1974**, *30*, 1127-1132.
172. Lindner, H. J. *Tetrahedron* **1976**, *32*, 753-757.
173. Lindner, H. J. *Tetrahedron* **1975**, *31*, 281-284.
174. Kessler, H.; Ott, W.; Lindner, H. J.; von Schnering, H. G.; Peters, E.-M.; Peters, K. *Chem. Ber.* **1980**, *113*, 90-103.
175. Allinger, N. L.; Wuesthoff, M. T. *Tetrahedron* **1977**, *33*, 3-10.
176. Dosen-Micovic, L.; Allinger, N. L. *Tetrahedron* **1978**, *34*, 3385-3393.
177. Burkert, U. *Tetrahedron* **1977**, *33*, 2237-2242; *ibid.* **1979**, *33*, 209-212, 691-695, 1945-1951.
178. Gagnaire, D.; Tran. V.; Vignon, M. *J. Chem. Soc., Chem. Commun.* **1976**, 6-7.
179. Romers, C.; Altona, C.; Buys, H. R.; Havinga, E. *Top. Stereochem.* **1969**, *4*, 39-97.
180. Tvaroska, I.; Bleha, T. *Can. J. Chem.* **1979**, *57*, 424-435.
181. Abe, A. *J. Am. Chem. Soc.* **1976**, *98*, 6477-6480.
182. Jeffrey, G. A.; Taylor, R. *J. Comput. Chem.* **1980**, *1*, 99-109.
183. Tvaroska, I.; Bleha, T. *Collect. Czech. Chem. Commun.* **1978**, *43*, 922-931.
183a. Levitt, M.; Warshel, A. *J. Am. Chem. Soc.* **1978**, *100*, 2607-2613.
184. Anet, F. A. L.; St. Jacques, M.; Henrich, P. M.; Cheng, A. K.; Krane, J.; Wong, L. *Tetrahedron* **1974**, *30*, 1629-1637.

185 (a) Schubert, W.; Schäfer, L.; Pauli, G. H. *J. Mol. Struct.* **1974**, *21*, 53-60. (b) Askari, M.; Pauli, G. H.; Schubert. W.; Schäfer, L. *ibid.* **1977**, *38*, 275-281. (c) Schäfer, L.; Chiu, N. S.; Askari, M. *ibid.* **1978**, *48*, 445-448. (d) Askari, M.; Ostlund, N. S.; Schäfer, L. *J. Am. Chem. Soc.* **1977**, *99*, 5246-5248.

186. Jacob, E. J.; Thompson, H. B.; Bartell, L. S. *J. Chem. Phys.* **1967**, *47*, 3736-3753.

187. Allinger, N. L.; Dosen-Micovic, L.; Viskocil, J. F. Jr.; Tribble, M. T. *Tetrahedron* **1978**, *34*, 3395-3399.

188. (a) Harris, J. M.; Smith, M. R. *J. Org. Chem.* **1978**, *43*, 3588-3596. (b) Harris, J. M.; Schafer, S. G.; Smith, M. R.; McManus, S. P. *Tetrahedron Lett.* **1979**, 2089-2092.

189. Eliel, E. *Angew. Chem.* **1972**, *84*, 779-791; *Angew. Chem. Int. Ed. Engl.* **1972**, *11*, 739-750.

190. Blackburne, I. D.; Duke, R. P.; Jones, R. A. Y.; Katritzky, A. R.; Record, K. A. F. *J. Chem. Soc., Perkin Trans. II* **1973**, 332-336.

191. Traetteberg, M.; Hilmo, I.; Abraham, R. J.; Ljunggren, S. *J. Mol Struct.* **1978**, *48*, 395-405.

192. Tourwe, D.; Laus, G.; Van Binst, G. *J. Org. Chem.* **1978**, *43*, 322-324.

193. Terui, Y. *J. Chem. Soc., Perkin Trans. II* **1975**, 118-127.

194. Snyder, J. P.; Crans, D. C., submitted for publication.

195. Karlsson, S.; Liljefors, T.; Sandström, J. *Acta Chem. Scand.* **1977**, *B31*, 399-406.

196. Berg, U.; Grimaud, M.; Sandström, J. *Nouv. J. Chim.* **1979**, *3*, 175-181.

197. Quellette, R. J. *J. Am. Chem. Soc.* **1974**, *96*, 2421-2425.

198. Hutchings, M. G.; Andose, J. D.; Mislow, K. *J. Am. Chem. Soc.* **1972**, *97*, 4553-4561, 4562-4570. Hummel, J. P.; Zurbach, E. P.; DiCarlo, E. N.; Mislow, K. *ibid.* **1976**, *98*, 7480-7483.

199. Hummel, J. P.; Stackhouse, J.; Mislow, K. *Tetrahedron* **1977**, *33*, 1925-1930.

200. Smith, Z.; Seip, H. M.; Hengge, E.; Bauer, G. *Acta Chem. Scand.* **1976**, *A30*, 697-702.

201. Abraham, R. J.; Tabony, J. *Tetrahedron Lett.* **1975**, 2095-2098.

202. Sundius, T. *J. Mol. Spectrosc.* **1977**, *64*, 47-55.

203. Heublein, G.; Kühmstedt, R.; Kadura, P.; Dawczynski, H. *Tetrahedron* **1970**, *26*, 81-90. Heublein, G.; Kühmstedt, R.; Dawczynski, H.; Kadura, P. *ibid.* **1970**, *26*, 91-98.

204. Fuchs, B.; Wechsler, P. S. *Tetrahedron* **1977**, *33*, 57-64.

205. Part I: Stølevik, R. *Acta Chem. Scand.* **1974**, *A28*, 299-314. Part XV: Braathen, M.; Christensen, D. H.; Klaeboe, P.; Seip, R.; Stølevik, R. *ibid.* **1979**, *A33*, 437-444.

206. (a) Meyer, A. Y. *J. Mol. Struct.* **1977**, *40*, 127-138. (b) Meyer, A. Y. *ibid.* **1978**, *49*, 383-394.

207. Kao, J.; Allinger, N. L. *J. Inorg. Chem.* **1977**, *16*, 35-41.

208. Samdal, S.; Seip, H. M.; Torgrimsen, T. *J. Mol. Struct.* **1979**, *57*, 105–121.

209. De Alti, G.; Decleva, P.; Sgamellotti, A. *J. Mol. Struct.* **1979**, *53*, 129–138.

210. Wilson, G. E., Jr. *J. Am. Chem. Soc.* **1974**, *96*, 2426–2429.

211. Jørgensen, F. S.; Snyder, J. P. *Tetrahedron* **1979**, *35*, 1399–1407. Jørgensen, F. S.; Snyder, J. P., submitted for publication.

212. Snyder, J. P.; Harpp, D. N. *Tetrahedron Lett.* **1978**, 197–200.

213. Deiters, J. A.; Gallucci, J. C.; Clark, T. E.; Holmes, R. R. *J. Am. Chem. Soc.* **1977**, *99*, 5461–5471. Cf. Holmes, R. R. *ibid.* **1975**, *97*, 5379–5385.

214. Marsh, F. J.; Weiner, P.; Douglas, J. E.; Kollman, P. A.; Kenyon, G. L.; Gerlt, J. A. *J. Am. Chem. Soc.* **1980**, *102*, 1660–1665. See also: Gerlt, J. A.; Gutterson, N. I.; Drews, R. E.; Sokolow, J. A. *J. Am. Chem. Soc.* **1980**, *102*, 1665–1670.

215. Lipari, G.; Tosi, C. *Theor. Chim. Acta (Berlin)* **1978**, *50*, 169–170.

216. Birnbaum, G. I.; Buchanan, G. W.; Morin F. G. *J. Am. Chem. Soc.* **1977**, *99*, 6652–6656.

217. Boyd, R. H.; Kesner, L. *J. Am. Chem. Soc.* **1977**, *99*, 4248–4256.

218. Buckingham, D. A.; Sargeson, A. M. *Top. Stereochem.* **1970**, *6*, 219–277.

219. (a) Snow, M. R. *J. Am. Chem. Soc.* **1970**, *92*, 3610–3617. (b) Buckingham, D. A.; Maxwell, I. E.; Sargeson, A. M.; Snow, M. R. *ibid.* **1970**, *92*, 3617–3626.

220. (a) McDougall, G. J.; Hancock, R. D.; Boeyens, J. C. A. *J. Chem. Soc., Dalton Trans.* **1978**, 1438–1444. (b) Boeyens, J. C. A.; Hancock. R. D.; McDougall, G. J. *S. Afr. J. Chem.* **1979**, *32*, 23–26. (c) Hancock R. D.; McDougall, G. J.; Marsicano, F. *Inorg. Chem.* **1979**, *18*, 2847–2852.

221. DeHayes, L. J.; Busch, D. H. *Inorg. Chem.* **1973**, *12*, 1505–1513.

222. Laier, T.; Larsen, E. *Acta Chem. Scand.* **1979**, *A33*, 257–264.

223. Liang, C. D.; Baran, J. S.; Allinger, N. L.; Yuh, Y. *Tetrahedron* **1976**, *32*, 2067–2069.

224. Dougherty, D. A.; Mislow, K.; Huffman, J. W.; Jacobus, J. *J. Org. Chem.* **1979**, *44*, 1585–1589.

224a. Holker, J. S. E.; Jones, W. R.; Leeming, M. G. R.; Holder, G. M.; Midgley, J. M.; Parkin, J. E.; Whalley, W. B. *J. Chem. Soc., Perkin Trans. I* **1978**, 253–260. Ferguson, G.; Restivo, R. J.; Lane, G. A.; Midgley, J. M.; Whalley, W. B. *J. Chem. Soc., Perkin Trans. II* **1978**, 1038–1042.

225. Allinger, N. L.; Burkert, U.; De Camp, W. H. *Tetrahedron* **1977**, *33*, 1891–1895. Burkert, U.; Allinger, N. L., *Tetrahedron* **1978**, *34*, 807–809.

226. Boeyens, J. C. A.; Bull, J. R.; Tuiman, A.; van Rooyen, P. H. *J. Chem. Soc., Perkin Trans. II* **1979**, 1279–1287.

227. Patterson, D. G.; Djerassi, C.; Yuh, Y.; Allinger, N. L. *J. Org. Chem.* **1977**, *42*, 2365–2370.

227a. Schneider, H.-J.; Gschwendtner, W.; Weigand, E. F. *J. Am. Chem. Soc.* **1979**, *101*, 7195–7198.

228. DeTar, D. F.; Luthra, N. P. *J. Am. Chem. Soc.* **1977**, *99*, 1232–1244.

229. White, D. N. J.; Guy, M. H. P. *J. Chem. Soc., Perkin Trans. II* **1975**, 43–46.
230. White, D. N. J.; Morrow, C. *Comput. Chem.* **1979**, *3*, 33–48.
231. Madison, V.; Young, P. E.; Blount, E. R. *J. Am. Chem. Soc.* **1976**, *98*, 5358–5364.
232. Hagler, A. T.; Stern, P. S.; Sharon, R.; Becker, J. M.; Naider, F. *J. Am. Chem. Soc.* **1979**, *101*, 6842–6852.
233. Urry, D. W.; Khaled, M. A.; Renugopalakrishnan, V.; Rapaka, R. S. *J. Am. Chem. Soc.* **1978**, *100*, 696–705.
234. Clark, T.; Knox, T. Mc O.; McKervey, M. A.; Mackle, H.; Rooney, J. J. *J. Am. Chem. Soc.* **1979**, *101*, 2404–2410.
235. Paquette, L. A. *Pure Appl. Chem.* **1978**, *50*, 1291–1301; *Top. Curr. Chem.* **1979**, *79*, 41–165.
236. Roth, W. R.; Klärner, F.-G.; Lennartz, H.-W. *Chem. Ber.* **1980**, *113*, 1818–1829.
237. Rogers, D. W.; Dagdagan, O. A.; Allinger, N. L. *J. Am. Chem. Soc.* **1979**, *101*, 671–676.
238. Dewar, M. J. S. *Chem. Br.* **1975**, *11*, 97–106.
239. Morokuma, K. *Acc. Chem. Res.* **1979**, *10*, 294–300.
240. DeTar, D. F.; Tenpas, C. J. *J. Am. Chem. Soc.* **1976**, *98*, 4567–4571.
241. DeTar, D. F.; Tenpas, C. J. *J. Am. Chem. Soc.* **1976**, *98*, 7903–7908.
242. DeTar, D. F.; Tenpas, C. J. *J. Org. Chem.* **1976**, *41*, 2009–2013.
243. Winans, R. E.; Wilcox, C. F., Jr. *J. Am. Chem. Soc.* **1976**, *98*, 4281–4285.
244. Danforth, C.; Nicholson, A. W.; James, J. C.; Loudon, G. M. *J. Am. Chem. Soc.* **1976**, *98*, 4275–4281.
245. Abraham, M. H.; Grellier, P. L.; Hogarth, M. J. *J. Chem. Soc., Perkin Trans. II* **1975**, 1365–1371.
246. DeTar, D. F.; McMullen, D. F.; Luthra, N. P. *J. Am. Chem. Soc.* **1978**, *100*, 2484–2493.
247. Abraham, M. H.; Grellier, P. L.; Hogarth, M. J. *J. Chem. Soc., Perkin Trans. II* **1977**, 221–224.
248. Tremelling, M. J.; Hopper, S. P.; Mendelowitz, P. C. *J. Org. Chem.* **1979**, *44*, 4770–4774.
249. Müller, P.; Perlberger, J. C. *Helv. Chim. Acta* **1976**, *59*, 1880–1885.
250. Perlberger, J. C.; Müller, P. *J. Am. Chem. Soc.* **1977**, *99*, 6316–6319.
251. Wipke, W. T.; Gund, P. *J. Am. Chem. Soc.* **1976**, *98*, 8107–8118.
252. Bürgi, H. B. *Angew. Chem.* **1975**, *87*, 461–475; *Angew. Chem. Int. Ed. Engl.* **1975**, *74*, 460–473. Bürgi, H. B.; Dunitz, J. D.; Lehn, J. M.; Wippf, G. *Tetrahedron* **1974**, *30*, 1563–1572. Baldwin, J. E. *J. Chem. Soc., Chem. Commun.* **1976**, 738–741.
253. Bingham, R. C.; Schleyer, P. v. R. *J. Am. Chem. Soc.* **1971**, *93*, 3189–3199.
254. Karim, A.; McKervey, M. A.; Engler, E. M.; Schleyer, P. v. R. *Tetrahedron Lett.* **1971**, 3987–3990.

255. Ōsawa, E.; Engler, E. M.; Godleski, S. A.; Inamoto, Y.; Kent, G. J.; Kausch, M.; Schleyer, P. v. R. *J. Org. Chem.* **1980**, *45*, 984–991.

256. Fry, J. L.; Engler, E. M.; Schleyer, P. v. R. *J. Am. Chem. Soc.* **1972**, *94*, 4628–4634.

257. Lomas, J. S.; Luong, P. K.; Dubois, J.-E. *J. Am. Chem. Soc.* **1977**, *99*, 5478–5480.

258. Ōsawa, E.; Furusaki, A.; Hashiba, N.; Matsumoto, T.; Singh, V.; Tahara, Y.; Wiskott, E.; Farcasiu, M.; Iizuka, T.; Tanaka, N.; Kan, T.; Schleyer, P. v. R. *J. Org. Chem.* **1980**, *45*, 2985–2995.

260. Smith, M. R.; Harris, J. M. *J. Org. Chem.* **1978**, *43*, 3588–3596.

261. Farcasiu, D. *J. Org. Chem.* **1978**, *43*, 3878–3882.

262. Harris, J. M.; Mount, D. L.; Smith, M. R.; McManus, S. P. *J. Am. Chem. Soc.* **1977**, *99*, 1283–1285.

263. Schneider, H. J.; Thomas, F. *J. Am. Chem. Soc.* **1980**, *102*, 1424–1425.

264. Ōsawa, E.; Aigami, K.; Takaishi, N.; Inamoto, Y.; Fujikura, Y.; Majerski, Z.; Schleyer, P. v. R.; Engler, E. M.; Farcasiu, M. *J. Am. Chem. Soc.* **1977**, *99*, 5361–5373.

265. McKervey, M. A. *Tetrahedron* **1980**, *36*, 971–992.

266. Fort, R. C., Jr. "Adamantane, the Chemistry of Diamond Molecules"; Dekker: New York, 1976.

267. Müller, P.; Perlberger, J. C. *J. Am. Chem. Soc.* **1976**, *98*, 8407–8413; *ibid.* **1975**, *97*, 6862–6863.

268. Müller, P. *Chimia* **1977**, *31*, 209–218.

269. Burns, W.; McKervey, M. A.; Rooney, J. J.; Sammon, N. G.; Collins, J.; Schleyer, P. v. R.; Ōsawa, E. *J. Chem. Soc., Chem. Commun.* **1977**, 95–96.

270. Ōsawa, E.; Schleyer, P. v. R.; Chang, L. W. K.; Kane, V. V. *Tetrahedron Lett.* **1974**, 4189–4192. Musso, H. *Chem. Ber.* **1975**, *108*, 337–356. Deppisch, B.; Guth, H.; Musso, H.; Ōsawa, E. *Chem. Ber.* **1976**, *109*, 2956–2959.

271. Ōsawa, E.; Aigami, K.; Inamoto, Y. *J. Chem. Soc., Perkin Trans. II* **1979**, 181–190.

272. Ōsawa, E.; Aigami, K.; Inamoto, Y. *Tetrahedron* **1978**, *34*, 509–515.

273. Barborak, J. C.; Khoury, D.; Maier, W. F.; Schleyer, P. v. R.; Smith, E. C.; Smith, W. F., Jr.; Wyrick, C. *J. Org. Chem.* **1979**, *44*, 4761–4766.

274. Huisgen, R.; Ooms, P. H.; Mingin, M.; Allinger, N. L. *J. Am. Chem. Soc.* **1980**, *102*, 3951–3953.

275. House, H. O.; Phillips, W. V.; van Derveer, D. *J. Org. Chem.* **1979**, *44*, 2400–2405.

276. Dauben, W. G.; Kellogg, M. S. *J. Am. Chem. Soc.* **1980**, *102*, 4456–4463.

277. Ōsawa, E.; Shimada, K.; Kodama, K.; Itō, S. *Tetrahedron Lett.* **1979**, 2353–2354.

278. (a) Shirahama, H.; Ōsawa, E.; Matsumoto, T. *Tetrahedron Lett.* **1978**, 1987–1990; *J. Am. Chem. Soc.* **1980**, *102*, 3208–3213. (b) Shirahama, H.; Ōsawa, E.; Matsumoto, T. *Tetrahedron Lett.* **1979**, 2245–2246.

279. Messerotti, W.; Pagnoni, U. M.; Trave, R.; Zanasi, R.; Andreetti, G. D.; Bocelli, G.; Sgarabotto, P. *J. Chem. Soc., Perkin Trans. II* **1978**, 217-224.
280. Bellesia, F.; Pagnoni, U. M.; Pinetti, A.; Trave, R. *Gazz. Chim. Ital.* **1978**, *108*, 39-44.
281. Terada, Y.; Yamamura, S. *Tetrahedron Lett.* **1979**, 1623-1626.
282. Terada. Y.; Yamamura, S. *Tetrahedron Lett.* **1979**, 3303-3306.
283. Das, T. K.; Dutta, P. C.; Kartha, G.; Bernassau, J. M. *J. Chem. Soc., Perkin Trans. II* **1977**, 1287-1295.
284. Rüchardt, C.; Beckhaus, H.-D. *Angew. Chem.* **1980**, *92*, 417-429; *Angew. Chem. Int. Ed. Engl.* **1980**, *19*, 429-440.
285. Hönig, H.; Allinger, N. L. *J. Org. Chem.* **1977**, *42*, 2330-2333.
286. White, D. N. J.; Sim, G. A. *Tetrahedron* **1973**, *29*, 3933-3938.
287. Guy, M. H. P.; Sim, G. A.; White, D. N. J. *J. Chem. Soc., Perkin Trans. II*, **1976**, 1917-1920.
288. Godleski, S. A.; Schleyer, P. v. R.; Ōsawa, E.; Wipke, W. T. *Prog. Phys. Org. Chem.*, **1981**, *13*, 63-117.
289. Paquette, L. A.; Klein, G.; Doesche, C. W. *J. Am. Chem. Soc.* **1978**, *100*, 1595-1596.
290. For example, see: Ferguson, J.; Mau, A. W.-H.; Whimp, P. O. *J. Am. Chem. Soc.* **1979**, *101*, 2370-2377.
291. Harano, K.; Ban, T.; Yasuda, M.; Ōsawa, E.; Kanematsu, K., *J. Am. Chem. Soc.* **1981**, *103*, 2310-2317.
292. Olah, G. A.; Liang, G.; Schleyer, P. v. R.; Engler, E. M.; Dewar, M. J. S.; Bingham, R. C. *J. Am. Chem. Soc.* **1973**, *95*, 6829-6831.
293. Martella, D. J.; Jones, M. Jr.; Schleyer, P. v. R.; Maier, W. F. *J. Am. Chem. Soc.* **1979**, *101*, 7634-7637. Maier, W. F.; Schleyer, P. v. R., *ibid.* **1981**, *103*, 1891-1900.
294. Cf. Burkert, U. *Chem. Ber.* **1977**, *110*, 773-777.
295. Forrest, T. P. *J. Am. Chem. Soc.* **1975**, *97*, 2628-2630.
296. Tokita, K.; Kondo, S.; Takeda, M. *J. Chem. Res. (S)* **1980**, 63.
297. (a) Johnston, M. D., Jr.; Raber, D. J.; DeGennaro, N. K.; D'Angelo, A.; Perry, J. W. *J. Am. Chem. Soc.* **1976**, *98*, 6042-6044. (b) Raber, D. J.; Janks, C. M.; Johnston, D. M., Jr.; Raber, N. K. *Tetrahedron Lett.* **1980**, 677-680.
298. DeTar, D. F.; Luthra, N. P. *J. Org. Chem.* **1979**, *44*, 3299-3305.
299. Wilson, N. K.; Stothers, J. B. *Top. Stereochem.* **1974**, *8*, 1-158.
300. Smith, D. H.; Jurs, P. C. *J. Am. Chem. Soc.* **1978**, *100*, 3316-3321.
301. Schneider, H.-J.; Weigand, E. F. *J. Am. Chem. Soc.* **1977**, *99*, 8362-8363; 8363-8364.
303. For example, see: Wilson, S. R.; Huffman, J. C. *J. Org. Chem.* **1980**, *45*, 560-566.
304. (a) "Computer-Assisted Drug Design," Olson, E. C.; Christoffersen, R. E., Eds.; American Chemical Society: Washington, D. C., 1979; ACS Symposium Series No. 112. (b) Gund, P.; Andose, J. D.; Rhodes, J. B.; Smith, G. M. *Science* **1980**, *208*, 1425-1430.

305. Dyott, T. M.; Stuper, A. J.; Zander, G. S. *J. Chem. Inf. Comput. Sci.* **1980**, *20*, 28-35.
306. Stuper, A. J.; Dyott, T. M.; Zander, G. S., in ref. 304a, pp. 383-414.
307. Smith, G. M.; Gund, P. *J. Chem. Inf. Comput. Sci.* **1978**, *18*, 207-210.
308. Gund, P. *Annu. Rep. Med. Chem.* **1979**, *14*, 299-308.
309. Nuss, M. E.; Marsh, F. J.; Kollman, P. A. *J. Am. Chem. Soc.* **1979**, *101*, 825-833.
310. Hagler, A. T.; Huler, E.; Lifson, S. *J. Am. Chem. Soc.* **1974**, *96*, 5319-5327.
311. For example, see: Weintraub, H. J. R. *Int. J. Quant. Chem.: Quant. Biol. Symp.* **1977**, *4*, 111-125.
312. Cf. Warshel, A. *J. Phys. Chem.* **1979**, *83*, 1640-1652.
313. Şimonetta, M. *Acc. Chem. Res.* **1974**, *7*, 345-350.
314. Warshel, A.; Lifson, S. *J. Chem. Phys.* **1970**, *53*, 582-594.
315. Lifson, S.; Levitt, M. *Comput. Chem.* **1979**, *3*, 49-50.
316. Williams, D. E.; Starr, T. L. *Comput. Chem.* **1977**, *1*, 173-177.
317. (a) Hagler, A. T.; Huler, E.; Lifson, S. *J. Am. Chem. Soc.* **1974**, *96*, 5319-5327. (b) Hagler, A. T.; Lifson, S. *ibid.* **1974**, *96*, 5327-5335.
318. (a) Hagler, A. T.; Lifson, S.; Dauber, P. *J. Am. Chem. Soc.* **1979**, *101*, 5122-5130. (b) Hagler, A. T.; Dauber, P.; Lifson, S. *ibid.* **1979**, *101*, 5131-5141.
319. Bernstein, J.; Hagler, A. T. *J. Am. Chem. Soc.* **1978**, *100*, 673-681.
320. Warshel, A. *J. Am. Chem. Soc.* **1979**, *101*, 744-746.
321. Weinstein, S.; Leiserowitz, L.; Gil-Av, E. *J. Am. Chem. Soc.* **1980**, *102*, 2768-2772.
322. Fyfe, C. A.; Harold-Smith, D. *Can. J. Chem.* **1976**, *54*, 769-782; 783-789.
323. Liljefors, T.; Wennerström, O. *Tetrahedron* **1977**, *33*, 2999-3003.
324. Ermer, O. *Angew. Chem.* **1977**, *89*, 431-432; *Angew. Chem. Int. Ed. Engl.* **1977**, *16*, 411-412.
324a. The synthesis of 1,16-dimethyldodecahedrane was reported after submission of the manuscript of this chapter. Paquette, L. A.; Balogh, D. W.; Usha, R.; Kountz, D.; Christoph, G. G. *Science*, **1981**, *211*, 575-576.
325. Wiberg, K. B. *Comput. Chem.* **1977**, *1*, 221-223.
326. White, D. N. J. *Comput. Chem.* **1977**, *1*, 225-233.
327. Allinger, N. L.; Hickey, M. J. *Tetrahedron* **1972**, *28*, 2157-2161.
328. Bartell, L. S.; Fitzwater, S.; Hehre, W. J. *J. Chem. Phys.* **1975**, *63*, 4750-4758.
329. Wilson, K. R. In "Computer Networking and Chemistry," Lykos, P., Ed.; American Chemical Society: Washington, D. C., 1975; ACS Symposium Series No. 19.
330. Allen, F. H.; Bellard, S.; Brice, M. D.; Cartwright, B. A.; Doubleday, H.; Higgs, H.; Hummelink, T.; Hummelink-Peters, B. G.; Kennard O.; Motherwell, W. D. S.; Rodgers, J. R.; Watson, D. G. *Acta Crystallogr., Sect. B* **1979**, *35*, 2331-2339.

331. DeTar, D. F. *Comput. Chem.* **1976**, *1*, 115–119.
332. MACCS: Molecular Design Ltd., 1122 B. St., Hayward, CA 94541.
333. For example, see: Versichel, W.; Geise, H. J. *Comput. Chem.* **1979**, *3*, 136.

Chiral Monolayers at the Air-Water Interface

MARTIN V. STEWART

Department of Chemistry and Physics
Middle Tennessee State University
Murfreesboro, Tennessee

EDWARD M. ARNETT*

Department of Chemistry
University of Pittsburgh
Pittsburgh, Pennsylvania

I. Introduction 196
II. The "Absolute" Method of Stereochemistry and Some Definitions 199
III. Monolayers at the Air-Water Interface 202
IV. Experimental Monolayer Chemistry 205
V. Enantiomer Discrimination in Monolayers 220
A. Simple Surfactants 221
B. More Complex Surfactants 241
VI. A Case in Point: Acid-Dependent Chiral Discrimination of the *N*-α-Methylbenzylstearamides 245
VII. Diastereomer Discrimination in Monolayers 249
VIII. Summary 253
Acknowledgments 254
References 254

*Present address: Department of Chemistry,
Gross Laboratory,
Duke University,
Durham, North Carolina.

I. INTRODUCTION

This chapter is an outgrowth of our longstanding interest in the stereochemistry of molecular interactions—the ways that molecules fit together in different environments. An especially interesting field for such studies is that of chiral monolayers, whose literature is relatively sparse, diffuse, and obscure. This topic involves the two disciplines of interfacial chemistry and stereochemistry between which there has been very little collaboration. It is our hope that by presenting the current state of this interdisciplinary area, we may interest some stereochemists in interfacial chemistry and some surface chemists in stereochemistry. Accordingly, we have described the relevant methodology of both fields more extensively than would be appropriate if we were writing only for experts in either one. We encourage the reader to brush over familiar material and hope that he or she will find the rest intriguing.

One of the most important problems in organic chemistry and biochemistry is the understanding and control of stereospecific reactions. The contrast between the stereospecificity of reactions in biological organisms (1–3) and the comparatively poor control of asymmetric synthesis (4–7) in the laboratory remains tantalizing despite the considerable progress that has been made recently (8). Obviously, dissymmetry at the level of biomolecules and their aggregates must play a major role in biochemical specificity (9), and the extensive employment of chiral assemblies in living systems implies that a high degree of survival value results from stereospecific interactions. Hence, a detailed knowledge of the stereochemistry of intermolecular and interionic organization is ultimately required for understanding the molecular processes that characterize life.

From the viewpoint of modern physical chemistry, the delineation of stereospecificity must ultimately come down to a detailed analysis of the strength and geometrical requirements of the forces that attract molecules and hold them together in complexes, aggregates, and transition states. These forces have been classified in their simplest terms in several reviews (10–12). They range from the relatively weak and nondirectional dispersion forces to hydrogen bonds and ion-dipole interactions, which have enough strength and direction to provide a good starting point for the prediction of stereospecificity. Before addressing the major topic of this chapter, we refer briefly to the large and scattered literature on chiral aggregation in various types of related complexes and note a few key papers and recent reviews.

Most chemists appreciate at once that there should be energetic differences between an assembly of chiral (i.e., right- and left-handed) molecules to form aggregates that are diastereomerically related and also those that are differentiated as pure enantiomers versus racemic modifications. However, there have been remarkably few authenticated physicochemical studies of discriminating chiral interactions in loose ionic or molecular complexes such as ordinary ion pairs or solvates, and all these indicate that chiral recognition factors in solution are energetically small (usually less than 0.5 kcal/mol). Horeau and Guetté (13) have rejected most of the reports in this field as inconclusive because of inadequate purification of materials or other failures in experimental approach. Their extensive review has been supplemented recently by Wynberg and Feringa (14), who stressed the effect of "antipodal interactions" on chemical reactivity and by Craig and Mellor (15), who provided a theoretical foundation for the calculation of short- and long-range interaction terms for chiral molecules.

Although the chiral recognition factor in such systems is relatively weak, there is no question that it is measurable and provides a useful approach to elucidating intermolecular interactions between nonreacting molecules.

Tanford (16) has recently summarized the evidence for hydrophobic bonding in biochemistry and has emphasized (17) that living matter depends on the hydrophobic interactions of amphipathic molecules in an aqueous environment for assembly into basic organizational units such as cell membranes. Considerable background on these matters is available in the six-volume treatise edited by Franks (18). Bender (19,20) and Breslow (21) have achieved partial stereochemical control of reactions using cyclodextrin inclusion compounds as models for enzyme-substrate complexes. More recently, the beautifully conceived "host-guest" experiments of Cram (22) and Lehn (23) have pointed the way to using multiply positioned hydrogen-bonding sites for the stereospecific resolution of amino acids. Pirkle (24) has demonstrated the use of chiral solvents for elucidating the configuration and enantiomeric purity of chiral solutes through the NMR spectra of diastereomeric solvates. Similarly, optical resolution of underivatized enantiomers has been achieved with liquid chromatography by the use of both chiral stationary and chiral mobile phases (25). Although we intentionally omit from this chapter the behavior of other types of chiral surfactant systems such as micelles (26-30), this is presently a lively and important field that deserves treatment as a separate topic (31).

The studies referred to above demonstrate the significance and potential power of hydrogen bonding, ion association, and hydrophobic bonding in stereospecific aggregation that could ultimately provide a means for controlling the stereochemical course of reactions. However, as matters stand now, there is only rudimentary information on the strength and geometrical requirements of these forces.

One may consider a series of physical states ranging from the crystalline, where molecular aggregation and orientation are large, to the dilute gaseous state, where there are no significant orientational limits. States of intermediate order are represented by micelles, liquid crystals, monolayers, ion pairs, and dipole-dipole complexes. In the crystalline state, the differences between pure enantiomers, racemic modifications, and diastereomeric complexes are clearly defined both structurally and energetically (32,33). At the other extreme, stereospecific interactions between diastereomerically related solvents and solutes, ion pairs, and other partially oriented systems are much less clearly resolved.

Diastereomeric transition states are, ipso facto, a special case because they cannot (by definition) be studied directly, although it is obvious that the reacting molecules must be limited to the proper spatial arrangement if they are to react at all. Much of the stereochemical literature of organic chemistry and biochemistry describes attempts to infer the relative energies and structures of diastereomeric transition states from reaction rates and the configurations of reactants and products. However, the reacting species must first approach each other, and any differences in the binding energy of diastereomeric complexes may contribute to their relative activation energies. Transition states can be studied indirectly through the combination of thermodynamic data for initial states with activation parameters (34–36). Thus, the thermodynamics of chiral aggregation may be highly relevant to kinetic studies of stereochemistry.

This chapter discusses stereospecific intermolecular interactions in monolayers at the air-water interface, where surface-active molecules (surfactants) are partially oriented with respect to each other by the cooperative combination of interionic, hydrophobic, and hydrogen-bonding forces. We believe that these reports should be of particular interest in relation to stereospecificity in assemblies such as micelles, vesicles, and bilayer membranes, where their significance has been largely ignored.

The ultimate goal of this work is to elucidate the contribution of shape and symmetry to the aggregation of molecules and ions. As

we have noted, intermolecular forces are often relatively weak and may be geometrically ill defined. Furthermore, the study of interfacial systems is notoriously vulnerable to the effects of impurities. Fortunately, a rationale is available that provides a powerful approach to these problems through the principles of classical stereochemistry. The stereochemical approach, which is the topic of Sect. II, also provides an *absolute* method to check for the effects of impurities and reduces the likelihood of problems from this source to a very low level.

II. THE "ABSOLUTE" METHOD OF STEREOCHEMISTRY AND SOME DEFINITIONS

Chiral molecules interact to form complexes that are related as enantiomers or as diastereomers. Enantiomers are perfect chemical models for each other except in their interactions with polarized light or with other chiral molecules, and this provides the basis for an absolute method for demonstrating subtle differences in physical properties that might otherwise be confused with the effects of impurities.

Let the subscript I denote the molecular structure of a chiral molecule possessing, to simplify discussion, a single chiral center. If the letters R and S specify absolute configuration according to the sequence rules of Cahn, Ingold, and Prelog (37), then R_I and S_I describe a pair of enantiomers (i.e., nonsuperposable mirror-image stereoisomers). Let a row of dots symbolize an intermolecular interaction between the indicated molecules and $M(\ )$ represent the numerical magnitude of any measurable physical property of the bulk sample.

The possible types of intermolecular associations between R_I and S_I are summarized in Table 1 using this notation. The first two interactions listed are related enantiomerically and are necessarily identical. The third interaction differs from the first two in that both enantiomers are involved.

If R_I and S_I display ideal behavior on mixing, then

$$M(R_I \cdots R_I) = M(S_I \cdots S_I) = M(R_I \cdots S_I)$$

If nonideal behavior is displayed, then

$$M(R_I \cdots R_I) = M(S_I \cdots S_I) \neq M(R_I \cdots S_I)$$

and a true binary mixture results. We refer to any measurable manifestation of nonideality in such a system as an *enantiomer discrimination*, for the physical properties of the bulk sample would exhibit a dependence on its optical purity. Nonideal behavior is frequently, but not always, detectable in highly oriented and strongly interacting systems such as crystalline solids and hydrogen-bonded liquids. Ideality is the general rule for enantiomeric mixtures that are gases, nonassociating liquids, or dilute solutions.

Although $M(R_I \cdots R_I) = M(S_I \cdots S_I)$ for both ideal and nonideal systems, the enantiomers R_I and S_I are differentiated by the presence of a second different chiral molecule (e.g., either R_{II} or S_{II}). Two pairs of enantiomers are capable of four other types of intermolecular association, in addition to the three already mentioned in Table 1. These are conveniently diagrammed in Figure 1,

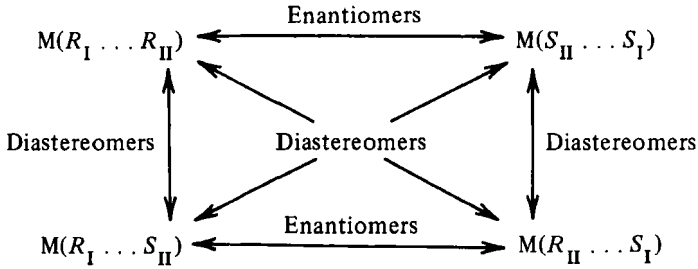


Figure 1. Schematic relationship of enantiomeric and diastereomeric interactions for two pairs of enantiomers.

where the double-headed arrows represent all possible comparisons between any measurable physical property of a bulk sample having the composition indicated by the interacting pairs. Obviously, these

Table 1
Intermolecular Associations of a Single Enantiomeric Pair

Interaction	Bulk Sample
$R_I \cdots R_I$	Optically pure R_I
$S_I \cdots S_I$	Optically pure S_I
$R_I \cdots S_I$	Optically impure sample, which is racemic when mol % R_I = mol % S_I

do not have to represent four unique measurements (i.e., six independent comparisons), but rather two different pairs of equivalent measurements (i.e., three independent comparisons), which can be used, if necessary, as checks on each other. For example, data obtained from the enantiomerically related pairs are necessarily related as

$$M(R_{\mathrm{I}} \cdots R_{\mathrm{II}}) = M(S_{\mathrm{II}} \cdots S_{\mathrm{I}}) \quad \text{and}$$
$$M(R_{\mathrm{I}} \cdots S_{\mathrm{II}}) = M(R_{\mathrm{II}} \cdots S_{\mathrm{I}})$$

This, in turn, demands the equivalence of the four ways in which the diastereomerically related pairs can be compared, namely,

$$\begin{aligned} M(R_{\mathrm{I}} \cdots R_{\mathrm{II}}) - M(R_{\mathrm{I}} \cdots S_{\mathrm{II}}) &= \\ M(S_{\mathrm{II}} \cdots S_{\mathrm{I}}) - M(R_{\mathrm{II}} \cdots S_{\mathrm{I}}) &= \\ M(S_{\mathrm{II}} \cdots S_{\mathrm{I}}) - M(R_{\mathrm{I}} \cdots S_{\mathrm{II}}) &= \\ M(R_{\mathrm{I}} \cdots R_{\mathrm{II}}) - M(R_{\mathrm{II}} \cdots S_{\mathrm{I}}) & \end{aligned}$$

We refer to any measurable difference between diastereomeric pairs as a *diastereomer discrimination*. We use the term *chiral discrimination* to include both enantiomer and diastereomer discrimination for the general case.

The absolute methodology, then, is applied by preparing chiral compounds, purifying them until the enantiomers exhibit identical physical properties, and comparing their properties with those of mixtures of the same pure enantiomers. Thus, an *enantiomer discrimination* will be revealed. When mixed with pure enantiomers of a second chiral compound, a *diastereomer* discrimination will be demonstrated. Chiral cross-checks (e.g., $R_{\mathrm{I}}S_{\mathrm{II}}$ vs. $R_{\mathrm{II}}S_{\mathrm{I}}$) will provide insurance against errors from artifacts or impurities. Similarly, an enantiomer discrimination is confirmed if identical results are observed for a racemic modification obtained by mixing equal amounts of optically pure enantiomers and also through chemical synthesis from a racemic precursor. For systems as sensitive to the presence of trace impurities as monolayers, the stereochemical approach can provide powerful protection against errors in interpretation. In Sect. V we provide an example of such a pitfall, drawn from an early study of chiral monolayers.

This strategy is "absolute" in the sense that it employs symmetry properties of perfectly corresponding pairs rather than approximate models based on extrapolation, analogy, homology, or calculations from "first principles." No other method is available in chemistry to provide such strong proof of internal consistency. Any measurable

difference is necessarily due to differences in the geometrical requirements and the strength of the forces by which the system aggregates. A considerable price may have to be paid, however, in terms of the extra labor involved in making the cross-chiral checks and purifying materials until the checks agree. For this reason, the method has been employed only rarely. Another obstacle to general use is that often only one enantiomer is easily available (e.g., as a natural product) and the antipode must be synthesized.

The only possible fallacy in this method is its inability to detect *directly* either an identical amount of the same impurity in all four samples or in any particular pair of enantiomers. However, since each sample must be purified independently, the accidental introduction of an equivalent amount of a potent impurity in either case is unlikely unless it is a common side product from a synthetic step.

III. MONOLAYERS AT THE AIR-WATER INTERFACE

Of all the many modes by which ions and molecules can aggregate, there is probably none that offers a greater opportunity for the controlled investigation of molecular orientation than is presented by monolayers at the air-water interface. Monolayers are films one molecule thick that are generated when certain types of surfactant molecules are spread on the surface of clean aqueous media, either pure water or electrolyte solutions. As a basic structural requirement, monolayer-forming compounds must have one or more hydrophilic head groups attached to a hydrophobic residue, which is often an *n*-alkyl chain of sufficient size to render the whole molecule or ion virtually insoluble in water. Such molecules are called amphipathic to emphasize the opposing hydrophilic and hydrophobic portions of their structure. If the hydrocarbon chain is short, say 6 to 10 methylene groups, the molecules will go into the aqueous phase, where they will aggregate to form micelles when their concentration exceeds the *critical micelle concentration* (CMC). If the chain is longer, most of the molecules are retained at the air-liquid interface. Provided intermolecular attractions are not too large, the molecules will then cover the liquid surface as a monolayer whose characteristics are roughly those of a two-dimensional gas, liquid, or solid, depending on the conditions of temperature, subphase composition, and the surface area of the subphase per molecule of surfactant.

The high degree of intermolecular order that is possible for sur-

factants in aqueous media results from a balance between the solvating requirements of the polar, hydrophilic head group and the opposing hydrophobic aggregation of the nonpolar hydrocarbon chains (16). The latter is caused by the relatively strong attraction of water molecules for each other to form an extended, three-dimensional, hydrogen-bonded network. The fatty, nonpolar portions of the amphipathic molecules are, in turn, weakly attracted by short-range dispersion forces, whereas their polar head groups are directed to maximize solvation. Thus, the hydrophobic groups are "squeezed out" of the solvent matrix and aggregate either in the form of micelles within the aqueous medium or as a monolayer adsorbed at the air-water interface.

The fundamental physical chemistry of monolayers was worked out several decades ago by Langmuir, Harkins, Rideal, Adam, Schulman, and others. In an excellent monograph, Gaines (38) has summarized the history and the state of knowledge up to 1966 of monolayers at air-liquid interfaces. Other good accounts of the subject can be found in several more general texts on surface chemistry (39–43). None, however, includes a discussion (or even a reference) to chirality in monolayers.

An extraordinary opportunity to manipulate molecular orientation is possible in a monolayer through variation of the surface area (the two-dimensional equivalent of volume, which is symbolized as A and has units of square angstroms per molecule). The properties most commonly related to surface area are surface pressure π, and surface tension γ, both having units of dynes per centimeter. We describe methods for studying the relation of these and other surface properties in the next section, where we also more fully define their meaning.

One end of each surface-active molecule in a monolayer is anchored firmly to the liquid surface by the attraction of the polar head group for the aqueous subphase, while the hydrophobic portion is displaced easily from it. If the molecules are separated widely as in a "gaseous monolayer," the simple two-dimensional gas law is approached, namely, $\pi A = kT$, where k is the Boltzmann constant. The hydrophobic chains are free to assume almost any orientation above the surface and may sweep out circles with radii as long as their tails by rotating around their point of attachment at the head group. However, intermolecular translational movements are restricted to the two-dimensional interfacial plane because the hydrophilic head groups cannot leave the aqueous surface.

As the available surface area is reduced, the hydrocarbon tails will collide with each other more frequently until there is no longer

enough space to accommodate the random orientations of the chains. At this area, molecular packing can proceed by having the chains lift off from the surface to assume various orientations, and a sharp increase in surface pressure is noted. As the area per molecule is reduced yet further, there is often a series of phase transitions that may be related, in some cases, to different molecular orientations in the so-called two-dimensional liquid or crystalline states. As we shall see later, these states may or may not be stable in the thermodynamic sense. As the area occupied by the monolayer is further decreased, the surface pressure increases to a maximum and then drops quickly, indicating the collapse of the film (Fig. 2). The ability to relate molecular shape to molecular packing, hence to physical properties, is precisely what makes monolayers so appealing to the physical chemist. Thus, the cross-sectional area for vertical fatty acid chains in the condensed solid states of many monolayers corresponds closely to that found in the crystal, ca. 20 $Å^2$ (44,45).

Reactions in monolayers (38b) also provide direct chemical evidence for the dependence of molecular orientation on the surface area. The rates of oxidation and halogenation of double bonds midway along the carbon chain of oleic acid, the rate of lactoniza-

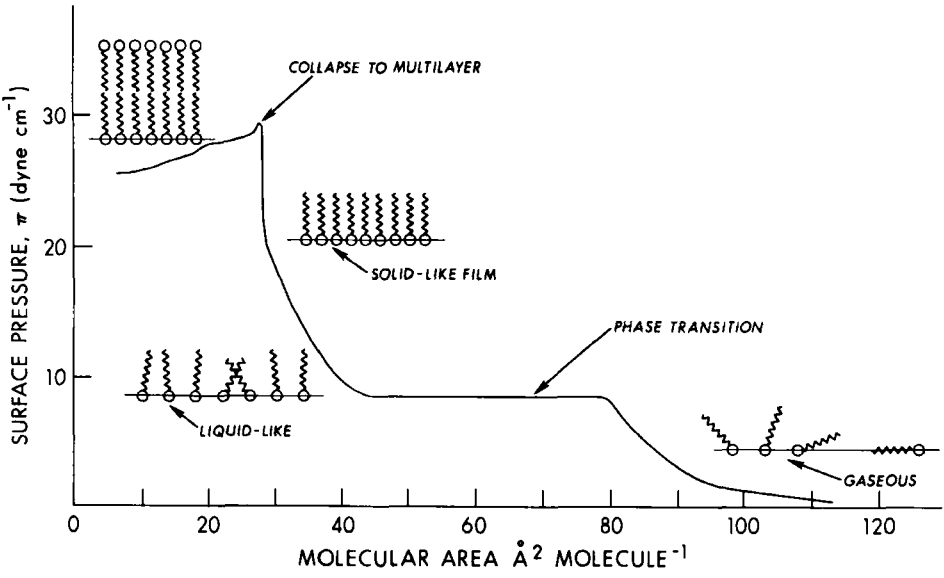


Figure 2. Typical force-area (π–A) curve for compression of a monolayer on a Langmuir film balance with molecular orientations often proposed for different regions.

tion of γ-hydroxystearic acid, and the attack of enzymes and snake venoms on monolayer substrates can be regulated, and in some cases stopped, by compressing the film with a barrier. The reaction resumes at its previous rate when the barrier is backed off to allow the film to expand. This is strong evidence that compressing the film causes the hydrophobic chains of the substrate molecules to lift off from the surface, thereby removing the reactive functions from the portion of the aqueous interface at which they are accessible to attack by the reagent. Clearly, some of the problems of random approach in three dimensions that complicate interpretations of rate phenomena in dilute solutions may be clarified when studied "two dimensionally" in monolayers.

The significance of monolayers to biochemistry lies in their close relation to the molecular interactions that take place at the interface between aqueous and hydrophobic systems such as cell membranes and within enzymes. The molecular alignment in monolayers is closely related to the lipid bilayer structure proposed for membranes (46). Since stereospecific chemical reactions of living organisms often take place at the cell boundaries, it is small wonder that during the past 25 years much monolayer research has been reported by biochemists, physiologists, and pharmaceutical chemists (47–51).

Surface-active lipids and the proteins that comprise biomembranes are all chiral, as are most of the biochemicals that travel through them. Therefore, if there are significant differences between the energetics of diastereomeric interactions between membrane components, chiral aggregation factors could play a key role in biological organization and membrane processes. This proposition is so obvious as to be nearly tautological. However, very few of the many studies of biochemically important molecules in membranes make explicit recognition of this fact.

The work reviewed here shows that chiral discrimination in monolayers is probably quite general and can be modulated by variations in the temperature and pH of the aqueous subphase. This property alone renders the many monolayer studies of racemic materials inconclusive for comparison with naturally occurring optically active systems (or vice versa).

IV. EXPERIMENTAL MONOLAYER CHEMISTRY

The basic equipment and methods for spreading and handling monolayer films at the air-water interface were developed initially by

Langmuir and Blodgett at the General Electric Company Research Laboratories. In a series of papers that truly deserve to be called "elegant" by virtue of their novelty, simplicity, and generality, the techniques for spreading, compressing, and transferring monolayers were worked out by these two scientists, whose names are still associated with the Langmuir film balance and the Blodgett dipping technique. Although steady refinement in the basic equipment and methods occurred over the half-century following Langmuir's seminal paper on fatty acid monolayers (52), published in 1917, several major improvements that considerably enhance the reliability of monolayer work have become possible only recently. Application of modern analytical instrumentation to this field has been fostered by the relevance of monolayers to biophysical studies of membrane bilayers on one hand, and on the other, to the sudden leap forward that the study of solid surfaces is now enjoying (47). Since monolayer films either at the air-water interface or transferred to a solid support provide an unusually simple heterogeneous system, they may be expected to share in the rapid development of surface science and to help in illuminating some aspects of it (53–58).

The most important property of a liquid-gas interface is its surface energy. Surface tension arises at the boundary because of the grossly unequal attractive forces of the liquid subphase for molecules at its surface relative to their attraction by the molecules of the gas phase. These forces tend to pull the surface molecules into the interior of the liquid phase and, as a consequence, cause liquids to minimize their surface area. If equilibrium thermodynamics apply, the surface tension γ is the partial derivative of the Helmholtz free energy of the system with respect to the area of the interface—when all other conditions are held constant. For a phase surface, the corresponding relation of γ to Gibbs free energy G and surface area A is shown in eq. [1].

$$\gamma = \left(\frac{\partial G}{\partial A}\right)_{T,\,P,\,N_J} \qquad [1]$$

Surface tension may be considered equally well as free energy per unit area or as force per unit length (39). Surface tension is manifested in the development of menisci, capillary rise, bubble growth, and the flow patterns of liquid jets. On a Langmuir film balance, the measured energy property that is studied as a function of area is the force exerted by the molecules in the monolayer against a floating barrier that separates a clean water surface from one supporting the mono-

layer. When a liquid surface is covered by an insoluble monolayer, its surface tension is lowered. A surface force against the barrier results from the difference in surface tension between the pure liquid surface γ_0 and the one covered by the film, γ. This surface force against the barrier is equivalent in two dimensions to pressure in three dimensions and is called the surface pressure π. For a system at equilibrium, the surface pressure can be measured directly by the difference in surface tension between the two surfaces separated by the floating barrier (38):

$$\pi = \gamma_0 - \gamma \qquad [2]$$

Since surface pressure is a free energy term, the energies and entropies of first-order phase transitions in the monolayer state may be calculated from the temperature dependence of the π-A curve using the two-dimensional analog of the Clausius-Clapeyron equation (59), where ΔH is the molar enthalpy change at temperature T and ΔA is the net change in molar area:

$$\Delta H = T\Delta A\frac{d\pi}{dT} \qquad [3]$$

Although the measurement of liquid surface tensions (i.e., surface energies) can be accomplished by many methods (39,60), only three are generally useful for the study of monolayers on aqueous solutions. These are the du Nouy ring detachment method, the Wilhelmy hanging-plate method, and the direct measurement of the surface pressure exerted against a floating barrier using a suitably arranged differential torsion balance.

The convenience of the ring detachment method lies in the availability of simple, inexpensive apparatus. A ring of platinum wire, freshly flamed to ensure cleanliness, is drawn vertically out of the solution's surface, using a torsion balance to measure the resisting force that opposes the increase in surface area of the adhering liquid. With practice, it is possible to obtain reproducible values for the force just necessary to remove the ring from the surface. By the use of appropriate tables and calibration factors (60), static surface tension may be determined with an error of about 1%. The crucial value of the force is at the catastrophic point where the meniscus breaks, and this is most difficult to observe objectively. To deal with this problem and a number of others, such as good temperature control, automated tensiometers are now available (Fig. 3). These

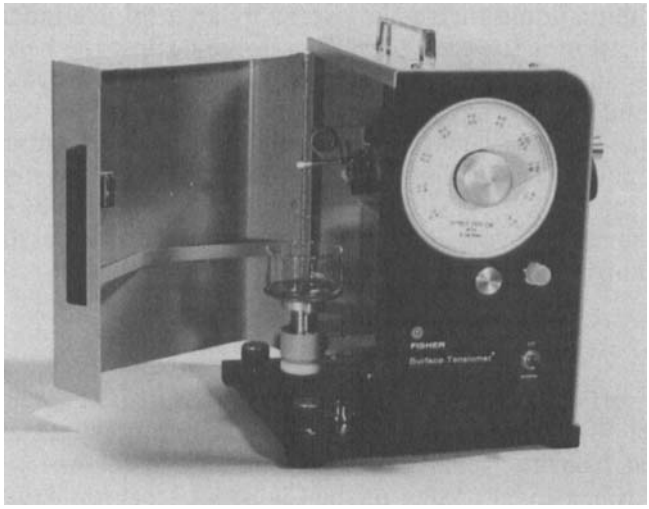


Figure 3. A modern automatic tensiometer. Photograph supplied by Fisher Scientific Co.

devices use a motor-driven table to lower the vessel containing the liquid surface from contact with the ring. The force on the ring is measured with a transducer, which is connected to a strip chart recorder to determine the exact restoring force at the instant of rupture. Surface tensions are claimed to be accurate and reproducible to ±0.04% by this arrangement.

The Wilhelmy plate method provides an extremely simple approach that, unlike the ring detachment method, permits the measurement of continuously varying or dynamic surface tensions. If a thin plate (e.g., a microscope slide, a strip of platinum foil, or even a slip of filter paper) is attached to a microbalance and suspended so that its lower edge is just immersed in a liquid, the measured apparent weight W_T is related to the actual weight of the plate W_P and the surface tension γ by the following simple equation:

$$W_T = W_P + \gamma \cdot p \qquad [4]$$

where p is the perimeter of the plate surface in contact with the liquid. For thin plates, this will obviously approximate twice the width of the plate. The recording microbalance (Fig. 4) can be used to follow changes in surface energy by this method, and it has become the technique most commonly employed with the Langmuir film balance.

The use of an automatically recording torsion balance (38,41,42, 55,61) to measure the force generated by a monolayer film against a floating barrier permits its determination with great sensitivity and accuracy to the millidyne level. Figure 5 shows a schematic of a Langmuir film balance. The two arms of a U-shaped fork, which is connected to a phosphor-bronze torsion strip, are inserted loosely through a Teflon floating barrier. Small lateral displacements of the barrier are directly proportional to the film pressure against it and can be converted to recorded voltage changes by the vertical movement of a tiny metal core that hangs in the cavity of a linearly variable differential transducer (LVDT). In practice, the torsion balance system is calibrated frequently by placing small class S weights on the pan suspended from the cross-arm of the torsion strip. The exact relationship between surface pressure in dynes per centimeter of barrier length and displacement of the strip chart recorder pen is thus assured. Alternatively (and preferably), the voltage output from the LVDT may be digitized with an analog-digital converter for storage and processing of the data by computer.

Since surface tension is affected greatly by temperature, there is little point in measuring it carefully unless the apparatus is well thermostatted and the surface and subphase have been brought to

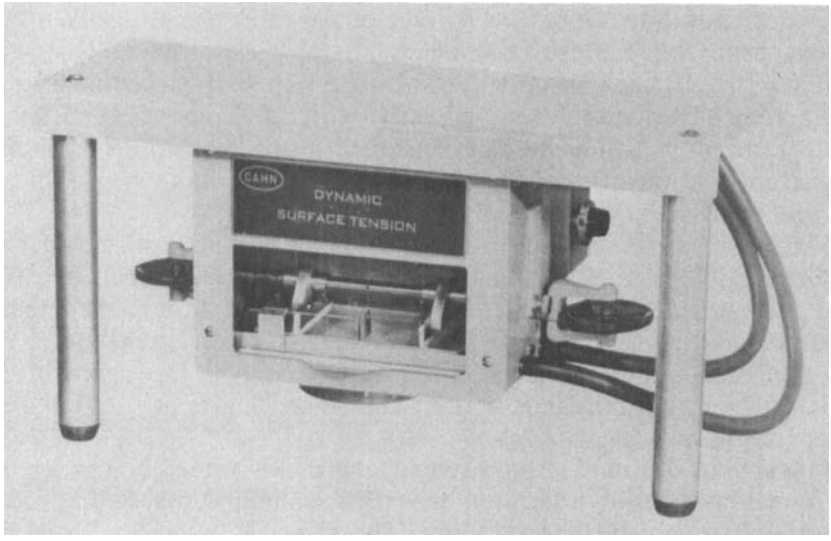


Figure 4. Automatic dynamic surface tension balance showing Wilhelmy plate suspended in surface. Photograph supplied by Cahn Instruments, Inc.

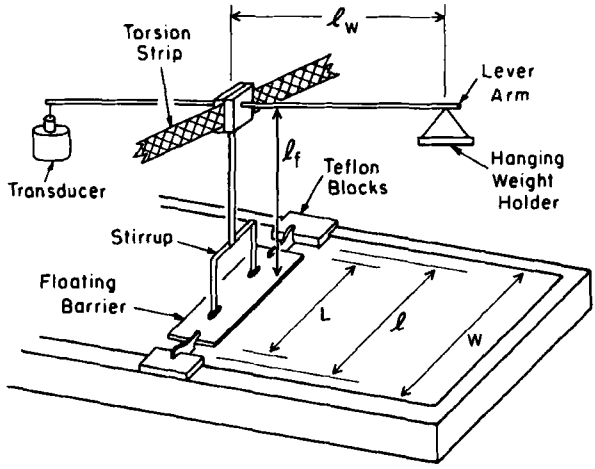


Figure 5. Schematic of a modern film balance. From Thompson (101).

thermal equilibrium. In view of the furious activity at the molecular level that must be associated with the passage of water molecules to and from the gas phase through the surface film, it is a moot point what the actual surface temperature may be or, for that matter, where the actual surface zone begins or ends in either phase. Obviously, unless the relative humidity of the air in the film balance case is 100%, evaporation from the surface must cause local cooling. A recent paper by Kellner (62) demonstrates the considerable error that can arise from failing to control the film balance temperature adequately. The careful comparison of force-area curves at various temperatures to study two-dimensional phase transitions was an important feature of several key studies on chiral monolayers which we discuss in Sect. V.

Figures 6 and 7 show a modern Langmuir film balance and its arrangement inside a Puffer-Hubbard temperature-controlled cabinet (63). Inside the cabinet, the film balance is protected further from circulating air currents by a Plexiglass case. At the bottom of the Teflon trough lies a serpentine glass coil through which water from a thermoregulator is circulated to help control subphase temperature.

Movement of the Teflon sweeping barrier is effected through a worm screw assembly mounted beneath the aluminum base that supports the trough during operation. The screw is driven by a sealed reversible motor with a precision feedback controller to maintain constant speed and torque. Force-area isotherms are actually gener-

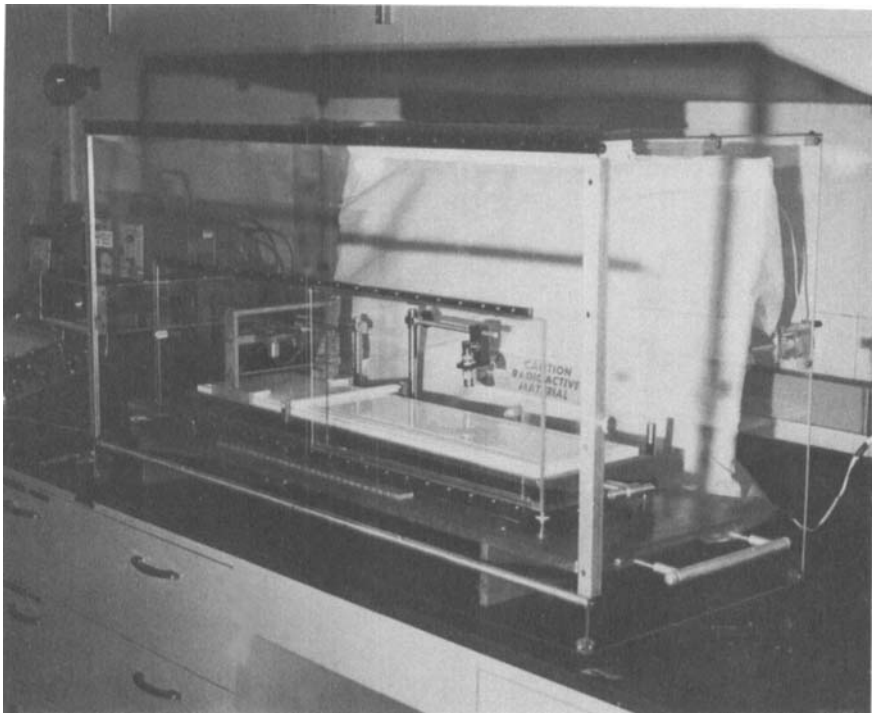


Figure 6. A modern automatic film balance. The ionizing source for the surface potential probe is shown on its swinging arm, out of the way at the rear of the trough. Readout equipment is at the far left.

ated by recording changes of surface pressure (as transmitted from the LVDT) as a function of running time on the strip chart. It is, therefore, essential that the relationship between distance on the strip chart and distance along the film balance trough be known exactly. Again, the rectangular configuration of the trough must be milled precisely from a Teflon block and bolted permanently into a heavy magnesium base to prevent gradual deformation of the Teflon. Only if all these factors are handled correctly in the design and construction of the trough can there be a rigorous relation between surface area and strip chart divisions.

Another property of monolayer films that can be continuously recorded as function of surface area is the surface potential (38,64). Although the exact interpretation of this property is not entirely clear, it is related to the orientation of the surfactant dipoles with respect to the subphase surface and is often followed simultaneously

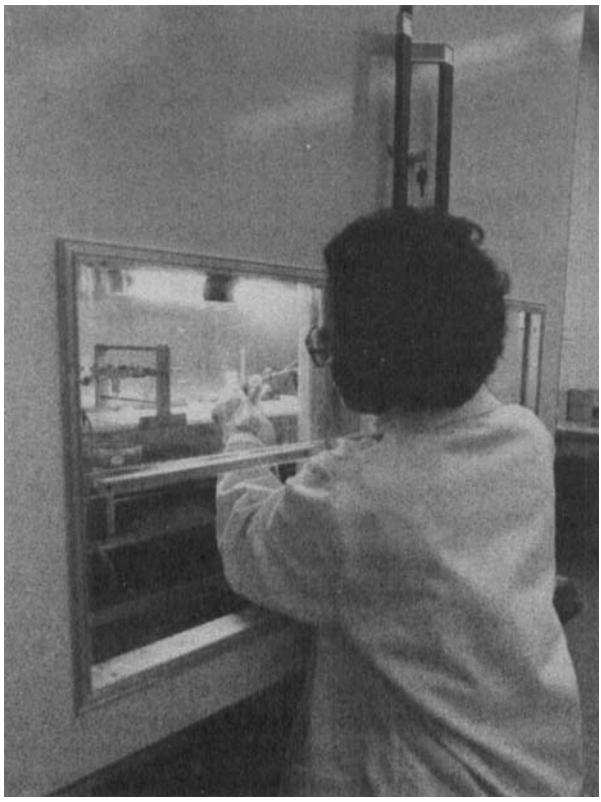


Figure 7. Spreading a film with a micrometer syringe. The film balance and its case are housed inside a temperature controlled cabinet.

with the changes in surface pressure by means of a two-pen recorder. It is also employed as a useful probe for examining the monolayer for any inhomogeneity such as the formation of patchy films. Surface potential is usually measured by employing a radioactive source to ionize the air gap between the aqueous surface and an electrode that is held just above it. The difference in Volta potential is found by comparison with an appropriate reference electrode immersed in the subphase solution.

Monolayer films are usually spread from a dilute solution in an appropriate volatile and highly purified solvent. Small droplets of solution are spotted at 40 or 50 points on the clean subphase surface using a micrometer syringe. Adequate time, say 20 min, must be allowed for the surfactant film to spread evenly and also for the solvent to evaporate completely. Since certain solvents are retained in some

types of film, it is advisable to make control runs from solutions in several solvents. For generating force-area curves, films are usually spread at large surface areas such as 150 to 200 $Å^2$/molecule from which the film will be compressed with the barrier to a final area of 10 to 20 $Å^2$/molecule. For an ordinary surfactant such as stearic acid spread on the usual initial trough area of, say, 550 cm^2, only about 30 μg is needed to produce a monolayer. Since the surface properties of a monolayer are often affected by the presence of 1% or less of some impurities, scrupulous care is required in the purification of all components in the system, and they must be protected carefully from contamination during handling (65). The exposed monolayer film itself is obviously vulnerable to airborne contamination during study (66) and must be isolated especially from aerosols such as tobacco smoke or grease particles from vacuum pumps. An important reason for employing chiral surfactants in the study of monolayer properties is the opportunity to use the absolute checks based on molecular symmetry described in Sect. II to eliminate errors due to impurities or other artifacts. Probably a fair percentage of the force-area curves presented in the general monolayer literature are not suitably reproducible because of the presence of impurities.

An important feature of surfactant monolayers is their transferability from the air-water interface to clean, smooth, solid supports such as glass or metal surfaces. Blodgett and Langmuir (67) developed this technique and employed it for building up multilayers whose thickness was that of a known number of molecular chain lengths. Recently, there has been considerable interest in the application of this technique to prepare "organized multilayers" for the study of optical, electrical, and catalytic properties of very thin films of known composition (47,53-55).

Figures 8 and 9 show two specially designed multicompartment Langmuir troughs that permit the treatment of a monolayer with a series of different subphase reagent solutions, thus producing a known series of chemical reactions in the film. Following these treatments, the films may be transferred to a solid support or subjected to quantitative analysis to determine the outcome of the reactions.

The ability to recover monolayers and subject them to meaningful analysis has become practical only in recent years because of the development of new methods of trace analysis. High-performance liquid chromatography and vapor phase chromatography allow separation and identification of such small quantities (54a). Attenuated total reflectance techniques for infrared analysis (56) and field desorption mass spectrometry (68) have been applied to the trans-

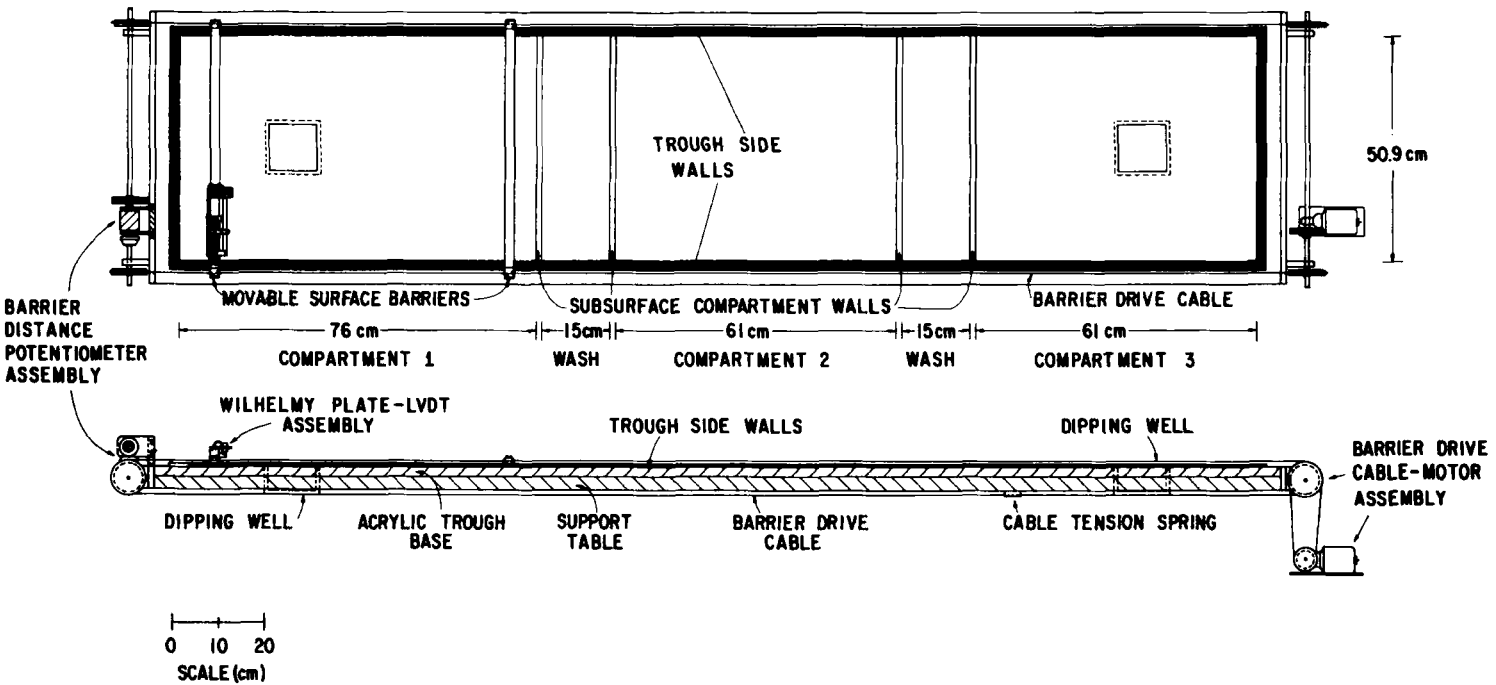


Figure 8. Multicompartment monolayer trough for manipulation of films on the surface. Schematic provided by Dr. S. J. Valenty of General Electric Co. and reprinted from *Journal of the American Chemical Society* **1979**, *101*, 1. Copyright 1979, American Chemical Society.

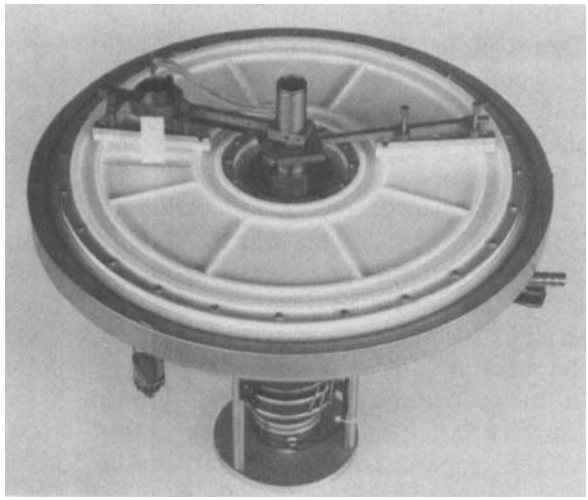


Figure 9. Fromherz circular multicompartment trough for transferring monolayer films to different subphases. Reproduced with permission of Dr. Fromherz and American Institute of Physics. See *Rev. Sci. Instrum.* **1975**, *46*, 1381.

ferred and recovered films. Absorption spectra of multilayer assemblies have also become a useful means for following reactions (55). Ellipsometry is a more classical method, which provides information on the molecular orientation at the interface (69).

It is not difficult to visualize, or to provide convincing evidence for the analogies of gaseous monolayers, at large areas per molecule, or of condensed or solid films at low molecular areas, to their three-dimensional counterparts of gases and crystalline solids. However, between these limiting conditions must lie a considerable range of other states that either are true thermodynamic phases or may be metastable in terms of various criteria. Just as the liquid and amorphous states in three dimensions are poorly defined in structural terms when compared to crystals or gases, so are the various intermediate states of monolayer and multilayer films.

The primary evidence for the conversion of gaseous monolayers at the air-water interface to other intermediate states lies in the abrupt changes found on the π-A isotherms of many film-forming compounds. So many of these isotherms have been reproduced in fine detail in a number of laboratories under a variety of conditions that they cannot possibly be rejected wholesale as artifacts. The sharp transitions from curves to plateaus, where the molecular area varies readily at constant surface pressure, may be related

reasonably to a first-order transition (59), where two states requiring different molecular areas are in equilibrium (since the surface free energy is constant). Often these transitions respond to changes in temperature or to the length or shape of the hydrocarbon portion of the molecule in a way that can be interpreted persuasively in terms of changes in molecular packing.

Much of the pioneering work of Langmuir (52), Adam (70), Harkins (71), and their followers was devoted to attempts at characterizing these intermediate states, first through empirical criteria and then to relating each phase to discrete modes of molecular packing. Gaines (38d) has summarized some of these ingenious attempts to develop categories of intermediate liquid films into subclassifications such as "liquid expanded" and "mesomorphous." Correlation of changes in surface potential and surface viscosity with film compressibility (and the response of all these properties to changes in temperature or variations of surfactant chain length) have been examined in considerable detail. However, the enormous variety of possible ways that the chains and polar head group can interact with each other and with the subphase leaves many detailed pictures of molecular packing in intermediate phases open to argument. Beyond that, the nagging question of metastability inevitably clouds the issue. If one recalls that the devitrification of a glass from a supercooled liquid to a crystalline solid takes a number of centuries, it would not be surprising to find that many metastable film states require months or even years to relax to their thermodynamically stable states. Obviously, no techniques are presently available to follow film changes over such long periods of time on a film balance.

Much of the original motivation for the investigation of chiral monolayers by the Swedish surface chemists Stenhagen and Lundquist, whose work we review in Sect. V, lay in testing the notion that lipid monolayers could undergo phase changes related to those in the crystalline forms. Lipid crystals are often polymorphic by virtue of the variety of ways that their long hydrocarbon chains can pack with respect to each other. It is currently believed that the different modes of orientation and packing of these chains in monolayers are similarly responsible for the relations between surface energy and surface area that are portrayed as phase transitions on π-A isotherms.

Most discussions, such as those cited above, of monolayer films are presented within the context of equilibrium thermodynamics. The applications of the "two-dimensional gas law," $\pi A = kT$, the phase rule, and relations between surface tension and surface pressure to free energy all assume reversibility. Perhaps it seems odd to

question such an assumption in view of the virtually instantaneous establishment of equilibrium due to the familiar rapid redistribution of energies and orientations that occurs during the compression of gases or the mixing of liquids. Small molecules of three-dimensional fluid systems have so few restrictions on their freedom to tumble or rotate that we think of reorientation as occurring very rapidly when compared to the rate of translational motion imposed by stirring, pouring, or compressing. Surfactant molecules in a film at the air-water interface are in quite a different situation, since the translational motion of the head groups is restricted to a plane defined by the subphase surface, whereas the hydrophobic tails can sweep out various figures of revolution above the plane.

As the film is compressed by the slowly moving barrier of the film balance, it is not hard to suppose that the time required for the hydrocarbon chains to stack together side by side into a homogeneously ordered sheet may be considerable. Any dissymmetries, kinks, branches, or double bonds in the chain will interfere with the rapid ordering of the film to a symmetrical two-dimensional array (38d). Slow surface reorganization is easily related conceptually to the well-known ability of membrane lipids containing cis-unsaturated fatty acid chains to maintain fluidity (16). Even if all the chains are saturated and are of equal length, it is not hard to imagine that there may be many orientations of nearly the same energy into which the C_{14} to C_{20} aliphatic chains of a surfactant could be packed during the course of an ordinary slow (30 min) compression of a monolayer. Although the average energies of the states associated with each distribution of orientations might be quite reproducible, as evidenced by reproducible π-A isotherms, they would be metastable (by definition) if their energy lay above the lowest possible surface energy for that monolayer at that particular temperature, area, and film pressure. The application of equilibrium thermodynamics in such circumstances is not rigorously appropriate if the film pressure at a given area is in any way dependent on the pathway by which the film reached that area or on any kinetic factor such as the rate of compression (74).

The discussion above points out the importance of characterizing the degree of metastability of a monolayer before attempting to draw thermodynamic inferences from π-A curves. Unfortunately, this precaution is mentioned only rarely in the monolayer literature. Undoubtedly, kinetic factors in molecular orientation are of great inherent interest, but first they should be clearly identified.

The best approach to a true thermodynamic equilibrium spreading

pressure (ESP) is to place well-formed crystals of the pure surfactant on a clean water surface at constant temperature and area. The change in surface tension or surface pressure as the molecules spread out from the crystal face may be recorded using a Wilhelmy plate, or a continuously reading torsion balance, until a constant value of the ESP is reached. Other techniques for spreading films at ESP are described by Gaines (38). Figure 10 shows the attainment of ESP for films of *N*-α-methylbenzylstearamide spread from crystals of racemic sample on 10*N* aqueous sulfuric acid.

An obvious, but again infrequently reported, approach to detecting kinetic factors in force-area isotherms is to compress spread films at different rates. Figure 11 shows the effect of a tenfold variation in the rate of compressing a film of optically active *N*-α-methylbenzylstearamide. Obviously, as the molecules become more crowded at the interface, their rate of reorientation is unable to keep up with the movement of the sweeping barrier, even though the fastest barrier rate is only 2 or 3 cm/min. Again, there is chiral discrimination in the rates of reorientation, since the racemic film shows no effect of changing compression rate over the same range.

The stability of films, even in thermodynamically metastable states, may be tested by stopping the barrier drive at intervals during compression of the film. If there is no drop in film pressure after several minutes, it is unlikely that the π-A relationships up to that point will be dependent on the compression rate. Figure 12 shows

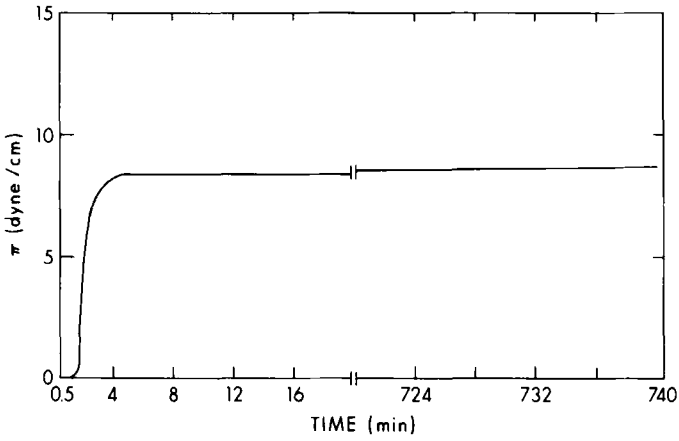


Figure 10. Development of equilibrium spreading pressure of film spread from pure crystals. Film pressure is measured on a Langmuir balance with barriers stationary. From Thompson (101).

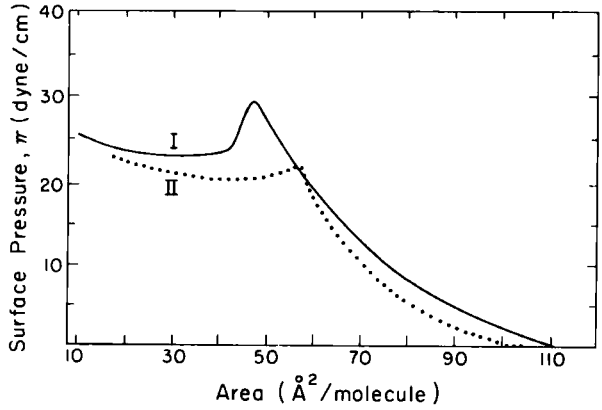


Figure 11. Effect of variation of compression rate on a film that shows kinetic effects of surface packing: curve I, tenfold variation of rate in curve II. From Thompson (101).

the difference between the stability of a film at low pressures and the pressure drop of the same film at the higher pressures and lower areas per molecule.

If kinetic factors due to slow molecular reorganization are important, hysteresis may be observed if a film is alternately compressed and expanded. Figure 13 shows the effect of compressing, expanding, and recompressing a film of optically pure *N*-α-methylbenzylstearamide.

Naturally, this section serves as only a very limited introduction to the present status of monolayer techniques. However, it should be

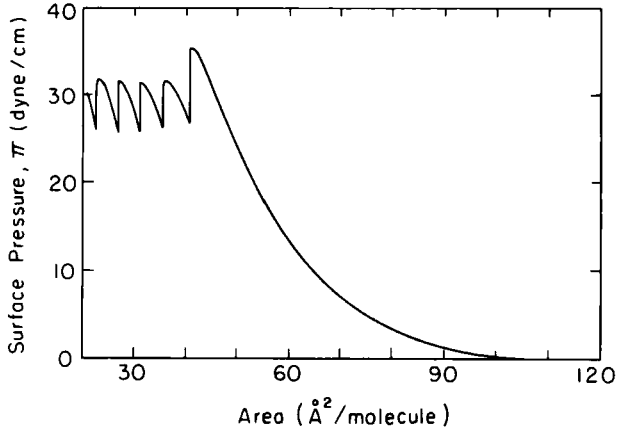


Figure 12. Pressure drop after regular intermittent compressions after film has been compressed beyond collapse point. From Thompson (101).

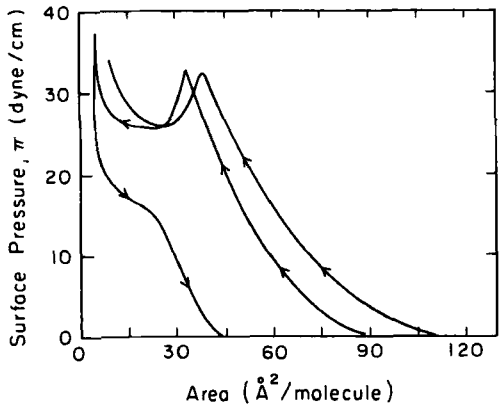


Figure 13. Film hysteresis showing failure of film to expand reversibly along its compression isotherm. Recompression of such a film follows an isotherm with reduced surface area at each pressure. From Thompson (101).

adequate for the discussion of studies concerning chiral monolayers that follows.

V. ENANTIOMER DISCRIMINATION IN MONOLAYERS

The ability of a chiral molecule to distinguish between its pair of mirror-image stereoisomers was defined in Sect. II as an *enantiomer discrimination.* Although the consequences of the geometrical isomerism of cis and trans olefins and carbocyclic functions have been explored in monolayer systems by a number of investigators, there have been very few stereochemical studies that compare the monolayer behavior of optically pure enantiomers with their corresponding racemic modifications. Many examples of observable differences in the surface pressure, surface potential, and surface viscosity of geometrical isomers such as the unsaturated erucic and brassidic acids (i.e., *cis*- and *trans*-13-docosenoic acids, respectively) or the epimeric steroids cholestan-3-ol and *epi*-cholestan-3-ol have been cited by Gaines (38d) and others (70,71a,72,75). Chapman (76) has studied phospholipids containing a double bond in the hydrocarbon chain to show that a given cis compound produces a monolayer that is considerably more expanded than that of the corresponding trans isomer. These studies attest to the sensitivity of monolayer properties to subtle differences in molecular structure; however, the comparisons

are being made between diastereomers, not between mirror-image isomers.

Since the subtler interactions between enantiomers have been overlooked by almost all workers in the field, the following references were unusually hard won and represent the fruits of some 15 years of literature searching. We have tried not only to describe how these results bear on the establishment of chiral discrimination in monolayers as general phenomena but also to indicate the diverse motivations of individual authors for engaging in these laborious studies, most of which were not originally directed toward a delineation of the role of stereochemistry in the packing of monolayers. Although we hope that our coverage has been complete, we realize the possibility of omission and apologize to any workers whose reports we have failed to locate.

A. Simple Surfactants

We limit this section to a discussion of stereochemical studies that sought to demonstrate discriminating enantiomeric interactions in monolayers of simple surfactants having one hydrophobic chain of methylenes and, generally, a single chiral center. Work in this area includes derivatives of long chain fatty acids, alcohols, or esters whose chiral center is included in the methylene chain.

The most intensive examinations known to us of chiral interactions in a monolayer are those reported by a group of Swedish surface scientists, notably Monica Lundquist (73,77–79) of the Institute of Medical Biochemistry (Gothenburg) and Stina and Einar Stenhagen (80,81) formerly of the Institute of Medical Chemistry (Uppsala), in a few scattered papers beginning in the mid-1940s. The Stenhagens, in their seminal paper of 1945, stated that they knew of no prior study of optically active surfactants, and we have not been able to locate any that predate this claim. Regrettably, even the most authoritative treatises on interfacial chemistry have ignored Lundquist's major contribution to this field despite its elegance and the basic implications it contains for subsequent monolayer studies of membranes. Gaines (38e) refers to the desirability of detailed stereochemical studies, but must have overlooked the Swedish work in that area notwithstanding the enormous scope of his book. In fact, the only citations to any of the Swedish work of which we are aware were in the recent articles by Tachibana and his co-workers (82,83) and the more obscure dissertation of Zeelen (84), whose results have not yet been presented in the journal literature.

A considerable controversy among surface scientists began over 50 years ago concerning possible analogies between the phase changes of three-dimensional crystals and the apparent two-dimensional phase changes that could be inferred from the force-area curves of monolayers (70,71,85–87). One of the basic issues was the suitability of regarding condensed monolayers as periodic arrays of a two-dimensional "crystalline" lattice. The Swedish workers, using specially designed and thermostatted film balances (61,88), set about testing this analogy by collecting the surface pressure versus temperature data necessary for plotting two-dimensional π-T phase diagrams of monolayers. A close relationship was reported between the kind of polymorphism found in the crystalline state and in monolayers for a variety of lipid types. For example, the packing of the hydrocarbon chains in monolayers of *n*-eicosyl and *n*-docosyl acetates produce three high-pressure, small-area phases (i.e., the so-called condensed solid, solid, and superliquid phases), which were shown to correspond to three clearly defined crystalline forms (89). Much of the early work through 1955 is summarized in Stenhagen's review (72), and a more current survey has been provided by Lundquist (73).

A clear message from this work is that monolayers can be considered to be "two-dimensional" only in the simplest sense, and it is the changes in three-dimensional orientation of the hydrocarbon chains above the water surface that are of primary importance in the detailed interpretation. Even though the film is only one molecule thick, the mode of intermolecular packing can be varied widely as a function of temperature and surface pressure to provide monomolecular phases and associated phase equilibria of many different types. As a corollary, we note that a rich fund of information about intermolecular packing can be obtained from π-T plots and that essential facts about stereochemistry in monolayers may be missed completely by working at only one temperature.

In view of their interest in the relationship between phase changes in the two-dimensional monolayer versus three-dimensional bulk phase systems, it is a small wonder that the Swedish groups were attracted to a strategy of comparing the behavior of optically pure surfactants with mixtures of stereoisomers. Analogy to the well-known phase-composition diagrams (33) for the melting of crystalline optical isomers is obvious and was stated clearly in the Stenhagens' original paper (80):

> A racemic modification may exist in three forms in the solid state, i.e., racemic compounds, racemic mixture, and racemic solid solution. Racemic compounds exist only in the solid state and have never been demonstrated

> in liquids at temperatures above the freezing point. If the antipodes and the racemic compound show different monolayer behavior it might, therefore, be concluded that the monolayers in question at least in this respect exhibit the properties of a solid. Furthermore, if both the racemic compounds and the corresponding enantiomorphs give liquid monolayers, the force-area curves ought to be identical as long as the monolayers are true liquids. If the state of the monolayers changes on compression, the force-area curves should begin to differ from the point where a more organized state sets in. From a study of different optically active molecules we might thus obtain fresh information regarding the state of condensed monolayers. . . . It follows that caution is necessary when monolayers of synthetic racemic products are compared with those of optically active natural products, as even if the structures are similar the monolayer behavior may be different.

Lundquist and the Stenhagens concentrated their efforts on the physical aspects of monolayer chemistry and did not elaborate their work much in the direction of structural variation of the surfactant molecules. Their results show clearly, however, that the response of chiral monolayers to changes in surface pressure and temperature is sharply dependent on both the molecular structure of the surfactant and the optical purity of the sample. The Stenhagens were keenly aware of the possible application of the monolayer technique to stereochemical and other structural problems (72); however, they failed to exploit the full potential suggested by their initial results and, instead, pursued the field of mass spectrometry, to which they made substantial contributions.

Consequently, the Stenhagens published only a single study of direct relevance to our review (80). Comparison of the monolayer behavior of optically active and racemic eicosan-2-ol showed intriguing differences, especially at low molecular areas and high surface pressures; however, this initial observation was later vitiated when one of the samples was found to be impure (90). Whereas the dextrorotary sample had been isolated in apparently pure form from a natural source, the synthetic racemic material was later shown to contain a by-product from the Grignard reaction of octadecylmagnesium bromide with acetaldehyde that could not be removed by chromatographic adsorption on alumina, distillation, or recrystallization. Hence, the origin of the differences observed in the earlier force-area curves became doubtful.

The later studies of Tachibana, and also those of Lundquist, employed the absolute method of chiral cross-checking of one enantiomer against another as outlined in Sect. II. The Stenhagens did not do this originally and probably would have been saved from the

intrusion of an impurity in their otherwise flawless experiment if they had had samples of both enantiomers available to make this test. For example, an equal mixture of the optical isomers would not have afforded results identical with the racemic sample because of the contamination of the latter. Nevertheless, the conceptual framework of their initial paper is so broadly stated and its implications so clearly perceived that the historical priority of their contribution is assured.

In a second paper, the Stenhagens compared the monolayer properties of several diastereomeric long chain compounds to demonstrate that diastereomers, as should be expected, can exhibit slightly different force-area curves when studied under the same conditions (81). Their observation that this much less subtle effect of stereochemistry is also dependent on the nature of the monomolecular film that is formed, however, is of greater interest. Diastereomeric (+)-2(*S*),9(*R*)- and (+)-2(*S*),9(*S*)-dimethyltetracosanoic acids exhibit *identical* force-area curves on both acidic and neutral subphases (0.01*N* HCl and 0.4m*M* $KHCO_3$ containing 0.03m*M* $BaCl_2$) over a wide range of temperatures (4–20°C). These monolayers behave as true liquids and were characterized as liquid-condensed at lower temperatures and liquid-expanded at higher temperatures. Mixtures containing the two diastereomers in different proportions gave results that were identical to those obtained with the pure compounds. On the other hand, force-area curves obtained from the corresponding diastereomeric 7-keto-2,9-dimethyltetracosanoic acids on both subphases at 20°C were identical during an initial expanded region, but began to differ significantly as a phase transition to a more condensed state set in. The Stenhagens concluded from this that the condensed monolayers of the latter surfactants were more closely packed and ordered than the liquid ones, since they were sensitive to the stereochemistry of the surfactant. They also suggested that such comparisons of force-area curves obtained from diastereomers could have general utility in defining the nature of phase transitions in monolayers.

The first irrefutable observation of a discriminating interaction between enantiomeric surfactants in monolayers was most probably made by Filippus Johannes Zeelen (84) in a detailed study concerning the synthesis, monolayer behavior, and photochemistry of a series of *N*-stearoylamino acid derivatives that were employed to model the conformation and photochemical decomposition of proteins. Although Zeelen was able to demonstrate significant differences in the force-area curves obtained from racemic and optically active forms of several of these derivatives, publication of this work in 1956 was

limited to 50 copies of his doctoral dissertation written in Dutch (under the direction of Prof. Havinga, State University of Leiden, Netherlands).

An interesting historic parallel (91) can be drawn to van't Hoff's proposal of the tetrahedral geometry for groups bound to a tetravalent carbon atom because its original appearance was also in the form of an obscure pamphlet in Dutch (Utrecht, 1874); however, van't Hoff's work was quickly translated into French (1875) and German (1876) for publication in vehicles having considerably wider circulation. In Zeelen's case, only the synthetic aspects of his dissertation were subsequently published in the journal literature (92). However, the later paper does provide a cautionary note that the surfactant compounds employed in the film balance studies may not have been optically pure because racemization during their synthesis was possible.

Zeelen found the extent of chiral discrimination to be dependent on the type of monomolecular phase that was formed. Thus, racemic and optically active samples displayed identical force-area curves (Fig. 14) when both formed liquid-expanded films, but showed considerably different curves (Fig. 15) under conditions where both samples formed a more highly condensed monolayer.

The monolayer behavior of *N*-stearoyltyrosine (Fig. 16) was more complex. Under conditions (0.01*N* HCl, 22°C) where the racemic material formed a condensed film having a limiting molecular area of 39 ± 2 Å^2, the force-area curve of L-(+)-*N*-stearoyltyrosine exhibited a liquid-expanded film at large areas (ca. 100–45 Å^2 per molecule) followed by a transition beginning at 16.5 dynes/cm surface pressure to a condensed phase having a smaller limiting molecular area of 34 ± 2 Å^2. However, both these latter samples exhibited only the liquid-expanded phase on distilled water alone.

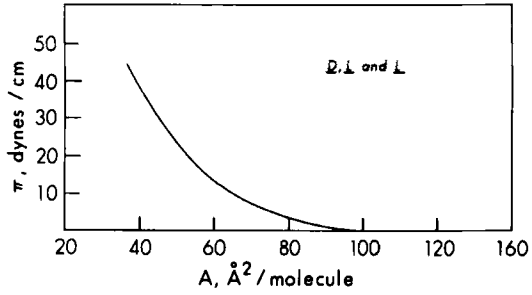


Figure 14. Films of L-and D,L-*N*-stearoylleucine; no enantiomer discrimination is discernible. From Zeelen (84).

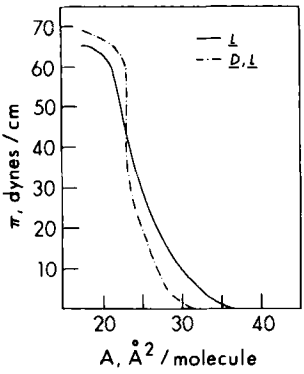


Figure 15. Comparison of L- and D,L-*N*-stearoylalanine films; enantiomeric discrimination is barely discernible. From Zeelen (84).

The values for the limiting area per molecule cited in the text were determined by extrapolation of the high-pressure part of the curve to zero pressure.

Zeelen demonstrated a fair degree of control over the occurrence of distinct monolayer phases not only through variation of the subphase pH, but also by structural modification of the surfactant head group. He was able to provide a consistent description of the properties of these compressed films using space-filling molecular models on the working hypotheses that the hydrophilic head groups are immersed in the aqueous subphase, the peptide group forms the greatest number of intermolecular hydrogen bonds, and the hydrophobic paraffin chains are closely packed in parallel arrays. He regarded this stereochemical approach as being the best means of specifying the nature of monolayer phases and criticized the Stenhagens' earlier classification of their eicosan-2-ol films (80) as being

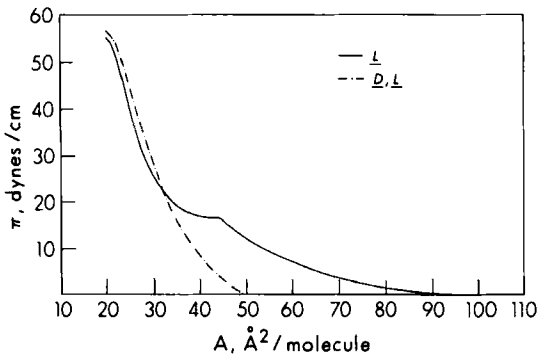


Figure 16. Comparison of films of L- and D,L-*N*-stearoyltyrosine showing clear enentiomeric discrimination. From Zeelen (84).

of a "viscous liquid" type when his own samples displayed enantiomer discrimination in the condensed phase only.

Neither Zeelen nor the Stenhagens pursued this exciting new approach to probing the intermolecular organization of monolayers beyond their initial investigations, and the prospects suggested by their pioneering efforts would have remained unrealized for 20 years, were it not for the tenacity of Monica Lundquist. Beginning in 1961, Lundquist published a series of 10 reviews and original papers that explored the molecular arrangement in condensed monolayers by establishing definite relationships between the phases and phase transitions of monomolecular films on water and the corresponding polymorphism in three-dimensional crystals. Three of these papers deal directly with the consequences of stereochemistry (77–79) and are based on the fundamental hypothesis of her Swedish compatriots that the observation of racemic compound formation in the compressible region of monolayers implies that "the molecules in the compressible states are not necessarily oriented at random." An initial survey of her approach (93) was followed 15 years later by a comprehensive review of her results and conclusions (73). It is unfortunate that Lundquist's work was not presented at a time or place where it could make its proper impact on the development of monolayer chemistry. Thus, many researchers who could have benefited from her results are unaware of her significant accomplishments.

These studies were remarkably thorough and involved the painstaking repetition of monolayer experiments on a film balance over a series of closely spaced temperatures, from which the thermodynamic parameters of enthalpy and entropy for the phase changes could be derived. The results were then compared with phase diagrams obtained for the bulk samples through X-ray powder diffraction and differential thermal analysis methods (89). Lundquist concluded that the close relationship observed between condensed monolayer phases and the corresponding crystalline forms displayed by the same substance in the three-dimensional bulk phases was primarily due to the arrangement of the hydrocarbon chains of the surfactant. The expanded state of a monolayer is compared to bulk liquids in that there is a random arrangement of the hydrocarbon chain. This idea was supported by the good correlation made between the heat of fusion determined calorimetrically for crystalline samples and the corresponding "melting heats" of their monolayers derived from film balance data through application of the two-dimensional Clausius-Clapeyron equation on the first-order transition of a condensed to an expanded film. Thus, the molecular mechanism involved in mono-

layer phase transitions, including multilayer formation, was gradually developed to satisfy the results of experiments such as these.

In addition to the expanded (E) and gaseous (G) monolayer states, six condensed phases were identified and described in terms of the packing arrays of their hydrocarbon chains: three having a vertical chain arrangement perpendicular to the subphase surface and three having tilted chains. Further distinctions were made within these groups by analogy to the well-established phase transitions observed in the common orthorhombic and high-temperature hexagonal polymorphic forms of *n*-hydrocarbons in three-dimensional crystals. The three vertical phases are characterized by their relative incompressibility and also by their existence at areas per molecule so small that the chains simply must be vertically oriented. The most condensed of these is the condensed solid (CS) orthorhombic-type phase followed by, in decreasing intermolecular order and chain-chain interaction, the slightly disordered solid (S) orthorhombic intermediate-type phase, and the superliquid (LS) hexagonal phase having some degree of orientational freedom about the long axis of the chain. The remaining liquid condensed L_2'', L_2', and L_2 phases are much more compressible, have a tilted chain arrangement, and are analogous to the corresponding vertical phases CS, S, and LS, respectively.

On compression of a tilted monolayer phase, a reorientation of the molecules into the vertical position takes place. These designations of the various monolayer phases are not unique to Lundquist, but have evolved during the historical development of surface chemistry. Although she proposed a new terminology (94) for the condensed monolayer phases (not employed herein), the fundamental contribution of other workers was clearly acknowledged in her review (73). Nevertheless, Lundquist stands alone as the single investigator during this 20 year period who successfully explored the nature of monolayer phases and phase transitions with a comprehensive stereochemical methodology.

In her initial investigation, Lundquist studied the monolayer behavior of racemic and optically active forms of both tetracosan-2-ol and its acetate derivative on 0.01*N* aqueous HCl over a considerable range of temperature (77). In each case, it was possible to demonstrate chiral discrimination between pure enantiomers versus the racemic substance. Furthermore, the extent of enantiomer discrimination was significantly temperature dependent, being enhanced at lower temperatures and frequently disappearing at higher ones. Under favorable conditions of temperature, however, the appearance of the force-area curves could be very sensitive to the optical purity

of the sample. For example, the optically pure enantiomers of tetracosan-2-ol formed solid-condensed films that exhibited no phase transitions over a temperature range of 3.3–27.5°C. The force-area curve of the racemic substance, on the other hand, showed a distinct plateau under these conditions: it could be made to appear in samples having an optical purity of less than 80%, and it faded away in all samples above a temperature of about 28°C. Above 32°C, the monolayer behavior of the racemic and the optically pure samples were virtually identical. When the composition of the binary mixture of enantiomers reached 1 : 1, the force-area curve of the racemic substance could be reproduced exactly at any temperature. Lundquist argued that the simplest interpretation of the plateau region is that it represents a phase transition from a racemic mixture to the formation of a true racemic compound in the monolayer. Thus, an ordered intermolecular arrangement can be inferred.

The force-area curves for racemic and (*S*)-(+)-2-tetracosanyl acetate recorded with a barrier speed of 5 cm/min are shown in Figures 17 and 18, respectively. Again, both enantiomers showed identical monolayer behavior. The film balance behavior of the racemic acetate was indistinguishable from that of the pure enantiomers at temperatures above about 27°C; however, below this temperature the force-area curves differed markedly even at low surface pressures, which indicates that racemic compound formation occurs at relatively large areas per molecule.

In a second paper, Lundquist observed that racemic and optically active forms of the methyl ester of 2-methylhexacosanoic acid show the same characteristics in their monolayer phase behavior as the 2-tetracosanyl acetates because of their closely analogous molecular structures (78). This laid the foundation for her interesting demonstration (Figs. 19 and 20) of quasi-racemate formation in monolayers (79), which is discussed in Sect. VI. The force-area curves of the methyl esters of racemic and (*S*)-(+)-2-methylhexacosanoic acid on 0.01*N* aqueous HCl are displayed in Figures 21 and 22 respectively. The surface pressures at characteristic points in these force-area curves are plotted against temperature in Figures 23 to 28 and are labeled with Lundquist's designations of the various monolayer phases and phase transitions. She observed considerable film instability in these phases transitions as shown by the rapid, exponential fall of surface pressure on stopping the moving barrier during compression, which indicates that true equilibrium surface pressures were not recorded during the normal conditions of these film balance experiments.

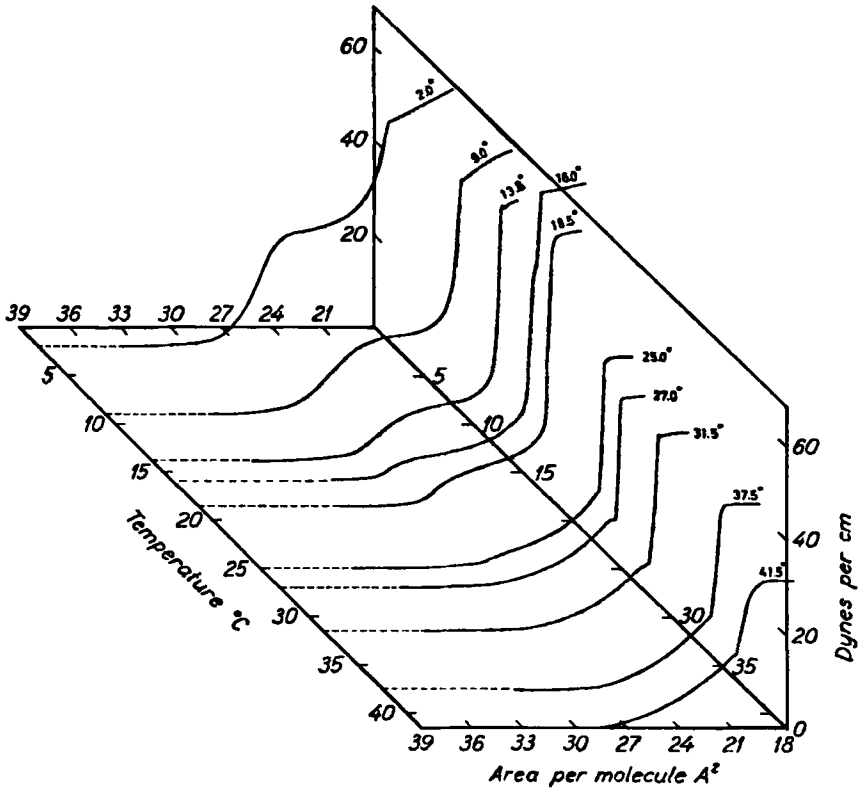


Figure 17. π-A curves for racemic 2-tetracosanyl acetate at different temperatures. From Lundquist (77). Permission of Stockholm University Library.

More recently, Tachibana and co-workers (82,83) have reported an especially well-defined example of an enantiomer discrimination involving monolayers of racemic, D-(−)-, and L-(+)-12-hydroxystearic acid, $CH_3(CH_2)_5$-$CHOH(CH_2)_{10}CO_2H$, whose absolute configuration was determined by Serck Hanssen (95) as (*S*)-(+). An unusual feature of this surfactant involves the position of the hydroxyl group, which is so far removed from the carboxyl head group that it can function as a second point of attachment to the aqueous subphase. The impetus for their detailed investigation of the monolayer characteristics of this system was derived from a longstanding interest in the inherent morphology of finely divided soap particles found in soap-oil dispersions.

Semisolid dispersions of soaps in mineral oils, usually prepared through *in situ* crystallization of metallic salts of long chain fatty

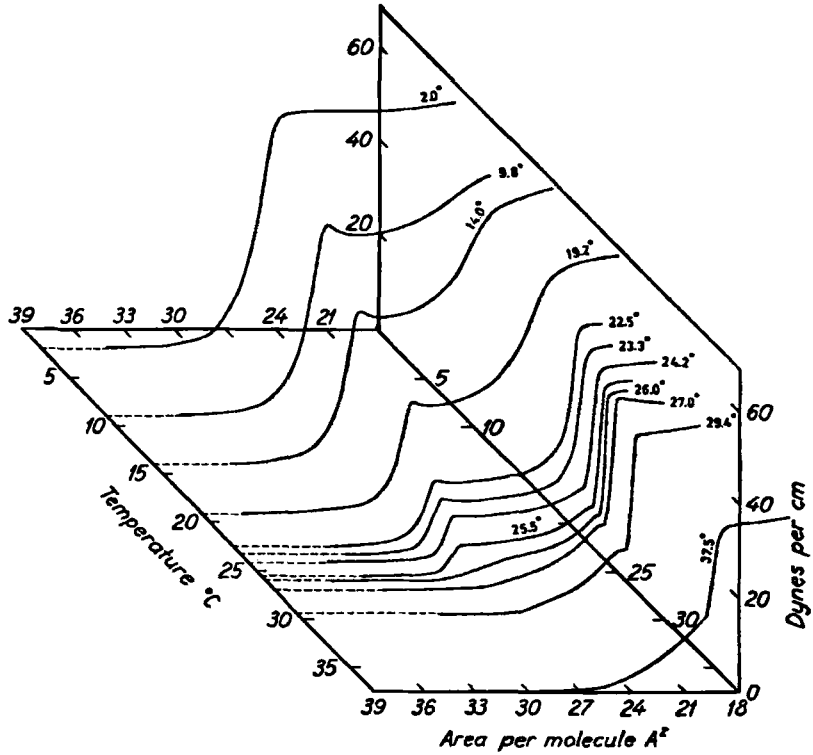


Figure 18. π-A curves for (*S*)-(+)-2-tetracosanyl acetate at different temperatures. From Lundquist (77). Permission of Stockholm University Library.

acids, display the desirable properties of solid gels for application as lubricating greases. Electron microscopic examination of the dispersed particles of optically active lithium 12-hydroxystearate prepared in this manner reveals microcrystalline aggregates in the shape of twisted fibers (96). Significantly, all fibers twist in the same direction when prepared from a single enantiomer. In their initial investigations, the Tachibana group (97,98) demonstrated both enantiomorphism and racemate formation from the external morphology of these twisted fibers: the lithium salt of L-(+)-12-hydroxystearic acid showing a left-handed twist, its enantiomer having a right-handed twist, and the racemic salt being flat platelets with no twist at all. The rubidium and cesium salts as well as the precursor carboxylic acid also produce twisted fibrous aggregates, but the chiral sense of their twist is *opposite* to that of the lithium soap of corresponding absolute configuration. Furthermore, the sodium and

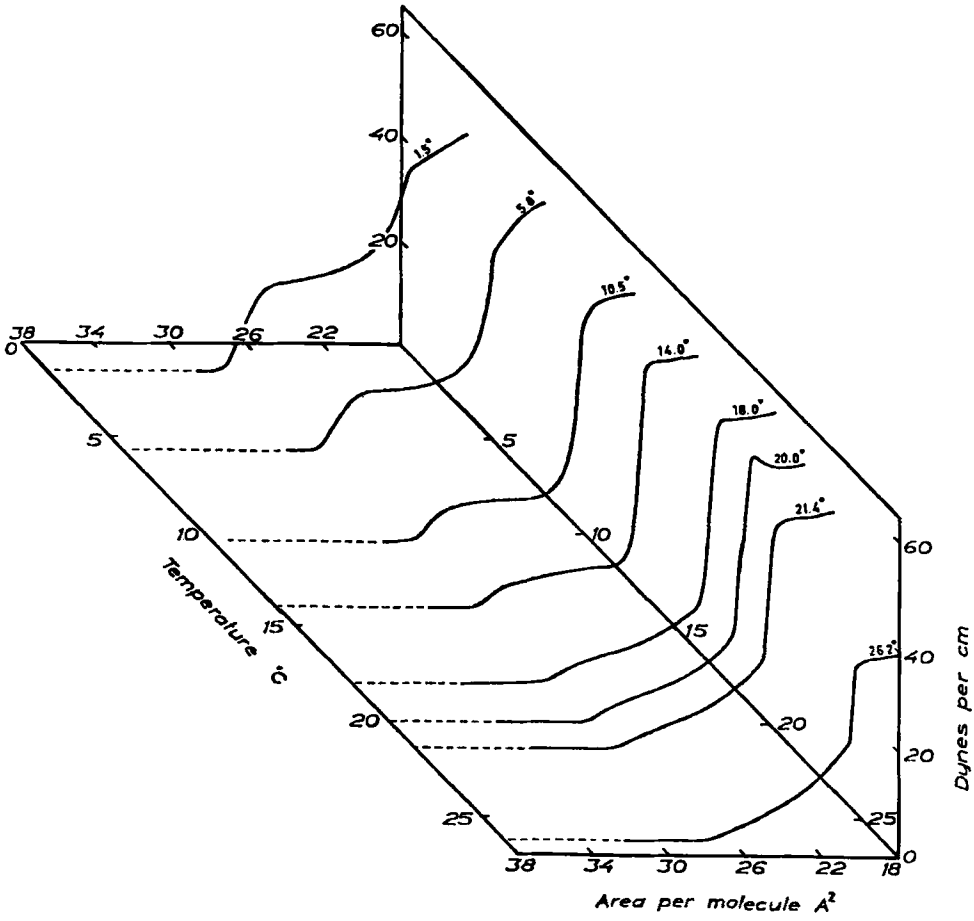


Figure 19. π-A curves for quasi-racemic equimolar mixture of (*S*)-(+)-2-tetracosanyl acetate (Fig. 18) and methyl ester of (*R*)-(−)-2methylhexacosanoic acid (Fig. 22) at various temperatures. From Lundquist (79). Permission of Stockholm University Library.

potassium soaps yield right-handed fibers together with left-handed ones even when prepared from an optically pure sample.

Electron microscopic examination of the gel-like precipitates obtained on recrystallization of these soaps from several common solvents showed that neither the concentration of the solution nor the polarity of the solvent played a role in determining the direction of the twist for the fibers of a particular sample. These results, together with later studies involving divalent metal soaps (98,99),

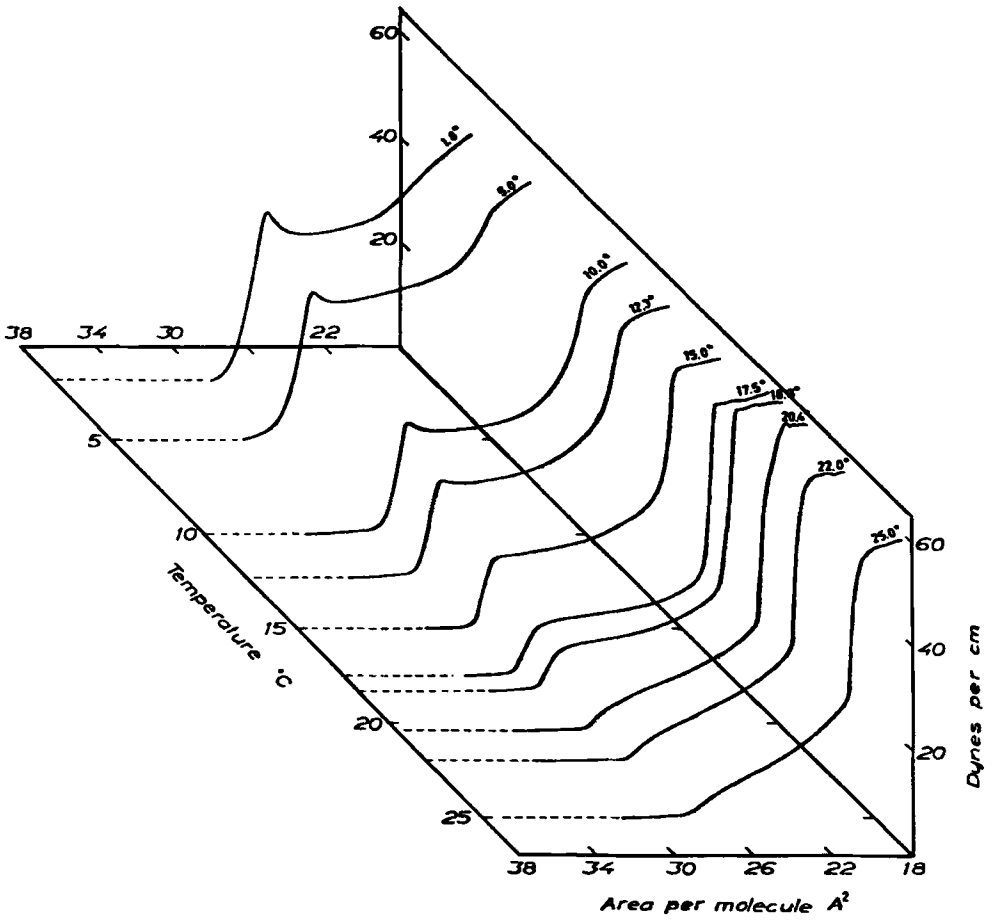


Figure 20. π-A curves for quasi-enantiomeric 1 : 1 mixture of (*S*)-(+)-2-tetracosanyl acetate and methyl ester of (*S*)-(+)-2-methylhexacosanoic acid at various temperatures. From Lundquist (79). Permission of Stockholm University Library.

indicate that the inherent chirality of the fibrous aggregates is determined by the cation, while the absolute configuration of the sample merely serves to maintain the chiral relationship of the pair of enantiomers, Electron micrographs (Fig. 29) obtained by Uzu and Sugiura (100) confirmed independently that 12-hydroxystearic acid forms gels built from fibrous aggregates having a left-handed twist when prepared from the D-(−) acid and a right-handed twist from the L-(+) acid, but appearing plate shaped from the racemic material. Using

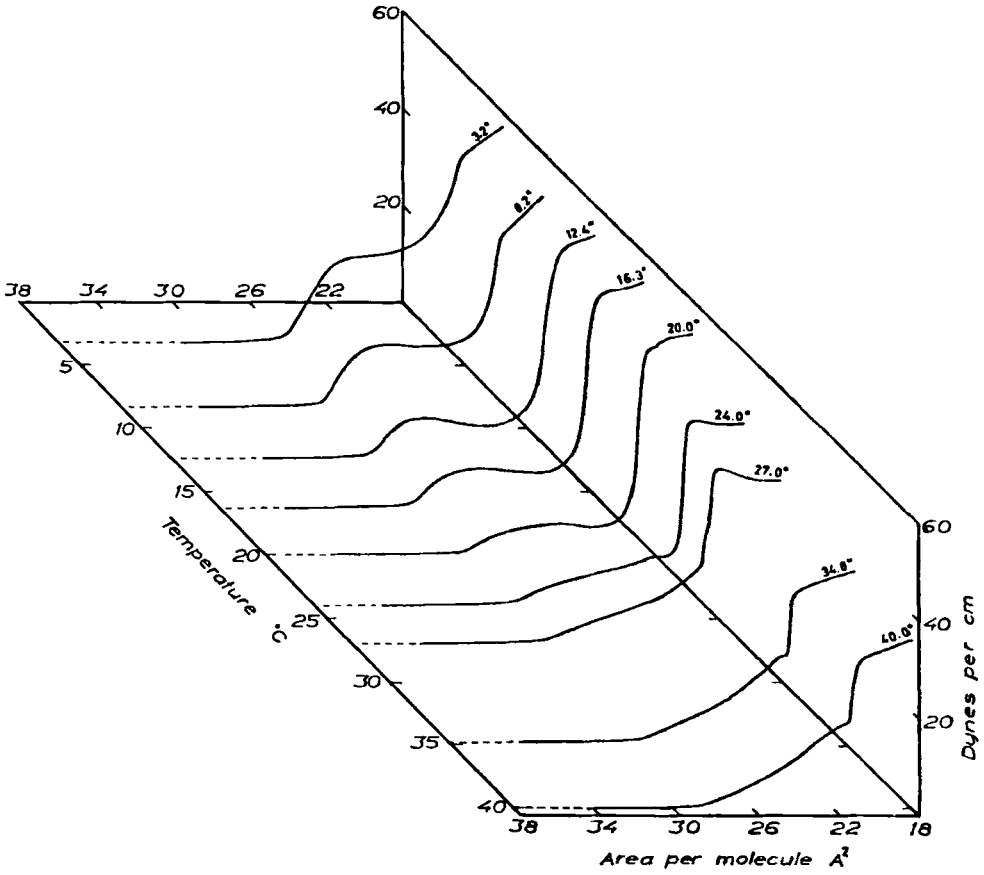


Figure 21. π-A curves for the racemic methyl ester of 2-methylhexacosanoic acid at various temperatures. From Lundquist (78). Permission of Stockholm University Library.

phase composition diagrams of differential scanning calorimetry data and powder diffraction patterns, these authors were able to support the appealing conclusion that the flat platelets represent the formation of a true racemic compound.

As an extension of their previous work, the Tachibana group (82, 83) studied the collapse fragments that occur when monolayers of 12-hydroxystearic acid are compressed slowly (18 Å^2/molecule • hr) at surface areas of less than 21 Å^2/molecule, the normal cross-sectional area of a hydrocarbon chain. The collapsed monolayers were transferred from the subphase to hydrophilic supports by a horizontal lifting method for electron microscopic observation, which revealed (Fig. 30) flat platelets when the sample was racemic and twisted

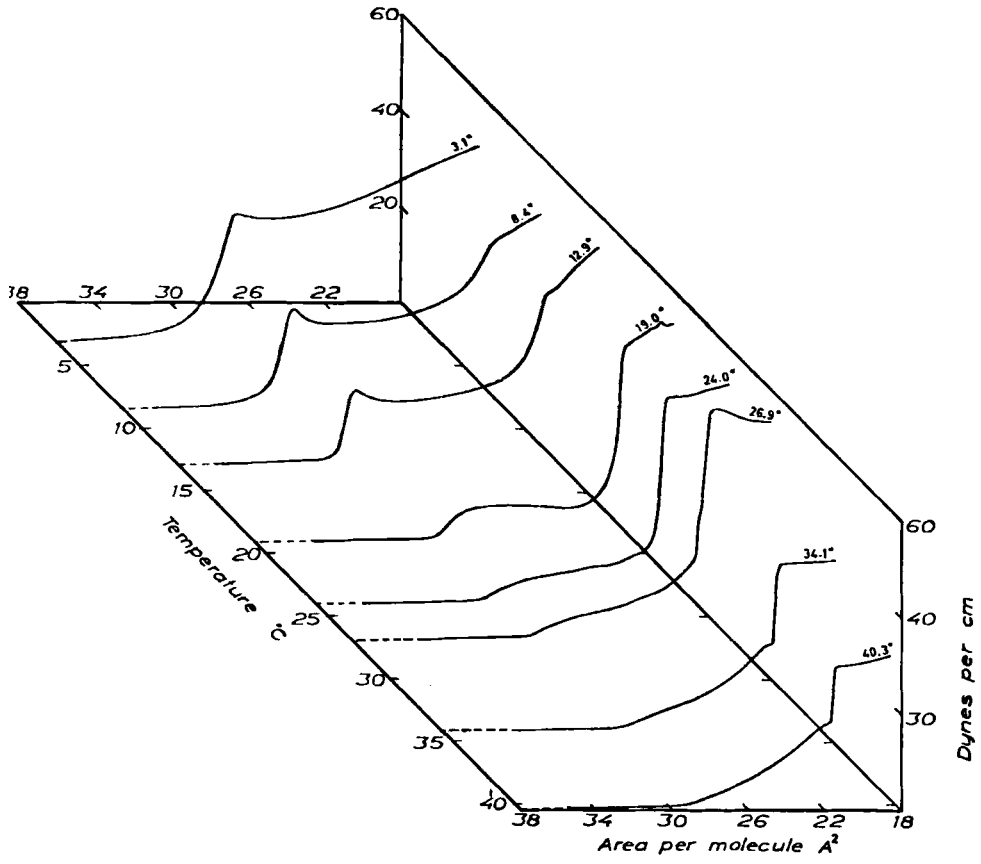


Figure 22. π-A curves for the methyl ester of (*S*)-(+)-2-methylhexacosanoic acid at various temperatures. From Lundquist (78). Permission of Stockholm University Library.

fibers when it was optically pure. The twisted fibers of the collapsed films bear an identical chiral relationship to those crystallized from solution.

The role of the hydroxyl group in determining cohesional properties and molecular aggregation was demonstrated by comparisons of the infrared spectra obtained from optically active and racemic samples in several phases: mulls of crystalline powder, isotropic solutions, gels, collapsed monolayers, and multilayers built up by the Blodgett technique. These spectra, together with a detailed packing analysis involving space-filling molecular models and powder diffraction data, established a close correspondence between the intermolecular association of the condensed and bulk states, and supported

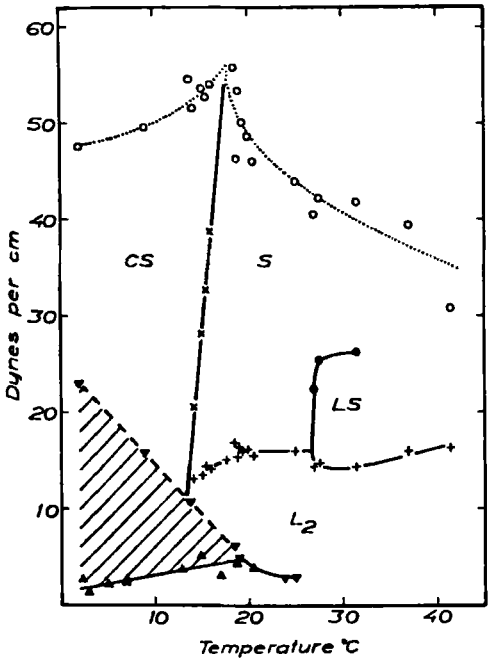


Figure 23. π-T diagram for racemic 2-tetracosanyl acetate. Derived from Figure 17. From Lundquist (77). Permission of Stockholm University Library.

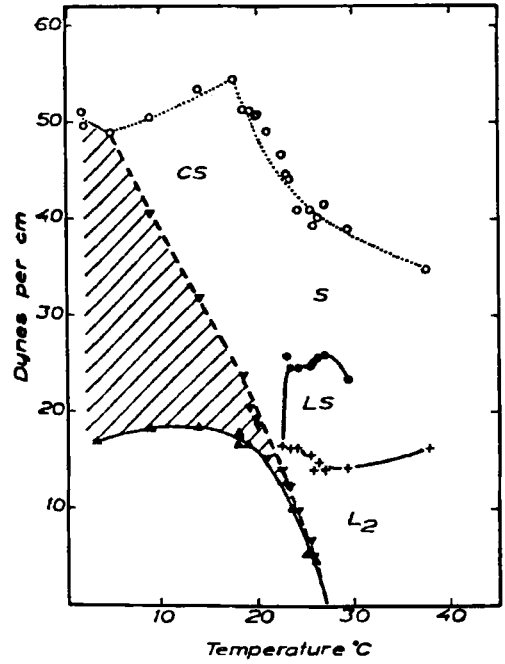


Figure 24. π-T diagram for (*S*)-(+)-2-tetracosanyl acetate. Derived from Figure 18. From Lundquist (77). Permission of Stockholm University Library.

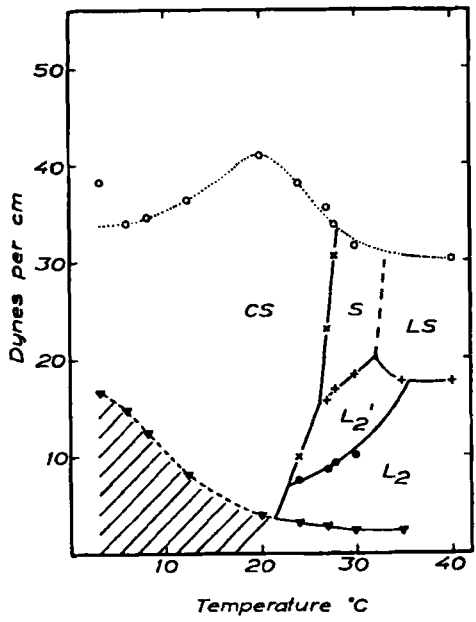


Figure 25. π-T diagram for racemic methyl ester of 2-methylhexacosanoic acid. Derived from Figure 21. Form Lundquist (78). Permission of Stockholm University Library.

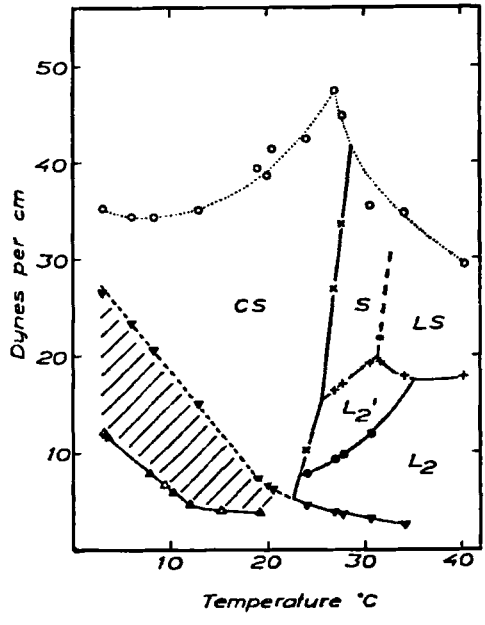


Figure 26. π-T diagram for methyl ester of (*S*)-(+)-2-methylhexacosanoic acid. Derived from Figure 22. From Lundquist (78). Permission of Stockholm University Library.

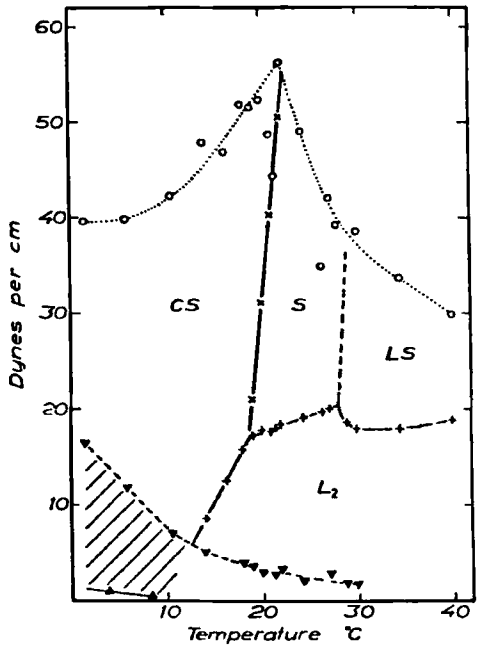


Figure 27. π-T diagram for quasi-racemic 1 : 1 mixture of (*S*)-(+)-2-tetracosanyl acetate and methyl ester of (*R*)-(−)2-methylhexacosanoic acid. From Lundquist (79). Permission of Stockholm University Library.

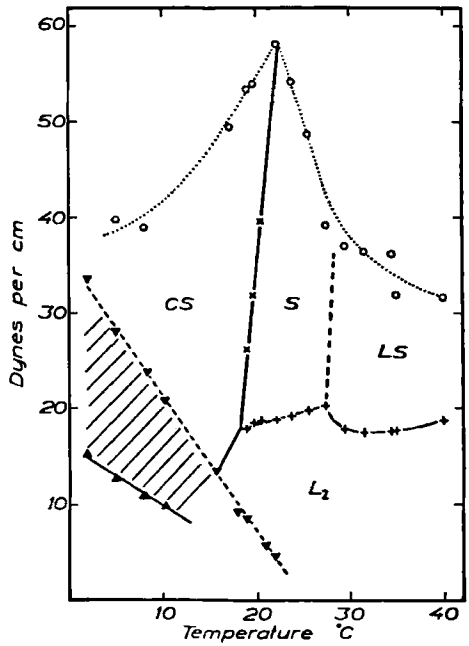


Figure 28. π-T diagram of quasi-enantiomeric 1 : 1 mixture of (*S*)-(+)-2-tetracosanyl acetate and methyl ester of (*S*)-(+)-2-methylhexacosanoic acid. From Lundquist (79). Permission of Stockholm University Library.

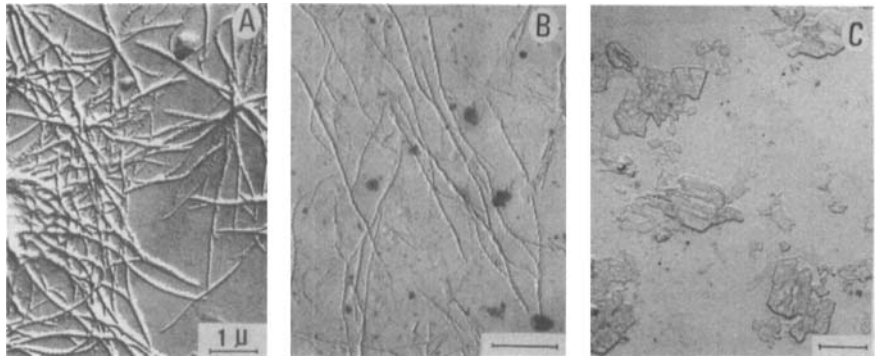


Figure 29. Electron micrographs of microcrystals crystallized from solutions of D- and L-12-hydroxystearic acids. (*A*) D : L = 8 : 2, (*B*) D : L = 3 : 7, (*C*) D : L = 1 : 1. From Uzu and Sugiura (100). Photographs supplied by Prof. Uzu. Permission of Academic Press, Inc.

the conclusion that the hydroxyl groups of a close-packed structure consisting of a single enantiomer are sterically favored to form extended hydrogen-bonded arrays, and those of the racemic compound are not. It was necessary to apply these convincing, but indirect, physical methods to infer the crystal packing because these compounds do not afford suitable single crystals for X-ray diffraction analysis.

The question arises as to whether the racemic compound was formed during the collapse of the monolayer or at a certain mono-

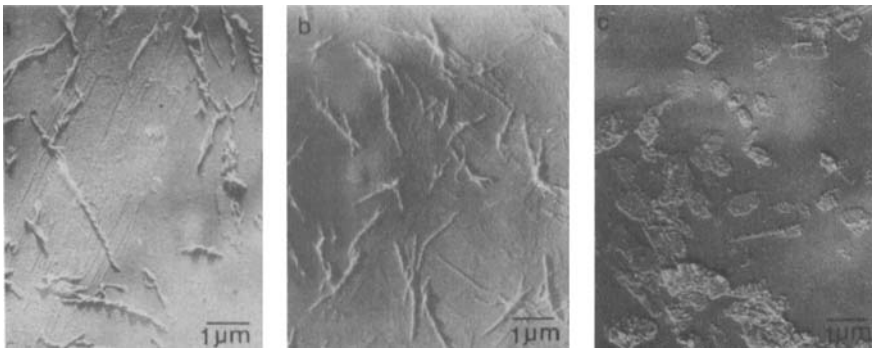


Figure 30. Electron micrographs of collapsed mololayers of 12-hydroxystearic acid. (*A*) D-acid, left-handed twist, (*B*) L-acid, right-handed twist, (*C*) D,L-acid. From Tachibana and Hori (82). Photographs supplied by Prof. Tachibana. Permission of Academic Press, Inc.

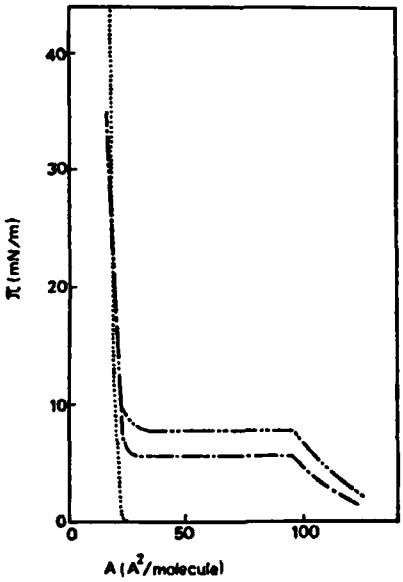


Figure 31. π-A curves for D-12-hydroxystearic acid (– - –), D,L-12-hydroxystearic acid (– - - –); and stearic acid (· · ·). From Tachibana and Hori (82). Permission of Academic Press, Inc.

layer state during compression. The π-A isotherm of the L-(+) acid on 0.01N HCl at 20°C was identical with that of the D-(-) acid in all details. Although significant differences can be seen in Figure 31 for the behavior of the racemic acid monolayer under identical conditions, both curves have the same general characteristics: a compressible region above 95 Å^2/molecule followed by a surface pressure plateau to a highly incompressible region whose extrapolated area at zero pressure is 24.0 ± 1.0 Å^2/molecule. The latter dimension is nearly identical with the limiting area of the condensed film of unsubstituted stearic acid, whereas the former closely approximates the packing area estimated from molecular models for a bent conformation having a $CH_3(CH_2)_5$- chain rising steeply from the water surface and both the carboxyl and hydroxyl groups immersed in the aqueous subphase.

It is, therefore, reasonable to interpret the plateau region as being a first-order, two-dimensional phase transition from the bent to an erect conformation where the fatty acid chains bearing the 12-hydroxyl group are being forced from the subphase to assume a nearly vertical arrangement by compression of the expanded monolayer to a condensed one at high surface pressure and low molecular areas. This view is consistent with the measured surface potential, which begins to decrease sharply from an almost constant value at the onset of the plateau and levels off to a value near that of a con-

densed stearic acid monolayer. The coexistence of the two phases from 95 to 24 $Å^2$/molecule is also suggested by application of the two-dimensional phase rule to the nearly constant pressure of the plateau at constant temperature. The plateau region for the racemic acid occurs at a higher pressure than that of the optically active sample. As might be expected from our discussion of the results obtained by Lundquist, this difference in surface pressure increases with decreasing temperature. The net change in molar internal energy ΔE, accompanying the phase transition, can be calculated from $\Delta H = \Delta E + \pi \Delta A$, where ΔA is the net change in molar area and ΔH is the molar enthalpy change accompanying the transition at this temperature as obtained from the two-dimensional Clausius-Clapeyron equation given in Sect. IV. The value of ΔE was -4.1 ± 0.1 and -3.3 ± 0.1 kcal/mol (-17.1 ± 0.3 and -14.0 ± 0.3 kJ/mol) for the D-(−) and racemic acids, respectively, showing that the condensed film of the former is thermodynamically more stable than the latter. Based on these results, Tachibana concluded that "the two-dimensional racemic compound formation occurs prior to the completion of the condensed film, probably in the plateau region."

We would only add to this the observation that unlike the original expectations of the Stenhagens, this system shows an enantiomeric interaction in the expanded film and pressure plateau region, but none in the subsequent condensed monolayer; the loss of the enantiomeric effect appears to coincide, perhaps fortuitously, with the removal of the chiral center from the aqueous surface. It is also worth noting that although these data have been treated in terms of thermodynamics, no tests for metastability were reported and, accordingly, the data may reflect a combination of terms from kinetics and classical thermodynamics.

B. More Complex Surfactants

The compounds most thoroughly investigated as monolayers at the air-water interface have been long chain derivatives of normal paraffins containing a carboxyl, hydroxyl, amino, or other polar head groups. However, a number of other compounds having a more complex molecular structure than these simple surfactants have also been studied as monolayers, frequently because of their biological significance and the unique ability of the film balance to relate the shape and dimensions of highly oriented molecules. The characteristics of stable monolayers have been reported for phospholipids, glycerides, polypeptides, synthetic polymers, porphyrins, fat-soluble

vitamins, bile acids, steroids, and other compounds with condensed ring systems. Gaines (38) has reviewed much of this literature through 1966. Although most of these compounds are chiral, the vast majority of the reports have ignored this significant factor of molecular structure in determining monolayer behavior.

Many of the studies have interesting stereochemical consequences but are beyond the scope of this chapter, which is limited to enantiomer and diastereomer discrimination as defined in Sect. II. For example, 13,14-dihydroxydocosanoic acid has two chiral centers and, therefore, exists as two diastereomerically related pairs of enantiomers. The force-area curves of racemic modifications of these diastereomers differ greatly, yet reaction of both *cis* and *trans*-13-docosenoic acid in the monolayer state over a subphase of dilute acidic permanganate has been reported in the early surface chemistry literature to afford the same 13,14-dihydroxy diastereomer (104). This result, which has not been reinvestigated, is unlike the stereoselective oxidation claimed for the analogous reaction in solution and gives some indication of the directive influence that molecular orientation at an interface may have on the stereochemical course of reactions. Beyond this, total asymmetric synthesis from achiral starting materials and reagents resulting from chiral packing arrangements in monolayers, as has already been realized in three-dimensional crystals (7), remains an unexplored and exciting possibility.

There are also several monolayer studies of polymers that deserve mention but do not represent true enantiomer or diastereomer discrimination. For example, atactic, isotactic, syndiotactic, and stereoblock samples of poly(methylmethacrylate) exhibit clear differentiation in their force-area curves attributable to the varying degree and kind of stereoregularity along the chain (105). It has been suggested that such monolayer studies may help to characterize the configuration of polymer chains (106). Differences in the monolayer behavior of poly(γ-benzyl-DL-glutamate), an atactic polypeptide prepared from the racemic amino acid, and poly(γ-benzyl-L-glutamate), an isotactic polypeptide prepared from the optically active amino acid, have also been reported (107). However, these comparisons are made among diastereomers and random polymers that would be expected to differ in all their physical properties including their monolayer behavior.

A genuine example of enantiomer discrimination has been reported for polypeptides by Malcolm (108,109). Mixed monolayers of enantiomerically related samples of isotactic poly(alanine), poly(γ-benzylglutamate), poly(β-benzylaspartate), and poly(ε-benzyloxycarbonyllysine) were studied to shed some light on the

characteristic transition plateau in their force-area curves. A detailed analysis of the differences observed between an optically pure polypeptide and the racemic modification were interpreted, in some cases, as indicating the occurrence of a racemic *mixture* in the monolayer. In such cases, the polypeptides were thought to interact more strongly with their own kind than with their enantiomer. An example of a diastereomer discrimination has also been reported for polypeptides by Shafer (110) and is discussed in Sect. VII.

Proteins occur in the interfacial system of cell membranes. Since protein molecules have very complicated structures, it is difficult to give more than a rough interpretation of their monolayer behavior. Thus, monolayers of synthetic polypeptides having a single chain of simple composition, such as those mentioned above, are frequently studied as a model system to explore the conformation and intermolecular packing of proteins in interfacial systems (109,111). A giant step in simplifying the attack on this frontier has come through the general recognition that biological membranes are a bilayer arrangement of two back-to-back phospholipid monolayers whose polar head groups form a hydrated sheath facing the two surfaces of the membrane and whose methylene chains are directed toward the hydrophobic interior of the membrane to intertwine and surround the individual protein molecules (16,46,48,49). Beyond this general description, however, the detailed structure of cell membranes is still a controversial matter of intensive current research.

In view of the well-developed techniques for studying monolayers of simple surfactants at the air-water interface, the logical application of the reductionist approach to simplifying the study of membranes has been to regard monolayers of phospholipids (both phosphoglycerides and sphingolipids) and also mixed monolayers of phospholipids with either polypeptides or steroids as being adequate models of lipoprotein biological membranes (50,51). Thus, the stated or implied objective of virtually all the many physical and chemical techniques that have been applied to phospholipid systems, including film balance experiments of monolayers at the air-water interface, has ultimately been a better understanding of the structure and function of cell membranes (112). However, extrapolation of the results obtained from these model systems to the membranes of living organisms must be applied with extreme caution.

Most film balance experiments involving phospholipids have been performed with single enantiomers having the 3-*sn* configuration (formerly called L) because this corresponds to the absolute configuration of virtually all phospholipid samples obtained from

natural sources (113,114). The useful literature in this area began in 1962, when van Deenen and his associates at the State University of Utrecht reported a comprehensive survey of the monolayer behavior of a number of synthetic phospholipids to demonstrate the effects of head group, chain length and position, unsaturation, and subphase pH (115). The studies by the preceding generation of surface scientists were carried out on poorly defined systems of natural origin, and real progress in characterizing phospholipid monolayers was not possible until synthetic samples having high chemical and optical purity became available (114,116). The Dutch group recognized the possible influence of stereochemistry in determining their results. Indeed, they found that although both enantiomers of 1-stearoyl-2-lauroyl-3-phosphatidylcholine gave force-area curves that were identical, they occupied a greater area per molecule at all surface pressures than did the racemic modification.

Phillips and Chapman (117), at the Unilever Research Laboratory at Welwyn, failed to find any differences due to enantiomer discrimination with monolayers of racemic and optically active dimyristoyl phosphatidylethanolamine. The negative result implied by the prestigious Unilever group appears to have laid to rest all further consideration that chiral discrimination might be an important factor in phospholipid monolayers. In his authoritative review (118) of 1970, Cadenhead suggested that the discrepancy between the Unilever group's results and those of the Dutch group may be due to an impurity in van Deenen's sample. He went on to state that, as far as chiral discrimination is concerned, ". . . no conclusive evidence yet exists for this particular effect on phospholipid isotherms." For this reason, Cadenhead dropped the use of configurational assignments throughout the rest of his review.

Critical appraisal of the available literature, however, suggests that the phenomenon of chiral discrimination in phospholipid monolayers has received only cursory attention and has not been tested suitably. On the basis of the results obtained from chiral monolayers of the simpler surfactants cited in the preceding section, as well as from our own work, we feel that there is some precedent for believing that chiral discrimination in phospholipid monolayers could be significant when examined under the proper conditions. On the other hand, we are also aware of the challenge issued to the community of scientists involved in the study of phospholipid monolayers by Horn and Gershfeld (119) in 1977. They questioned the significance of many of the previous studies in this area and attributed the variability of the force-area curves obtained by different groups to the

coexistence of several nonequilibrium monolayer states under the common conditions of film balance experiments. Negative results after a truly exhaustive search for chiral discrimination in phospholipid monolayers, then, may well suggest that disorder and fluidity are characteristic of their intermolecular packing according to the original premise of the Stenhagens (80), quoted earlier.

VI. A CASE IN POINT: ACID-DEPENDENT CHIRAL DISCRIMINATION OF THE *N*-α-METHYLBENZYLSTEARAMIDES

The literature reviewed in the preceding section is related directly to our own research activities over the past 5 years. We describe some of our results here, since they illustrate for one system many of the principles and phenomena for which there are only scattered reports elsewhere.

Our motivation for this work lay in the singular opportunities to study intermolecular stereochemistry that chiral monolayers seemed to offer and the heuristic challenge of discovering new phenomena with potentially significant implications in a virgin field of inquiry. In view of a lack of precedent, there were virtually no guidelines to suggest the appropriate structural features that would elicit the phenomena we hoped to discover. With so little to go on, we simply combined two of the most thoroughly explored systems: α-phenethylamine from the field of stereochemistry and stearic acid from surface chemistry. The ready availability of both enantiomers of the amine, their well-established configurations, and the relation of the amine to the series of simple chiral pharmaceuticals such as amphetamine, ephedrine, pseudoephedrine, and DOPA were added incentives. The enantiomeric *N*-α-methylbenzylstearamides were easily prepared by aminolysis of highly purified methyl stearate and were subjected to repeated recrystallization until all physical properties were essentially identical.

Initial attempts to spread the amide as a monolayer film on aqueous subphases failed. Since patches of microcrystals could be observed by careful inspection, it was concluded that the aggregation forces in the solid phase were too great to permit significant expansion of the molecules onto the adjacent surface of the air-water interface. It is well known that amides are weak bases that are protonated on the carbonyl oxygen by moderately strong aqueous acid. Accordingly, a series of subphases prepared from carefully purified sulfuric acid–

water mixtures was tried, on the notion that the protonation of the amide head groups would cause mutual repulsion of positive charges at the interface and, accordingly would produce expansion to form a stable film.

The success of this approach was demonstrated immediately by surface tension measurements, which moreover revealed an interesting and potentially important new phenomenon. Surface active behavior began to be manifested by racemic *N*-α-methylbenzylstearamide on 3.5*N* H_2SO_4 with decreasing of surface tension as the acid strength was increased. However, surfactant behavior for the pure enantiomeric amides began to be seen only at acid strengths greater than 6*N*. Thus, chiral discrimination at the surface was established for this system, and furthermore, it was shown to be acid dependent. The dependence of surface tension lowering as a function of subphase acidity is depicted in Figure 32.

Encouraged by the results from static surface tension measurements, we next ran force-area curves on 3*N*, 6*N*, and 10*N* acids. As Figure 33 indicates, there is pronounced discrimination between the racemic and enantiomeric monolayers, and those differences are sharply dependent on the subphase acidity, as had been implied by the surface tension behavior.

Figure 33 is particularly instructive because it shows the drastically different responses to compression of the racemic monolayer and the enantiomeric ones. Consistent with static surface tension results (Fig. 32), the enantiomeric amide does not even spread as a monolayer on 3*N* H_2SO_4. On all three acid subphases, the racemic material

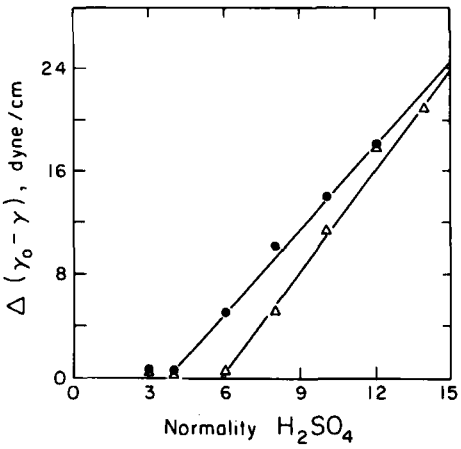


Figure 32. Variation of the lowering of the surface free energy of sulfuric acid solutions, with acid concentration, by the racemic (●) and enantiomeric (△) *N*-α-methylbenzylstearamides. From Thompson (101).

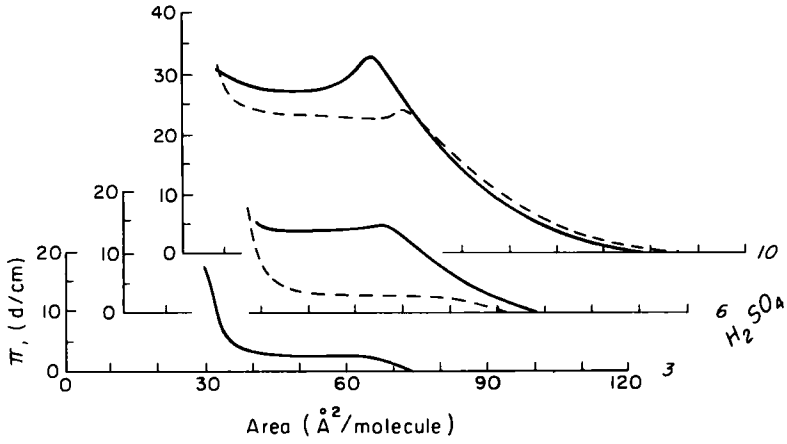


Figure 33. π-A isotherms of the chiral N-α-methylbenzylstearamides on 3, 6, and 10N H_2SO_4 at 25 ± 1°C. Compression rate, 7.2 Å²/molecule • min; initial molecular area, 120 Å². Solid lines depict behavior of racemate; broken lines depict behavior of enantiomers. From Thompson (101).

shows a greater proclivity to expand as a film, since its surface pressure π is greater at each molecular area than are those of the enantiomers. A plateau region running from about 35 to 70 Å²/molecule is defined clearly on 3N and 6N acids. This suggests strongly that a first-order transition between two monolayer phases is taking place (at constant surface free energy) at the π's of the plateaus. On 6N H_2SO_4 a difference of about 10 dynes/cm is seen between the plateau pressure of the racemic film at 15 dynes/cm and the enantiomers at 5 dynes/cm. This difference corresponds to about 1 kcal/mol at 70 Å²/molecule and half that at 35 Å²/molecule. This is roughly equivalent to the statistical entropy difference, R ln 2, which is an inherent contribution to a racemic system from its enantiomers at comparable conditions. However, the behavior on 10N acid removes most of the difference seen at lower acidities and with it any simple explanation in terms of entropy. Comparison of racemic and enantiomeric films from other systems (Figs. 14–22) removes any lingering notion that higher film pressures from racemic systems is a general rule.

Equilibrium spreading pressures, like static surface tension measurements, provide a means to determine surface energies under equilibrium conditions. On 10N H_2SO_4, racemic crystals (Fig. 10) spread within 5 min to an equilibrium pressure of 8.6 dynes/cm, whereas about 8 hr was required by either (*R*)-(+)- or (*S*)-(-)- crystals to spread to a final pressure of 5.5 dynes/cm.

The sharply different rates at which equilibrium was reached clearly implied that kinetic factors as well as thermodynamic ones could be involved in the expansion or compression of these films. It was therefore important to test them for stability using the criteria described in Sect. IV.

Figure 11 shows that a tenfold increase in compression rate has a decided effect on the shape of the π-A isotherm of (*R*)-(+)-*N*-α-methylbenzylstearamide films. At rapid compression, a higher film pressure is produced at any given molecular area than at slow compression. It should be remembered that the enantiomeric amides are much slower to spread than are the corresponding racemic materials, and the former give every evidence of being more closely and firmly packed at any given area. Figure 11 implies that the enantiomer molecules have a rather slow rate of reorganization under compression as a surface film. The time required for the molecules to pack into low-energy arrangements at a given molecular area is actually of the same order as the compression rate. In three dimensions this would be equivalent to the slow response of a liquid or gas to compression by a piston. Such behavior is usually only seen for very viscous liquid systems. In contrast to the behavior shown in Figure 11, the π-A isotherm for the racemic stearamide shows no variation with compression rate over the same range used to study the enantiomers.

Another test of film stability is shown in Figure 13, where compressed films were expanded and recompressed. The hysteresis pattern was observed for both enantiomer films and racemate films at 15°C but not at 25°C (101). This indicates again the relatively high viscosity of surface films and the sensitivity of molecular reorganization to changes in structure and conditions.

Given such evidences of nonthermodynamic behavior of compressed monolayers, it was important to test film stability at various points along the π-A isotherms for the normal rate of slow compression. The racemic film maintained a steady film pressure over at least 10 min after the barrier drive was stopped, showing little or no tendency to relax from the compressed state to one of lower energy. The enantiomer film in contrast showed a tendency to relax steadily from a compressed metastable state to a more stable and better packed condition approaching the equilibrium spreading pressure.

The metastable compressed films described above bear rough analogy to a supersaturated solution, since a larger number of molecules are contained per unit area than would be stable under true equilibrium conditions in the presence of a second denser phase. On

the strength of this analogy a "two-dimensional resolution" in the surface was attempted.

A racemic film was compressed nearly to its collapse point. It was then seeded by sprinkling crystals of pure enantiomeric amide on the surface. A rapid decrease in surface pressure was observed approaching the equilibrium spreading pressure of the enantiomer. A control experiment in which racemic crystals were sprinkled on the compressed racemic film produced a pressure drop that slowly approached, but did not reach, the ESP of the racemic film. The observed behavior was consistent with what would be expected if the enantiomer seed crystals had removed molecules of the same enantiomer from the racemic film, leaving a monolayer composed mainly of molecules of the opposite configuration.

An interesting possibility raised by this experiment is that of spontaneous resolution in chiral monolayers. If this were a reasonably common phenomenon, it would give yet another possible answer to the perennial question of the chiral environment for the primordial stereospecific condensation reaction that produced the first chiral biopolymers. As our knowledge of chiral monolayers develops, we should have a better perspective on the likelihood of a racemic film spontaneously unmixing to produce patches of enantiomeric film at lower surface energy. The relevance of such a result to the "origin of terrestrial life" problem will have to remain eternally speculative and untestable.

VII. DIASTEREOMER DISCRIMINATION IN MONOLAYERS

The ability of a chiral molecule to distinguish between the enantiomers of a second (different) chiral molecule was defined in Sect. II as a *diastereomer discrimination*. This phenomenon may be observed in a mixed monolayer of two chiral surfactants and may also occur when a chiral substance is dissolved in the aqueous subphase under the monolayer of a second chiral substance. As before, examples of such chiral discrimination would not include those whose difference in monolayer behavior results only from the gross structural differences of diastereomers such as the different force-area characteristics exhibited by mixed monolayers of 1-oleoyl-2-stearoyl-3-*sn*-phosphatidylcholine with epimeric steroids (120). The relevant experiment, that of comparing the monolayer behavior of mixed monolayers of cholesterol with enantiomeric phospholipids, has been reported (121). As might be anticipated from our previous discussion of

phospholipid monolayers, however, no differences were observed beyond the errors of the technique.

Shafer (110) studied the interaction of 16 different polypeptides with 11 different lipid monolayers to examine the role of molecular structure in the binding of polypeptides to lipid monolayers. The lipid monolayer was spread at constant area and a solution of the polypeptide was added to the gently stirred subphase with a syringe; then the change in surface pressure was continuously recorded while the area of the monolayer remained constant. Penetration of the protein molecule into the monolayer would be expected to cause an increase in the surface pressure, whereas binding without penetration (i.e., adsorption) would not. As part of this study, identical experiments were conducted with the isotactic poly(L-lysine) and poly(D-lysine), the atactic poly(DL-lysine), and the racemic modification formed by mixing the enantiomers in equal amounts. On obtaining significantly different results for the two enantiomers, Shafer concluded that "such discrimination, if it is the result of the isomerism, is mostly likely to occur if the isomeric carbon atoms of the phospholipid and polyamino acid molecules are localized in close proximity to each other."

The relevance of such a diastereomer discrimination to the transport of chiral molecules, such as pharmaceuticals or biochemicals, through hydrophobic barriers, such as cell membranes, is obvious. Furthermore, since poly(DL-lysine) followed the same general pattern of behavior displayed by the other three samples, the observed surface-pressure changes probably were not due to helicalization of the polypeptide. Whereas poly(L-lysine) and poly(D-lysine) form helices with opposite screw sense, the random copolymer poly(DL-lysine) is to a large extent prevented from forming helices.

An interesting kinetic study of the hydrolysis of phosphatidylcholine monolayers with phospholipase A_2 enzyme has been reported by Zografi, Verger, and de Haas (122). Here, the monolayer was spread on a solution of the enzyme; then the surface pressure was set by compression to a constant value and the depletion of the film during the course of the reaction was followed by its change in surface area. As part of this work, the rate of hydrolysis of mixed monolayers of 1,2-dioctanoyl-3-*sn*-phosphatidylcholine and its enantiomer were measured in various proportions. Surprisingly, the investigators found that the rate of hydrolysis was unaffected by the optical purity of the sample. Although the 1-*sn* enantiomer is totally insensitive to the action of the enzyme, it does function as a pure competitive inhibitor in the bulk phase. Zografi et al. suggested that

this is probably an artifact of the film balance technique, where only a tiny fraction of the total bulk enzyme is involved in the reaction. Thus, even a powerful inhibitor in the mixed monolayer could not deplete the enormous reservoir of enzyme in the subphase.

Probably the most interesting and important example of diastereomer discrimination known to us is part of the body of work conducted by Monica Lundquist, whose enormous contribution to the area of chiral discrimination in monolayers is discussed in Sect. V. In her third paper (79), she demonstrated that Fredga's method of quasi-racemates (33) can be applied to the two-dimensional organization of chiral surfactants in monolayers.

Plots of melting point against optical purity are commonly referred to as phase-composition diagrams. The direct proportionality of melting point with heat of fusion has also been employed to construct similar plots based on thermal analysis data. The classification of racemic modifications into three different types with regard to their crystal packing (32) can be made based on the overall shape of these plots as follows:

1. *Racemic mixture*. The phase-composition diagram exhibits a minimum; thus, the molecules having identical absolute configurations have the greatest affinity and, in effect, a chiral molecule regards its enantiomer as an impurity.
2. *Racemic compound or racemate*. The phase-composition diagram exhibits a maximum; thus, the molecules of opposite configuration have the greatest affinity. This is the most commonly encountered type of behavior.
3. *Racemic solid solution*. The phase-composition diagram has a zero slope across the whole composition range; thus, there is little difference in the affinity among molecules of either configuration (i.e., no chiral discrimination).

Phase-composition diagrams may also be plotted for mixtures of optically pure samples that are structurally similar, but not identical. Such plots have been employed frequently as an empirical correlation to absolute configuration, which is referred to as the method of quasi-racemates. The details, variations, limitations, and numerous examples of this method have been presented by others (33). We merely note here that if a phase-composition diagram of the racemic compound type were obtained for a particular pair of enantiomers having known configuration, and if the phase-composition diagram of mix-

tures of one of these enantiomers and an enantiomer of another structurally similar molecule were also of the racemic compound type, there is strong evidence that these compounds are in the opposite configurational series. However, if this plot indicates that a racemic mixture (or a solid solution) was obtained, the conclusion follows that these substances have the same absolute configuration. Obviously, for this method to have any reliability, the compounds compared must be chemically very similar. The functional groups attached to the chiral center not only must be similar in size, but must be similar in such features as dipole-dipole interactions and hydrogen-bonding capacity. Despite its rather severe limitations, the history of stereochemistry has shown the method of quasi-racemates to be a valuable technique.

The force-area curves for racemic and (*S*)-(+)-2-tetracosanyl acetate were shown in Figures 17 and 18, respectively, while those of methyl esters of racemic and (*S*)-(+)-2-methylhexacosanoic acid are found in Figs. 21 and 22, respectively. All these curves were obtained under identical experimental conditions at the various temperatures indicated in the figures. Simple inspection shows that the force-area curves of the two racemic samples are very similar, as are those for both optically pure samples. Lundquist suggested that this is merely a result of the very similar shapes and molecular structures of these chiral surfactants. Apart from the chain length, the only structural difference is limited to a reversal of the positions of the carbonyl group and ester oxygen.

Figure 20 shows the force-area curves obtained from an equimolar mixture of (*S*)-(+)-2-tetracosanyl acetate and the methyl ester of (*S*)-(+)-2-methylhexacosanoic acid. Comparison with either Figure 18 or Figure 22 demonstrates that the force-area curve of the mixed monolayer has the same general appearance as those of the individual pure enantiomers.

Figure 19 shows the force-area curves obtained from an equimolar mixture of (*S*)-(+)-2-tetracosanyl acetate and the methyl ester of (*R*)-(−)-2-methylhexacosanoic acid. Comparison with either Figure 17 or Figure 21 reveals that the mixed monolayer now exhibits the same general characteristics as the racemic samples of the individual components. The surface pressures at characteristic points in the force-area curves of the mixed monolayers are displayed in Figures 27 and 28, and may be compared with those obtained from the racemic and optically active components in Figures 23 to 26. The logical conclusion of this beautiful experiment is that the force-area curves of Figure 19 represent the formation of a quasi-racemate in a monolayer. Lundquist (79) summarized the significance of this result by noting:

The differences observed between the quasi-racemic mixture and the mixture of enantiomers with the same configuration are analogous to the differences between the racemic and the optically active forms of the pure compounds. Thus, a kind of two-dimensional isomorphy exists between the molecular systems in question. The different properties of optically active and racemic forms in solid surface phases have been taken as evidence of an orderly arrangement of the molecules in some kind of two-dimensional crystalline lattice.

VIII. SUMMARY

Monolayers of surfactants at the air-water interface provide an unparalleled opportunity to study energy changes due to differences in orientation of the surfactant molecules as they are packed within various areas on the surface. The work reviewed here, from a small number of studies that have been widely scattered through the literature, shows that the surface properties of monolayers are quite sensitive to stereochemistry.

Thus, chiral discrimination may be observed that differentiates the force-area curves of the enantiomers of some surfactants from their racemic modifications. Apparent phase changes in the monolayer can be related to parallel behavior in the crystalline state through X-ray diffraction and differential scanning calorimetry. Formation of racemic compounds and quasi-racemates can be observed in some cases.

The states produced by compression of monolayers are not necessarily at thermodynamic equilibrium, but may be metastable. In some cases, this is manifested clearly by different force-area curves being produced at different rates of compression. Slow reorganization of monolayer molecules is also apparent as hysteresis when films are repeatedly compressed and expanded. In chiral monolayers, the *rates* of molecular reorganization may be stereospecific as well as the thermodynamic behavior.

These facts are of potential importance to biochemistry because most of the components of bilayer membranes are chiral. It is reasonable that stereospecific packing in the membrane may affect the way its components fit together and the way that chiral biomolecules are transferred through the membranes. To date the possible relevance of stereospecific intermolecular aggregation of chiral lipids has received little, if any, attention from biochemists. We hope that this review will help to bring greater recognition to the interesting possibilities that are offered by the study of chiral monolayers.

ACKNOWLEDGMENTS

We are grateful for support from National Institutes of Health (grant GM-20386), the National Science Foundation (grant CHE-7622369), and the R. J. Reynolds Industries Fund during various phases of our laboratory and literature research in this field. Our colleagues Drs. Orlean Thompson and Barbara Kinzig provided expert advice as well as most of the experimental background for our work. Jeffrey Gold and Patricia Zingg provided much help in preparation of this manuscript.

REFERENCES

1. (a) Floss, H. G.; Tsai, M.-D. *Adv. Enzymol.* **1979**, *50*, 243-302. (b) Hanson, K. R.; Rose, I. A. *Acc. Chem. Res.* **1975**, *8*, 1-10. (c) Cornforth, J. W. *Tetrahedron* **1974**, *30*, 1515-1524. (d) Battersby, A. R.; Staunton, J. *ibid.* **1974**, *30*, 1707-1715. (e) Goodwin, T. W. *Essays Biochem.* **1973**, *9*, 103-160.
2. (a) Alworth, W. L. "Stereochemistry and Its Application in Biochemistry"; Wiley-Interscience: New York, 1972. (b) Popják, G. In "The Enzymes," 3rd ed.; Boyer, P. D., Ed.; Academic Press: New York, 1970; Vol. 2, Chapter 3.
3. (a) Bentley, R. "Molecular Asymmetry in Biology"; Academic Press: New York, 1969; Vol. 1. (b) Bentley, R. *ibid.* 1970; Vol. 2.
4. (a) Izumi, Y.; Tai, A. "Stereo-differentiating Reactions: The Nature of Asymmetric Reactions"; Academic Press: New York, 1977. (b) Morrison, J. D.; Mosher, H. S. "Asymmetric Organic Reactions"; Prentice-Hall: Englewood Cliffs, NJ, 1971.
5. Kagan, H. B.; Fiaud, J. C. *Top. Stereochem.* **1978**, *10*, 175-285.
6. (a) Szabo, W. A.; Lee, H. T. *Aldrichim. Acta* **1980**, *13*(1), 13-20. (b) Valentine, D.; Scott, J. W. *Synthesis* **1978**, 329-356. (c) Wynberg, H. *Chimia* **1976**, *30*, 445-451. (d) Scott, J. W.; Valentine, D. *Science* **1974**, *184*, 943-952. (e) Eliel, E. L. *Tetrahedron* **1974**, *30*, 1503-1513. (f) Izumi, Y. *Angew. Chem.* **1971**, *83*, 956-966; *Angew. Chem., Int. Ed. Engl.* **1971**, *10*, 871-881. (g) Inch, T. D. *Synthesis* **1970**, 466-473. (h) Morrison, J. D. *Surv. Prog. Chem.* **1966**, *3*, 147-182.
7. For a summary of recent attempts to achieve asymmetric synthesis from the chirality of crystal packing and in similarly organized cholesteric media, see: (a) Green, B. S.; Lahav, M.; Rabinovich, D. *Acc. Chem. Res.* **1979**, *12*, 191-197. (b) Eskenazi, C.; Nicoud, J. F.; Kagan, H. B. *J. Org. Chem.* **1979**, *44*, 995-999. (c) Thomas, J. M.; Morsi, S. E.; Desvergne, J. P. *Adv. Phys. Org. Chem.* **1977**, *15*, 63-151. (d) Paul, I. C.; Curtin, D. Y. *Science* **1975**, *187*, 19-26.
8. Meyers, A. I. *Acc. Chem. Res.* **1978**, *11*, 375-381.
9. Engström, A.; Strandberg, B., Eds. "Symmetry and Function of Biological

Systems at the Macromolecular Level"; Wiley-Interscience: New York, 1969.

10. (a) Israelachvili, J. N.; Ninham, B. W. *J. Colloid Interface Sci.* **1977**, *58*, 14–25. (b) Israelachvili, J. N.; Tabor, D. *Prog. Surf. Membrane Sci.* **1973**, *7*, 1–55.
11. Jencks, W. P. "Catalysis in Chemistry and Enzymology"; McGraw-Hill: New York, 1969.
12. Kauzmann, W. *Adv. Protein Chem.* **1959**, *14*, 1–63.
13. Horeau, A.; Guetté, J. P. *Tetrahedron* **1974**, *30*, 1923–1931.
14. Wynberg, H.; Feringa, B. *Tetrahedron* **1976**, *32*, 2831–2834.
15. Craig, D. P.; Mellor, D. P. *Top. Curr. Chem.* **1976**, *63*, 1–48.
16. Tanford, C. "The Hydrophobic Effect: Formation of Micelles and Biological Membranes," 2nd ed.; Wiley-Interscience: New York, 1980.
17. Tanford, C. *Science* **1978**, *200*, 1012–1018.
18. (a) Franks, F., Ed. "Water, A Comprehensive Treatise"; Plenum: New York, 1972; Vol. 1. (b) Franks, F., Ed. *ibid.* 1973; Vol. 2. (c) Franks, F., Ed. *ibid.* 1973; Vol. 3. (d) Franks, F., Ed., *ibid.* 1975; Vol. 4. (e) Franks, F., Ed. *ibid.* 1975; Vol. 5 (f) Franks, F., Ed. *ibid.* 1979; Vol. 6.
19. (a) Bender, M. L.; Komiyama, M. "Cyclodextrin Chemistry"; Springer-Verlag: Berlin, 1978. (b) Harada, A.; Furue, M.; Nozakura, S.-I. *J. Polym. Sci., Polym. Chem. Ed.* **1978**, *16*, 189–196.
20. (a) Komiyama, M.; Bender, M. L. *Bioorg. Chem.* **1979**, *8*, 249–254. (b) Komiyama, M.; Bender, M. L. *J. Am. Chem. Soc.* **1978**, *100*, 4576–4579.
21. (a) Breslow, R. *Acc. Chem. Res.* **1980**, *13*, 170–177. (b) Breslow, R.; Czarniecki, M. F.; Emert, J.; Hamaguchi, H. *J. Am. Chem. Soc.* **1980**, *102*, 762–770.
22. (a) For Part 22 of this continuing series, see: Peacock, S. S.; Walba, D. M.; Gaeta, F. C. A.; Helgeson, R. C.; Cram, D. J. *J. Am. Chem. Soc.* **1980**, *102*, 2043–2052. (b) Cram, D. J.; Cram, J. M. *Acc. Chem. Res.* **1978**, *11*, 8–14. (c) Cram, D. J.; Cram, J. M. *Science* **1974**, *183*, 803–809. (d) Stoddart, J. F. *Chem. Soc. Rev.* **1979**, *8*, 85–142. (e) Prelog, V. *Pure Appl. Chem.* **1978**, *50*, 893–904.
23. (a) Lehn, J.-M. *Pure Appl. Chem.* **1979**, *51*, 979–997. (b) Lehn, J.-M. *ibid.* **1978**, *50*, 871–892. (c) Lehn, J.-M.; Simon, J.; Moradpour, A. *Helv. Chim. Acta* **1978**, *61*, 2407–2418. (d) Lehn, J.-M. *Acc. Chem. Res.* **1978**, *11*, 49–57.
24. (a) Pirkle, W. H.; Adams, P. E. *J. Org. Chem.* **1979**, *44*, 2169–2175. (b) Pirkle, W. H.; Rinaldi, P. L. *ibid.* **1979**, *44*, 1025–1028. (c) Pirkle, W. H.; Rinaldi, P. L. *ibid.* **1978**, *43*, 4475–4480. (d) Pirkle, W. H.; Rinaldi, P. L. *ibid.* **1977**, *42*, 3217–3219. (e) Pirkle, W. H.; Sikkenga, D. L. *ibid.* **1977**, *42*, 1370–1374. (f) Pirkle, W. H.; Hoover, D. J., *Top. Stereochem.*, **1982**, *13*, 263–331.
25. (a) Pirkle, W. H.; House, D. W.; Finn, J. M. *J. Chromatogr.* **1980**, *192*, 143–158. (b) Davankov, V. A. *Adv. Chromatogr.* **1980**, *18*, 139–195. (c) Pirkle, W. H.; House, D. W. *J. Org. Chem.* **1979**, *44*, 1957–1960. (d) Krull, I. S. *Adv. Chromatogr.* **1978**, *16*, 175–210. (e) Lochmüller, C. H.; Souter, R. W. *J. Chromatogr.* **1975**, *113*, 283–302.

26. (a) Fendler, J. H. *J. Phys. Chem.* **1980**, *84*, 1485–1491. (b) Bunton, C. A. *Pure Appl. Chem.* **1977**, *49*, 969–979. (c) Menger, F. M. *Bioorg. Chem.* **1977**, *3*, 137–152.

27. (a) Moss, R. A.; Lee, Y.-S.; Lukas, T. J. *J. Am. Chem. Soc.* **1979**, *101*, 2499–2501. (b) Goldberg, S. I.; Baba, N.; Green, R. L.; Pandian, R.; Stowers, J.; Dunlap, R. B. *ibid.* **1978**, *100*, 6768–6769. (c) Sugimoto, T.; Matsumura, Y.; Imanishi, T.; Tanimoto, S.; Okano, M. *Tetrahedron Lett.* **1978**, 3431–3434.

28. (a) Miyagishi, S.; Nishida, M. *J. Colloid Interface Sci.* **1978**, *65*, 380–386. (b) Massé, J.; Parayre, E. *C. R. Hebd. Seances Acad. Sci., Ser. C* **1977**, *284*, 45–48.

29. (a) Kunitake, T.; Nakashima, N.; Hayashida, S.; Yonemori, K. *Chem. Lett.* **1979**, 1413–1416. (b) Doiuchi, T.; Minoura, Y. *Kagaku (Kyoto)* **1979**, *34*, 332–335; *Chem. Abstr.* **1979**, *91*, 141252z. (c) Radley, K.; Saupe, A. *Mol. Phys.* **1978**, *35*, 1405–1412. (d) Doiuchi, T.; Minoura, Y. *Macromolecules* **1977**, *10*, 260–265.

30. (a) Menger, F. M.; Boyer, B. J. *J. Am. Chem. Soc.* **1980**, *102*, 5936–5938. (b) Tachibana, T.; Kurihara, K. *Naturwissenschaften* **1976**, *63*, 532–533.

31. Massé, J.; Parayre, E. *Actual. Chim.* **1978**, No. 6, 7–13; *Chem. Abstr.* **1978**, *89*, 91407q.

32. (a) Kitaigorodskii, A. I. *Chem. Soc. Rev.* **1978**, *7*, 133–163. (b) Kitaigorodskii, A. I. "Molecular Crystals and Molecules"; Academic Press: New York, 1973. (c) Kitaigorodskii, A. I. *Adv. Struct. Res. Diffr. Methods* **1970**, *3*, 173–247. (d) Kitaigorodskii, A. I. "Organic Chemical Crystallography"; Consultants Bureau: New York, 1961. (e) Mills, H. H.; Speakman, J. C. *Prog. Stereochem.* **1969**, *4*, 273–298. (f) Speakman, J. C. *ibid.* **1958**, *2*, 1–38 (g) Hägg, G. In "The Svedberg Anniversary Volume," Tiselius, A.; Pedersen, K. O., Eds.; Almqvist & Wiksells: Uppsala, Sweden, 1944; pp. 140–154.

33. (a) Eliel, E. L. "Stereochemistry of Carbon Compounds"; McGraw-Hill: New York, 1962; Chapter 4 and pp. 106–110. (b) Leclercq, M.; Collet, A.; Jacques, J. *Tetrahedron* **1976**, *32*, 821–828. (c) Fredga, A. *ibid.* **1960**, *8*, 126–144. (d) Fredga, A., in ref. 32g, pp. 261–273.

34. Buncel, E.; Wilson, H. *Acc. Chem. Res.* **1979**, *12*, 42–48.

35. Abraham, M. H. *Prog. Phys. Org. Chem.* **1974**, *11*, 1–87.

36. Arnett, E. M.; McKelvey, D. R. *Rec. Chem. Prog.* **1965**, *26*, 185–199.

37. (a) Cahn, R. S.; Ingold, C.; Prelog, V. *Angew. Chem.* **1966**, *78*, 413–447; *Angew. Chem., Int. Ed. Engl.* **1966**, *5*, 385–415. (b) Cahn, R. S.; Ingold, C. K.; Prelog, V. *Experientia* **1956**, *12*, 81–94. (c) Cahn, R. S.; Ingold, C. K. *J. Chem. Soc.* **1951**, 612–622.

38. (a) Gaines, G. L. "Insoluble Monolayers at Liquid-Gas Interfaces"; Interscience: New York, 1966. (b) Gaines, G. L. *ibid.* Chapter 7. (c) Gaines, G. L. *ibid.* Chapter 1. (d) Gaines, G. L. Chapters 4 and 5. (e) Gaines, G. L. pp. 256–257, 272–273.

39. Adamson, A. W. "Physical Chemistry of Surfaces," 3rd ed.; Wiley-Interscience: New York, 1976.

40. (a) Aveyard, R.; Haydon, D. A. "An Introduction to the Principles of

Surface Chemistry"; Cambridge University Press: London, 1973. (b) For a brief and highly readable account of the techniques and practical applications of film balance experiments, see: Cadenhead, D. A. *Ind. Eng. Chem.* **1969**, *61*(4), 22–28.

41. Alexander, A. E.; Hibberd, G. E. In "Techniques of Chemistry," 4th ed.; Weissberger, A.; Rossiter, B. W., Eds.; Wiley-Interscience: New York, 1971; Vol. 1, Part 5, pp. 557–589.
42. Gershfeld, N. L. In "Techniques of Surface and Colloid Chemistry and Physics," Good, R. J.; Stromberg; R. R., Patrick; R. L., Eds.; Dekker: New York, 1972; Chapter 1.
43. Davies, J. T.; Rideal, E. K. "Interfacial Phenomena," 2nd ed.; Academic Press: New York, 1963.
44. (a) Malta, V.; Celotti, G.; Zannetti, R.; Martelli, A. F. *J. Chem. Soc., B* **1971**, 548–553. (b) MacGillavry, C. H.; Wolthuis-Spuy, M. *Acta Crystallogr., Sect. B* **1970**, *26*, 645–648. (c) Larsson, K. *J. Am. Oil Chem. Soc.* **1966**, *43*, 559–562. (d) Abrahamsson, S. *Acta Crystallogr.* **1959**, *12*, 301–304; *ibid.* 304–309. (e) Ref. 32b, pp. 48–62. (f) Ref. 32d, pp. 177–215.
45. For X-ray crystal structures of surfactants having a more complicated molecular structure, see: (a) Abrahamsson, S.; Dahlén, B.; Löfgren, H.; Pascher, I.; Sundell, S., in ref. 48, pp. 1–23. (b) Weinstein, S.; Leiserowitz, L. *Acta Crystallogr., Sect. B* **1980**, *36*, 1406–1418. (c) Hitchcock, P. B.; Mason, R.; Shipley, G. G. *J. Mol. Biol.* **1975**, *94*, 297–299. (d) Hitchcock, P. B.; Mason, R.; Thomas, K. M.; Shipley, G. G. *J. Chem. Soc., Chem. Commun.* **1974**, 539–540. (e) Hybl, A.; Dorset, D. *Acta Crystallogr., Sect. B* **1971**, *27*, 977–986.
46. (a) Stackpole, C. W. *Prog. Surf. Membrane Sci.* **1978**, *12*, 1–182. (b) Singer, S. J., in ref. 48, pp. 443–461. (c) Jain, M. K.; White, H. B. *Adv. Lipid Res.* **1977**, *15*, 1–60. (d) Singer, S. J.; Nicolson, G. L. *Science* **1972**, *175*, 720–731.
47. Agarwal, V. K. *Thin Solid Films* **1978**, *50*, 3–12.
48. Abrahamsson, S.; Pascher, I., Eds. "Structure of Biological Membranes"; Plenum: New York, 1977.
49. (a) Tien, H. T. "Bilayer Lipid Membranes (BLM): Theory and Practice"; Dekker: New York, 1974. (b) Jain, M. K. "The Bimolecular Lipid Membrane: A System"; Van Nostrand Reinhold: New York, 1972.
50. (a) Gershfeld, N. L. *Annu. Rev. Phys. Chem.* **1976**, *27*, 349–368. (b) Montal, M. *Annu. Rev. Biophys. Bioeng.* **1976**, *5*, 119–175. (c) Chapman, D. *Q. Rev. Biophys.* **1975**, *8*, 185–235. (d) Phillips, M. C. *Prog. Surf. Membrane Sci.* **1972**, *5*, 139–221. (e) Shah, D. O. *Adv. Lipid Res.* **1970**, *8*, 347–431.
51. For recent discussion of the role that phospholipid head groups play in biological assemblies, see: (a) Hauser, H.; Phillips, M. C. *Prog. Surf. Membrane Sci.* **1979**, *13*, 297–413. (b) Yeagle, P. L. *Acc. Chem. Res.* **1978**, *11*, 321–327.
52. (a) Langmuir, I. *J. Am. Chem. Soc.* **1917**, *39*, 1848–1906. (b) For a brief history of earlier experiments with monolayers by Benjamin Franklin, Agnes Pockels, and Lord Rayleigh, see: ref. 38c.

53. (a) Sauer, K. *Acc. Chem. Res.* **1978**, *11*, 257-264. (b) De Levie, R. *J. Electroanal. Chem.* **1976**, *69*, 265-297. (c) Drexhage, K. H. *Prog. Opt.* **1974**, *12*, 163-232. (d) Srivastava, V. K. *Phys. Thin Films* **1973**, *7*, 311-397. (e) Larsson, K. *Surf. Colloid Sci.* **1973**, *6*, 261-285.

54. (a) Valenty, S. J. *J. Am. Chem. Soc.* **1979**, *101*, 1-8. (b) Valenty, S. J. *J. Colloid Interface Sci.* **1979**, *68*, 486-491. (c) Valenty, S. J., in ref. 57a, pp. 69-95. (d) Russell, J. C.; Costa, S. B.; Seiders, R. P.; Whitten, D. G. *J. Am. Chem. Soc.* **1980**, *102*, 5678-5679. (e) Whitten, D. G.; Mercer-Smith, J. A.; Schmehl, R. H.; Worsham, P. R., in ref. 57a, pp. 47-68. (f) Richard, M. A.; Deutch, J.; Whitesides, G. M. *J. Am. Chem. Soc.* **1978**, *100*, 6613-6625.

55. Möbius, D.; Bücher, H. In "Techniques of Chemistry," 4th ed.; Weissberger, A.; Rossiter, B. W., Eds.; Wiley-Interscience: New York, 1972; Vol. 1, Part 3B, pp. 577-702.

56. (a) Harrick, N. J. "Internal Reflection Spectroscopy"; Wiley-Interscience: New York, 1967. (b) Takenaka, T.; Harada, K.; Matsumoto, M. *J. Colloid Interface Sci.* **1980**, *73*, 569-577. (c) Boerio, F. J.; Chen, S. L. *J. Colloid Interface Sci.* **1980**, *73*, 176-185. (d) Raupach, M.; Emerson, W. W.: Slade, P. G. *J. Colloid Interface Sci.* **1979**, *69*, 398-408. (e) Chollet, P.-A. *Thin Solid Films* **1978**, *52*, 343-360. (f) Müller, H.; Friberg, S.; Hellsten, M. *J. Colloid Interface Sci.* **1970**, *32*, 132-140. (g) Loeb, G. I.; Baier, R. E. *J. Colloid Interface Sci.* **1968**, *27*, 38-45. (h) Flournoy, P. A.; Schaffers, W. J. *Spectrochim. Acta* **1966**, *22*, 5-13; Flournoy, P. A.; Schaffers, W. J. *ibid.* **1966**, *22*, 15-20.

57. (a) Wrighton, M. S., Ed. "Interfacial Photoprocesses: Energy Conversion and Synthesis"; American Chemical Society: Washington, D.C., 1980; Advances in Chemistry Series No. 184. (b) Goddard, E. D., Ed. "Monolayers"; American Chemical Society: Washington, D.C., 1975; Advances in Chemistry Series No. 144. (c) Blank, M., Ed. "Surface Chemistry of Biological Systems"; Plenum: New York, 1970. (d) Goddard, E. D., Ed. "Molecular Association in Biological and Related Systems"; American Chemical Society: Washington, D.C., 1968; Advances in Chemistry Series No. 84.

58. (a) Castner, D. G.; Somorjai, G. A. *Chem. Rev.* **1979**, *79*, 233-252. (b) Buchholz, J. C.; Somorjai, G. A. *Acc. Chem. Res.* **1976**, *9*, 333-338.

59. (a) Motomura, K. *J. Colloid Interface Sci.* **1967**, *23*, 313-318. (b) Ekwall, P.; Ekholm, R.; Norman, A. *Acta Chem. Scand.* **1957**, *11*, 693-702; Ekwall, P., Ekholm, R.; Norman, A. *Acta Chem. Scand.* **1957**, *11*, 703-709. (c) Glazer, J.; Alexander, A. E. *Trans. Faraday Soc.* **1951**, *47*, 401-409. (d) Vavruch, I. *J. Colloid Interface Sci.* **1980**, *73*, 267-269.

60. (a) Alexander, A. E.; Hayter, J. B. In "Techniques of Chemistry," 4th ed.; Weissberger, A.; Rossiter, B. W., Eds.; Wiley-Interscience: New York, 1971; Vol. 1, Part 5, pp. 501-555. (b) Jasper, J. J. In "Treatise on Analytical Chemistry," Kolthoff, I. M.; Elving, P. J., Eds.; Interscience: New York, 1967; Vol. 7, Part 1, pp. 4611-4760.

61. Andersson, K. J. I.; Ställberg-Stenhagen, S.; Stenhagen, E. In "The Svedberg Anniversary Volume," Tiselius, A.; Pedersen, K. O., Eds.; Almqvist & Wiksells: Uppsala, Sweden, 1944; pp. 11-32.

62. (a) Kellner, B. M. J. *J. Colloid Interface Sci.* **1980**, *74*, 308-309. (b) For an especially detailed account of the methods and problems involved in temperature and humidity control during film balance experiments, see: Cowden, M. W. Ph.D. Dissertation, State University of New York at Buffalo, 1975; *Diss. Abstr. Int. B* **1975**, *36*, 1559.

63. This film balance was designed by Dr. Barbara J. Kinzig (presently at the Optical Sciences Division, Naval Research Laboratory, Washington, D.C.) and was built by Dennis Sicher and Robert Muha at the University of Pittsburgh. See ref. 101 for a more detailed description of the apparatus.

64. (a) Bergeron, J. A.; Gaines, G. L. *J. Colloid Interface Sci.* **1967**, *23*, 292-294. (b) Bewig, K. W. *Rev. Sci. Instrum.* **1964**, *35*, 1160-1162. (c) Pethica, B. A.; Standish, M. M.; Mingins, J.; Smart, C.; Iles, D. H.; Feinstein, M. E.; Hossain, S. A.; Pethica, J. B., in ref. 57b, pp. 123-134.

65. (a) Pomerantz, P.; Clinton, W. C.; Zisman, W. A. *J. Colloid Interface Sci.* **1967**, *24*, 16-28. (b) Rouser, G.; Kritchevsky, G.; Whatley, M.; Baxter, C. F. *Lipids* **1966**, *1*, 107-112. (c) Rouser, G.; Kritchevsky, G.; Heller, D.; Lieber, E. *J. Am. Oil Chem. Soc.* **1963**, *40*, 425-454. (d) Gaines, G. L. *J. Phys. Chem.* **1959**, *63*, 1322-1324.

66. (a) Mysels, K. J.; Florence, A. T. *J. Colloid Interface Sci.* **1973**, *43*, 577-582. (b) Mysels, K. J.; Florence, A. T. In "Clean Surfaces: Their Preparation and Characterization for Interfacial Studies," Goldfinger, G., Ed.; Dekker: New York, 1970; pp. 227-268.

67. (a) Blodgett, K. B. *J. Am. Chem. Soc.* **1935**, *57*, 1007-1022. (b) Blodgett, K. B.; Langmuir, I. *Phys. Rev.* **1937**, *51*, 964-982. (c) Blodgett, K. B. *Phys. Rev.* **1939**, *55*, 391-404. (d) Langmuir, I. *Proc. R. Soc. London, Ser. A* **1939**, *170*, 1-39.

68. Ligon, W. V.; Valenty, S. J. *J. Am. Chem. Soc.* **1979**, *101*, 1612-1614.

69. (a) Minc, S. *J. Electroanal. Chem. Interfacial Electrochem.* **1975**, *62*, 291-296. (b) Rothen, A. *Prog. Surf. Membrane Sci.* **1974**, *8*, 81-118. (c) Bashara, N. M.; Hall, A. C.; Buckman, A. B. In "Techniques of Chemistry," 4th ed.; Weissberger, A.; Rossiter, B. W., Eds.; Wiley-Interscience: New York, 1972; Vol. 1, Part 3C, pp. 453-504.

70. Adam, N. K. "The Physics and Chemistry of Surfaces," 3rd ed.; Oxford University Press: London, 1941.

71. (a) Harkins, W. D. "The Physical Chemistry of Surface Films," 2nd ed.; Reinhold: New York, 1954. (b) Harkins, W. D. In "Physical Methods of Organic Chemistry," Weissberger, A., Ed.; Interscience: New York, 1945; Vol. 1, pp. 211-252.

72. Stenhagen, E. In "Determination of Organic Structure by Physical Methods," Braude, E. A.; Nachod, F. C., Eds.; Academic Press: New York, 1955; pp. 325-371.

73. Lundquist, M. *Prog. Chem. Fats Other Lipids* **1978**, *16*, 101-124; *Chem. Abstr.* **1978**, *89*, 95289a.

74. (a) Müller-Landau, F.; Cadenhead, D. A.; Kellner, B. M. J. *J. Colloid Interface Sci.* **1980**, *73*, 264-266. (b) Jalal, I.; Zografi, G. *J. Colloid Interface Sci.* **1979**, *68*, 196-198. (c) Bienkowski, R. S., Ph.D. Dissertation, State University of New York at Stony Brook, 1973; *Diss. Abstr. Int. B* **1974**,

34, 4555. (d) See ref. 119 for metastable states in phospholipid monolayers.

75. Welles, H. L.; Zografi, G.; Scrimgeour, C. M.; Gunstone, F. D. in ref. 57b, pp. 135–152.
76. Chapman, D.; Owens, N. F.; Walker, D. A. *Biochim. Biophys. Acta* **1966**, *120*, 148–155.
77. Lundquist, M. *Ark. Kemi* **1961**, *17*, 183–195; *Chem. Abstr.* **1962**, *56*, 10939e.
78. Lundquist, M. *Ark. Kemi* **1963**, *21*, 395–406; *Chem. Abstr.* **1964**, *60*, 4000e.
79. Lundquist, M. *Ark. Kemi* **1965**, *23*, 299–306; *Chem. Abstr.* **1965**, *63*, 5505c.
80. Ställberg-Stenhagen, S.; Stenhagen, E. *Ark. Kemi, Mineral. Geol. A* **1945**, *18*, 1–8; *Chem. Abstr.* **1947**, *41*, 1598h.
81. (a) Ställberg-Stenhagen, S.; Stenhagen, E. *Acta Chem. Scand.* **1951**, *5*, 481–484. (b) For a later application of the film balance technique to distinguish between diastereomers for structural elucidation, see: Bruun, H. H.; Stenhagen, E. *Acta Chem. Scand.* **1959**, *13*, 832–834.
82. Tachibana, T.; Hori, K. *J. Colloid Interface Sci.* **1977**, *61*, 398–400.
83. Tachibana, T.; Yoshizumi, T.; Hori, K. *Bull. Chem. Soc. Jpn.* **1979**, *52*, 34–41.
84. Zeelen, F. J., Doctoral Thesis "Stearoyl-Aminozuren: Synthese, Spreiding, en Photochemie"; Rijksuniversiteit te Leiden (State University of Leiden): Leiden, Netherlands, 1956. We thank Dr. Zeelen (presently with Organon Scientific Development Group, Netherlands) for generously supplying us with a copy of his thesis and for permission to reproduce figures from it.
85. (a) Harkins, W. D.; Copeland, L. E. *J. Chem. Phys.* **1942**, *10*, 272–286. (b) Copeland, L. E.; Harkins, W. D.; Boyd, G. E. *ibid.* **1942**, *10*, 357–365. (c) Harkins, W. D.; Boyd, E. *J. Phys. Chem.* **1941**, *45*, 20–43. (d) Harkins, W. D.; Boyd, E. *J. Chem. Phys.* **1940**, *8*, 129–130.
86. Dervichian, D. G. *ibid.* **1939**, *7*, 931–948.
87. Joly, M. *J. Colloid Sci.* **1950**, *5*, 49–70.
88. Ställberg-Stenhagen, S.; Stenhagen, E. *Nature (London)* **1947**, *159*, 814–815.
89. (a) Lundquist, M. *Chem. Scr.* **1971**, *1*, 5–20; *Chem. Abstr.* **1971**, *75*, 11447a. (b) Lundquist, M. *Ark. Kemi* **1970**, *32*, 27–41; *Chem. Abstr.* **1970**, *73*, 14007b. (c) Lundquist, M. *Proc. Scand. Symp. Surf. Activ., 2nd, Stockholm* **1964**, 294–305; *Chem. Abstr.* **1967**, *66*, 14284v.
90. Serck-Hanssen, L.; Ställberg-Stenhagen, S.; Stenhagen, E. *Ark. Kemi* **1953**, *5*, 203–221. For the rejection of the monolayer data collected from this sample, see: ref. 77.
91. Mason, S. F. *Top. Stereochem.* **1976**, *9*, 1–34.
92. Zeelen, F. J.; Havinga, E. *Rec. Trav. Chim. Pays-Bas* **1958**, *77*, 267–272.
93. Lundquist, M. *Fin. Kemistsamf. Medd.* **1963**, *72*, 14–27; *Chem. Abstr.* **1964**, *60*, 39e.
94. Lundquist, M. *Chem. Scr.* **1971**, *1*, 197–209; *Chem. Abstr.* **1972**, *76*, 145958x.

95. Serck-Hanssen, K. *Chem. Ind. (London)* **1958**, 1554.
96. (a) McClellan, A. L. *J. Chem. Phys.* **1960**, *32*, 1271–1272. (b) Hotten, B. W.; Birdsall, D. H. *J. Colloid Sci.* **1952**, *7*, 284–294.
97. (a) Tachibana, T.; Kitazawa, S.; Takeno, H. *Bull. Chem. Soc. Jpn.* **1970**, *43*, 2418–2421. (b) Tachibana, T.; Kambara, H. *ibid.* **1969**, *42*, 3422–3424. (c) Tachibana, T.; Kambara, H. *J. Colloid Interface Sci.* **1968**, *28*, 173–174. (d) Tachibana, T.; Kambara, H. *J. Am. Chem. Soc.* **1965**, *87*, 3015–3016.
98. Tachibana, T.; Kayama, K.; Takeno, H. *Bull. Chem. Soc. Jpn.* **1972**, *45*, 415–422.
99. Uzu, Y.; Hattori, M. *Bull. Chem. Soc. Jpn.* **1972**, *45*, 3476–3478.
100. Uzu, Y.; Sugiura, T. *J. Colloid Interface Sci.* **1975**, *51*, 346–349.
101. Thompson, O. I., Ph.D. Dissertation, University of Pittsburgh, 1980.
102. Arnett, E. M.; Chao, J.; Kinzig, B.; Stewart, M.; Thompson, O. *J. Am. Chem. Soc.* **1978**, *100*, 5575–5576.
103. Arnett, E. M.; Thompson, O. *J. Am. Chem. Soc.* **1981**, *103*, 968–970.
104. (a) Marsden, J.; Rideal, E. K. *J. Chem. Soc.* **1938**, 1163–1171. (b) Gilby, A. R.; Alexander, A. E. *Aust. J. Chem.* **1956**, *9*, 347–363.
105. (a) Beredjick, N.; Ries, H. E. *J. Polym. Sci.* **1962**, *62*, S64–S68. (b) Beredjick, N.; Ahlbeck, R. A.; Kwei, T. K.; Ries, H. E. *ibid.* **1960**, *46*, 268–270.
106. Beredjick, N. In "Newer Methods of Polymer Characterization," Ke, B., Ed.; Interscience: New York, 1964; Chapter 16.
107. (a) Isemura, T.; Hamaguchi, K. *Bull. Chem. Soc. Jpn.* **1954**, *27*, 125–130. (b) For a review of this area that summarizes the contribution of these workers, see: Joly, M. *Prog. Surf. Membrane Sci.* **1964**, *1*, 1–50.
108. Malcolm, B. R. *Adv. Chem.* **1975**, *145*, 338–359.
109. Malcolm, B. R. *Prog. Surf. Membrane Sci.* **1973**, *7*, 183–229.
110. Shafer, P. T. *Biochim. Biophys. Acta* **1974**, *373*, 425–435.
111. (a) Miller, I. R.; Bach, D. *Surf. Colloid Sci.* **1973**, *6*, 185–260. (b) Miller, I. R. *Prog. Surf. Membrane Sci.* **1971**, *4*, 299–350.
112. (a) Wiegel, F. W.; Kox, A. J. *Adv. Chem. Phys.* **1980**, *41*, 195–228. (b) Luzzati, V.; Tardieu, A. *Annu. Rev. Phys. Chem.* **1974**, *25*, 79–94.
113. For configurational specification of phospholipids as recommended by the IUPAC-IUB Commission on Biochemical Nomenclature, see: *Biochim. Biophys. Acta* **1968**, *152*, 1–9.
114. Kates, M. *Methods Membrane Biol.* **1978**, *8*, 219–290.
115. van Deenen, L. L. M.; Houtsmuller, M. T.; de Haas, G. H.; Mulder, E. *J. Pharm. Pharmacol.* **1962**, *14*, 429–444.
116. Slotboom, A. J.; Bonsen, P. P. M. *Chem. Phys. Lipids* **1970**, *5*, 301–397.
117. Phillips, M. C.; Chapman, D. *Biochim. Biophys. Acta* **1968**, *163*, 301–313.
118. Cadenhead, D. A. *Prog. Surf. Membrane Sci.* **1970**, *3*, 169–192.
119. (a) Horn, L. W.; Gershfeld, N. L. *Biophys. J.* **1977**, *18*, 301–310. (b) For a differing point of view, see: Müller-Landau, F.; Cadenhead, D. A. *Chem. Phys. Lipids* **1979**, *25*, 299–314.

120. Demel, R. A.; Bruckdorfer, K. R.; van Deenen, L. L. M. *Biochim. Biophys. Acta* **1972**, *215*, 311-320.

121. (a) Ghosh, D.; Lyman, R. L.; Tinoco, J. *Chem. Phys. Lipids* **1971**, *7*, 173-184. For related studies, see: (b) Ghosh, D.; Tinoco, J. *Biochim. Biophys. Acta* **1972**, *266*, 41-49. (c) Ghosh, D.; Williams, M. A.; Tinoco, J. *ibid.* **1973**, *291*, 351-362.

122. Zografi, G.; Verger, R.; de Haas, G. H. *Chem. Phys. Lipids* **1971**, *7*, 185-206.

NMR Chiral Solvating Agents

WILLIAM H. PIRKLE and DENNIS J. HOOVER*

The Roger Adams Laboratory,
School of Chemical Sciences,
University of Illinois,
Urbana, Illinois

I. Introduction 264
II. Types of Chiral Solvating Agents (CSA) 265
III. Characteristics of CSA-Induced Nonequivalence 267
A. Origins and Intrinsic Features 267
B. Solvent, Temperature, and Concentration Effects 269
C. Effect of CSA Structure 272
D. The CSA Experiment 275
IV. Correlation of Absolute Configuration 278
A. General Considerations 278
B. Fluoroalcohol CSAs 280
1. The Dibasic Solute Model 280
2. Exceptions to the Dibasic Solute Model 293
3. Monobasic Solutes 295
C. Amine CSAs 298
1. Diastereomeric Solvates 298
2. Diastereomeric Salts 303
D. Other CSAs 307
E. Consequences of "Three-Point" Interactions 308
F. Nonequivalence in Nuclei Other Than ^{1}H 313
V. Self-Induced Nonequivalence 316
VI. Miscellaneous Applications 319
VII. Comparison of CSAs with CLSRs 322
References 327

*Present address: Harvard University,
Department of Chemistry,
Cambridge, Massachusetts.

I. INTRODUCTION

Chemists have long appreciated that in principle, a chiral environment might dissimilarly perturb the properties of enantiomeric molecules, alter the stereochemical course of reactions, or imbue otherwise achiral molecules with chiral properties. This principle has been embodied in many forms in the practical applications of selectively preparing, separating, and determining the absolute configuration and enantiomeric purity of optical isomers. It is a matter of record, however, that this appreciation is often matched with little more than a vague understanding of the mechanism whereby chiral recognition arises. *Chiral recognition*, the ability of one chiral molecule to somehow "recognize" the chirality of another, is a term used for its convenience rather than its semantic soundness (the observer does the recognizing, not the molecules).

Chiral recognition has been studied most often in the liquid phase. There are a number of methods for detecting diastereomeric interactions in solution (1). Extrinsic properties, such as boiling point, density, and dipole moment differences between the separate enantiomers and mixtures thereof, have little practical application and contribute scarcely at all to the understanding of these interactions. Such an understanding, however, is a prerequisite to the rational design of new and more effective applications. Not surprisingly, methods that have been of most value in the study of these interactions have also been of most value in a practical sense. These techniques reveal spectral differences between enantiomers in a chiral environment or measure differences in the energies with which the enantiomers interact with that environment.

NMR spectroscopy is a sensitive probe for the occurrence of solvent-solute and solute-solute interactions, and it has provided some of the most detailed information concerning the nature of these interactions. Before 1966, several groups of workers independently considered the possibility that although enantiomeric molecules could not be distinguished by NMR spectroscopy, this task might be accomplished if a chiral solvent were used. Mislow and Raban were the first to suggest this possibility in the literature (2). The first realization of this phenomenon was reported by Pirkle, who observed separate ^{19}F NMR resonances for the enantiomers of (trifluoromethyl) phenylcarbinol in optically active 1-phenylethylamine solvent (3). Numerous reports of enantiomer NMR nonequivalence followed shortly thereafter, forming the basis of an early review (4). The technique has recently emerged as a facile alternative to classical solutions (5) of

the often difficult problem of determining enantiomeric purity and absolute configuration.

Two conceptually similar classes of chiral additives have been developed. In this chapter, we are concerned with the use of diamagnetic chiral *solvating* agents (CSAs) to dissimilarly perturb the NMR spectra of enantiomeric solutes. Since the applications of paramagnetic chiral lanthanide *shift* reagents (CLSRs) have been recently reviewed (6), we restrict our discussion of this important class of chiral additives to a comparison of their attributes and shortcomings with those of various diamagnetic CSAs.* The discussion focuses primarily on the origins and practical applications of this nonequivalence. The studies discussed are ones of diastereomeric interactions that are "fast" (fast vs. slow exchange) on the NMR time scale, a distinction that serves primarily to separate our discussion from that of NMR studies of covalent diastereomers (7, 8), in which interactions would be intramolecular, rather than intermolecular. Our coverage is intended to be comprehensive rather than exhaustive, although we have attempted to provide complete referencing of relevant literature through mid-1980.

II. TYPES OF CHIRAL SOLVATING AGENTS (CSA)

Since the first report of the nonequivalence phenomenon, approximately 40 chiral substances have been reported to induce enantiomeric nonequivalence in the NMR spectra of a host of solutes. These CSAs are encountered in subsequent discussions. Two qualities considered to be essential in the design of the first reported experiment (3) are evident in nearly all CSA-solute combinations. In all cases, the CSA and the solute have the common feature of complementary functionality, which permits their interaction. Both are in general hydrogen bond donors or acceptors: the CSAs are acids, amines, alcohols, sulfoxides, or cyclic compounds such as cyclodextrins, crown ethers, or peptides, which attractively interact with appropriate enantiomeric solutes, engendering different spatial environments for their nuclei. In nearly every case the CSA contains a group of high diamagnetic anisotropy near its asymmetric center, a feature

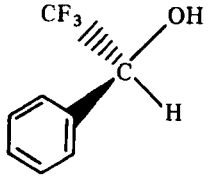
*We maintain a distinction between "shift" and "solvating" agents both for the difference in the respective additive-solute association mechanisms and for the difference in the origin and appearance of the spectral perturbations that are induced (see Sect. VII).

that is advantageous in translating the different average spatial environments of solute nuclei into different magnetic environments measurable by the NMR method.

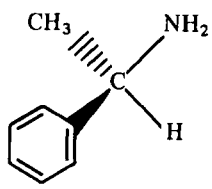
In our discussion, "solute" refers to the substance whose resonances are being discussed (which may be racemic, enantiomerically enriched, or even a single enantiomer), and "CSA" to the substance whose chirality influences solute spectral behavior. Occasionally, for a given pair of compounds, these roles may be interchangeable.

The CSAs may be solids or liquids that are added to an achiral solvent containing the solute of interest. Liquid CSA may also serve as the solvent for the experiment.

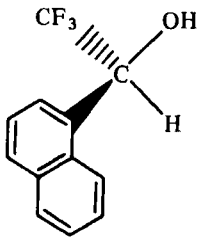
The CSAs that have been used most widely are 2,2,2-trifluoro-1-phenylethanol (TFPE, 1a), 2,2,2-trifluoro-1-(1-naphthyl)ethanol (TFNE, 1b), 2,2,2-trifluoro-1-(9-anthryl)ethanol (TFAE, 1c), 1-phenylethylamine (PEA, 2a), and 1-(1-naphthyl)ethylamine (NEA, 2b). Both enantiomers of TFPE, TFAE (9), PEA, and NEA are commercially available. The fluoroalcohols are relatively acidic and interact strongly with solutes having one or more basic sites (Sect. IV-B). Amines 2 have been used most often as CSAs for organic acids or other acidic solutes (Sect. IV-C). A number of analogs of TFAE have been studied (Sect. III-C).



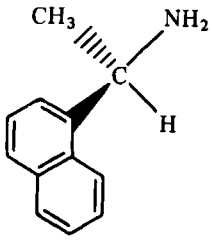
TFPE
(*S*)−(+)−**1a**



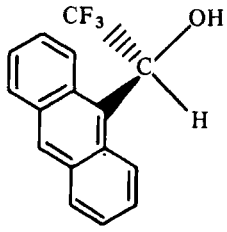
PEA
(*R*)−(+)−**2a**



TFNE
(*S*)−(+)−**1b**



NEA
(*R*)−(+)−**2b**



TFAE
(*S*)−(+)−**1c**

III. CHARACTERISTICS OF CSA-INDUCED NONEQUIVALENCE

A. Origins and Intrinsic Features

Equations [1] and [2] describe the interaction of enantiomeric solutes A and A′ with chiral solvating agent S. Solvates (or association complexes) are formed that are diastereomeric and thus can, in principle, have different properties. Relevant differences are those in

$$A + S \underset{}{\overset{K}{\rightleftharpoons}} AS \qquad [1]$$

$$A' + S \underset{}{\overset{K'}{\rightleftharpoons}} A'S \qquad [2]$$

NMR spectral parameters and in stability. When these equilibria are fast on the NMR time scale, a single "average" species is observed for each of the two systems. The chemical shifts for previously enantiotopic (10) nuclei (which are now diastereotopic in the presence of the CSA) may differ in the two systems. This nonequivalence in the spectra of A and A′ may be induced by S through a combination of several factors. First, the diastereomeric solvates may have intrinsically nonidentical spectra. Second, if a chemical shift perturbation occurs upon solvation, a difference in K and K' such that one solute enantiomer is solvated to a greater extent than is the other can also result in nonequivalence between the rapidly averaging species. No intrinsic spectral difference need be invoked (although it may be present) in the second case. More convoluted situations might be imagined. The solute enantiomers might themselves associate, thus forming a different type of diastereomeric complex, the various complexes possibly having nonidentical spectra or formation constants. The spectral consequences of solute-solute interactions contribute to the time-averaged "nonequivalence pool." Since solute-solute association is second (or higher) order in solute concentration, whereas solute-CSA association is first order in solute concentration, the extent to which the two processes compete depends on the concentration of each solute enantiomer, even if K and K' are equal. In general, the effects of solute-solute interaction are minimal and can be ignored, especially when an excess of a strongly solvating CSA is employed. Hence, the overall nonequivalence that is observed is a function of the differences between the spectra of the diastereomeric solvates and the uncomplexed enantiomers, and of their relative

populations (hence the component concentrations and equilibrium constants K and K').

Nonequivalence magnitude is described by eq. [3]:

$$\Delta\delta = \frac{[AS]}{[A]}\delta^{AS} - \frac{[A'S]}{[A']}\delta^{A'S} \qquad [3]$$

where δ^{AS} and $\delta^{A'S}$ are the shift differences between the respective solvates and the uncomplexed enantiomers. The equation defining nonequivalence magnitude and sense in terms of original CSA and solute enantiomer concentrations does not lend itself to a general analytic solution.

An example of the nonequivalence represented by eq. [3] is shown in Figure 1. In the 100 MHz NMR spectrum of a mixture of (*S*)-enriched methyl alanate and 2 equiv of (*R*)-TFPE, nonequivalence is observed in the amino ester *C*-methyl, H_a, and *O*-methyl resonances, with magnitudes of 0.028, 0.023, and 0.013 ppm, respectively (11). Two other intrinsic features of this nonequivalence are the relative intensities of the nonequivalent signals, and their relative field positions or *sense* of nonequivalence. The former reflects the enantiomeric composition of the solute, which is in this case a 1.43:1 mixture of enantiomers (17.8% enantiomeric excess) measured from the relative peak heights of the expanded *C*-methyl or *O*-methyl resonances. The latter is indicative of absolute configuration. In this sample, the *C*-methyl resonance of the major solute enantiomer (*S*) occurs at lower field than that of its antipode; this behavior is conveniently termed lowfield (or downfield) nonequivalence. Accordingly, the methoxy and H_a protons exhibit a highfield (or upfield) sense of nonequivalence. Nonequivalence sense for a particular CSA-solute combination depends on the configuration of each component; reversed senses of nonequivalence (relative to those of Fig. 1) would be observed for the (*S*)-enriched ester in the presence of (*S*)-TFPE, or for the combination of (*R*)-ester and (*R*)-TFPE. As a consequence of the fast-exchange process, the enantiomeric purity of the CSA affects only the magnitude of spectral nonequivalence between the enantiomeric solutes (when the CSA is racemic, solute enantiomers are solvated to the same extent by *both* CSA enantiomers, and no nonequivalence is observed). Since the CSA need not be enantiomerically pure for nonequivalence to arise, enantiomeric purity determination by this method is absolute in the sense that no reference to a standard of known optical purity is required.

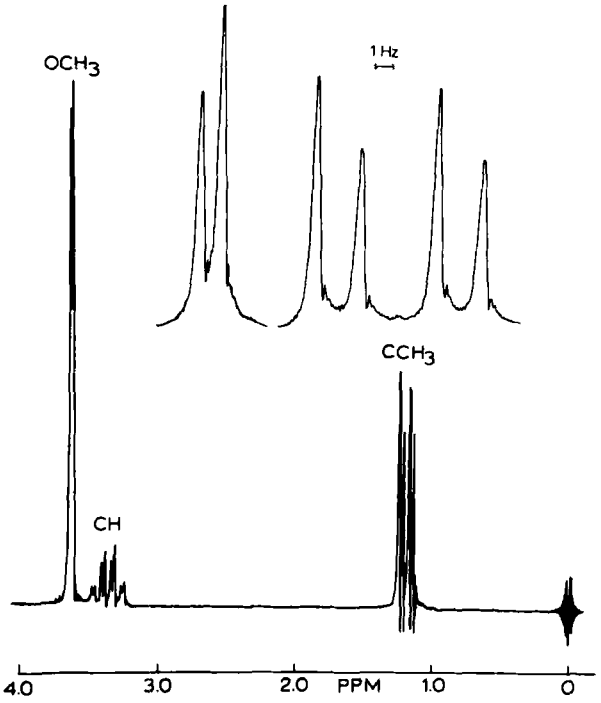


Figure 1. Portions of the 100 MHz NMR spectrum of partially resolved (*S*)-methyl alanate in (*R*)-(-)-TFPE. The upper traces are scale expansions of the *O*-methyl (*left*) and *C*-methyl (*right*) resonances. Reprinted with permission from *J. Am. Chem. Soc.* **1969**, *91*, 5150-5155. Copyright by the American Chemical Society.

B. Solvent, Temperature, and Concentration Effects

Variables other than CSA optical purity may affect nonequivalence magnitudes by changing either the populations or the intrinsic spectra of the diastereomeric solvates.

The earliest studies of diastereomeric solvates verified the importance of hydrogen bonding to the CSA-solute interaction. For example, although fluorine nonequivalence is observed for racemic TFPE in optically active NEA, no nonequivalence is observed for its methyl ether under the same conditions. Similarly, the magnitude of fluorine nonequivalence observed for a series of trifluoromethylarylcarbinols in PEA was smallest for the α-pyridyl analog, in which a considerable amount of intramolecular hydrogen bonding occurs (12). Vapor

osmometric apparent molecular weight measurements on dilute cyclohexane solutions containing TFPE and PEA and infrared studies of the interaction of various aryltrifluoromethylcarbinols with PEA have confirmed the presence of a hydrogen bond between these components and indicate a 1:1 stoichiometry for the interaction (13). Accordingly, solvent effects are generally dramatic. Association is much stronger (and nonequivalence accordingly larger) in nonpolar solvents. Addition of even a small quantity of a polar material (e.g., dimethylsulfoxide or methanol) will severely reduce or eliminate nonequivalence to the extent that the polar material competes with the solute for CSA or to the extent that it alters conformations of the solvates that give rise to nonequivalence (14–16). With diastereomeric salts, in which interaction between chiral counterions is very strong, nonequivalence has been observed in absence of CSA even in relatively polar solvents such as pyridine (17) or tetrahydrofuran (18). Here too, nonequivalence diminishes with increasing solvent polarity, but often for a reason different from that which applies to diastereomeric solvates (Sect. IV-C-2). Another example is peculiar but understandable: β-cyclodextrin induces nonequivalence in the ^{15}N nuclei of the enantiomers of 8-benzyl-5,6,7,8-tetrahydroquinoline in dimethylsulfoxide solution (18). The interaction in this case is probably one of solute intercalation into the cyclodextrin ring.

The concentration of CSA (for a given solute concentration) also substantially influences nonequivalence magnitude. Nonequivalence increases with an increase in CSA concentration until the solute is completely solvated by the CSA. Although the concentration required to produce this effect depends on the interaction strength of the solvent-solute pair, with type 1 fluoroalcohols, for example, many solutes have association constants so great that at typical NMR solute concentrations, maximum nonequivalence is observed at CSA-solute ratios between 2 and 5. The typical behavior is shown in Figure 2 for isopropylmethylsulfoxide in the presence of TFPE (19). Nonequivalence for each resonance increases with added CSA, until approximately 3 equiv is present, after which little increase is achieved. Nonequivalence arises under these circumstances only from spectral differences in the diastereomeric solvates, not from different degrees of association of the solute enantiomers with the CSA, since no diminution of nonequivalence is observed even at high CSA concentrations. An achiral diluent is essential if a solid CSA is to be used, and its use is preferable even with liquid CSA, since increased spectral resolution is gained by diminishing sample viscosity. Nonequivalence

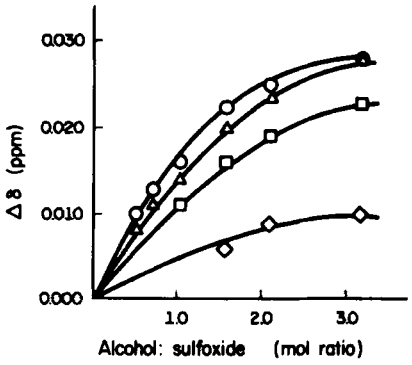
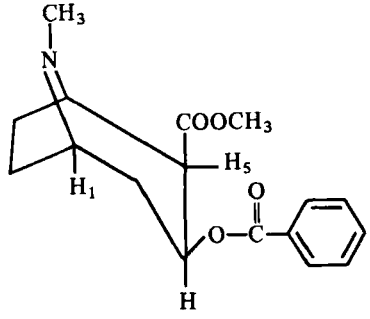


Figure 2. Plots of the chemical shift differences between the enantiomers of 1.25*M* isopropyl methylsulfoxide in the presence of (-)-TFPE at 28° in CCl_4. Each of the four proton sets shows nonequivalence: ○, $S\underline{CH_3}$; △, $C\underline{CH_3}$; ◇, $C\underline{CH_3}$; □, C<u>H</u>. Reprinted with permission from *Tetrahedron Lett.* **1974**, 2295–2298.

decreases, however, with increased dilution at constant CSA-solute ratio, since CSA concentration is the important factor.

Temperature reduction generally provides a severalfold enhancement of nonequivalence magnitude (15,16,19). Cocaine (**3**) at 20°C shows methylphenylcarbinol-induced nonequivalence in H_1 and H_5, and in the *N*-methyl and *O*-methyl resonances of 0.14, 0.03, 0.01, and 0.05 ppm, respectively (15). On lowering the temperature to -40°C, these differences increase to 0.47, 0.06, 0.12, and 0.17 ppm. Only the nonequivalence for H_5 changes in sense (zero nonequivalence is observed for H_5 at 0°C). Although the increase in nonequivalence magnitude with a reduction of temperature can be attributed in some cases to an increase in the equilibrium constants for CSA-solute association, such enhancement is observed even when the CSA is present in such excess as to cause essentially complete solvation of the enantiomeric solutes (doubtless **3** is such an example). Here, temperature reduction must also increase the intrinsic spectral differ-



3

ence of the diastereomeric solvates, by increasing the populations of specific conformations that give rise to nonequivalence.

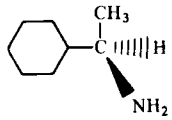
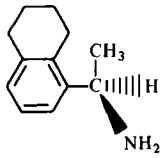
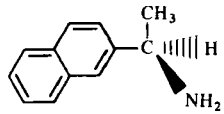
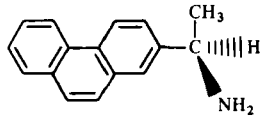
C. Effect of CSA Structure

A number of structural features of CSAs 1 and 2 have been pinpointed as conducive to large nonequivalence magnitudes.

The enhanced acidity of carbinols 1 over their nonfluorinated analogs [the pK_a of TFPE is 11.9 (20)] makes these compounds much more efficient as CSAs since less is required to saturate a given solute. This primary effect is not the sole contribution of the perfluoroalkyl group, however. Compounds 1 induce larger nonequivalence than the nonfluorinated analogs even when the latter are used in large excess [e.g., as solvent (21)]. Substituting heptafluoropropyl for the trifluoromethyl of TFPE increases the maximum nonequivalence attainable for a given solute (22). These effects are attributed primarily to an enhancement of the slight acidity of the carbinyl hydrogen. The increased acidity increases the population of specific nonequivalence-engendering conformations that arise through interaction of the carbinyl hydrogen with a second basic site in the solute. This secondary interaction and the exact nature of these conformations have been better understood through study of nonequivalence behavior of solutes of known configuration, as discussed in Sect. IV. An added virtue of the trifluoromethyl group is that it generally does not obscure solute resonances.

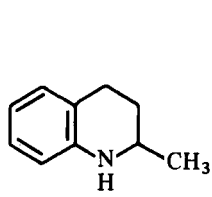
The nature of the aryl group has a substantial effect on nonequivalence magnitudes for both fluoroalcohol and amine CSA. Table 1 outlines this dependence for various type 2 CSAs using TFPE as solute. The importance of having an anisotropic group in the CSA is demonstrated by the near-zero nonequivalence observed with the cyclohexyl analog 2c. Partial removal of anisotropy (cf. NEA with 2d) affects only the nonequivalence magnitude of the trifluoromethyl group, leaving senses of nonequivalence unchanged. Total anisotropy is less important than the orientation of the anisotropic group. PEA, β-NEA, and the 2-phenanthryl analog 2f give similar values that are substantially less than those obtained with NEA. This effect is attributed to a steric barrier to aryl rotation imposed by the peri proton of the 1-naphthyl group of NEA. Steric interference by peri protons in naphthalene derivatives is well documented (23). Larger nonequivalence ensues as fewer conformations are available to the diastereomeric solvates. In reality, the remaining conformations must be those that enhance spectral nonequivalence in the diastereomeric

Table 1
Magnitudes and Senses of Nonequivalence Observed for
(*R*)-(-)-Enriched TFPE (**1a**) in Some Chiral Amine Solvating Agents[a]

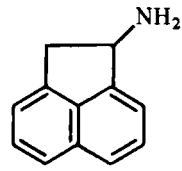
CSA	Nonequivalence and Sense[b]	
	$\lvert\Delta\delta\rvert$(C<u>H</u>)(Hz at 60 MHz)	$\lvert\Delta\delta\rvert$(C<u>F</u>$_3$)(Hz at 54.6 MHz)
(*R*)-PEA	ca. 0.3 (H)	2.1 (H)
 (*R*)-2c	0.0	ca. 0.4 (H)
(*R*)-NEA	2.1 (L)	3.3 (H)
 (*R*)-2d	2.4 (L)	ca. 0.5 (H)
 (*R*)-2e (β-NEA)	0.0	2.2 (H)
 (*R*)-2f	ca. 0.7 (H)	2.4 (H)

[a] Data from Ref. 13.
[b] (H), highfield; (L), lowfield.

solvates, if an increase in nonequivalence with decreased conformational variability is to be observed. The aspect of this reduced variability that is most important to solute nonequivalence is probably the orientation of the CSA aromatic substituent into a position where it more highly shields specific solute nuclei. Resolved compounds 4 and 5 (the latter a model for one conformation of rotationally restricted NEA) do not induce nonequivalence in TFPE (13), demonstrating



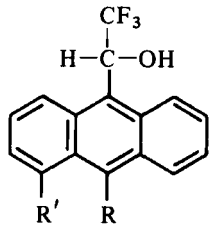
4



5

that restricted rotation alone is insufficient. Apparently, the only solvate conformations assumed by these compounds are those in which the diastereotopic solvate nuclei are nearly equally shielded. Anet and co-workers (16) invoked this restricted rotation to account for the progressively larger values of carbinyl proton nonequivalence observed for phenyl-, β-naphthyl-, α-naphthyl-, and 9-anthrylmethylcarbinols *as solutes* in the presence of several optically active sulfoxide CSAs. This increase is probably qualitatively different in origin from that described above.

9-Anthryl, because of the more severe peri interactions (and greater anisotropy), is yet better than α-naphthyl as a CSA substituent. Various substituted analogs of TFAE (**1d–1i**) have been prepared (24), and their relative efficiencies as CSA for several solutes are compared in Table 2. Of these CSAs, only **1i** stands out as more powerful than TFAE, but this difference is usually marginal. The 9-anthrylcarbinols outperform TFPE or TFNE for these and other solutes where nonequivalence is observed.



	R	R′
1d	Me	H
1e	Br	H
1f	Bz	H
1g	SMe	H
1h	Ph	H
1i	H	Ph

D. The CSA Experiment

The procedure for conducting a CSA-NMR experiment consists simply of mixing the CSA and the substrate in an appropriate solvent and recording the NMR spectrum. For best results, several precautions entailing only minimal effort should be taken.

Solute concentration alone is not particularly important, and generally only as much sample is used as is required for adequate signal strength. This minimizes the quantity of CSA required. Solvent must dissolve both the CSA and the substrate; it must be free of resonances that would obscure those of the solute, and it must not interfere with the CSA-solute interaction mechanism. Benzene,

Table 2
Magnitudes of Nonequivalence Induced in Three Representative Solutes by Various Type 1 CSAs[a]

			$\lvert\Delta\delta\rvert$ (Hz at 100 MHz)[b]			
CSA[c]	$\underline{CH}_3$—S(O)—C($\underline{CH}_3$)$_3$		Ph—$\underline{CH}$(OH)COO$\underline{CH}_3$		Ph—$\underline{CH}$(NH_2)$\underline{CH}_3$	
1a	2.6	1.2[d,e]	–	–	1.7	0.0[e,f]
1c	9.5	4.0	1.5	7.6	13.6	2.2
1d	6.5[g]	3.0[g]	0.0[h]	4.0[h]	9.9	2.9
1e	6.9	1.0	3.9[i]	3.9[i]	11.7[j]	1.1[j]
1f	7.2	3.8	Obscure	3.3	9.9	0.3
1g	8.9	4.1	0.6	5.9	14.9	2.0
1h	7.3	4.0	3.6	7.5	6.8	3.0
1i	8.9	3.8	2.6	8.3	15.2	3.0

[a] Data from ref. 24 unless otherwise indicated.
[b] Values are for the underlined nuclei in each solute shown and were determined in carbon tetrachloride with the exception of values for **1d**, which were obtained in chloroform-d, at CSA concentrations of about 0.4*M*.
[c] Chiral solvating agent; each agent was determined to be more than 90% enantiomerically pure, except for **1d** and **1e** whose purity was found to be ca. 80%; hence data obtained by these two fluoroalcohols has been corrected to 100%. Unless otherwise noted, the molar ratio of CSA to solute is between 2.4 and 3.3.
[d] From ref. 21.
[e] CSA/solute, 2.0; $CFCl_3$ solvent.
[f] From ref. 30.
[g] CSA/solute, 3.6.
[h] CSA/solute, 4.7.
[i] CSA/solute, 4.0.
[j] CSA/solute, 2.1

carbon tetrachloride, fluorotrichloromethane, and carbon disulfide are typically satisfactory, as are chloroform and methylene chloride, which however reduce nonequivalence magnitudes somewhat. Benzene-d_6 is generally the best choice when using TFAE, because of its exceptionally high capacity for this material (ca. 350 mg of TFAE dissolves in 1 ml of benzene) and its low polarity. If the solvates being examined are diastereomeric salts, a nonpolar solvent is also generally desired, but under certain conditions, nonequivalence may be observed in polar solvents (18) or enhanced by adding pyridine or using pyridine as solvent (17). Addition of a minimum amount of internal standard is suggested when nearby solute resonances are to be examined since overall upfield shifts of 0.5 ppm are not uncommon upon addition of CSA. Consequently highfield solute signals such as those of methyls may occur so near TMS that an intense TMS signal (or its sidebands) may interfere with accurate determination of enantiomeric excess. Other internal standards may be used as well, as long as they do not interfere with the interaction of solute and CSA. Likewise, solute impurities that would compete with the solute for CSA (residual alcoholic or ethereal solvents are a frequently encountered annoyance) should be removed.

The choice of CSA depends, of course, on the nature of the solute, but unless precedent suggests otherwise, TFAE is a logical first choice for solutes containing at least one basic site. If low-temperature work is anticipated, the more soluble TFPE or TFNE may prove to be advantageous. If the solute is a carboxylic acid or contains acidic functionality, NEA may be useful. For many solutes, the selection of these CSAs over their less effective analogs may well define the difference between a successful experiment and an inconclusive one.

As in any NMR work where high resolution is desired, the sample should contain no solid particles. Therefore, it is good practice to filter the sample through a small plug of glass wool before obtaining the spectrum on a well-tuned spectrometer. Addition of the CSA should have at most a very minor effect on resolution. When exchangeable protons obscure a particular spectral area (e.g., the hydroxyl resonance of TFAE occurs between 3 and 4 ppm), they may be exchanged for deuterium by shaking with D_2O in the usual fashion. A stock solution of CSA prepared in the appropriate solvent and exchanged several times with D_2O is especially convenient. This procedure has no detrimental effect on nonequivalence magnitudes because of the water stability of the CSA and the insolubility of water in the sample itself.

In measuring enantiomeric excess (e.e.) one must first ascertain

that the signals being compared truly represent the enantiomeric ratio. Rigorously, areas under peaks are to be compared in making the e.e. determinations. In practice, however, precision is often much more easily achieved by comparing peak heights of the diastereotopic resonances. This approximation is accurate with diamagnetic CSAs, since the diastereotopic signals have essentially identical line widths. Such an approximation should not be made with the paramagnetic CLSRs, where differential broadening is often considerable. In making this measurement in the continuous wave mode, averaging a number of scans in both upfield and downfield sweep directions is desirable. The experimenter can easily determine the accuracy of this measurement for the compound in question if a sample of known enrichment (e.g., the racemate) is available. In favorable instances, precision can approach ± 1%. As little as 0.02 ppm nonequivalence is adequate for a ± 2% determination of e.e. on well-resolved singlets at 100 MHz (11) (and proportionally less at higher spectrometer frequencies). Snatzke and co-workers (25) have shown that with CSAs, peak height measurements even of overlapping multiplets can also give accuracy within 2%. If the spectra are obtained by computer averaging, the precaution of employing sufficient data points must be taken if the plotted signal intensities are to correspond accurately to component concentrations.

As a rule, it is profitable to examine first the nonequivalence behavior of the racemic solute, if it is available. In doing so, one readily determines the resonances for which nonequivalence may be observed and the conditions that are optimal for examining a particular pair of resonances. When different sets of solute resonances are closely spaced, maximum nonequivalence is not always desired on first examination, for resonances may "cross over" one another, making nonequivalence sense determination ambiguous or an e.e. measurement impossible. In the case of highly enriched samples, this experiment becomes imperative, since one must be certain to correctly identify the signal from the minor enantiomer. In the latter case the signal may also be identified by addition of the racemate or the opposite solute enantiomer.

When working with natural products, for example, it frequently happens that the racemate or a sample of different enrichment is not available. When this is the case, the positions of both diastereotopic resonances may still be determined, by examining the solute in the presence of first one, then the other CSA enantiomer (15). Since, in this circumstance, one is comparing actual field positions of a single resonance in different spectra and these differences may be

small, the samples must be identical in every respect (including the enantiomeric purity of the CSA), and they must be measured under identical conditions if the observed difference is to be meaningful. Slight concentration variations between the samples are less critical when a large excess of CSA is employed.

Finally, when determining the sense of nonequivalence of either very closely spaced diastereotopic resonances or resonances superimposed on other solute signals, it is wise to examine solute behavior using first one, then the other CSA enantiomer under the same conditions. This minimizes the possibility of instrumental error, from impurities, or from otherwise unanticipated sources. Incremental addition of racemate is another good check on the reality of a tenuous observation.

For assignment of absolute configuration, the determination of nonequivalence sense should always be performed using excess CSA (Sect. IV-A).

IV. CORRELATION OF ABSOLUTE CONFIGURATION

A. General Considerations

There are a number of ways to determine whether two samples of a chiral substance are enriched in the same enantiomer. Traditionally, configurational analysis is achieved through comparison of the signs of optical rotation. Polarimetric measurements can also provide information concerning the enantiomeric purity and absolute configuration of a sample in hand, provided the magnitude and the sign of rotation expected for enantiomerically pure material of a given absolute configuration are known.

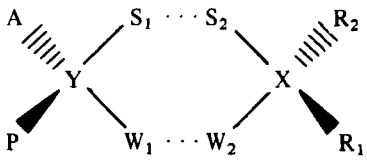
Configurational comparison may also be made by the NMR-CSA method. The relative configurations of two samples of a chiral substance may be determined through observed senses of nonequivalence in the presence of a given CSA. If the nonequivalence behavior of any resonance of a configurationally known compound has been reported, one need determine only the sense of nonequivalence for this resonance (with the same CSA type) to assign the absolute configuration to a sample of the same substance.

The reported determinations of nonequivalence sense for configurationally known compounds are presented or referenced in this section. The NMR method of absolute configuration determination, when it works, is often more reliable and positive than chiroptic

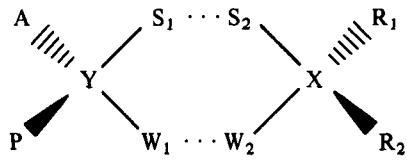
methods. One needs only sufficient sample for a good NMR spectrum, and sample purity is dictated only by this consideration in the spectral area of interest.

To use the CSA-NMR technique to *assign* absolute configuration from the observed senses of nonequivalence of new solutes, one must have a precise understanding of the relative contribution of the various nonequivalence mechanisms that are operating, and come to grips with the specific CSA-solute interactions that engender these differences. Nonequivalence for a given CSA-solute system is a complicated function of the spectral differences between the diastereomeric solvates and the free enantiomers, the relative concentrations of the enantiomeric solutes, and the equilibrium constants for formation of the solvates. The situation is simplified considerably when there is enough excess of CSA present to drive the solvation essentially to completion, as nonequivalence contributions originating in differential association constants or from a partially resolved solute become minimal. As discussed earlier, this condition is achieved for most solutes (at normal NMR sample concentrations) with less than 5 equiv of type 1 or 2 CSA. By evaluating nonequivalence sense only under these conditions, one essentially confines its origin to the intrinsic spectral differences of the diastereomeric solvates. One can frequently understand the origin of nonequivalence (and thus its sense) if one understands the conformational behavior of the diastereomeric solvates derived from a CSA of known absolute configuration. This understanding allows assignment of absolute configuration to the solute from the observed nonequivalence sense or senses.

Spectral nonequivalence in diastereomeric solvates results from the population of conformations that place at least one set of chemically equivalent nuclei in different positions with respect to a CSA substituent capable of perturbing their magnetic environment. Having three "points of interaction" or reference is a general requirement for chiral recognition (26). The manner in which this requirement is met is readily understood in terms of complexes **6** and **7** through



6



7

which, in general terms, the ability of the CSA to dissimilarly perturb the NMR behavior of enantiomeric solutes may be rationalized. Two simultaneous interactions occur between solute and CSA that populate chelatelike conformations in the diastereomeric solvates. These interactions, which must show some specificity for one another (S_1 for S_2 and W_1 for W_2), constitute two of the three necessary reference points. Previously enantiotopic solute nuclei are now in different positions relative to a chemical shift-perturbing group P, whose effect on their magnetic environment constitutes the third reference point. In the several generalized models that account for the nonequivalence senses of the majority of CSA-solute combinations thus far examined, this shift perturber P is an aromatic substituent whose anisotropy imparts a diamagnetic shift to solute nuclei R_1 and R_2 that come within its domain. When in certain cases the shift perturber also assumes the role of W_1, it must impart a rotational preference for the other three CSA substituents if chiral recognition is to arise. In some cases, the anisotropic perturbation may dissimilarly affect nuclei of S_2, W_2, and X.

The perturber P may also function by interacting either attractively or repulsively with R_1 or R_2. In some cases this third interaction may cause one solvate to deviate somewhat from the conformation depicted. Stereochemically dependent third interactions allow chiral recognition not only on an NMR basis, but on an energetic basis as well (Sect. IV-E).

The perturber P also may function by influencing rotational or conformational dispositions of an R substituent so as to change its spectral properties or those of other solute nuclei by changing their *intra*molecular relationship to anisotropic groups.

In all cases, correct predictions of the nonequivalence sense (or senses) requires an accurate assessment of CSA-solute conformation(s), and a precise knowledge of the effect of the shift-perturber P. In many cases, sufficient information has been accumulated (in the form of nonequivalence senses determined from CSAs and solutes of known configurations) to allow "models" approximating these conformations to be used in assignment of absolute configuration.

B. Fluoroalcohol CSAs

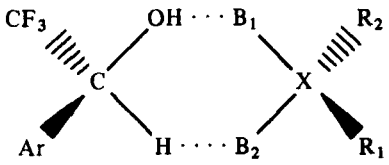
1. The Dibasic Solute Model

One model uniformly correlates the absolute configurations of a wide variety of solutes with the sense of nonequivalence observed in

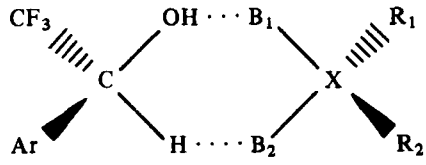
the presence of type 1 fluoroalcohols. The acidic carbinol function interacts strongly with a hydrogen bond receptor in the enantiomeric solutes. The carbinyl hydrogen, also somewhat acidic because of the electronegative character of the perfluoroalkyl substituent, seeks interaction with a secondary basic site in the solutes. The secondary site may be the π electrons of aromatic rings or multiple bonds, or the unshared electron pairs of heteroatoms. Evidence for conformational control by the intramolecular variation of this type of interaction, termed "carbinyl hydrogen bonding" (CHB), has also been reported (27).

In very general terms, solute enantiomers having appropriately situated basic sites B_1 and B_2, will, by simultaneous interaction with the hydroxyl and carbinyl hydrogens of the fluoroalcohol, assume chelatelike conformations depicted by 8 and 9. Owing to the shielding effect of the aromatic substituent of the fluoroalcohol, the time-averaged chemical shifts of nuclei in R_1 will occur at higher field when R_1 is cis to the aromatic group (as in 8) than when it is trans (as in 9). Thus, a sample enriched in the solute enantiomer of solvate 8 will show an upfield sense of nonequivalence for the R_1 resonance. One readily sees that resonances of R_2 in this sample will show an opposite (downfield) sense of nonequivalence. No differences in size or nature of R_1 and R_2 need be present for nonequivalence to be observed. Accordingly, even achiral compounds (e.g., dimethylsulfoxide) may show nonequivalence for their enantiotopic nuclei, as well as compounds that are chiral by virtue of isotopic labeling (29). This model readily accounts for the greater scope and power of TFAE compared to its phenyl and naphthyl analogs, and accounts for the inability of cyclohexyltrifluoromethylcarbinol to induce perceptible nonequivalence (28).

Circumstantial evidence for such specific conformations comes from the previously mentioned temperature effect: an increase in nonequivalence with reduction of temperature seems to be a general behavioral characteristic of CSA-solute combinations, even when a large excess of CSA is present. The temperature dependence of nonequivalence for isopropylmethylsulfoxide (Fig. 3) additionally sug-



8



9

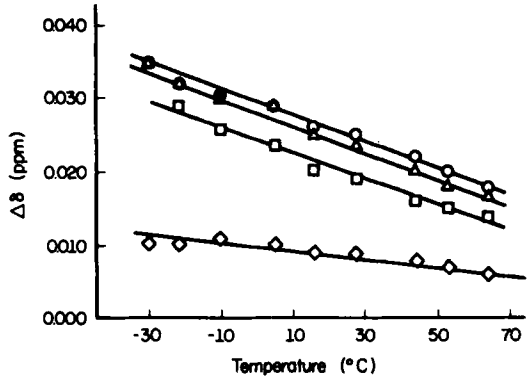


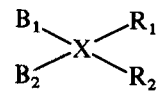
Figure 3. Effect of temperature on the magnitude of the chemical shift difference between isopropyl methyl sulfoxide enantiomers in the presence of (-)-TFPE in CCl_4. Molar ratio of alcohol to sulfoxide to solvent is 2 : 1 : 5. Symbols are as in Figure 2. Reprinted with permission from *Tetrahedron Lett.* **1974**, 2295-2298.

gests that at least in this case *one* conformation causes most of the nonequivalence (19). The magnitude of nonequivalence for each nucleus changes by the same factor on lowering the temperature (2.1 ± 0.25 over the interval between 70 and -30°C). If a variety of conformations made dissimilar contributions to the nonequivalence of all four proton sets, temperature reduction would most probably cause a dissimilar change in each.*

Many types of solute meet the requirements of this model. The chiral center X may be carbon, nitrogen, sulfur, phosphorus, or a group of atoms. A number of functional groups themselves possess two basic sites, for example, sulfoxides, oximes, hydrazones, lactones, sulfinates, and oxaziridines. Table 3 lists the nonequivalence behavior of configurationally known representative examples of a variety of general solute types that are accommodated by this model, together with the relevant B_1 and B_2 assignments. Two general features of these data are especially noteworthy. In every case, the nonequivalence observed in R_1 is opposite in sense to that observed in R_2. In accord with the general model, the substituents designated as such are those that occur on either side of the B_1–X–B_2 plane and need not necessarily be attached to the chiral center X. This characteristic behavior is the hallmark of this and other solvation models where (as

*The nonequivalence observed in cocaine (**3**) suggests two or more conformations: the nonequivalences for the H_1 and *O*-methyl increase by a factor of about 3.3, *N*-methyl by about 12, and a change in sense was observed for H_5 (no nonequivalence at 0°C) on lowering the temperature from 20 to -40°C.

Table 3

Solutes  Conforming to the Dibasic Solute Fluoroalcohol Model

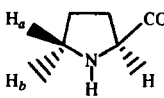
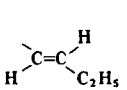
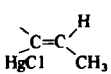
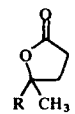
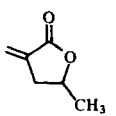
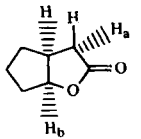
Entry	X or Structure	B_1	B_2	R_1	R_2	AC[c]	CSA	Nonequivalence (ppm)[a] and Sense[b] R_1	R_2	B_1, B_2	Ref. and Examples[d]
1	$ArCHNH_2R$	NH_2	α-Naphthyl	CH_3	H	*R*	(*R*)-**Ib**	0.015 (H)	0.062 (L)		28 (5)
2	$PhCHNH_2CH_3$	NH_2	Ph	CH_3	H	*R*	(*S*)-**Id**	0.032 (L)	0.100 (H)		24
3	$PhCH_2CHNH_2CH_3$	NH_2		CH_3	H	*R*	(*S*)-**Id**	0.020 (L)	Obscure	0.00 – 0.020 (H)	24
4	$RCHNH_2COOCH_3$	NH_2	$COOCH_3$	CH_3	H	*S*	(*R*)-**Ia**	0.028 (L)	0.023 (H)	0.013 (H)	11 (14)
5	$PhCH_2CHNH_2COOCH_3$	NH_2	$COOCH_3$		H	*S*	(*R*)-**Ia**	0.025 (L) – 0.022 (L)	0.022 (H)	0.023 (H)	11
6	$(CH_3)_2CHCHNH_2COOCH_3$	NH_2	$COOCH_3$		H	*R*	(*R*)-**Ia**	0.011 (H) 0.009 (H) 0.009 (H)	0.041 (L)	0.041 (L)	11
7		NH	$COOCH_3$		H	*S*	(*R*)-**Ia**	0.066 (L) 0.046 (L)	0.060 (H)	0.028 (H)	11
8	C	OH	Ph	D	H	*R*	(*S*)-**Id**	–	0.051 (H)	–	24
9	C	OH	Ph	CH_3	H	*R*	(*S*)-**Id**	0.018 (L)	0.089 (H)	–	24
10	C	OCH_3	Ph	CH_3	H	*R*	(*S*)-**Ie**	0.016 (L)	0.025 (–)	5.0 (H)	24

Table 3 continued

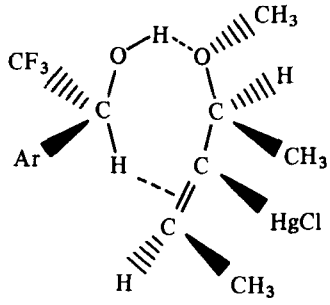
Entry	X or Structure	B_1	B_2	R_1	R_2	AC[c]	CSA	Nonequivalence (ppm)[a] and Sense[b]			Ref. and Examples[d]
								R_1	R_2	B_1, B_2	
11	C	OH	$COOCH_3$	CH_3	H	*R*	(*S*)-Ie	0.029 (L)	0.070 (H)	0.044 (H)	24
12	C	OH	$COOCH_3$	$(CH_3)_3C$	H	*R*	(*S*)-Ie	0.0	0.094 (H)	0.071 (H)	24
13	C	OCH_3	$COOCH_3$	CH_2(CH$_3$)	CH_3	*R*	(*S*)-Ic	0.054 (L) –	0.036 (H)	0.00, 0.014 (H)	31
14	RCHOHC≡CH	OH	C≡CH	CH_3	H	*R*	(*S*)-Ic	0.037 (L)	0.03 (H)	0.0	24 (1)
15	C	OH		CH_2(CH$_3$)	CH_3	*S*	(*S*)-Ic	–	0.025 (L)	–	31
16	$RCH(OCH_3)C(X)=CHR$	OCH_3		CH_3	H	*S*	(*S*)-Ic	–	–	0.016 (H)	32
17		C=O	–O–	CH_2(CH$_3$)	CH_3	*R*	(*R*)-Ic	0.042 (L) –	0.010 (H)	–	33 (1)
18		C=O	–O–	CH_2(CH$_3$)	H	*R*	(*R*)-Ic	0.038 (H) –	–	–	33 (2)
19		C=O	–O–	CH_3	H	*R*	(*R*)-Ic	0.018 (L)	–	–	34

20		C=O	–O–	–	H_a H_b	2(*S*), 3 (*S*)	(*R*)-Ic	–	0.030 (L) 0.005 (L)	–	33 (1)
21	ArN(O)EtMe	O	α-Naphthyl	CH_3 | CH_2	CH_3	*R*	(*S*)-Ib	0.019 (L) 0.017 (L)	0.029 (H)	–	35 (1), 36
22	$PhP(O)CH_3R$	O	Ph	CH_3CH_2	CH_3	*R*	(*S*)-Ia	–	0.019 (H)	–	35 (5), 37
23	$PhPCH_3R$	P	Ph	CD_3	CH_3	*R*	(*S*)-Ia	–	0.004 (L)	–	35 (2)
24	P	O	Ph	CH_2Ph	CH_3	*R*	(*S*)-Id	–	0.121 (H)	–	35
25	$RS(O)CH_3$	O	S	$(CH_3)_3$	CH_3	*R*	(*R*)-Ia	0.012 (H)	0.026 (L)	–	21 (3)
26	$ArS(O)CH_3$	O	S	Ph	CH_3	*R*	(*R*)-Ia	–	0.012 (L)	–	21 (3)
27	S	O	S	$PhCH_2$	CH_3	*R*	(*R*)-Ia	–	0.025 (L)	–	21
28	$CH_3S(O)OR$	O	$O(CH_3)_3$	CH_3	S	*R*	(*S*)-Ia	0.030 (H)	–	0.014 (L)	22 (2)
29	*p*-TolS(O)OR	O	$O(CH_3)_3$	$CH_3C_6H_4$	S	*S*	(*S*)-Ib	0.067 (L)	–	0.093 (H)	22 (4)

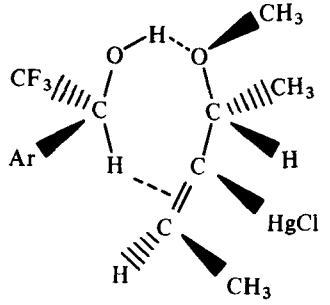
[a] Because of differences in temperature (25–40°C), CSA concentration (at least 2 equiv CSA/equiv solute), and achiral diluent, relative nonequivalence magnitudes are only roughly comparable between entries.
[b] (H), highfield; (L), lowfield.
[c] Independently established configuration.
[d] Number of additional configurationally known examples of the solute types studied in the respective references given in parentheses.

a first approximation) only two points of interaction (either attractive or repulsive) exist between CSA and solute.

Second, nonequivalence may be observed in B_1 or B_2 substituents, for example, in ethers (entries 10, 13, and 16 in Table 3), in carboxylic esters (entries 4–7, 11–14), and in sulfinate esters (entries 28 and 29). In every case, this nonequivalence is of the same sense as that of the smaller R_1 or R_2 substituent (or opposite to that of the larger of these groups). The origin of this trend is the preference for these compounds to populate rotamers in which the B_1 or B_2 substituent is turned away from the larger of the R_1 or R_2 groups. In the diastereomeric solvates, as illustrated by solvates **10** of (*S*)-TFAE and the



(*S,S*)—**10**



(*S,R*)—**10**

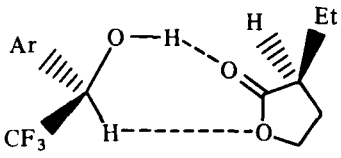
major methoxymercurial of 1,3-dimethylallene (entry 16), the B_1 substituent will be disposed preferentially to the face of the chelate-defined plane bearing the smaller R_1 or R_2 group (in this case hydrogen), hence will have the same sense of nonequivalence as this substituent.

Aminoester entries 4 to 6 show that the nonequivalence magnitude of the B_2 substituent increases on changing R from methyl to benzyl to isopropyl, indicating an increased preference (on a time-averaged basis) for this rotameric disposition. Which oxygen of the ester function actually serves as B_2 is inconsequential. A similar trend is noted for hydroxy esters (entries 11 and 12).

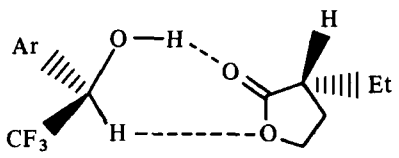
In correlating senses of nonequivalence to solute absolute configuration, B_1 and B_2 must be correctly identified. Inverting these assignments inverts the prediction of nonequivalence senses for a given set of CSA-solute absolute configurations. With many dibasic solutes—for example, with alkylarylamines (entries 1–3), alkylarylcarbinols (entries 8 and 9), propargylic alcohols (entry 14), allylic alcohols and ethers (entries 15 and 16), dialkylsulfoxides (entry 25), and monoaryl

amine and phosphine oxides (entries 21-23)—the correct choices of B_1 and B_2 are obvious. The nonequivalence behavior of configurationally known solutes of this type establishes the general validity of this model.

When ambiguity exists, the study of model solutes of known configuration becomes particularly important before a "solvation model" for the particular solute type can be assigned. Lactones, for example, possess two oxygen atoms whose relative basicity is not immediately apparent. A study of configurationally known examples (33) indicated the primary basic site to be the carbonyl oxygen. The lactone model, illustrated by solvates 11 for an α-substituted butyrolactone



(*R*,*R*)–**11**

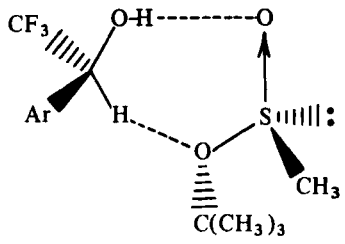


(*R*,*S*)–**11**

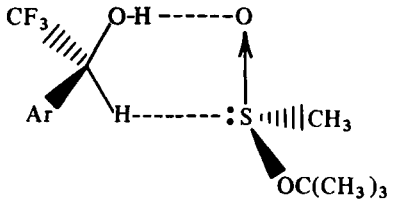
(entry 18), holds for γ-substituted butyrolactones as well (33). Since butyrolactones are roughly planar and on a time-averaged basis are thus coplanar with the approximate plane of the chelate ring, substituents extending on either side of this plane (including ring protons) may show appreciable nonequivalence.

Lactones of larger ring size, however, deviate considerably from planarity, and the consequences of their conformations must be taken into consideration in any assignment of absolute configuration. Few δ-lactones have been examined. Although several δ-lactones are asserted to show nonequivalence in accord with the γ-lactone model (38, 39), we recommend that this model not be used for assignment of absolute configuration to δ-lactones.

Another frequently encountered problem is that of the solute that contains more than one possible site of secondary interaction. In such cases, one B_2 generally "dominates" the other, and its incorrect identification often leads to incorrect configurational assignment to the solute. Acyclic sulfinate esters, for example, have two potential sites that could serve as B_2, the electron pair on sulfur and the alkoxy oxygen. The nonequivalence predictions one would make in choosing either as B_2 are different. Solvates 12 and 13 are the two possible solvation modes for *t*-butyl (*R*)-methanesulfinate and an (*S*)-carbinol (1). Principal operation of model 12 predicts a highfield

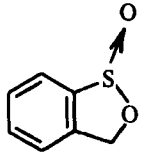


12

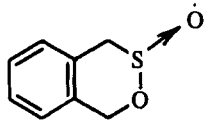


13

sense of nonequivalence for the (*S*)-methyl, and lowfield nonequivalence for the *t*-butyl group in an (*R*)-enriched sulfinate–(*S*)-CSA sample. If the secondary interaction is at sulfur, the prediction (from model 13) is reversed. The actual observation (Table 3, entry 28) is in accord with model 12, indicating that B_2 is the alkoxy oxygen. Obviously, nonequivalence magnitudes of sulfinate esters and those of any compound with two proximate B_2 sites depend on the relative populations of the two possible solvation modes resulting from these secondary interactions. With sultines 14 and 15 the secondary inter-



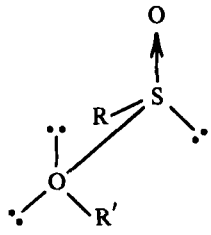
14



15

action at sulfur appears to be of increased importance relative to that in sulfinate esters (22). Some contribution from solvate 13 is apparent, however, with the latter compounds. As previously noted, the sense of alkoxy nonequivalence indicates that sulfinate esters preferentially populate rotamers 16, where the alkoxy substituent is approximately trans to the sulfinyl substituent. Larger alkoxy groups produce greater nonequivalence magnitudes of predictable senses in both sulfur and alkoxy substituent resonances, possibly owing to an increase in the basicity of the oxygen to which the larger group is appended. However, an increase in alkoxy bulk must also decrease the competing interaction at sulfur by more heavily populating rotamer 16, in which the approach to sulfur is hindered by the alkoxy substituent.

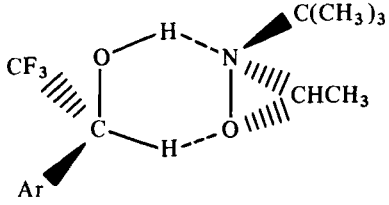
In this and other cases of a third basic site being near the chiral center, the relative importance of this site must be ascertained before



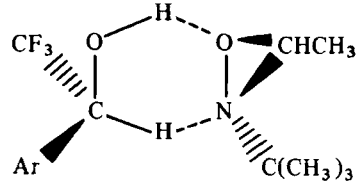
16

assigning absolute configuration from the solvation model. In general, a remote third basic site should have little effect on nonequivalence unless it competes with B_1 for the primary hydrogen bond. In such cases, nonequivalence should diminish without changing senses unless there is a two-point interaction at the remote site. In most cases, a site is rendered "remote" by merely one methylene group; benzylphenylmethylphosphine oxide, for example, shows substantial nonequivalence, utilizing the phenyl, not benzyl, as B_2 (entry 24). The data in Table 3 for compounds that contain three basic sites (those that have functionality in R_1 and R_2) suggest that an "ordering" of the relative basicities of various B_1 and B_2 substituents might be achieved. Sulfoxides, for example, maintain a secondary interaction at sulfur even in the presence of aryl, benzyl, and vinyl substituents (21). In sulfinate esters, B_2 is the alkoxy oxygen regardless of potential aryl or sulfur interactions. Blind application of such rules to new solute classes, however, should be avoided, especially when more than two basic sites are present. Secondary interactions are quite sensitive to the steric environments about the sites of interaction, and solvation models cannot be so naively predicted.

Oxaziridine nonequivalence is an interesting case in point. Oxaziridines have attracted considerable stereochemical attention because of the dissymmetric nitrogen and its appreciable barrier to inversion, and a variety of enantiomerically enriched samples have been prepared by a number of methods (40). Studies of the CSA-induced nonequivalence of these compounds have been reported by two groups (40–43). Fluoroalcohols 1 induce large nonequivalence in both carbon and nitrogen resonances of oxaziridines, so that a determination of enantiomeric purity by this method is easily accomplished. Initially, an understanding of oxaziridine nonequivalence behavior was not straightforward. Oxaziridines, like lactones, have two heteroatoms that may serve as B_1 and B_2, and the site of primary interaction is not obvious. The model based on a primary interaction at nitrogen (17) predicts upfield nonequivalence for the *t*-butyl group of

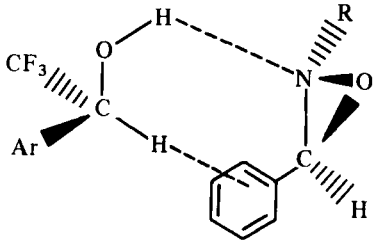


(*S,S*)−17

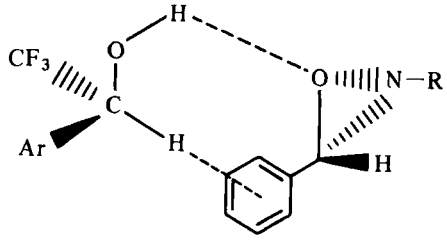


(*S,S*)−18

(*S*)-enriched oxaziridine **19a** with an (*S*)-fluoroalcohol, whereas the alternative model **18** predicts a lowfield sense of nonequivalence for this group. The presence of aryl substituents further complicates spectral interpretation, since a second potential B_2 site is introduced and interactions such as **20** or **21** might occur. Initial efforts to decipher the nonequivalence behavior shown by a series of oxaziridines derived from the corresponding imines by (*S*)-(+)-monopercamphoric acid (MPCA) oxidation (40) were additionally hampered by a lack of suitable configurationally known models for comparison. Table 4 outlines the nonequivalence behavior shown by some of these compounds.



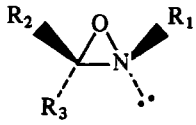
(*S,S*)−20



(*S,S*)−21

An independent solution to the problem of defining the site of primary interaction may in some cases be achieved by studying solute behavior toward achiral lanthanide shift reagents (LSRs). The primary interaction in lactones, for example, with both LSRs and CSAs is the carbonyl oxygen (33); intuitively, one expects a general correlation between basicities of functional groups toward LSRs and toward carbinols 1. The study of a series of oxaziridines (44) revealed that an LSR binds to nitrogen unless a bulky nitrogen substituent or a bulky ring carbon substituent syn to the nitrogen lone pair is present, in which case coordination to oxygen is observed. Inasmuch as the steric requirement of a hydroxyl is considerably less than that of the

Table 4
Nonequivalence of Oxaziridines from (+)-MPCA Oxidation of Imines[a]



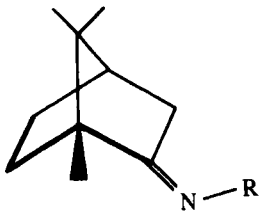
19

Compound	R_1	R_2	R_3	CSA	Nonequivalence (Hz at 100 MHz, 25°C)[b] and Sense[c] R_1	R_2	R_3
19a	*t*-Bu	H	CH_3	le	7.5 (H)	3.0 (L)	15.0 (L)
19b	*t*-Bu	H	H	ld	9.0 (H)	35.0 (L)	30.0 (L)
	CH_3				14.1 (H)		
	|						
19c	CH–		$-(CH_2)_5-$	ld	1.6 (H)	–	–
	|						
	CH_3				3.2 (H)		
			CH_3				47.0 (L)
			|			
19d	*t*-Bu	H	CH–	le	23.0 (H)	14.0 (H)	–
			|			
			CH_3				35.0 (L)
19e	*t*-Bu	H	Ph	ld	6.7 (L)	0.0	–
19f	*t*-Bu	H	*p*-BrC_6H_4	le	2.2 (L)	0.0	3.0 (L)
19g	*t*-Bu	H	*p*-$NO_2C_6H_4$	le	3.5 (L)	0.0	3.0 (L)
19h	*t*-Bu	H	*p*-MeC_6H_4	le	4.5 (L)	0.5 (L)	0.5 (L)
19i	CH_3	H	Ph	le	2.5 (L)	1.5 (L)	–
19j	CH_3	Ph	H	le	8.5 (H)	–	12.0 (L)
	CH_3				8.0 (H)		
	|						
19k	CH–	Ph	H	le	–	–	12.0 (L)
	|						
	CH_3				5.0 (H)		

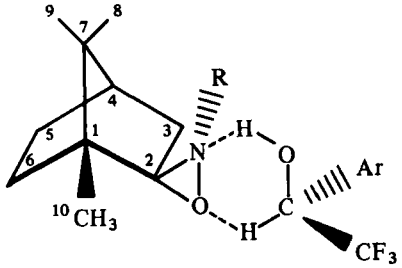
[a]Data from ref. 41.
[b]Nonequivalence measured in the presence of approximately threefold excess of (*S*)-(+)-CSA in a dilute CCl_4 solution of oxaziridine.
[c](H), highfield; (L), lowfield.

LSR, nitrogen, the more basic of the heteroatoms, appeared to be the site of primary interaction. This conclusion was simultaneously corroborated by the nonequivalence behavior of several configurationally established oxaziridines reported independently by two groups (41,42). These oxaziridines were prepared by peracid oxida-

tion of imines 22 derived from (+)-(1*R*,4*R*)-enriched camphor. In the presence of (*S*)-fluoroalcohols 1, these oxaziridines exhibit upfield nonequivalence for the nitrogen substituent, and downfield nonequivalence for the 10-methyl resonance, in accord with solvation model 23, where the primary interaction occurs at nitrogen. The alkyloxaziridines of Table 4 (**19a–19d**) were accordingly assigned the (*S*)-configuration at nitrogen, as depicted in the table.



22



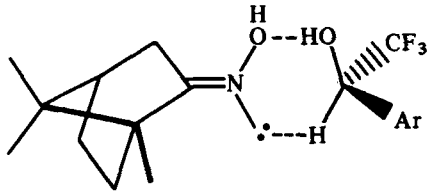
23

Various independent experiments suggested that the aryl-substituted oxaziridines of Table 4 (**19e–19k**) are of the same (*S*)-configuration at nitrogen. Of these compounds, the cis isomers **19j** and **19k** behave like the alkyloxaziridines **19a** to **19d**, while the nonequivalence sense for the nitrogen substituent of the trans compounds **19e** to **19i** deviates from this pattern. The solvation mode accounting for the observed senses of nonequivalence in the trans isomers is as shown in 20, where an aryl group syn to the nitrogen lone pair blocks access to oxygen but offers an acceptable alternative site for the secondary interaction. The anti relationship of the lone pair and the aryl group precludes this solvation mode for *cis*-3-aryloxaziridines, so that nonequivalence in these compounds, as with alkyloxaziridines, originates from solvation mode 17.

Five configurationally known oxaziridines derived from imines of PEA display nonequivalence behavior that is in general accord with this model, though occasional unpredictable deviations attributed to internal magnetic anisotropic effects were noted (41).

Oximes are another solute type having nitrogen and oxygen as basic sites. From the one available example (24), the primary and secondary interactions appear to be at oxygen and nitrogen, respectively. Nonequivalence shown by the three methyl resonances of the oxime derived from *d*-enriched camphor are of the same sense but opposite that shown by the endo-H_2 proton. These nonequivalences are of the sense expected of solvate **23a**. This example suggests a

potentially general (but untested) method for determining the absolute configuration and enantiomeric excess of cyclic ketones.



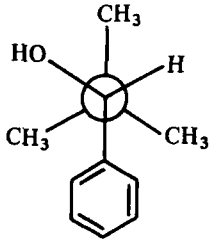
23a

Fluoroalcohols 1 have been employed in assigning absolute configuration of amines (30), benzothiophene oxides (45), lactones (33, 46), oxaziridines (41), and an amine oxide (47).

2. *Exceptions to the Dibasic Solute Model*

A few solutes of the types generally accommodated by the fluoroalcohol–dibasic solute model deviate from the general rule that R_1 and R_2 exhibit opposite senses of nonequivalence. With (*S*)-1e, (*R*)-enriched phenyl-*tert*-butylcarbinol shows, as expected, highfield nonequivalence (0.15 ppm) in the carbinyl resonance, but the *tert*-butyl group also shows highfield nonequivalence (0.03 ppm) (24).

This result can be satisfactorily rationalized by assuming that the *tert*-butyl group influences the rotational disposition of the phenyl substituent, so that rotamer 24 is heavily populated. In the diastereomeric solvates, the solute chiral center is no longer in the chelate



24

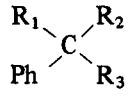
plane. The *tert*-butyl and proton substituents lie on the same side of this plane, thus having the same sense of nonequivalence. Analogous behavior is observed for the isopropyl and carbinyl resonances of 2-methyl-1-phenylpropylamine with TFPE. Although this deviation

has not been systematically examined, it seems reasonable to expect that such deviations will be encountered only in solutes so sterically hindered about B_2 that the orientation of this group is affected. In such cases, the smaller of R_1 or R_2 is still expected to show the "correct" sense of nonequivalence.

The behavior of the *ortho*-methyl resonances of diarylsulfoxides is also exceptional (48). For example, both methyls of *o*-tolyl-*p*-tolylsulfoxide show nonequivalence of the same sense as that expected for the *p*-methyl group on the basis of the general sulfoxide model. The senses observed for *o*-methyl groups in several other *o*-tolylsulfoxides are also inverted, whereas those of other resonances are normal. This behavior, which may result from an intramolecular shielding of these groups by either sulfinyl or aromatic moieties in rotamers whose populations are affected by the CSA, is not well understood.

Table 5 presents nonequivalence data for several α-amino, α-hydroxy, and α-methoxyphenylacetates to illustrate some additional deviations that are not well defined. Presuming that the amine, alcohol, and ether functions serve as B_1, each solute has two potential

Table 5
Fluoroalcohol-Induced Nonequivalence for Substituted Phenylacetates[a]



			Configuration		Nonequivalence (ppm) and Sense[b]		
R_1	R_2	R_3	Solute	CSA[c]	R_1	R_2	R_3
OH	$COOCH(CH_3)_2$	H	*S*	*S*	–	0.01 (L) 0.01 (L) 0.01 (L)	0.04 (L)
OH	$COOCH_3$	H	*R*	*S*	–	0.08 (H)	0.02 (H)
OCH_3	$COOCH_3$	H	*S*	*S*	0.04 (H)	0.02 (L)	–
OH	$COOCH_3$	CH_3	*S*	*S*	–	–	0.03 (H)
OCH_3	$COOCH_3$	CH_3	*S*	*R*	0.05 (H)	0.12 (L)	0.06 (L)
NH_2	$COOCH_3$	H	*S*	*S*	–	0.12 (L)	0.01 (H)

[a] Data from ref. 24.
[b] (H), highfield; (L), lowfield.
[c] Excess of **Ic**, **Id**, or **Ie** in CCl_4 is approximately threefold.

B_2 sites. Choosing the ester as B_2, one predicts lowfield nonequivalence for nuclei in R_1, R_2, and R_3 for an *S,S* CSA-solute combination (or highfield for *S,R*). This works nicely for the first two entries, but fails for one or more resonances of the others. Alternatively, choosing phenyl as B_2, one predicts for an *R,S* (or *S,R*) CSA-solute combination low-, high-, and lowfield nonequivalences for R_1, R_2, and R_3 nuclei, respectively (or high, low, high for *S,S*), which corresponds precisely to observations for the third, fourth, and last entries only. Obviously, more systematic study is needed before solvation mode(s) of these compounds can be postulated. These examples reemphasize our caution that a simple "ordering" of three or more basic sites that has been deduced from only a few configurationally known solutes is not a firm basis for a CSA configurational assignment.

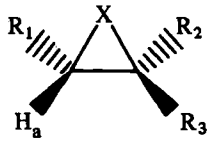
All these deviations have one similarity: they occur in compounds having relatively crowded chiral centers bearing at least one highly anisotropic substituent. The differential effect of the CSA on the intramolecular anisotropic environment of a given nucleus (e.g., on aryl rotation) cannot presently be stated.

Another general type of deviation is discussed in Sect. IV-E.

3. Monobasic Solutes

Solutes need not possess two basic sites to show fluoroalcohol-induced nonequivalence. The first pertinent claim in this regard is that of nonequivalence for the endo-α-keto proton of (+)-camphor (5 Hz at 100 MHz), measured from the differences in the spectra obtained at -65°C with first one, then the other enantiomer of methylphenylcarbinol (15). Five other monobasic solutes, methyl- and *tert*-butyl oxiranes (49), and methyl-, *tert*-butyl-, and *trans*-2,3-dimethylthiiranes, (50), are reported to show nonequivalence in the presence of TFPE. Moretti and Torre (49, 50) have studied the nonequivalence behavior of these and other epoxides, episulfides, and episulfoxides, and have noted as the only obvious configurational trend a consistent nonequivalence sense for protons on substituted ring carbons [lowfield for (*S*)-solute-(*R*)-CSA combinations, Table 6]. Though many of these solutes have two or more basic sites, the usual fluoroalcohol model does not correctly predict nonequivalence for all resonances in any of these solutes that show nonequivalence in more than one nucleus. Carbinyl hydrogen bonding by solute ring protons to the CSA phenyl group is probably an important secondary interaction with these solutes.

Table 6
TFPE-Induced Nonequivalence of Epoxides, Episulfides, and Episulfoxides[a]



Solute					Nonequivalence (Hz at 60 MHz, 25°C)[c] and Sense[d]			
X	R_1	R_2	R_3	AC[b]	H_a	R_1	R_2	R_3
O	Me	H	H	*S*	0.5 (L)	–	–	–
O	*t*-Bu	H	H	*S*	1.9 (L)	0.6 (H)	1.0 (H)	1.0 (H)
O	Ph	H	H	*S*	2.4 (L)	–	0.5 (L)	0.6 (H)
O	Ph	H	Me	1*S*, 2*S*	2.1 (L)	–	–	–
O	Ph	Me	H	1*S*, 2*R*	1.8 (L)	–	0.8 (H)	0.9 (H)
O	Ph	H	Ph	*S*, *S*	1.0 (L)	–	1.0 (L)	–
S	Me	H	H	*S*	0.9 (L)	–	–	0.5 (H)
S	Me	H	Me	*S*, *S*	0.6 (L)	–	0.6 (L)	–
S	*t*-Bu	H	H	*S*	1.2 (L)	0.3 (L)	0.0	0.7 (H)
S	Ph	H	H	*S*	0.8 (L)	–	0.0	0.6 (H)
S	Ph	H	Ph	*S*, *S*	0.0	–	0.0	–
SO	Me	H	H	1*S*, 2*S*	0.9 (L)	0.5 (H)	0.2 (H)	0.5 (H)
SO	*t*-Bu	H	H	1*S*, 2*S*	1.5 (L)	0.6 (L)	0.2 (L)	0.8 (H)
SO	Ph	H	H	1*S*, 2*S*	2.1 (L)	–	1.6 (L)	0.7 (L)
SO	Ph	H	H	2*S*, 3*S*	0.0	–	1.0 (L)	–

[a] Date from refs. 49 and 50.
[b] Absolute configuration of solute.
[c] Sample composition, 2:1:ca. 3 molar ratio of (*R*)-(-)-TFPE to solute to CCl_4, respectively.
[d] (H), highfield; (L), lowfield.

Very recently (51), nonequivalence has been found in a variety of additional monobasic solutes whose configurational analysis was thought earlier to lie outside the scope of the CSA technique. 2-Butanol, for example, when dissolved in benzene saturated with TFAE, shows nonequivalence in both methyl resonances. A variety of other chiral and prochiral compounds such as 2-propanol, methyl 2-propyl sulfide, 2-aminobutane, and 2-methyl-1-butanol show nonequivalence for their enantiotopic methyl groups under these conditions. The magnitudes of nonequivalence in these instances are small (0.02–0.03 ppm) but, as illustrated in Figure 4 for enriched 2-butanol,

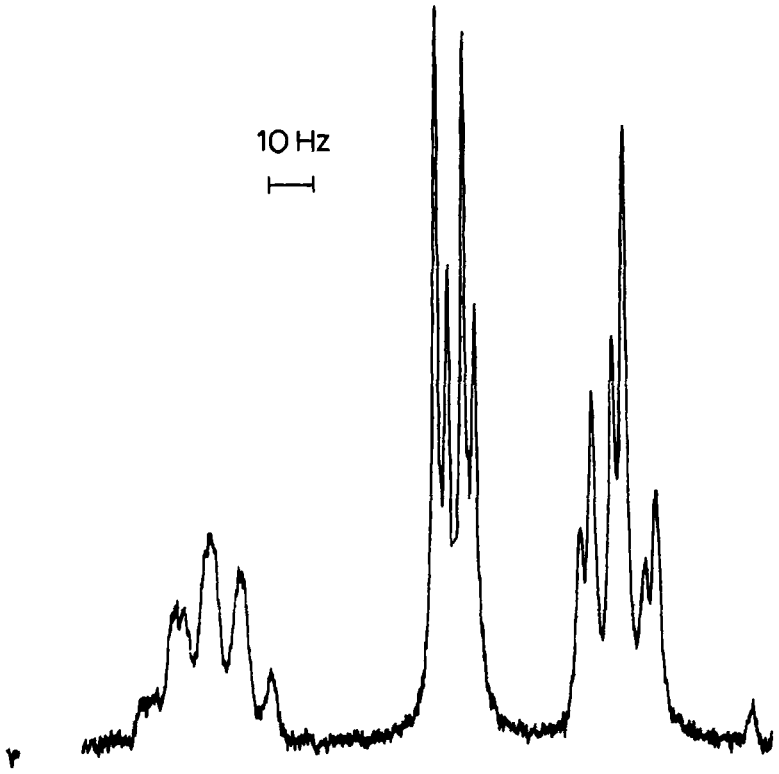
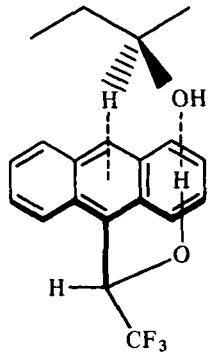


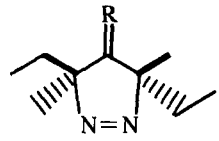
Figure 4. Methyl resonances of (*S*)-(+)-enriched 2-butanol in benzene saturated with (*R*)-TFAE (220 MHz).

at high field strength they do suffice for nonequivalance sense determination. In favorable instances, enantiomeric purity can be measured as well. Several monobasic nitrogen heterocycles show much larger nonequivalence. For example, the nonequivalences in the methyl groups of 1,2,2,5-tetramethylpiperidine are 0.05, 0.11, 0.0, and 0.12 ppm, respectively, in the presence of 3 equiv of TFAE in benzene at 25°C.

Model 25, invoking a preferential rotameric disposition of TFAE dictated by peri interactions, and solvate conformations resulting from CHB between the solute carbinyl proton and the anthryl ring, correctly predicts the senses of nonequivalence observed for 2-butanol (Fig. 4), and for 2-octanol as well. In these conformations, the substituent over the larger portion of the anthryl ring is the more shielded.



25



26

R = H, H
R = O
R = H, OH

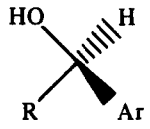
Monobasic solutes that have *no carbinyl hydrogens* may also show nonequivalence. 3-Methyl-2-butanone, 4-methyl-2-pentanone, 2-methylpropanal, methyl 2-methylbutyrate, 2,2,6,6-tetramethylpiperidine, methyldiisopropylcarbinol, and methylethyl-*n*-butylcarbinol in TFAE-saturated benzene all show nonequivalence of sufficient magnitude (0.01–0.03 ppm) to allow nonequivalence sense determination at 220 MHz. An especially striking example is that provided by pyrazolines **26**. With only a severalfold excess of (*S*)-TFAE, 3(*S*),5(*S*)-enriched samples of these compounds show nonequivalence in their methyl resonances (downfield sense for the singlets and upfield sense for the triplets) sufficient for enantiomeric purity determination at 90 MHz (52).

These examples indicate that a much larger variety of solutes fall within the purview of the CSA technique than has been realized, immediately enhancing its value as a reliable alternative to chiroptic and CLSR methods as a means of comparing configurations of monobasic solutes and determining their enantiomeric purity. Studies of more configurationally known solutes will doubtless expand the utility of the CSA method in assignment of absolute configuration to these solutes as well.

C. Amine CSAs

1. Diastereomeric Solvates

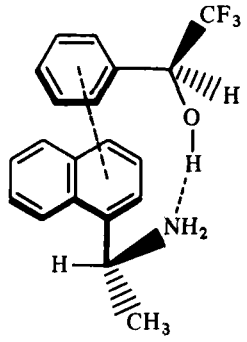
Historically, (*R*)-(+)-α-NEA served as the CSA for the first configurational correlations made by the NMR-CSA method (30). Thirteen enriched alkylarylcarbinols were examined; the carbinyl proton resonances of enantiomers with stereochemistry **27** were observed at



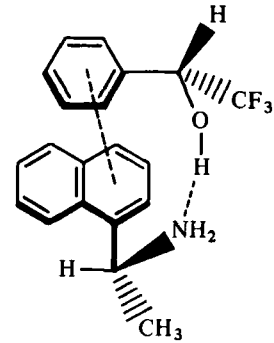
27

higher field than those of their mirror images. Additionally, nonequivalence in the fluorine resonances of enantiomers 27 having trifluoromethyl as R was of the lowfield sense. On the basis of this correlation, the configurations of nine analogous carbinols were assigned.

This spectral nonequivalence for the diastereomeric solvates was originally rationalized in terms of conformers 28 (shown for TFPE as solute) where (*R*)-NEA as its preferred rotamer (dictated by the peri interaction) interacts primarily with the carbinol hydroxyl and populates the conformers shown through an aryl-aryl attraction. Thus, in (*S*,*R*)-28, the carbinyl proton is held more closely to the naphthyl ring, whereas in (*R*,*R*)-28 its position is reversed. This situation results in the observed highfield sense of nonequivalence for the carbinyl proton of carbinols 27 and accounts for the opposite sense shown by the fluorine resonances. In one instance, aryl nonequivalence was also identified. All three ring protons of trifluoromethyl-α-thienylcarbinol (13) show the same nonequivalence sense as the carbinyl proton (opposite to that of trifluoromethyl). Such also is expected from the proposed interactions 28, since the aryl substituent



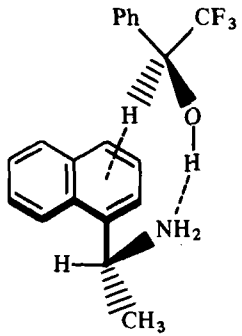
(*S*,*R*)−28



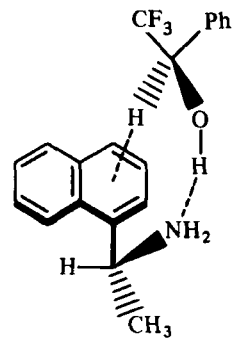
(*R*,*R*)−28

will be more heavily shielded in the (*S*,*R*)- than in the (*R*,*R*)-solvate because it may approach the naphthyl ring more closely. Moreover, the (*S*,*R*)-conformer may be the more heavily populated for this reason.

This conformational hypothesis, though accounting satisfactorily for the observations, was advanced before extensive data had been obtained for fluoroalcohols 1 *as CSA*, and was made without appreciation for the conformational control asserted by carbinyl hydrogen bonding (CHB). Recognition of this possibility suggests two alternative solvation modes for consideration, since two carbinyl hydrogens may be considered. The first (29), using the solute carbinyl hydrogen, is the conformation arrived at from interactions suggested previously (with imposition of a preferred naphthyl disposition) during discussion of the fluoroalcohol–dibasic solute nonequivalence mechanism. Model 29 correctly predicts the sense of nonequivalence for trifluoromethyl substituents [downfield for a sample enriched in the (*S*,*R*)-solvate] and accounts for the sense observed for an aromatic

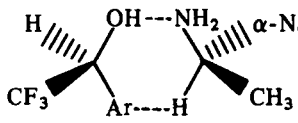


(*S*,*R*)−29

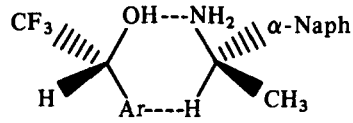


(*R*,*R*)−29

substituent. No nonequivalence is expected for the carbinyl proton unless the (*R*,*S*)-conformer is more heavily populated than its (*R*,*R*)-counterpart. The second possibility, 30, invoking CHB between the amine methine and the fluoroalcohol aromatic group, correctly predicts the senses of both carbinol carbinyl and trifluoromethyl resonances. What prediction should be made for the sense of aryl nonequivalence is less obvious. The disposition of the naphthyl group (omitted for clarity), is not vital to nonequivalence sense in this case (although it would certainly affect nonequivalence magnitude). All three conformations, perhaps others as well, are potential contributors to the observed nonequivalence. Since CHB should be stronger in conformers 29 than in 30, the former are probably more heavily populated. Carbinyl proton nonequivalence (and its sense) can be understood in terms of conformers 29, where an additional aryl-aryl attraction [from conformer (*R*,*S*)-29] increases the population of



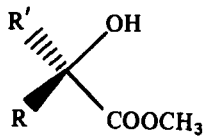
(*S*,*R*)–30



(*R*,*R*)–30

the (*R*,*S*)-conformer relative to that of (*R*,*R*), hence more heavily shielding the carbinol carbinyl proton of the former. In terms of this model, the origin of NEA-induced fluorine nonequivalence in methyl-, *t*-butyl-, and cyclohexyltrifluoromethylcarbinols is apparent (12). Model 29 also accounts for the senses of nonequivalence in the *t*-butyl and cyclohexyl compounds (13), though the origin of carbinyl nonequivalence (still opposite in sense to that of trifluoromethyl) in these two alcohols is not obvious. Our "revision" of this model is a refinement of the hypothetical conformations accounting for nonequivalence made as a result of the reassessment of the relative importance of two secondary interactions. Several propargylic and allylic alcohols also show nonequivalence (53), which may be rationalized on the basis of this model.

Another correlation is observed in the carbomethoxy resonances of various hydroxyesters 31 (Table 7) (53,54). With (*R*)-NEA, compounds having the absolute stereochemistry of 31 (R > R′) show highfield nonequivalence for the carboxy methyl resonance. This generalization, while correct, is a misleading simplification. The correlation may be understood for entries 1 to 10 with a rationale similar to that arrived at for secondary carbinols: conformations 32 populated by CHB between the solute and the CSA aryl group will result in a highfield signal for the carbomethoxy resonance of the (*R*)-configured solute (entry 9 is a deviation in nomenclature only). Carbinyl nonequivalence of the same sense (entries 4 and 10 are exceptions) would result from increased population of the (*R*,*R*)-conformer as a result of an attractive carbomethoxy-aryl interaction (54). Entries 11 to 15 of Table 7 are satisfactorily understood in terms of conformers 33, populated by a secondary carbomethoxy-aryl attraction (55), with added aryl-aryl attraction



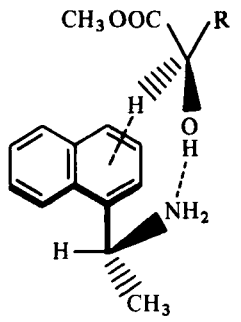
31

Table 7
NMR Spectral Nonequivalence of Methyl Glycolates in the Presence of (*R*)-(+)-NEA[a]

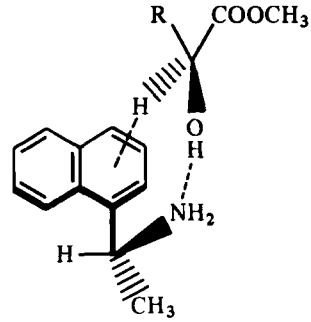
	$R_1R_2C(OH)COOCH_3$			Nonequivalence[b] $\Delta\delta$ (Hz at 100 MHz, 29°C, unless otherwise specified)[c] and Sense[d]	
Entry	R_1	R_2	AC[e]	R_2	$COOCH_3$
1	CH_3	H	*S*	1.3 (L)	2.3 (L)
2	$(CH_3)_2CH$	H	*R*	0.5 (H)	2.2 (H)
3	Cyclohexyl	H	*R*		1.9 (H)
4	$CH_3O_2CCH_2$	H	*S*	0.9 (H)	2.3 (L)
5	$CH_3O_2CCH(OH)$	H	*R*	1.1 (H)	2.0 (H)
6	Ph	H	*R*		3.5 (H)
7	*o*-ClC_6H_4	H	*S*	1.2 (L)	3.4 (L)
8	*m*-$NO_2C_6H_4$	H	*R*		4.1 (H)
9	α-Thienyl	H	*R*		3.2 (L)
10	α-Naphthyl	H	*R*	1.3 (L)	3.2 (H)
11	Cyclohexyl	CF_3	*R*	1.4[f] (L)	0.0[g]
12	Ph	CH_3	*R*		0.9[h] (H)
13	Ph	CCl_3	*S*		0.3[h] (L)
14	Ph	$CH(CH_3)_2$	*R*		0.7[h] (H)
15	Ph	Cyclohexyl	*R*		0.3[h] (H)

[a] Data from ref. 53.
[b] Sample composition of amine, ester, and $CFCl_3$ was in a 2:1:ca. 3 molar ratio.
[c] No entry indicates that nonequivalence could not be observed under these conditions.
[d] (H), highfield; (L), lowfield.
[e] Known absolute configuration.
[f] Hertz at 56.4 MHz, 40°C.
[g] No perceptible broadening at 100 MHz, 29°C.
[h] Hertz at 60 MHz, 40°C.

to stabilize the *R,R* conformers. In these and in entries 6 to 10, a secondary aryl-aryl attraction might do as well, but such a model would not account for fluorine nonequivalence in entry 11, and is not required for entries 6 to 10. The observation of highfield carbomethoxy nonequivalence and lowfield fluorine nonequivalence—which, together with other information, was used to assign the (*R*)-configuration to (–)-methyl-α-hydroxy-α-trifluoromethylphenyl



(*R*,*R*)−32



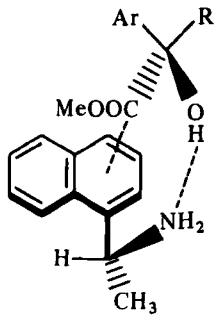
(*S*,*R*)−32

acetate (34) (54)—fits this hypothesis. A simpler model accounting for all carbomethoxy nonequivalences in Table 7 might be conformer 35, where the carbomethoxy is disposed preferentially away from the larger R substituent and toward the face of the chelate ring shielded by the naphthyl substituent. This model, however, does not correctly predict the sense of fluorine nonequivalence in entry 12, nor in compound 34.

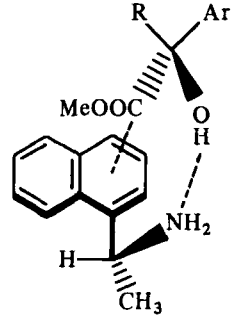
Snatzke and co-workers (25) have also reported a general correlation for the α-proton of a series of α-substituted propionamides in PEA. Several other correlations have been made for carboxylic and phosphorus thioacids; these are separately discussed in the next section.

2. *Diastereomeric Salts*

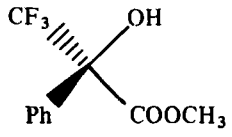
Salts of the various optically active aromatic acids and amines employed extensively as resolving agents frequently exhibit large nonequivalence (17,18,56-69). Since a fast-exchange process is



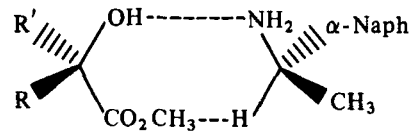
(*R*,*R*)−33



(*S*,*R*)−33



34



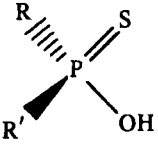
35

occurring in this type of CSA-solute combination as well, relative intensities of signals stemming from diastereotopic groups correspond to enantiomeric excess, providing a convenient method (when nonequivalence can be observed) for monitoring the progress of a classical resolution. Nonequivalence for salts is severely diminished or nonexistent in polar solvents. This is generally not a problem, since salts with one aromatic component are often readily soluble in benzene or chloroform, or are of sufficient solubility in these solvents to allow computer-averaged spectra to be obtained. Salt nonequivalence has also been employed in enantiomeric purity determination of ketones (56) and alcohols (57) after their derivatization to oximes (with *O*-aminoglycolic acid) or phthalate half-esters, respectively.

Several correlations between absolute configuration and nonequivalence sense in diastereomeric salts have been reported. The benzylic protons of the (*R*)-NEA salts of three (*S*)-α-alkylphenylacetic acids show upfield nonequivalence (58). The α-protons of *N*-phthalimido derivatives of eight naturally occurring α-amino acids show highfield nonequivalence (as their (*S*)-PEA salts (59)). Mikołajczyk *et al.*, (17,60,61) have shown that a correlation exists in the salts of a series of phosphorus thioacids (**36**). Table 8 shows data taken from ref. 17. Both *P*-methyl and *O*-methyl resonances of (*S*)-enriched *O*-alkylmethyl- (**36a–36d**) and (*S*)-*O*-methylalkylphosphorus thioacids (**36e–36g**) show downfield nonequivalence. The methyl groups on phosphorus show the larger effect. This series of salts also shows downfield ^{31}P nonequivalence. The size of the phosphorus nonequivalence appears to decrease as the bulk of the R group increases in the *O*-alkyl series (consider **36a**, **36e**, and **36f**) and to increase with an increase in the bulk of OR (**36a–36d**). In another series (**36h–36j**) three (*R*)-alkylphenylphosphorus thioacids (configurationally related to **36a** to **36g** by interchange of phenyl and alkoxyl), nonequivalence was reversed: a downfield sense of ^{31}P nonequivalence was observed for the (*R*)-naphthylethylamine salts.

No models to account for salt nonequivalence have been proposed. Although the aforementioned correlations between absolute configuration and nonequivalence sense might appear to justify assign-

Table 8
^{1}H and ^{31}P Nonequivalence of Phosphorus Thioacid Salts[a]

Compound		R	R^1	^{1}H $\Delta\delta R^{b,c}$	^{1}H $\Delta\delta R^{1\,b,c}$	^{31}P $\Delta\delta^{d}$
	**36a**	Me	MeO	0.153	0.015	0.082
	36b	Me	EtO	0.315	—[e]	0.086
	36c	Me	*i*-PrO	0.115	—[e]	0.263
	36d	Me	*n*-BuO	0.186	—[e]	0.144
	36e	Et	MeO	—[e]	0.048	0.086
	36f	*i*-Pr	MeO	—[e]	0.010	0.049
(*S*)-**36a–36g**	**36g**	*t*-Bu	MeO	—[e]	0.042	—[e]
(*R*)-**36h–36j**	**36h**	Me	Ph	0.144[f]	—[e]	0.272[g]
	36i	Et	Ph	—[e]	—[e]	0.210[g]
	36j	*t*-Bu	Ph	—[e]	—[e]	1.00[g]

[a] Data from ref. 17.
[b] Given in parts per million for racemates with 1 equiv (*S*)-(-)-PEA in CCl_4.
[c] Lowfield nonequivalence with (*S*)-(-)-enriched thioacid, except for **36h–36j**.
[d] In PhH, 1 equiv (*S*)-(-)-NEA; e.e. of **36** not specified, from ^{1}H decoupled spectrum.
[e] Not reported.
[f] Lowfield nonequivalence with (+)-PEA.
[g] (*R*)-(+)-thioacid with (*R*)-(+)-NEA, lowfield nonequivalence.

ment of absolute configuration based on nonequivalence senses in diastereomeric salts, two possible complications are present for salts that are absent from the diastereomeric solvates considered so far. Potentially, these complications can affect the reliability of absolute configuration assignment from nonequivalence sense (62). First, salts exist in nonpolar solvents as aggregates of ion pairs. Since the composition of ion-pair aggregates can affect the chemical shift of salts (63), the senses of nonequivalence may in principle depend on the composition and size of the aggregate. Aggregate size might vary between salts of different compounds.

The magnitude of nonequivalence exhibited by diastereomeric salts depends on solvent polarity (57,60,64), this effect stemming from dissociation of the ion pairs. Equations [4] and [5] describe the equilibria that occur in systems of diastereomeric salts. When weakly basic enantiomeric solutes interact with weakly acidic CSAs, the dissociation of the diastereomeric solvates AHS and A'HS into

$$A + HS \underset{}{\overset{K_1}{\rightleftharpoons}} AHS \overset{K_3}{\rightleftharpoons} AH^+ + S^- \qquad [4]$$

$$A' + HS \underset{}{\overset{K_2}{\rightleftharpoons}} A'HS \overset{K_4}{\rightleftharpoons} A'H^+ + S^- \qquad [5]$$

ion pairs is negligible (i.e., $K_3 \approx K_4 \approx 0$), and if an excess of HS is used, differences in K_1 and K_2 become irrelevant as the equilibria are shifted completely to the right. Nonequivalence observed under these circumstances arises solely from the nonequivalent spectra of the diastereomeric solvates. In the case of diastereomeric salts, the assumption may generally be made that $K_1 \approx K_2 \approx \infty$, thus no nonequivalence increase will generally be observed beyond addition of 1 equiv of CSA, as has been noted (64). However, K_3 and K_4, may be appreciable and need not be equal. Hence, dissociation of the ion pairs may contribute to the observed nonequivalence.

Phenomena originating from this dissociation have been observed even when nonpolar solvents are used. Ejchart and Jurczak (65) have found a concentration dependence and a linear correlation between solute enantiomeric purity and nonequivalence magnitude in the spectral behavior of PEA salts of 2-acetoxyphenylacetic acid and methylphenylphosphinothioic acid. Nonequivalence magnitudes in these salts also depend on the relative amine-acid configurations. These workers have been careful to note that variations in nonequivalence magnitudes attendant with changes in enantiomeric purity and concentration for any given set of salts are not accompanied by a change in nonequivalence sense (65,66). Nonequivalence sense can thus be used to reliably compare configurations of two samples of the same salts.

The problem, however, arises in comparing nonequivalence senses of different salt pairs. In assigning configurations on this basis, in addition to assuming a correlation between intrinsic nonequivalence and different solute structures, one must assume that a sufficient correlation exists in the magnitude and relative ratios of the dissociation constants of the various salts being considered, and in the net contribution of aggregation in the various systems, to prevent these factors from overriding intrinsic nonequivalence.* In cases where intrinsic spectral nonequivalence is small, these factors increase in importance, and a "correlation" in nonequivalence sense may well reflect instead a correlation in dissociation constants.† For these reasons, correlations in diastereomeric salts should be regarded as strictly empirical.

D. Other CSAs

Few correlations between solute configuration and nonequivalence sense have been found for CSAs other than 1 and 2. Harger (70) reports that resolved methylphenylphosphinamide and its *N*-phenyl analog induce nonequivalence in the R (alkyl) resonances of various analogs, the sense of which may be predicted by model 37, invoking

---

*Assuming that K_1 and $K_2 = \infty$, the situation reduces to that of enantiomeric solutes in the presence of 1 equiv of CSA. The pertinent relationships are

$$K_3 = \frac{[AH^+][S^-]}{[AHS]} \quad [6]$$

$$K_4 = \frac{[A'H^+][S^-]}{[A'HS]} \quad [7]$$

$$[S^-] = [AH^+] + [A'H^+] \quad [8]$$

$$[AHS] = C - [AH^+] \quad [9]$$

$$[A'HS] = C' - [A'H^+] \quad [10]$$

where C and C′ are the total concentrations of the enantiomeric components. By substituting eqs. [8] and [9] into eq. [6], and eqs. [8] and [10] into eq. [7], one obtains eqs. [11] and [12], respectively. After solving eq. [12] for $[A'H^+]$

$$K_3 = \frac{[AH^+]([AH^+] + [A'H^+])}{C - [AH^+]} \quad [11]$$

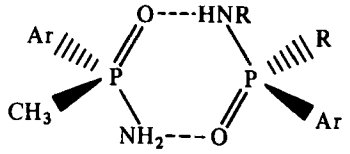
$$K_4 = \frac{[A'H^+]([AH^+] + [A'H^+])}{C' - [A'H^+]} \quad [12]$$

and substituting this value into eq. [11], eq. [13] is derived.

$$[AH^+]^3(K_3 - K_4) + [AH^+]^2(K_3^2 - K_3C - K_3K_4 - K_4C') - [HA^+](2K_3^2C - K_3K_4C) + K_3^2C^2 = 0 \quad [13]$$

Nonequivalence magnitudes for given K_3, K_4, C, and C′, and intrinsic spectral differences between free and uncomplexed components ($\delta^{AHS} - \delta^{AH^+}$, $\delta^{A'HS} - \delta^{A'H^+}$) can be calculated iteratively using eqs. [13], [12], and [3] (Sect. III-A). As the intrinsic spectral difference between the diastereomers ($\delta^{AHS} - \delta^{A'HS}$) becomes smaller, it becomes increasingly easy to invert the nonequivalence sense (sign of $\Delta\delta$) by changing the K_3/K_4 ratio from greater to less than unity.

†Such is perhaps the case for phosphorus nonequivalence in phosphorus thioacid salts (see Sect. IV-F).



37

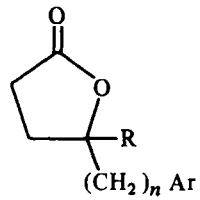
a "head-to-tail" arrangement populated by interactions between acidic and basic sites in CSA and solute. Methyl- and *tert*-butylphenylphosphinothioic acids induce in phosphorus amides nonequivalence (71) whose sense may be similarly explained. The origin of nonequivalence induced in a phosphoryl ester by these thioacids is unclear (72).

Cram and co-workers have experimented extensively with chiral recognition in crown ethers derived from various β-binaphthols (73). In nonpolar solvents, these chiral ethers complex salts of PEA and various chiral α-amino esters (with fast exchange), inducing nonequivalence in their NMR spectra. The senses of proton nonequivalence induced in these solutes have been used to support proposed structures of the diastereomeric solvates (74).

E. Consequences of "Three-Point" Interactions

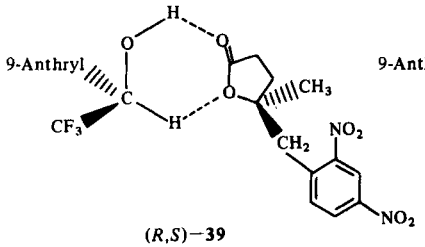
In the framework of a well-established model, predicting nonequivalence sense of a given solute is often as simple as predicting the primary and secondary interactions, and the anisotropic environment of the nucleus in question. In this simple picture, the diastereomeric solvates are considered to be of equal stability. In reality, one or more additional interactions may be present. These additional interactions can be stereochemically dependent and can result in differential stability of the solvates. We have encountered models (Sect. IV-C) in which increased stability by a third "augmenting" interaction was invoked to account for nonequivalence senses of certain nuclei. In these cases, the third interaction had only a minor effect on the structures of the solvates. In using any model, one must be prepared for additional interactions having sufficient strength to significantly alter the structure of one or both of the solvates. In such cases, the expected correlation between stereochemistry and observed senses of nonequivalence may break down.

Several exceptions of this type have been found. Lactones 38 bearing nitrophenyl or nitrobenzyl substituents (Table 9) have been shown to depart from the two-point lactone model (Sect. IV-B) (75).

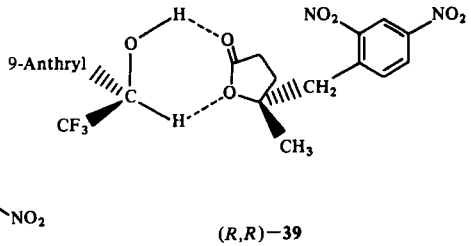


38

In the presence of a severalfold excess of (*R*)-TFAE, an (*S*)-enriched sample of lactone **38a** shows lowfield nonequivalence for the benzyl methylene hydrogens and highfield nonequivalence for the methyl group, in accord with the model. However (*S*)-enriched samples of the nitrated lactones afford different results not predicted by the usual model (solvates **39**). The senses of methyl nonequivalence for



(*R*,*S*)−**39**



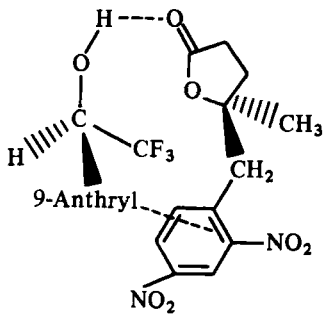
(*R*,*R*)−**39**

these lactones are inverted and are the same as the sense of the benzyl methylene groups. This behavior is ascribed to an additional attractive π-π interaction between the nitrated aromatic substituent of the lactone and the fluoroalcohol anthryl substituent. This third interaction does little to alter the structure of the (*R*,*R*)-solvate, since both secondary interactions may occur simultaneously, but it offers an alternative conformation (*R*,*S*-**40**) to the (*R*,*S*)-solvate, which may well compete with the expected conformation (*R*,*S*)-**39**. Population of conformer (*R*,*S*)-**40** at the expense of (*R*,*S*)-**39** (the conformation expected to provide the shielding responsible for the "normal" upfield sense of methyl nonequivalence) is probably the cause of the "inverted" senses of nonequivalence shown by the methyls of the nitroaryl lactones. From solvates **39** and **40**, it is evident that the (*R*,*R*)-solvate can simultaneously experience three bonding interactions, whereas the (*R*,*S*)-solvate can simultaneously experience but two. Such reasoning leads one to anticipate that the former will be the more stable. This stability difference may be demonstrated in several ways. The ^{13}C nonequivalence (discussed

Table 9
Fluoroalcohol-Induced Nonequivalence of Nitrolactones[a]

Lactone					Nonequivalence (ppm)[b] and Sense[c]						
							Ar				
Compound	R	*n*	Ar	AC[d]	R	CH_2	H_2	H_3	H_4	H_5	H_6
38a	CH_3	1	Ph	*S*	0.07 (H)	0.03 (L)	–	–	–	–	–
38b	CH_3	1	*o*-$NO_2C_6H_4$	*S*	0.04 (L)	0.08 (L)	–	–	–	–	–
38c	CH_3	1	*p*-$NO_2C_6H_4$	*S*	0.02 (L)	0.08 (L)	–	–	–	–	–
38d	CH_3	1	*o,p*-$(NO_2)_2C_6H_3$	*S*	0.02 (L)	0.11 (L)	–	–	–	–	0.20 (L)
38e	H	0	*o,p*-$(NO_2)_2C_6H_3$	*S*	0.13 (L)	–	–	0.03 (L)	–	0.22 (L)	0.22 (L)

[a]Data from refs. 33 and 75.
[b]2–4 Equivalents (*R*)-(-)-TFAE in CCl_4.
[c](H), highfield; (L), lowfield.
[d]Configuration of solute.

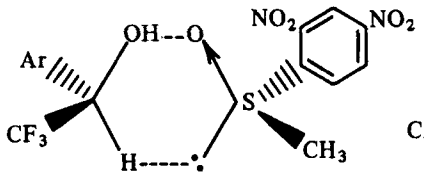


(*R,S*)—**40**

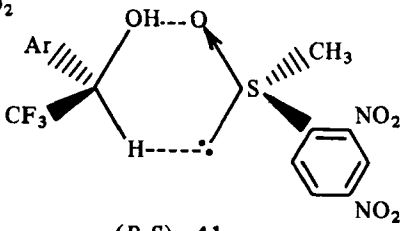
further in Sect. IV-F), provides circumstantial evidence for this hypothesis. Chromatography of the racemic nitroaryllactones on silica using a carbon tetrachloride solution of (*R*)-TFAE *as eluent* gives (*S*)-enriched samples of these lactones in the low-R_f fractions. This elution order would be expected if the mechanism of chromatographic resolution reflected the relative stabilities of the two diastereomeric solvates.

Differential stability of these solvates has also been demonstrated by NMR through use of an *achiral* lanthanide shift reagent *in conjunction with* TFAE. Incremental addition of $Eu(fod)_3$ to a solution of (*R*)-TFAE and the dinitrolactone shifts the resonances of the (*S*)-enantiomer more rapidly downfield than those of the (*R*)-enantiomer. Nonequivalence increase in this manner arises by a preferential disruption of the least stable (*R,S*) solvate. In the case of the nonnitrated parent, addition of the LSR gradually attenuates nonequivalence, as both solvates (of approximately equal stability) are equally disbanded.

This LSR-CSA technique (discussed in detail in ref. 76) has also been applied to a series of sulfoxides. Nitroarylsulfoxides are also capable of a strong three-point interaction with fluoroalcohols **1**, an ability that is responsible for a considerable difference in stability between the solvates. Mixtures of **1d** and 2,4-dinitrophenyl methyl sulfoxide are red, and the intensity of this color is inversely proportional to temperature, consistent with formation of π-π complexes. Crystallization of the racemic sulfoxide from carbon tetrachloride solutions of (*R*)-**1d** leaves mother liquor enriched in the (*R*)-sulfoxide enantiomer, that predicted by the usual solvation model (41), to form the more stable solvate. With this compound it is also apparent that the (*R,S*)-solvate may differ considerably from the predicted conformation, by population of **42**. This additional interaction,



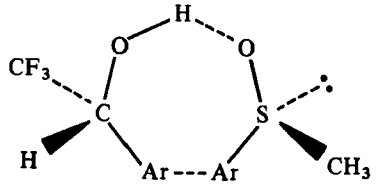
(*R,R*)−**41**



(*R,S*)−**41**

however, does not cause the nonequivalence sense of the (*S*)-methyl resonance to deviate from "normality". Figure 5 shows the nonequivalence behavior of various nearly racemic sulfoxides in the presence of **1e**, as a function of added LSR. Nonequivalence of methyl trideuteriomethyl sulfoxide, chiral by virtue of isotopic substitution, is attenuated completely after addition of about 1 equiv of LSR, indicative of the similar stability of the solvates and the much higher affinity of the sulfoxide for the LSR than for the CSA. The behavior of the other sulfoxides belies a complicated set of interrelated nonequivalence mechanisms (76), but a common feature is present: a minimum occurs when the LSR concentration equals that of the enantiomer forming the least stable solvate. The shape of each curve reflects the differential ability of the LSR to remove sulfoxide from the least stable solvate and is related to the nonidentical energies of solvation of the sulfoxide enantiomers. The nitrophenyl sulfoxides exhibit the largest differences in solvate stability.

In general, the observation of opposite senses of nonequivalence for substituents on opposite faces of the plane defined by primary and secondary interactions will be the hallmark of a normal solvation model. Deviations are of no consequence for enantiomeric purity determinations but should raise questions concerning the validity of the usual model for the assignment of absolute configuration based on the observed senses of nonequivalence. Since knowledge of solute structure often allows anticipation of such "third interactions,"



(*R,S*)−**42**

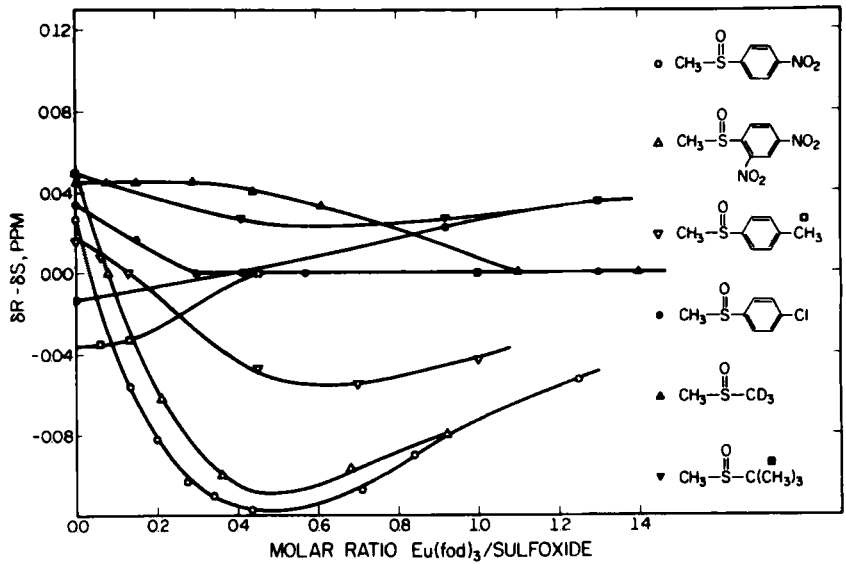


Figure 5. The influence of $Eu(fod)_3$ concentration on the magnitudes and senses of nonequivalence of several methyl sulfoxides (0.2*M*) in the presence of (*R*)-ld. Reprinted with permission from *J. Org. Chem.* 1975, *40*, 3430-3434. Copyright by the American Chemical Society.

rational interpretation of observed senses of nonequivalence is often possible even when these deviations occur.

When NMR assignment of absolute configuration is desired, the strong three-point interaction is generally unwelcome. Such chiral recognition on an energetic basis, however, is fundamental to asymmetric reactions and to the direct chromatographic separation of enantiomers. Several groups have employed NMR in the study and development of methods for separating optical isomers (73,74,77, 78,82). Chromatographic and partitioning methods exploiting diastereomeric interactions of the same types discussed in this chapter are especially valuable both for their practical applications and for the different vantage point they provide for studying chiral recognition.

F. Nonequivalence in Nuclei Other Than ^1H

Table 10 lists reported CSA-solute combinations for which nonequivalence has been observed in ^{19}F, ^{31}P, ^{13}C, and ^{15}N nuclei. Anisotropic shielding of a given nucleus "remains essentially constant (in ppm) no matter what nucleus is being considered" (84). Since

Table 10
Nonequivalence in Nuclei Other than Hydrogen

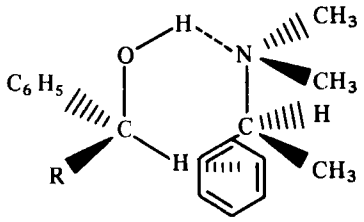
Nucleus	CSA	Solute	Ref.
^{13}C	*N,N*-Dimethyl PEA	ArCHOHR	79
^{13}C	TFAE	Lactone **38d**	75
^{13}C	Cyclo-(L-ProGly)$_n$ Peptides	α-Amino ester salts	80
^{13}C	L-Valine, L-leucine ureides	o-$C_2H_5C_6H_4NHCOOCF_3$	81
^{13}C	Carbohydrate-derived crown ethers	PEA-HPF_6	82
^{13}C	NEA	Phosphorus thioacids	17
^{15}N	β-Cyclodextrin and various acids	8-Benzyl-5,6,7,8-tetrahydroquinoline	18
^{19}F	PEA, NEA	$ArCHOHCF_3$, $RCHOHCF_3$	3, 28
^{19}F	TFNE	$PhCHNH_2CF_3$	30
^{19}F	NEA	$Ph(CF_3)COHCOOCH_3$	54
^{19}F	NEA	c-$C_6H_{11}CF_3COHCOOCH_3$	53
^{19}F	NEA	$RCHOHCF_3$	12
^{31}P	PEA	Phosphorus thioacids	17, 61
^{31}P	TFPE	Pyrophosphoramides	83

chemical shifts of these nuclei appear over a much wider range than those of protons, the relative contribution of anisotropic shielding by the CSA to the chemical shifts of solute nuclei diminishes.

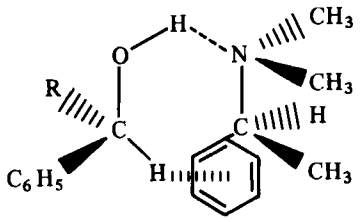
Only fluorine and carbon nuclei have been studied in combinations for which solvation modes are understood. Fluorine appears to be the more well behaved. NEA-induced nonequivalence senses in fluorine nuclei of trifluoromethylarylcarbinols are correctly predicted by the "usual" solvation model (Sect. IV-C) (28).

^{13}Carbon nonequivalence induced by *N,N*-dimethyl PEA in various halomethylarylcarbinols has been suggested to arise by differential crowding of the carbinol *R* substituent by the methyl group of the CSA in solvates **43** (79). Accordingly, nonequivalence magnitudes for the halomethyl carbons parallel the size and polarizability of the halogen substituents. Where configurations were known, this halomethyl resonance originating from the (*R,S*)-solvate was at higher field than that of the (*S,S*)-solvate; and opposite senses of nonequivalence were observed for the C_1 aromatic resonances. In only one instance was nonequivalence at the asymmetric carbon observed.

(*S*)-enriched dinitrobenzyl lactone **38d** (Sect. IV-E), in the presence of a severalfold excess of (*R*)-TFAE, shows nonequivalence in every carbon except that of the methyl group (Table 11). Only the carbonyl and carbinyl carbons are shifted downfield, consistent with a lowering of electron density resulting from hydrogen and carbinyl hydrogen



(*R*,*S*)−**43**



(*S*,*S*)−**43**

bonding to the adjacent oxygens. The lowfield sense of nonequivalence shown by all carbons in the 2,4-dinitrobenzyl substituent is in accord with a greater degree of diamagnetic shielding and electron donation by π-π complexing in the (*R*,*R*)-solvate. The highfield nonequivalence shown by carbonyl, α-, β-, and γ-carbons also suggests greater hydrogen bonding and CHB for this solvate.

The origin of the correlation reported for phosphorus nonequivalence in diastereomeric phosphorthioic acid salts (17,61) is unclear. A direct anisotropic effect of the CSA aromatic substituent on the

Table 11
^{13}C NMR Nonequivalence of (*S*)-(+)-Enriched **38d** in the Presence of (*R*)-TFAE[a]

Carbon	Δppm[b]	Nonequivalence Magnitude (Hz at 25.2 MHz) and Sense[c]
C=O	+2.469	8.62 (H)
α	-0.571	1.98 (H)
β	-0.285	Shoulder (H?)
γ	+1.134	4.66 (H)
$-CH_3$	-1.035	0.0
Benzyl	-1.009	4.13 (L)
Aromatic[d]		
C_1	-0.846	4.13 (L)
C_2	-1.052	4.12 (L)
C_3	-0.553	3.05 (L)
C_4	-0.871	4.67 (L)
C_6	-0.842	3.24 (L)

[a] Data from ref. 75.
[b] Difference in presence and absence, respectively, of TFAE (in CCl_4).
[c] (H), highfield; (L), lowfield.
[d] C_5 not assignable.

resonance of the single asymmetric atom is intuitively minimal, and this correlation may well reflect a trend in differential dissociation of the diastereomeric salts into ion pairs (Sect. IV-C-2).

V. SELF-INDUCED NONEQUIVALENCE

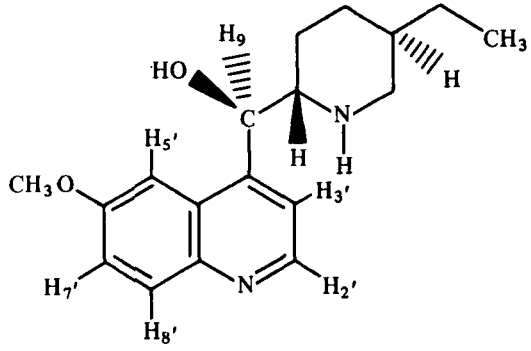
Partially resolved samples of certain compounds show enantiomeric NMR nonequivalence in an otherwise achiral medium, and do so in magnitudes proportional to their enantiomeric purity. This phenomenon, termed "self-induced nonequivalence" or "autononequivalence," has been observed for compounds shown in Table 12. Dihydroquinine (44) was the first of these examples to be reported (14). Figure 6 shows portions of the 100 MHz spectra of optically pure, naturally occurring dihydroquinine, a 1:1 mixture of the natural product and synthetic racemate, and the racemate alone, all at approximately the same concentration in $CDCl_3$ solution. The three spectra are different; Figure 6b shows nonequivalence for the $H_{2'}$, $H_{3'}$, $H_{8'}$, and H_9 resonances, the intensities corresponding to the optical purity of the sample (33%, e.e.).

In such cases the CSA is the solute itself. By external comparison, solute enantiomers A and A′ are in different average environments,

Table 12
Compounds Showing Self-Induced Nonequivalence

Compound[a]	Ref.
Dihydroquinine **(44)**	14
1d	24
$Ph(C\underline{H}_3)P(O)NHR$(R=H,Ph,*p*-$NO_2C_6H_4$)	70
$Ph(C\underline{H}_3)P(S)OH$	71
$pH(C\underline{H}_3)_3P(S)OH$	71
o-$HOCH_2C_6H_4S(O)C\underline{H}_3$	85
o-$HOC(C\underline{H}_3)_2C_6H_4S(O)Ph$	86
$HO_2CC\underline{H}_2C(CH_3)(C_2H_5)COOH$	1
$HO_2CC\underline{H}_2C(CH_3)(CH(CH_3)_2)COOH$	1
$C_2H_5O(CH_3)P(Y)SCH_2C(O)N(R)CH(CH(CH_3)_2)COX$	87
Y, R, X = S, H, OH; S, H, OC_2H_5; S, CH_3, OH; S, CH_3, OC_2H_5; O, H, OH; O, H, OC_2H_5	

[a] Nonequivalence in underlined nuclei.



44

since they are associated predominantly with major enantiomer A,

$$A + A \rightleftharpoons AA \qquad [14]$$

$$A' + A \rightleftharpoons A'A \qquad [15]$$

and for reasons cited earlier, different signals may be observed for each. As the enrichment of such a sample increases, both the intensity of the major resonance (relative to the minor one) and the nonequivalence between them ($\Delta\delta$) increase.

Decreasing the enantiomeric purity of the enriched sample causes the nonequivalent resonances to tend toward equality in intensity (as the sample approaches racemic composition) and to approach one another (as the nonequivalence magnitude decreases). As evidenced by Figures 6*a* and 6*c*, the chemical shifts for the nuclei in the racemic and enantiomerically pure material need not be identical.

Observed senses of nonequivalence for the various resonances of compounds in Table 12 are *not* dependent on which enantiomer is in preponderance. Inverting the predominant configuration of the sample inverts the configuration of both "CSA" and "solute," leaving this observation unchanged. Absolute configuration therefore cannot thereby be assigned, unless a configurationally known sample of the same substance is available for addition to the unknown. In this event, after each of two incremental additions, spectra must be taken, the second to ascertain whether the resulting decrease (or increase) in enantiomeric purity after the first addition has been accompanied by a net inversion of configuration.

The lowfield sense of nonequivalence for the methyl doublet of methylphenylphosphinothioic acid studied by Harger (71) is readily

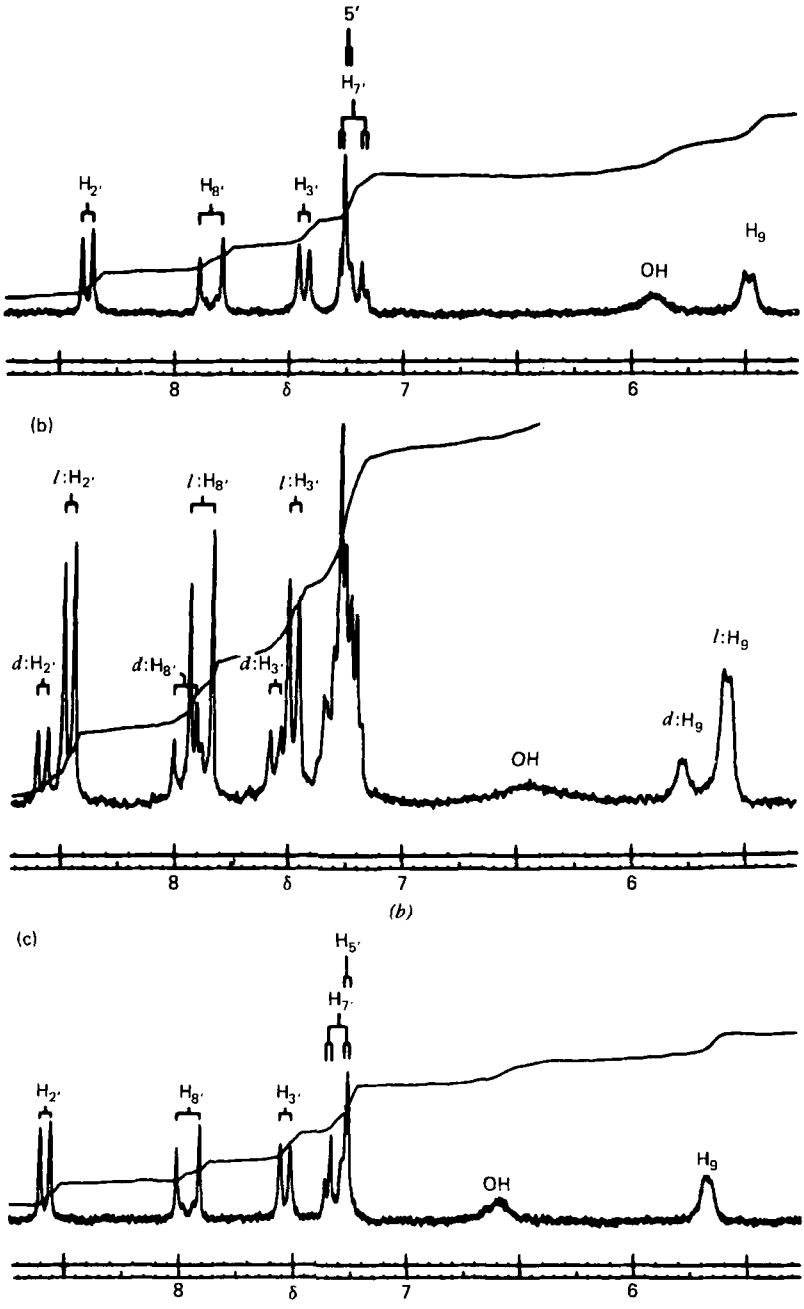
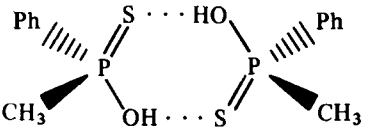
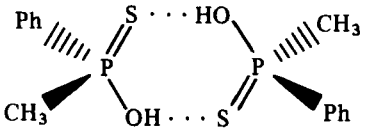


Figure 6. Portion of the 100 MHz NMR spectra of (*a*) natural (-)-dihydroquinine (0.36*M*), (*b*) an artificial 1 : 1 mixture of racemic and natural (-)-dihydroquinine (0.27*M*), and (*c*) racemic dihydroquine (0.35*M*) in $CDCl_3$ solution. Reprinted with permission from *J. Am. Chem. Soc.* **1969**, *91*, 1871-1872. Copyright by the American Chemical Society.

understood in terms of solvates 45, illustrated for the (*S*)-enriched case. Both enantiomers will on the average be associated with a molecule of the (*S*)-configuration, the methyl group of the *R* (minor) enantiomer being the more shielded. The behavior of other phosphinothioic acids and amides has been similarly rationalized (70,71). Since other entries in Table 12 contain both acidic and basic sites, "two-point" interactions can be reasonably expected to occur in these cases as well.



(*S,S*)—45



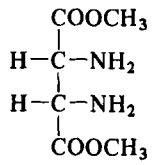
(*S,R*)—45

The dependence of this phenomenon on temperature and concentration has been studied in detail (70,71,87) and treated mathematically (87). In principle any compound capable of self-association might be capable of self-induced nonequivalence. These cases should be sufficient to suggest due caution on the part of those who would establish the identity of a racemate (e.g., a synthetic "natural product"), by comparison of its NMR spectrum with that of the naturally derived optically pure substance. This phenomenon is not restricted to solutes with aromatic substituents, as evidenced by Table 12. Self-induced nonequivalence may be eliminated by addition of polar solvents or by dilution of the sample. Under these conditions, as has been shown for dihydroquinine (14), spectra of racemic, optically pure, and enriched material become identical.

VI. MISCELLANEOUS APPLICATIONS

CSAs have found stereochemical applications in areas other than those of enantiomeric purity and absolute configuration determination.

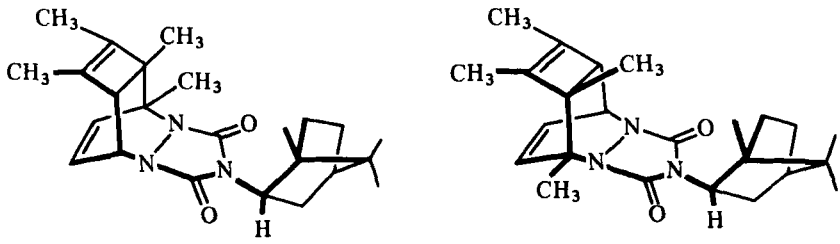
As mentioned in Sect. IV-B, enantiotopic groups even in achiral substances may show nonequivalence. For example, this property sometimes can be used to distinguish meso compounds from their chiral isomers. Thus in the presence of TFPE, the meso isomer of dimethyl 2,3-diaminosuccinate (46) shows two equally intense methoxy singlets and an AB quartet for the now diastereotopic methine hydrogens (88). This coupling clearly shows 46 to be the



46

meso isomer. The racemate would show at most two lines for the methine resonance (a singlet for the methine protons of each enantiomer), since these nuclei within each enantiomer are enantiotopic, hence isochronous, even in the presence of CSA. Thus, no coupling is observed. The meso-*dl* assignment cannot be made if only uncoupled signals (e.g., those of the methoxy groups) are considered.

In principle, separation of resonances of diastereomeric compounds (such as *dl* and meso isomers) may be increased simply through use of an appropriate *achiral* solvent. Chiral solvents may in some cases be especially effective in producing a separation, particularly if the diastereomers differ in configuration about a center that is amenable to analysis by the CSA method. Kaehler and Rehse (89) give a detailed account of conditions necessary for measurement of the ratio of *meso*- and *dl*-tartaric acid employing *N,N*-dimethyl PEA. Bornyl acetate used as solvent for 1,2-difluoro-1,2-dichloroethane (90) allows ^{19}F measurement of the diastereomeric composition. Paquette and co-workers (91,92), using TFAE, were able to determine the diastereomeric purity of the recrystallized adducts 47 of

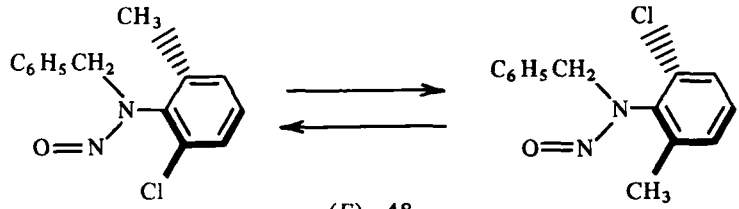


47

(–)-*endo*-bornyltriazolindione and 1,2,3,4-tetramethylcyclooctatetraene, thereby monitoring the resolution of this olefin. Joesten (83), using TFPE, observed phosphorus nonequivalence in several diastereomeric pyrophosphoramides.

A number of compounds cannot be obtained in an enantiomerically enriched state because of their rapid racemization at ambient temperatures. Although their chirality cannot be proved by optical

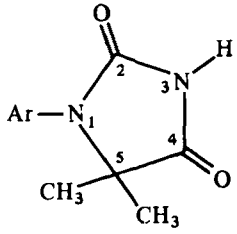
methods, it can be demonstrated by NMR using an appropriate CSA. For example, the enantiomers of both the (*E*)- and (*Z*)-isomers of *N*-nitrosoamine **48** interconvert rapidly by rotation about the *N*-aryl



(*E*)—**48**

bond. Mannschreck has shown (69,93) that in the presence of (+)-TFPE the enantiomers of both isomers are distinguishable. By measuring nonequivalence as a function of temperature, one can measure rates of racemization on *racemic samples*. These workers use this approach to determine the barriers to rotation about the *N*-aryl bond of the (*E*)-enantiomers of **48**. Since nonequivalence magnitudes almost always increase as temperature is lowered, the appearance of enantiomeric nonequivalence for interconverting enantiomers below a certain "coalescence" temperature may stem either from "freezing out" the interconversion of enantiomers or from increased population of the nonequivalence-engendering conformers of the diastereomeric solvates. Mannschreck minimized this ambiguity by using different CSAs, each of which afforded essentially the same rotational barriers.

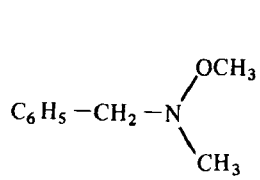
Similarly, TFPE was used in measuring the rotational barriers to interconversion of the enantiomers of several 1-arylhydantoins **49** (94). The free energies of activation thus measured (18–21 kcal/mol) were in accord with those obtained by measurement of the coalescence temperatures of the diastereotopic methyl protons. When CSAs are employed in this capacity, the presence of diastereotopic



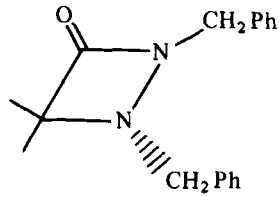
49

	Ar
49a	2-Methylphenyl
49b	2,3-Dimethylphenyl
49c	2,4-Dimethylphenyl
49d	2,5-Dimethylphenyl

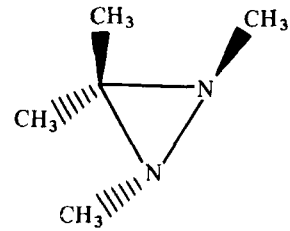
nuclei in the substrate is not required. The enantiomers of methoxylamine **50** (35), diazetidinone **51** (69), and diaziridine **52** (68), all rapidly interconverting at ambient temperature, have been observed by NMR in the presence of various CSAs.



50

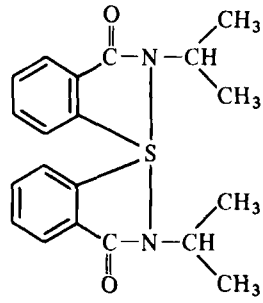


51



52

CSAs may also be valuable in providing proof of chirality as structural support for novel or unknown compounds. Martin and coworkers (95) have demonstrated the chirality of various sulfuranes, such as **53**, by observing their nonequivalence in the presence of TFPE and TFAE.



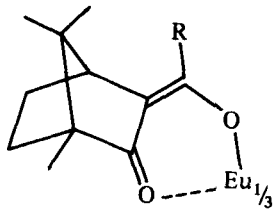
53

VII. COMPARISON OF CSAs AND CLSRs

The use of chiral lanthanide shift reagents (CLSRs) for NMR enantiomeric purity determination has become very popular (6) since the first of these compounds (**54a**) was reported by Whitesides and Lewis (96). Reagents **54b** [$Eu(hfbc)_3$ or $Eu(hfc)_3$] and **54c** [$Eu(facam)_3$ or $Eu(tfc)_3$] subsequently independently introduced by Fraser (97) and Goering (98), are most widely used, and are commercially available.

The CLSRs unquestionably are of broader scope than are CSAs in

enantiomeric purity determination. The advantage of the former is their ability to induce generally much larger nonequivalence in enantiomeric solutes. Table 13 compares nonequivalence magnitudes of several representative solutes for CLSRs **54** and several fluoro-



54

R
54a *t*-Butyl
54b $CF_2CF_2CF_3$
54c CF_3

alcohol CSAs. This difference is especially advantageous for solutes lacking singlet resonances, since complete separation of complex multiplets may often be achieved. The CLSRs will be also more generally applicable to enantiomeric purity determination in monofunctional or very weakly basic solutes, where CSAs often fail to induce nonequivalence, though as discussed in Sect. III-B-3, CSAs are not necessarily unsuited for such solutes.

The relative effects of CLSRs and CSAs on solute spectral behavior differ dramatically. Figures 7 and 8 illustrate these effects for 2-phenyl-2-butanol. With a CLSR (Fig. 7), separation of resonances of enantiotopic nuclei is accompanied by a large downfield shift of the same general magnitude as observed for achiral paramagnetic LSRs (100) (or upfield with the praseodymium analogs). Since

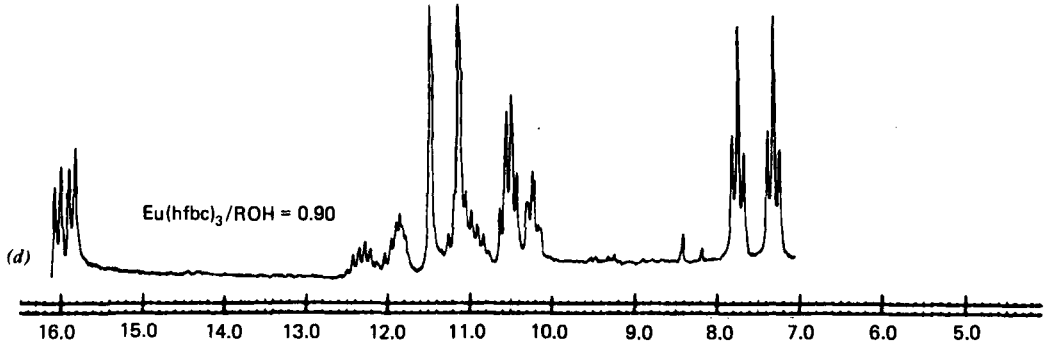
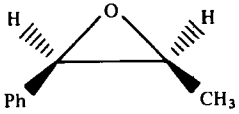


Figure 7. NMR spectrum of *dl*-2-phenyl-2-butanol in CCl_4 in the presence of CLSR **54b**(60 MHz). The downfield doublets are the resonances of the *ortho*-aromatic protons. Reprinted with permission from *J. Am. Chem. Soc.* **1974**, *96*, 1493–1501. Copyright by the American Chemical Society.

Table 13
Comparison of CLSR- and CSA-Induced Nonequivalence for Certain Solutes

Solute	Nucleus	CLSR	$\Delta\delta$ (ppm)[a]	CSA	$\Delta\delta$ (ppm)[b]
$PhCH(NH_2)CH_3$	CH	**54c**	0.18	**1d**	0.10
	CH_3		0.92		0.03
$CH_3CH(NH_2)COOCH_3$	CH	**54c**	0.26	**1e**	0.06[c]
	CH_3		0.06		0.05
	OCH_3		0.05		0.03
PhCHDOH	CH	**54b**	0.15	**1d**	0.05
$PhCH(OH)CH_3$	CH	**54b**	0.07	**1d**	0.09
	CH_3		0.05		0.02
$PhCH(OH)C(CH_3)_3$	CH	**54b**	0.09	**1e**	0.15[c]
	CH_3		0.14		0.03
$CH_3CH(OH)CH_2CH_3$	$CHCH_3$	**54b**	0.06	**1c**	0.01[d]
	CH_2CH_3		0.00		0.01
	CH_3	**54c**	0.27	**1a**	0.02
Styrene oxide	α-H	**54b**	0.31	**1a**	0.04[e]
	trans-β-H		0.75		0.01
	cis-β-H		0.15		0.01

[a] Data from Ref. 6.
[b] Data from Table 3 unless otherwise indicated.
[c] Ref. 24.
[d] Ref. 51.
[e] Ref. 49.

resonances nearest the basic site are more highly shifted, these may cross over less affected signals. With a diamagnetic CSA (Fig. 8) only small upfield shifts (ca. 0.5 ppm) are usually encountered.

Nonequivalence magnitude with CLSRs are critically dependent on the ratio of CLSR to substrate and do not typically maximize with excess CLSR; a decrease is usually observed past a certain ratio. This critical ratio varies considerably for different solutes and may occur in some instances at very low (<0.1 equiv) CLSR levels. More effort is thus generally required to optimize the CLSR experiment, both in carefully controlling the addition of CLSR, and in obtaining repetitive spectra, to keep track of the highly shifted resonances. Comparison of the configurations of two samples is also a more difficult task with CLSRs, since care must be taken to employ the same ratios of CLSR to solute when comparing the nonequivalence sense

of two samples. Since both CLSR enantiomers are not readily available, comparing nonequivalence senses for highly enriched samples is likely to be an insurmountable problem if both solute enantiomers are not available.

The broadening of solute resonances with increased amounts of additive is a problem inherent in the CLSR (but not the CSA) technique. As discussed in Sect. III-D, this prevents e.e. determination by peak height measurement, since the CLSR generally differentially broadens enantiomer resonances, and requires complete separation of the signals. In contrast, broadening with CSA, when observed, leads to only a minor loss of spectral resolution due to increased viscosity or to an increased average molecular size (because of solvate formation), which is equal for both enantiomers. Thus, smaller nonequivalence magnitudes suffice for e.e. determination by the CSA method.

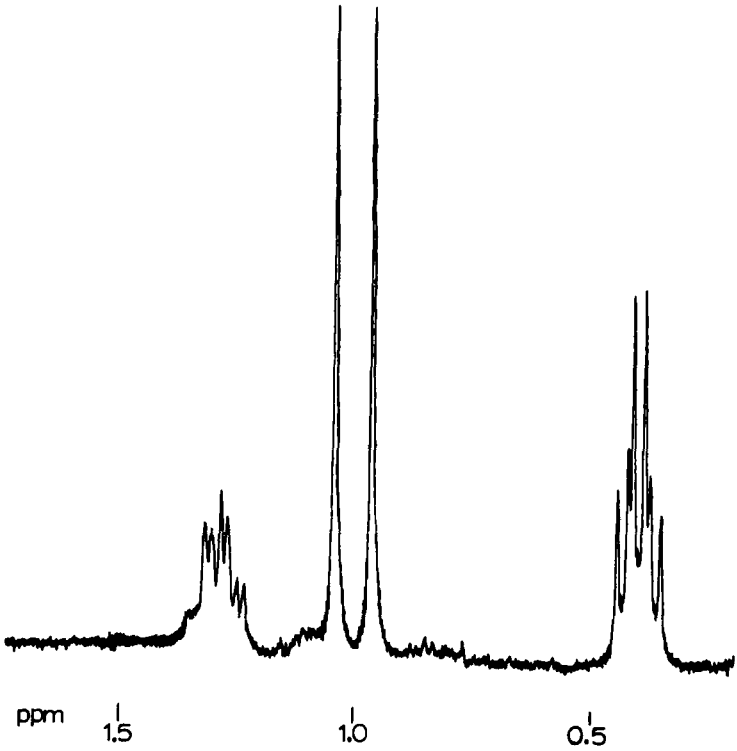


Figure 8. Upfield portion of the NMR spectrum of 2-phenyl-2-butanol (racemic) in benzene solution saturated with CSA (*R*)-TFAE (220 MHz).

CLSR proton resonances (generally 1 to −1 ppm) seldom obscure those of the solute. Resonances of various CSAs may overlap some solute signals, especially in the aromatic region.

In contrast to the CLSRs, which are hygroscopic and require the use of dry solvents,* CSAs require no special care in storage or handling although exposure of TFAE to strong light should be avoided, and amines **2** should be stored in an inert atmosphere to prevent carbamic acid formation. Chromatography of collected samples for fluoroalcohol (or substrate) recovery is routine, as are D_2O exchanges performed directly in the NMR tube.

For enantiomeric purity determination, the CSA and CLSR techniques are complementary. When both methods work for a given solute, the CSA method is the more easily implemented.

CLSRs are inferior to CSAs for assignment and comparison of absolute configuration. Nonequivalence induced by CLSR originates by a variety of mechanisms. Whitesides (96), noting the same sense of nonequivalence for all resonances of enriched PEA with CLSR **54a**, suggested that a difference in stabilities of the complexes, with a greater shift for the amine resonances of the more stable complex, might account for nonequivalence. Goering (98) suggested that an intrinsic spectral difference was responsible for opposite senses of nonequivalence for different sets of nuclei in the same molecule. Both groups of investigators later concurred in the view that both mechanisms contribute and that the relative importance of each depends on CLSR, solute, and conditions (102, 103).

Whitesides and Goering additionally presented evidence for the presence of 2:1 or higher substrate-CLSR adducts. Differential formation constants of higher adducts plus the possibility of intrinsic spectral nonequivalence of such species are additional mechanisms that may contribute to overall nonequivalence. The behavior of the enantiotopic methyl resonances of dimethyl sulfoxide, where nonequivalence varies unpredictably with CLSR-substrate ratio, presumably inverting in sense, illustrates this complication, insofar as nonequivalence cannot in this case originate from a difference in association constants (103). In any event, use of large excess of CLSR to minimize the effects of differences in formation constants and stoichiometry is not an attractive alternative, because nonequivalence is not necessarily optimum and line broadening generally becomes severe.

*Granot and Reuben report an example of an "aqueous chiral shift reagent." In water, several proton resonances of norepinephrine exhibit nonequivalence in the presence of cobaltous adenosine-5′-triphosphate (101).

The picture of the CLSR-solute interaction is further complicated by the structural uncertainty of the CLSR. Four diastereomers are possible for octahedral complexes with three dibentate ligands (104) which, in the case of CLSR, rapidly interconvert on the NMR time scale (105). The configurational composition of the europium need not be the same in the solute complexes, and the shielding exerted by differing configurations need not be similar (106).

Nevertheless, correlations have been found in four β-hydroxyesters (107), eight aminoesters (108), primary α-deuterioalcohols (109), and secondary carbinols (110). Even in a closely related series, exceptions have been found (110) in search of a predictable pattern. A study of nonequivalence in methyl alkyl sulfoxides with CLSR **54c** (48) revealed a diminution of nonequivalence on increasing alkyl bulk with an inversion of sense between *n*-propyl and isopropyl. Changes in nonequivalence sense in several cases with different CSA-solute ratios were also observed. Presently, these CLSR configurational correlations remain totally empirical.

We concur with Whitesides (111) that in view of the complexity of lanthanide-solute systems, CLSR correlations are likely to prove neither general nor reliable, and with Mosher (110) in asserting that this technique should not be applied outside a closely related series of compounds. Even when proper precautions are taken, configurations assigned by the CLSR method should not be held above suspicion.

REFERENCES

1. Horeau, A.; Guetté, J. P. *Tetrahedron* **1974**, *30*, 1923–1931.
2. Raban, M.; Mislow, K. *Tetrahedron Lett.* **1965**, 4249–4253.
3. Pirkle, W. H. *J. Am. Chem. Soc.* **1966**, *88*, 1837.
4. Ejchart, A.; Jurczak, J. *Wiad. Chem.* **1970**, *24*, 857–872.
5. Raban, M.; Mislow, K. *Top. Stereochem.* **1967**, *2*, 199–230.
6. Sullivan, G. R. *Top Stereochem.* **1978**, *10*, 287–329.
7. Dale, J. A.; Dull, D. L.; Mosher, H. S. *J. Org. Chem.* **1969**, *34*, 2543–2549. Dale, J. A.; Mosher, H. S. *J. Am. Chem. Soc.* **1968**, *90*, 3732–3738; *ibid.* **1973**, *95*, 512–519.
8. Pirkle, W. H.; Simmons, K. A.; Boeder, C. W. *J. Org. Chem.* **1979**, *44*, 4891–4896. Pirkle, W. H.; Hauske, J. R. *ibid.* **1977**, *42*, 1839–1844.
9. Aldrich Chemical Co., Milwaukee, WI.
10. Mislow, K.; Raban, M. *Top. Stereochem.* **1967**, *1*, 1–38.
11. Pirkle, W. H.; Beare, S. D. *J. Am. Chem. Soc.* **1969**, *91*, 5150–5155.
12. Pirkle, W. H.; Burlingame, T. G. *Tetrahedron Lett.* **1967**, 4039–4042.

13. Burlingame, T. G., Ph.D. Dissertation, University of Illinois, Urbana, 1968.
14. Williams, T.; Pitcher, R. G.; Bommer, P.; Gutzwiller, J.; Uskokovic, M. *J. Am. Chem. Soc.* **1969**, *91*, 1871–1872.
15. Jochims, J. C., Taigel, G.; Seeliger, A. *Tetrahedron Lett.* **1967**, 1901–1908.
16. Anet, F. A. L.; Sweeting, L. M.; Whitney, T. A.; Cram, D. J. *Tetrahedron Lett.* **1968**, 2617–2620.
17. Mikołajczyk, M.; Omelanczuk, J.; Leitloff, M.; Drabowicz, J.; Ejchart, A.; Jurczak, J. *J. Am. Chem. Soc.* **1978**, *100*, 7003–7008.
18. Dyllick-Brenzinger, R.; Roberts, J. D. *J. Am. Chem. Soc.* **1980**, *102*, 1166–1167.
19. Pirkle, W. H.; Beare, S. D.; Muntz, R. L. *Tetrahedron Lett.* **1974**, 2295–2298.
20. Stewart, R.; van der Linden, R. *Can. J. Chem.* **1960**, *38*, 399–406.
21. Pirkle, W. H.; Beare, S. D. *J. Am. Chem. Soc.* **1968**, *90*, 6250–6251.
22. Pirkle, W. H.; Hoekstra, M. S. *J. Am. Chem. Soc.* **1976**, *98*, 1832–1839.
23. Balasubramanian, V. *Chem. Rev.* **1966**, *66*, 567–641.
24. Pavlin, M. S., Ph.D. Dissertation, University of Illinois, Urbana, 1977.
25. Snatzke, G.; Fox, J. E.; El-Abadelah, M. M. *Org. Magn. Reson.* **1973**, 413–417.
26. Ogston, A. G. *Nature (London)* **1948**, *162*, 963.
27. Pirkle, W. H.; Hauske, J. R. *J. Org. Chem.* **1976**, *41*, 801–805.
28. Pirkle, W. H.; Beare, S. D. *J. Am. Chem. Soc.* **1967**, *89*, 5485–5487.
29. Pirkle, W. H.; Pavlin, M. S. *J. Chem. Soc., Chem. Commun.* **1974**, 274–275.
30. Pirkle, W. H.; Burlingame, T. G.; Beare, S. D. *Tetrahedron Lett.* **1968**, 5849–5852.
31. Pirkle, W. H.; Hoover, D., unpublished observations.
32. Pirkle, W.; Boeder, C. W. *J. Org. Chem.* **1977**, *42*, 3697–3700.
33. Pirkle, W. H.; Sikkenga, D. L.; Pavlin, M. S. *J. Org. Chem.* **1977**, *42*, 384–387.
34. Pirkle, W. H., unpublished observations.
35. Muntz, R. L., Ph.D. Dissertation, University of Illinois, Urbana, 1972.
36. Muntz, R. L.; Pirkle, W. H.; Paul, I. C. *J. Chem. Soc., Perkin Trans. II* **1972**, 483–488. Pirkle, W. H.; Muntz, R. L.; Paul, I. C. *J. Am. Chem. Soc.* **1971**, *93*, 2817–2819.
37. Pirkle, W. H.; Beare, S. D.; Muntz, R. L. *J. Am. Chem. Soc.* **1969**, *91*, 4575.
38. Pirkle, W. H.; Adams, P. E. *J. Org. Chem.* **1978**, *43*, 378–379.
39. Pirkle, W. H.; Adams, P. E. *J. Org. Chem.* **1979**, *44*, 2169–2175. Pirkle, W. H.; Adams, P. E., *J. Org. Chem.*, **1980**, *45*, 4117–4121.
40. Pirkle, W. H.; Rinaldi, P. L. *J. Org. Chem.* **1977**, *42*, 3217–3219, and references therein.
41. Pirkle, W. H.; Rinaldi, P. L. *J. Org. Chem.* **1978**, *43*, 4475–4480.
42. Forni, A.; Moretti, I.; Torre, G. *Tetrahedron Lett.* **1978**, 2941–2944.

43. Montanari, F.; Moretti, I.; Torre, G. *Gazz. Chim. Ital.* **1973**, *103*, 681–690.
44. Pirkle, W. H.; Rinaldi, P. L; Simmons, K. A. *J. Magn. Reson.* **1979**, *34*, 251–264.
45. Whitney, T. A.; Pirkle, W. H. *Tetrahedron Lett.* **1974**, 2299–2300.
46. Epstein, W. W.; Gaudioso, L. A. *J. Org. Chem.* **1979**, *44*, 3113–3117.
47. Moriwaki, M.; Yamamoto, Y.; Oda, J.; Inouye, Y. *J. Org. Chem.* **1976**, *41*, 300–303.
48. Sikkenga, D. L., Ph.D. Dissertation, University of Illinois, Urbana, 1976.
49. Moretti, I.; Taddei, F.; Torre, G. *J. Chem. Soc., Chem. Commun.* **1973**, 25–26.
50. Bucciarelli, M.; Forni, A.; Moretti, I.; Torre, G. *Tetrahedron* **1977**, *33*, 999–1002.
51. Pirkle, W. H.; Hoover, D. J., manuscript in preparation.
52. Hoover, D. J., Ph.D. Dissertation, University of Illinois, Urbana, 1980.
53. Beare, S. D., Ph.D. Dissertation, University of Illinois, Urbana, 1969.
54. Pirkle, W. H.; Beare, S. D. *Tetrahedron Lett.* **1968**, 2579–2582.
55. Ledaal, T. *Tetrahedron Lett.* **1968**, 1683–1688.
56. Mamlok, L.; Marquet, A.; Lacombe, L. *Tetrahedron Lett.* **1971**, 1039–1042.
57. Guetté, J.-P.; Lacombe, L.; Horeau, A. *C. R. Hebd. Seances Acad. Sci. Ser. C* **1968**, *267*, 166–169.
58. Horeau, A.; Guetté, J.-P. *C. R. Hebd. Seances Acad. Sci. Ser. C* **1968**, *267*, 257–259.
59. Ejchart, A.; Jurczak, J.; Bankowski, K. *Bull. Acad. Pol. Sci.* **1971**, *19*, 731–734.
60. Mikołajczyk, M.; Para, M.; Ejchart, A.; Jurczak, J. *J. Chem. Soc., Chem. Commun.* **1970**, 654.
61. Mikołajczyk, M.; Omelanczuk, J. *Tetrahedron Lett.* **1972**, 1539–1541.
62. Pirkle, W. H. *J. Chem. Soc., Chem. Commun.* **1970**, 1525–1526.
63. Buckson, R. L.; Smith, S. G. *J. Phys. Chem.* **1964**, *68*, 1875–1878.
64. Ejchart, A.; Jurczak, J. *Bull. Acad. Pol. Sci.* **1970**, *18*, 445–447.
65. Mikołajczyk, M.; Ejchart, A.; Jurczak, J. *Bull. Acad. Pol. Sci.* **1971**, *19*, 721–724.
66. Ejchart, A.; Jurczak, J. *Bull. Acad. Sci. Pol.* **1971**, *19*, 725–730.
67. Baxter, C. A. R.; Richard, H. C. *Tetrahedron Lett.* **1972**, 3357–3358.
68. Mannschreck, A.; Seitz, W. *IUPAC, 23rd Int. Congr. Pure Appl. Chem.* **1971**, *2*, 309–323.
69. Mannschreck, A.; Jonąs, V.; Kolb, B. *Angew. Chem. Int. Ed. Engl.* **1973**, *12*, 583–584; *Angew. Chem.* **1973**, *85*, 590–592.
70. Harger, M. J. P. *J. Chem. Soc., Perkin Trans. II* **1977**, 1882–1886; *J. Chem. Soc., Chem. Commun.* **1976**, 555–556.
71. Harger, M. J. P. *J. Chem. Soc. Perkin Trans. II* **1978**, 326–331.
72. Harger, M. J. P. *Tetrahedron Lett.* **1978**, 2927–2928.
73. Cram, D. J.; Helgeson, R. C.; Sousa, L. R.; Timko, J. M.; Newcomb, M.;

Moreau, P.; deJong, F.; Gokel, G. W.; Hoffman, D. H.; Domeier, L. A.; Peacock, S. C.; Madan, K.; Kaplan, L. *Pure Appl. Chem.* **1975**, *43*, 327-349. Cram, D. J.; Cram, J. M. *Acc. Chem. Res.* **1978**, *11*, 8-14.

74. Kyba, E. B.; Koga, K.; Sousa, L. R.; Siegel, M. G.; Cram, D. J. *J. Am. Chem. Soc.* **1973**, *95*, 2692-2693. Helgeson, R. C.; Timko, J. M.; Moreau, P.; Peacock, S. C.; Mayer, J. M.; Cram, D. J. *ibid.* **1974**, *96*, 6762-6763. Peacock, S. C.; Domeier, L. A.; Gaeta, F. C. A.; Helgeson, R. C.; Timko, J. M.; Cram, D. J. *ibid.* **1978**, *100*, 8190-8202. Kyba, E. P.; Timko, J. M.; Kaplan, L. J.; deJong, F.; Gokel, G. W.; Cram, D. J. *ibid.* **1978**, *100*, 4555-4568.
75. Pirkle, W. H.; Sikkenga, D. L. *J. Org. Chem.* **1977**, *42*, 1370-1374.
76. Pirkle, W. H.; Sikkenga, D. L. *J. Org. Chem.* **1975**, *40*, 3430-3434.
77. Pirkle, W. H.; Sikkenga, D. L. *J. Chromatogr.* **1976**, *123*, 400-404.
78. Pirkle, W. H.; House, D. W. *J. Org. Chem.* **1979**, *44*, 1957-1960. Pirkle, W. H.; House, D. W.; Finn, J. M. *J. Chromatogr.* **1980**, *192*, 143-158.
79. Pirkle, W. H.; Hoekstra, M. S. *J. Magn. Reson.* **1975**, *18*, 396-400.
80. Deber, C. M.; Blout, E. R. *J. Am. Chem. Soc.* **1974**, *96*, 7566-7568.
81. Lochmuller, C. H.; Harris, J. M.; Souter, R. W. *J. Chromatogr.* **1972**, *71*, 405-413.
82. Curtis, W. D.; King, R. M.; Stoddart, J. F.; Jones, G. H. *J. Chem. Soc., Chem. Commun.* **1976**, 284-285. Curtis, W. D.; Laidler, D. A.; Stoddart, J. F.; Jones, G. H. *J. Chem. Soc., Perkin Trans. I* **1977**, 1756-1769. Curtis, W. D.; Laidler, D. A.; Stoddart, J. F.; Jones, G. H. *J. Chem. Soc., Chem. Commun.* **1975**, 835-837.
83. Joesten, M. D.; Smith, H. E.; Vix, V. A. *J. Chem. Soc., Chem. Commun.* **1973**, 18-19.
84. Levy, G. C.; Nelson, G. L. "Carbon-13 Nuclear Magnetic Resonance for Organic Chemists"; Wiley: New York, 1972.
85. Pirkle, W. H.; Hoekstra, M. S.; unpublished observations.
86. Martin, J. C.; Balthazor, T. M.; private communication.
87. Kabachnik, M. I.; Mastryukova, T. A.; Fedin, E. I.; Vaisberg, M. S.; Morozov, L. L.; Petrovskii, P. V.; Shipov, A. E. *Usp. Khim.* **1978**, *47*, 1541-1564; *Russ. Chem. Rev.*, **1978**, *47*, 821-834; *Tetrahedron* **1976**, 1719-1728.
88. Kainosho, M.; Ajisaka, K.; Pirkle, W. H.; Beare, S. D. *J. Am. Chem. Soc.* **1974**, *94*, 5924-5926.
89. Kaehler, H.; Rehse, K. *Tetrahedron Lett.* **1968**, 5019-5022.
90. Abraham, R. J.; Siverns, T. M. *Org. Magn. Reson.* **1973**, *5*, 253-254.
91. Gardlik, J. M.; Paquette, L. A. *Tetrahedron Lett.* **1979**, 3597-3600.
92. Paquette, L. A.; Gardlik, J. M.; Johnson, L. K.; McCullough, K. J. *J. Am. Chem. Soc.* **1980**, *102*, 5026-5032.
93. Mannschreck, A.; Jonas, V.; Kolb, B. *Angew. Chem.* **1973**, *85*, 994-996; *Angew. Chem. Int. Ed. Engl.* **1973**, *12*, 909-910.
94. Colebrook, L. D.; Icli, S.; Hund, F. H. *Can. J. Chem.* **1975**, *53*, 1556-1562.
95. Adzima, L. J.; Chiang, C. C.; Paul, I. C.; Martin, J. C. *J. Am. Chem. Soc.* **1978**, *100*, 953-962. Martin, J. C.; Adzima, L. J. *J. Org. Chem.*, **1977**,

42, 4006-4016. Lam, W. Y.; Martin, J. C. *J. Am. Chem. Soc.* **1977**, *99*, 1659-1660.

96. Whitesides, G. M.; Lewis, D. W. *J. Am. Chem. Soc.* **1970**, *92*, 6979-6980.
97. Fraser, R. R.; Petit, M. A.; Saunders, J. K. *J. Chem. Soc., Chem. Commun.* **1971**, 1450-1451.
98. Goering, H. L.; Eikenberry, J. N.; Koermer, G. S. *J. Am. Chem. Soc.* **1971**, *93*, 5913-5914.
99. Montanari, F.; Moretti, I.; Torre, G. *Gazz. Chim. Ital.* **1974**, *104*, 7-15.
100. Hofer, O. *Top. Stereochem.* **1975**, *9*, 111-197.
101. Granot, J.; Reuben, J. *J. Am. Chem. Soc.* **1978**, *100*, 5209-5210.
102. McCreary, M. D.; Lewis, D. W.; Wernick, D. L.; Whitesides, G. M. *J. Am. Chem. Soc.* **1974**, *96*, 1038-1054.
103. Goering, H. L.; Eikenberry, J. N.; Koermer, G. S.; Lattimer, C. J. *J. Am. Chem. Soc.* **1974**, *96*, 1493-1501.
104. King, R. M.; Everett, G. W. *Inorg. Chem.* **1971**, *10*, 1237-1241.
105. Denning, R. G.; Rossoti, F. J. C.; Sellars, P. J. *J. Chem. Soc., Chem. Commun.* **1973**, 381-382.
106. Shapiro, B. L.; Hlubucek, J. R.; Sullivan, C. R.; Johnson, J. F. *J. Am. Chem. Soc.* **1971**, *93*, 3281-3285. Demarco, D. V.; Elzey, T. K.; Lenis, R. B.; Wenkert, E. *J. Am. Chem. Soc.* **1970**, *92*, 5734-5737, 5737-5739.
107. Dongala, E. B.; Solladie-Cavallo, A.; Solladie, G. *Tetrahedron Lett.* **1972**, 4233-4236.
108. Ajisaka, K.; Kamisaku, M.; Kainosho, M. *Chem. Lett.* **1972**, 857-858.
109. Cervinka, O.; Malon, P.; Trska, P. *Collect. Czech. Chem. Commun.* **1973**, *38*, 3299-3301.
110. Sullivan, G. R.; Ciavarella, D.; Mosher, H. *J. Org. Chem.* **1974**, *39*, 2411-2416.
111. Whitesides, G. M.; Lewis, D. W. *J. Am. Chem. Soc.* **1971**, *93*, 5914-5916.

Chiral Organosulfur Compounds

MARIAN MIKOŁAJCZYK and JÓZEF DRABOWICZ

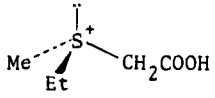
Centre of Molecular and Macromolecular Studies,
Polish Academy of Sciences,
Department of Organic Sulfur Compounds,
Lodz, Poland

I. Introduction and Scope 334
II. Optically Active Organosulfur Compounds 335
A. Sulfoxides 336
1. Resolution of Racemic Sulfoxides 336
2. Asymmetric Synthesis of Sulfoxides 340
3. Kinetic Resolution of Sulfoxides 345
4. Stereospecific Synthesis of Sulfoxides 348
B. Sulfinates 352
C. Thiosulfinates 355
D. Sulfinamides 357
E. Sulfinyl Chlorides 359
F. Sulfimides 360
G. Sulfinimidoates and Sulfinimidamides 362
H. Sulfurous Acid Derivatives 363
1. Sulfites 364
2. Amidosulfites and Amidothiosulfites 365
I. Sulfonium Salts 366
J. Sulfonium Ylides 371
K. Oxosulfonium Salts 373
L. [$^{16}O^{18}O$] Sulfones and [$^{16}O^{18}O$] Sulfonates 374
M. Sulfoximides 375
N. Sulfonimidoyl Chlorides, Sulfonimidoates, and Sulfonimidamides 381
O. Sulfuranes 384
III. Determination of Absolute Configuration and Optical Purity of Chiral Sulfur Compounds 386
A. Determination of Chirality at Sulfur by Chemical Methods 387
B. Determination of Absolute Configuration by Spectrometric Methods 394
1. Nuclear Magnetic Resonance 394
2. Optical Rotatory Dispersion and Circular Dichroism 397
3. Ultraviolet and Infrared Spectroscopy 398
4. X-Ray Analysis 399

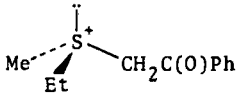
5. Other Methods 402
C. Determination of Optical and Enantiomeric Purity 402
IV. Basic Problems of the Dynamic Stereochemistry of Chiral Sulfur Compounds 406
A. Racemization 406
1. Thermal Racemization 406
2. Photochemical Racemization 411
3. Racemization Induced by Chemical Reactions 411
a. Reactions with Hydrogen Halides 411
b. Reactions with Other Acids 414
c. Reactions with Carboxylic Acid Anhydrides 415
d. Other Reactions 416
B. Nucleophilic Substitution at Chiral Tri- and Tetracoordinate Sulfur 418
C. Reactions of Chiral Sulfur Compounds with Electrophilic Reagents 431
V. Asymmetric Induction in Transfer of Chirality from Sulfur to Other Centers 435
VI. Final Remarks 457
References 457

I. INTRODUCTION AND SCOPE

Although the first optical resolutions of chiral organosulfur compounds, sulfonium salts 1 and 2, were reported in 1900 by Pope and Peachey (1) and by Smiles (2), the stereochemistry of organosulfur compounds is a relatively new field, which has developed mostly



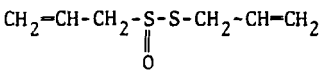
1



2

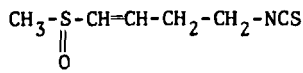
during the past three decades. The isolation, around 1950, of many chiral sulfinyl compounds such as **3**, **4**, **5**, and **6** from natural sources (3,4) resulted in intense activity in the preparation and study of new chiral organosulfur structures.

However, the major factor stimulating the rapid development of static and dynamic sulfur stereochemistry was the interest in the mechanism and steric course of nucleophilic substitution reactions at chiral sulfur. Very recently, chiral organic sulfur compounds have attracted much attention as useful and efficient reagents in asymmetric synthesis.



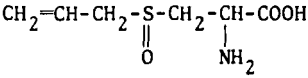
3

(C. J. Cavallito, J. H. Bailey, 1944)



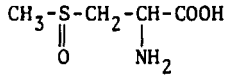
4

(H. Schmidt, P. Karrer, 1948)



5

(A. Stoll, E. Seebeck, 1948)



6

(R. L. M. Synge, J. C. Wood, 1956)

Although many previous reviews (5–12) and literature compilations (13–16) have dealt with sulfur stereochemistry, we decided to write a new report on chiral sulfur compounds to provide a survey of the topic with emphasis on the most recent findings. This chapter consists of four major parts treating syntheses of chiral sulfur compounds, methods for determination of their absolute configuration and optical purity, the dynamic stereochemistry of organosulfur compounds, and the use of chiral sulfur compounds in asymmetric synthesis.

This chapter covers only the chiral compounds that are cited in the literature by virtue of their optical activity. To keep the chapter to an acceptable length, a discussion of the stereochemical properties of sulfenamides showing axial chirality is omitted (17). Similarly, to limit the scope of the review, the chemistry of penicillin, cephalosporin sulfoxides and related compounds (14,18,19), steroidal sulfoxides (15,16), and other naturally occurring chiral sulfur compounds (4) is not discussed. For the same reason, only selected results are discussed and in some cases only references are given to recent papers and review articles on special topics.

II. OPTICALLY ACTIVE ORGANOSULFUR COMPOUNDS

In this section we present a survey of the different types of optically active organosulfur compounds and the synthetic approaches to them. Although sulfur forms a variety of structures differing in number of ligands ($N = 1$–6) and in valency (7), the overwhelming majority of organic sulfur compounds obtained in an optically active state belong to the tricoordinate (three different substituents and the lone electron pair on S) and tetracoordinate (four different ligands on S)

classes, both having distorted tetrahedral geometry. Optically active tetracoordinate sulfur compounds having trigonal bipyramidal structure (sulfuranes) have become available relatively recently.

A. Sulfoxides

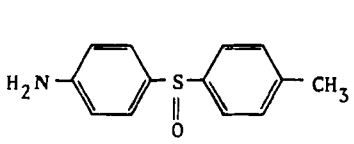
Chiral sulfoxides play a key role in sulfur stereochemistry. Therefore, much effort has been devoted to elaboration of convenient methods for their synthesis. Until now, chiral sulfoxides have been obtained in the following ways:

1. Optical resolution.
2. Asymmetric synthesis.
3. Kinetic resolution.
4. Stereospecific synthesis.

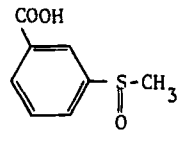
These methods are briefly presented below.

1. Resolution of Racemic Sulfoxides

In 1926 Harrison et al. (20) described the first resolutions of 4'-amino-4-methyldiphenyl sulfoxide 7 and *m*-carboxyphenyl methyl sulfoxide 8 into the enantiomeric forms via formation and crystal-

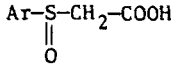


7



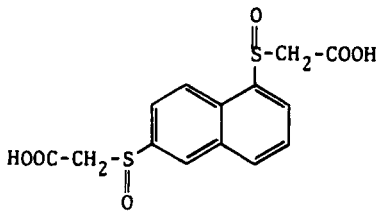
8

lization of the diastereomeric salts with *d*-camphorsulfonic acid and brucine, respectively. A few years later, Suszko and his collaborators (21) and more recently Janczewski and his group (22) published a large number of papers on the synthesis, resolution, and optical properties of α-substituted sulfinylacetic acids of general structure 9. Similarly, Kiełczewski (23) resolved the derivatives of 1,6- and 1,8-

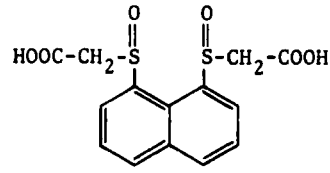


9

naphthyldisulfinylacetic acid **10** and **11** into their enantiomeric forms using the carboxylic groups for salt formation with optically active amines. Bohman and Allenmark (24) have reported the resolu-

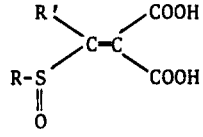


10



11

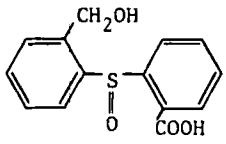
tion of a series of sulfoxide derivatives of unsaturated malonic acids of general structure **12**. The classical method of resolution, that is, the formation of diastereomeric salts with cinchonine and quinine,



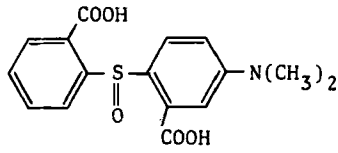
12

also has been used by Kapovits (25) to resolve sulfoxides **13** to **16**, which are starting materials for the synthesis of chiral sulfuranes. Very recently, Mikołajczyk and his co-workers (26) succeeded in the optical resolution of sulfoxide **17** utilizing a phosphonic acid moiety as the resolving "handle." Holmberg (27) has described the resolution of racemic sulfinylacetic acid **18**, which has an additional center of chirality on the α-carbon atom. Optically active 2-hydroxy- and 4-hydroxyphenyl alkyl sulfoxides were obtained by Wagner and Bohme (28) by separation of the diastereomeric 2- or 4-(tetra-*O*-acetyl-β-D-glucopyranosyloxy)phenyl alkyl sulfoxides **19**. The optically active sulfoxides were recovered from **19** by deacetylation with base and cleavage of the acetal. An interesting synthesis of optically active 1,3-dithian-1-oxide **20** was achieved recently by the addition of the 2-lithio derivative of **20** to (+)-camphor followed by separation of the diastereomeric alcohols and regeneration of sulfoxide **20** with potassium hydroxide in *t*-butyl alcohol (29).

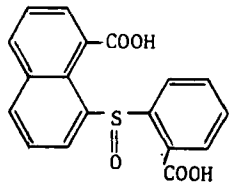
In addition to the classical resolution of sulfoxides via diastereo-



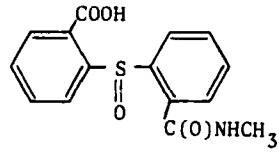
13



14

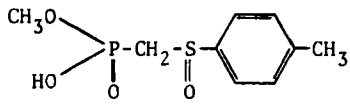


15

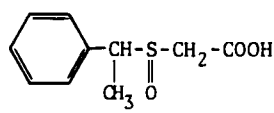


16

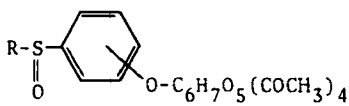
meric salts or derivatives, as illustrated by the selected examples given above, other–nonclassical–procedures are known that allow the resolution of racemic sulfoxides that do not contain acidic or basic functional groups. The first example of this type was reported by Backer and Keuning as early as 1934 (30). They resolved 2,5-dithiaspiro[3,3]heptane-2,5-dioxide 21 by means of a cobalt complex with *d*-camphorsulfonic acid as ligand. Later on, Cope and Caress (31) reported the total resolution of ethyl *p*-tolyl sulfoxide 22 through



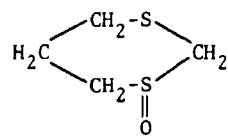
17



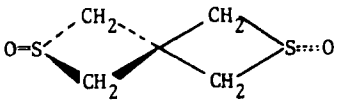
18



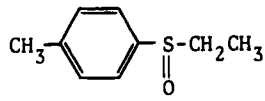
19



20



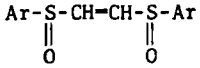
21



22

formation and separation of the diastereomeric complexes of 22 with *trans*-dichloroethylene platinum(II) containing optically active α-methylbenzylamine as ligand.

Owing to its conceptual simplicity and manifest utility, the direct liquid chromatographic separation of enantiomeric sulfoxides on chiral columns has also been attempted. Thus, Montanari et al. (32) found that racemic unsaturated vinyl disulfoxides 23 may be par-

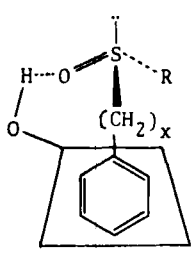


23

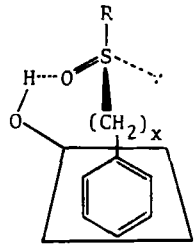
tially resolved by this method on activated α-lactose. Wudl (33) has used a polymer prepared from chiral methyl *p*-styryl sulfoxide for the chromatographic separation of sulfoxides. In extension of their studies on the NMR determination of enantiomeric purity and absolute configuration of chiral sulfoxides, Pirkle and House (34) recently introduced a silica gel-bonded chiral fluoroalcoholic stationary phase for the direct separation of enantiomeric sulfoxides. The successful chromatographic resolution devised by Pirkle is conceptually based on three types of stereochemically dependent interaction between the chiral fluoroalcoholic moiety of a stationary phase and the enantiomeric sulfoxides to be separated. These interactions include two hydrogen bonds and a π—π donor-acceptor interaction between the aromatic substituents of a chiral alcohol and sulfoxide. These interactions are discussed in Sect. III-B-1.

A different approach to the resolution of sulfoxides was recently reported by Mikołajczyk and Drabowicz (35). It takes advantage of the fact that sulfoxides as well as other sulfinyl compounds very easily form inclusion complexes with β-cyclodextrin. Since β-cyclodextrin (the host) is chiral, its inclusion complexes with racemic guest substances are mixtures of diastereomers that can be formed in unequal amounts. In this way a series of alkyl phenyl, alkyl *p*-tolyl, and alkyl benzyl sulfoxides has been resolved. However, the optical

purities of the partially resolved sulfoxides do not exceed 15% after just one inclusion process. It is interesting to note that the relationship observed between the stereospecificity of inclusion of sulfoxides in β-cyclodextrin and the structure of the preferentially included sulfoxide may be rationalized by assuming that two inclusion complexes (**24a** and **24b**) are concurrently formed in a ratio that depends on the nature of the alkyl substituent at sulfur. In the case of *t*-butyl aryl sulfoxides, the inclusion complex **24b** is favored for steric reasons.



24a

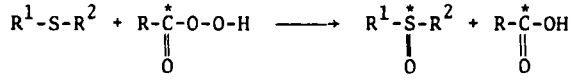


24b

x=0,1

2. *Asymmetric Synthesis of Sulfoxides*

An attractive route to chiral sulfoxides is based on asymmetric oxidation of unsymmetrical sulfides by means of chiral oxidizing reagents. The first asymmetric oxidation of sulfides with optically active peracids (eq. [1])* has been independently described in 1960 by two groups headed by Montanari (36) in Italy and by Balenovic (37) in

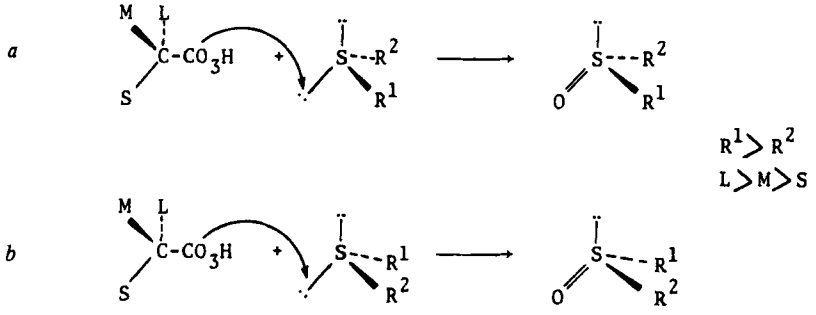


[1]

Yugoslavia. An excellent monograph by Morrison and Mosher (38) provides a comprehensive review of the pre-1969 literature on this subject. The formation of sulfoxides in the asymmetric reaction shown above typically occurred with quite low optical purities (not higher than 10%). The detailed and extensive studies of Montanari and

*Throughout, an asterisk (*) denotes a chiral, optically active center.

co-workers (39) on peracid oxidation revealed that the chirality in the predominantly formed sulfoxide enantiomer depends on the absolute configuration of the peracid used. This led Montanari to propose a topographic description for the diastereomeric transition states involved in this asymmetric oxidation. This is shown in Scheme 1.



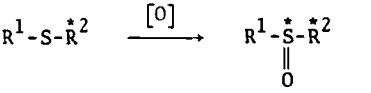
Scheme 1

According to this correlation model, in which the principles of steric control of asymmetric induction at carbon (40) are applied, the stereoselectivity of oxidation should depend on the balance between one transition state [Scheme 1(*a*)] and a more hindered transition state [Scheme 1(*b*)] in which the groups R^1 and R^2 at sulfur face the moderately and least hindered regions of the peroxy acid, respectively. Based on this model and on the known absolute configuration of (+)-percamphoric acid and (+)-1-phenylperpropionic acid, the correct chirality at sulfur (+)-*R* and (−)-*S* was predicted for alkyl aryl sulfoxides, provided asymmetric oxidation is performed in chloroform or carbon tetrachloride solution. Although the correlation model for asymmetric oxidation of sulfides to sulfoxides is oversimplified and has been questioned by Mislow (41), it may be used in a tentative way for predicting the chirality at sulfur in simple sulfoxides.

In contrast to asymmetric oxidation of unsymmetrical sulfides with chiral peracids, microbial oxidation usually gives much better results. Thus, optically active phenyl benzyl sulfoxide was prepared by oxidation of the parent sulfide via fermentation with *Aspergillus niger*, NRRL 337, with 18% optical purity (42). Similarly, asymmetric

$$R^1\text{-}S\text{-}R^2 \xrightarrow{\text{microorganism}} R^1\text{-}\overset{*}{\underset{\underset{O}{\|}}{S}}\text{-}R^2 \qquad [2]$$

induction during oxidation of 7-α-methylthioandrostone to the sulfoxide by fermentation with *Calonectria decora* (CBS) was observed (43). As a result of their extensive studies, Henbest and co-workers (44) found that the chemical yield and stereoselectivity of the oxidation by *Aspergillus niger* depend on the structure of sulfide and on the efficiency with which the enzymatic oxidation system can accommodate the reacting sulfide. The trend in stereoselectivity is best illustrated by the results involving the oxidation of alkyl *p*-tolyl sulfides. The highest optical purity (99%) was observed in the case of *t*-butyl *p*-tolyl sulfoxide and the lowest (32%) for methyl *p*-tolyl sulfoxide. Very recently, the oxidation of alkyl *p*-tolyl sulfides by *Mortierella isabellina,* RRLL 1757, and *Helminthosporium sp.*, NRRL 4671, was found (45) to give the corresponding sulfoxides with 100% optical purity.



[3]

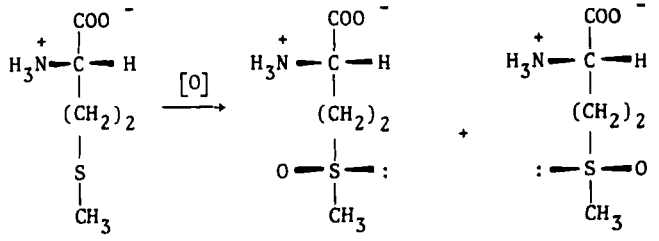
Asymmetric induction at sulfur is also observed when sulfides that are chiral at carbon are treated with achiral oxidizing agents. The first example of this internal induction was reported by Cram and Pine (46), who oxidized (*R*)-2-octyl phenyl sulfide with *t*-butyl hydroperoxide. Two diastereomeric sulfoxides **25** were found to be formed in the ratio 1.6:1. It is interesting to note that the original configurational assignments of the chirality at sulfur in **25** were later invalidated by Mislow (47). This points out that the principle of steric control of asymmetric induction developed for carbon does not allow unqualified predictions of absolute configuration at sulfur. Nishio and Nishihata (48) recently came to the same conclusion in connection with an investigation of the oxidation of optically active 1-phenylethyl alkyl(phenyl) sulfides with various oxidizing agents. In every reaction studied the predominantly formed diastereomeric sulfoxide **26** was shown to have the configuration S_cR_s. Moreover, it was found that the proportion of the diastereomeric sulfoxides **26** was not significantly affected by a change in the nature of the oxidant. In the



25 **26**

case of alkyl derivatives, the product ratio (S_cR_s)-**26** to (S_cS_s)-**26** varies from 3.1 for R = Me to 49 for R = *t*-Bu.

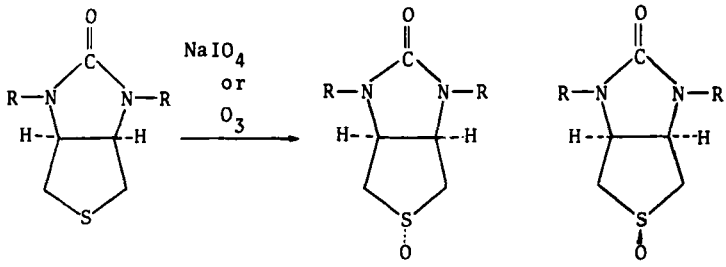
An interesting example of asymmetric induction at sulfur concerns the oxidation of (*S*)-methionine **27** to the corresponding sulfoxides **28**. Christensen and Kjaer (49) found that upon oxidation of (*S*)-**27**



(*S*)–**27** (S_cS_s)–**28** (S_cR_s)–**28**

[4]

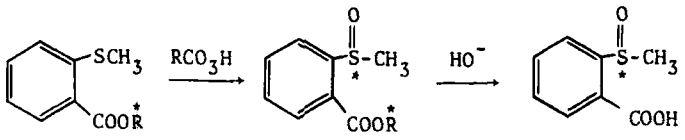
with hydrogen peroxide, nearly equal amounts of diastereomeric sulfoxides **28** were produced. However, Bordignan (50) reported recently that the use of $HAuCl_4$ as oxidant provides a method for the completely stereospecific conversion of (*S*)-**27** into the methionine sulfoxide (S_cS_s)-**28**. In the course of studies on the total synthesis of biotin, Marquet and her co-workers (51) observed that the key intermediate sulfide **29** undergoes a highly stereoselective oxidation with sodium metaperiodate or ozone to give the two diastereomeric sulfoxides *cis*-**30** and *trans*-**30** in a 90:10 ratio. The oxidation of optically active esters of *o*-methylthiobenzoic acid **31** by achiral peroxyacids, followed by hydrolysis, resulted in the formation of



29 *cis*–**30** *trans*–**30**

[5]

R=$PhCH_2$, $CH_2=CH_2-CH_2$

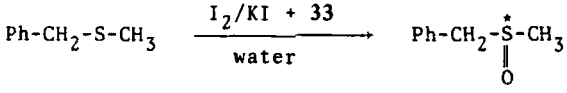


[6]

31 32

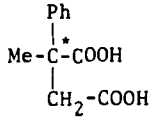
optically active *o*-methylsulfinylbenzoic acid 32 (52). The use of 2,4,6-trimethylperbenzoic acid and bulky inducing alcohols in the ester moiety lead to higher optical purities (up to about 40%) of sulfoxide 32.

Asymmetric oxidation of sulfides to sulfoxides occurs in the presence of chiral catalysts. It was found (53) that oxidation of benzyl methyl sulfide with iodine suspended in (*R*)-2-methyl-2-phenylsuccinate 33 buffer gives optically active benzyl methyl sulfoxide 34 having 6.35% optical purity. Much higher asymmetric



[7]

34



33

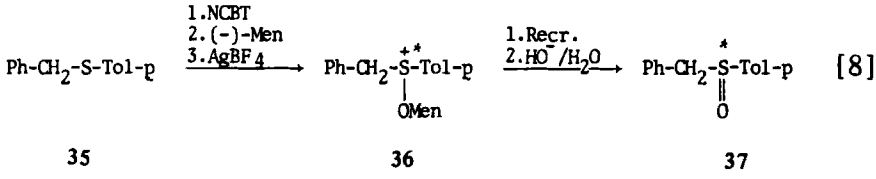
induction was observed (54,55) in the two-phase oxidation of alkyl aryl sulfides and dithioacetals of formaldehyde by sodium metaperiodate in the presence of such proteins as bovine serum β-globulin and egg albumin. Optical purities of the sulfoxides so formed ranged between 20 and 60%.

Low asymmetric induction (e.e. 0.3–2.5%) was found (56) to occur when unsymmetrical sulfides were electrochemically oxidized on an anode modified by treatment with (-)-camphoric anhydride or (*S*)-phenylalanine methyl ester.

Similarly, the metal-catalyzed oxidation of aryl alkyl sulfides by *t*-butyl hydroperoxide carried out in a chiral alcohol gives rise to optically active sulfoxides of low optical purity (e.e., 0.6–9.8%) (57).

Chiral alcohols have also been used to induce optical activity in sulfoxides during halogenation of sulfides. Thus, Johnson (58) found

that treatment of benzyl *p*-tolyl sulfide **35** with *N*-chlorobenzotriazole (NCBT) followed by sequential addition of (-)-menthol and silver tetrafluoroborate afforded optically active menthoxysulfonium salt **36**, which upon recrystallization and hydrolysis gave benzyl *p*-tolyl sulfoxide **37** with 87% optical purity. Oae et al., (59) reported similar



[8]

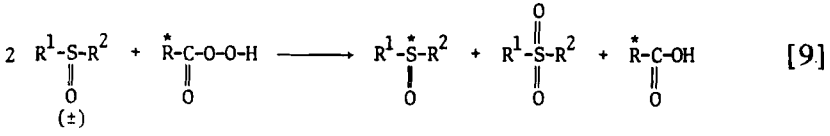
35 **36** **37**

asymmetric synthesis of chiral diaryl sulfoxides (e.e. up to 20%) using (-)-menthol and *t*-butyl hypochlorite.

Very recently, other Japanese workers applied *N*-bromocaprolactam and a chiral alcohol as solvent for the same purpose as well as chiral *N*-chlorocaprolactam and water as oxidant (60,61). In both cases optically active sulfoxides were obtained in low optical and chemical yields.

3. Kinetic Resolution of Sulfoxides

Since in principle the reactions of enantiomeric sulfoxides with a chiral reagent are expected to proceed at unequal rates, a possibility exists for obtaining chiral sulfoxides, especially when the reacting racemic sulfoxide is used in excess in relation to the chiral reagent. A typical example of such a kinetic resolution of a racemic sulfoxide is its reaction with a deficiency of chiral peracid, affording a mixture of optically active sulfoxide and achiral sulfone (62,63). However,

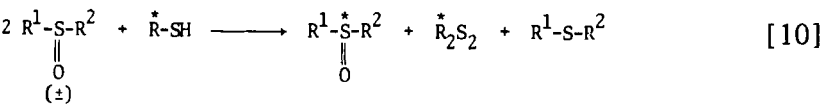


[9]

the very low optical purity of the recovered sulfoxides (up to 5%) constitutes a serious limitation of this method. In connection with the asymmetric oxidation of sulfides to sulfoxides, it is interesting to note that the sulfoxide enantiomer formed preferentially in the asymmetric oxidation of sulfide undergoes slower oxidation to sulfone. In accord with expectations, higher optical purities (up to 30%)

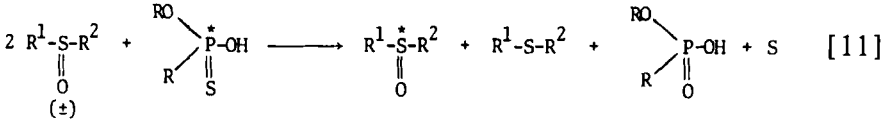
were noted when racemic sulfoxides were exposed to growing cultures of *Aspergillus niger* (64).

Optically active sulfoxides can also be obtained when a racemic sulfoxide is reduced with an insufficient amount of a chiral reagent. Balenovic and Bregant (65) found that L-cysteine reacted with racemic sulfoxides to produce a mixture of sulfide, L-cystine, and nonreduced optically active starting sulfoxide. Mikołajczyk and Para



[10]

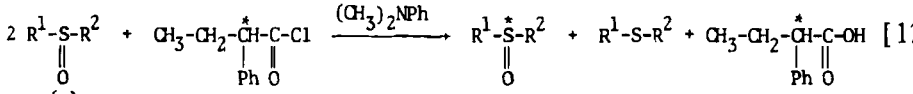
(66) used optically active phosphonothioic acids as asymmetric reducing agents in reactions with racemic sulfoxides according to eq. [11]. Although optical purities of the nonreduced sulfoxides



[11]

were quite low (<5%), a clear relationship was found between the chirality of the reducing *P*-thioacid and the recovered sulfoxide. This observation may be exploited, with some reservation for configurational correlations, even though it is not certain that the correlation will apply in all cases. Partial asymmetric reduction of racemic sulfoxides also occurs when a complex of $LiAlH_4$ with chiral alcohols or amino alcohols (ephedrine, cinchonidine) is used (67).

Recently, Juge and Kagan (68) reported that a more efficient kinetic resolution of racemic sulfoxides takes place in the Pummerer-type reaction with optically active α-phenylbutyric acid chloride **38** in the presence of *N,N*-dimethylaniline. In contrast to the asym-

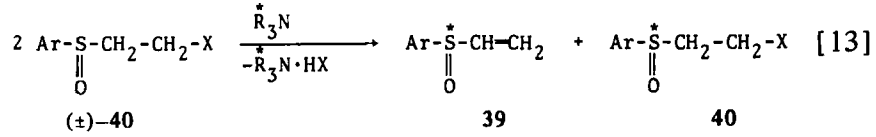


[12]

38

metric reductions of racemic sulfoxides discussed above, this procedure afforded the nonreduced sulfoxides in optical yields up to 70%.

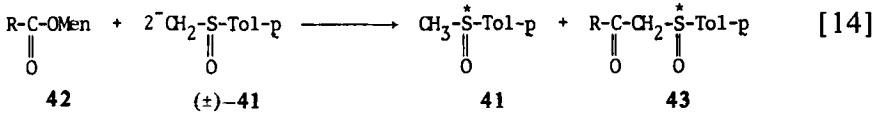
A very interesting approach to chiral α,β-unsaturated sulfoxides **39** based on a kinetic resolution was elaborated by Marchese (69), who found that asymmetric elimination of racemic β-halogenosulfoxides **40** takes place in the presence of chiral tertiary amines.



[13]

(±)–**40** **39** **40**

The optically active sulfoxides **39** and **40** were formed in optical yields up to 20% and with opposite configurations at sulfur. The reaction of the carbanion derived from racemic methyl *p*-tolyl sulfoxide (**41**) with 0.5 molar equivalent of (–)-menthyl carboxylates **42** was found (70) to occur asymmetrically to give the corresponding optically active β-ketosulfoxide **43** and methyl *p*-tolyl sulfoxide **41**, having opposite configurations at sulfur. The degree of stereo-

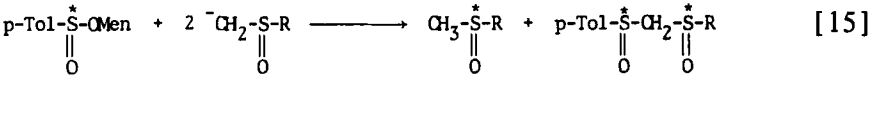


[14]

42 (±)–**41** **41** **43**

selectivity in this reaction is strongly dependent on the nature of the R group in **42**. Thus, the β-ketosulfoxide is formed with an optical yield of 1.3% for R = Et. In the case of R = *t*-Bu, the optical yield was increased to 71.5%.

A reaction similar to that discussed above occurs between 2 equivalents of the sulfoxide carbanion **44** and diastereomerically pure menthyl *p*-toluenesulfinate **45** and results in the formation of optically active disulfoxide **46** and starting sulfoxide **44** (71).



[15]

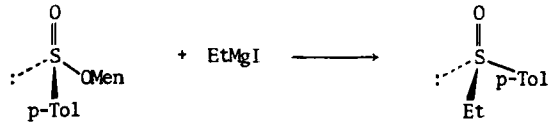
45 (±)–**44** **44** **46**

Finally, it is interesting to note that partial photochemical decomposition of racemic alkyl aryl sulfoxides in the presence of chiral amines as sensitizers (72) gave optically active sulfoxides with optical purities of about 3%. The use of cholesteric liquid crystalline

reaction media has been claimed (73) to change the enantiomeric composition of racemic sulfoxides at high temperatures. However, the latter observations could not be reproduced (74).

4. Stereospecific Synthesis of Sulfoxides

The most important and widely used approach to chiral sulfoxides is the method developed by Andersen (5) based on the reaction between the diastereomerically pure (or strongly enriched in one diastereomer) menthyl arenesulfinates and Grignard reagents. The first stereospecific synthesis of optically active (+)-(*R*)-ethyl *p*-tolyl sulfoxide **22** was accomplished in 1962 by Andersen (75) from (−)-(*S*)-menthyl *p*-toluenesulfinate **45** and ethylmagnesium iodide.

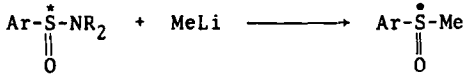


[16]

(−)-(*S*)-**45** (+)-(*R*)-**22**

Soon after that, a variety of chiral alkyl aryl and diaryl sulfoxides (47,76–78) were synthesized from **45** and other optically active arenesulfinates. In accord with Andersen's original assumption, this highly stereospecific Grignard reaction proceeds with inversion of configuration at sulfinyl sulfur, as rigorously proved by Mislow (79) and other investigators (80,81). The stereospecific conversion of menthyl arenesulfinates into chiral methyl aryl sulfoxides may also be achieved by means of methyllithium (82,83). Very recently, Harpp (84) found that a cleaner reaction results from the use of lithium-copper reagents (R_2CuLi) instead of Grignard reagents.

The Andersen synthesis of chiral sulfoxides has also been extended to diastereomerically or enantiomerically pure arenesulfinamides, which on treatment with methyllithium give optically active methyl aryl sulfoxides (83,85). The use of menthyl sulfinates in the synthesis of sulfoxides has been exploited in the preparation of optically active sulfoxides **47** and **48**, which are chiral by virtue of isotopic substitution, H→D (86), and $^{12}C \rightarrow {}^{13}C$ (87), respectively. More recent



[17]

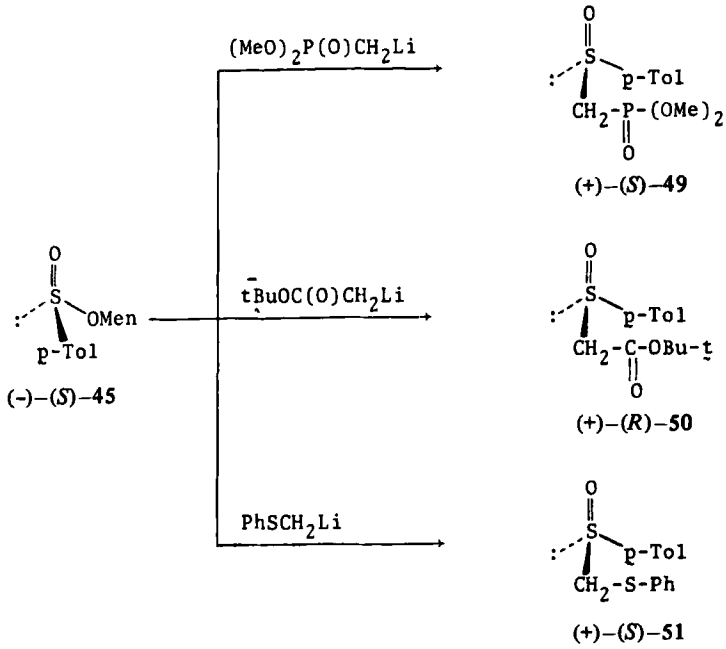
$$CH_3\text{-}\overset{\overset{O}{\|}}{S}\text{-OMen} + CD_3MgI \longrightarrow CH_3\text{-}\overset{\overset{O}{\|}}{S}\text{-}CD_3 \quad [18]$$

47

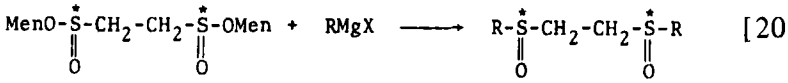
$$Ph\text{-}{}^{12}CH_2\text{-}\overset{\overset{O}{\|}}{S}\text{-OMen} + Ph\text{-}{}^{13}CH_2MgCl \longrightarrow Ph\text{-}{}^{12}CH_2\text{-}\overset{\overset{O}{\|}}{S}\text{-}{}^{13}CH_2\text{-}Ph \quad [19]$$

48

examples of stereospecific syntheses of optically active sulfoxides from (–)-(*S*)-**45** include the syntheses of α-phosphoryl sulfoxide **49** (26), β-ketosulfoxide **50** (89), and dithioacetal monoxide **51**(90) (see Scheme 2). A stereospecific synthesis of chiral aliphatic disulfoxides **52** is illustrated by the reaction between dimenthyl ethane-1,2-disulfinate **53** and aliphatic Grignard reagents (91). In this



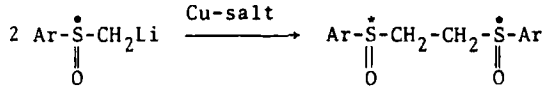
Scheme 2 In the original work (26), the (*R*)–configuration was incorrectly assigned to the sulfoxide (+)–(*S*)–**49**.



[20]

53 52

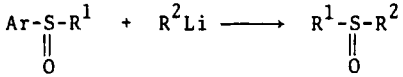
context, it is interesting to mention that a one-step synthesis of aromatic disulfoxides **54** has been worked out by Mislow (92). It involves the copper-catalyzed oxidative coupling of α-carbanions derived from chiral methyl aryl sulfoxides.



[21]

54

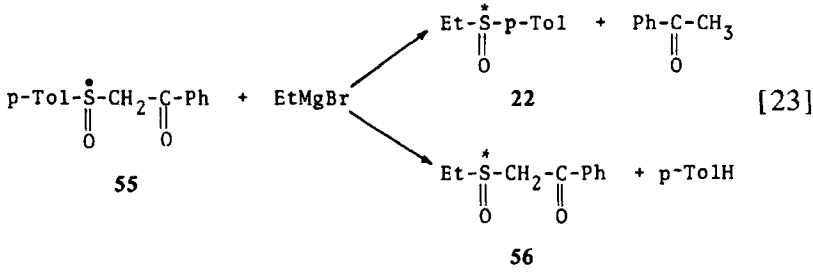
Optically active dialkyl sulfoxides of high optical purity (>95%), which could not be prepared from menthyl alkanesulfinates, have been synthesized by Johnson et al. (93) via reaction of chiral alkyl aryl sulfoxides with alkyllithium reagents. The exchange of the



[22]

aryl group by alkyl takes place with inversion of configuration at sulfur. When (+)-(*R*)-*p*-toluenesulfinylacetophenone **55** was used as substrate, two possible cleavage modes were observed (94) in the reaction with ethylmagnesium bromide, leading to chiral ethyl *p*-tolyl sulfoxide **22** and ethylsulfinylacetophenone **56**.

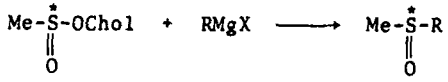
An alternative route to enantiomeric methyl alkyl sulfoxides (95) is based on the reaction of aliphatic Grignard reagents with the dia-



[23]

55 22 56

stereomerically pure (−)-(*S*) and (+)-(*R*)-cholesteryl methanesulfinates **57**, having $[\alpha]_{589}$ − 113.95° and $[\alpha]_{589}$ + 77.35°, respectively. A different and general approach to the stereospecific synthesis of chiral

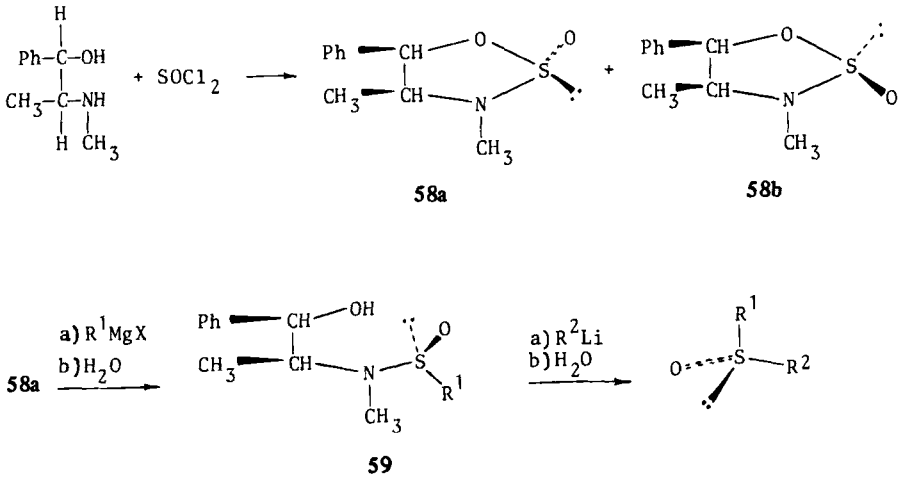


[24]

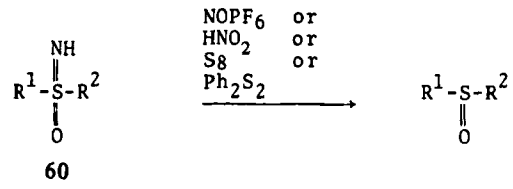
57

sulfoxides was reported by Wudl and Lee (96,97) in 1972. Key intermediates in their procedure are cyclic diastereomeric amidosulfites **58** prepared from *l*-ephedrine and thionyl chloride. The selective cleavage of the S–O bond in **58** with Grignard reagent leads to a chiral sulfinamide **59**, which on subsequent treatment with an appropriate alkyllithium reagent affords a chiral sulfoxide (Scheme 3). Since both reactions take place with inversion of configuration at sulfur, it is obvious that the order of introduction of the groups R^1 and R^2 determines the configuration of the chiral sulfoxide formed.

In addition to the stereospecific sulfoxide syntheses mentioned above, optically active sulfoxides of high optical purity may be prepared from optically active sulfoximides **60**, which are sufficiently basic to form salts with optically active sulfonic acids and can be easily resolved into enantiomers. The stereospecific conversion of sulfoximides **60** into the corresponding sulfoxides was effected by



Scheme 3

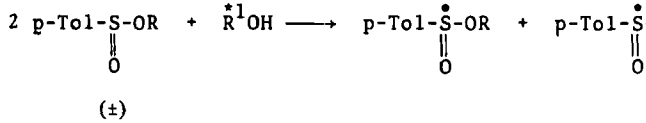


[25]

Cram (98) using nitrosyl hexafluorophosphate or nitrous acid. Oae and his group (99) also have reported a method for the stereospecific deimination of **60** by means of elemental sulfur or diphenyl disulfide at 160°C. All these procedures give chiral sulfoxide with the same configuration at sulfur as that of the starting sulfoximides **60**.

B. Sulfinates

Chiral sulfinates are important intermediates that are widely applied in the synthesis of other classes of chiral organosulfur compounds and in their configurational correlations. Optically active sulfinates were first prepared in 1925 by Phillips (100) in two ways. The first consisted in the transesterification of racemic alkyl *p*-toluenesulfinates with chiral alcohols such as (–)-menthol and (–)-2-octanol yielding a mixture of two optically active sulfinates as shown in eq. [26]. The

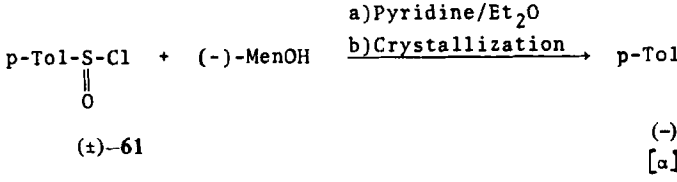


[26]

R= Et,n-Bu

second route comprised the condensation of *p*-toluenesulfinyl chloride **61** with chiral alcohols to give a mixture of diastereomeric sulfinates in unequal amounts. In this way Phillips prepared the first mixture of diastereomeric menthyl *p*-toluenesulfinates **45**, from which he isolated the pure diastereomer (–)-(*S*)-**45**.

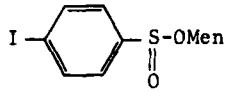
Since (–)-(*S*)-**45** is a common precursor to many chiral organosulfur



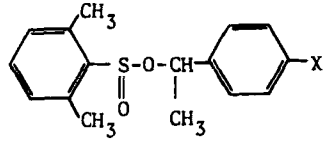
[27]

compounds, especially sulfoxides, other investigators were prompted to improve the synthetic approach to this ester. Thus Estep and Tavares (101) found that it is advantageous to perform the reaction described in eq. [27] at room temperature. The pure diastereomer (-)-(*S*)-**45** formed can be isolated after one crystallization in high yield. Recently, it was reported (102) that the use of a trimethylsilyl derivative of menthol and sulfinyl chloride **61** results in the predominant formation of the desired ester (-)-(*S*)-**45**, which is easily isolated in the pure state by a single crystallization.

In 1958 Herbrandson and Cusano (103) prepared menthyl esters of *p*-iodobenzenesulfinic acid **62**. Darwish and McLearen (104) described the synthesis and separation of diastereomeric esters **63** from optically active α-methylbenzyl alchols. Similarly, methanesulfinyl chloride **64** was found to react with cholesterol to give a

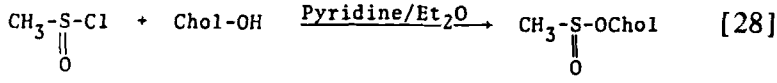


62



63

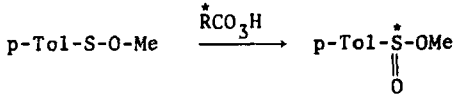
mixture of crystalline diastereomeric cholesteryl methanesulfinates **57** that can be separated into pure diastereomers (95).



[28]

(±)-**64** **57**

During the past decade much attention was paid to the synthesis of chiral sulfinates with the sulfur atom as a sole center of chirality. A little earlier, Fava (105) had reported the asymmetric oxidation of methyl *p*-toluenesulfenate with (+)-monopercamphoric acid, yielding the corresponding sulfinate **65**. The optical purity of the product was, however, very small (ca. 3%).



[29]

65

An attempt to directly resolve alkyl alkanesulfinates via β-cyclodextrin inclusion complexes was only partly successful (35,106). In the majority of cases, the optical purity of the isolated esters was in the 5 to 10% range. In the case of isopropyl methanesulfinate, however, inclusion was highly stereospecific and afforded the ester with 68% optical purity.

A new and general approach to chiral aliphatic or aromatic sulfinates has been recently described by Mikołajczyk and Drabowicz (107). It consists of the asymmetric condensation of racemic sulfinyl chlorides at low temperature with achiral alcohols in the presence of chiral tertiary amines as asymmetric reagents. The optical purity (up to 45%) of the sulfinates formed is strongly dependent on the structure of all the reaction components.

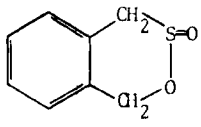
$$R\text{-}\overset{\overset{O}{\|}}{S}\text{-}Cl + R^1OH \xrightarrow[-(CH_3)_2\overset{*}{N}R\cdot HCl]{(CH_3)_2\overset{*}{N}R} R\text{-}\overset{\overset{O}{\|}}{\overset{*}{S}}\text{-}OR^1 \qquad [30]$$

It is worth mentioning that the extent of asymmetric induction in the sulfinate synthesis is comparable with that observed in the reaction of sulfinyl chlorides with optically active alcohols. However, in this case, the sulfinate products contain only one chiral center on sulfur; the chiral-inducing amine is very easily recovered as the hydrochloride.

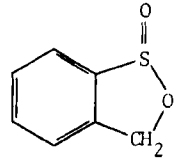
Another approach to chiral sulfinates was developed by Pirkle and Hoekstra (108); it is based on incomplete but stereoselective reaction of racemic sulfinates with chiral Grignard reagents. This kinetic resolution affords the unreacted sulfinates enriched in the (*S*)-enantiomers with optical purities in the 8–64% range. The chiral cyclic sulfinates **66** and **67** were first obtained by this method.

$$2\ R\text{-}\overset{\overset{O}{\|}}{S}\text{-}OR + \overset{*}{R}MgX \longrightarrow R\text{-}\overset{\overset{O}{\|}}{\overset{*}{S}}\text{-}R^1 + R\text{-}\overset{\overset{O}{\|}}{\overset{*}{S}}\text{-}OR \qquad [31]$$

(±)

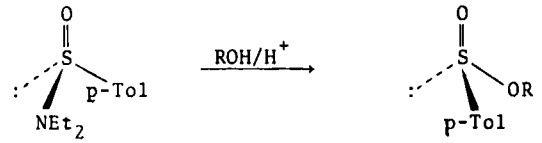


66



67

Chiral *p*-toluenesulfinates of high optical purity were recently prepared by Mikołajczyk and Drabowicz (109) in a stereospecific manner starting from chiral (+)-(*S*)-*N*,*N*-diethyl *p*-toluenesulfinamide **68**. Treatment of **68** with achiral alcohols in the presence of strong acids (CF_3CO_2H, $PhSO_3H$, $HSbF_6$, CF_3SO_3H) as catalysts gives the corresponding sulfinates in very high chemical yield and with inversion of configuration at sulfur. The stereospecificity of this process was found to be dependent on the structure of the alcohol used. Full stereospecificity in the acid-catalyzed alcoholysis of **68** was



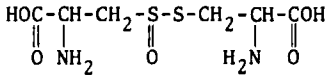
[32]

(+)–(*S*)–**68**

observed with primary alcohols. In an extension of this work, it was demonstrated (110) that it is possible to synthesize both enantiomers of methyl *p*-toluenesulfinate **65**, using (–)-(*S*)-**45** as starting material.

C. Thiosulfinates

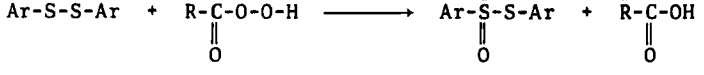
The separation of the diastereomeric cystine-*S*-monoxides **69** by Savige et al. (111) in 1964 demonstrated that the chiral, pyramidal configuration at the sulfinyl sulfur in thiosulfinates can be maintained.



69

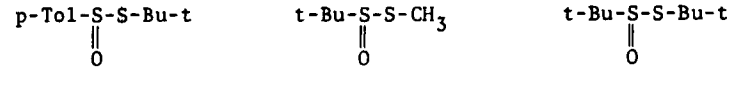
However, the synthetic approaches to simple chiral thiosulfinates with sulfur as a sole center of chirality are relatively few in number, and for the most part their applicability is limited.

Optically active aromatic thiosulfinates were first prepared by asymmetric oxidation of diaryl disulfides with (+)-percamphoric acid (105,112). Apart from the fact that the optical purity of diaryl



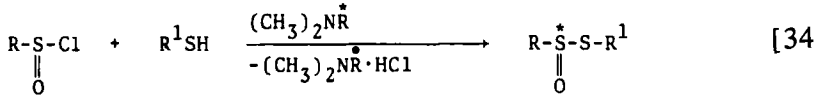
[33]

thiosulfinates prepared in this way was very low (up to 5%), the method failed in the synthesis of optically active dialkyl thiosulfinates, which are chemically not very stable compounds (113). For the first time, simple, optically stable thiosulfinates (70–72) containing the *t*-butyl group—a factor that increased their chemical and optical stability—have been obtained by partial optical resolution of racemates via β-cyclodextrin inclusion complexes (35). More conveniently,



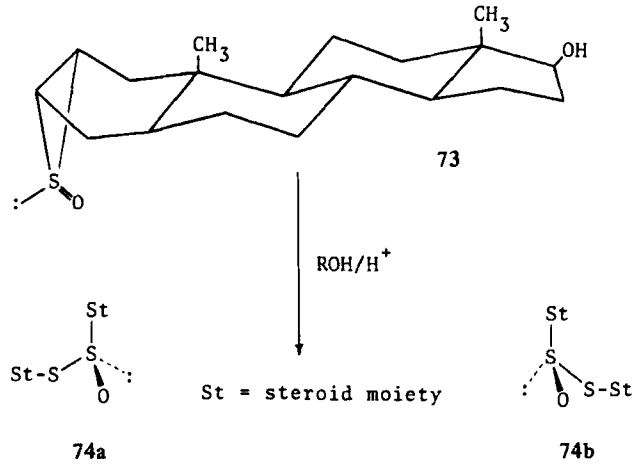
70 71 72

they may be prepared by the asymmetric condensation of racemic sulfinyl chlorides with achiral thiols in the presence of optically active tertiary amines (114). Recently, Kishi (115) found that the



[34]

reaction of the thiosteroid episulfoxide 73 (shown in eq. [35]) with methanol or ethanol in the presence of catalytic amounts of sulfuric acid leads to diastereomeric forms of the corresonding disulfide-*S*-monoxide 74.



[35]

D. Sulfinamides

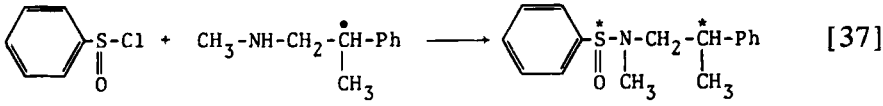
Optically active *N*-*p*-toluenesulfinyl piperidine **75** prepared in low optical purity by oxidation of *N*-*p*-toluenesulfenyl piperidine with (+)-percamphoric acid represents the first example of a chiral sulfinamide (105). As in the case of asymmetric oxidation of sulfides and sulfenates, the synthetic utility of this method is strongly limited by its low stereoselectivity.



[36]

75

Jacobus and Mislow (85) reported that racemic benzenesulfinyl chloride reacts with chiral *N*-methyl-2-phenylpropylamine to yield a mixture of the corresponding diastereomeric sulfinamides **76** that can be separated into pure components by fractional crystallization.

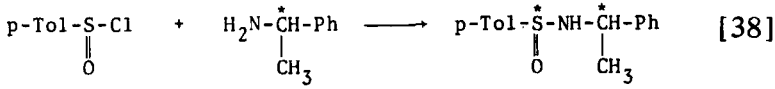


[37]

(±) **76**

In this connection, it is interesting to note that the extent of asymmetric induction in this reaction is strongly temperature dependent. Thus, the condensation carried out at 0°C yielded the mixture of diastereomeric sulfinamides **76** in a 3:1 ratio, whereas this ratio was 1:1 when the reaction was performed at -70°C. Diastereomeric *N*-α-methylbenzyl-*p*-toluenesulfinamides **77** were also prepared by Cram and Nudelman (116) in the reaction between sulfinyl chloride **61** and chiral (-)-α-methylbenzyl amine.

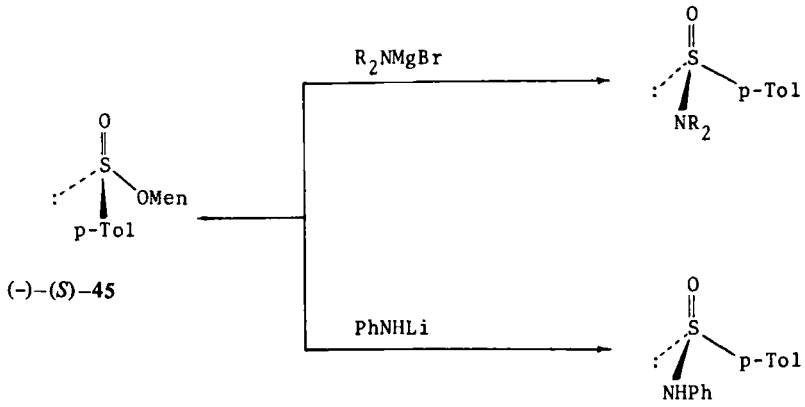
(-)-(*S*)-Menthyl *p*-toluenesulfinate **45**, a key compound in the stereospecific synthesis of sulfoxides, was also found to be a very convenient starting material for chiral sulfinamides. Montanari



[38]

(±)–**61** **77**

and co-workers (83) showed that the reaction of (–)-(*S*)-**45** with dialkylaminobromomagnesium reagents is highly stereospecific and proceeds with inversion at sulfur to give the corresponding sulfinamides (Scheme 4). Similar reaction of (–)-(*S*)-**45** with lithium anilide results in the stereospecific formation of the corresponding anilide **78** (116).

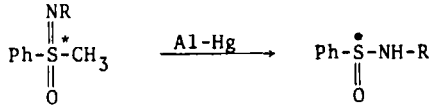


(–)-(*S*)-**45**

78

Scheme 4

A different approach to the stereospecific synthesis of sulfinamides described by Johnson (117,118) is based on the conversion of suitable chiral tetracoordinate sulfur compounds into sulfinamides. It was shown (117) that optically active methyl phenyl sulfoximide undergoes a clean and stereospecific reduction to the corresponding sulfinamide by means of aluminum amalgam. On the other hand,



[39]

R = CH_3, H, Tos

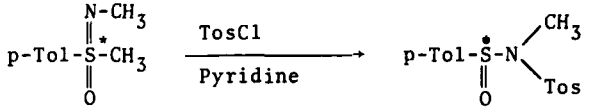
optically active *N,N*-dimethyl-*p*-toluenesulfinamide **79** was obtained (118) in a stereospecific way in the reaction of dimethyl fumarate with the ylide prepared from (dimethylamino)methyl-*p*-tolueneoxosulfonium tetrafluoroborate.



[40]

79

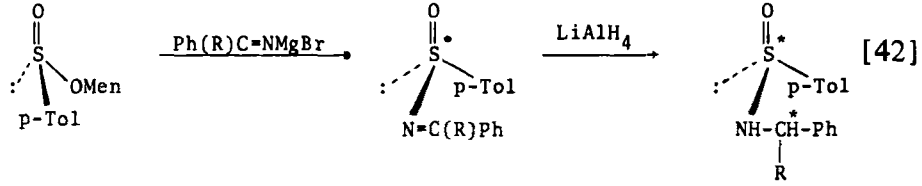
Optically active *N*-tosyl-*N*-methyl-*p*-toluenesulfinamide **80** was prepared (119) in low chemical yield by the reaction of optically active methyl *p*-tolyl sulfoximide **81** with 2 equiv of tosyl chloride in pyridine as solvent. The process of demethylation takes place with retention of configuration at sulfur.



[41]

81 **80**

Very recently, Cinquini and Cozzi (120,121) described an interesting synthesis of chiral sulfinamides starting from (–)-(*S*)-**45**. They found that treatment of (–)-(*S*)-**45** with imino-Grignard reagents results in the formation of the corresponding optically active *N*-alkylidenesulfinamides **82** which, in turn, were converted into a mixture of the diastereomeric sulfinamides **83** upon reduction by



[42]

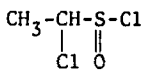
(–)-(*S*)-**45** **82** **83**

$LiAlH_4$. It is interesting to note that a substantial asymmetric induction at the carbon atom was observed in the last reaction.

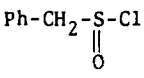
E. Sulfinyl Chlorides

The chiral nature of the chlorosulfinyl grouping was first demonstrated by NMR spectroscopy. King and Beatson (112) found that the proton NMR spectrum of α-chloroethanesulfinyl chloride **84** indicated clearly the presence of two diastereomers due to the

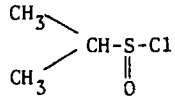
presence of two chiral centers—one at carbon and one at sulfur. Later on, observation of the magnetic nonequivalence of geminal protons or groups of protons in phenylmethanesulfinyl chloride **85** and 2-propanesulfinyl chloride **86** as well as in other simple sulfinyl chlorides provided additional evidence of the chiral stability in these compounds (123–125).



84

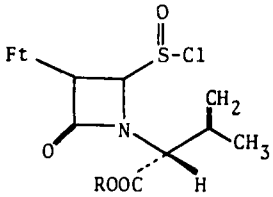


85



86

The first optically active sulfinyl chloride was prepared (126) by treatment of 7-phthalimidopenicillanate 1-oxide with sulfuryl chloride. The formation of a mixture of diastereomeric sulfinyl chlorides **87** in a 2:1 ratio indicates that the chlorosulfinyl grouping is demonstrably chiral.

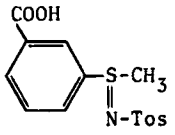


87

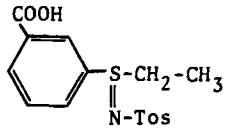
F. Sulfimides

The replacement of the oxygen atom in sulfoxides by nitrogen leads to a new class of chiral sulfur compounds, namely, sulfimides, which recently have attracted considerable attention in connection with the stereochemistry of sulfoxide-sulfimide-sulfoximide conversion reactions and with the steric course of nucleophilic substitution at sulfur. The first examples of chiral sulfimides, **88** and **89**, were prepared and resolved into enantiomers by Phillips (127,128) by means of the brucine and cinchonidine salts as early as 1927. In the same way, Kresze and Wustrow (129) were able to separate the enantiomers of other structurally related sulfimides.

The best and most versatile method for the synthesis of chiral sulfimides takes advantage of the stereospecific reaction of chiral

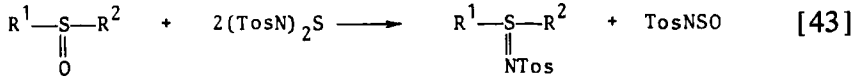


88

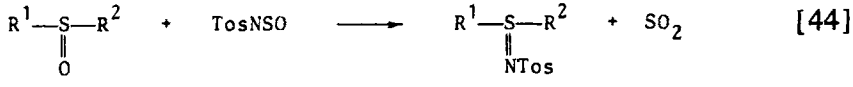


89

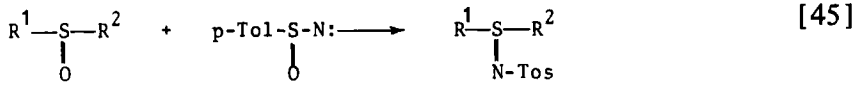
sulfoxides with various iminating reagents such as bis(*N*-tosylsulfurdiimine), *N*-sulfinyl-*p*-toluenesulfonamide, and *p*-toluenesulfinylnitrene (130–136). With all these reagents the sulfoxide-sulfimide



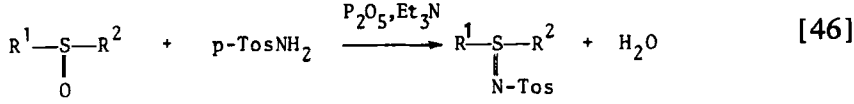
[43]



[44]



[45]



[46]

conversion occurs with retention of configuration at sulfur. However, when pyridine is used as solvent, the reaction of sulfoxides with bis(*N*-tosylsulfurdiimine) and *N*-sulfinyl-*p*-toluenesulfonamide proceeds with inversion of configuration in accordance with the original observation of Cram and Day (130).

An alternative stereospecific synthesis of chiral sulfimides reported by Nudelman (137) consists of the reaction of the diastereomeric menthyl *p*-toluenesulfinimidoates **90** with Grignard reagents giving the optically active sulfimide **91**. This reaction, like the Andersen synthesis of chiral sulfoxides, proceeds with inversion of configura-

$$\text{p-Tol-}\overset{*}{\underset{\|}{\text{S}}}\text{-OMen} \quad (\text{N-Tos}) \quad + \quad CH_3MgBr \longrightarrow \text{p-Tol-}\overset{*}{\underset{\|}{\text{S}}}\text{-}CH_3 \quad (\text{N-Tos}) \qquad [47]$$

90 91

tion at sulfur. There are also two papers in the literature describing the asymmetric synthesis of sulfimides. Oae (59,138) has reported that unsymmetrical diaryl sulfides, on treatment with *t*-butyl hypochlorite and menthol followed by the sodium salt of *p*-toluenesulfonamide, give optically active sulfimides.

$$Ar^1\text{-S-}Ar^2 \xrightarrow[2.\text{MenOH}]{1.t\text{-BuOCl}} Ar^1\text{-}\overset{*}{\underset{\|}{\text{S}}}\text{-}Ar^2 \quad (\text{N-Tos}) \qquad [48]$$

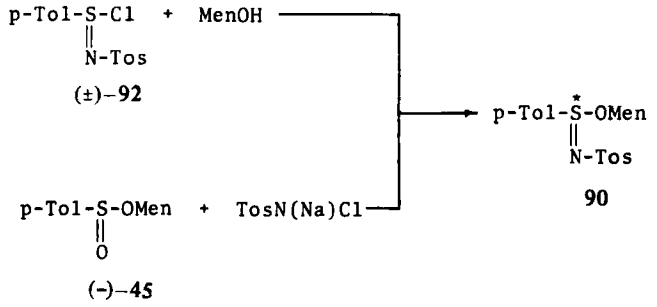
The second work (139) deals with the asymmetric desulfimination of racemic alkyl aryl *N*-tosylsulfimides by chiral thiols.

$$2R^1\overset{}{\underset{\|}{\text{S}}}\text{-Ar} \quad (\text{N-Tos}) \quad (\pm) \quad + \quad 2\overset{*}{R}^2SH \longrightarrow R^1\overset{*}{\underset{\|}{\text{S}}}\text{-Ar} \quad (\text{N-Tos}) \quad + \quad R^1\text{S-Ar} \quad + \quad \overset{*}{R}^2_2S_2 \quad + \quad TosNH_2 \qquad [49]$$

G. Sulfinimidoates and Sulfinimidamides

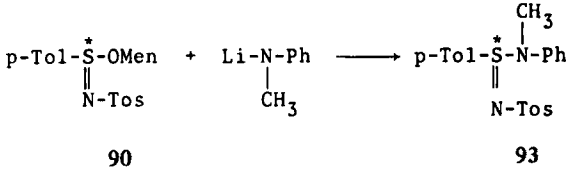
In addition to sulfimides, the nitrogen analogs of sulfinates and sulfinamides are chiral and have been obtained as optically active compounds. For instance, the synthesis of diastereomeric menthyl *p*-toluenesulfinimidoates **90** mentioned above was effected by Cram and his collaborators (18,137) on two ways. The first comprised the reaction of racemic *N*-tosyl-*p*-tolueneiminosulfinyl chloride **92** with menthol, followed by separation of the diastereomers of **90**, whereas in the second method the reaction of the ester (–)-**45** with chloramine T was utilized.

In extension of this work, the synthesis of enantiomeric and diastereomeric sulfinimidamides was also described. Treatment of the diastereomerically pure menthyl ester **90** with the lithium salt of *N*-methylaniline was found to give the corresponding sulfinimidamide

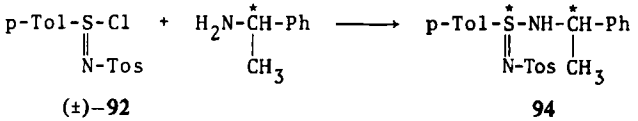


[50]

93, in which the sulfur atom is the sole center of chirality. A mixture of the closely related diastereomeric sulfinimidamides **94** was obtained (140) as a result of the reaction of the racemic chloride **92** with chiral α-methylbenzylamine. Its crystallization gave the pure diastereomers of **94**.



90 **93** [51]



(±)-**92** **94** [52]

H. Sulfurous Acid Derivatives

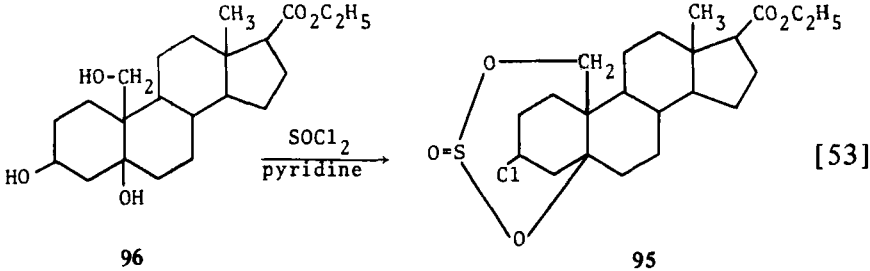
All the chiral sulfinyl compounds discussed above are the derivatives of achiral sulfinic acid **94a**. Another class of chiral sulfinyl compounds may be derived from achiral sulfurous acid **94b** via replacement of the hydroxy groups by suitable substituents. A brief survey of such chiral sulfinyl compounds is presented next.



94a **94b**

1. Sulfites

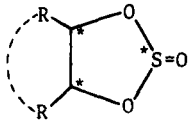
In 1952 Herzig and Ehrenstein (141) obtained chiral sulfites for the first time. They found that a mixture of the cyclic diastereomeric sulfites **95**, separated by chromatography, is obtained on treatment of 3-β-5,19-trihydroxyetiocholanate **96** with thionyl chloride in the



[53]

96 **95**

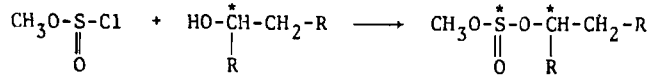
presence of pyridine. A variety of cyclic diastereomeric sulfites having the general formula **97** were later synthesized from thionyl chloride and other chiral diols (142–146).



97

Pritchard and co-workers (147) reported the preparation of an acyclic chiral sulfite, **98**, which is formed as a mixture of diastereomers in the reaction between racemic methyl chlorosulfite and (+)-diphenacyl malate. The pure diastereomers of **98** were isolated by fractional crystallization.

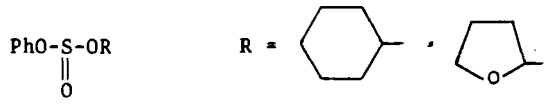
A very interesting method for the synthesis of chiral sulfites with the sulfur atom as the only chiral center was reported by Reid and



[54]

R = $PhC(O)CH_2OC(O)O$-

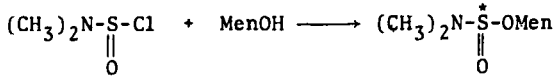
Fahrney (148). The pepsin-catalyzed hydrolysis of the racemic phenyl cycloalkyl sulfites **99** was found to be highly enantioselective, and it gave the unreacted sulfites **99** in optically active form.



99

2. Amidosulfites and Amidothiosulfites

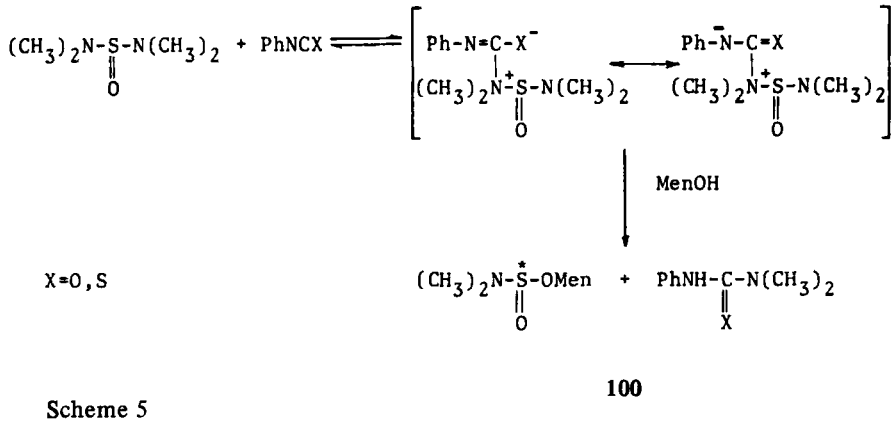
Wudl and Lee (96,97) reported the first preparation and resolution of the cyclic diastereomeric amidosulfites **58**, which have been successfully used in the synthesis of chiral sulfoxides. A mixture of diastereomeric menthyl dimethylamidosulfites (**100**) was obtained in the reaction of racemic dimethylaminosulfinyl chloride (**101**) with menthol in the presence of pyridine (149). The degree of asymmetric



[55]

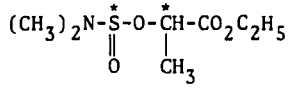
(±)–101 **100**

induction in this reaction was rather low, and the highest ratio of diastereomers was found to be 55:45. It is interesting that the same diastereomeric mixture of amidosulfites **100** was produced by the more complicated reaction shown in Scheme 5. Similar experiments



Scheme 5

were carried out with (–)-ethyl lactate, leading to the corresponding diastereomeric amidosulfites **102**.



102

The first examples of optically active acyclic alkyl dimethylamidosulfites **103** with sulfur as the sole chiral atom were prepared (149) according to the reaction sequence shown in Scheme 5 from achiral alcohols and (+)-α-phenylethyl isothiocyanate as an asymmetric reagent. Optically active amidothiosulfites **104** were also synthesized using the same approach (150).

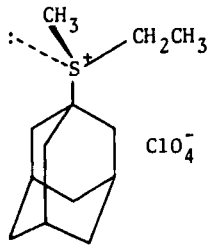


103 **104**

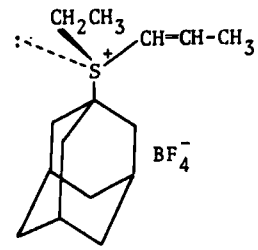
I. Sulfonium Salts

Sulfonium salts also belong to the group of chiral tricoordinate sulfur compounds. As mentioned in the introduction, methylethylthetine **1** and methylethylphenacyl **2** ions were the first optically active organosulfur compounds to be prepared. Their optical resolution was accomplished in 1900 (1,2) through conventional separation of the diastereomeric salts formed by **1** and **2** with chiral camphor- or bromocamphorsulfonic acids. The successful optical resolution of sulfonium ions **1** and **2** was of great contemporary importance in the development of the theory of optical activity based on the tetrahedral model, even though in the case of sulfonium salts the role of a fourth substituent is played by the unshared pair of electrons on the sulfur atom.

More than 60 years later Darwish and co-workers (151,152) prepared a series of chiral trialkylsulfonium, dialkylarylsulfonium, and diarylalkylsulfonium perchlorates by resolution of the corresponding (–)-dibenzoyl hydrogen tartrate salts followed by replacement of the optically active acid anion by perchlorate. At the same time, 1-adamantylethylmethylsulfonium perchlorate **105** (153) and 1-adamantylethylpropenylsulfonium tetrafluoroborate **106** (154) were resolved

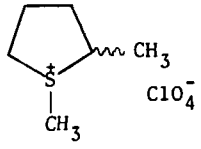


105

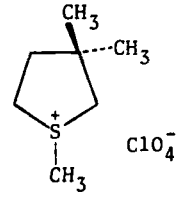


106

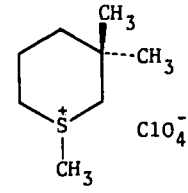
into their enantiomers via diastereomeric salts with (–)-malic acid and (–)-dibenzoyltartaric acid, respectively. More recently, the partial optical resolution of the cyclic five- and six-membered sulfonium salts **107**, **108**, and **109** (–)-di-*o*-toluoyltartaric acid as the chiral resolving agent has been described (155).



107



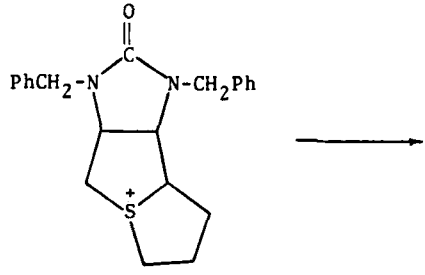
108



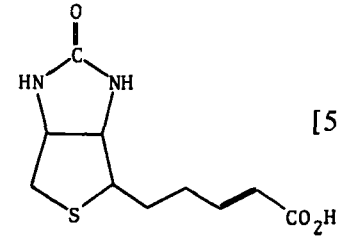
109

From the synthetic viewpoint the optical resolution of sulfonium salt **110** is of great interest because its enantiomers served as starting material for the synthesis of chiral α-dehydrobiotin **111** (156).

It is interesting to note that asymmetric synthesis of the sulfonium salt **112** was recently reported by Kobayashi (157). He found that



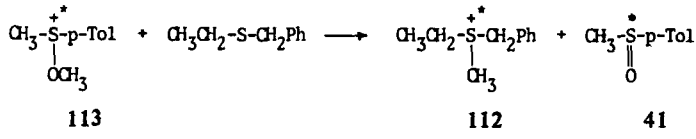
110



111

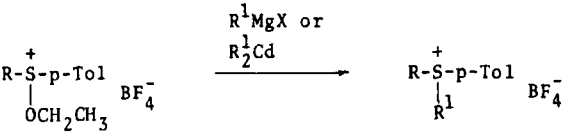
[56]

when benzyl ethyl sulfide is reacted with the chiral methoxysulfonium salt **113**, asymmetric methylation takes place at dicoordinate sulfur yielding the chiral benzylethylmethylsulfonium salt **112** with an optical purity of 60%, as well as chiral methyl *p*-tolyl sulfoxide **41**.



113 **112** **41** [57]

In addition to routes involving resolution and asymmetric synthesis, optically active sulfonium salts have been prepared in a stereospecific way by Andersen (158,159). Thus, synthesis of the optically active dialkyl-*p*-tolylsulfonium salts **114** from the optically active ethoxysulfonium salt **115** was accomplished by the addition of alkyl Grignard or dialkylcadmium reagents. This reaction occurs with inversion

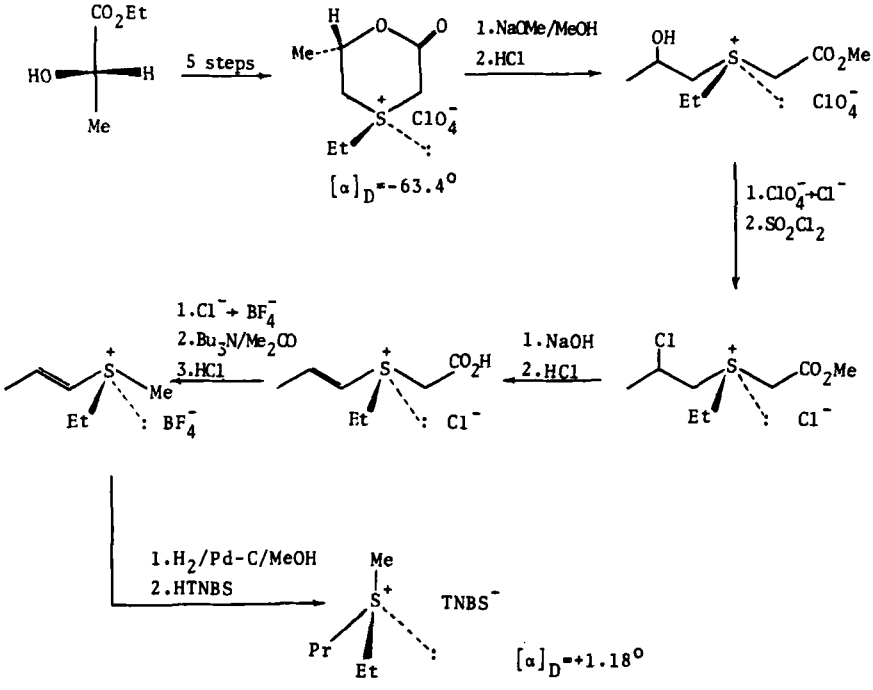


115 **114** [58]

of configuration at sulfur, although some racemization takes place. Despite the successful application of this procedure in the synthesis of various dialkylaryl or diarylalkylsulfonium salts, all attempts to prepare optically active triarylsulfonium salts resulted in the formation of racemic mixtures.

A multistep stereospecific synthesis of ethylmethylpropylsulfonium 2,4,6-trinitrobenzenesulfonate **116** from (-)-(*S*)-ethyl lactate was recently elaborated by Kjaer and his co-workers (160) and is shown in Scheme 6.

In their elegant studies on sulfoxides, Johnson and co-workers have described a general method for the synthesis of chiral alkoxysulfonium salts consisting of the *O*-alkylation of chiral sulfoxides by triethyloxonium tetrafluoroborate (161). This method is illustrated by eq. [59], which shows the synthesis of ethoxybenzyl-*p*-tolylsulfonium tetrafluoroborate **117**. Subsequently, it was found that other "hard" alkylating agents such as FSO_3CH_3 or $CF_3SO_3CH_3$ may be used for this purpose. Extension of the foregoing approach to



116

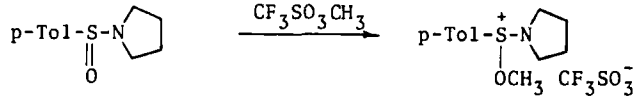
Scheme 6

chiral sulfinates made it possible (162) to prepare chiral dialkoxysulfonium salts **118**.

Similarly, the *O*-alkylation reaction of chiral sulfinamides leads to chiral alkoxyaminosulfonium salts. For instance, methoxypyrrolidino-*p*-tolylsulfonium salt **119** was formed when chiral sulfinamide **120**

$$\underset{\underset{\underset{\mathrm{O}}{\|}}{\mathrm{PhCH_2\text{-}S\text{-}p\text{-}Tol}}}{\mathbf{37}} \xrightarrow{\mathrm{Et_3O^+BF_4^-}} \underset{\underset{\underset{\mathrm{OCH_2CH_3}}{|}}{\mathrm{Ph\text{-}CH_2\text{-}S^+\text{-}p\text{-}Tol}}}{\mathbf{117}}\ \mathrm{BF_4^-} \qquad [59]$$

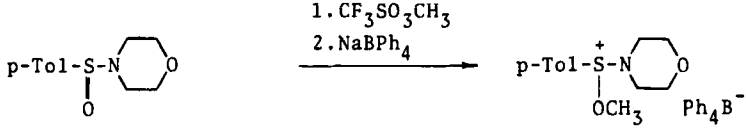
$$\underset{\underset{\underset{\mathrm{O}}{\|}}{\mathrm{R\text{-}S\text{-}OR^1}}}{} \xrightarrow{\mathrm{CF_3SO_3CH_3}} \underset{\underset{\underset{\mathrm{OCH_3}}{|}}{\mathrm{R\text{-}S^+\text{-}OR^1}}}{\mathbf{118}}\ \mathrm{CF_3SO_3^-} \qquad [60]$$



[61]

(+)-(*S*)-**120** (*S*)-**119**

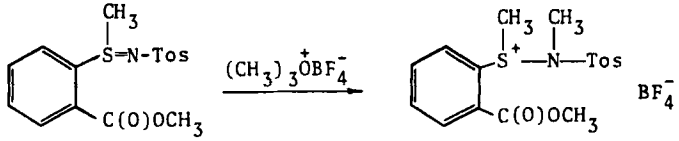
was treated with methyl trifluoromethanesulfonate (110). The reaction of chiral sulfinamide **121** with the same methylating agent gave the corresponding sulfonium salt **122**, which was isolated and characterized as a tetraphenylborate (163).



[62]

(+)-(*S*)-**121** (+)-(*S*)-**122**

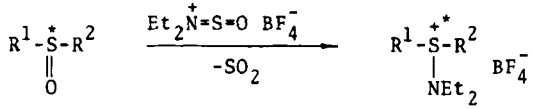
Two methods are described for the preparation of chiral aminosulfonium salts. The first is based on the alkylation of nitrogen in chiral sulfimides. In this way the optically active aminosulfonium salt **123** was obtained from sulfimide **124**, as shown in eq. [63] (164).



[63]

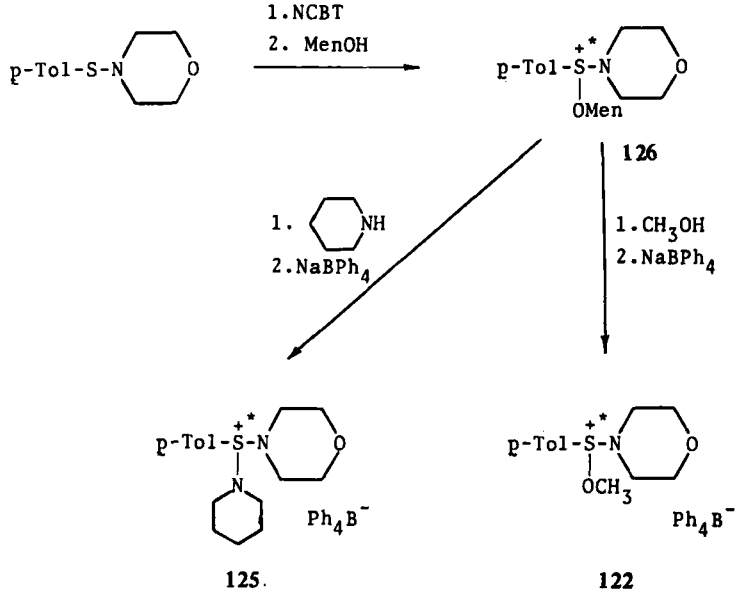
(-)-(*S*)-**124** (-)-(*S*)-**123**

The second approach to chiral aminosulfonium salts consists of the conversion of chiral sulfoxides into aminosulfonium salts by means of *N,N*-diethylaminosulfinyl tetrafluoroborate (165). The reaction occurs with predominant retention of configuration at sulfur with dialkyl and alkyl aryl sulfoxides. However, its stereospecificity is strongly dependent on the nature of substituents in the starting sulfoxide. In the case of diaryl sulfoxides this method failed to give chiral aminodiarylsulfonium salts.



[64]

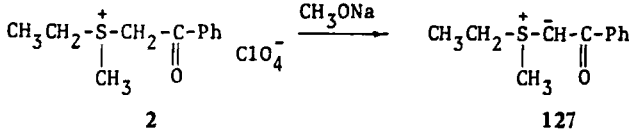
Quite recently, an asymmetric synthesis of alkoxyaminosulfonium salt **122** and diaminosulfonium salt **125** was accomplished (163) by way of menthoxysulfonium salt **126**, obtained by treating *N*-*p*-toluenesulfenylmorpholine with 1-chlorobenzotriazole (NCBT), followed by menthol. The subsequent addition of methanol and sodium tetraphenylborate gave the optically active salt **122** (Scheme 7). When **126** was treated with piperidine instead of methanol, the optically active diaminosulfonium salt **125** was formed.



Scheme 7

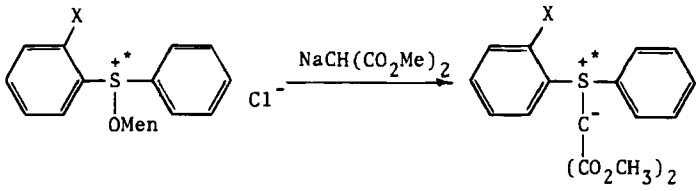
J. Sulfonium Ylides

Darwish and Tomilson (166) first reported that deprotonation of optically active methylethylphenacylsulfonium perchlorate (2) by means of sodium methoxide affords the optically active ethylmethylsulfonium phenacylide **127**. The ylide **127** has also been resolved into optically active forms via diastereomeric salts with chiral dibenzoyltartaric acid monohydrate (167).



2 127 [65]

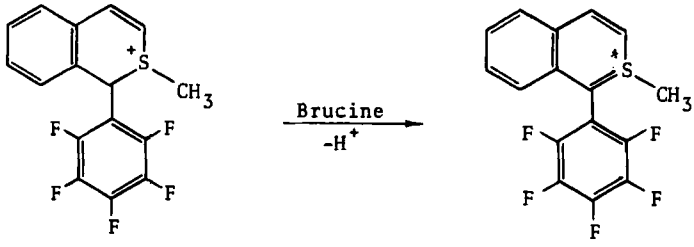
More recently, the chiral *o*-substituted diarylsulfonium ylides **128** were obtained from menthoxysulfonium salts **129** and sodium dimethylmalonate (59). The desired sulfonium salts **129** were prepared from the corresponding sulfides and menthol in the presence of *t*-butyl hypochlorite and used further without isolation.



[66]

129 X=OCH$_3$, CH$_3$ **128**

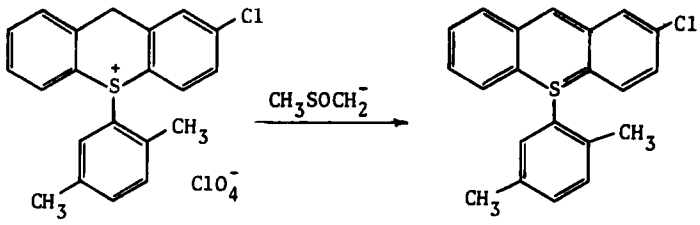
Among the compounds to be discussed in this subsection we also encounter thiabenzene systems that, according to Mislow (168), are best described as cyclic sulfonium ylides. 1-Pentafluorophenyl-2-methyl-2-thianaphthalene **130** the first example of an optically active thiabenzene, was prepared by Mislow and co-workers (169) by deprotonation of thiochromenium tetrafluoroborate **131** with brucine in anhydrous dimethylsulfoxide.



[67]

131 **130**

In further studies on thiabenzenes, Mislow and co-workers (170) demonstrated that deprotonation of optically active 2-chloro-10-(2,5-xylyl)-10-thioxanthenium perchlorate **132**, resolved via the (+)-camphor-10-sulfonate salt, affords optically active 2-chloro-10-(2,5-xylyl)thiaanthracene **133**, which subsequently rearranges to the corresponding 9-substituted thioxanthene.

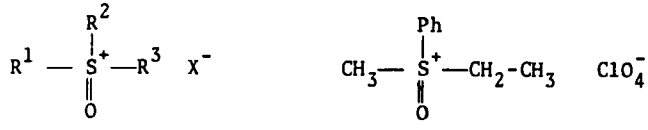


[68]

132 133

K. Oxosulfonium Salts

Oxosulfonium salts of the general formula shown in **134** belong to a group of tetrahedral tetracoordinate sulfur compounds with four different ligands. Therefore, they are chiral at sulfur and can exist in the form of optical isomers. Thus far, however, methylethylphenyl-



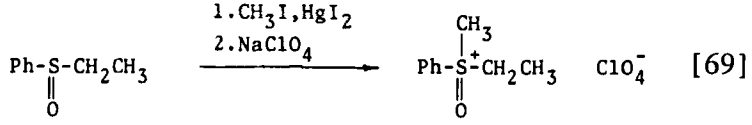
134 135

oxosulfonium perchlorate **135** is the only compound of this type whose enantiomers have been isolated. Three methods are available to prepare optically active **135**, and all were worked out by Kobayashi and co-workers (171–173). The first method (171) is based on the separation of diastereomeric salts formed by methylethylphenyloxosulfonium mercuritriiodide and (+)-camphor-10-sulfonic acid. Upon treatment with sodium perchlorate, the enantiomers of **135** were isolated.

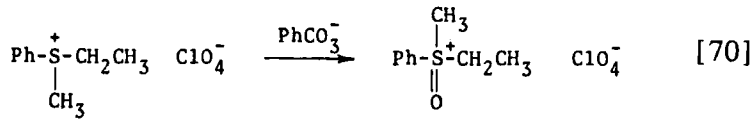
Sulfoxides are known to form both *O*-alkyl and *S*-alkyl derivatives. The latter are obtained when so-called soft alkylating agents are employed. This behavior of sulfoxides was utilized (172) in the stereospecific synthesis of chiral **135**. The reaction of the optically active (+)-ethyl phenyl sulfoxide **136** with methyl iodide in the presence of mercuric iodide followed by anion exchange was found to give the optically active salt **135**.

An alternative stereospecific synthesis of optically active (+)-**135**

consists in the oxidation of (+)-methylethylphenylsulfonium perchlorate **137** with perbenzoic acid (173).



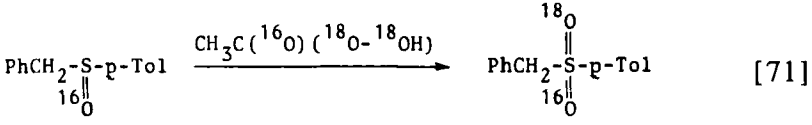
(+)–136 (+)–135 [69]



(+)–137 (+)–135 [70]

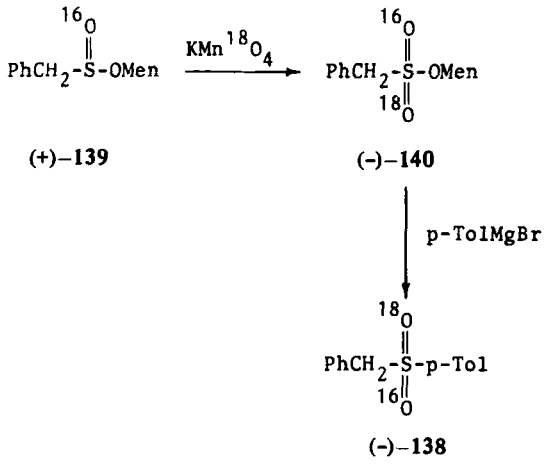
L. [$^{16}O^{18}O$] Sulfones and [$^{16}O^{18}O$] Sulfonates

Substitution of one of the two ^{16}O oxygen atoms in the sulfonyl group by ^{18}O leads to a chiral sulfonyl group. The first example of a sulfone whose optical activity is due to such isotopic substitution was reported by Stirling (77) as early as 1963. The oxidation of (+)-benzyl *p*-tolyl sulfoxide **37** with ^{18}O-labeled peracetic acid was found to give (–)-benzyl *p*-tolyl [$^{16}O^{18}O$] sulfone **138**. The same chiral



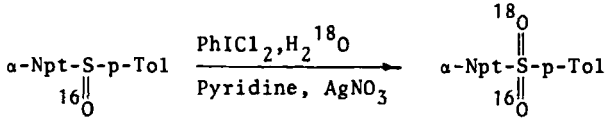
(+)–37 (–)–138 [71]

sulfone was later obtained by Sabol and Andersen (174) by a two-reaction sequence. In the first step (+)-menthyl phenylmethanesulfinate **139** was oxidized with $KMn^{18}O_4$ to give the corresponding (–)-menthyl phenylmethanesulfonate **140**. This ester, in turn, upon treatment with *p*-tolylmagnesium bromide furnished the identical levorotatory sulfone **138**. Recently, two other approaches became available for the synthesis of chiral [$^{16}O^{18}O$] sulfones, both of which were developed by Cinquini et al. (175). One of these is the oxidation of optically active (–)-α-naphthyl *p*-tolyl sulfoxide **141** with



(+)–139 (–)–140 (–)–138 [72]

iodobenzene dichloride in the presence of silver nitrate in pyridine containing ^{18}O-labeled water.



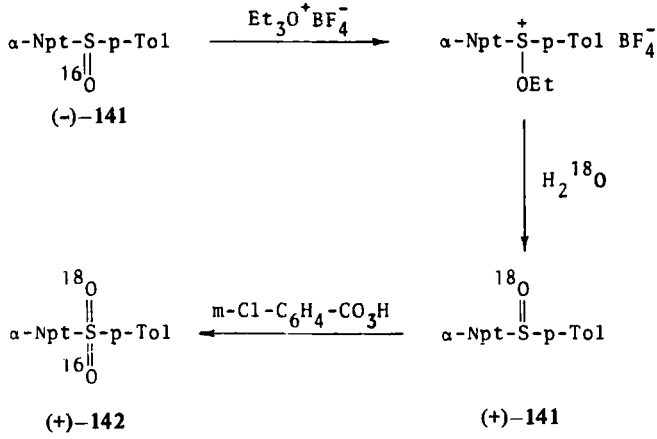
(–)–141 (–)–142 [73]

The second synthesis of the enantiomer of this sulfone entails two transformations. First, (–)-α-naphthyl *p*-tolyl [^{16}O] sulfoxide **141** was converted into the corresponding [^{18}O] sulfoxide **141** by the method of Johnson (with inversion of configuration). Its oxidation with *m*-chloroperbenzoic acid afforded the chiral sulfone (+)-**142** (Scheme 8). The latter procedure was also used for the preparation of chiral (–)-[$^2H_2$]benzyl *p*-tolyl [$^{16}O^{18}O$]sulfone (**143**) from (–)-[$^2H_2$]-benzyl *p*-tolyl sulfoxide **37**.

M. Sulfoximides

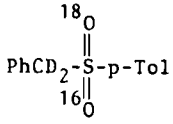
Among chiral tetracoordinate sulfur compounds, most information is available on sulfoximides, which may be considered to be the mononitrogen analogs of sulfones.

The first example of an optically active sulfoximide was reported by Barash (176) in 1960. He was able to effect the separation of the



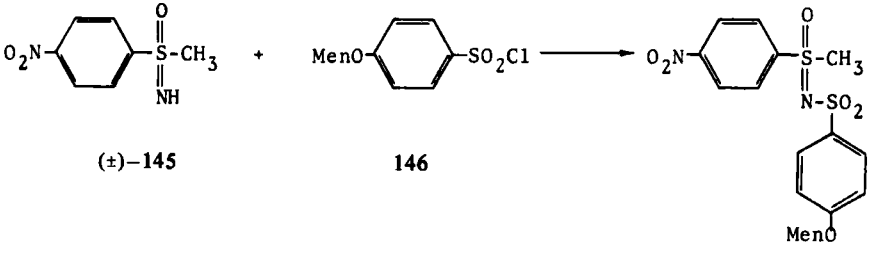
Scheme 8

diastereomeric sulfoximides **144** obtained by condensation of the racemic methyl-*p*-nitrophenylsulfoximide **145** with the optically active sulfonyl chloride **146**. Slightly later, Kresze and Wustrow (129)

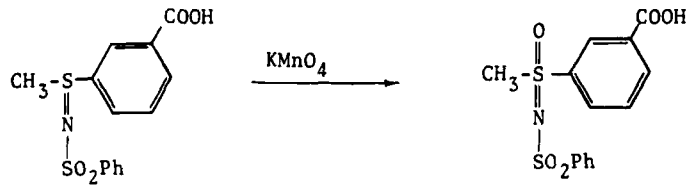


(-)-**143**

reported the optical resolution of the racemic sulfoximide **147**, containing a carboxyl group, via diastereomeric salts with α-methylbenzylamine. Moreover, they prepared the enantiomers of this sulfoximide by oxidation of optically active forms of the corresponding sulfimide **148** with potassium permanganate and showed that the reaction pro-



(±)-**145** **146** **144** [74]



[75]

148 147

ceeded with retention of configuration at sulfur. Fusco and Tenconi (177) took advantage of the basic nature of the imino group of "free" sulfoximides and resolved methylphenylsulfoximide **149** by means of (+)-camphor-10-sulfonic acid. Mesitylmethylsulfoximide **150** was resolved by Johnson and Schroeck (118) in a similar way.

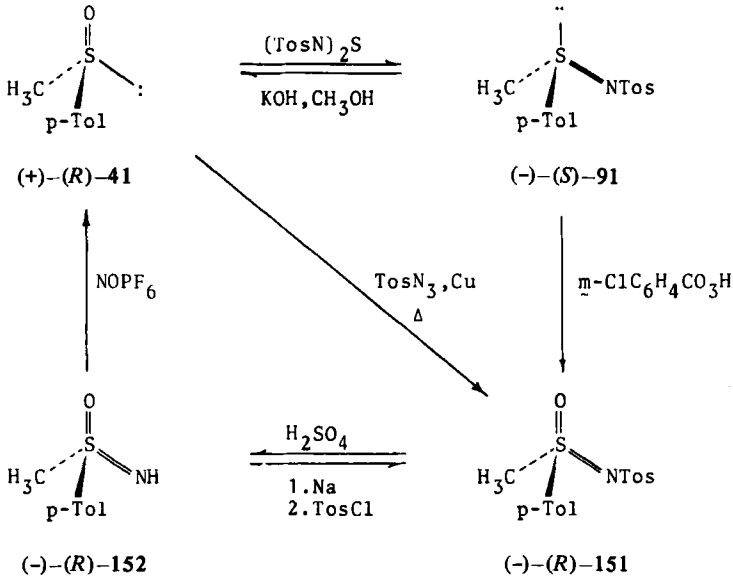


149 150

Recent studies on chiral sulfoximides, espcially in the laboratories of Cram, Johnson, Andersen, and Stirling, have been centered on the stereospecific interconversions between chiral sulfoxides, sulfimides, and sulfoximides, as well as on the construction of new stereochemical cycles. For the sake of brevity, only some selected results from these extensive studies are presented here to illustrate various stereospecific syntheses of chiral sulfoximides.

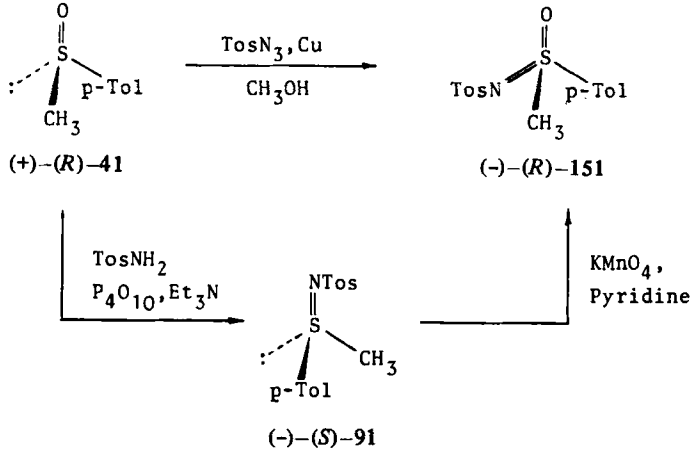
The procedure most commonly used for the stereospecific preparation of optically active sulfoximides involves the reaction of optically active sulfoxides with arylsulfonyl azides in the presence of copper (98,118,131,178,179). This reaction occurs with retention of configuration at sulfur and with high stereospecificity. The stereospecific sulfoxide-sulfoximide conversion is a key reaction in the stereospecific sulfoxide-sulfimide-sulfoximide set of interconversions carried out by Cram and co-workers (98) and shown in Scheme 9. A similar cycle of interconversions studied independently by Andersen and co-workers (179) was used to determine the stereochemical course of the sulfoxide-sulfoximide transformation (see Scheme 10).

Another stereospecific synthesis of chiral sulfoximides, reported



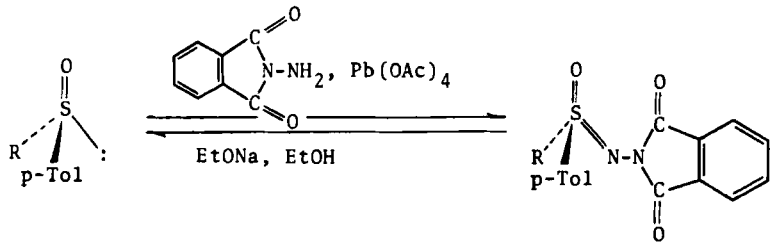
Scheme 9

by Colonna and Stirling (180), is based on the reaction of chiral sulfoxides with *N*-aminophthalimide, which affords the corresponding *N*-phthalimidosulfoximides **153**, with retention of configuration at



Scheme 10

sulfur. The starting sulfoxides may be regenerated from **153** by treatment with sodium ethoxide.

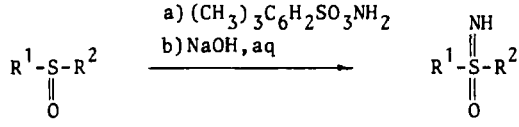


[76]

R = benzyl, vinyl, α–naphthyl

153

Optically active *N*-tosylsulfoximides produced in the copper-catalyzed reaction of chiral sulfoxides with tosyl azide may be hydrolyzed with strong acid (H_2SO_4) to optically active "free" sulfoximides. However, this procedure often fails and/or results in decomposition. It is interesting to note in this connection that a simple one-step method for the preparation of optically active unsubstituted sulfoximides has been reported recently by Johnson and co-workers (180). It involves the reaction between optically active sulfoxides and *O*-mesitylsulfonylhydroxylamine and results in sulfoximides **60** of high optical purity. As expected, this imidation process occurs with retention of configuration at sulfur.



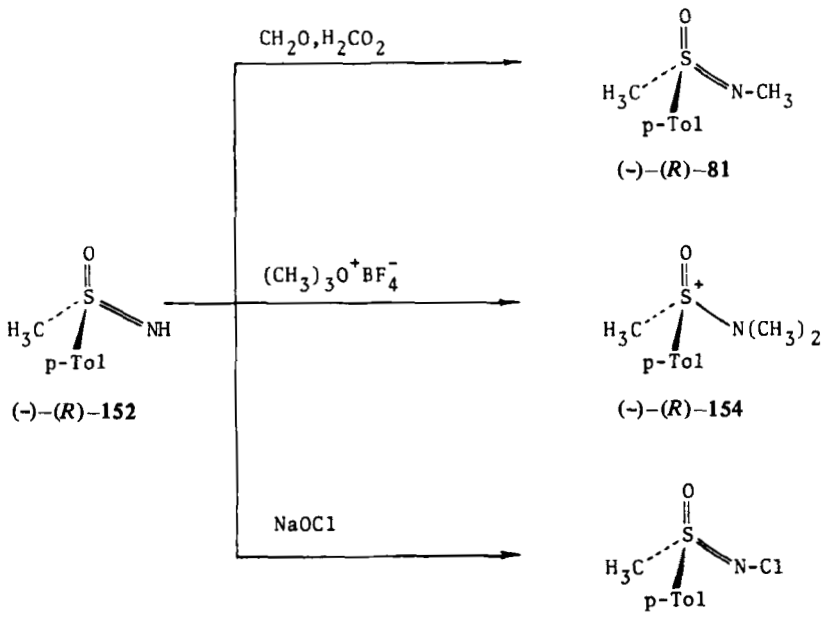
[77]

60

Optically active unsubstituted sulfoximides react with electrophilic reagents at the nitrogen atom, yielding a variety of the *N*-substituted sulfoximides. The monomethylation (119), dimethylation (118), and chlorination (98) reactions of (–)-(*R*)-methyl-*p*-tolylsulfoximide **152** best illustrate this type of modification (Scheme 11).

Very recently, Oae et al. (182) found that alkaline hydrolysis of *N*-chlorosulfimide **156** affords the corresponding sulfoximide **157** with almost full retention of configuration at sulfur.

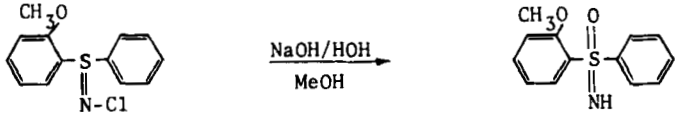
In an extension of their prolific work on chiral sulfoximides, Cram and co-workers (133,182,183) have also prepared the optically active



(-)-(*R*)-152 (-)-(*R*)-81 (-)-(*R*)-154 (-)-(*R*)-155

Scheme 11

cyclic sulfoximides **158** and **159**. The sulfoximide **158** was obtained (133) in optically active form via treatment of the racemate with (+)-camphor-10-sulfonyl chloride followed by separation of diastereomers and removal of the sulfonyl grouping. The optically active sulfoximide **159** (182) was synthesized in a stereospecific way by reacting the sodium salt of (-)-(*R*)-methyl-*p*-tolylsulfoximide **152**

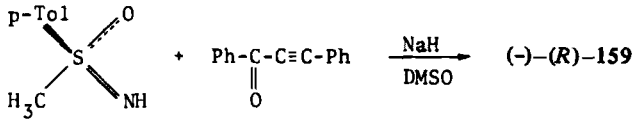


[78]

156 **157**



158 **159**

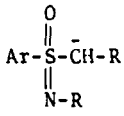


[79]

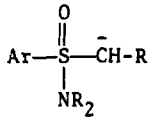
(-)-(*R*)-**152** **160**

with the ketone **160**. It is evident that after the first addition step an intramolecular cyclization takes place to form a six-membered ring.

Finally, it should be noted that in contrast to optically labile sulfonium ylides, the oxosulfonium ylides derived from chiral sulfoximides and related compounds are configurationally stable. Johnson and co-workers (184) have obtained a large number of chiral oxosulfonium ylides having the general structures **161** and **162** and have used them as nucleophilic alkylidene transfer agents for asymmetric synthesis. These results are discussed in the last part of this chapter.



161



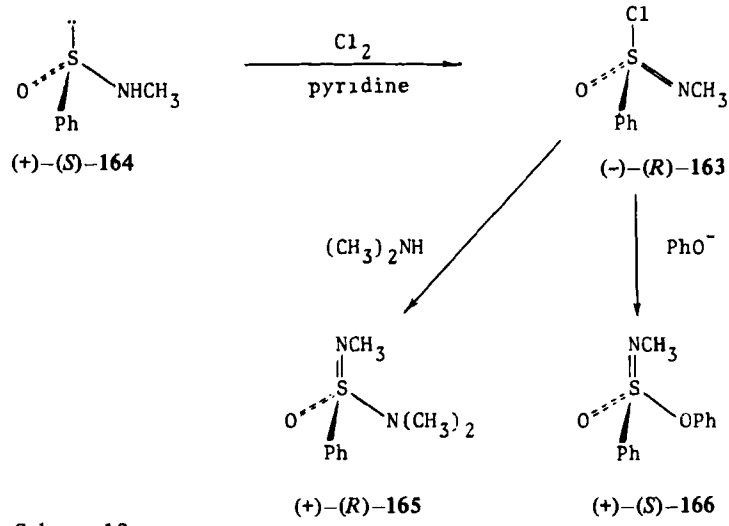
162

N. Sulfonimidoyl Chlorides, Sulfonimidoates, and Sulfonimidamides

In this section we briefly mention other classes of sulfur compounds that are optically active as a consequence of the attachment of four different groups to the central sulfur atom.

Of great importance was the discovery by Johnson et al. (185) of the stereospecific synthesis of optically active sulfonimidoyl chlorides, which are key substrates for making new types of sulfonimidoyl compounds. The method involves chlorination of readily available chiral sulfinamides with chlorine or *N*-chlorobenzotriazole. Scheme 12 summarizes the synthesis of (-)-(*R*)-*N*-methylphenylsulfonimidoyl chloride **163** from (+)-(*S*)-*N*-methyl benzenesulfinamide **164** and its reactions with sodium phenoxide and dimethylamine.

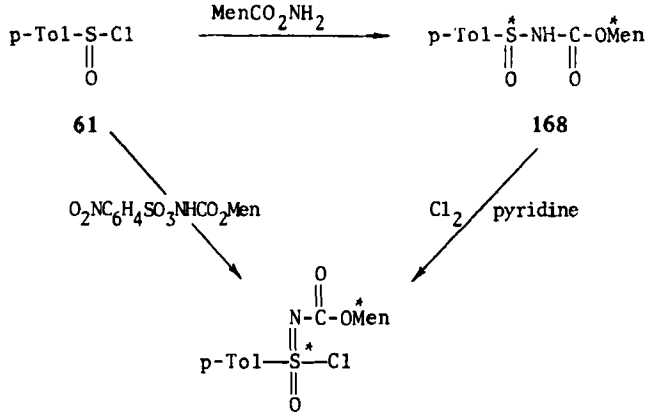
Johnson demonstrated that the conversion of (+)-(*S*)-**164** into (-)-(*R*)-**163** takes place with retention of configuration, whereas the nucleophilic substitution reactions occurred with inversion of configuration at sulfur. The only drawback to this study involved the



Scheme 12

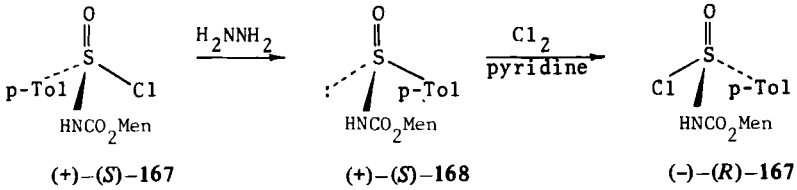
fact that the chloride **163** was an optically unstable compound and could not be isolated in a pure state.

Jones and Cram (186) subsequently reported the preparation of the two optically pure crystalline diastereomers of *N*-carbomenthoxy-*p*-toluenesulfonimidoyl chloride **167**. A mixture of diastereomeric chlorides was obtained as shown in Scheme 13, from which (+)-(*S*)-**167** was isolated by chromatography and crystallization. The second diastereomerically pure isomer of chloride **167** was synthesized by



Scheme 13

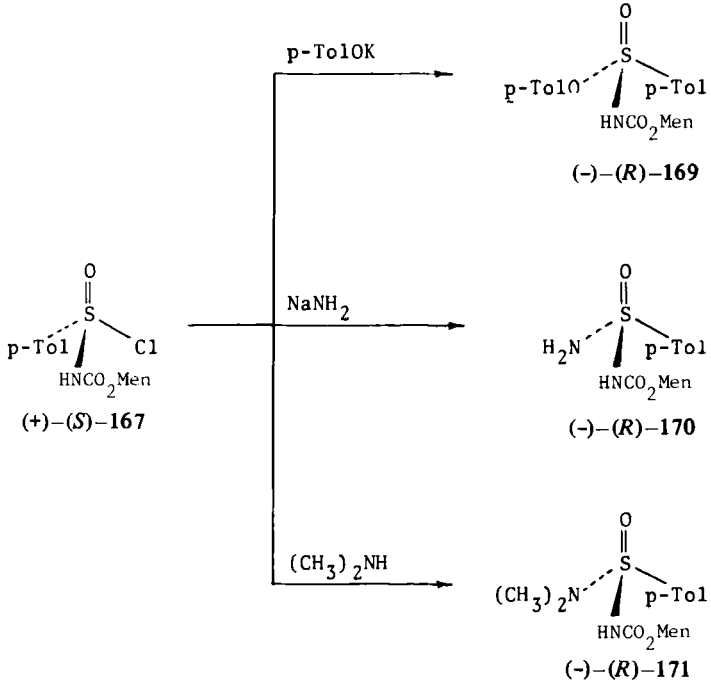
treatment of (+)-(*S*)-**167** with hydrazine and subsequent chlorination of the *N*-carbomenthoxy-*p*-toluenesulfinamide **168**, which was formed.



(+)-(*S*)-**167** (+)-(*S*)-**168** (-)-(*R*)-**167** [80]

When pure (+)-(*S*)-**167** was reacted with potassium *p*-cresylate, sodium amide, and dimethylamine, the corresponding nucleophilic substitution products **169**, **170**, and **171** were formed (Scheme 14). In each case, complete or almost complete inversion of configuration at chiral sulfur was observed.

With regard to optically active sulfonimidamides, reference should also be made to compounds **172** and **173**. They are sufficiently acidic to form salts with organic bases and were resolved into optical anti-



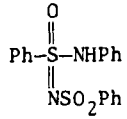
(+)-(*S*)-**167**

(-)-(*R*)-**169**

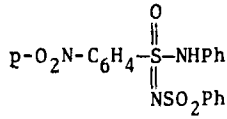
(-)-(*R*)-**170**

(-)-(*R*)-**171**

Scheme 14

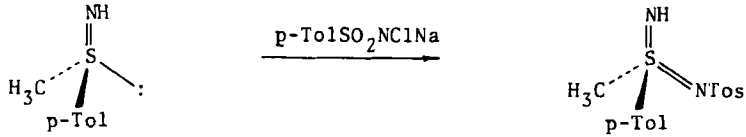


172



173

podes by Levchenko and Kozlov (187) via their α-methylbenzylamine salts as early as 1963. Recently, the stereospecific synthesis of *N*-tosylmethyl-*p*-tolylsulfonimidamide **174** was accomplished by Christensen and Kjaer (188) by treatment of the optically active sulfimide **175** with chloramine T in liquid ammonia.

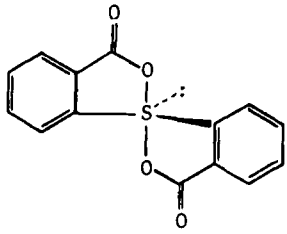


(+)-(*R*)-**175** (-)-(*S*)-**174** [81]

O. Sulfuranes

Tetracoordinate sulfur compounds containing a lone pair of electrons at sulfur possess a more or less distorted trigonal-bipyramidal structure, in common with the vast majority of other pentacoordinated molecules of the main group elements (189,191,199). A common name, sulfurane, is generally accepted for this type of compound. In principle, sulfuranes are chiral. However, both the number of optically active isomers and their optical stability depend on the nature of substituents bonded to the central sulfur atom, the apicophilicity of the substituents, and the energy required for permutational isomerization processes. In this context it is interesting to note that acyclic sulfuranes with four different ligands should exist in 20 isomeric forms.

The first indication of the chirality of sulfuranes was provided by the X-ray analysis of spirosulfurane **176** (192). This work clearly demonstrated the presence of enantiomeric pairs of **176** in the crystal lattice. In 1975, the optically active chlorosulfurane **177**, the first example of an optically active tetracoordinate sulfurane, was synthesized by Martin and Balthazor (194,195) by the route indicated in Scheme 15. Reaction of (-)-(*S*)-menthyl benzenesulfinate **178** with the protected Grignard reagent **179** gave the corresponding sulfoxide alcohol (-)-(*S*)-**180** which was cyclized to the chlorosul-

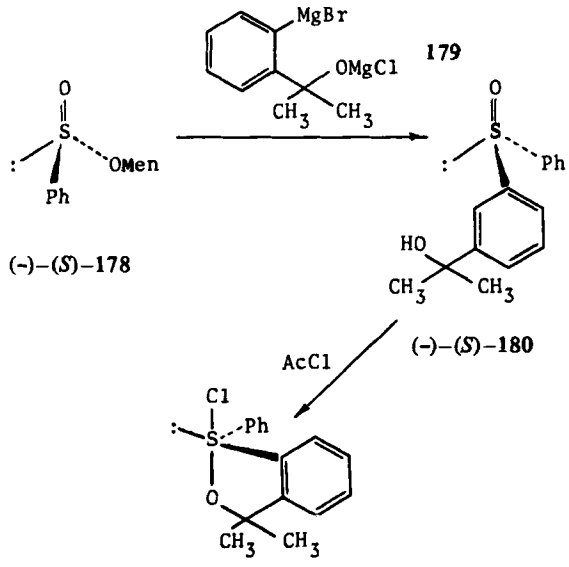


176

furane (+)-177 by treatment with acetyl chloride at low temperature. According to this procedure it was possible to obtain optically active (+)-177 in 95% enantiomeric purity.

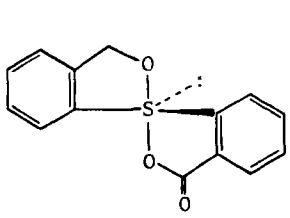
Since the first reaction undoubtedly proceeds with inversion of configuration at sulfur, and since additional experiments demonstrated that the formation of chlorosulfurane 177 from sulfoxide 180 takes place with retention at sulfur, (*S*)-chirality was assigned to (+)-177. As for the designation of absolute configuration, Martin and Balthazor (195) proposed a system of nomenclature for optically active pentacoordinate species.

Recently, Kapovits et al. (25) prepared the enantiomers of the spirosulfuranes 181, 182, 183, and 184 by treating the (-)- and

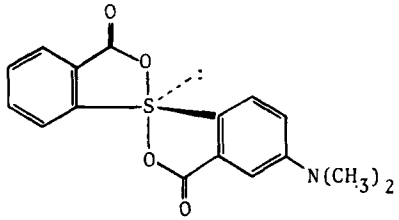


Scheme 15

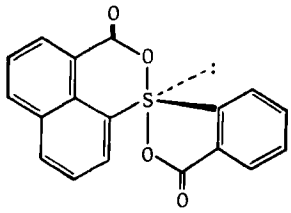
(+)-sulfoxides **13**, **14**, **15**, and **16** mentioned above with *N,N*-dichloro-*p*-toluenesulfonamide in pyridine at low temperatures. So far, the optical purities and absolute configurations of the spirosulfuranes so prepared are unknown.



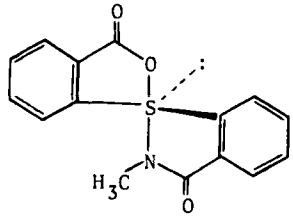
181



182



183



184

The stereochemistry of chiral sulfuranes is in its infancy, and further studies in this field are both expected and desirable.

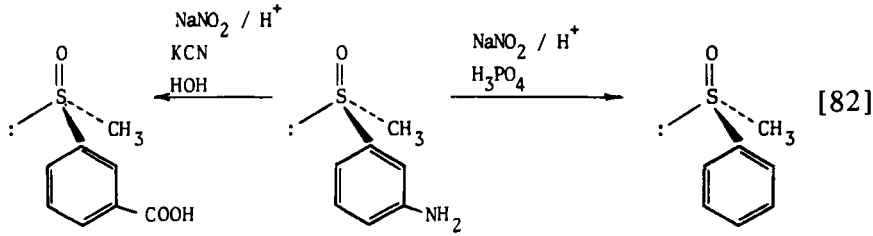
III. DETERMINATION OF ABSOLUTE CONFIGURATION AND OPTICAL PURITY OF CHIRAL SULFUR COMPOUNDS

The development of sulfur stereochemistry is closely connected to the determination of absolute and relative configurations and to a knowledge of the optical purities of organic sulfur compounds. A knowledge of the absolute configuration of the chiral sulfur center and the correct evaluation of its optical purity is required not only by chemists studying static or dynamic sulfur stereochemistry but also by biochemists, because many chiral sulfur compounds have been isolated from natural sources in recent years. Consequently, the past two decades have seen a very rapid development of methods for the determination of absolute configuration and optical purity in that group of compounds. Generally, these methods can be clas-

sified in two groups. The first includes methods utilizing chemical transformations and the second is based on spectrometric techniques. Now we discuss specific methods for determining the absolute configuration and optical purity of chiral organosulfur compounds. One should note that, in most cases, several methods are used simultaneously in such assignments.

A. Determination of Chirality at Sulfur by Chemical Methods

The conventional method of establishing the absolute configuration of chiral compounds, consisting of the conversion of the tested compound into another of known configuration in a sequence of reactions that does not affect the center of chirality, has been utilized for the determination of the absolute configuration of alkyl aryl sulfoxides and benzyl alkyl sulfoxides containing amino or carboxylic group in the meta position in the aromatic ring (196). In this correlation, optically active (–)-*m*-aminophenyl methyl sulfoxide **185** was diazotized, and the diazonium salt obtained was decomposed *in situ* with phosphoric acid to give (–)-methyl phenyl sulfoxide **186**. Since the levorotatory sulfoxide **186** has the (*S*)-configuration at the sulfur atom, the same configuration should be assigned to sulfoxide (–)-**185** and to (–)-*meta*-carboxyphenyl methyl sulfoxide (8) prepared from (–)-**185** in a similar way.

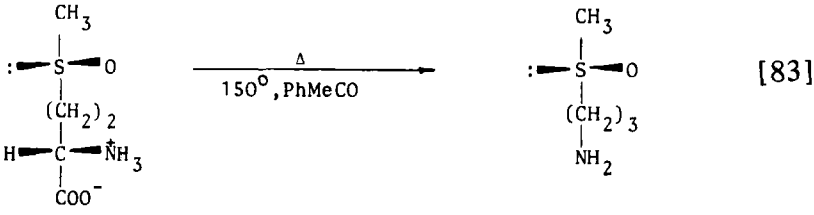


[82]

(–)-(*S*)-**8** (–)-(*S*)-**185** (–)-(*S*)-**186**

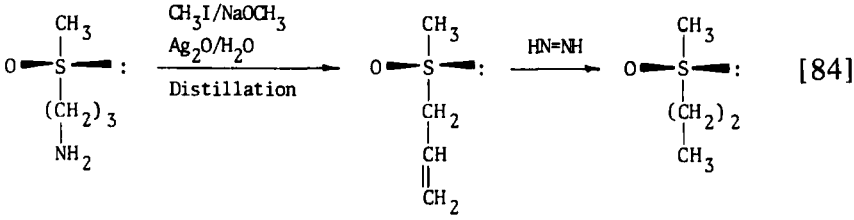
The (*S*)-configuration at the sulfur atom was assigned (49) to the naturally occurring L-methionine sulfoxide **28** based on the results of its thermal decarboxylation, leading to the formation of the dextrorotatory enantiomer of 3-methylsulfinylpropylamine **187** of known absolute (*S*)-configuration at chiral sulfur.

The configurational relationship between (–)-(*R*)-**187**, (+)-alkyl methyl sulfoxide **188**, and methyl *n*-propyl sulfoxide **189** was established (79) by the chemical method shown in eq. [84].



[83]

(-)-(*S*)-28 (+)-(*S*)-187



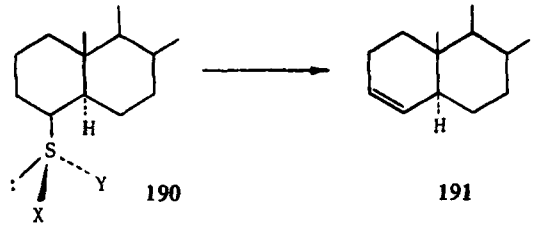
[84]

(-)-(*R*)-187 (+)-(*R*)-188 (-)-(*R*)-189

A different chemical method that allows the absolute configuration of sulfoxides and other sulfinyl compounds to be established is based on the well-known fact that these compounds undergo stereospecific syn elimination, yielding olefins through a five-center cyclic transition state (197,198). In sulfoxides containing an additional center of chirality on carbon, the transition states leading to syn elimination are diastereomeric. Analysis of the reaction products and of the relative stability of the diastereomeric transition states may lead in favorable cases to the assignment of absolute configuration at sulfur in compounds subjected to pyrolysis.

The pyrolytic method was first used to establish the chirality at sulfur in steroidal sulfoxide derivatives of 5α-cholestane (199). It was found that behavior of the diastereomeric sulfoxides **190**, derivatives of 4β-phenylsulfinyl-5α-cholestane having opposite configurations at sulfur, is quite different when the compounds are heated in boiling benzene. One of them, **190a**, undergoes complete decomposition, affording 5α-cholest-3-ene **191**, but the second diastereomer is quite inert under these conditions.

This significant difference in the reactivity of the diastereomeric sulfoxides **190** is due to nonbonding interactions occurring in the transition state between the aromatic ring and the methyl group and

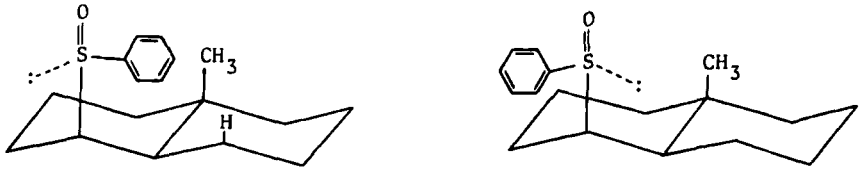


[85]

190 191

	X	Y
190a	Ph	O
190g	O	Ph

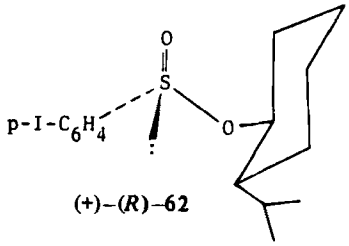
the hydrogen atom of the steroid moiety. Analysis of Dreiding models reveals that these interactions are strong in **190b**, where the chirality at sulfur is *S*, and completely absent in the case of its isomer, as shown. The utility of the pyrolytic elimination for configurational assignments to steroidal sulfoxides and sulfinates was further demonstrated many times by Jones and his co-workers (200–203).



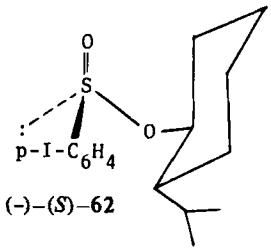
190b **190a**

O-Menthyl *p*-iodobenzenesulfinate **62** exists in two diastereomeric forms having $[\alpha]_D$ + 46° and -146° (79,103). Herbrandson and Cusano (103) determined their absolute configurations on the basis of kinetic studies of the hydrogen chloride-catalyzed equilibration (+)-**62** ⇌ (-)-**62** and ethanolysis of both diastereomeric esters. They found that the equilibration reaction carried out in nitrobenzene at room temperature results in the formation of a mixture containing 59 ± 3% of the dextrorotatory diastereomer. On the other hand, the rate of ethanolysis of the thermodynamically more stable (+)-**62** isomer was found to be twice as large as that of the (-)-isomer.

The findings discussed above led Herbrandson and Cusano to the conclusion that the thermodynamically less stable diastereomer (-)-**62** has the (*S*)-configuration because in this structure there is a strong destabilizing interaction between the aromatic ring and the isopropyl group of the menthyl residue. X-Ray analysis of (-)-**62** confirmed the correctness of this assignment (204).

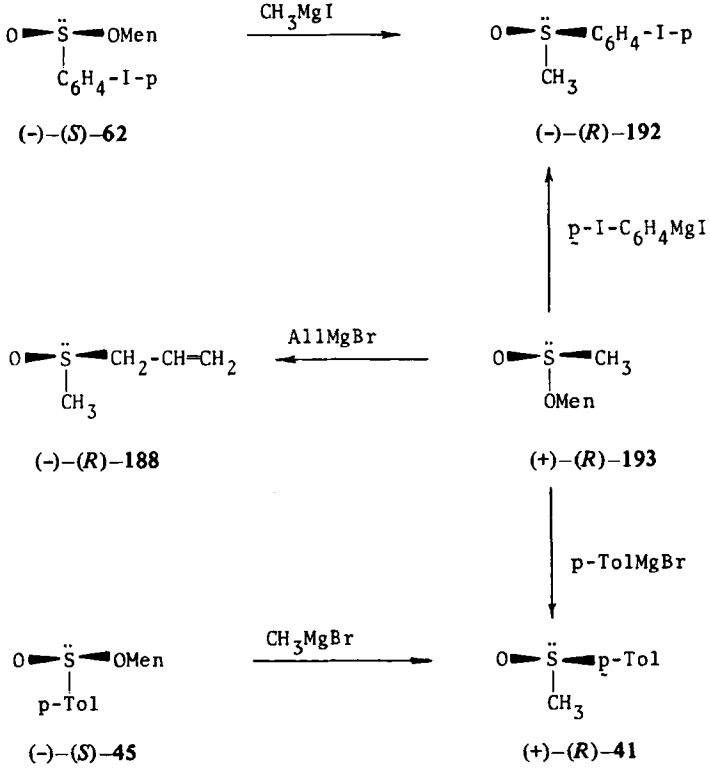


(+)-(*R*)-62



(-)-(*S*)-62

Based on the known absolute configuration of menthyl *p*-iodobenzenesulfinate 62, Mislow and his co-workers (79) linked the absolute configurations of sulfoxides and sulfinates using stereochemical cycles involving an odd number of Grignard reactions. The sequence of reactions given in Scheme 16 illustrates this general and perhaps most important method of configurational correlations.



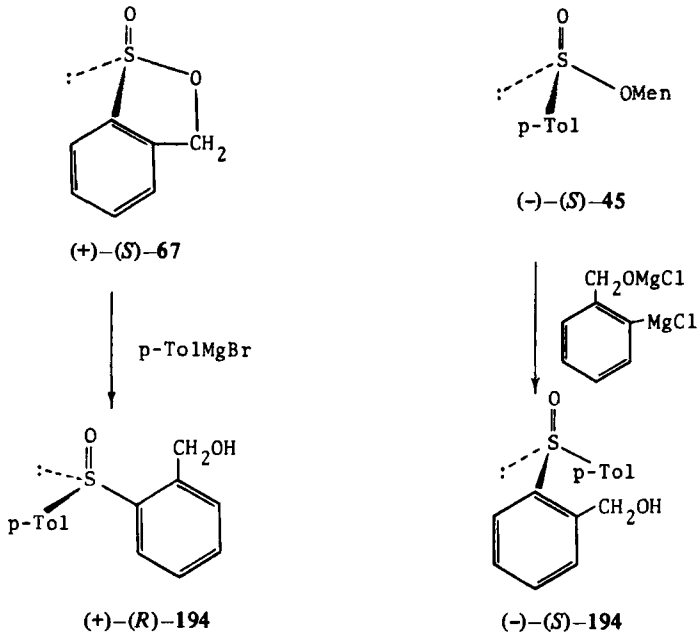
Scheme 16

Since reaction of (–)-**62** with methylmagnesium iodide gives methyl *p*-iodophenyl sulfoxide **192** with the same sign of rotation as that of the sulfoxide **192** obtained from reaction of (+)-menthyl methanesulfinate **193** with *p*-iodophenylmagnesium iodide, the two menthyl esters (–)-**62** and (+)-**193** must have opposite configurations at sulfur. From this it follows that (+)-**193** has the (*R*)-configuration. For the same reason, (–)-menthyl *p*-toluenesulfinate **45** and (+)-**193** also differ in chirality at sulfur because both are precursors of (+)-methyl *p*-tolyl sulfoxide (**41**). Hence, (–)-**45** has the (*S*)-configuration at sulfur. Furthermore, since the absolute configuration of (+)-**41** has been established (80,81) to be *R* by X-ray analysis and the configuration of (+)-**188** was related to (–)-iberin, which had been assigned the (*R*)-configuration by X-ray analysis (205), this reaction sequence also provided unequivocal evidence that the reaction of sulfinic esters with Grignard reagents occurs with inversion of configuration at sulfur.

The stereospecific conversion of sulfinates into sulfoxides of known chirality has been applied as a general method for determining the absolute configuration of a wide range of optically active sulfinic esters. For example, the absolute configurations of a series of alkyl alkanesulfinates obtained by asymmetric synthesis (107) or resolution via β-cyclodextrin inclusion complexes (106) were determined by this method.

The assumption that the Grignard reaction with cyclic sulfinates (sultins) proceeds with inversion of configuration at sulfinyl sulfur constitutes a basis for establishing the absolute configuration of the optically active ester **67**. Scheme 17 gives the correlation. At first, the absolute configuration of the sulfoxide (–)-**194** was established as *S* on the basis of the reaction of (–)-(*S*)-menthyl *p*-toluenesulfinate **45** with the Grignard reagent obtained from 2-bromobenzyl alcohol. The fact that the reaction of (+)-**67** with *p*-tolylmagnesium bromide gave sulfoxide (+)-(*R*)-**194** and the assumption that this reaction also occurs with inversion of configuration at sulfur led Pirkle and Hoekstra (108) to the conclusion that the ester under consideration has the (*S*)-configuration.

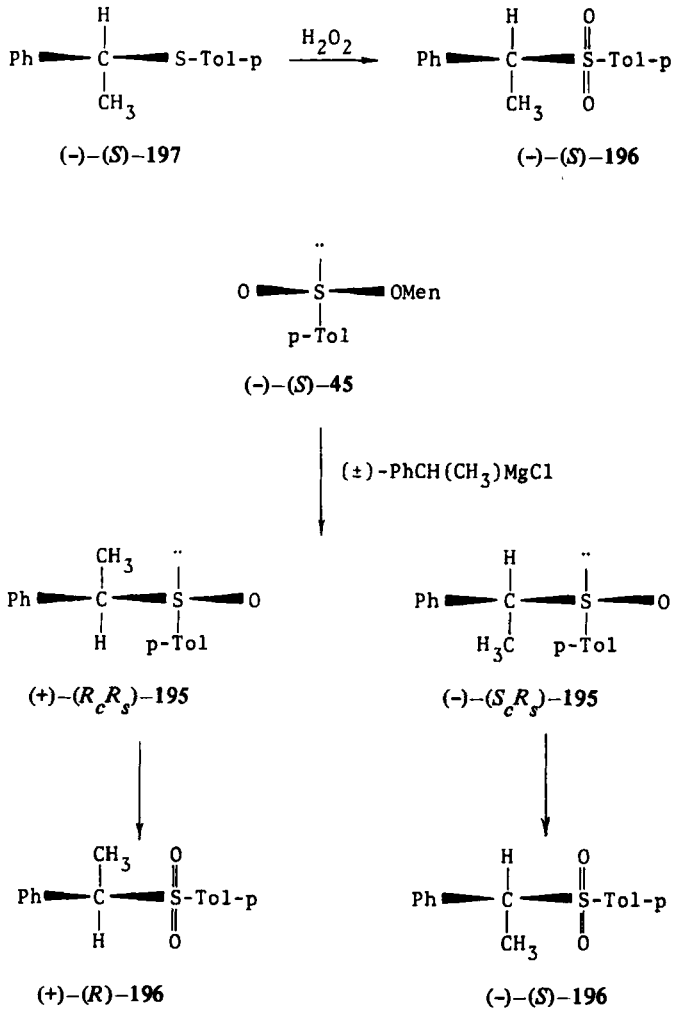
An interesting example of a chemical method for determining the absolute configuration of diastereomeric α-phenylethyl *p*-tolyl sulfoxides **195** based on the stereospecific sulfinate-sulfoxide conversion has been reported by Nishio and Nishihata (206). In this work optically active α-phenylethyl *p*-tolyl sulfoxides **195** and the corresponding sulfones **196** were prepared in two different ways and their specific rotations compared (see Scheme 18). Thus, oxidation of (–)-(S_c)-α-phenylethyl *p*-tolyl sulfide **197** with hydrogen peroxide



Scheme 17

gave (-)-(S_c)-α-phenylethyl *p*-tolyl sulfone **196**. On the other hand, (-)-(*S*)-menthyl *p*-toluenesulfinate **45**, on treatment with racemic α-phenylethylmagnesium chloride, yielded a mixture of diastereomeric α-phenylethyl *p*-tolyl sulfoxides **195** that have the same (*R*)-configuration at sulfur and are epimeric at the α-carbon atom. After separation, both (+)- and (-)-sulfoxides **195** were oxidized to the corresponding enantiomeric (+)- and (-)-sulfones **196**. Since the levorotatory sulfone **196** has the (*S*)-configuration at carbon, the same configuration should be assigned to its precursor (-)-sulfoxide **195**. In view of this result, Nishio and Nishihata (206) corrected their earlier assignment (207) of the absolute configuration to α-phenylethyl *p*-tolyl sulfoxides **195** which was based on steric considerations.

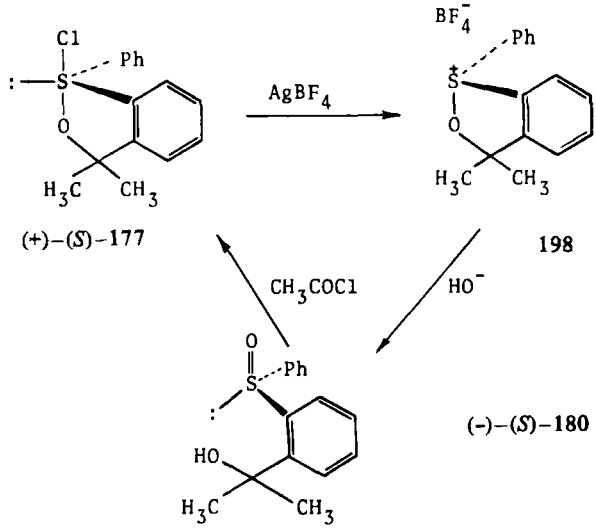
In their important work on the synthesis and properties of optically active chlorosulfurane (+)-**177**, Martin and Balthazor (195) deduced its absolute configuration by means of chemical correlations. Reaction of (+)-**177** with silver tetrafluoroborate yields cyclic sulfonium salt **198**, which was hydrolyzed without isolation under alkaline conditions to give sulfoxide (-)-(*S*)-**180**, from which (+)-**177** was obtained. Assuming that the conversion (+)-**177** → **198** proceeds with



Scheme 18

retention of configuration at sulfur and that hydrolysis of 198 is accompanied by inversion at sulfur, as was demonstrated earlier for basic hydrolysis of acyclic alkoxysulfonium salts (161), the absolute configuration of (+)-177 was established as that shown in Scheme 19.

Finally, it should be stressed that various nucleophilic and electrophilic reactions that lead from sulfoxides and sulfinates of known absolute configuration to new chiral tri- and tetracoordinate sulfur compounds and follow a stereochemically unambiguous course can be utilized for configurational assignments. Some of these reactions



Scheme 19

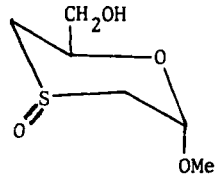
were discussed earlier and are also considered in the section devoted to dynamic sulfur stereochemistry.

B. Determination of Absolute Configuration by Spectrometric Methods

In addition to chemical correlations discussed above, several physical methods are now available for the determination of the relative and absolute configurations of chiral sulfur compounds. Among these, NMR, infrared (IR), optical rotatory dispersion (ORD), circular dichroism (CD), and X-ray analysis are the most important. Sections III-B-1 to III-B-5 outline applications of these techniques for establishing the chirality around the sulfur atom.

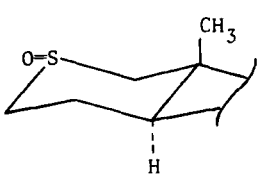
1. Nuclear Magnetic Resonance

The deshielding effect exerted by the sulfinyl group, observed initially in 1961 in the ^{1}H NMR spectra of cyclic sulfites (208), was utilized successfully for establishing the absolute configuration at sulfur of diastereomeric sulfinyl compounds and especially of sulfoxides. Detailed analysis of ^{1}H NMR spectra of the diastereomeric 1,4-oxathiane sulfoxides **199**, in which the anisotropic effect of the sulfinyl group on the neighboring protons was taken into account, made it possible to assign configurations to both epimers (209).

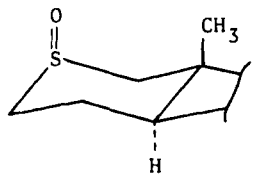


199

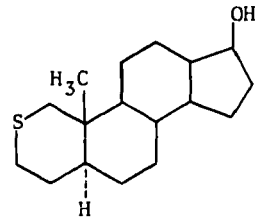
The absolute configurations of the diastereomeric sulfoxides **200a** and **200b** derived from 2-thio-5α-androstan-17β-ol **201** were assigned on the basis of the chemical shift differences of the 19-methyl protons of the steroid moiety (210). The values of the chemical shift were found to be 1.137, 1.046, and 1.418 ppm for the parent thiosteroid **201** and the sulfoxides **200a** and **200b**, respectively, indicating the absolute configurations *S* for **200a** and *R* for the epimer **200b**.



200a



200b

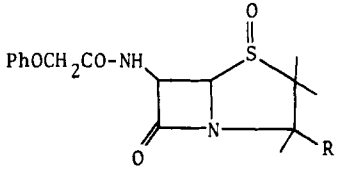


201

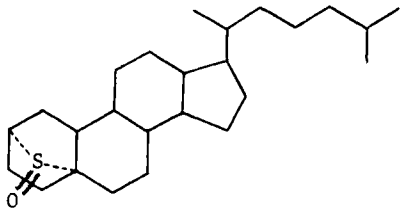
The ^{1}H NMR spectra of sulfoxides **200a** and **200b** obtained in benzene confirmed additionally the validity of these configurational assignments as the values of $\Delta\delta^{CDCl_3}_{C_6H_6}$ were found to be 19 and 4 Hz for **200a** and **200b**, respectively.

In this context, it should be pointed out that the correlation between aromatic solvent-induced shifts (ASIS) and the axial or equatorial orientation of protons in cyclic sulfoxides and sulfites is quite distinct (211–213) and may be utilized in the assignment of configurations. For instance, the absolute configuration *S* at sulfur was assigned to the penicillin sulfoxide **202** based on analysis of the effect of aromatic solvents on the chemical shifts of protons of the thiazolidine ring (214,215).

The recently introduced lanthanide-induced shift (LIS) technique has also found useful application in configurational studies of sulfur compounds. For example, the absolute configurations of a new type of bridged steroidal sulfoxide **203**, which is epimeric at sulfur, were



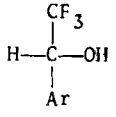
202



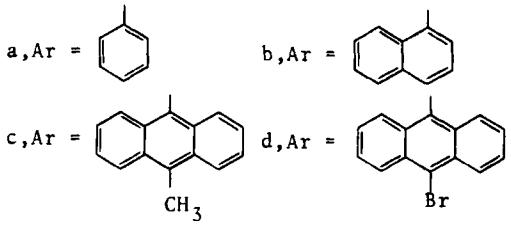
203

determined by means of this method by measuring the ^1H NMR spectra in the presence and absence of the shift reagent, $Eu(dpm)_3$ (216).

NMR spectroscopy was found to be a valuable technique for differentiation between the enantiomers of optically active compounds. The principles of the methods used to distinguish between enantiomers by means of NMR have been developed and reviewed by Mislow and Raban (217). The best results from the point of view of the determination of optical purity and absolute configuration of chiral sulfur compounds, especially of sulfinyl compounds, have been obtained with the help of chiral solvents (218). Pirkle (86) was the first to demonstrate that enantiomeric sulfoxides have nonidentical NMR spectra when dissolved in chiral alcohols having the following general formula:

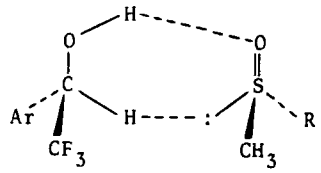


204

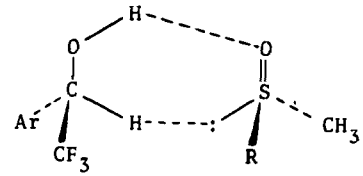


The ratio of the intensities of the appropriate diastereotopic signals of the chiral sulfoxide investigated is a measure of the enantiomeric content. The empirical correlation found between the sense of nonequivalence and the configuration of methyl alkyl and methyl aryl sulfoxides provided a basis for applying this method to configurational assignments. The specific solvation model proposed by Pirkle (219) to explain the sense and magnitude of nonequivalence (219a) is represented by **205a** and **205b**.

It was assumed that the preferred conformations of diastereomeric



205a



205b

solvates **205a** and **205b** are stabilized by hydrogen bonding between the hydroxy and sulfinyl groups, by interaction between the weakly acidic methine proton of the fluoroalcohol and the electron pair on sulfur (carbinyl hydrogen bonding), and also by $\pi-\pi$ interactions between the aromatic rings (R = aryl). In terms of this model the methyl protons of methyl alkyl and methyl aryl sulfoxides having the (*R*)-configuration at sulfur would appear in ^{1}H NMR spectra at lower field than those of the (*S*)-enantiomers, while the opposite situation should be observed for the proton resonance signals of the alkyl group R. Since this clear-cut relationship was observed in a dozen or so analyzed cases, it was possible to deduce the absolute configuration of sulfoxides from the sense of nonequivalence (220).

Recently, a similar simple conformational model was successfully used to assign the absolute configurations of acyclic and cyclic sulfinic esters (108).

2. *Optical Rotatory Dispersion and Circular Dichroism*

Between 1926 and 1962, numerous ORD curves of optically active sulfoxides were described in the literature for the visible and ultraviolet (UV) regions. However, down to about 250 nm all compounds investigated showed plain curves with $[\phi]$ increasing toward shorter wavelengths, and this limited their diagnostic value for the determination of the absolute configuration of these compounds.

Andersen (75,76), as well as Mislow (221), discovered that the ORD curves of alkyl aryl sulfoxides show a strong Cotton effect in the region below 250 nm. An extensive study by Mislow and his coworkers (47) led to the following empirical rules, correlating the sign of the Cotton effect with the absolute configurations of chiral dialkyl, alkyl aryl, and diaryl sulfoxides, as well as menthyl esters of aromatic sulfinic acids:

1. (–)-Methyl alkyl sulfoxides that do not contain other strongly perturbing groups have negative Cotton effects centered at the strong absorption band near 200 nm and have the (*R*)-configuration.
2. In alkyl aryl sulfoxides the Cotton effect corresponding to the UV primary band occurring at about 235 to 255 nm has a high molecular amplitude and the positive sign characterizes the absolute configuration *R*.
3. In menthyl arenesulfinates, the Cotton effect corresponding to the primary band has a high molecular amplitude and the negative sign characterizes the absolute configuration *S*.

It must be stressed, however, that the methyl alkyl sulfoxide rule is not valid for alkyl benzyl and alkyl allyl sulfoxides (222–224), where the electronic, steric, and solvent effects exert influences on the chiroptical phenomena in a way that is difficult to rationalize. This rule was found to be satisfactory and was used for the assignment of absolute configurations of steroidal (200,201,225), penicillin (226), and amino acid (227–230) sulfoxides.

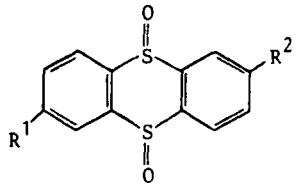
The ORD and CD curves of chiral sulfinamides derived from aromatic sulfinic acids show a strong Cotton effect centered at 240 to 256 nm (83). The position of this Cotton effect, its dependence on the solvent used, and the amplitude reveal a complete analogy with that observed in alkyl aryl sulfoxides and aromatic menthyl sulfinates. Thus, the positive sign of the Cotton effect observed in the ORD curves of dextrorotatory sulfinamides is indicative of the (*S*)-configuration around sulfur in these compounds.

Recently, the chiroptical properties of sulfimides have been described (130,138). In this case too, a clear correlation exists between the absolute configuration at sulfur and the sign of the Cotton effect observed at 270 to 285 nm.

Detailed discussions of ORD and CD spectra of chiral sulfur compounds may be found in the reviews of Laur (7) and Ziffer (231).

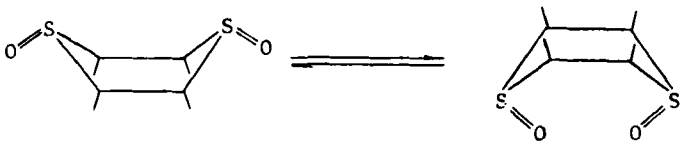
3. Ultraviolet and Infrared Spectroscopy

Mislow and co-workers (232) have shown that the assignment of configuration in the series of diastereomeric *cis*- and *trans*-thianthrene-5,10-dioxides **206** substituted in the aromatic ring is possible on the basis of UV or IR spectra. The authors cited found that the principal absorption band in the UV spectra of the trans isomer of **206** is shifted with respect to that of the cis isomer toward longer wave-

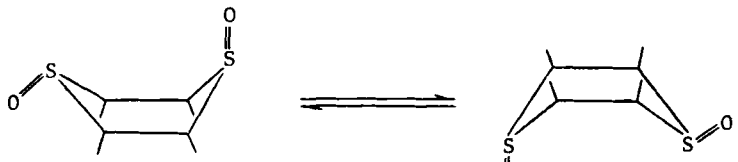


206

a-d, $R^1=R^2=H$, Cl, CH_3, CH_2COOCH_3
e, $R^2=H$, $R^2=Br$
f, $R^1=H$, $R^2=COOCH_3$
g, $R^1=H$, $R^2=COOH$



anti-cis syn-cis



trans trans

lengths (from 212 to 221 nm). Similarly, the IR spectra of the diastereomeric disulfoxides **206** show characteristic differences; the cis isomers of **206** have a strong absorption band at 1087 to 1094 cm^{-1}, whereas the corresponding trans compounds absorb at 1018 to 1044 cm^{-1} and 1070 to 1079 cm^{-1}. These differences were used to establish the geometry of two isomeric 2-carboxythianthrene-5,10-dioxides **206**, trans (m.p. 250–252°C) and cis (m.p. 303–304°C), which were resolved by Janczewski (233) into two sets of enantiomers.

4. X-Ray Analysis

The most reliable method for the determination of absolute configurations is based on the X-ray diffraction technique, which recently has become more accessible and efficient because of the availability of electronic computers and of automatic and semiautomatic diffractometers.

Among chiral sulfur compounds, (+)-methyl-L-cysteine sulfoxide **28** was the first whose configuration was determined by X-ray analysis (234,235). Since the chiral center on the α-amino carbon has the (*S*)-configuration, the configuration at the chiral sulfur atom was established by internal comparison as (*S*). Unfortunately, the complex structure of this compound eliminated it as a standard in studies of the determination of the absolute configuration of other optically active sulfur compounds. In this regard, the determination of the absolute configuration at sulfur in (–)-menthyl *p*-iodobenzenesulfinate **62** by X-ray diffraction (47,204) was an important step forward, since this ester could be used as a configurational standard in the chemical correlations discussed above. In this case the absolute configuration at sulfur was established by internal comparison. However, the absolute configuration of (+)-methyl *p*-tolyl sulfoxide **41** has been determined directly by means of the Bijvoet method (80, 81). Table 1 lists the chiral sulfur compounds, inclusive of natural products, whose absolute configurations have been established by X-ray analysis.

Table 1
Optically Active Sulfur Compounds; Absolute Configuration at Sulfur Determined by X-Ray Analysis

Entry	Compound	Absolute Configuration at Sulfur	Ref.
1	(+)-Methyl L-cysteine sulfoxide	*S*	*Chem. Ind. (London)* **1956**, 1428; *Acta Crystallogr.* **1962**, *15*, 635
2	(–)-Menthyl *p*-iodobenzenesulfinate	*S*	*J. Am. Chem. Soc.* **1964**, *86*, 3395
3	(–)-*N*-[(1-phenylethyl)-*N'*-3-*n*-propyl] methyl sulfoxide thiourea	*R*	*J. Chem. Soc., Chem. Commun.* **1965**, 100
4	(+)-(2*R*,6*S*)-2-Hydroxymethyl-6-methoxy-1,4-oxathian-*S*-oxide	*S*	*J. Chem. Soc., Chem. Commun.* **1966**, 759; *J. Chem. Soc. B*, **1971**, 1692
5	(+)-Methyl *p*-tolyl sulfoxide	*R*	*Angew. Chem. Int. Ed. Engl.* **1969**, *8*, 612; *Acta Crystallogr.; Sect. B.* **1970**, *26* 846

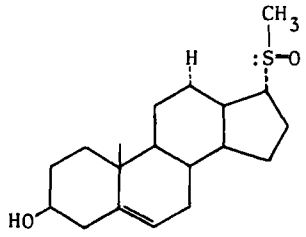
Table 1 continued

Entry	Compound	Absolute Configuration at Sulfur	Ref.
6	Phenoxymethyl penicillin sulfoxide methanol solvate	*S*	*J. Am. Chem. Soc.* **1969**, *91*, 1408
7	(+)-2-(*S*)-Methionine sulfoximide	*R*	*J. Chem. Soc.; Chem. Commun.* **1969**, 169; *J. Chem. Soc. B*, **1970**, 694
8	(+)-*N*-[(3-*endo*)-bromo-2-oxo-9-bornanesulfonyl]-methyl-*p*-tolylsulfoximide	*R*	*J. Am. Chem. Soc.* **1970**, *92*, 7369
9	(+)-Methyl-6-deoxy-6-methylsulfinyl α-D-glucopyranoside	*S*	*Acta Chem. Scand.* **1971**, *25*, 1139
10	(+)-*N*-Phthalimido-2-bromo-(2*S*)-octyl-*p*-tolylsulfoximide	*R*	*Cryst. Struct. Commun.* **1973**, *2* 171
11	(-)-*o*-Carboxyphenyl methyl sulfoxide	*S*	*Acta Crystallogr.* **1974**, *30*, 642
12	(+)-Ethylsulfinyltryptophan	*R*	*Justus Liebigs Ann. Chem.* **1974**, 1570
13	(-)-(*S*)-Ethyl-6-methyl-1,4-oxathian-2-one 2,4,6-trinitrobenzenesulfonate	*S*	*J. Chem. Soc., Chem. Commun.* **1975**, 629
14	(+)-*N*-Phthalimido-*p*-tolyl-α-naphthyl-sulfoximide	*S*	*Cryst. Struct. Commun.* **1975**, *4* 393
15	(+)-1,2-Dibromo-2-phenylethyl *p*-tolyl sulfoxide	*S*	*Bull. Soc. Chem. Jpn.* **1975**, *48*, 944
16	(+)-Methyl-tri-*O*-acyl-6-deoxy-6-methyl-sulfinyl α-D-glucopyranoside	*S*	*Acta Crystallogr. Sect. B*, **1976**, *32* 2017
17	(-)-α-Chlorobenzyl *t*-butyl sulfoxide	*S*	*Cryst. Struct. Commun.* **1977**, *6*, 85
18	(+)-[((3*S*)-3-Amino-3-carboxypropyl) (carboxymethyl)methylsulfonium] 2,4,6-trinitrobenzenesulfonate	*R*	*J. Am. Chem. Soc.* **1977**, *99*, 7292
19	(-)-(2*R*)-S-[(1*S*,2*R*)-1,3-dithian-2-yl]-isoborneol-1-oxide	*S*	*J. Org. Chem.* **1978**, *43*, 90

5. *Other Methods*

The measurements of dipole moments and retention times in chromatography were found to be especially useful in assigning the configuration (cis-trans geometry) of cyclic four-, five-, and six-membered sulfoxides (236,237). These methods were also applied to the determination of configuration of steroidal sulfoxides (216,238).

A different mass spectral fragmentation pattern has been reported for diastereomeric steroidal sulfoxides (239). For instance, the sulfoxide **207** undergoes fragmentation to give a more abundant $[M-CH_3-SOH]^+$ ion than the other three diastereomeric sulfoxides. This indicates that in some cases the correlation of mass spectra with configuration is possible.



207

In addition to other methods, the quasi-racemate method was used (98) to determine the absolute configuration of *N*-tosyl methyl-*p*-tolylsufimide **91**.

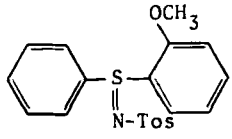
It is also interesting to note that circular differential Raman scattering, circular intensity differential (CID), has been reported for a series of optically active sulfoxides and a correlation found between the absolute configuration at sulfur and the differential scattering (240). Thus, all (*R*)-alkyl *p*-tolyl sulfoxides investigated show a common (positive) CID feature in the 300 to 400 cm^{-1} region.

C. Determination of Optical and Enantiomeric Purity

As in the case of other chiral compounds, the optical and enantiomeric purity of chiral organosulfur compounds can be determined by various methods (241). The simplest and most common method for the determination of optical purity of a mixture of enantiomers is based on polarimetric measurements. However, this method requires a knowledge of the specific rotation of the pure enantiomer. In the

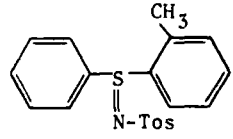
absence of other criteria, 100% optical purity is ascribed when the melting point and the optical rotation of a crystalline enantiomer or its diastereomeric precursor do not change upon crystallization. Although in the majority of cases such maximal optical rotation obtained in the resolution of enantiomers corresponds to optical purity, examples are known where this criterion is invalid. Thus, in contrast to (–)-menthyl *p*-toluenesulfinate **45**, which can be obtained as a diastereomerically pure sample by crystallization, (+)-menthyl *p*-iodobenzenesulfinate **62**, $[\alpha]_D + 25°$, does not change its properties ($[\alpha]_D$ and melting point) during crystallization, though it contains only 91% of the dextrorotatory epimer (79).

Crystallization of optically active sulfimides **208** and **209** prepared by asymmetric synthesis results in a gradual increase of their melting points and optical rotations until the values given below are attained (138). The failure of successive crystallizations to affect these values



208

$[\alpha]_D$+98°; mp 161.5-162°C



209

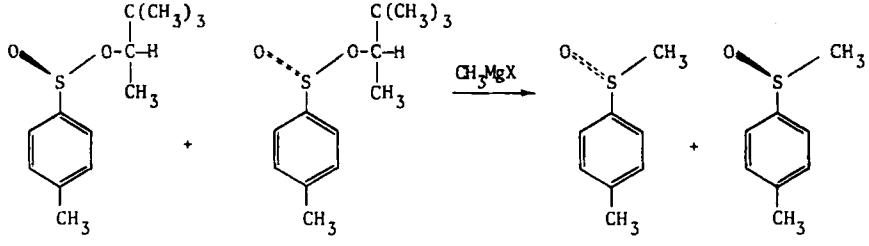
$[\alpha]_D$+41°; mp 122-122.5°C

was taken as evidence of 100% optical purity of both sulfimides purified in this way. Similarly, the observation that optically active methylphenylsulfoximide **149** with $[\alpha]_D + 36.5°$ obtained by separation of diastereomeric salts with (+)-camphor-10-sulfonic acid does not change its optical rotation upon crystallization is considered to be proof of the completeness of resolution and of optical purity of **149** (118).

The polarimetric method, in combination with the results of chemical correlation, made it possible to determine the optical purity of a range of chiral sulfinates (105–107), thiosulfinates (35,105), and sulfinamides (83) with the sulfur atom as a sole center of chirality. These compounds were converted by means of Grignard or alkyllithium reagents into sulfoxides of known specific rotations. This approach to the determination of optical purity of chiral sulfinyl compounds has at least two limitations. The first is that it cannot be applied to sterically hindered compounds [e.g., *t*-butyl *t*-butanethiosulfinate **72** does not react with Grignard reagents]. Second, this

method requires the assumption that the Grignard reaction is fully stereospecific, which is not necessarily true.

An interesting method for the estimation of optical purity of sulfoxides, which consists of the combination of chemical methods with NMR spectroscopy, was elaborated by Mislow and Raban (241). The optical purity is usually determined by the conversion of a mixture of enantiomers into a mixture of diastereomers, the ratio of which may be easily determined by NMR spectroscopy. In contrast to this, Mislow and Raban used as starting material for the synthesis of enantiomeric sulfoxides a diastereomeric mixture of pinacolyl *p*-toluenesulfinates **210**. The ratio of the starting sulfinates **210** was 60.5:39.5, as evidenced by the ^{1}H NMR spectrum. Since the Grignard reaction occurs with full stereospecificity, the ratio of enantiomers of the sulfoxide formed is expected to be almost identical to that of **210**. This corresponds to a calculated optical purity of the sulfoxide of 20%. In this way the specific rotations of other alkyl or aryl *p*-tolyl sulfoxides can conveniently be determined.

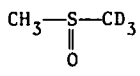


210a **210b** **41a** **41b**

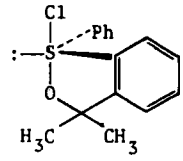
As was already mentioned, the phenomenon of nonequivalence of NMR spectra of enantiomers in chiral solvents is a basis for the determination of enantiomeric purity of a variety of chiral sulfur compounds. This method, developed by Pirkle, has the advantage over other methods of being absolute; that is, the chemical shift difference between enantiotopic nuclei induced by the chiral solvent increases with increasing optical purity of the solvent, whereas the relative intensities of the signals that are used to measure the enantiomeric composition of the solute are not affected.

NMR spectral differentiation of enantiomers as solutes in chiral solvents has been achieved with sulfoxides, sulfinates, thiosulfinates, sulfinamides, and sulfites (86,108,242). The usefulness and high sensitivity of this method is confirmed by its successful application

to the determination of the enantiomeric purity of methyl trideuteriomethyl sulfoxide **47**, whose optical activity is due to the isotopic H → D substitution (86). Recently, the enantiomeric purity of op-



47



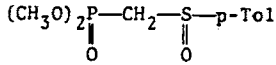
177

tically active chlorosulfurane (+)-(*S*)-**177** was also determined by the method of Pirkle using (+)-(*S*)-1-(10-methyl-9-anthryl)-2,2,2-trifluoroethanol **204c** (195).

Similar differentiation between enantiomers by means of NMR can also be achieved by the use of chiral lanthanide shift reagents (243). Tris-[3-(heptafluoropropylhydroxymethylene)-*d*-camphorato]-europium was used for the first time (244) for determining the enantiomeric content of benzyl methyl sulfoxide **34**. The enantiomeric composition of the partially resolved methyl *p*-tolyl sulfoxide **41** was estimated using tris-[3-(*t*-butylhydroxymethylene)-*d*-camphorato]-europium (245). Another complex of europium, tris-[3-(trifluoromethylhydroxymethylene)-*d*-camphorato] europium (TFMC), in contrast to those mentioned above, was effective in the differentiation of various enantiomeric mixtures of chiral sulfinates (107), thiosulfinates (35), and sulfinamides (246).

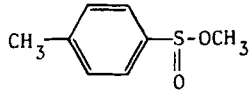
It is of interest to note that the magnetic nonequivalence of the enantiomers of the α-phosphoryl sulfoxide **49** in the presence of TFMC was observed (88) not only in ^{1}H but also in ^{31}P and ^{13}C NMR spectra. With regard to the accuracy of the NMR method, the $^{31}P\{^{1}H\}$ NMR spectra proved very useful in this case, since only two well-separated singlets that were due to enantiomeric sulfoxides **49** were observed.

Finally, one should note that the determination of enantiomeric purity by means of chiral shift reagents appears to be more advantageous than the method of Pirkle because the magnitude of nonequivalence $\Delta\delta$ is generally greater, thus leading to a more accurate



49

estimation of the enantiomeric content. The $\Delta\delta$ values for methyl *p*-toluenesulfinate **65** observed in the chiral alcohol **204b** and in the presence of TFMC best illustrate these differences.



65

(−)-**65** + **204b** (at 220 MHz)	(+)-**65** + TFMC (at 60 MHz)
$\Delta\delta_{OCH_3}$ = 2.9 Hz	$\Delta\delta_{OCH_3}$ = 21 Hz
$\Delta\delta_{CH_3}$ = 1.8 Hz	$\Delta\delta_{CH_3}$ = 5 Hz

IV. BASIC PROBLEMS OF THE DYNAMIC STEREOCHEMISTRY OF CHIRAL SULFUR COMPOUNDS

This section surveys the most important reactions of chiral organosulfur compounds. Some of these were touched on in the previous sections. For the sake of convenience, a variety of reactions occurring at the chiral sulfur center are divided into three main types of reactions: racemization, nucleophilic substitution reactions, and electrophilic reactions.

A. Racemization

Racemization, which results in the loss of optical activity of a chiral compound, is considered to be one of the fundamental processes in dynamic stereochemistry. Quite generally, racemization can be caused by supplying adequate energy by heating or irradiation, or it may be effected by chemical reactions.

As a result of recent extensive studies, especially that of Mislow (247) on the stereomutation of sulfoxides, it is recognized that racemization of optically active organosulfur compounds occurs under various conditions and according to different mechanisms.

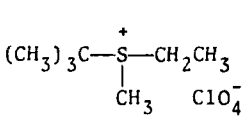
1. Thermal Racemization

Pyramidal inversion is perhaps the simplest way to cause racemization. In this process the conversion of one enantiomer into another

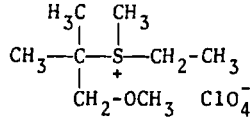
takes place without splitting the bonds between the central chiral atom and the substituents occupying the corners of a tetrahedron.

All diaryl sulfoxides, some alkyl aryl sulfoxides (e.g., methyl *p*-tolyl sulfoxide, **41**), and some dialkyl sulfoxides (e.g., methyl 1-adamantyl sulfoxide), were found to undergo racemization according to the pyramidal inversion mechanism. Mislow and co-workers (248) have found that for most of the compounds investigated, irrespective of the nature of the substituents attached to sulfur, the first-order rate constant for racemization in *p*-xylene at 210°C is about 3×10^{-5} sec^{-1}, corresponding to a half-life of about 6 hr. Moreover, the activation parameters do not show significant differences and their values were contained in a narrow range: $\Delta H^{\ddagger}$ 35 to 42 kcal/mol and $\Delta S^{\ddagger}$ -8 to +4 e.u. Even though the racemization rate constants differ slightly, their distinct dependence on the steric and to a lesser extent on the electronic effects of the substituents bonded to the sulfinyl sulfur atom was noted. It deserves adding that the activation volume for racemization of methyl *p*-tolyl sulfoxide **41**, $\Delta V^{\ddagger} \sim 0$ ml/mol, is also consistent with the pyramidal inversion mechanism (249).

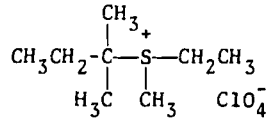
Kinetic studies on the thermal racemization of the sulfonium salt **211** revealed that the process requires much lower activation energies when compared with thermal racemization of sulfoxides. Comparison of the relative rates for racemization of sulfonium salts **211**, **212**, and **213** was taken (151) as evidence that racemization of **211** is the result of pyramidal inversion, not of an alternative dissociation mechanism. On the other hand, Brower and Wu (249) concluded that the volume of activation for the racemization of sulfonium ion **211**, $\Delta V^{\ddagger}$ = +6.4 ml/mol, is more compatible with a transition state in which partial dissociation has occurred.



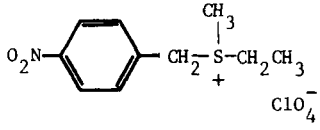
211



212



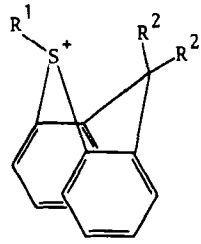
213



214

A pyramidal inversion mechanism was proposed for the racemization of 1-adamantylethylmethylsulfonium **105**, benzylethylmethylsulfonium (**112**), *p*-nitrobenzylethylmethylsulfonium (**214**) and phenacylethylmethylsulfonium 2 perchlorates (152,153).

Thermal racemization of a range of the cyclic sulfonium salts **215** was studied by the dynamic NMR method (250), and that of the cyclic sulfonium salts **107**, **108**, and **109** by the polarimetric method (155). It was reported that the rates of thermal racemization of cyclic sulfonium salts are several orders of magnitude smaller than those of acyclic analogs. This finding is again consistent with the pyramidal inversion mechanism for racemization of this group of compounds, since an increase in ring strain is expected on going from the tetrahedral ground state to a planar transition state for pyramidal inversion.



R^1=alkyl or aryl

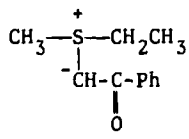
R^2=CH_3 or H

215

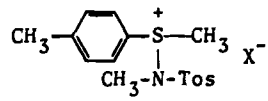
Oae (251,252) as well as Darwish and Datta (253) investigated the process of thermal racemization of chiral alkylarylsulfimides and diarylsulfimides. It was found to proceed at temperatures as low as 65 to 100°C with a rate constant of the order 1 to 10×10^{-5} sec^{-1}, which corresponds to an activation energy of about 23 to 30 kcal/mol. These data indicate that the thermal racemization of sulfimides is much faster than that of analogous sulfoxide systems. The racemization of sulfimides is a unimolecular reaction practically independent of the polarity of the solvent; this property, coupled with the absence of decomposition products, supports the view that racemization of sulfimides occurs by pyramidal inversion.

The studies of Darwish et al. (166,253) have shown that the sulfonium ylide **127** and the aminosulfonium salts **216** also undergo racemization at 50 to 90°C by pyramidal inversion.

Benzyl *p*-tolyl sulfoxide **37** undergoes racemization in *p*-xylene with a measurable rate at 130 to 150°C—far below the temperature required for the pyramidal inversion of the sulfoxides discussed



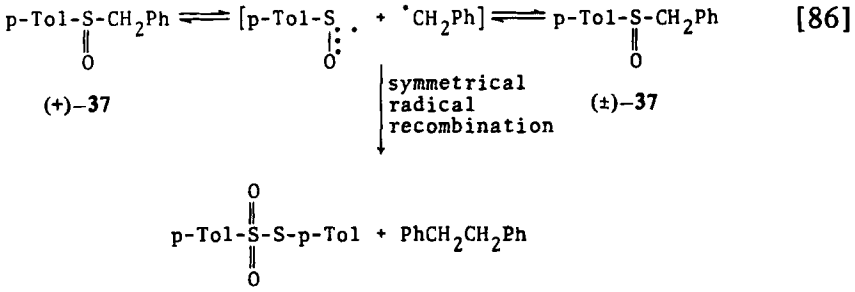
127



216

a, X=BF_4
b, X=CF_3SO_3
c, X=TNBS

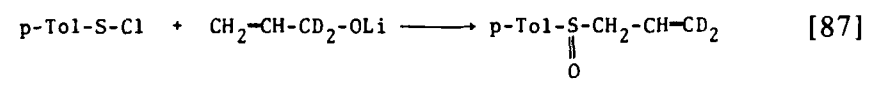
above. It was found (254) that a high activation energy and a strongly positive activation entropy ($\Delta H^{\ddagger}$ = 43.0 kcal/mol; $\Delta S^{\ddagger}$ = 24.6 e.u.) are characteristic of this process. Furthermore, the racemization of 37 is accompanied by extensive decomposition and results in the formation of *p*-tolyl *p*-toluenethiolsulfonate and bibenzyl in addition to other products. These and other observations have been rationalized by Mislow (254) in terms of a homolytic scission mechanism. Thus, the homolysis of the benzylic carbon-sulfur bond in optically active 37 leads to a radical pair that on cage recombination affords the enantiomeric sulfoxide 37 as shown in eq. [86]. The acti-



[86]

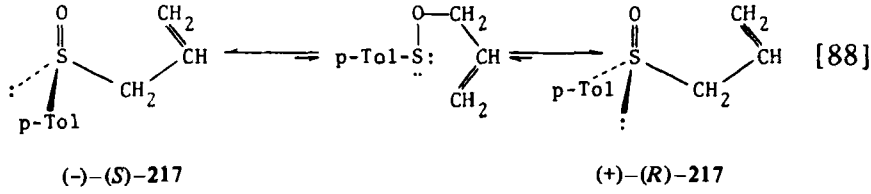
vation volume for thermal racemization of benzyl *p*-tolyl sulfoxide 37, $\Delta V^{\ddagger}$ = +26 ml/mol, is in good agreement with the proposed mechanism (249).

In contrast to benzyl *p*-tolyl sulfoxide 37, allyl *p*-tolyl sulfoxide 217 racemizes between 50 and 70°C. The values of the activation energy and the entropy ($\Delta H^{\ddagger}$ = 23 kcal/mol; ΔS = -4.9 e.u.) as well as the absence of decomposition products are indicative of a different racemization mechanism for this sulfoxide. In this connection, it is interesting to note that the condensation of *p*-toluenesulfenyl chloride with allyl alcohol labeled in the α-position with deuterium



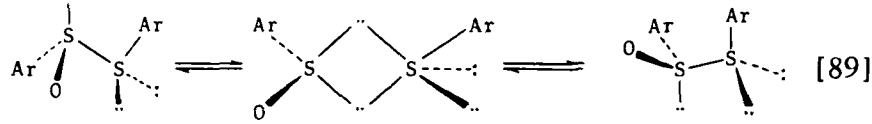
[87]

affords allyl-γ-$^2H_2$ *p*-tolyl sulfoxide 217. Based on these results, Mislow (255) proposed a cyclic rearrangement mechanism, ([2,3] sigmatropic process) for the racemization of allyl sulfoxides involving an achiral sulfenate ester as an intermediate.



[88]

An extraordinarily easy thermal racemization was observed for aryl arenethiosulfinates (256). It occurs at a convenient rate at about 50°C. The following activation parameters were estimated for the racemization of *p*-tolyl *p*-toluenethiosulfinate 218: $\Delta H^{\ddagger}$ = 23 kcal/mol; $\Delta S^{\ddagger}$ = –4 e.u. Thus, the rate of racemization is about 10^{11} times greater than that of diaryl sulfoxides. An internal displacement of sulfenyl sulfur rather than pyramidal inversion was proposed as the mechanism. Recent studies on the chemistry and stereochemistry



[89]

of thiosulfinates (113,114) suggest, however, that the rapid racemization of thiosulfinates may be caused by chemical reaction, for example, with the corresponding sulfenic acid present in trace amounts.

The configurational stability of sulfinamides was investigated by Cram and Booms (257). They found that sulfinamides undergo racemization at room temperature but with a very long induction time. This indicates that the racemization process is a consequence of a homolytic scission of the sulfur-nitrogen bond involving the formation of an achiral sulfinyl radical. The free radical mechanism of the racemization of sulfinamides is supported by the fact that they initiate the polymerization of styrene and methyl methacrylate.

2. *Photochemical Racemization*

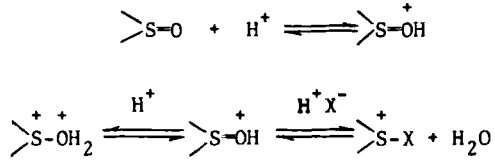
Mislow and co-workers (258) and Hammond (259) have shown that optically active diaryl sulfoxides, which are configurationally stable in the dark at 200°C, lose their optical activity after 1 hr at room temperature on irradiation with ultraviolet light. Similarly, an easy conversion of the trans isomer of thianthrene-5,10-oxide **206a** into the thermodynamically more stable cis isomer takes place upon irradiation in dioxane for 2 hr. However, the behavior of α-naphthylethyl *p*-tolyl sulfoxide under comparable irradiation conditions is different, namely, it is completely decomposed after 4 min. These differences are not surprising because the photochemical racemization of diaryl sulfoxides occurs by way of the pyramidal inversion mechanism whereas decomposition of the latter sulfoxide occurs via a radical mechanism with the cleavage of the sulfur-carbon bond. It is interesting to note that photoracemization may be a zero-order process in which the rate depends only on the intensity of the radiation and on the quantum yield.

3. *Racemization Induced by Chemical Reactions*

Very often racemization of chiral sulfur compounds is effected by diverse chemical agents. Much attention has been paid to the elucidation of the mechanisms of such chemically induced racemization processes. A brief summary of the results obtained in this field is given next.

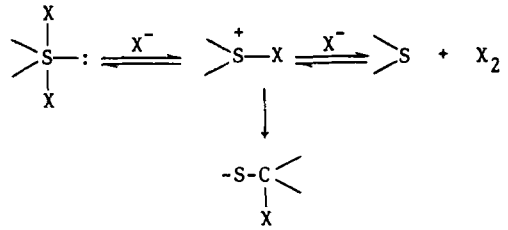
a. Reactions with Hydrogen Halides. The epimerization of optically active L-methionine sulfoxides catalyzed by hydrogen chloride was reported by Iselin in 1961 (260). Soon after that, Mislow et al. (261) found that alkyl aryl sulfoxides undergo racemization in a solution of hydrochloric acid in dioxane or tetrahydrofuran at room temperature. Later on, several groups of workers carried out extensive studies on the mechanism of racemization of sulfoxides catalyzed by hydrogen halides using chiral alkyl aryl or diaryl and ^{18}O-labeled sulfoxides as model compounds (10). Generally, it was found that sulfoxides do not racemize in the presence of hydrofluoric acid, whereas in hydrobromic acid racemization is accompanied by reduction, which is the sole reaction in the case of hydroiodic acid. Furthermore, it was established that racemization is accompanied by the exchange of ^{18}O and the rate constants for both processes are equal. All the results obtained indicate that three concurrent reactions

–racemization, oxygen exchange, and reduction–are initiated by protonation of the sulfoxide. In the next step the protonated sulfoxide can form a halogenosulfonium salt or may be again protonated. The halosulfonium ion may be reduced to sulfide and/or



[90]

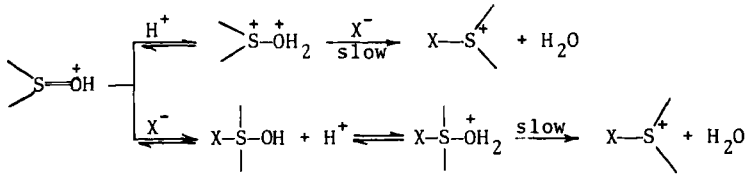
transformed into a dihalogenosulfurane intermediate on reacting with a second halide ion, or it may undergo the Pummerer type of rearrangement. The position of equilibrium of eq. [91] determines



[91]

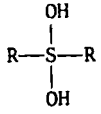
whether reduction or racemization will predominate. In the case of iodide ion this equilibrium is shifted to the right, which leads exclusively to reduction. With chloride and bromide ions equilibrium is usually shifted to the left, and predominant racemization and oxygen exchange are observed.

With regard to the rate-determining step of the reaction between sulfoxides and hydrohalic acids, there are some conflicting opinions. Since the rate of racemization of sulfoxides catalyzed by hydrochloric acid decreases markedly with increasing the steric hindrance around sulfur, Mislow (261) assumed that the formation of the dihalogenosulfurane intermediate is the rate-determining step. However, racemization is a first-order reaction with respect to halide ions and is second-order with respect to protons; this realization led other workers (262,263) to propose that the formation of halosulfonium salt (eq. [92]) is the rate-determining step. According to Oae and co-workers (264), the second protonation (of the hydroxysulfurane intermediate) is the slowest step in this reaction. It is also of interest to note that Kwart and Omura (265) suggested the formation of a di-



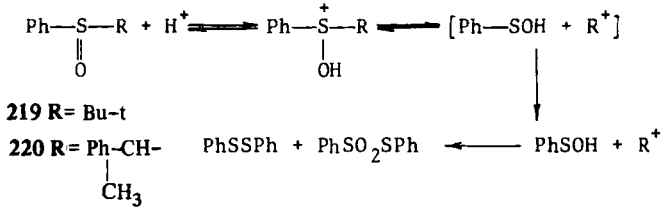
[92]

hydroxysulfurane intermediate **218** in the hydrochloric acid-catalyzed racemization of sulfoxides.



218

The behavior of chiral phenyl *t*-butyl sulfoxide **219** and α-phenylethyl phenyl sulfoxide **220** is completely different in strongly acidic media and in the presence of halide ions. Two reactions were found (266) to occur in parallel. One results in the loss of optical activity, and the second leads to the decomposition of the sulfoxide. It was observed that the racemization process is not accompanied by [^{18}O]oxygen exchange. In the case of sulfoxide **220** the complete loss of optical activity at chiral sulfur is accompanied by partial racemization at the chiral carbon center. These results are consistent with a sulfenic acid-ion-pair mechanism formulated by Modena and co-workers (266) as follows (it is obvious that the formation of achiral sulfenic acid is responsible for racemization).



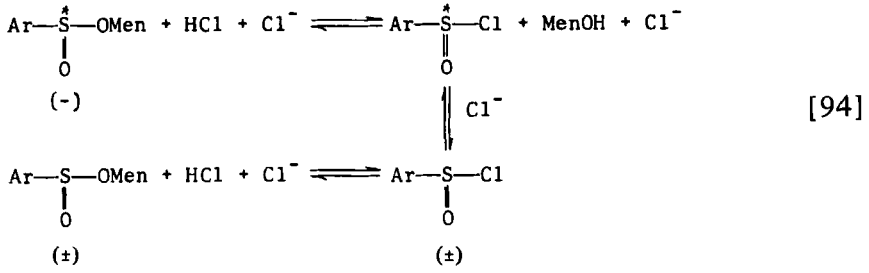
[93]

219 R= Bu-t

220 R= Ph-CH(CH$_3$)-

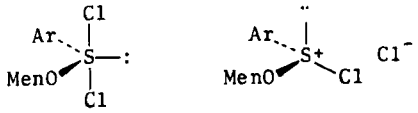
Hydrogen chloride was also found to catalyze the racemization of chiral sulfinates. Herbrandson and Dickerson (267) found that diastereomerically pure menthyl arenesulfinates undergo epimerization in nitrobenzene in the presence of hydrogen chloride and chloride ions. On the basis of kinetic studies they proposed a mecha-

nism involving a transient formation of sulfinyl chloride that may racemize rapidly via the chloride-chloride exchange reaction at sulfur.



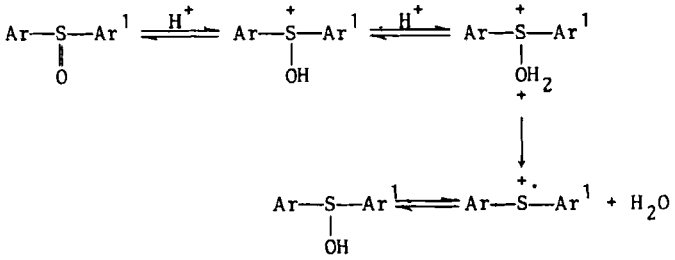
[94]

Mislow and his co-workers (261) suggested, however, that epimerization of menthyl sulfinates occurs via either a sulfurane intermediate 221 or a sulfonium salt 222.



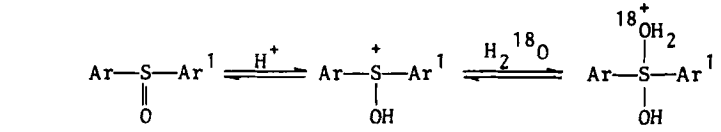
221 **222**

b. Reactions with Other Acids. Oae and Kunieda (268,269) demonstrated that the oxygen exchange and racemization of sulfoxides in sulfuric acid proceeds by two different mechanisms. In 96% sulfuric acid the racemization and oxygen exchange rates are almost the same, and the entropies of activation are positive or very small negative values. These observations support an A-1 mechanism in which the sulfur-oxygen bond fission occurs as a slowest step of the reaction. The fact that electron spin resonance signals have been observed for solutions of parasubstituted diphenyl sulfoxides in concentrated sulfuric acid is indicative of a radical cation intermediate. At lower

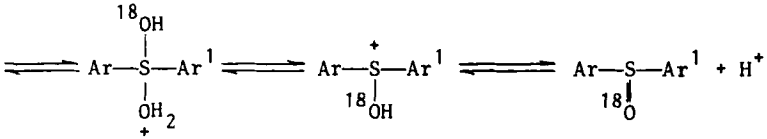


[95]

concentrations of sulfuric acid the ratio k_{ex}/k_{rac} becomes approximately 0.5 and the activation entropy values are strongly negative. These data are consistent with an A-2 type of mechanism in which the nucleophilic attack of water on the conjugate acid is the rate-determining step.



[96]

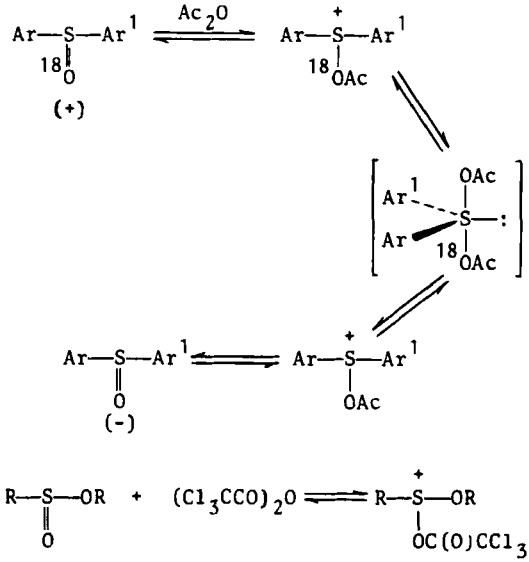


Racemization of diaryl and alkyl aryl sulfoxides accompanied by oxygen exchange was also observed in α-halogenoacetic acids (270, 271) and phosphoric acid (272).

c. **Reactions with Carboxylic Acid Anhydrides.** Heating chiral sulfoxides containing ^{18}O in the sulfinyl group with acetic anhydride results in three different reactions: racemization, oxygen exchange, and Pummerer rearrangement. The detailed studies of this process by Oae and co-workers (273–275) showed that the rate of racemization of sulfoxides is first order in both acetic anhydride and sulfoxide concentration, the ratio k_{ex}/k_{rac} is about 0.5, and the reaction is characterized by a high negative entropy. These data are best explained by assuming the mechanism in eq. [97], in which the formation of a symmetrical diacyloxysulfurane intermediate is a crucial step.

The acceleration of racemization of sulfoxides in acetic anhydride by adding Lewis acids, such as $AlCl_3$ (271,276,277), is consistent with the mechanism above, since the formation of acetoxysulfonium ion is facilitated.

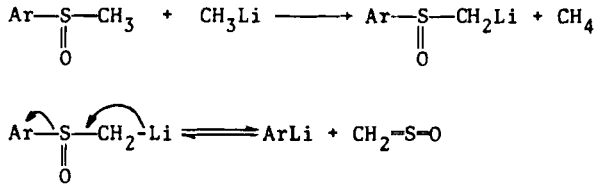
Diastereomeric menthyl arenesulfinates as well as enantiomeric alkyl alkanesulfinates racemize in the presence of trichloroacetic anhydride even at room temperature (278). A mechanism based on kinetic investigations was proposed in which the formation of alkoxyacyloxysulfonium salt is the rate-determining step.



[97]

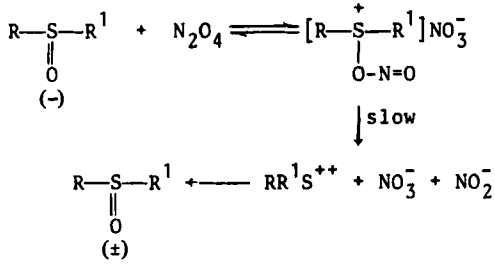
[98]

d. Other Reactions. Mislow and Jacobus (82) discovered that chiral sulfoxides containing labile α-hydrogens undergo substantial decomposition accompanied by partial racemization when treated with methyllithium in dimethoxyethane at room temperature. The mechanism proposed to explain the racemization and decomposition reactions involves the formation of an arenesulfinylmethide ion, from which methylenesulfine is subsequently eliminated. Since the latter is an achiral intermediate, its recombination with aryllithium would result in the formation of racemic starting sulfoxide. The formation of racemic methyl phenyl sulfoxide **186** in the reaction of (–)-menthyl methanesulfinate **193** with phenyllithium may be explained in a similar way.



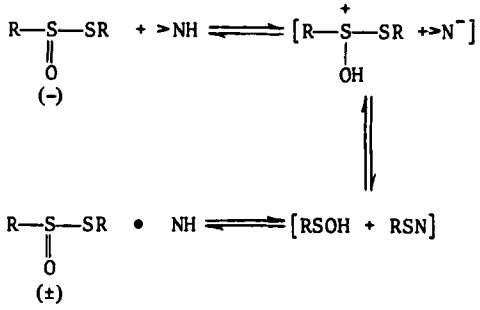
[99]

Nitrogen tetroxide also causes rapid racemization of sulfoxides; however, the reaction takes place without decomposition (279,280). This process is initiated by the formation of a sulfonium salt, which then undergoes partial ionization to form a dication intermediate.



[100]

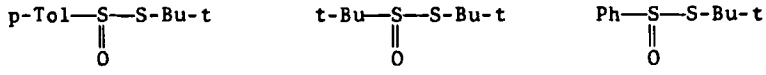
Much attention has been devoted to the acid- and nucleophile-catalyzed racemization of thiosulfinates. As a result of the extensive studies by Kice and his co-workers (112) and by Fava (281), it is clear now that the easy racemization of thiosulfinates caused by acids and bases (e.g., pyridine) is related to the scission of the sulfur-sulfur bond and the formation of sulfenic acid or its anion as an achiral intermediate. As expected, introduction of steric hindrance



[101]

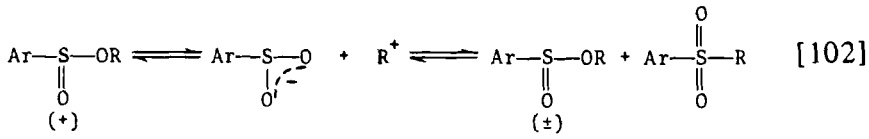
around one or both sulfur atoms in thiosulfinates leads to a considerable increase of their optical stability (114). Thus, no racemization of the thiosulfinates **70**, **72**, and **223** was observed in pyridine solution at room temperature, in benzene solution containing trifluoroacetic acid at room temperature, or under reflux in benzene solution for 10 hr.

Fava et al. (282) observed that, after brief heating in polar solvents, optically active benzhydryl *p*-toluenesulfinates undergo racemization accompanied by rearrangement to the corresponding sulfones. The



70 **72** **223**

common step for both reactions is the formation of carbonium and sulfinate ions, which can undergo return to either the oxygen or sulfur atoms of the ambident sulfinate anion.



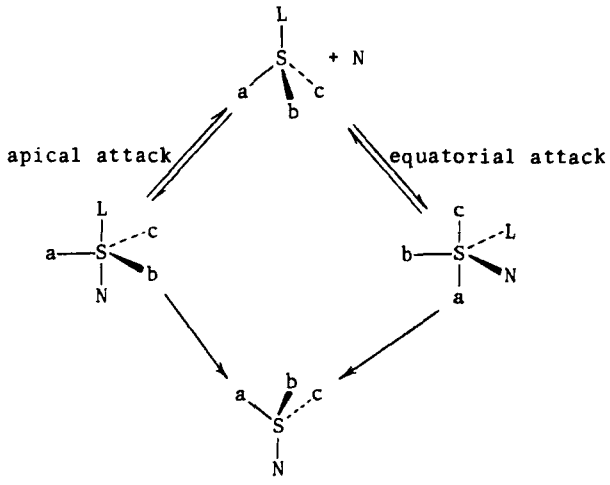
[102]

B. Nucleophilic Substitution at Chiral Tri- and Tetracoordinate Sulfur

The most frequently encountered reactions in organic sulfur chemistry are nucleophilic displacement reactions. The mechanism and steric course of S_N-*S* reactions have been the main points of interest of research groups all over the world, in particular, Andersen, Cram, Johnson, and Mislow in the United States; Kobayashi and Oae in Japan; Kjaer in Denmark; and Fava and Montanari in Italy. The results of these investigators have been discussed exhaustively in many reviews on sulfur stereochemistry. In a recent report on nucleophilic substitution at tricoordinate sulfur, the literature was covered by Tillett (10) to the end of 1975. Therefore only some representative examples of nucleophilic substitution reactions at chiral sulfur are discussed here. However, recent results obtained in the authors' laboratory are included.

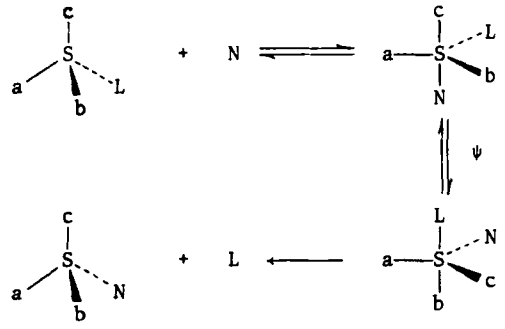
In the overwhelming majority of cases, nucleophilic substitution at chiral tri- and tetracoordinate sulfur results in inversion of configuration. It is customary to consider that such reactions occur synchronously by an S_N2-*S* mechanism involving a transition state, or stepwise by an addition-elimination mechanism (A-E) involving a trigonal-bipyramidal sulfurane intermediate that is formed by addition of the nucleophile (N) opposite to the leaving group (L) occupying the apical position and decomposed before any ligand reorganizations (pseudorotations) have taken place. An alternative explanation for nucleophilic displacement reactions at sulfur accompanied by inversion of configuration consists in the formation of a transient sulfurane with diequatorial disposal of N and L.

The addition-elimination mechanism also provides a reasonable explanation for nucleophilic substitution reactions at sulfur that occur with retention of configuration. It is assumed that nucleophilic attack occurs at sulfur in an apical position opposite a substituent



[103]

that is not the leaving group. This results in the formation of a sulfurane intermediate having the axial-equatorial arrangement of the nucleophile and the leaving group, respectively. After ligand reorganization by a single Berry pseudorotation, a new sulfurane intermediate is formed in which the leaving group occupies the apical position from which it departs. The overall process depicted in eq. [104] leads to retention of configuration.



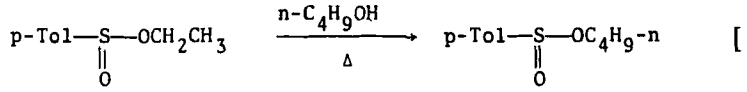
[104]

In addition to the foregoing explanation of retention of configuration, two possibilities may be taken into account. The first is that apical entry is followed by basal departure, and vice versa. Second, the sulfurane intermediate formed may have the structure of a square basal pyramid. In both cases nucleophilic substitution reactions may occur with retention of configuration without ligand reorganization. It appears that the apicophilicity of substituents in sulfurane species

and leaving group ability are among the important factors that determine the steric course of nucleophilic substitution at chiral sulfur.

Finally, although sulfurane intermediates have been proposed in many cases, they have not been isolated from nucleophilic substitution reactions. However, the concept of an addition-elimination mechanism is supported by the independent syntheses of a number of stable sulfuranes; these compounds have a trigonal-bipyramidal structure and in some cases the ligand reorganization was found to occur very easily (189–191).

Historically, the thermal transesterification of (–)-ethyl *p*-toluenesulfinate 224 with *n*-butanol affording (+)-*n*-butyl *p*-toluenesulfinate 225 described by Phillips in 1925 (100) is the first nucleophilic substitution reaction at chiral sulfur involving a Walden-type inversion. The evidence for inversion of configuration in this reaction was based on the assumption that both (–)-esters 224 and 225 obtained from the kinetic resolution have the same configuration.



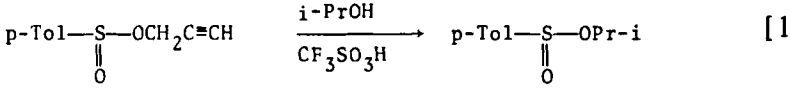
[105]

(–)-224 (+)-225

$[\alpha]_{546}$ -5.81° (ee 2.6%) $[\alpha]_{546}$ +0.32° (ee 0.1%)

Although recent studies on chiral sulfinates confirmed the original assumptions by Phillips concerning the steric course of transesterification as well as relative configurations of 224 and 225, attempts to reproduce the transesterification experiment failed (283).

It was found recently (283) that alcoholysis of chiral sulfinates proceeds at room temperature in the presence of strong acids with predominant inversion of configuration or racemization. The latter result is most probably due to the competitive symmetrical alkoxy-alkoxy exchanges in the starting and produced sulfinates. The reaction of (–)-*S*-propargyl *p*-toluenesulfinate (226) with isopropyl alcohol best illustrates these experiments.

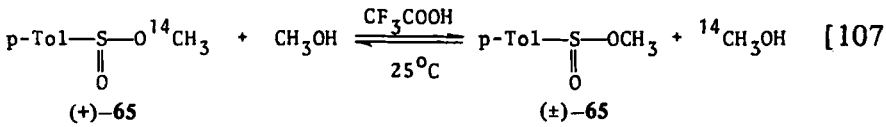


[106]

(–)-(*S*)-226 (+)-(*R*)-227

$[\alpha]_D$ -24.2° (ee 21.7%) $[\alpha]_D$ +17.6° (ee 8.7%)

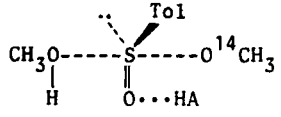
More rigorous evidence supporting the inversion in the transesterification of sulfinates was provided by kinetic measurements in which the rate of the acid-catalyzed racemization of (+)-methyl *p*-toluenesulfinate **65** in methanol was compared with that of isotopic methoxy-methoxy exchange under exactly the same conditions.



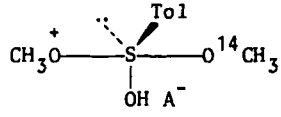
[107]

$$k_{rac} = (6.25 \pm 0.01) \cdot 10^{-5} \text{ sec}^{-1}$$
$$k_{ex} = (2.94 \pm 0.04) \cdot 10^{-5} \text{ sec}^{-1}$$

Sulfinate **65** loses its optical rotation almost twice as fast as it loses the radioactive methoxy group, thus proving unequivocally that the methoxy-methoxy exchange at the sulfinyl sulfur proceeds stereospecifically with net inversion of configuration. This result is compatible with an S_N2-*S* mechanism involving a transition state **228** or with the A-E mechanism involving a transient dialkoxysulfurane intermediate **229**, which should undergo decomposition faster than pseudorotation because the positions of all substituents at sulfur in the trigonal bipyramid are already optimally located from the point of view of apicophilicity.

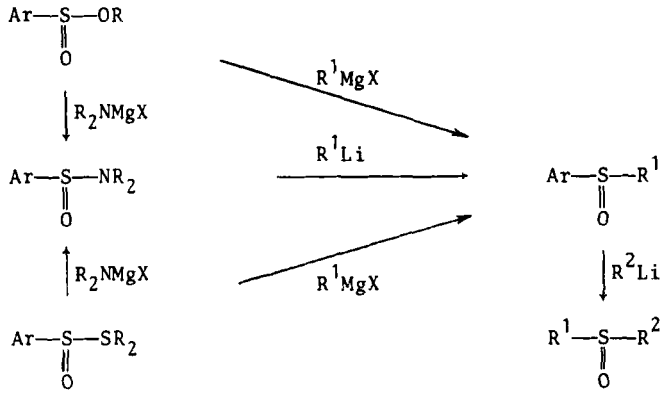


228



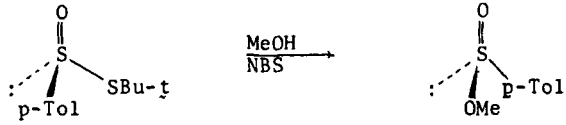
229

The reactions of chiral sulfinic esters with organometallic reagents also belong to the category of nucleophilic substitution reactions at sulfur and occur as a rule with inversion of configuration. Thus, the Andersen synthesis of sulfoxides (75,76) and the closely related reactions of sulfinamides (83,85,116) and thiosulfinates (105,114) with Grignard or alkyl (aryl) lithium reagents all proceeded with inversion of configuration and with high stereospecificity (see Scheme 20). An interesting synthesis of chiral dialkyl sulfoxides (93) based on the reaction of chiral alkyl aryl sulfoxides with alkyllithium reagents also proceeds with inversion of configuration.



Scheme 20

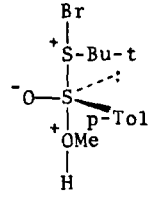
With regard to nucleophilic substitution at sulfur in thiosulfinates, it is interesting to note that methanolysis of (-)-(*S*)-*t*-butyl *p*-toluenethiosulfinate **70** in the presence of *N*-bromosuccinimide (NBS) proceeds with predominant inversion at the sulfinyl center. Most



[108]

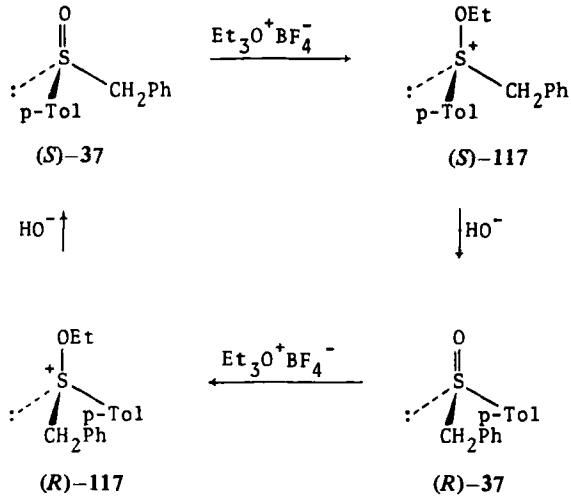
(-)-(*S*)-**70** $[\alpha]_D$ -31.5° (ee 11.3%)

(+)-(*R*)-**65** $[\alpha]_D$ +12.75° (ee 5.8%)



230

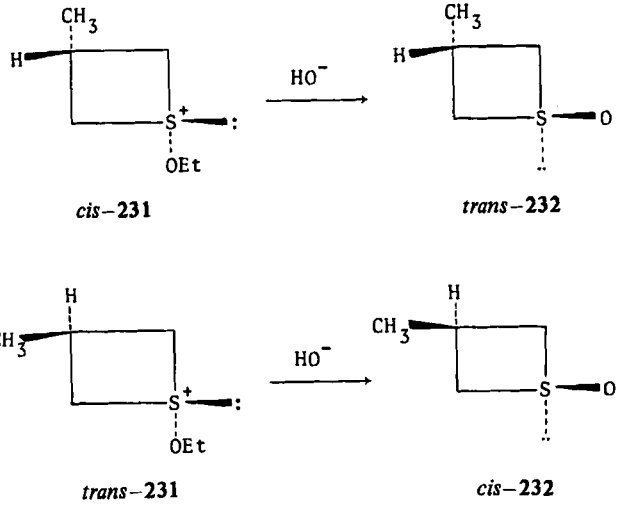
probably the reaction is initiated by the formation of the *S*-bromosulfonium salt and the inversion arises from a trigonal bipyramidal intermediate (transition state) **230**, with an apical-apical arrangement of entering and leaving groups.



Scheme 21

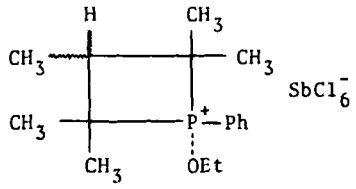
Johnson and McCants (161) were the first to show that the alkaline hydrolysis of alkoxysulfonium salts, obtained by *O*-alkylation of sulfoxides, proceeds with inversion of configuration at sulfur. This method was employed to interconvert (*R*)- and (*S*)-benzyl *p*-tolyl sulfoxides 37 as shown in Scheme 21. In contrast to the hydroxide anion, the chloride, bromide, and iodide anions as well as the nitrogen atom of pyridine react with chiral ethoxydiarylsulfonium salts, not at sulfur but at the α-carbon atom of the ethoxy group, yielding the starting sulfoxide with retained configuration (284). On the other hand, the nucleophilic attack of the fluoride anion is directed at sulfur as in the case of the hydroxide anion (285).

The alkaline hydrolyses of both *cis*- and *trans*-1-ethoxy-3-methylthietanium ions 231 also proceed with complete inversion of configuration at sulfur (Scheme 22) as was demonstrated by Tang and Mislow (286). This rather unexpected finding is of considerable mechanistic importance, especially since alkaline hydrolysis of analogous cyclic phosphorus compounds, *cis*- and *trans*-1-ethoxy-1-phenyl-2,2,3,4,4-pentamethylphosphetanium hexachloroantimonates 233 is accompanied by retention of configuration at phosphorus. This result is in harmony with the concept pf pseudorotation of the intermediate phosphorane 234, in which the four-membered ring is placed in the most favorable, strain-free, apical-equatorial position. However, the formation of the analogous sulfurane inter-

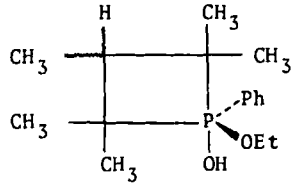


Scheme 22

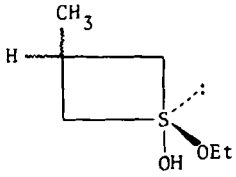
mediate 235 in the course of alkaline hydrolysis of cyclic sulfonium salts 231 must be excluded because it should give, after pseudorotation and decomposition, the cyclic sulfoxides 232 with retention of configuration at sulfur.



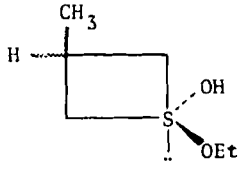
cis– and *trans*–233



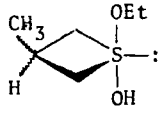
234



235

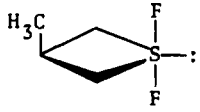


236



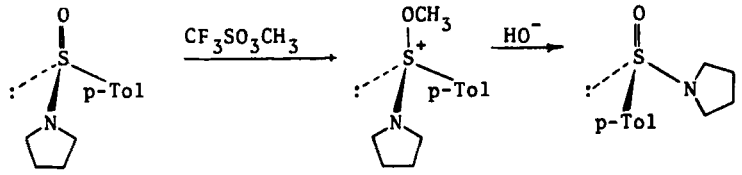
237

Between 236 and 237, the two other sulfurane intermediates that may be responsible for inversion at sulfur, 237 appears to be the more probable candidate for two reasons. The first is that the ethoxy and hydroxy groups occupy the proper apical positions in accord with their high apicophilicities, and the lone electron pair is placed equatorially, consistent with all the available structural data on sulfuranes. Second, the four-membered ring in a stable cyclic difluorosulfurane 238 was found by Denney et al. (287) to occupy a diequatorial position.



238

The original observation of Johnson that alkaline hydrolysis of alkoxysulfonium salts takes place with inversion of configuration at sulfur was utilized recently (110) to invert the configuration of sulfinamides. As was already mentioned, (+)-(*S*)-*p*-toluenesulfinylpyrrolidine 120 was treated with methyl triflate to give the corresponding methoxypyrrolidino-*p*-tolylsulfonium triflate 119. The crude salt 119 was then subjected to mild alkaline hydrolysis and gave the enantiomeric sulfinamide (-)-(*R*)-120. This two-reaction sequence takes place with at least 91% inversion.



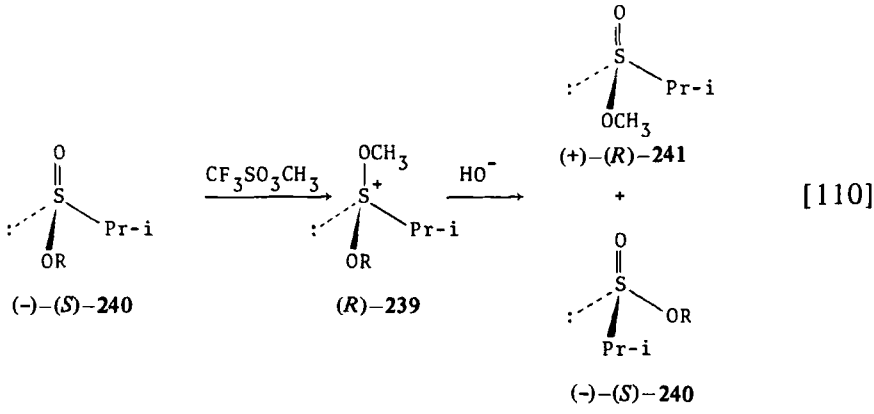
[109]

(+)-(*S*)-120 (*S*)-119 (-)-(*R*)-120

In the hope of gaining further experimental insight into the mechanism of nucleophilic displacement at sulfur, the alkaline hydrolysis of chiral dialkoxysulfonium salts was investigated (162). At least two interesting features of these model systems for nucleophilic substitution studies should be accentuated: both alkoxy groups are of comparable leaving group ability, and there are essentially two identical tetrahedral faces to be attacked by the nucleophile.

The alkaline hydrolysis of a series of chiral methoxyalkoxyiso-

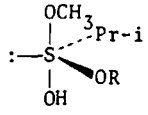
propylsulfonium triflates, $(CH_3O)(RO)$-*i*-PrS^+ $CF_3SO_3^-$ **239** (R = Et, *n*-Pr, *i*-Pr, *n*-Bu, Neopentyl), obtained *in situ* by methylation of the chiral sulfinates **240** with methyl triflate, was found to give two possible sulfinates with configurations inverted with respect to that of the starting sulfonium salt. It should be noted, however, that the



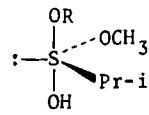
[110]

optical purities of **240** and **241**, the esters formed, are much lower than that of the starting sulfinate (+)-(*R*)-**240**. This is due to a competitive attack of hydroxide anion at the methoxy carbon atom (as evidenced by ^{18}O experiments) and eventually to some racemization of the starting sulfonium salt **239** under the reaction conditions.

The displacement of both alkoxy groups at sulfur in **239** with predominant inversion of configuration can be explained by the simultaneous formation of two different intermediates (or transition states) **242** and **243**, which undergo decomposition before pseudorotation. In this context, it is interesting to note that the formation and decomposition of only one such sulfurane intermediate would give two sulfinate products with inverted and retained configuration at sulfur.



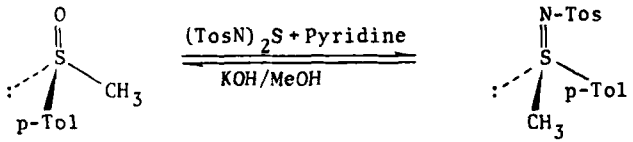
242



243

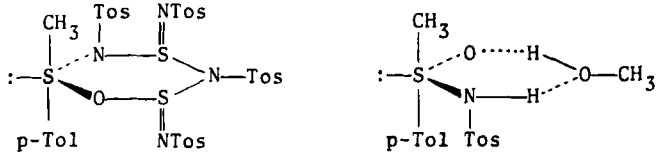
The sulfoxide-sulfimide interconversion is of considerable interest in connection with the possible geometries of the transition states or intermediates that might arise from nucleophilic substitution at

sulfur. Cram and Day (130) showed that the reaction of chiral methyl *p*-tolyl sulfoxide (**41**) with bis(tosylsulfurdiimide) in pyridine affords the corresponding sulfimide **91** with inversion of configuration at sulfur. They also found that the alkaline hydrolysis of the latter proceeds with inversion at sulfur and yields the starting sulfoxide.



(−)-(*S*)-**41** (+)-(*R*)-**91** [111]

Taking into account that the sulfoxide → sulfimide conversion in pyridine is second order in sulfurdiimide, Cram and co-workers proposed the mechanism involving a trigonal-bipyramidal intermediate **244** with an equatorial-equatorial arrangement of entering and leaving groups forming a ring system. It has been suggested that a similar



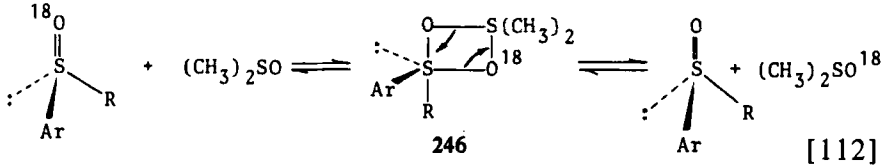
244 **245**

type of intermediate, **245**, with diequatorial disposal of entering and departing groups, is formed during the alkaline hydrolysis of the sulfimide **91** in methanol (98).

A more detailed discussion on the mechanisms and steric courses of imide-oxygen ligand transfer reactions may be found in a paper by Cram and co-workers (8).

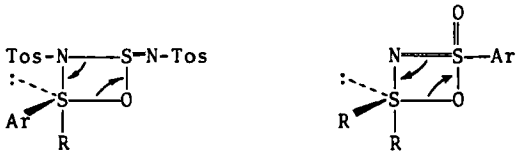
Oae and co-workers (288) were the first to show that nucleophilic displacement at sulfur is accompanied by retention of configuration. They found that chiral ^{18}O-labeled alkyl aryl sulfoxides exchange oxygen with dimethylsulfoxide at about 150°C, almost without racemization. To explain the steric course (retention) of this reaction, the formation of a trigonal-bipyramidal intermediate **246** was postulated in which the entering and departing oxygen atoms occupy apical and equatorial positions, respectively.

Later on, Christensen (134,135) showed that the reaction of chiral sulfoxides with *N*-sulfinyl-*p*-toluenesulfonamide in benzene as well as



246 [112]

the reaction of chiral sulfoxides with bis(tosylsulfurdiimide) carried out in the same solvent proceed with retention of configuration to give sulfimides. In this case, too, the operation of an apical-equatorial substitution mechanism with the formation of the transient sulfurane 247 was proposed. A similar mechanism was advanced by Maricich

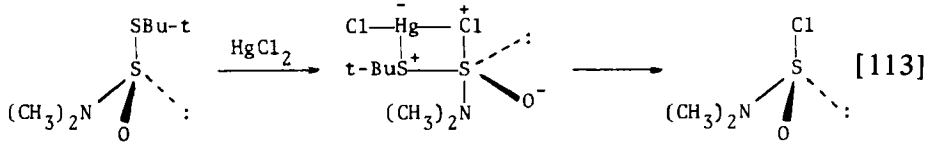


247 248

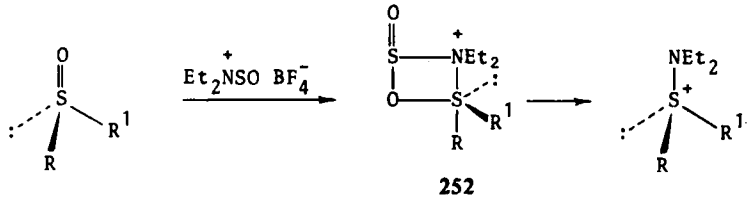
and Hoffman (136) to explain retention at sulfur in the reaction of a sulfoxide with *p*-toluenesulfinylnitrene leading also to a sulfimide via 248.

Recently, two other examples of substitution with retention at sulfur have been reported. The first concerns the reaction of the optically active amidothiosulfite 249 with mercury dichloride, yielding the optically active aminosulfinyl chloride 250 (150). The second comprises the conversion of chiral sulfoxides into aminosulfonium salts using *N,N*-diethyl-*N*-sulfinylammonium tetrafluoroborate as reagent (165). In both cases the observed retention at sulfur could have arisen from the trigonal-bipyramidal intermediates 251 and 252 with an equatorial-apical (or apical-equatorial) arrangement of entering and leaving groups.

Analysis of all the examples discussed here involving retention of configuration at sulfur strongly suggests that a tendency of the four-



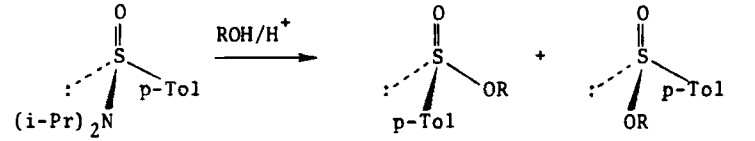
(-)-249 251 250 [113]



252 [114]

membered rings to occupy an apical-equatorial position in a trigonal-bipyramidal intermediate is a decisive factor in determining the course of nucleophilic substitution.

In this connection it is interesting that the steric course of the acid-catalyzed alcoholysis of the optically active (–)-(*S*)-*N*,*N*-diisopropyl-*p*-toluenesulfinamide **253** depends on the structure of the alcohol used. The results so far obtained are listed in Table 2 (246).

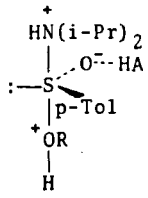


(–)–(*S*)–**253** (*S*) (*R*) [115]

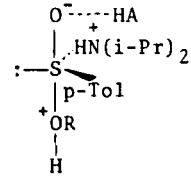
Inspection of the results in Table 2 shows that the predominant retention of configuration was observed in the cases of isopropanol, cyclopentanol, and cyclohexanol. These preliminary data may be rationalized in terms of the parallel formation of two sulfurane intermediates (**254** and **255**), which are responsible for inversion and retention at sulfur, respectively. The relative stabilities of these inter-

Table 2
Acid-Catalyzed Alcoholysis of (+)-(*S*)-**253**

Alcohol	Inversion (%)	Retention (%)
Methanol	69	31
Ethanol	54	46
n-Propanol	58	42
Isopropyl alcohol	41	59
Isobutyl alcohol	51.5	48.5
Pentanol-3	52.5	47.5
Cyclopentanol	48	52
Cyclohexanol	26	74



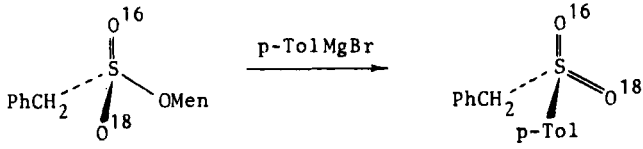
254



255

mediates, which determine the steric course of the reaction, appear to be dependent in a complex way on steric factors.

In contrast to the widely investigated stereochemistry of nucleophilic substitution at optically active tricoordinate sulfur, there have been few similar studies with optically active tetracoordinate sulfur systems. Sabol and Andersen (174) were the first to show that the reaction of *p*-tolylmagnesium bromide with (–)-menthyl phenylmethane[^{16}O-^{18}O]sulfonate **140** proceeds with inversion of configuration. Thus, the Grignard reaction at the sulfinyl and sulfonyl centers takes place with the same stereochemistry.

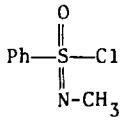


[116]

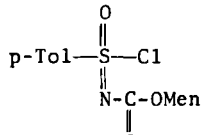
(–)-(*R*)-**140** (–)-(*S*)-**138**

Recently, Johnson and Jonsson (185) as well as Jones and Cram (166) demonstrated that the replacement of chlorine in the optically active sulfonimidoyl chlorides **163** and **167** by phenoxy or dimethylamino groups occurs with inversion of configuration. The syntheses of both chlorides and displacement reactions are shown in Schemes 12 and 13 (see page 382).

Finally, we cite an important paper by Martin and Balthazor (195) on nucleophilic substitution at tetracoordinate sulfur in chloro-



163



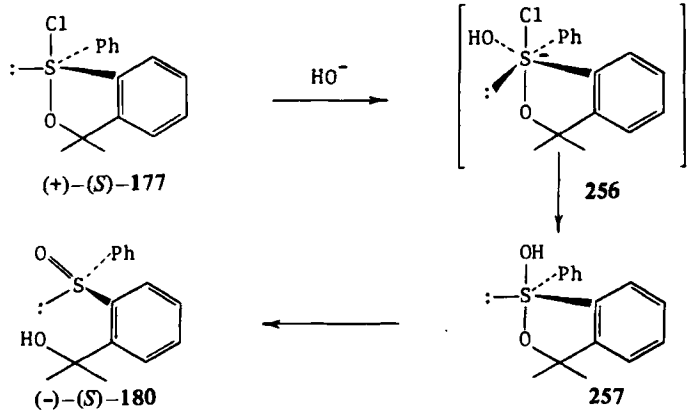
167

sulfurane 177. These investigators found that hydrolysis of (+)-(*S*)-177 in the presence of diisopropylethylamine or *N*,*N*-dimethylaniline yielding sulfoxide (-)-(*S*)-180 is accompanied by retention at sulfur. Based on additional kinetic studies of the hydrolysis of chlorosulfurane 177 and related compounds, Martin and Balthazor proposed an associative mechanism involving an octahedral sulfur anion transition state 256, which decomposes via hydroxysulfurane 257 to the final substitution product—the sulfoxide 180 (Scheme 23).

C. Reactions of Chiral Sulfur Compounds with Electrophilic Reagents

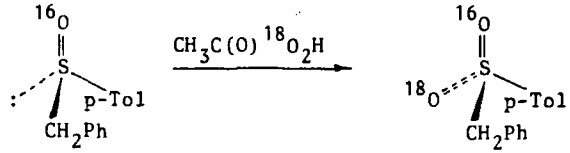
As the last point in Sect. IV, we discuss briefly the reactions of chiral sulfur compounds with electrophilic reagents. In contrast to nucleophilic substitution reactions, the number of known electrophilic reactions at sulfur is very small and practically limited to chiral tricoordinate sulfur compounds that on reacting with electrophilic reagents produce more stable tetracoordinate derivatives. It is generally assumed that the electrophilic attack is directed on the lone electron pair on sulfur and that the reaction is accompanied by retention of configuration. As typical examples of electrophilic reactions at tricoordinate sulfur, we mention oxidation, imination, alkylation, and halogenation. All these reactions were touched on in the section dealing with the synthesis of chiral tetracoordinate sulfur compounds.

The first example of stereospecific oxidation of sulfoxides was described by Stirling (77), who was able to synthesize (-)-(*S*)-benzyl



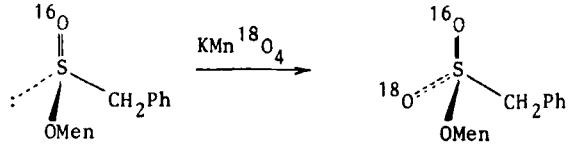
Scheme 23

p-tolyl [^{16}O-^{18}O]sulfone **138** by oxidation of (+)-(*R*)-benzyl *p*-tolyl sulfoxide **37** with ^{18}O-labeled peracetic acid. Later on, Sabol and



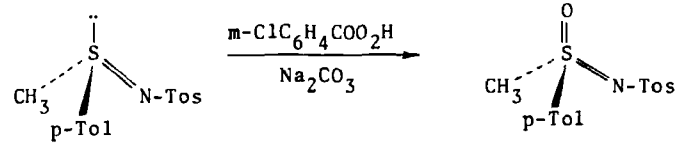
(+)-(*R*)-**37** (-)-(*S*)-**138** [117]

Andersen (174) reported that oxidation of (+)-(*R*)-methyl phenylmethanesulfinate **139** with potassium permanganate containing ^{18}O gives (-)-(*R*)-menthyl phenylmethanesulfonate **140**. In both cases retention of configuration in the oxidation step was assumed.



(+)-(*R*)-**139** (-)-(*R*)-**140** [118]

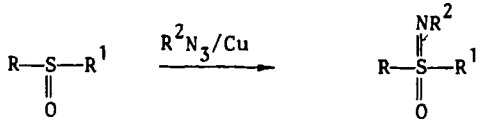
The oxidative conversion of the (-)-(*S*)-*N*-tosyl methyl-*p*-tolylsulfimide **91** to the corresponding (-)-(*R*)-sulfoximide **151** is of considerable interest because the absolute configurations of the substrate and product were established by the quasi-racemate method and by X-ray analysis (98), respectively. Therefore, the stereochemical result of this experiment indicates unequivocally that oxidation of chiral tricoordinate sulfur compounds proceeds with retention of configuration.



(-)-(*S*)-**91** (-)-(*R*)-**151** [119]

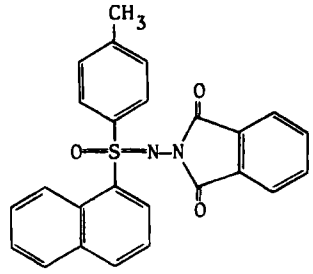
Another reaction belonging to the category of electrophilic reactions is the reaction of sulfoxides with nitrenelike reagents leading to sulfoximides (98,178,179).

The determination of the absolute configuration of (-)-(*S*)-*N*-



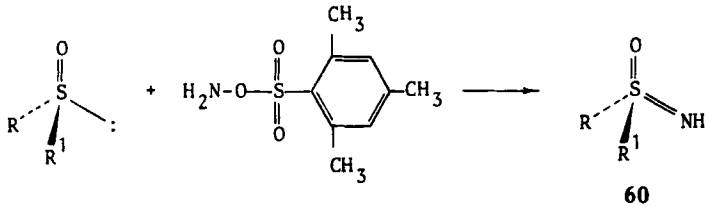
[120]

phthalimido-α-naphthyl-*p*-tolyl sulfoximide **153** by X-ray analysis (289) gave a final proof of retention of configuration in the process of nitrenation of sulfoxides.



153

The synthesis of *N*-unsubstituted sulfoximides in the reaction of chiral sulfoxides with *O*-mesitylsulfonylhydroxylamine follows the same steric course (180). Similarly, the reaction of (+)-(*R*)-methyl-*p*-

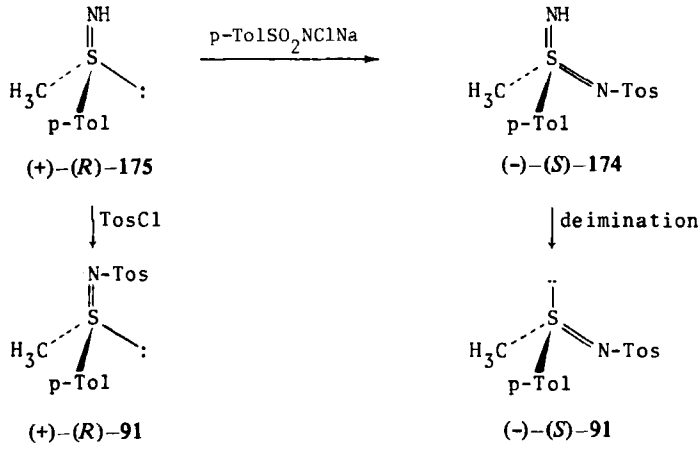


[121]

60

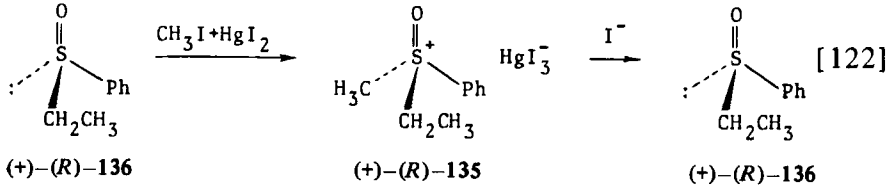
tolyl sulfimide **175** with chloramine T in liquid ammonia involving the electrophilic attack of nitrogen on the unshared sulfur electron pair also proceeds with retention of configuration, as evidenced by the chemical correlation shown in Scheme 24 (188).

As mentioned earlier (see page 373), methylation of (+)-(*R*)-ethyl phenyl sulfoxide **136** with methyl iodide in the presence of mercury iodide affords the corresponding oxosulfonium salt (+)-(*R*)-**135** (172). That its demethylation by iodide anion yields sulfoxide **136** with the same configuration as that of the starting one indicates that *S*-methylation of sulfoxides occurs with retention of configuration.



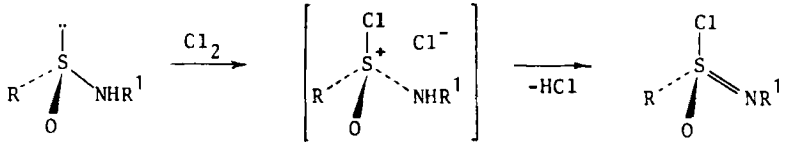
Scheme 24

Finally, chlorination of chiral sulfinamides (185,186) which may be classified as electrophilic reaction at a tricoordinate sulfur, proceeds with retention at sulfur, yielding chiral sulfonimidoyl chlorides. This reaction is exemplified by the synthesis of sulfonimidoyl



[122]

chlorides (-)-(*R*)-163 and (+)-(*S*)-167 depicted in Schemes 12 and 13. Most probably the process of chlorination of sulfinamides involves at first the formation of a chlorosulfonium salt, which is then stabilized by proton abstraction from the nitrogen atom by means of chloride anion.



[123]

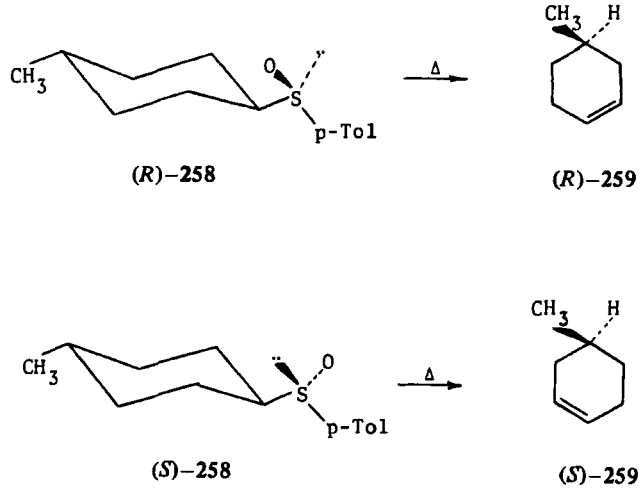
The formation of halogenosulfonium salts is considered to be the first step in the α-halogenation of sulfoxides. The mechanism and stereochemistry of α-halogenation of sulfoxides are discussed in detail by Montanari in his recent review paper (9).

V. ASYMMETRIC INDUCTION IN TRANSFER OF CHIRALITY FROM SULFUR TO OTHER CENTERS

In the last two decades optically active sulfur compounds have found wide application in asymmetric synthesis. This is mainly because organic sulfur compounds are quite readily available in optically active form. Moreover, the chiral sulfur groupings that induce optical activity can be removed from the molecule easily, under fairly mild conditions, thus presenting an additional advantage in the asymmetric synthesis of chiral compounds. This section deals with reactions in which asymmetric induction in transfer of chirality from sulfur to other centers was observed. This subject has been treated only in a cursory manner in recent reviews on asymmetric synthesis (290-292).

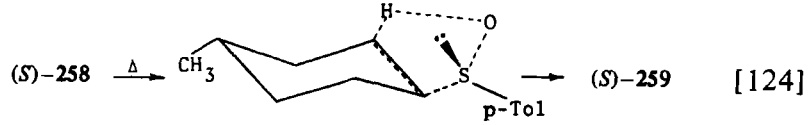
Various criteria may be used to classify such reactions. In our survey the most general criterion was used, that is, the further fate of the chiral sulfur moiety inducing optical activity. According to this criterion all the reactions, which can be defined as the processes of transfer of chirality from the chiral sulfur atom to the newly formed chiral carbon or heteroatomic center, can be divided into three groups. The first group includes such reactions as result in the formation of new chiral, sulfur-free compounds. The second group includes reactions in the course of which the formation of a new chiral center is accompanied by disappearance of the chirality at sulfur, although the achiral sulfur moiety constitutes an integral part of the new optically active molecule. To the third group belong reactions resulting in the formation of diastereomeric systems where the inducing chiral sulfur center preserves fully or partly its optical activity.

The first example of asymmetric induction in transfer of chirality from the chiral sulfur atom to the prochiral carbon atom was described by Goldberg and Sahli in 1965 (197). It concerns the pyrolysis of the optically active *p*-tolyl *trans*-4-methylcyclohexyl sulfoxides **258**. It was found that on pyrolysis at 200 to 250°C, optically active sulfoxides (*R*)-**258** and (*S*)-**258** yield optically active 4-methylcyclohexenes-1 **259**, with the absolute *R* and *S* configurations, respectively, at the newly formed chiral carbon atoms (Scheme 25). The optical purities of the 4-methylcyclohexenes-1 that were formed depended largely on the temperature of pyrolysis. Thus, the values of 42 and 70% optical purity were noted for **259** at 250° and 200°C, respectively. The formation of the cycloolefins **259**, whose absolute configurations are the same as those of the starting optically active sulfoxides **258**, indicates that the pyrolysis reaction proceeds



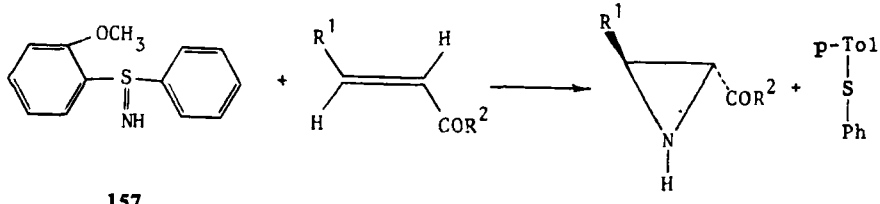
Scheme 25

through a transition state with the smallest interactions between the axial ring protons and the substituents at the chiral sulfur atom.



[124]

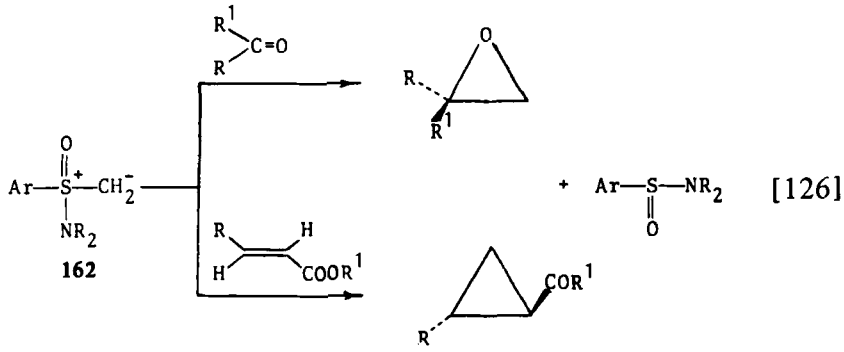
In the asymmetric synthesis of the optically active α-acylaziridines **260** described recently by Furukawa et al. (293), the optically active *o*-methoxyphenylphenylsulfimide **157**, which plays the role of the optical activity inducing agent, is converted to the corresponding sulfide. In this reaction, which involves a typical Michael addition of **157** to the carbon-carbon double bond followed by elimination of sulfide, the optical purities of the chromatographically purified



157 **260** [125]

α-acylaziridines **260** reach about 30% and are practically independent on the solvent used for the reaction. This asymmetric synthesis can be applied only in the case of strongly electrophilic olefins such as α, β-dicarbonyl ethylene derivatives, which seriously limits its utility.

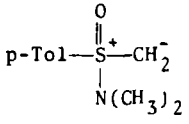
A very convenient asymmetric synthesis of cyclopropane or epoxide systems developed by Johnson (184) is based on the use of chiral sulfur ylides as the agents that induce optical activity. Generally, this method consists of the asymmetric addition of a chiral sulfur ylide to the C=C or C=O bond and subsequent cyclization of the addition product to form a chiral cyclopropane or epoxide system together with chiral sulfinamide. A wide range of chiral



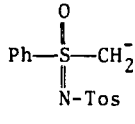
[126]

oxosulfonium ylides (**162a–162g**) have been used as nucleophilic alkylidene transfer agents for the asymmetric synthesis discussed here. The reaction of ylide **162a** with benzaldehyde yields styrene epoxide with the absolute configuration *R* at the carbon atom and 20% optical purity. Analogous reactions of ylide **162a** with *p*-chlorobenzaldehyde, *n*-heptanal, and acetophenone produce the corresponding chiral epoxides; however, so far their absolute configurations and optical purities are unknown (118). Optically active cyclopropanes obtained by asymmetric reaction of chiral sulfur ylides with olefins are listed in Table 3.

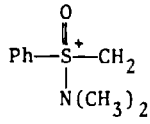
It is interesting to note that the reaction of *trans*-benzalacetophenone with ylide **162a** affords (1*S*,2*S*)-phenylcyclopropane with 35.3% optical purity, whereas its enantiomer having the (1*R*,2*R*)-configuration is formed when *trans*-benzalacetophenone is reacted with ylide **162b**. Studies on the relationship between the steric requirements of the substituents attached to the chiral ylide sulfur atom and the optical purity of the cyclopropane rings formed have shown that increases in the steric size of the *N*,*N*-dialkylamino



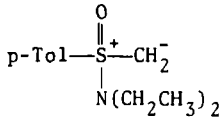
162a



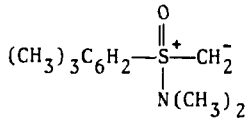
162b



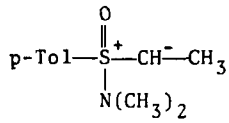
162c



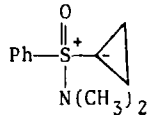
162d



162e



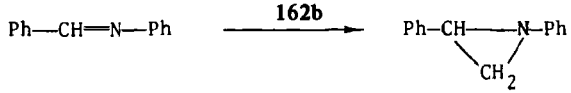
162f



162g

group and of the aromatic substituent in the ylide result in the lowered optical purity of cyclopropanes.

When benzylideneaniline is reacted with ylide **162b**, optically active *N*-phenyl-2-phenylaziridine **261** of unknown absolute configuration and optical purity is produced (294).



[127]

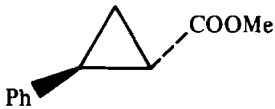
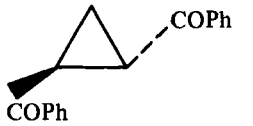
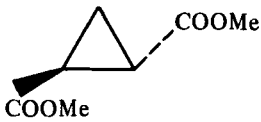
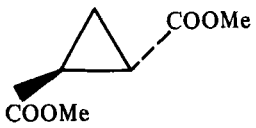
261, $[\alpha]_D^{-12.9^\circ}$

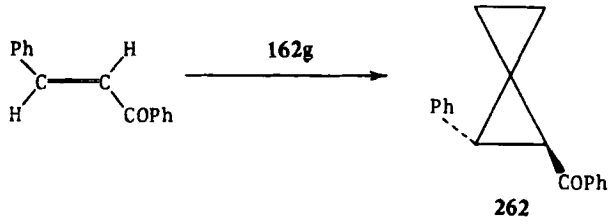
Both the reaction of ylide **162f** with methyl acrylate and the reaction of ylide **162c** with methyl methacrylate produce, after hydrolysis, the same optically active *trans*-2-methylcyclopropanecarboxylic acid with optical purities of 43.2 and 11.9%, respectively (295).

It is of some interest that optically active spiroketone **262** is formed when *trans*-benzalacetophenone is treated with ylide **162g** (295). The absolute configuration and optical purity of this ketone are unknown.

The reaction of the sulfonium salt **263** with methyl cyanoacetate in the presence of sodium methoxide was found to give exclusively the *E*-isomer of (1*S*,2*R*)-1-cyano-2-phenylcyclopropanecarboxylic acid methyl ester **264** of 25.5% optical purity (296).

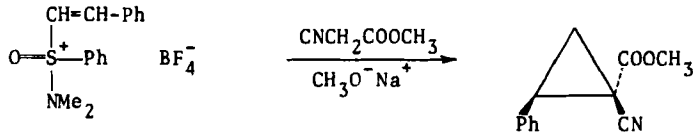
Table 3
Asymmetric Synthesis of Chiral Cyclopropane Derivatives

Substrate	Ylide	Product		
			Absolute Configuration	e. e. (%)
Methyl *trans*-cinnamate	**162a**		1*S*,2*S*	30.4
trans-1,4-Diphenyl-2-butene-1,4-dione	**162a**		1*S*,2*S*	–
Dimethyl fumarate	**162a**		1*S*,2*S*	15.2
Dimethyl maleate	**162a**		1*S*,2*S*	17.8
Methyl *trans*-crotonate	**162c**		1*R*,2*R*	11.9
trans-Benzalacetophenone	**162b**		1*R*,2*R*	49
trans-Benzalacetophenone	**162a**		1*S*,2*S*	35
trans-Benzalacetophenone	**162c**		1*S*,2*S*	7



262

[128]



263,

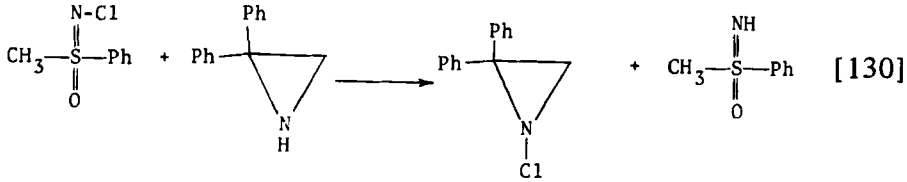
$[\alpha]_D$ -5.7°

(1*S*, 2*R*)–264,

$[\alpha]_{546}$ +64°

[129]

In recent years three other examples of asymmetric induction have been described in the literature in which the chiral sulfur reagent that induces optical activity is converted into another chiral sulfur compound. The first reaction of this type is the chlorination of 2,2-diphenylaziridine (**265**) by means of the optically active *N*-chlorophenylmethylsulfoximide (**266**), affording optically active *N*-chloro-2, 2-diphenylaziridine (**267**) and the unsubstituted sulfoximide **149** (197). In this case asymmetric induction is observed on the nitrogen atom.



266,

$[\alpha]_D$ +195°

265

267,

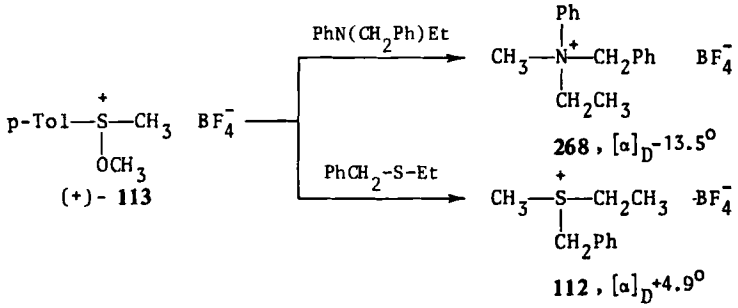
$[\alpha]_D$ +4.3°

149

[130]

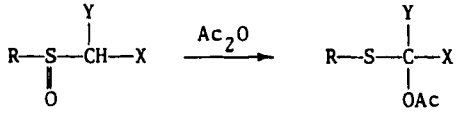
Another example of asymmetric induction in the transfer of chirality from tricoordinate sulfur to the nitrogen atom was reported by Kobayashi (157), who found that methylation of benzylethylaniline with (+)-methoxymethyl-*p*-tolylsulfonium salt **113** yields (–)-benzylethylmethylphenylammonium tetrafluoroborate **268**. A similar asymmetric methylation reaction was observed with benzyl ethyl sulfide. Chiral ammonium **268** and sulfonium salts **112** were formed

with 69 and 60% optical purity, respectively, indicating that the extent of asymmetric induction was rather high.



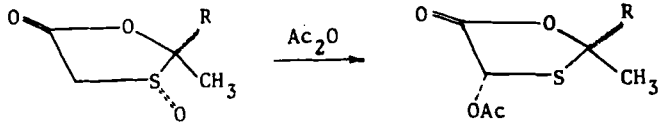
[131]

The Pummerer reaction depicted schematically in eq. [132] is a typical conversion in which the chirality at sulfur disappears and a new chiral center on the α-carbon atom to sulfur is created (298).



[132]

A stereoselective Pummerer reaction was first observed with the diastereomeric cyclic sulfoxides **269**. It was found (299) that when the *cis*- or *trans*-sulfoxides **269** are heated for several hours with acetic anhydride, the corresponding *cis*- or *trans*-acetoxysulfides **270** are formed with a stereospecificity exceeding 85%.



[133]

269 **270**

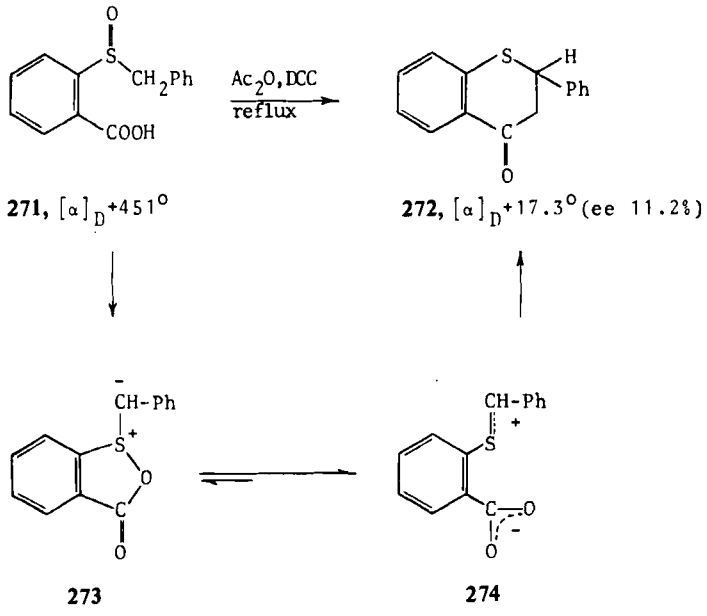
In 1974 the first example of asymmetric induction in an intramolecular Pummerer reaction was observed and reported. Stridsberg and Allenmark (300) treated optically pure *o*-benzylsulfinylbenzoic acid **271** with acetic anhydride in the presence of dicyclohexylcarbodiimide (DCC) and found that the Pummerer reaction product, 3,1-benzoxathian-4-one **272**, was optically active. The sign and optical rotation values ($[\alpha]_D$ varied from +42° to -11°) of **272**

depended on the reaction conditions. In the mechanism proposed by the authors cited, the formation of a cyclic acyloxysulfonium ylide 273, which yields optically active 272 via 274, is the step responsible for the transfer of chirality from sulfur to carbon (Scheme 26).

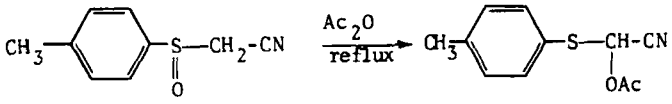
Recently, new examples of asymmetric induction in the Pummerer reaction of chiral sulfoxides have been described. Oae and Numata (301) reported that the optically active α-cyanomethyl *p*-tolyl sulfoxide 275 undergoes a typical Pummerer rearrangement upon heating with excess of acetic anhydride at 120°C, to give the optically active α-acetoxy sulfide 276. The optical purity at the chiral α-carbon center in 276, determined by means of ^{1}H- NMR spectroscopy using a chiral shift reagent, was 29.8%.

A similar extent of asymmetric induction was observed (88) in the Pummerer reaction of optically active α-phosphoryl sulfoxide 49, which results in the formation of the corresponding optically active α-acetoxy α-phosphorylmethyl sulfide 277.

In the course of further studies it was found (302) that the Pummerer reaction of α-phosphoryl sulfoxide 49 catalyzed by bromine or carried out in the presence of dicyclohexylcarbodiimide

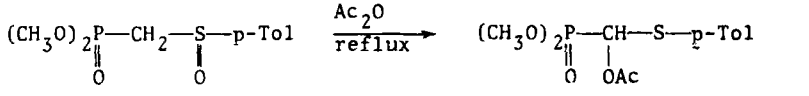


Scheme 26



[134]

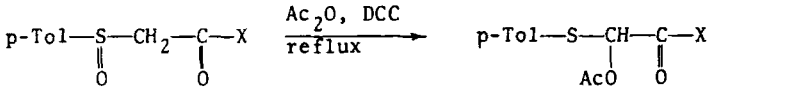
275, $[\alpha]_D^{+252^\circ}$ 276, $[\alpha]_D^{+26.8^\circ}$ (ee 29.8%)



[135]

49, $[\alpha]_D^{+144^\circ}$ 277, $[\alpha]_D^{-4^\circ}$ (ee 24%)

(DCC) proceeds with much higher enantioselectivity (e.e. up to 45%). Likewise, a much higher degree of asymmetric induction was observed in the Pummerer reaction of optically active α-carbonyl-substituted sulfoxides carried out in the presence of DCC (303) to give the α-acetoxy-α-*p*-toluenesulfenylacetic acid derivatives 278.



[136]

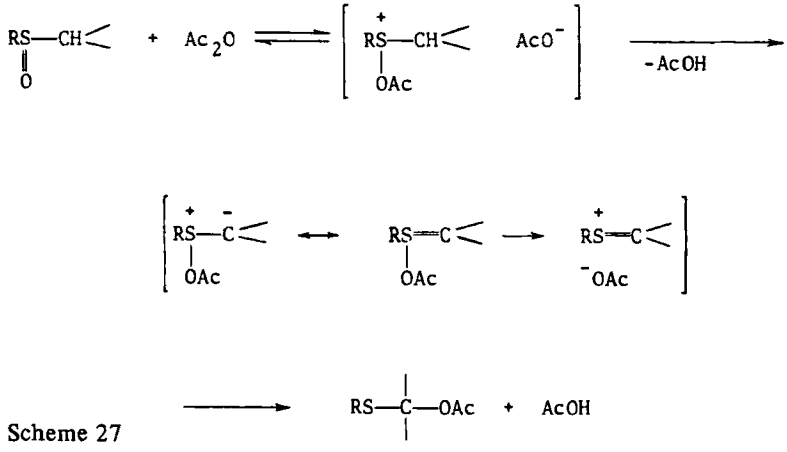
278, (ee up to 70%)

X=$N(CH_3)_2$, OEt, OPh

It is now commonly accepted that the Pummerer reaction consists of three main steps (Scheme 27), the formation of the acyloxysulfonium salt followed by the sulfonium ylide, which in the last step undergoes the rearrangement to give the final reaction products. The observation of substantial asymmetric induction in the Pummerer reaction strongly suggests that the migration of the acetoxy group from sulfur to carbon [1,2-shift] occurs to a large extent by an intramolecular process presumably via the five-membered cyclic transition state shown as 279. A more detailed discussion of the stereochemical and mechanistic aspects of the Pummerer reaction may be found in the article by Oae (298).

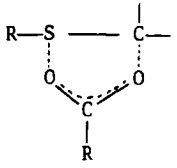
One of the most interesting reactions in sulfur chemistry is the reversible [2,3]sigmatropic rearrangement of allyl sulfoxides to the corresponding sulfenate esters, which are achiral at sulfur. However, in the case of suitably substituted allyl sulfoxides a new chiral center may be generated at the α-carbon in this process, as shown in eq. [137].

The fact that the sulfenate esters formed can be converted under



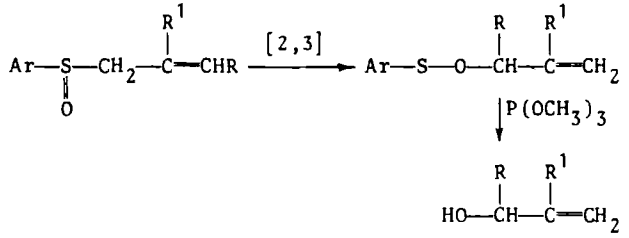
Scheme 27

mild conditions into the corresponding allyl alcohols by treatment with trimethyl phosphite or dimethylamine hydrochloride in methanol (304) has made it possible to exploit the [2,3]sigmatropic rearrangement of optically active allyl aryl sulfoxides for asymmetric

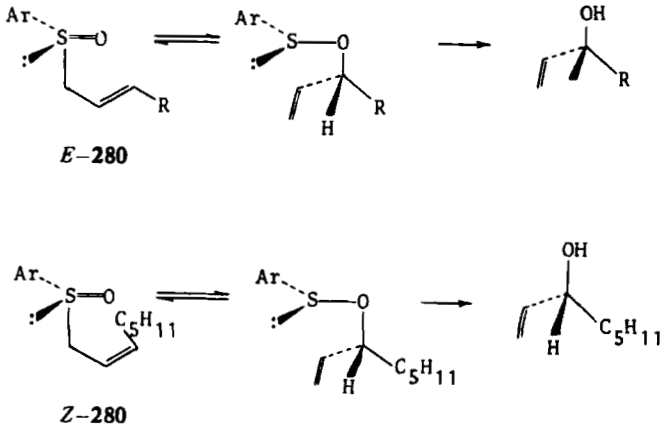


279

synthesis of optically active allyl alcohols. According to Hoffman et al. (305-307), who carried out extensive studies on the stereochemistry of this rearrangement, the enantioselectivity of the allyl sulfoxide to sulfenate conversion depends mainly on the geometry of the carbon-carbon double bond in acyclic allyl sulfoxides and on the steric requirements of the cyclic allyl system bonded to the sulfinyl



[137]

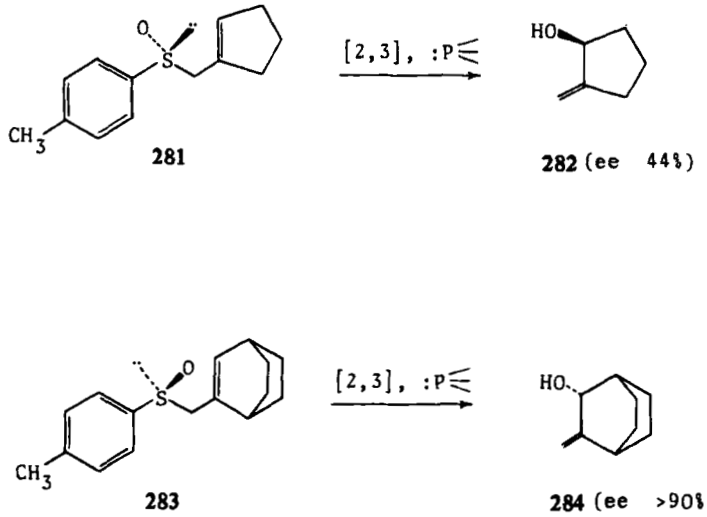


E–280

Z–280

Scheme 28

sulfur atom. For instance, the rearrangement of the 3-*E*-substituted allyl sulfoxides **280** proceeds with low enantioselectivity to allyl alcohols, whereas the rearrangement of the 3-*Z*-substituted allyl sulfoxides **280** leads to the corresponding alcohols of 42% optical purity (Scheme 28). On the other hand, in this way the cyclic five-membered allyl sulfoxide **281** gives allyl alcohol **282** of 44% optical purity while the optical purity of bicyclic alcohol **284** obtained from sulfoxide **282** exceeded 90% (Scheme 29).



281

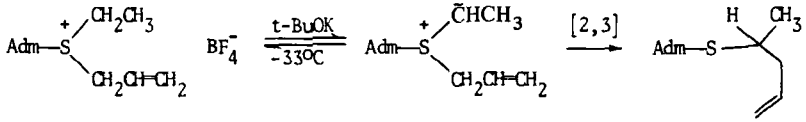
282 (ee 44%)

283

284 (ee >90%)

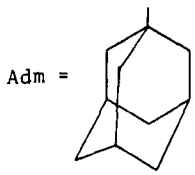
Scheme 29

A very high degree of asymmetric induction was observed by Trost and Hammen (154) in the [2,3]sigmatropic rearrangement of ylide 285 derived from optically active 1-adamantylallylethylsulfonium tetrafluoroborate 286. They found that the optically active 1-adamantyl-2-pent-4-enyl sulfide 287 formed in this process has at



[138]

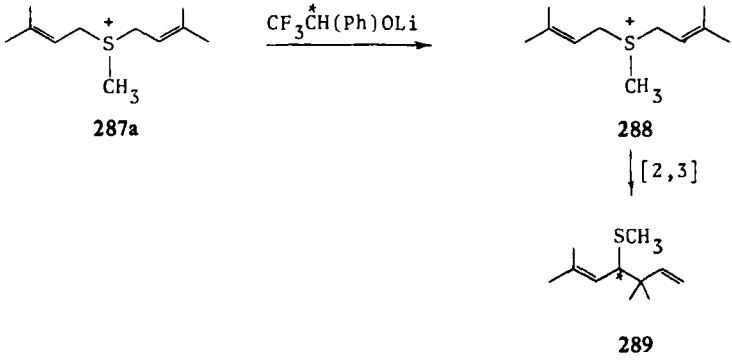
286 285 287, $[\alpha]_{365}$ -6.86°



least 94% optical purity. Such efficient asymmetric synthesis undoubtedly results from the concerted character of the rearrangement.

It is interesting to note that asymmetric induction was also observed (308) during generation of ylide 288 from achiral sulfonium salt 287a by means of chiral lithium 2,2,2-trifluoromethyl-α-phenylethoxide. The [2,3]sigmatropic rearrangement of the chiral ylide 288 obtained *in situ* in this way leads to optically active sulfide 289 of 5% optical purity.

The most numerous group of asymmetric syntheses includes reactions of chiral sulfur compounds leading to diastereomeric systems as a result of the generation of a new chiral center and the preserva-



[139]

287a 288 289

tion of chirality at sulfur. From the point of view of asymmetric synthesis it is interesting to remove the chirality at the sulfur atom in the next step. This may be accomplished in three different ways:

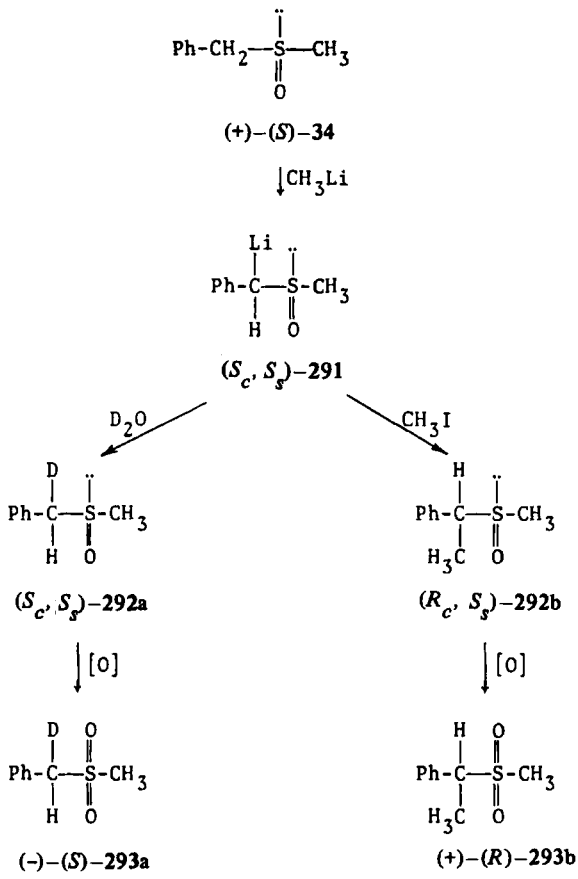
1. By oxidation of the chiral sulfur moiety to the sulfonyl grouping.
2. By reduction of the chiral sulfur moiety to dicoordinate sulfur derivatives.
3. By complete desulfuration.

Procedures 1 and 2 yield new organosulfur compounds whose chirality is due to the presence of the newly formed chiral carbon atom or heteroatom; procedure 3 affords optically active sulfur-free compounds. The third procedure is most attractive from the preparative point of view.

Durst and co-workers (309) investigated in detail the stereochemistry of deuteration and methylation of carbanions derived from optically active (+)-(*S*)-benzyl methyl sulfoxide **34** and (+)-(*R*)-benzyl *t*-butyl sulfoxide **290**. The reactions, which allowed the extent of asymmetric induction on the α-carbon atom as well as the stereochemistry of deuteration and methylation to be determined, are summarized in Schemes 30 and 31.

Since earlier investigations (310–312) have shown that deuteration of sulfinyl carbanions proceeds with retention of configuration at the α-carbon atom, the formation of α-deuterosulfones (–)-(*S*)-**293a** and (+)-(*R*)-**296a** proved that the diastereomeric lithium salts **291** and **294** have the configuration S_cS_s and R_cR_s respectively. This result also indicates that methylation of these salts proceeds with inversion of configuration at the α-carbon atom. The optical purities of the α-deuterosulfoxides **292a** and **295a** are unknown, whereas those of the α-methyl sulfones **293b** and **296b** are 81 and 99%, respectively. This points to the almost complete asymmetric induction at the α-carbon atom in the generation of sulfoxide carbanions.

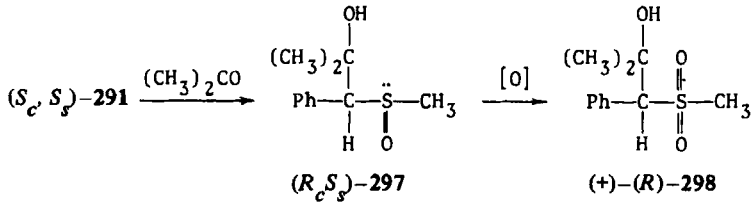
A highly efficient asymmetric induction was also observed in the addition of the lithium salt of (+)-(*S*)-**34** to acetone (313). The addition product **297** (optical purity ca. 80%) was then oxidized to the corresponding sulfone **298**, whose absolute configuration was established as *R* by means of chemical correlations. The formation of sulfone **298** with the absolute configuration *R* at carbon proves that, unlike methylation, the addition reaction takes place with retention of configuration. It is worthy of note that the optically active



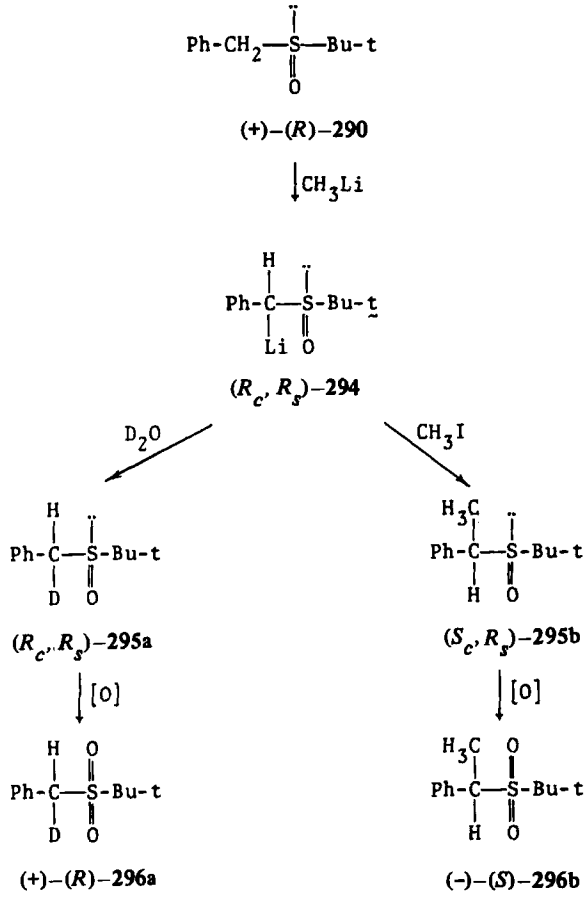
Scheme 30

β-hydroxysulfoxide **297** has been used for the synthesis of optically active epoxides.

Addition of the lithium salt **299** obtained from chiral methyl *p*-tolyl sulfoxide **41** to carbonyl and imino systems as well as to epoxides was thoroughly studied by Tsuchihashi and co-workers.

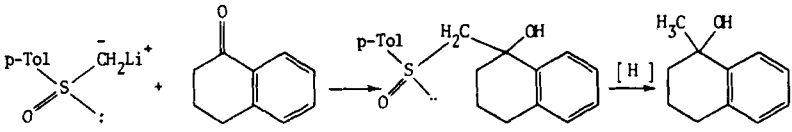


[140]



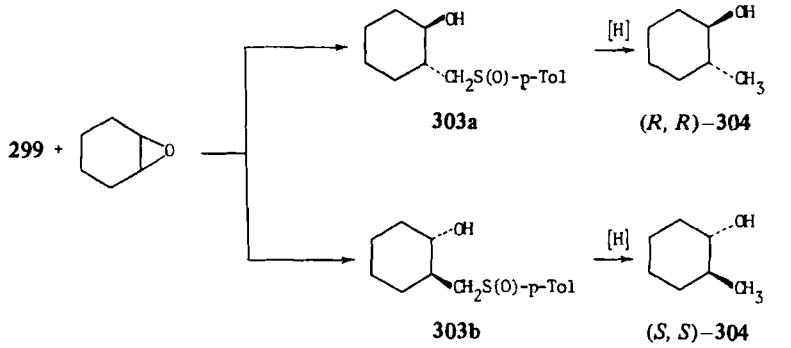
Scheme 31

Reaction of **299** with benzaldehyde was found to give an equimolar mixture of diastereomeric β-hydroxysulfoxides (314). Addition of **299** to α-tetralone **300** was more satisfactory, since the corresponding diastereomeric β-hydroxysulfoxides **301** were formed in a 1.8:1 ratio. Their subsequent desulfuration with Raney nickel yielded levorotatory 1-hydroxy-1-methyl-1,2,3,4-tetrahydronaphthalene **302** of unknown absolute configuration and optical purity. Similarly, addition of **299** to cyclohexene oxide leads to the formation of diastereomeric β-hydroxysulfoxides **303** in a 2:1 ratio which, after separation, may be desulfurized to give (*R*,*R*)- and (*S*,*S*)- *trans*-2-methylcyclohexanols **304**, respectively. Analysis of ^{1}H NMR spectra of the



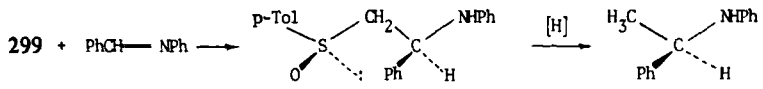
299 300 301 (-)-302 [141]

addition product of **299** to benzylideneaniline has shown that only one diastereomer of the β-amino sulfoxide **305** is formed (315). Since on reduction it gave (-)-(*R*)-*N*-phenyl-α-methylbenzylamine **306**, it follows that it has the (R_cS_s)-configuration.



303a (*R*, *R*)-**304**

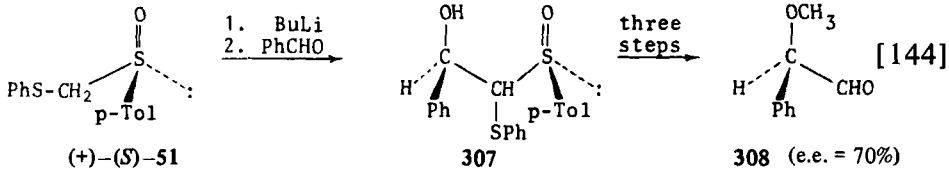
303b (*S*, *S*)-**304** [142]



(R_c, S_s)-**305** (-)-(*R*)-**306** [143]

Recently, much attention has been devoted to the use of carbanions derived from optically active α-substituted sulfoxides in asymmetric synthesis. Thus, the condensation of the lithium salt of the optically active dithioacetal mono-*S*-oxide **51** with benzaldehyde yields a mixture of diastereomeric adducts **307**, which were converted in high chemical yield into the corresponding optically active α-methoxyaldehyde **308**, having 70% optical purity (316).

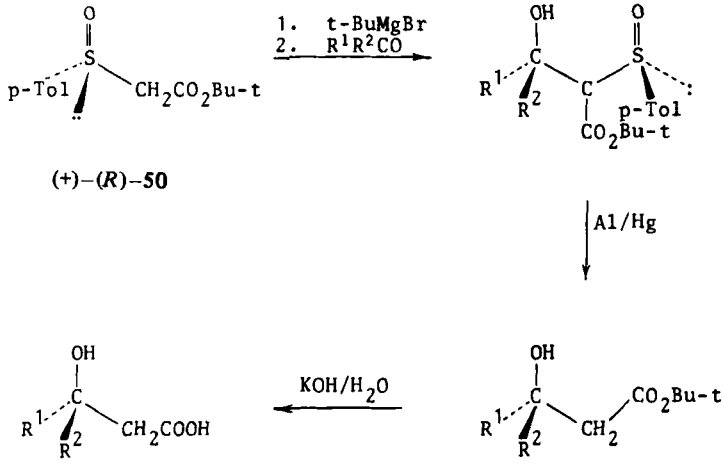
A closely related reaction of ketones and ketoesters with chiral *t*-butyl (+)-(*R*)-*p*-toluenesulfinylacetate **50** was utilized for the synthesis of chiral β-hydroxy acids as shown in Scheme 32 (317). The optical purities of the final reaction products varied from 8.5 to 91%.



[144]

(+)–(*S*)–51 307 308 (e.e. = 70%)

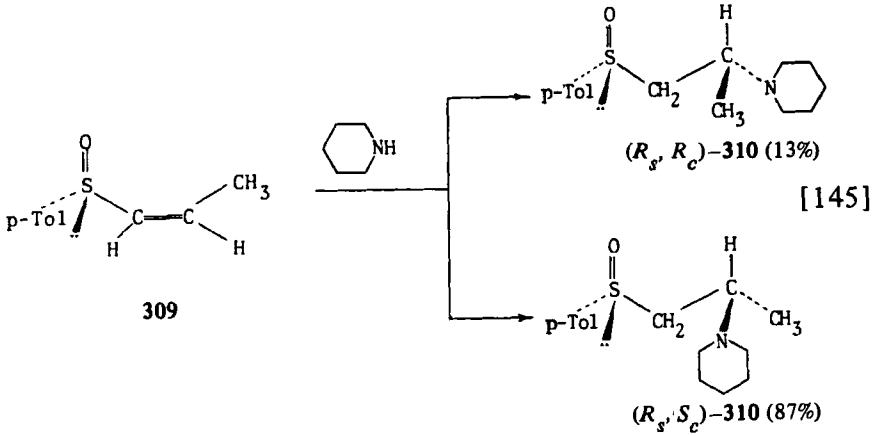
The addition reactions of nucleophilic and electrophilic reagents to optically active α,β-unsaturated sulfoxides have also been found to proceed in an asymmetric way. Addition of piperidine to chiral (*R*)-*cis*-propenyl *p*-tolyl sulfoxide **309** affords a 87:13 mixture of diastereomeric sulfoxides **310** (318). The configuration at the β-carbon atom of the predominant diastereomer (R_sS_c)-**310** was determined by means of chemical correlation starting from optically



Scheme 32

active alanine. The reaction of sodium diethyl malonate with (*R*)-*trans*-β-styryl *p*-tolyl sulfoxide **311** yields the diastereomeric sulfoxides **312** in an 8:2 ratio (319).

In the Michael addition reaction depicted in eq. [146] the diastereomeric sulfoxides **312** are formed under kinetic control conditions, therefore, the addition of sodium diethyl malonate is an irreversible process. On the contrary, addition of sodium methoxide to the sulfoxide **311** is a thermodynamically controlled process and leads to a mixture of diastereomeric β-methoxysulfoxides **313** in a 31:69 ratio (320).

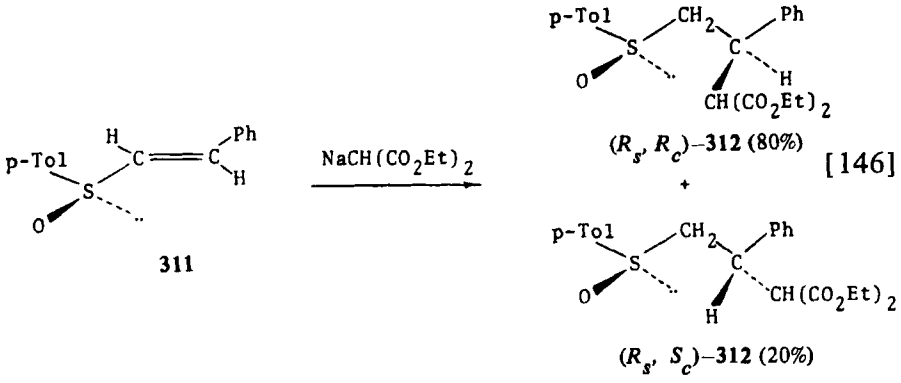


309

(R_s, R_c)–**310** (13%)

(R_s, S_c)–**310** (87%)

[145]



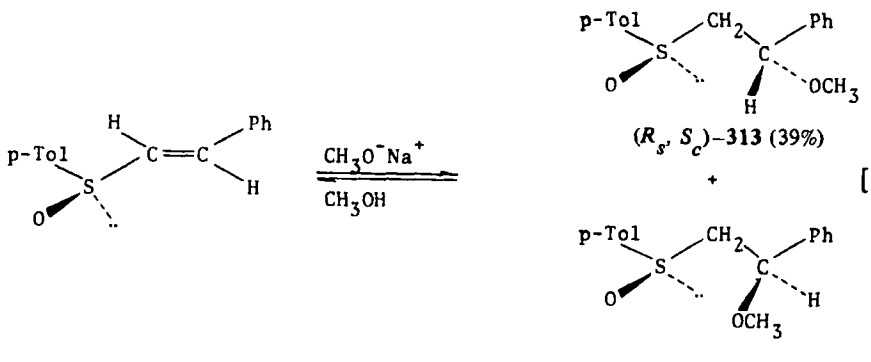
311

(R_s, R_c)–**312** (80%)

+

(R_s, S_c)–**312** (20%)

[146]



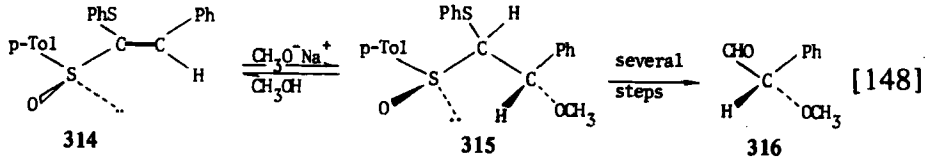
(R_s, S_c)–**313** (39%)

+

(R_s, S_c)–**313** (61%)

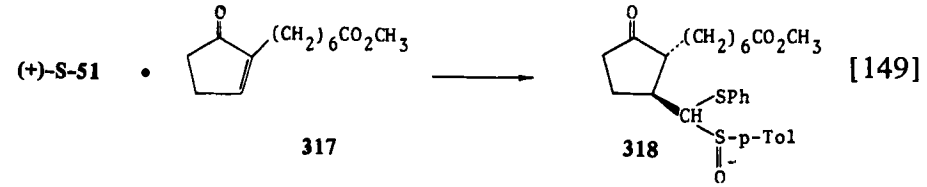
[147]

Quite recently, the addition of methoxy anion to the optically active styryl sulfoxide **314** was found to give a mixture of diastereomeric dithioacetal mono-*S*-oxides **315**, which were converted to the optically active α-methoxyaldehyde **316**, having 59.6% optical purity (316).



314 **315** **316** [148]

The Michael addition of (+)-(*S*)-**51** to the α,β-unsaturated ketone **217** constitutes a key step in the asymmetric synthesis of the optically active cyclopentanone **318**, which is precursor of the 11-deoxyprostaglandins (321).

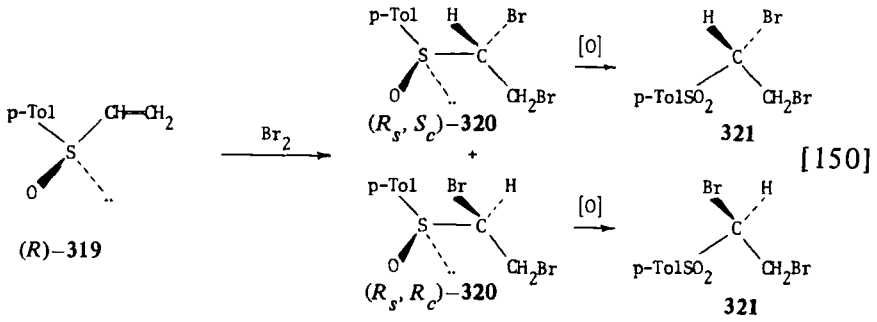


317 **318** [149]

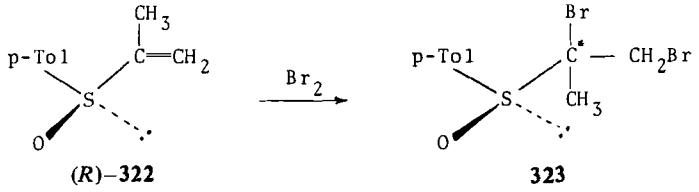
The addition of electrophilic reagents to chiral α,β-unsaturated sulfoxides is also accompanied by asymmetric induction. Stirling and Abbott (318,322) found that the addition of bromine to the optically active (*R*)-vinyl-*p*-tolyl sulfoxide **319** yields a mixture of diastereomeric α,β-dibromosulfoxides **320**. Oxidation of this mixture gives the optically active sulfone **321**, with a center of chirality at the α-carbon atom only. The optical purity (32%) of this sulfone was estimated by comparing its specific rotation with that obtained as a result of oxidation of diastereomerically pure sulfoxide (R_sS_c)-**320**. The assignment of configuration at the α-carbon atom was based on the analysis of the polarizabilities of substituents.

The reaction of bromine with the optically active (*R*)-α-methylvinyl *p*-total sulfoxide **322** also yields a mixture of diastereomeric sulfoxides **323**; their ratio, estimated by the NMR method, was 71.5:28.5.

A very high degree of asymmetric induction was observed in the addition of hypobromous acid and methyl hypobromite to the optically active styryl sulfoxide (*R*)-**311** (323). The ratio of diastereomeric β-hydroxy sulfoxides **324** formed in the first reaction was



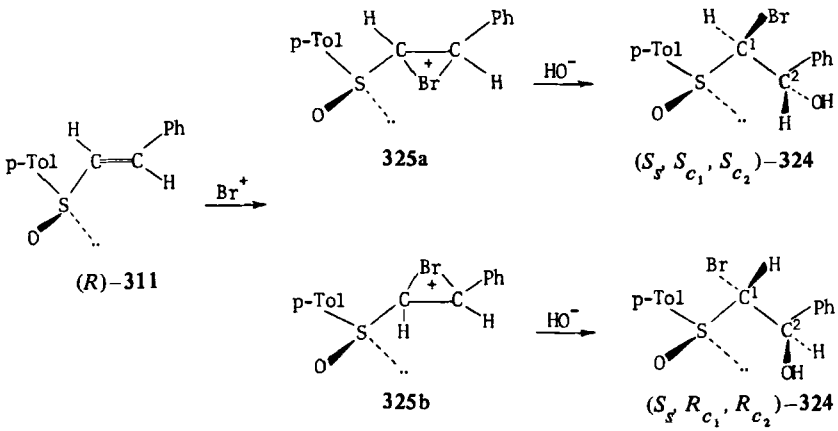
[150]



[150a]

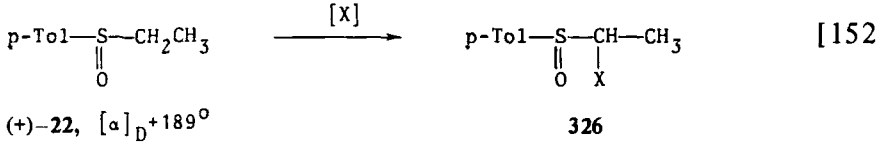
90:10, whereas the analogous diastereomeric β-methoxysulfoxides were obtained in the second reaction in a 95:5 ratio. Such almost complete asymmetric induction is due to the reaction mechanism involved. In the first step bromonium ion Br^+ attacks the carbon-carbon double bond to give a cyclic bromonium compound **325**, which subsequently reacts with a nucleophile ^-OH at the β-carbon, leading to the α-bromo-β-hydroxysulfoxide **324**. The formation of **325a** is strongly preferred over **325b** for steric reason.

Finally, we briefly mention the asymmetric induction that occurs in the α-halogenation of sulfoxides. The mechanism and stereochem-



[151]

istry of this reaction have been investigated in detail by Montanari and his group. Montanari and co-workers (324) were the first to show that the conversion of (+)-ethyl *p*-tolyl sulfoxide 22 into the corresponding α-halogeno derivatives 326 is accompanied by asymmetric induction at the α-carbon atom, since the sulfones 327 obtained from them were in all cases optically active. Some experimental results are shown in eqs. [152] and [153] to illustrate the relationship between the extent of asymmetric induction in

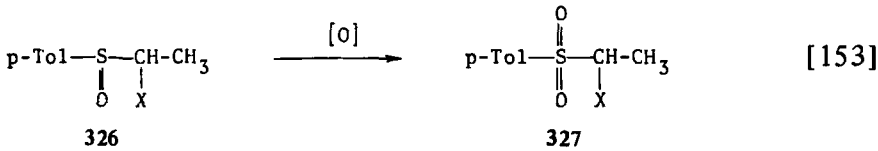


[152]

(+)-**22**, $[\alpha]_D$ +189°

326

X=PhICl$_2$ a, X=Cl, $[\alpha]_D$ -7°
X=PhICl$_2$+AgNO$_3$ a, X=Cl, $[\alpha]_D$ -153°
X=Br$_2$ b, X=Br, $[\alpha]_D$ -83°
X=Br$_2$+AgNO$_3$ b, X=Br, $[\alpha]_D$ -115°



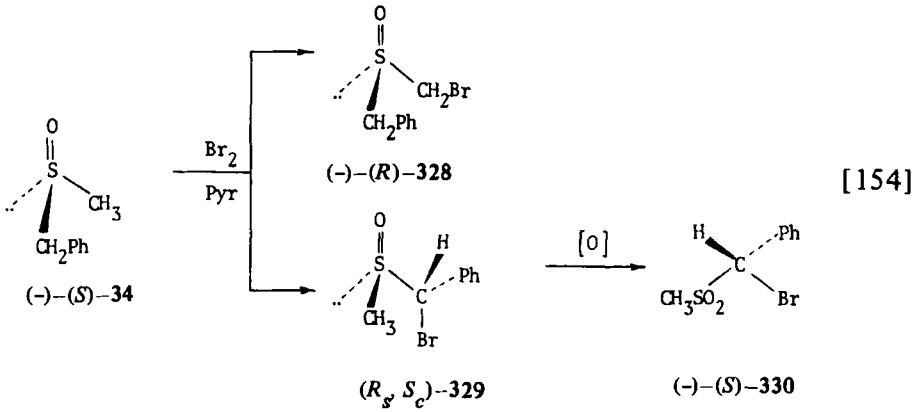
[153]

326 **327**

a, X=Cl, $[\alpha]_D$ -7° a, X=Cl, $[\alpha]_D$ -0.5°
a, X=Cl, $[\alpha]_D$ -153° a, X=Cl, $[\alpha]_D$ -6.9°
b, X=Br, $[\alpha]_D$ -115° b, X=Br, $[\alpha]_D$ -14.9°

α-halogenation and the nature of halogenating agent. It was demonstrated that chlorination of (+)-22 by $PhICl_2$ in the presence and absence of $AgNO_3$ leads to identical structures of 326a; differences in optical activity are due to the formation of different ratios of enantiomers, not to different ratios of diastereomers.

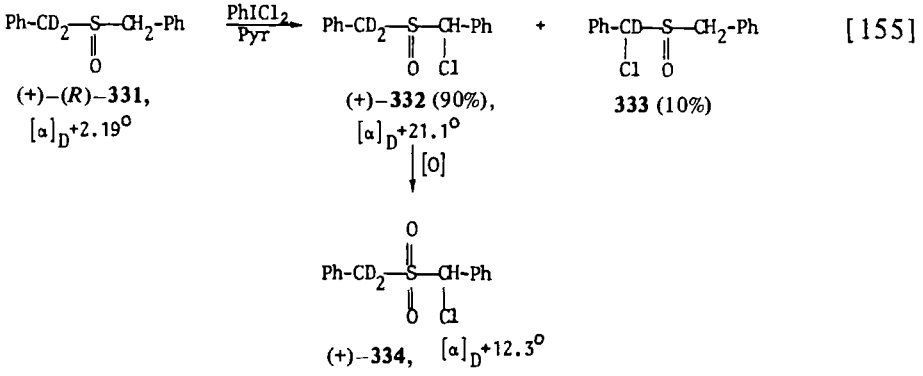
Bromination of (–)-(*S*)-benzyl methyl sulfoxide 34 with bromine in pyridine affords a mixture of two regioisomers: α-bromomethyl benzyl sulfoxide 328 and α-bromobenzyl methyl sulfoxide 329, in a molar ratio of 3:2 (325). Oxidation of the latter gives the corresponding sulfone (–)-(*S*)-330, the absolute configuration of which was determined by X-ray analysis. In this context, it is interesting to point out that the formation of the sulfoxide 328 is accompanied by retention at sulfur, whereas 329 is formed with inversion at sulfur.



[154]

A rare case of asymmetric induction caused by isotopic substitution was observed (326) when optically active (+)-(*R*)-α,α-dideuteriodibenzyl sulfoxide **331** was chlorinated with dichloroiodobenzene in pyridine, α,α-Dideuteriobenzyl α′-chlorobenzyl sulfoxide **332** was obtained as a major regioisomer with at least 78% isotopic purity. The high stereospecificity of the reaction is indicated by formation of essentially only one of the possible diastereomers. Oxidation of sulfoxide **332** affords the sulfone **334**, which has high optical rotation.

These and other examples of intramolecular asymmetric induction by the sulfinyl group have been discussed by Montanari in his review paper (9).



[155]

VI. FINAL REMARKS

We hope that this review of chiral sulfur compounds will be useful to chemists interested in various aspects of chemistry and stereochemistry. The facts and problems discussed provide numerous possibilities for the study of additional stereochemical phenomena at sulfur. As a consequence of the extent of recent research on the application of organosulfur compounds in synthesis, further developments in the field of sulfur stereochemistry and especially in the area of asymmetric synthesis may be expected. Looking to the future, it may be said that the static and dynamic stereochemistry of tetra- and pentacoordinate trigonal-bipyramidal sulfur compounds will be and should be the subject of further studies. Similarly, more investigations will be needed to clarify the complex nature of nucleophilic substitution at tri- and tetracoordinate sulfur. Finally, we note that this chapter was intended to be illustrative, not exhaustive; therefore, we apologize to the authors whose important work could not be included.

REFERENCES

1. Pope, W. J.; Peachey, S. J. *J. Chem. Soc.*, **1900**, *77*, 1072–1075.
2. Smiles, S. *J. Chem. Soc.*, **1900**, *77*, 1174–1179.
3. Challenger, F. "Aspects of the Organic Chemistry of Sulphur"; Butterworths: London, 1959.
4. Kjaer, A. *Pure Appl. Chem.* **1977**, *49*, 137–152.
5. Andersen, K. K. *Int. J. Sulfur Chem. B*, **1971**, *6*, 69–76
6. Sorensen, O. N. *Int. J. Sulfur Chem. B*, **1971**, *6*, 321–344.
7. Laur, P. H. In "Sulfur in Organic and Inorganic Chemistry," Vol. 3, Chapter 24, Senning, A., Ed.; Dekker: New York, 1972.
8. Cram, D. J.; Day, J.; Garwood, D. C.; Rayner, D. R.; von Schriltz, D. M.; Williams, T. R.; Nudelman, A.; Yamagishi, F. G.; Booms, R. E.; Jones, M. R. *Int. J. Sulfur Chem. C*, **1972**, *7*, 103–109.
9. Montanari, F. In "Organic Sulphur Chemistry," Stirling, C. J. M., Ed.; Butterworths: London, 1975; pp. 181–202.
10. Tillett, J. G. *Chem. Rev.*, **1976**, *76*, 747–772.
11. Whistler, R. L.; De, K. K. J. *Carbohydrates Nucleosides Nucleotides*, **1979**, *6*, 199–237.
12. Wenschuh, E., Dolling, K.; Mikołajczyk, M.; Drabowicz, J. *Z. Chem.* **1980**, *20*, 122–132.
13. Johnson, C. R.; Sharp, J. C. *Rep. Sulfur Chem.*, **1969**, *4*, 1–32.
14. Nudelman, A. *Int. J. Sulfur Chem. B*, **1971**, *6*, 1–39.

15. Nudelman, A. *Int. J. Sulfur Chem. B*, **1972**, *7*, 241-267.
16. Nudelman, A. *Phosphorus Sulfur*, **1976**, *2*, 51-94.
17. Raban, M.; Yamamoto, G. *J. Am. Chem. Soc.*, **1979**, *101*, 5890-5895, and references cited therein.
18. Flynn, E. H. "Cephalosporins and Penicillins, Chemistry and Biology"; Academic Press: New York, 1972.
19. Barton, D. H. R. *Pure Appl. Chem.*, **1973**, *33*, 1-15.
20. Harrison, P. W. B.; Kenyon, J.; Phillips, H. *J. Chem. Soc.*, **1926**, 2079-2090.
21. Piechulek, W.; Suszko, J. *Rocz. Chem.*, **1933**, *13*, 520-529. Janczewski, M.; Suszko, J. *ibid.*, **1952**, *26*, 394-406.
22. Janczewski, M.; Maziarczyk, H. *Rocz. Chem.*, **1977**, *51*, 891-906, and earlier references.
23. Kiełczewski, M. *Bull. Acad. Pol. Sci., Ser. Chem.*, **1966**, *14*, 813-818.
24. Bohman, O.; Allenmark, S. *Ark. Kemi*, **1969**, *31*, 299-303.
25. Huszthy, P.; Kapovits, I.; Kucsman, A.; Radic, L. *Tetrahedron Lett.*, **1978**, 1853-1856. Kapovits, I., private communication, 1980.
26. Mikołajczyk, M.; Midura, W.; Grzejszczak, S.; Zatorski, A.; Chefczynska, A. *J. Org. Chem.*, **1978**, *43*, 473-478.
27. Holmberg, B. *Ark. Kemi, Min. Geol.*, **1939**, *13A*(1).
28. Wagner, G.; Boehme, S. *Z. Chem.*, **1962**, *2*, 278-279. Wagner, G.; Boehme, S. *Arch. Pharm.*, **1964**, *297*, 257-267.
29. Bryan, R. F.; Carey, F. A.; Dailey, O. D., Jr.; Maher, R. J.; Miller, R. W. *J. Org. Chem.*, **1978**, *43*, 90-96.
30. Backer, H. J.; Keuning, K. J. *Rec. Trav. Chim. Pays-Bas*, **1934**, *53*, 798-807.
31. Cope, A. C.; Caress, E. A. *J. Am. Chem. Soc.*, **1966**, *88*, 1711-1713.
32. Farina, G.; Montanari, F.; Negrini, A. *Gazz. Chim. Ital.*, **1959**, *89*, 1548-1563.
33. Wudl, F. *Diss. Abstr.*, **1968**, *28*, 3363B.
34. Pirkle, W. H.; House, D. W. *J. Org. Chem.*, **1979**, *44*, 1957-1960.
35. Mikołajczyk, M.; Drabowicz, J. *J. Am. Chem. Soc.*, **1978**, *100*, 2510-2515. Mikołajczyk, M.; Drabowicz, J.; Cramer, F. *J. Chem. Soc.D*, **1971**, 317-318.
36. Mayr, A.; Montanari, F.; Tramontini, M. *Gazz. Chim. Ital.*, **1960**, *90*, 739-749. Maccioni, A.; Montanari, F.; Secci, M.; Tramontini, M. *Tetrahedron Lett.*, **1961**, 607-611.
37. Balenovic, K.; Bregant, N.; Francetic, D. *Tetrahedron Lett.*, **1960** (6), 20-22. Balenovic, K.; Bregovec, I.; Francetic, D.; Monkovic, I.; Tomasic, V. *Chem. Ind. (London)*, **1961**, 469-470.
38. Morrison, J. D.; Mosher, H. S. "Asymmetric Organic Reactions"; Prentice-Hall: Englewood Cliffs, NJ, 1971.
39. Folli, U.; Iarossi, D.; Montanari, F.; Torre, G. *J. Chem. Soc., C* **1968**, 1317-1322.
40. Cram, D. J.; Abd Elhafez, F. A. *J. Am. Chem. Soc.*, **1952**, *74*, 5828-5835.

41. Mislow, K.; Green, M.; Raban, M. *J. Am. Chem. Soc.*, **1965**, *87*, 2761–2762.
42. Dodson, R. M.; Newman, N.; Tsuchiya, H. M. *J. Org. Chem.*, **1962**, *27*, 2707–2708.
43. Holmlund, C. E.; Sax, K. J.; Nielsen, B. E.; Hartman, R. E.; Evans, R. H., Jr.; Blank, R. H. *J. Org. Chem.*, **1962**, *27*, 1468–1470.
44. Auret, B. J.; Boyd, D. R.; Henbest, H. B.; Ross, S. *J. Chem. Soc., C*, **1968**, 2371–2374.
45. Abushanab, E.; Reed, D.; Suzuki, F.; Sih, C. J. *Tetrahedron Lett.*, **1978**, 3415–3418.
46. Cram, D. J.; Pine, S. H. *J. Am. Chem. Soc.*, **1963**, *85*, 1096–1100.
47. Mislow, K.; Green, M. M.; Laur, P.; Melillo, J. P.; Simmons, T.; Ternay, A. L., Jr.; *J. Am. Chem. Soc.*, **1965**, *87*, 1958–1976.
48. Nishihata, K.; Nishio, M. *J. Chem. Soc., Perkin Trans. II*, **1973**, 758–762.
49. Christensen, B. W.; Kjaer, A. *J. Chem. Soc., Chem. Commun.*, **1965**, 225–226.
50. Bordignon, E.; Cattalini, L.; Natile, G.; Scatturin, A. *J. Chem. Soc., Chem. Commun.*, **1973**, 878–879.
51. Lavielle, S.; Bory, S.; Moreau, B.; Luche, M. J.; Marquet, A. *J. Am. Chem. Soc.*, **1978**, *100*, 1558–1563.
52. Barbieri, G.; Davoli, V.; Moretti, I.; Montanari, F.; Torre, G. *J. Chem. Soc., C*, **1969**, 731–735.
53. Higuchi, T.; Pitman, I. H.; Gensch, K. H. *J. Am. Chem. Soc.*, **1966**, *88*, 5676–5677.
54. Sugimoto, T.; Kokubo, T.; Miyazaki, J.; Tanimoto, S.; Okano, M. *J. Chem. Soc., Chem. Commun.*, **1979**, 402–403.
55. Ogura, K.; Fujita, M.; Iida, H. *Tetrahedron Lett.*, **1980**, 2233–2236.
56. Firth, B. E.; Miller, L. L.; Mitani, M. M.; Rogers, T.; Lennox, J.; Murray, R. W. *J. Am. Chem. Soc.*, **1976**, *98*, 8271–8272. Firth, B. E.; Miller, L. L. *ibid.*, **1976**, *98*, 8272–8273.
57. Di Furia, F.; Modena, G.; Curci, R. *Tetrahedron Lett.*, **1976**, 4637–4638.
58. Johnson, C. R.; Bacon, C. C.; Kingsbury, W. D. *Tetrahedron Lett.*, **1972**, 501–504.
59. Moriyama, M.; Oae, S.; Numata, T.; Furukawa, N. *Chem. Ind. (London)*, **1976**, 163–164.
60. Kinoshita, M.; Sato, Y.; Kunieda, N. *Chem. Lett.*, **1974**, 377–380.
61. Sato, Y.; Kunieda, N.; Kinoshita, M. *Chem. Lett.*, **1976**, 563–566.
62. Kobayashi, M.; Yobe, A. *Bull. Chem. Soc. Jpn.*, **1967**, *40*, 224–225.
63. Folli, U.; Iarossi, D; Montanari, F. *J. Chem. Soc., C*, **1968**, 1372–1374.
64. Auret, B. J.; Boyd, D. H.; Henbest, H. B. *J. Chem. Soc. C*, **1968**, 2374–2376.
65. Balenovic, K.; Bregant, N. *Chem. Ind. (London)*, **1964**, 1577–1578.
66. Mikołajczyk, M.; Para, M. *J. Chem. Soc., Chem. Commun.*, **1969**, 1192–1193.
67. Mikołajczyk, M.; Leitloff, M. *Usp. Khim.*, **1975**, *44*, 1419–1453; *Russ. Chem. Rev. Engl. transl.*, **1975**, *44*, 670–698.

68. Juge, S.; Kagan, H. B. *Tetrahedron Lett.*, **1975**, 2733–2736.
69. Marchese, G.; Naso, F.; Ronzini, L. *J. Chem. Soc., Chem. Commun.*, **1974**, 830–831.
70. Kunieda, N.; Motoki, H.; Kinoshita, M. *Chem. Lett.*, **1978**, 713–716.
71. Kunieda, N.; Nokami, J.; Kinoshita, M. *Bull. Chem. Soc. Jpn.*, **1976**, *49*, 256–259.
72. Kagan, H. B.; Balavoine, G.; Maradpour, A. *J. Mol. Evol.*, **1974**, *4*, 41–48.
73. Pirkle, W. H.; Rinaldi, P. L. *J. Am. Chem. Soc.*, **1977**, *99*, 3510–3511.
74. Eskenazi, C.; Nicoud, J. F.; Kagan, H. B. *J. Org. Chem.*, **1979**, *44*, 995–999.
75. Andersen, K. K. *Tetrahedron Lett.*, **1962**, 93–95.
76. Andersen, K. K. *J. Org. Chem.*, **1964**, *29*, 1953–1956. Andersen, K. K.; Gaffield, W.; Papanikolaou, N. E.; Foley, J. W.; Perkins, R. I. *J. Am. Chem. Soc.*, **1964**, *86*, 5637–5646.
77. Stirling, C. J. M. *J. Chem. Soc.*, **1963**, 5741–5745.
78. Oae, S.; Khim, Y. H. *Bull. Chem. Soc. Jpn.*, **1967**, *40*, 1716–1719.
79. Axelrod, M.; Bickart, P.; Jacobus, J.; Green, M. M.; Mislow, K. *J. Am. Chem. Soc.*, **1968**, *90*, 4835–4842.
80. Hope, H.; de la Camp, U.; Homer, G. D.; Messing, A. W.; Sommer, L. H. *Angew. Chem.*, **1969**, *81*, 619; *Angew. Chem. Int. Ed. Engl.*, **1969**, *8*, 612–613.
81. de la Camp, U.; Hope, H. *Acta Crystallogr., Sect. B.*, **1970**, *26*, 846–853.
82. Jacobus, J.; Mislow, K. *J. Am. Chem. Soc.*, **1967**, *89*, 5228–5234.
83. Colonna, S.; Giovini, R.; Montanari, F. *Chem. Commun.*, **1968**, 865–866.
84. Harpp, D. N.; Vines, S. M.; Montillier, J. P.; Chan, T. H. *J. Org. Chem.*, **1976**, *41*, 3987–3992.
85. Jacobus, J.; Mislow, K. *Chem. Commun.*, **1968**, 253–254.
86. Pirkle, W. H.; Beare, S. D. *J. Am. Chem. Soc.*, **1968**, *90*, 6250–6251.
87. Andersen, K. K.; Colonna, S.; Stirling, C. J. M. *J. Chem. Soc., Chem. Commun.*, **1973**, 645–646.
88. Mikołajczyk, M.; Zatorski, A.; Grzejszczak, S.; Costisella, B.; Midura, W.; *J. Org. Chem.*, **1978**, *43*, 2518–2521.
89. Mioskowski, C.; Solladie, G. *Tetrahedron Lett.*, **1975**, 3341–3342.
90. Colombo, L.; Gennari, C.; Narisano, E. *Tetrahedron Lett.*, **1978**, 3861–3862.
91. Nieuwenhuyse, H.; Louw, R. *J. Chem. Soc., Perkin Trans. I*, **1973**, 839–841.
92. Maryanoff, C. A.; Maryanoff, B. E.; Tang, R.; Mislow, K. *J. Am. Chem. Soc.*, **1973**, *95*, 5839–5840.
93. Lockard, J. P.; Schroeck, C. W.; Johnson, C. R. *Synthesis*, **1973**, 485–486.
94. Nokami, J.; Kunieda, N.; Kinoshita, M. *Chem. Lett.*, **1977**, 249–252.
95. Andersen, K. K.; O'Brien, J. B., unpublished results quoted in Ph.D. thesis of O'Brien, 1968. Mikołajczyk, M.; Drabowicz, J. unpublished results quoted in Ph.D. thesis of Drabowicz, 1974.
96. Wudl, F.; Lee, T. B. K. *J. Chem. Soc., Chem. Commun.*, **1972**, 61–62.
97. Wudl, F.; Lee, T. B. K. *J. Am. Chem. Soc.*, **1973**, *95*, 6349–6358.

98. Cram, D. J.; Day, J.; Rayner, D. R.; von Schriltz, D. M.; Duchamp, D. J.; Garwood, D. C. *J. Am. Chem. Soc.*, **1970**, *92*, 7369–7384.
99. Oae, S.; Tsuchida, Y.; Furukawa, N. *Bull. Chem. Soc. Jpn.*, **1973**, *46*, 648–649.
100. Phillips, H. *J. Chem. Soc.*, **1925**, *127*, 2552–2587.
101. Estep, R. E.; Tavares, D. J. *Int. J. Sulfur Chem.*, **1973**, *8*, 279–280.
102. Harpp, D. N.; Friedlander, B. T.; Larsen, C.; Steliou, K.; Stockton, A. *J. Org. Chem.*, **1978**, *43*, 3481–3485.
103. Herbrandson, H. F.; Cusano, C. M. *J. Am. Chem. Soc.*, **1961**, *83*, 2124–2128.
104. Darwish, D.; McLaren, R. A. Abstracts, 14th National Meeting of the American Chemical Society, Chicago; September 1964; p. 445.
105. Sagramora, L.; Koch, P.; Garbesi, A.; Fava, A. *J. Chem. Soc., Chem. Commun.*, **1967**, 985–986.
106. Mikołajczyk, M.; Drabowicz, J. *Tetrahedron Lett.*, **1972**, 2379–2382.
107. Mikołajczyk, M.; Drabowicz, J. *J. Chem. Soc., Chem. Commun.*, **1974**, 547–548.
108. Pirkle, W. H.; Hoekstra, M. S. *J. Am. Chem. Soc.*, **1976**, *98*, 1832–1839.
109. Mikołajczyk, M.; Drabowicz, J.; Bujnicki, B. *J. Chem. Soc., Chem. Commun.*, **1976**, 568–569.
110. Mikołajczyk, M.; Bujnicki, B., Drabowicz, J. *Bull. Acad. Pol. Sci., Ser. Chem.*, **1977**, *25*, 267–269.
111. Savige, W. E., Eager, J.; Maclaren, J. A.; Roxburgh, C. M. *Tetrahedron Lett.*, **1964**, 3289–3293.
112. Kice, J. L.; Large, G. B. *Tetrahedron Lett.*, **1965**, 3537–3541.
113. Block, E.; O'Connor, J. *J. Am. Chem. Soc.*, **1974**, *96*, 3921–3929; *ibid.*, **1974**, *96*, 3929–3944.
114. Mikołajczyk, M.; Drabowicz, J. *J. Chem. Soc., Chem. Commun.*, **1976**, 220–221.
115. Kishi, M.; Ishihara, S.; Komeno, T. *Tetrahedron*, **1974**, *30*, 2135–2142.
116. Nudelman, A.; Cram, D. J. *J. Am. Chem. Soc.*, **1968**, *90*, 3869–3870.
117. Schroeck, C. W.; Johnson, C. R. *J. Am. Chem. Soc.*, **1971**, *93*, 5305–5306.
118. Johnson, C. R.; Schroeck, C. W. *J. Am. Chem. Soc.*, **1973**, *95*, 7418–7423.
119. Williams, T. R.; Booms, R. E.; Cram, D. J. *J. Am. Chem. Soc.*, **1971**, *93*, 7338–7340.
120. Cinquini, M.; Cozzi, F. *J. Chem. Soc., Chem. Commun.*, **1977**, 502–503.
121. Cinquini, M.; Cozzi, F. *J. Chem. Soc., Chem. Commun.*, **1977**, 723–724.
122. King, J. F.; Beatson, R. P. *J. Chem. Soc. D*, **1970**, 663–664.
123. Canalini, G.; Maccagnani, G.; Taddei, F. *Tetrahedron Lett.*, **1971**, 3035–3036.
124. Mikołajczyk, M.; Drabowicz, J. *Z. Naturforsch.*, **1971**, *26b*, 1372–1374.
125. Gupta, R. P.; Pizey, J. S.; Symeonides, K. *Tetrahedron*, **1976**, *32*, 1917–1920.
126. Kukolja, S.; Lammert, S. R. *Angew. Chem.*, **1973**, *85*, 40–41; *Angew. Chem., Int. Ed. Engl.*, **1973**, *12*, 67–68. Kukolja, S.; Lammert, S. R.; Gleissner, M. R. B.; Ellis, A. I. *J. Am. Chem. Soc.*, **1976**, *98*, 5040–5041.

127. Clarke, S. G.; Kenyon, J.; Phillips, H. *J. Chem. Soc.*, **1927**, 188–194.
128. Holloway, J.; Kenyon, J.; Phillips, H. *J. Chem. Soc.*, **1928**, 3000–3006.
129. Kresze, G.; Wustrow, B. *Chem. Ber.*, **1962**, *95*, 2652–2659.
130. Day, J.; Cram, D. J. *J. Am. Chem. Soc.*, **1965**, *87*, 4398–4399.
131. Rayner, D. R.; von Schriltz, D. M.; Day, J.; Cram, D. J. *J. Am. Chem. Soc.*, **1968**, *90*, 2721–2723.
132. Garwood, D. C.; Cram, D. J. *J. Am. Chem. Soc.*, **1970**, *92*, 4575–4583.
133. Yamagishi, F. G.; Rayner, D. R.; Zwicker, E. T.; Cram, D. J. *J. Am. Chem. Soc.*, **1973**, *95*, 1916–1925.
134. Christensen, B. W.; Kjaer. A. *J. Chem. Soc., Chem. Commun.*, **1969**, 934–935.
135. Christensen, B. W. *J. Chem. Soc., Chem. Commun.*, **1971**, 597–598.
136. Maricich, T. J.; Hoffman, V. L. *J. Am. Chem. Soc.*, **1974**, *96*, 7770–7781; Maricich, T. J.; Hoffman, V. L. *Tetrahedron Lett.*, **1972**, 5309–5312.
137. Nudelman, A. *Diss. Abstr.*, **1969**, *29*, 1049B; *Chem. Abstr.*, **1970**, *72*, 131905h.
138. Moriyama, M.; Yoshimura, T.; Furukawa, N.; Numata, T.; Oae, S. *Tetrahedron*, **1976**, *32*, 3003–3013.
139. Guanti, G.; Dell'Erba, C.; Gaiani, G. *Phosphorus Sulfur*, **1976**, *1*, 179–180.
140. Williams, T. R.; Nudelman, A.; Booms, R. E.; Cram, D. J. *J. Am. Chem. Soc.*, **1972**, *94*, 4684–4691.
141. Herzig, P. T.; Ehrenstein, M. *J. Org. Chem.*, **1952**, *17*, 724–736.
142. De la Mare, P. B. D.; Klyne, W.; Millen, D. J.; Pritchard, J. G.; Watson, D. *J. Chem. Soc.*, **1956**, 1813–1817.
143. Coxon, J. M.; Dansted, E.; Hartshorn, M. P.; Richards, K. E. *Tetrahedron*, **1968**, *24*, 1193–1197.
144. Coxon, J. M.; Hartshorn, M. P.; Lewis, A. J. *Aust. J. Chem.*, **1971**, *24*, 1009–1112.
145. Rowland, A. T.; Altland, H. W.; Creasy, W. S.; Dyott, T. M. *Tetrahedron Lett.*, **1970**, 4409–4412.
146. Rowland, A. T.; Adams, T. B.; Altland, H. W.; Creasy, W. S.; Dressner, S. A.; Dyott, T. M. *Tetrahedron Lett.*, **1970**, 4405–4409.
147. Hargreaves, M. K.; Modi, P. G.; Pritchard, J. G. *Chem. Commun.*, **1968**, 1306–1307.
148. Reid, T. W.; Fahrney, D. *J. Am. Chem. Soc.*, **1967**, *89*, 3941–3943.
149. Mikołajczyk, M.; Drabowicz, J. *Int. J. Sulfur Chem.*, **1973**, *8*, 349–357.
150. Mikołajczyk, M.; Drabowicz, J. *J. Chem. Soc., Chem. Commun.*, **1974**, 775–776.
151. Darwish, D; Tourigny, G. *J. Am. Chem. Soc.*, **1966**, *88*, 4303–4304.
152. Darwish, D.; Hui, S. H.; Tomilson, R. *J. Am. Chem. Soc.*, **168**, *90*, 5631–5632.
153. Scartazzini, R.; Mislow, K. *Tetrahedron Lett.*, **1967**, 2719–2722.
154. Trost, B. M.; Hammen, R. F. *J. Am. Chem. Soc.*, **1973**, *95*, 962–964.
155. Garbesi, A.; Corsi, N.; Fava, A. *Helv. Chim. Acta*, **1970**, *53*, 1499–1502.

156. Field, G. F.; Zally, W. J.; Sternbach, L. H. *J. Am. Chem. Soc.*, **1970**, *92*, 3520–3521.
157. Tsumori, K.; Minato, H.; Kobayashi, M. *Bull. Chem. Soc. Jpn.*, **1973**, *46*, 3503–3507.
158. Andersen, K. K. *J. Chem. Soc. D*, **1971**, 1051.
159. Andersen, K. K.; Caret, R. L.; Ladd, D. L. *J. Org. Chem.* **1976**, *41*, 3096–3100.
160. Kelstrup, E.; Kjaer, A.; Abrahamsson, S.; Dahlen, B. *J. Chem. Soc., Chem. Commun.* **1975**, 629–630.
161. Johnson, C. R; McCants, D., Jr., *J. Am. Chem. Soc.* **1965**, *87*, 5404–5409.
162. Mikołajczyk, M.; Drabowicz, J.; Bujnicki, B., unpublished results.
163. Okuma, K.; Minato, H.; Kobayashi, M. *Bull. Chem. Soc. Jpn.*, **1980**, *53*, 435–437.
164. Bohman, O.; Allenmark, S. *Chem. Scr.* **1973**, *4*, 202–206.
165. Drabowicz, J.; Bujnicki, B.; Mikołajczyk, M. *J. Org. Chem.*, **1981**, *46*, 2788–2790.
166. Darwish, D.; Tomilson, R. L. *J. Am. Chem. Soc.*, **1968**, *90*, 5938–5939.
167. Campbell, S. J.; Darwish, D. *Can. J. Chem.*, **1974**, *52*, 2953–2959.
168. Senkler, G. H., Jr.; Maryanoff, B. E.; Stackhouse, J.; Andose, J. D; Mislow, K. In "Organic Sulphur Chemistry," Stirling, C. J. M., Ed.; Butterworths: London, 1975; pp. 157–179.
169. Maryanoff, B. E.; Stackhouse, J.; Senkler, G. H., Jr.; Mislow, K. *J. Am. Chem. Soc.*, **1975**, *97*, 2718–2742.
170. Maryanoff, C. A.; Hayes, K. S.; Mislow, K. *J. Am. Chem. Soc.*, **1977**, *99*, 4412–4417.
171. Kobayashi, M.; Kamiyama, K.; Minato, H.; Oishi, Y.; Takada, Y.; Hattori, Y. *J. Chem. Soc. D*, **1971**, 1577–1578.
172. Kamiyama, K.; Minato, H.; Kobayashi, M. *Bull. Chem. Soc. Jpn.*, **1973**, *46*, 3895–3896.
173. Kobayashi, M., lecture delivered at the IX International Symposium on Organic Sulphur Chemistry, Riga, USSR, 1980.
174. Sabol, M. A.; Andersen, K. K. *J. Am. Chem. Soc.*, **1969**, *91*, 3603–3605.
175. Annunziata, R.; Cinquini, M.; Colonna, S. *J. Chem. Soc., Perkin Trans. I*, **1972**, 2057–2059.
176. Barash, M. *Nature (London)*, **1960**, *187*, 591.
177. Fusco, R.; Tenconi, A. *Chim. Ind. (Milan)*, **1965**, *47*, 61–63; *Chem. Abstr.* **1965**, *62*, 10357h.
178. Sabol, M. A.; Davenport, R. W.; Andersen, K. K. *Tetrahedron Lett.*, **1968**, 2159–2160.
179. Colonna, S.; Stirling, C. J. M. *J. Chem. Soc., Perkin Trans. I*, **1974**, 2120–2122.
180. Johnson, C. R.; Kirchhoff, R. A.; Corkins, H. G. *J. Org. Chem.*, **1974**, *39*, 2458–2459.
181. Akasaka, T.; Yoshimura, T.; Furukawa, N.; Oae, S. *Chem. Lett.*, **1978**. 417–418.
182. Williams, T. R.; Cram, D. J. *J. Am. Chem. Soc.*, **1971**, *93*, 7333–7335.

183. Williams, T. R.; Cram, D. J. *J. Org. Chem.*, **1973**, *38*, 20-26.
184. Johnson, C. R. *Acc. Chem. Res.*, **1973**, *6*, 341-347.
185. Jonsson, E. U.; Johnson, C. R. *J. Am. Chem. Soc.*, **1971**, *93*, 5308-5309.
186. Jones, M. R.; Cram, D. J. *J. Am. Chem. Soc.*, **1974**, *96*, 2183-2190.
187. Levchenko, E. S.; Kozlov, E. S. *J. Gen. Chem. USSR*, **1963**, *33*, 3551-3554; *Chem. Abstr.*, **1964**, *60*, 7946h.
188. Christensen, B. W.; Kjaer, A. *J. Chem. Soc., Chem. Commun.*, **1975**, 784.
189. Holms, R. R. *Acc. Chem. Res.*, **1979**, *12*, 257-265.
190. Martin, J. C.; Perrozzi, E. F. *Science*, **1976**, *191*, 154-159.
191. Martin, J. C. In "Topics in Organic Sulphur Chemistry," Tisler, M., Ed.; University Press: Ljubljana, Yugoslavia, 1978; pp. 187-206.
192. Kapovits, I.; Kalman, A. *J. Chem. Soc. D*, **1971**, 649-650.
193. Kalman, A.; Sasavari, I.; Kapovits, *I. Acta Crystallogr., Sect. B*, **1973**, *29*, 355.
194. Balthazor, T. M.; Martin, J. C. *J. Am. Chem. Soc.*, **1975**, *97*, 5634-5635.
195. Martin, J. C.; Balthazor, T. M. *J. Am. Chem. Soc.*, **1977**, *99*, 152-162.
196. Folli, U.; Iarossi, D. *Gazz. Chim. Ital.*, **1969**, *99*, 1297-1305.
197. Goldberg, S. I.; Sahli, M. S. *J. Org. Chem.*, **1967**, *32*, 2059-2062.
198. Kingsbury, C. A.; Cram, D. J. *J. Am. Chem. Soc.*, **1960**, *82*, 1810-1819.
199. Jones, D. N.; Green, M. J. *J. Chem. Soc., C*, **1967**, 532-542.
200. Jones, D. N.; Green, M. J.; Saeed, M. A.; Whitehouse, R. D. *J. Chem. Soc., C*, **1968**, 1362-1372.
201. Jones, D. N.; Green, M. J.; Whitehouse, R. D. *Chem. Commun.*, **1968**, 1634-1636.
202. Jones, D. N.; Green, M. J.; Whitehouse, R. D. *J. Chem. Soc., C*, **1969**, 1166-1173.
203. Jones, D. N.; Mundy, D.; Whitehouse, R. D. *J. Chem. Soc., C*, **1969**, 1668-1677.
204. Fleischer, E. B.; Axelrod. M.; Green, M.; Mislow, K. *J. Am. Chem. Soc.*, **1964**, *86*, 3395-3396.
205. Cheung, K. K.; Kjaer, A.; Sim, G. A. *Chem. Commun.*, **1965**, 100-102.
206. Nishio, M.; Nishihata, K. *J. Chem. Soc., D*, **1970**, 1485-1486.
207. Nishio, M. *J. Chem. Soc., D*, **1969**, 51-52.
208. Pritchard, J. G.; Lauterbur, P. C. *J. Am. Chem. Soc.*, **1961**, *83*, 2105-2110.
209. Foster, A. B.; Inch, T. D.; Qadir, M. H.; Webber, J. M. *Chem. Commun.* **1968**, 1086-1089.
210. Sollman, P. B.; Nagarajan, R.; Dodson R. M. *Chem. Commun.*, **1967**, 552-554.
211. Fraser, R. R.; Durst, T.; McClory, M. R.; Viau, R.; Wigfield, Y. Y. *Int. J. Sulfur Chem.*, **1971**, *1*, 133-137.
212. Ledaal, T. *Tetrahedron Lett.*, **1968**, 1683-1688.
213. Lett, R.; Bory, S.; Moreau, B.; Marquet, A. *Bull. Soc. Chim. Fr.*, **1973**, 2851-2856.
214. Cooper, R. D. G.; de Marco, P. V.; Cheng, J. C.; Jones, N. D. *J. Am. Chem. Soc.*, **1969**, *91*, 1408-1415.

215. Cooper, R. D. G.; de Marco, P. V.; Spry, D. O. *J. Am. Chem. Soc.*, **1969**, *91*, 1528–1529.
216. Kishi, M.; Tori, K.; Komeno, T.; Shingu, T. *Tetrahedron Lett.*, **1971**, 3525–3528.
217. Mislow, K.; Raban M. In "Topics in Stereochemistry," Vol. 1, Allinger, N. L.; Eliel, E. L., Eds.; Interscience; New York, 1967; pp. 1–50.
218. Campbell, J. R. *Aldrichim. Acta*, **1972**, *5*, 29–33.
219. Pirkle, W. H.; Beare, S. D.; Muntz, R. L. *Tetrahedron Lett.*, **1974**, 2295–2298.
219a. Pirkle, W. H.; Hoover, D. J. *Top. Stereochem.*, **1982**, *13*, 263–331.
220. Bucciarelli, M.; Forni, A.; Moretti, I.; Torre, G. *Tetrahedron*, **1977**, *33*, 999–1002.
221. Mislow, K.; Ternay, A. L., Jr.; Melillo, J. T. *J. Am. Chem. Soc.*, **1963**, *85*, 2329–2340.
222. Folli, U.; Montanari, F.; Torre, G. *Tetrahedron Lett.*, **1966**, 5037–5043.
223. Axelrod, M.; Bickart, P.; Goldstein, M. L.; Green, M. M.; Kjaer, A.; Mislow, K. *Tetrahedron Lett.*, **1968**, 3249–3252.
224. Henson, P. D.; Mislow, K. *J. Chem. Soc. D*, **1969**, 413–414.
225. Jones, D. N.; Helmy, E. E.; Taylor, R. J. K.; Edmonds, A. C. F. *J. Chem. Soc. D*, **1971**, 1401–1402.
226. Lisowski, J.; Siemion, I. Z.; Tyran, B. *Rocz. Chem.*, **1973**, *47*, 2035–2043.
227. Fowden, L.; Scopes, P. M.; Thomas, R. N. *J. Chem. Soc., C*, **1971**, 833–840.
228. Gaffield, W.; Wong, F. F.; Carson, J. F. *J. Org. Chem.*, **1965**, *30*, 951–952.
229. Barnsley, E. A. *Tetrahedron*, **1968**, *24*, 3747–3752.
230. Wieland, T.; de Urries, M. P. J.; Indest, H.; Faulstich, H.; Gieren, A.; Sturm, M.; Hoppe, W. *Justus Liebigs Ann. Chem.*, **1974**, 1570–1579.
231. Ziffer, H. In "Sulfur Reports," Senning, A., Ed.; Harwood Academic Publisher: New York, forthcoming.
232. Mislow, K.; Schneider, P.; Ternay, A. L., Jr. *J. Am. Chem. Soc.*, **1964**, *86*, 2957–2958.
233. Janczewski, M.; Dec, M. *Bull. Acad. Pol. Sci., Ser. Chim.* **1962**, *10*, 605–612.
234. Hine, R.; Rogers, D. *Chem. Ind. (London)*, **1956**, 1428–1430.
235. Hine, R. *Acta Crystallogr.*, **1962**, *15*, 635–638.
236. Johnson, C. R.; McCants, D., Jr. *J. Am. Chem. Soc.*, **1965**, *87*, 1109–1114.
237. Siegl, W. O.; Johnson, C. R. *J. Org. Chem.*, **1970**, *35*, 3657–3663.
238. Kishi, M.; Komeno, T. *Tetrahedron Lett.*, **1971**, 2641–2644.
239. Dodson, R. M.; Cahill, P. J.; Nelson, V. C. *Chem. Commun.*, **1968**, 620–621.
240. Boucher, H.; Brocki, T. R.; Moskovits, M.; Bosnich, B. *J. Am. Chem. Soc.*, **1977**, *99*, 6870–6873.
241. Raban, M.; Mislow, K. In "Topics in Stereochemistry," Vol. 2, Allinger, N. L.; Eliel, E. L. Eds.; Interscience: New York, 1968, pp. 199–230.
242. Pirkle, W. H.; Beare, S. D.; Muntz, R. L. *J. Am. Chem. Soc.*, **1969**, *91*, 4575.

243. Cockerill, A. F.; Davies, G. L. O.; Harden, R. C.; Rackham, D. M. *Chem. Rev.*, **1973**, *73*, 553–588.
244. Fraser, R. R.; Petit, M. A.; Saunders, J. K. M. *J. Chem. Soc. D*, **1971**, 1450–1451.
245. Nozaki, H.; Yoshino, K.; Oshima, K.; Yamamoto, Y. *Bull. Chem. Soc. Jpn.*, **1972**, *45*, 3495–3496.
246. Mikołajczyk, M.; Drabowicz, J.; Bujnicki, B., unpublished results.
247. Mislow, K. *Rec. Chem. Prog.*, **1967**, *28*, 217–240.
248. Rayner, D. R.; Gordon, A. J.; Mislow, K. *J. Am. Chem. Soc.*, **1968**, *90*, 4854–4860.
249. Brower, K. R.; Wu, T. *J. Am. Chem. Soc.*, **1970**, *92*, 5303–5305.
250. Andersen, K. K.; Cinquini, M.; Papanikolaou, N. E. *J. Org. Chem.*, **1970**, *35*, 706–710.
251. Furukawa, N.; Harada, K.; Oae, S. *Tetrahedron Lett.*, **1972**, 1377–1380.
252. Moriyama, M.; Furukawa, N.; Numata, T.; Oae, S. *Chem. Lett.*, **1976**, 275–278.
253. Darwish, D.; Datta, S. K. *Tetrahedron*, **1974**, *30*, 1155–1160.
254. Miller, E. G.; Rayner, D. R.; Thomas, H. T.; Mislow, K. *J. Am. Chem. Soc.*, **1968**, *90*, 4861–4868.
255. Bickart, P.; Carson, F. W.; Jacobus, J.; Miller, E. G.; Mislow, K. *J. Am. Chem. Soc.*, **1968**, *90*, 4869–4876.
256. Ciuffarin, E.; Isola, M.; Fava, A. *J. Am. Chem. Soc.*, **1968**, *90*, 3594–3595.
257. Booms, R. E.; Cram, D. J. *J. Am. Chem. Soc.*, **1972**, *94*, 5438–5446.
258. Mislow, K. Axelrod, M.; Rayner, D. R.; Gotthardt, H.; Coyne, L. M.; Hammond, G. S. *J. Am. Chem. Soc.*, **1965**, *87*, 4958–4959.
259. Cooke, R. S.; Hammond, G. S. *J. Am. Chem. Soc.*, **1968**, *90*, 2958–2959.
260. Iselin, B. Helv. Chim. Acta, **1961**, *44*, 61–78.
261. Mislow, K.; Simmons, T.; Melillo, J. T. Ternay, A. L., Jr. *J. Am. Chem. Soc.*, **1964**, *86*, 1452–1453.
262. Landini, D.; Modena, G.; Montanari, F.; Scorrano, G. *J. Am. Chem. Soc.*, **1970**, *92*, 7168–7174.
263. Landini, D.; Modena, G.; Quintily, U.; Scorrano, G. *J. Chem. Soc., B*, **1971**, 2041–2044.
264. Yoshida, H.; Numata, T.; Oae, S. *Bull. Soc. Chem. Jpn.* **1971**, *44*, 2875–2876.
265. Kwart, H.; Omura, H. *J. Am. Chem. Soc.*, **1971**, *93*, 7250–7256.
266. Modena, G.; Quintily, U.; Scorrano, G. *J. Am. Chem. Soc.*, **1972**, *94*, 202–208.
267. Herbrandson, H. F.; Dickerson, R. T., Jr. *J. Am. Chem. Soc.*, **1959**, *81*, 4102–4106.
268. Oae, S.; Kunieda, N. *Bull. Chem. Soc. Jpn.*, **1968**, *41*, 696–701.
269. Kunieda, N.; Oae, S. *Bull. Chem. Soc. Jpn.*, **1973**, *46*, 1745–1751.
270. Oae, S.; Yokoyama, M.; Kise, M. *Bull. Chem. Soc. Jpn.*, **1968**, *41*, 1221–1224.

271. Jonsson, E. *Acta Chem. Scand.*, **1967**, *21*, 1277–1280.
272. Kunieda, N.; Oae, S. *Bull. Chem. Soc. Jpn.*, **1968**, *41*, 1025–1026.
273. Oae, S.; Kise, M. *Tetrahedron Lett.*, **1967**, 1409–1413.
274. Oae, S.; Kise, M. *Bull. Chem. Soc. Jpn.*, **1970**, *43*, 1416–1420.
275. Kise, M.; Oae, S. *Bull. Chem. Soc. Jpn.*, **1970**, *43*, 1426–1430.
276. Kise, M.; Oae, S. *Bull. Chem. Soc. Jpn.*, **1969**, *43*, 1804–1808.
277. Jonsson, E. *Tetrahedron Lett.*, **1967**, 3675–3678.
278. Drabowicz, J.; Oae, S. *Tetrahedron*, **1978**, *34*, 63–66.
279. Johnson, C. R.; McCants, D., Jr. *J. Am. Chem. Soc.*, **1964**, *86*, 2935–2936.
280. Kunieda N.; Sakai, K.; Oae, S. *Bull. Chem. Soc. Jpn.*, **1969**, *42*, 1090–1094.
281. Savige, W. E.; Fava, A. *Chem. Commun.*, **1965**, 417–418.
282. Koch, P.; Fava, A. *J. Am. Chem. Soc.*, **1968**, *90*, 3867–3868.
283. Mikołajczyk, M.; Drabowicz, J.; Slebocka-Tilk, H. *J. Am. Chem. Soc.*, **1979**, *101*, 1302–1303.
284. Annunziata, R.; Cinquini, M.; Colonna, S. *J. Chem. Soc., Perkin Trans. I*, **1973**, 1231–1233.
285. Annunziata, R.; Cinquini, M.; Colonna, S. *J. Chem. Soc., Perkin Trans. I*, **1975**, 404–406.
286. Tang, R.; Mislow, K. *J. Am. Chem. Soc.*, **1969**, *91*, 5644–5645.
287. Denney, D. B.; Denney, D. Z.; Hsu, Y. F. *J. Am. Chem. Soc.*, **1973**, *95*, 4064–4065.
288. Oae, S.; Yokoyama, M.; Kise, M.; Furukawa, N. *Tetrahedron Lett.*, **1968**, 4131–4134.
289. Andreetti, G. D.; Bocelli, G; Coghi, L.; Sgarabotto, P. *Cryst. Struct. Commun.*, **1975**, *4*, 393–397.
290. Kagan, H.; Fiaud, J. C. In "Topics in Stereochemistry," Vol. 10, Allinger, N. L.; Eliel, E. L., Eds.; Interscience: New York, 1978; pp. 175–285.
291. Valentine, D., Jr.; Scott, J. W. *Synthesis*, **1978**, 329–356.
292. ApSimon, J. W.; Seguin, R. P. *Tetrahedron*, **1979**, *35*, 2797–2842.
293. Furukawa, N.; Yoshimura, T.; Ohtsu, M.; Akasaka, T.; Oae, S. *Tetrahedron*, **1980**, *36*, 73–80.
294. Johnson, C. R.; Kirchhoff, R. A.; Reischer, R. J.; Katekar, G. F. *J. Am. Chem. Soc.*, **1973**, *95*, 4287–4291.
295. Johnson, C. R.; Janiga, E. R. *J. Am. Chem. Soc.*, **1973**, *95*, 7692–7700.
296. Johnson, C. R.; Lockhard, J. P. *Tetrahedron Lett.*, **1971**, 4589–4592.
297. Annunziata, R.; Fornasier, R.; Montanari, F. *J. Chem. Soc., Chem. Commun.*, **1972**, 1133–1134.
298. Oae, S. In "Topics in Organic Sulphur Chemistry," Tisler, M., Ed.; University Press, Ljubljana, Yugoslavia, 1978; pp. 289–336.
299. Glue, S.; Kay, I. T.; Kipps, M. R. *J. Chem. Soc. D*, **1970**, 1158.
300. Stridsberg, B.; Allenmark, S. *Acta Chem. Scand., B*, **1976**, *30*, 219–227.
301. Numata, T.; Oae, S. *Tetrahedron Lett.*, **1977**, 1337–1340.

302. Mikołajczyk, M.; Midura, W.; Grzejszczak, S., unpublished results.
303. Numata, T.; Itho, S.; Oae, S. *Tetrahedron Lett.*, **1979**, 1869–1870.
304. Evans, D. A.; Andrews, G. C. *Acc. Chem. Res.*, **1974**, *7*, 147–155.
305. Goldmann, S.; Hoffmann, R. W.; Maak, N.; Geueke, K. J. *Chem. Ber.*, **1980**, *113*, 831–844.
306. Hoffmann, R. W.; Goldmann, S.; Gerlach, R.; Maak, N. *Chem. Ber*, **1980**, *113*, 845–855.
307. Hoffmann, R. W.; Gerlach, R.; Goldmann, S. *Chem. Ber.*, **1980**, *113*, 856–863.
308. Trost, B. M.; Biddlecom, W. G. *J. Org. Chem.*, **1973**, *38*, 3438–3439.
309. Durst, T.; Viau, R.; McClory, M. R. *J. Am. Chem. Soc.*, **1971**, *93*, 3077–3078.
310. Nishihata, K.; Nishio, M. *J. Chem. Soc. D*, **1971**, 958–959.
311. Durst, T.; Fraser, R. R.; McClory, M. R.; Swingle, R. B.; Viau, R.; Wigfield, Y. Y. *Can. J. Chem.*, **1970**, *48*, 2148–2150.
312. Baldwin, J. E.; Hackler, R. E.; Scott, R. M. *J. Chem. Soc. D*, **1969**, 1415–1416.
313. Durst, T.; Viau, R.; van den Elzen, R.; Nguyen, C. H. *J. Chem. Soc. D*, **1971**, 1334–1336.
314. Tsuchihashi, G.; Iriuchijima, S.; Maniwa, K. *Tetrahedron Lett.*, **1972**, 4605–4608.
315. Tsuchihashi, G.; Iriushijima, S.; Ishibashi, M. *Tetrahedron Lett.*, **1973**, 3389–3392.
316. Colombo, L.; Gennari, G.; Guanti, G.; Narisano, E.; Scolastico, G. IX International Symposium on Organic Sulphur Chemistry, Riga, USSR, 1980; Abstracts Book, p. 217.
317. Mioskowski, C.; Solladie, G. *Tetrahedron*, **1980**, *36*, 227–236.
318. Abbott, D. J.; Colonna, S.; Stirling, C. J. M. *J. Chem. Soc., Perkin Trans. I*, **1976**, 492–498.
319. Tsuchihashi, G.; Mitamura, S.; Ogura, K. *Tetrahedron Lett.*, **1976**, 855–858.
320. Tsuchihashi, G.; Mitamura, S.; Ogura, K. *Tetrahedron Lett.*, **1973**, 2469–2470.
321. Colombo, L.; Gennari, C.; Resnati, G.; Scolastico, C. IX International Symposium on Organic Sulphur Chemistry, Riga, USSR, 1980; Abstracts Book, p. 225.
322. Abbott, D. J.; Colonna, S.; Stirling, C. J. M. *J. Chem. Soc. D*, **1971**, 471.
323. Tsuchihashi, G.; Mitamura, S.; Ogura, K. *Tetrahedron Lett.*, **1974**, 455–458.
324. Calzavara, P.; Cinquini, M.; Colonna, S.; Fornasier, R.; Montanari, F. *J. Am. Chem. Soc.*, **1973**, *95*, 7431–7436.
325. Cinquini, M.; Colonna, S.; Montanari, F. *J. Chem. Soc., Perkin Trans. I*, **1974**, 1719–1723.
326. Cinquini, M.; Colonna, S. *J. Chem. Soc., Chem. Commun.*, **1974**, 769–770.

Subject Index

Ab initio MO method, 118, 119, 129, 137, 147, 148, 153, 177
Absolute configuration, assignment of, 278
  by chiral LSR, 326
  by CSA, 293
  models for, 280
Acetate enolate synthon, chiral, 89, 95
N-Acetylproline methyl ester, 151, 172
Acyclic transition state, in aldol condensation, 13
α-Acylaziridines, asymmetric synthesis of, 436
N-Acyloxazolidine-2-ones, 46
Adamantane, 123, 164, 175
Adamantanoid molecules, 158
Adamantene, dimerization of, 164
1-Adamantyl 2-pent-4-enyl sulfide, asymmetric synthesis of, 446
1-Adamantylethylmethylsulfonium perchlorate, racemization of, 408
  resolution of, 366
1-Adamantylethylpropenylsulfonium tetrafluoroborate, resolution of, 366
Ageratriol, 166
Agerol and diepoxide, 166
Air-water interface, monolayers at, 202
Alcohols, configuration of, 327
  and CSA, 295, 314, 327
  enantiomeric excess, determination of, 304
  force field calculations with, 147
Aldehyde diastereoface selection, 104
Aldehydes, chiral condensation with achiral enolates, 66
Aldimines, cross-condensation of, 63
Aldolate equilibrium, steric factors in, 12
Aldol condensation, acid catalyzed, 4
  catalyzed by tetra-*n*-butylammonium fluoride, 55
  catalyzed by titanium tetrachloride, 55, 63, 73
  catalyzed by trimethylsilyl triflate, 57
  crossed, 4
  diastereoselection in, 4
  effect of solvent polarity on, 45
  enantioselection in, 4
  independent of enolate geometry, 50
  kinetically controlled, 13, 51
  stereoselective, factors in, 21
    steric model for, 82
  thermodynamically controlled, 7
  with zinc enolates, 8
Aldol product stereochemistry, assignment of, 5
  effect of enolate geometry on, 14
Aldols, equilibration of, 11
Aldol transition states, HOMO-LUMO interactions in, 33
Alkanes, methyl substituted, 158
α-Alkoxyaldehydes, 71
Alkoxyaminosulfonium salts, asymmetric synthesis of, 371
  stereochemistry of alkaline hydrolysis of, 423
Alkyl aryl sulfimides, chiral, thermal racemization of, 408
Alkyl aryl sulfoxides, chiral, reaction with alkyllithium reagents, 350
Alkyl bromides, relative S_N2 reaction rates of, 162
N-Alkylidenesulfinamides, stereospecific synthesis of, 359
Allenes, and CSA, 286
Allinger force field, 121-123, 125, 130, 139, 154, 155, 158, 164, 169, 171, 176. *See also* MMI; MMPI; MM2
Allyl alcohols, asymmetric synthesis of, 445
  and CSA, 284, 286, 301
Allylboranes, addition reactions of, 101, 105
Allyl sulfoxides, [2,3] sigmatropic rearrangement of, 443
Allyl *p*-tolyl sulfoxides, racemization of, 409
Aluminum enolates, 19
Amide hydrolysis, hydroxyl assisted, 92

Amides: chiral, 88
enolates of, 26, 27, 30
force field parameters for, 150, 157, 175
Amine oxides, absolute configuration of, 293
and CSA, 285, 286
Amines, absolute configuration of, 293
chiral, in asymmetric elimination, 347
in asymmetric synthesis of sulfinates, 354
of thiosulfinates, 356
as sensitizers, in photochemical decomposition of sulfoxides, 347
and CSA, 275, 283, 286, 314
α-Amino acids, absolute configuration of, 304
2-Aminobutane, and CSA, 296
1-Aminodeoxyribose, 148
α-Amino esters, complex with chiral crown ethers, 308
configuration of, 327
and CSA, 269, 283, 286, 294
4'-Amino-4-methyldiphenyl sulfoxide, resolution of, 336
α-Aminophenylacetates, and CSA, 294
(−)-*m*-Aminophenyl methyl sulfoxide, absolute configuration of, 387
1-Aminoribose, 140
Amphipathic molecules, 197, 202
Andersen synthesis, of sulfinamides, steric course of, 421
of sulfoxides, 348
Anh transition state model, 67
Anisotropic groups, importance of, in CSA, 272
Anisotropic perturbation, 280
Anomeric effect, 120, 147
Anthracenophanes, 143
9-Anthrylcarbinols, as CSA's, 274
Aromatic hydrocarbons, non-benzenoid, 146
Aryl arenethiosulfinates, racemization of, 410
Aryl-aryl attraction, 300
Arylcarbinols, and CSA, 283, 286, 298, 325
Association complexes, 267
Association, degree of, in use of CSA, 271
Asteranes, 177
Asymmetric induction, in aldol condensation, 66, 69
Asymmetric oxidation, diastereomeric transition states in, 341
of sulfides, 344
Asymmetric reduction, of sulfoxides, 346
(*S*)-Atrolactic acid, 85
Autononequivalence, 316
Azomethine-enolate condensations, 59

Bartell's force field, 129
Basic sites, of CSA substrates, 281, 288
9-BBN enolates, 46
9-BBN triflate, 46
Benzenesulfinyl chloride, reaction with chiral-*n*-methyl-1-phenyl-2-propylamine, 357
Benzhydryl *p*-toluenesulfinates, racemization of, 417
Benzothiophene oxides, absolute configuration of, 293
3,1-Benzoxathiane-4-one, asymmetric synthesis of, 441
(+)-(*R*)-Benzyl *t*-butyl sulfoxide, stereochemistry of deuteration and methylation of, 447
Benzyl-^{12}C benzyl-^{13}C sulfoxides, stereospecific synthesis of, 348, 349
(−)-Benzylethylmethylphenylammonium tetrafluoroborate, asymmetric synthesis of, 440
Benzylethylmethylsulfonium salts, asymmetric synthesis of, 440
racemization of, 408
Benzyl methyl sulfoxide, asymmetric synthesis of, 344
reaction with bromine, 455
stereochemistry of deuteration and methylation, 447
o-Benzylsulfinylbenzoic acid, Pummerer reaction of, 441
Benzyl *p*-tolyl sulfide, asymmetric oxidation of, 345
(−)-Benzyl *p*-tolyl[^{16}O^{18}O]-sulfone, 374
(−)-Benzyl[$^{2}H_2$] *p*-tolyl [^{16}O^{18}O]-sulfone, 375
Benzyl *p*-tolyl sulfoxides, interconversion of enantiomers of, 423
oxidation of, with ^{18}O-labeled peracetic acid, 432
thermal racemization of, 408
Bianthrone, 138
Bicyclo[4.4.0]decane, 134
Bicycloheptanes, 131, 132

Bicyclo[2.2.0]hexane, 129
Bicyclo[2.1.1]hexene, 165
Bicyclononanes, 129, 133
Bicyclo[3.3.1]nonan-9-ol, 133
Bicyclo[3.3.1]nonan-9-one, 172
Bicyclo[3.3.1]nonan-3-yl tosylates, 133
Bicyclononenes, 171
Bicyclo[4.2.0]octane, 132
Bicycloundecanes, 135
BIGSTRN, 123, 139, 142, 143. *See also* Schleyer force field
Bilayer, 243
β-Binaphthols, 308
1,1'-Binaphthyl, 14
Biotin precursors, 343
Biphenyl, 141
Blodgett dipping technique, 206
Boat conformation, 155
Boat transition states, in aldol condensation, 18
Boron enolates, 37
  in aldol condensations of acyclic ketones, 42
  chiral, 80, 88
  diastereoselectivity of, 42
  generation of, 38
  stability of, 42
Boron ligand structure, effect of, on aldol diastereoselection, 46
Boryl enolates, *see* Boron enolates
Boyd's force field, 124, 131, 134, 153, 154, 160, 172
Bredt's rule, 171, 175
B Strain relief, 160
Bubble growth, 206
Butadiene, 137
n-Butane, 127, 130
2-Butanol, and CSA, 296
  and $Eu(fod)_3$, 299
1-Butene, 137
(*Z*)-2-Butenyldiethylalane, 75
6-*t*-Butyl-decalone-1, 165
t-Butyl dimethylamidothiosulfite, reaction with mercury dichloride, 428
t-Butyl (+)-(*R*)-*p*-toluenesulfinylacetate, use in asymmetric synthesis, 450
(−)-(*S*)-*t*-Butyl *p*-toluenethiosulfinate, stereochemistry of methanolysis of, 422

Camphor, and CSA, 295
Capillary rise method, for measuring surface tension, 206
Carbinyl hydrogen bonding, 281, 295, 300. *See also* CHB
N-Carbomenthoxy *p*-toluenesulfonimidoyl chloride, diastereomers of, 282
Carbomethoxy-aryl attraction, 301
Carbon-carbon bonds, elongated, 170
Carbon(^{13}C)nonequivalence, 309, 314
Carbonium ions (carbocations), applications of molecular mechanics to, 148, 149, 163, 164
Carbonyl compounds, conformation of, 148
Carboxylic acids, enediolates of, 31
  force field calculations in, 175
(−)-*meta*-Carboxyphenyl methyl sulfoxide, absolute configuration of, 387
  resolution of, 336
Catalytic hydrogenolysis of strained cage compounds, 164
Catenanes, 177
Cell membranes, 205
CFF (consistent force field), 124, 133, 137, 138, 141, 147, 148, 153, 154, 157, 175-177
Chair transition state, in aldol condensation, 14, 19
Charge interactions, 146
CHB (Carbinyl Hydrogen Bonding), 281, 295, 297, 300, 315
Chelating agents, chiral, 106
  effect on aldol condensation, 31, 32
Chelating centers, effect of, 29
Chiral additives, 265
Chiral alcohols, use in asymmetric oxidation of sulfides, 344
Chiral catalysts, in asymmetric oxidation of sulfides, 344
Chiral centers, crowded, 295
Chiral discrimination, 201
Chiral environment, 265
Chirality, proof of, 321
Chiral lanthanide shift reagents, *see* LSR, chiral
Chiral mobile phase, for HPLC, 197
Chiral recognition, 200, 264, 280. *See also* Enantiomer discrimination
  energetic basis of, 313
Chiral solvating agents, *see* CSA
Chiral solvents, 197
Chiral stationary phases, for HPLC, 197

Chiral surface-active lipids, 205
Chiral surfactants, 221
N-(*p*-Chlorobenzylidene)-*p*-chloroaniline, 175
N-Chlorocaprolactam, chiral, in asymmetric oxidation of sulfides, 345
1-Chloro-3,3-dimethyl-1-phenyl[3H-2,1-benzoxathiole, absolute configuration at sulfur in, 393
  stereospecific synthesis of, 384
N-Chloro-2,2-diphenylaziridine, asymmetric synthesis of, 440
α-Chloroethanesulfinyl chloride, NMR nonequivalence in, 359
Chlorophylls, 175
Chlorosulfurane hydrolysis, stereochemistry of, 431
2-Chloro-10-(2,5-xylyl)thiaanthracene, chiral, 372
Cholesterol, 121
Cholesteryl methanesulfinates, 351, 353
Chromic acid, oxidation of alcohols with, 164
Circular differential Raman scattering (CID), of chiral sulfoxides, 402
[8]Circulene, 175
Clausius-Clapeyron equation, 207
  two-dimensional, 227, 241
^{13}C NMR spectra, analysis of, 172, 173
Cocaine, shift nonequivalence in, 282
Cogwheeling, 144
Condensed phases, in monolayers, 228
CONFI, 124
Configuration of chiral sulfur compounds, by NMR, 396
Conformational analysis, 125
Conformational control, 166
  in carbinyl hydrogen bonding, 281, 300
Conformational energy calculations, 120, 130
Conformations, chelate-like, 280, 281
  lifetimes of, 271
  non-equivalence engendering, in CSA, 272
Conjugated π-systems, molecular mechanics in, 138
Consistent force field, 124
Consonant asymmetric synthesis, 66, 78, 81, 104
Cope rearrangements, 167
Correlated rotation, 142
Coulombic charge interaction terms, 157
Coupling, "through bond," 170
Cram's rule, 66
Critical micelle concentration (CMC), 202
Cross-sectional area, of fatty acid chain, 204
Crowded olefins, 137
Crown ethers, chiral recognition with, 308
Crystalline lattice, two-dimensional, 222
CSA (Chiral Solvating Agent), achiral diluent in use of, 266, 271
  choice of, 276
  concentration, effect of, 270, 275
  diamagnetic, 265
  enantiomeric purity of, 278
  hydrogen bonding with, 269
  infrared studies with, 270
  interaction with chiral substrate, 265, 280
  solvent effects on, 270
α-Cyanomethyl *p*-tolyl sulfoxide, Pummerer reaction of, 442
(1*S*,2*R*)-1-Cyano-2-phenylcyclopropanecarboxylic acid methyl ester, asymmetric synthesis of, 438
3',5'-Cyclic adenosine monophosphate, 152
Cyclic difluorosulfurane, structure of, 425
Cyclic sulfinates, chiral, 354
Cyclic sulfonium salts, resolution of, 367
Cyclic sulfoximides, optically active, 379, 380
Cyclobutane, 129, 172
Cyclobutene, 129
1,2,6,7-Cyclodecatetraene, 131
β-Cyclodextrin, inclusion compounds with, 197
  NMR non-equivalence induced by, 270
  in resolution of sulfinates, 354
  in resolution of sulfoxides, 339
  in resolution of thiosulfinates, 356
Cyclodi-β-alanyl, 157
Cyclododecane, 131
trans,trans,trans-1,5,9-Cyclododecatriene, 131
cis-Cyclododecene, 131
Cyclododecyne, 131
Cycloheptane, 153
Cyclohexadecane, 130
Cyclohexane, 132, 139, 172
Cyclohexanone, enolates of, 23
  force field calculation in, 162
Cyclohexyltrifluoromethylcarbinol, 281
Cyclononadienes and -trienes, 131

Cyclooctadienes and -trienes, 131
Cyclopentadecane, 131
Cyclopentane, 151, 172
Cyclopentasilane, 151
Cyclophanes, 122, 142, 144, 168
Cyclopropane, coupling constants in, 172
Cyclopropanes, asymmetric synthesis of, 437
Cyclotetraglycyl, 157
Cyclotridecane, 131
Cycloundecane, 131
L-Cysteine, reaction with racemic sulfoxides, 346
Cystine-2-monooxides, resolution of, 355
Cytidyl(3′-5′)guanosine monophosphate, 174

Decalin, 131
Decalins, substituted, 134
trans-2-Decalone, 148
Dehydroisocalamendiol, 166
DeTar's molecular calculation system, *see* MOLMEC
α-Deuterioalcohols, configuration of, 326
Deuterium exchange, 276
Dewar benzene, 129
Dialkylboryl trifluoromethanesulfonate esters, 41
Dialkyl sulfoxides, stereospecific synthesis of, 350
Dialkyl *p*-tolyl-sulfonium salts, stereospecific synthesis of, 368
Diamagnetic chiral solvating agents, *see* CSA
Diamagnetic shift, 280
Diamantane, 164
Diaminosulfonium salts, asymmetric synthesis of, 371
Diamond lattice theory, 130
Diaryl disulfides, asymmetric oxidation of, 355
  resolution of, 337
Diaryl sulfimides, chiral thermal racemization of, 408
Diaryl sulfoxides, and CSA, 294
Diastereoface selection, 66
  in aldehydes, 68
  effect of metal enolate structure on, 80
  for proprionyl imides, mechanism of, 90
anti-Diastereomer, definition, 4
Diastereomer discrimination, 201, 249
Diastereomeric interactions, 264
Diastereomeric salts, 270, 276, 303
Diastereomeric solvates, conformational behavior of, 279
  relative stabilities of, 311
  spectral differences of, 267, 271, 272
Diastereomeric transition states, 198
Diastereomers, distinction of, by CSA, 320
Diastereoselectivity, of boron enolates, 42
Diastereotopic faces, 66
Diboryl enediolates, 47
1,2-di-*t*-Butylcyclohexane, 129
di-*t*-Butylmethane, 129
trans-1,2-Dichlorocyclohexane, 146
Dicyclopentane, 169
(+)-(*R*)-α,α-Dideuteriodibenzyl sulfoxide, chlorination of, 456
Diethylboryl pivalate, 41
(+)-(*S*)-N,N-Diethyl *p*-toluenesulfinamide, in stereospecific synthesis of sulfinates, 355
Differential transducer, linearly variable (LVDT), 209
1,2-Difluoro-1,2-dichloroethane, 320
Dihydroquinine, self-induced nonequivalence in, 316
13,14-Dihydroxydocosanoic acid, stereoisomers of, 342
(−)-(*S*)-N,N-Diisopropyl *p*-toluenesulfinamide, stereochemistry of acid-catalyzed alcoholysis of, 429
Dimesityl 2,4,6-trimethoxyphenylmethane, 127
Dimethoxymethane, 147
2,3-Dimethylbutane, 127
anti-3,7-Dimethyl-*cis,cis*-1,5-cyclooctadiene, 131
di-Menthyl ethane-1,2-disulfinate, reaction with Grignard reagents, 349
4,4-Dimethyl-3-keto steroids, 154
3,3-Dimethyl-2,4-pentanedione, 149
Dimethylphosphate anion, 153
1-Dimethylphosphono-1-hydroxycycloheptane, 153
Dimethyltetracosanoic acids, diastereomeric, 224
N,N-Dimethyl *p*-toluenesulfinamide, stereoselective synthesis of, 358
Dimyristoylphosphatidylethanolamine, 244
Dinucleoside monophosphates, 174

1,2-Dioctanoyl-3-*sn*-phosphatidylcholine, 250
1,3-Dioxathiolane, 152
Diphenyldisulfide, deimination of sulfoxides with, 351, 352
1,2-Diphenylethane, 139
2,6-Diphenylhomotropylidene, 146
Dipole-dipole complexes, 198
Dissonant asymmetric synthesis, 66, 78, 104
Disulfides, 152
Disulfoxides, chiral, 349, 350
1,3-Dithian 1-oxide, resolution of, 337
2,5-Dithia-spiro[3.3]heptane 2,5-dioxide, resolution of, 338
Dithioacetal monooxides, stereospecific synthesis of, 349
Dithioacetals of formaldehyde, asymmetric oxidation of, 344
DNA, intercalation in, 174
13-Docosenoic acid, permanganate oxidation of, 242
Dodecahedrane, 176
Double bonds, halogenation of, 204
  oxidation of, 204
Drug design, 173
du Nouy ring-detachment method, 207
Dynamic NMR, molecular mechanics applied to, 127, 131

e.e., *see* Enantiomeric excess
EENY, 140
EFF–EHMO hybrid approach, 124, 139
Eicosan-2-ol, 223, 226
Electrochemical oxidation, asymmetric, 344
Electron diffraction analysis (ED), 125, 127, 132
  molecular mechanics constrained, 137
Electronic effects, 170
Ellipsometry, 215
Empirical force field, *see* Molecular mechanics; *specific force fields*
Enantiomer discrimination, 200, 201, 228
  in polypeptides, 242
  see also Chiral recognition
Enantiomeric excess, determination of, 268, 276, 277, 326
Enantiomeric purity, *see* Enantiomeric excess
Enantiomeric solutes, interaction with CSA, 267
Enantiomer pairs, intermolecular association of, 200
Enantiomers, chromatographic separation of, 313
  highly enriched, 277
  NMR spectra of, in chiral solvents, 404
Enantiotopic faces, 66
Enantiotopic ligands, and CSA, 296, 319
Enantiotopic nuclei, 281
Enediolates, dilithium, 10
  magnesium, 13
  metal, of carboxylic acids, 31
Enermol, 125, 147
Engler-Schleyer force field, 123, 129, 135, 139. *See also* Schleyer force field
(*E*)-enolate, 5
(*Z*)-enolate, 5
Enolate geometry, effect of, on aldol stereochemistry, 14
Enolates, aluminum, 19
  of amides, 26, 27, 88
  boron, 37, 38, 80
  chiral, 77, 79, 80, 88
    condensation with aldehydes, 76
  of cyclohexanones, 23
  of esters, 26, 79
    Claisen rearrangement of, 36
  α-heteroatom-substituted, 49
  hydrazone derived, chiral, 100
  of ketones, 22, 80
  lithium, 15, 23, 80
    of amides, 30
  magnesium, 20
  of phenylacetic acid, 10
  stereochemical nomenclature of, 5
Enolate structure, as factor in diastereoselection, 16
Enolate substituents, steric influence of, 22
Enolate substitution, 70
Enolization, of dialkylthioamides, 28
Enolization model, 27
Enolsilanes, 55
  cross condensation of, 63
EPEN, 177
1-Ephedrine, reaction with thionyl chloride, 351
Episulfides, and CSA, 295, 296
Episulfoxides, and CSA, 295, 296
Epoxides, asymmetric synthesis of, 437

and CSA, 295, 296
Equilibration of aldols, mechanism of, 11
of metal aldolates, 9, 10
Equilibrium spreading pressure, 217, 218
of *n*-α-methylbenzystearamide, 247
E_2 reaction, 161
Erythro chirally selective ketone enolates, 83
Erythro diastereomer, definition, 4
Erythronolides, 2
Erythro-threo equilibration, of metal aldolates, 9, 12
of hydroxy esters, 10
Esterification, 159
Esters, in aldol condensations, 26
enolates of, 26, 36, 79
α-heteroatom substituted, 33
Ethers, and CSA, 282, 286, 294
force field calculations in, 147
1-Ethoxy-3-methylthietanium ions, alkaline hydrolysis of, 423
1-Ethoxy-1-phenyl-2,2,3,4,4-pentamethylphosphetanium hexachloroantimonates, alkaline hydrolysis of, 423
Ethyl ketones, chiral, derived from carbohydrates, 86
Ethylmethylphenacylsulfonium perchlorate, chiral, deprotonation of, 371
Ethylmethylphenyloxosulfonium perchlorate, chiral, 373
(+)-Ethylmethylphenylsulfonium perchlorate, oxidation of, with perbenzoic acid, 374
Ethylmethylpropylsulfonium 2,4,6-trinitrobenzenesulfonate, stereospecific synthesis of, 368
Ethylmethylsulfonium phenacylide, resolution of, 371
synthesis of chiral, 371
(+)-(−)-Ethyl phenyl sulfoxides, methylation of, 433
reaction with methyl iodide, 373
(−)-Ethyl *p*-toluenesulfinate, transesterification of, 420
(+)-(*R*)-Ethyl *p*-tolyl sulfoxide, α-halogenation of, 455
resolution of, 338
stereospecific synthesis of, 348
E_S values, 160

Fast-exchange process, 268
Felkin model, 67, 71
Field desorption mass spectrometry, 213
Film balance, *see* Langmuir film balance
Film compressibility, 216
Films, condensed solid, 215
stability, tests for, 218
First-order transition, 216
Fluorine (^{19}F) nonequivalence, 301, 312, 314
Fluoroalcohols, chiral, 396
as CSA's, 275, 293
recovery of, 326
silica gel bonded, 339
Force-area curves, for 1-stearoyl-2-lauroyl-3-phosphatidylcholine, 244
Force field, 120, 121
F strain, 161
Functionality, complementary, 265

Gas law, two dimensional, 216
gauche-interaction, in transition state, of aldol condensation, 17
Gaussian, 80, 118
Gear effect, 143
GEMO, 125, 166
GEOM, 137
Geometrical isomers, surface properties of, 220
Geometrical optimization, 121
GEOP, 122
Germacrene, 166, 167
Germacronolides, 169
Global minimum energy conformation, 157, 166, 167, 169, 176
GMEC, *see* Global minimum energy conformation
Grignard reagents, chiral reaction with racemic sulfinates, 354

Halides, force field calculations with, 151
Halogenation, of double bonds, 204
β-Halogenosulfoxides, asymmetric elimination reactions of, 347
Heat: of formation, 119, 158
of hydrogenation, 158
Hedycaryol, 167
Heteroatom parameters, 122, 146ff
Hexadecamethylbicyclo[3.3.1]nonasilane, 151
n-Hexadecane, 126, 127
Hexahelicene, 144

Hexamethylbenzene, 143
1,2,3,4,5,6-Hexamethylbicyclo[2.2.0]-hexane, 129
Hexamethyldisilane, 126
Hexamethylethane, 125-127
2,2,3,3,4,4-Hexamethylpentane, 123
Hexaphenylethane, 128
High-performance liquid chromatography (HPLC), 213
Homoketonization, 164
HOMO–LUMO interactions, in aldol transition states, 33
Host-guest complexes, 197
Hückel MO calculations, extended (EHMO), 124, 155
Humulene, 123
Hydrazone enolates, chiral, 100
Hydrocoumarin, 164
Hydrogen bonding, 174, 175, 270, 281
Hydrolysis, 159
Hydrophobic interactions, 197, 203
β-Hydroxyacids, 88
α-Hydroxyesters, and CSA, 275, 284, 286, 294, 301, 302, 314
β-Hydroxyesters, configuration of, 326
  erythro-threo equilibration of, 10
(−)-1-Hydroxy-1-methyl-1,2,3,4-tetrahydronaphthalene, asymmetric synthesis of, 449
α-Hydroxyphenylacetates, and CSA, 294
12-Hydroxystearic acid, 230, 233, 239
  alkali salts of, 231
  first-order two-dimensional phase transition in, 240
γ-Hydroxystearic acid, lactonization of, 204, 205
Hysteresis, 219, 220

Imide enolates, chiral, 88
Imine enolates, chiral, 99
Imines, chiral, condensation of, 64
Infrared studies, of hydrogen bonding, 270
Intramolecular shielding, 294
Intrinsic spectral differences, 326
p-Iodobenzenesulfinic acid, menthyl esters of, 353
Ionic complexes, chiral interactions in, 197
Ion pairs, 198, 305, 316
Isobutane, 127
Isopropanesulfinyl chloride, NMR nonequivalence in, 360
Isopropyl methanesulfinate, resolution by β-cyclodextrin inclusion complexes, 354
Isopropyl methyl sulfoxide, 281
Isotope effect, secondary, 160
Isotopic labeling, 281
Isotopic substitution, chirality due to, 312
Ivanov reaction, stereochemistry of, 13
Izumi-Tai nomenclature, 66

7-Keto-2,9-dimethyltetracosanoic acids, 224
Ketones, and CSA, 293
  enantiomeric excess, determination of, 293, 304
  enolates of, 22, 80
  equilibration of, 9, 10
  unsaturated, 122
Δ^8-11-Ketosteroids, 155
β-Ketosulfoxides, asymmetric synthesis of, 347
  stereospecific synthesis of, 349
Kinetically controlled aldol diastereoselection, 13, 51
Kinetic resolution, of sulfoxides, 345

Lactones, absolute configuration of, 293 and CSA, 287, 293, 308, 310, 314, 315
Lagrange multiplier method, 131
Langmuir film balance, 206, 209-211
Langmuir troughs, multi-compartment, 213
Lanost-8-en-3-one, 155
Lanthanide induced shifts (LIS), 172. *See also* LSR
Lasalocid-A, 78
Lepidopterene, 170
Lifson's force field, 129, 134
Lipid bilayer, 205
Lipid monolayers, interaction with polypeptides, 250
Lipids, chiral, surface active, 205
Liquid crystals, 198
Liquid films, "liquid-expanded" and "mesomorphous", 216
LIS, *see* Lanthanide induced shift; LSR
Lithium enediolates, 10
  enolates, 15, 80, 88
Lithium ester enolates, condensation with imines, 63
Lithium 12-hydroxystearate, twisted fibers of, 231

LSR (Lanthanide Shift reagents), achiral, 290, 311
aqueous, 326
chiral, 265, 277, 322, 405
LVDT, *see* Differential transducer, linearly variable

Magnesium enolates, 20, 72
Magnetic non-equivalence of geminal protons, 360
(*S*)-Mandelic acid, 85
Manxane, 135
Maytansine, 98
Menisci, development of, 206
Menthyl arenesulfinates, conversion into sulfoxides, 348
Menthyl dimethylamidosulfites, synthesis of, 365
(+)-Menthyl *p*-iodobenzenesulfinate, absolute configuration of, 389, 400
optical purity of, 403
(−)-Menthyl phenylmethane[$^{16}O^{18}O$]-sulfonate, reaction with *p*-tolylmagnesium bromide, 430
(−)-(*S*)-Menthyl *p*-toluenesulfinate, reaction with Grignard reagents, 348
in stereospecific synthesis of sulfinamides, 357
synthesis of, 352
Mesitylmethylsulfoximide, resolution of, 377
Meso compounds, 319
Metacyclophane, 144
Metal-center chirality transfer, 101
Metal-center steric effects, 49, 83
Metal chelates, 153
Metal enolate structure, effect on diastereoface selection, 71, 80
Metal ligand effects, 37
Metalloenamines, 99
L-Methionine, oxidation of, 343
L-Methionine sulfoxide, 343
absolute configuration at sulfur of, 387
epimerization of, 411
Methoxyalkoxyisopropylsulfonium triflates, chiral, alkaline hydrolysis of, 425, 426
Methoxybenzyl-*p*-tolylsulfonium tetrafluoroborate, synthesis of, 368
α-Methoxyesters, and CSA, 284, 294
Methoxymercurials, and CSA, 284
Methoxy-methoxy exchange, isotopic, in (+)-methyl *p*-toluenesulfinate, 421
Methoxymorpholino-*p*-tolylsulfonium salt, synthesis of, 370
α-Methoxy-α-phenylacetaldehyde, asymmetric synthesis of, 450, 453
α-Methoxyphenylacetates, and CSA, 294
Methoxypyrrolidino-*p*-tolylsulfonium salts, synthesis of, 369, 370
Methyl 1-adamantyl sulfoxide, racemization of, 407
(+)-(*S*)-1-(10-methyl-9-anthryl)-2,2,2-trifluoroethanol, in determination of enantiomeric purity, 405
N-α-Methylbenzylstearamide, 219, 245-247
N-α-Methylbenzyl *p*-toluenesulfinamides, synthesis of, 357
2-Methyl-1-butanol, and CSA, 296
trans-2-Methylcyclohexanols, asymmetric synthesis of, 449
trans-2-Methylcyclopropanecarboxylic acid, asymmetric synthesis of, 438
(+)-Methyl L-cysteine sulfoxide, x-ray analysis of, 400
Methylenecyclobutene, 129
Methylenesulfine, as intermediate in racemization, 416
Methylethylphenacyl salt, resolution of, 366
Methylethylthetine salt, resolution of, 366
8-Methylhydrindane, 156
(−)-Methyl α-hydroxy-α-trifluoromethylphenylacetate, configuration of, 302
11β-Methyllynestrenole, 156
Methyl 2-methylhexacosanoate, 229, 234, 237, 238, 252
Methyl *p*-nitrophenyl sulfoximide, resolution of, 376
(+)-(*R*)-Methyl phenylmethanesulfinate, oxidation of, 432
(*R*)-2-Methyl-2-phenylsuccinate, 344
(−)-(*R*)-N-Methylphenylsulfonimidoyl chloride, synthesis of, 381
Methyl phenyl sulfoximide, optical purity of, 403
reduction to sulfinamide, 358
resolution of, 377
Methyl 2-propyl sulfide, and CSA, 296
Methyl *p*-styryl sulfoxide, chiral, polymer of, 339
o-Methylsulfinylbenzoic acid, optically active, 344

3-Methylsulfinylpropylamine, absolute configuration of, 387
1,1-bis(Methylthio)ethylene, 152
Methyl *p*-toluenesulfenate, asymmetric oxidation of, 353
Methyl *p*-toluenesulfinate, acid-catalyzed racemization of, 421
  stereospecific synthesis of, 355
Methyl *p*-tolyl sulfimide, alkaline hydrolysis of, 427
  reaction with chloramine-T, 433
Methyl *p*-tolyl sulfoxide, absolute configuration of, 400
  racemization of, 407
  reaction with bis(tosylsulfurdiimide), 427
  use in asymmetric synthesis, 449
(−)-(*R*)-Methyl *p*-tolyl sulfoximide, reaction of, 379
Methyl trideuterioethyl sulfoxide, enantiomeric purity of, 405
  stereospecific synthesis of, 348, 349
9-Methyltriptycene, 143
Methylvinyl sulfide, 152
(*R*)-α-Methylvinyl *p*-tolyl sulfoxide, reaction with bromine, 453
(*R*)-Mevalonolactone, 98
Micelles, 198, 202
Microbial oxidation, of racemic sulfoxides, 346
  of sulfides, 341
MM, *see* Molecular mechanics
MMI, 121, 122, 129, 143, 147, 149-152, 154, 155, 166-169, 172, 173, 177. *See also* Allinger force field
MMI/MMPI, *see* MMI; MMPI
MMPI, 121, 122, 138, 141-144, 175. *See also* Allinger force field
MM2, 122, 123, 125, 129, 132, 133, 150, 151, 158, 165, 168, 176, 177. *See also* Allinger force field
MNDO, 119
MO calculations, *see Ab initio;* Hückel MO calculations; Semiempirical MO methods
MODELS, 125, 151
MODELS-2, 150
Molecular builder, 124
Molecular complexes, chiral interactions in, 197
Molecular mechanics, 118-121
Molecular orientations, 204
  kinetic factors in, 217
MOLMEC, 124
Monensin, 70, 74
Monobasic solutes, 295
Monolayer behavior, of poly(γ-benzyl-dl-glutamate), 242
Monolayer-forming compounds, basic structural requirements for, 202
Monolayer phases, 228
Monolayers, 198
Monolayer studies, of polymers, 242
  definition of, 202
  effect of impurities on, 213
  enantiomer discrimination in, 220
  enantiomeric, 246
  fundamental physical chemistry of, 203
  gaseous, 203, 215
  heat of fusion and "melting heat" of, 227
  history of, 203
  intermediate states of, 215
  metastability in, 217
  mixed, 249
  phospholipid, 243
  quasi-racemate formation in, 229
  racemic, 246
  recovered, analysis of, 213
  transferred, 213
Monolayer trough, 214, 215
MSE, 146, 149, 151
MUB-2, 124, 125
Multiband drive technique, 134
Multilayers, 213

Naphthalene ring, deformed, 142
Naphthoquinone, 140
Naphthyldisulfinylacetic acid, resolution of, 336, 337
N-(*R*)-α-(1-Naphthyl)ethylamine, 175
1-(1-Naphthyl)ethylamine, as CSA, 266
α-Naphthylethyl *p*-tolyl sulfoxide, irradiation of, 411
(−)-α-Naphthyl *p*-tolyl[$^{16}O^{18}O$] sulfone, 374
NEA, *see* 1-(1-Naphthyl)ethylamine
Neopentane, 127
Newton-Raphson minimization, 121, 123, 131
Nitric acid, deimination of sulfoxides with, 351, 352
Nitroaryllactones, NMR non-equivalence in, 311

p-Nitrobenzylethylmethylsulfonium perchlorate, racemization of, 408
Nitrogen, chiral, 289, 290, 293, 321
Nitrogen-containing molecules, force fields for, 150
Nitrogen heterocyclics, and CSA, 297
Nitrosyl hexafluorophosphate, deimination of sulfoxides with, 351
NMR spectra and force field calculations, 171. *See also* Nonequivalence
Nonbenzenoid aromatic hydrocarbons, 146
Nonbonded H...H distances, 133, 135
Nonbonded interaction theory, 138
Nonequivalence (NMR), of aryl protons, 299
  in carbon NMR, 309, 314
  of enantiomers, 264, 265, 267, 268
  in fluorine NMR, 301, 312, 314
  magnitude of, 268, 277, 324
  mechanism of, 279
  in phosphorus NMR, 304, 305, 314, 315, 320
  relative signal position and intensity in, 268
  self-induced, 316, 317
  sense of, 268, 278, 281, 282, 293, 297, 312
Norbornene, 165
(1*S*,2*R*)-Norephedrine, 88
Nucleophilic additions, 161
Nucleophilic substitution, 161

2-Octanol, and CSA, 297
(*R*)-2-Octyl phenyl sulfide, oxidation of, 342
Olefin strain, 171
1-Oleoyl-2-stearoyl-2-*sn*-phosphatidylcholine, 249
O-mesitylsulfonylhydroxyamine, reaction with sulfoxides, 379
O-methyl *p*-toluenesulfinylmethanephosphonic acid, resolution of, 337
One-ring flip mechanism, 127
Ophiobolins, 168
Optical purity of chiral sulfur compounds, determination by NMR, 396
Optical rotation, 278
Organized multilayers, 213
Orthoacid model, 160
Overcrowded hydrocarbons, 125-128, 168
1,4-Oxathiane sulfoxides, ^{1}H NMR spectra of, 394
Oxaziridines, absolute configuration of, 293 and CSA, 289-293
Oxazoline enolates, chiral, 95
Oxidation, of double bonds, 204
Oximes, and CSA, 292
  enantiomeric excess, determination of, 304
Oxiranes, *see* Epoxides
11-Oxoestradiol 3-benzyl ether, 154
Oxosulfonium ylides, chiral, 381
  use in asymmetric synthesis, 437
Oxygen exchange in sulfoxides, stereochemistry of, 427

π-π complexes, 309, 311, 315
Paracyclophanes, 144
Paramagnetic chiral lanthanide shift reagents (CLSR), *see* LSR, chiral
Paramagnetic shift, 323
Partition functions, 158
PEA, *see* 1-phenylethylamine
Peak heights, in NMR, 277
Penicillin sulfoxide, configuration at sulfur in, 395
1-Pentafluorophenyl-2-methyl-2-thianaphthalene, synthesis of, 372
Pepsin-catalyzed hydrolysis of racemic phenyl cycloalkyl sulfites, 365
Peracids, chiral, asymmetric oxidation of sulfides with, 340
Perchlorotriphenylamine, 128
Perhalophosphazenes, 153
Perhydrotriptycene, 136
Pericyclic transition state, in aldol condensation, 13
Peri protons, steric interference by, 272
Pestalotin, 73
Pharmacophoric pattern, 173
Phase-composition diagrams, 222
Phase transitions, 216, 228
Phenacylethylmethylsulfonium perchlorate, racemization of, 408
Phenanthrene, hydrogenation products of, 168
Phenylacetic acid, enolate of, 10
Phenylacetic acids, absolute configuration of, 304
N-Phenyl-*N*-benzenesulfonyl-*p*-nitrophenylsulfonimidamide, resolution of, 383

N-Phenyl-*N*-benzenesulfonylphenylsulfonimidamide, resolution of, 383
Phenyl-*t*-butylcarbinol, 293
Phenyl *t*-butyl sulfoxide, racemization of, 413
1-Phenylbutyric acid chloride, optically active, reaction with racemic sulfoxides, 346
3-Phenylcyclohexane, 139
Phenylcyclopropane, asymmetric synthesis of, 437
2-Phenyl-1,3-dioxane, 139
1-Phenylethyl alkyl(phenyl) sulfides, oxidation of, 342
1-Phenylethylamine, as CSA, 264, 266
α-Phenylethyl phenyl sulfoxides, racemization of, 413
α-Phenylethyl *p*-tolyl sulfoxides, diastereomeric, absolute configuration at sulfur in, 391
Phenylglutaric anhydride, 139
Phenylmethanesulfinyl chloride, NMR nonequivalence in, 360
(−)-(*R*)-N-Phenyl-α-methylbenzylamine, asymmetric synthesis of, 450
N-Phenyl-2-phenylaziridine, asymmetric synthesis of, 438
Phenylpropionates, 2,6-disubstituted, 30
Phenyl ring orientation, 139
Phenyl substituent, rotational disposition of, 293
4β-Phenylsulfinyl-5α-cholestane sulfoxides, thermal elimination in, 388
(+)-(*S*)-Phenylthiomethyl *p*-tolyl sulfoxide, use in asymmetric synthesis, 450
Phosphate monoanion, 152
Phosphatidylcholine monolayers, 250
Phosphine oxides, and CSA, 285, 287
Phosphines, and CSA, 285
  force field calculations in, 152
Phosphoglycerides, monolayers in, 243
Phospholipase A_2 enzyme, 250
Phospholipid monolayers, 220, 243, 244
  chiral discrimination in, 244
Phosphonothioic acids, chiral, reaction with racemic sulfoxides, 346
Phosphoranes, 152
Phosphorus amides, and CSA, 308
Phosphorus–containing molecules, force field for, 152
Phosphorus (^{31}P) nonequivalence, 304, 305, 314, 315, 320
Phosphorus thioacids, absolute configuration of, 304
  and CSA, 305, 308, 319
α-Phosphoryl sulfoxide, ^{1}H, ^{31}P, and ^{13}C NMR spectra in presence of TFMC, 406
  Pummerer reaction of, 442
  stereospecific synthesis of, 349
(−)-(*S*)-N-Phthalimido-α-naphthyl *p*-tolyl sulfoximide, absolute configuration of, 432, 433
7-Phtalimidopenicillanate 1-oxide, chlorination of, 360
Pinacolyl *p*-toluenesulfinates, use in determination of optical purity of sulfoxides, 404
Piperidines, 150
Poly(γ-benzyl-DL-glutamate), monolayer behavior of, 242
Poly(lysine), 250
Polymers, monolayer studies of, 242
Polymethylhydrocoumaric acid, 160
Polymorphic forms of normal hydrocarbons, 228
Polyolefins, non-planar, 122
Polypeptides, enantiomer discrimination in, 242
  force-field calculation with, 157
  interaction with lipid monolayers, 250
Polyphenylethanes, 139
Polysaccharides, 147
Potential surface search, 131
PRDDO, 119
Preisocalamendiol, 166
Prelog-Djerassi lactonic acid, 84
Prochiral compounds and CSA, 296
Product development control, 161, 162
Proline, 172
Prolinol amides, 92
2-Propanol, and CSA, 296
(−)-(*S*)-Propargyl *p*-toluenesulfinate, steric course of reaction with isopropyl alcohol, 420
Propargylic alcohols, and CSA, 284, 286, 301
Propellers, molecular, 126
(*R*)-*cis*-Propenyl *p*-tolyl sulfoxide, reaction with piperidine, 451
Propionamides, 303
Propionyl imides, 88

Protons, exchangeable, 276
Pseudorotation, 151
Pummerer reaction, asymmetric, 441, 442
Pyranosides, 147
1-Pyrazolines, and CSA, 298

QCFF/PI, 124, 141, 148, 152
QCPE, *see* Quantum chemistry program exchange
Quantum chemistry program exchange (QCPE), 118, 119, 124
Quasi-racemates, 251
  formation in monolayers, 229, 252

Racemate, *see* Racemic compound
Racemic compound, 234, 251
Racemic mixture, 251
Racemic solid solution, 251
Racemization, degenerate, 320, 321
Racemization rates, 321
Reaction mechanism, 158
Reflex effect, 130, 156
Reformatsky reaction, 10, 68, 107
  with imines, 60
Resolution, two-dimensional, 249
Retro-aldol process, 16
RNA, intercalation in, 174
Rotation, restricted, 274
Rotational barriers, 321

Santonins, 169
Schleyer force field, 122, 123, 149, 157-161, 163, 169, 176. *See also* BIGSTRN; Engler-Schleyer force field
Self-association, 319
Self-induced non-equivalence, 316
Semiempirical MO methods, 118
Shielding effects, 281
[2,3] Sigmatropic rearrangement, of allyl sulfoxides, 443
Silanes, 150
Smith-Eyring method, modified (MSE), 146
Snake venoms, 205
sn-configuration, 243
Solid phase, slightly disordered, 228
Solute resonances, broadening of, 325
Solvates, diastereomeric, spectral differences of, 267, 271, 272
  differential stability of, 308
Solvation models, 282, 287
Solvent effects, 151, 270
Solvent polarity, effect on aldol stereoselection, 45
Spectral differences, of diastereomeric solvates, 267, 271, 272
Sphingolipids, monolayers in, 243
Spirosulfuranes, stereospecific synthesis of, 385, 386
S_E2 reaction, 161
S_N2 reaction, 161
S_N–S reactions, mechanism of, 418
Stabilomer, 169
Stearic acid, limiting film area of, 240
N-Stearoylalanine, 226
N-Stearoylamino acid, 224
1-Stearoyl-2-lauroyl-3-phosphatidyl choline, force area curves for, 244
N-Stearoylleucine, 225
N-Stearoyltyrosine, 225, 226
Stereochemical nomenclature, of enolates, 5
Stereodifferentiation: consonant, 81, 104
  dissonant, 104
  double, 78, 81, 104
Stereopopulation control, 160
Stereospecificity, and intermolecular forces, 196
Sterically hindered solutes, 294
Steric approach control, 161, 162
Steric congestion and steric hindrance, 163
Steric effects, 170
Steric energy distribution, 121
Steric factors, in aldolate equilibrium, 12
  remote, effect on asymmetric induction, 69
Steric model, for aldol diastereoface selection, 82
Steric strain, in carbonium ion, 163
Steroids, epimeric, 249
  force field calculations in, 153-155
Strain energy, 119, 164
Stretch-bend cross term, 177
Styrene epoxide, asymmetric synthesis of, 437
(*R*)-*trans*-β-Styryl *p*-tolyl sulfoxide, reaction with sodium diethyl malonate, 451
Sulfides, asymmetric oxidation of, 340, 344
Sulfimides, chiral, by resolution, 360
Sulfinamides, chiral: chlorination of, 434
  ORD and *CD* curves of, 398
  racemization of, 410

Sulfinate esters, and CSA, 282, 285, 287-289
Sulfinates, chiral, racemization of, 413
Sulfinylacetic acids, α-substituted, resolution of, 336
N-Sulfinyl *p*-toluenesulfonamide, 361
Sulfonimidoyl chlorides, replacement of chlorine in, stereochemistry of, 430
Sulfonium salts, thermal racemization of, 407
Sulfoxides, asymmetric reduction of, 347
  chiral, 336
    reaction with *N*-aminophthalamide, 378
  circular differential Raman scattering of, 402
  configuration of, 327
  conversion into aminosulfonium salts of, 428
  and CSA's, 275, 285, 286, 289, 311, 327
  and $Eu(fod)_3$, 313
  α-halogenation of, 453, 454
  imidation of, 379
  imination of, 361
  kinetic resolution of, 345
  microbial oxidation of, 346
  NMR spectra of, in chiral solvents, 396
  ORD curves of, 397
  racemization of, in carboxylic anhydrides, 415
    by hydrogen halides, 411
    by nitrogen tetroxide, 416
    in sulfuric acid, 414
  resolution of, by chromatography, 339
  stereospecific synthesis of, 349-351
  and sulfinates, absolute configuration of, 390, 391
  α,β-unsaturated, kinetic resolution of, 347
Sulfoxide-sulfoximide interconversion, stereochemical course of, 351, 352, 377
Sulfoximides, cyclic, chiral, 379, 380
Sulfuranes, chirality of, 322
Sulfur, elemental, deimination of sulfoxides with, 352
Sulfur-containing molecules, 151
Sulfur ylides, chiral, 437
Sultines, and CSA, 288
Superliquid (LS) hexagonal phase, 228
Surface area, 203
Surface energy, 206
Surface potential, 211, 212
Surface pressure, 203
  as function of temperature, 222
  and reversible thermodynamics, 216
Surface tension, 203, 206
  measurement of, 207
  and reversible thermodynamics, 216
SYMIN, 163
syn Diastereomer, definition, 4

Taft's E_S values, 160
Tartaric acids, and CSA, 320
Temperature, effect of, on CSA, 271, 281
Tensiometers, automated, 207, 208
Terpenes, force field calculations for, 153, 166
4-(Tetra-O-acetyl-β-D-glucopyranosyloxy)-phenyl alkyl sulfoxides, 337
1,1,2,2-Tetraalkylethanes, 128
1,1,2,2-Tetraarylethanes, 128
Tetra-*n*-butylammonium fluoride catalyzed aldol condensations, 55
Tetra-*t*-butylethylene, 137
Tetra-*t*-butyltetrahedrane, 135
2-Tetracosanyl acetate, 228-233, 236, 238, 252
Tetracosan-2-ol, 228
Tetracyclohexylsilane, 128
Tetrahedrane, 135
Tetramethylbutane, 125-127
1-X-2,2,4,4-Tetramethylcyclohexane, 130
Tetrasilane, 151
TFAE, *see* 2,2,2-Trifluoro-1-(9-anthryl)-ethanol
TFMC (trifluoromethylphenylcarbinol), *see* 2,2,2-Trifluoro-1-phenylethanol
TFNE, *see* 2,2,2-Trifluoro-1-(1-naphthyl)-ethanol
TFPE, *see* 2,2,2-Trifluoro-1-phenylethanol
Thermodynamically controlled aldol diastereoselection, 7
Thiabenzene systems, chiral, 372
Thianthrene 5,10-dioxides, IR spectra of, 398, 399
  photochemical epimerization of, 411
  UV spectra of, 398, 399
Thienamycin, 26
Thiiranes, *see* Episulfides
2-Thio-5α-androstan-17β-ol sulfoxides, ^1H NMR spectra of, 395

Thioamides, enolization of, 28
Thioboronite esters, 40
Thiosulfinates, racemization of, 417
Three-point interactions, 308
Threo diastereomer, definition, 4
Titanium enolates, 63
Titanium tetrachloride catalyzed aldol condensations, 55, 63, 73
(+)-(*R*)-*p*-Toluenesulfinylacetophenone, reaction with Grignard reagents, 350
p-Toluenesulfinylnitrene, 361
p-Toluenesulfinylpiperidine, asymmetric synthesis of, 357
(+)-(*S*)-*p*-Toluenesulfinylpyrolidine, conversion into its enantiomer, 425
p-Tolyl *trans*-4-methylcyclohexyl sulfoxides, chiral, pyrolysis of, 435
Torsional energy surface, 173
Torsion balance, automatically recording, 208
  differential, 207
Torsion-bend cross term, 177
N-Tosyl-*N*-methyl *p*-tolylsulfimide, determination of absolute configuration of, 402
  stereoselective synthesis of, 357
  steric course of oxidation of, 432
N-Tosyl-N-methyl *p*-toluenesulfinamide, stereoselective synthesis of, 359
N-Tosylmethyl-*p*-tolylsulfonimidamide, 384
bis(Tosylsulfurdiimide), reaction of chiral methyl *p*-tolyl sulfoxide with, 427
bis(N-Tosylsulfurdiimine), 361
N-Tosyl *p*-tolueneiminosulfinyl chloride, reaction with menthol, 362
Transition state in aldol condensation, acyclic, 13
  for allylborane addition reactions, 105
  chair, 14
  pericyclic, 13
  produce-like and reactant like, 164
  simulated, 159
Trialkylboranes, "conjugate addition" of, to α,β-unsaturated ketones, 39
2,4,6-Tribromo-1,3,5-trineopentylbenzene, 140
Tri-*t*-butylmethane, 126, 127
Tri-*t*-butylsilane, 127
Tricyclo [9.3.0$_{3,7}$] tetradecane, 168
2,2,2-Trifluoro-1-(9-anthryl)ethanol, as CSA, 266
Trifluoromethylphenylcarbinol, *see* 2,2,2-Trifluoro-1-phenylethanol
2,2,2-Trifluoro-1-(1-naphthyl)ethanol, as CSA, 266
2,2,2-Trifluoro-1-phenylethanol, as CSA, 264, 266
3-β,S,19-Tri-hydroxyetiocholanate, reaction with thionyl chloride, 364
Trimesitylamine, 128
4,4,14α-Trimethylpregnan-6,11-diols, 155, 156
Trimethylsilyl triflate catalyzed aldol condensations, 57
1,3,5-Trineopentylbenzene, 139
Tris(dialkylamino)borane, 127
Tris-[3-(heptafluoropropylhydroxymethylene)-D-camphorato] europium, 405
Trisulfides, 152
Two-point attraction, 286
Two-ring flip mechanism, 127

Unsaturated ketones, 122
Urey-Bradley force field, 120, 124
UTAH-5, 125

Valence force field, 120
van der Waals forces, 139
(*S*)-Vaninol, 88
Vapor osmometric studies, of hydrogen bonding, 269, 270
(*R*)-Vinyl *p*-tolyl sulfoxide, reaction with bromine, 453
Volta potential, 212

Westheimer method, 120
White-Boyill force field, 123, 133, 158, 169
Wilhelmy hanging plate, 207-209
WMIN, 125, 140

X-Ray crystal analysis, 174

Zimmerman model, 16
Zinc enolates, 60, 79
  in aldol condensation, 8
Zirconium aldol condensations, 93
  mechanism of, 51-55
Zirconium enolates, 50, 92

Cumulative Index, Volumes 1-13

	VOL.	PAGE
Absolute Configuration of Planar and Axially Dissymmetric Molecules *(Krow)*	5	31
Absolute Stereochemistry of Chelate Complexes *(Saito)*	10	95
Acetylenes, Stereochemistry of Electrophilic Additions *(Fahey)*	3	237
Aldol Condensations, Stereoselective *(Evans, Nelson* and *Taber)*	13	1
Analogy Model, Stereochemical *(Ugi* and *Ruch)*	4	99
Asymmetric Synthesis, New Approaches in *(Kagan* and *Fiaud)*	10	175
Asymmetric Synthesis Mediated by Transition Metal Complexes *(Bosnich* and *Fryzuk)*	12	119
Atomic Inversion, Pyramidal *(Lambert)*	6	19
Axially and Planar Dissymmetric Molecules, Absolute Configuration of *(Krow)*	5	31
Barriers, Conformational, and Interconversion Pathways in Some Small Ring Molecules *(Malloy, Bauman,* and *Carreira)*	11	97
Barton, D. H. R., and Hassel, O.–Fundamental Contributions to Conformational Analysis *(Barton, Hassel)*	6	1
Carbene Additions to Olefins, Stereochemistry of *(Closs)*	3	193
Carbenes, Structure of *(Closs)*	3	193
sp^2-sp^3 Carbon-Carbon Single Bonds, Rotational Isomerism about *(Karabatsos* and *Fenoglio)*	5	167
Carbonium Ions, Simple, the Electronic Structure and Stereochemistry of *(Buss, Shleyer* and *Allen)*	7	253
Chelate Complexes, Absolute Stereochemistry of *(Saito)*	10	95
Chirality Due to the Presence of Hydrogen Isotopes at Noncyclic Positions *(Arigoni* and *Eliel)*	4	127
Chiral Lanthanide Shift Reagents *(Sullivan)*	10	287
Chiral Monolayers at the Air-Water Interface *(Steward* and *Arnett)*	13	195
Chiral Organosulfur Compounds *(Mikolajczyk* and *Drabowicz)*	13	333
Chiral Solvating Agents, in NMR *(Pirkle* and *Hoover)*	13	263
Classical Stereochemistry, The Foundations of *(Mason)*	9	1
Conformational Analysis, Applications of the Lanthanide-induced Shift Technique in *(Hofer)*	9	111
Conformational Analysis–The Fundamental Contributions of D. H. R. Barton and O. Hassel *(Barton, Hassel)*	6	1
Conformational Analysis of Intramolecular Hydrogen-Bonded Compounds in Dilute Solution by Infrared Spectroscopy *(Aaron)*	11	1
Conformational Analysis of Six-membered Rings *(Kellie* and *Riddell)*	8	225
Conformational Analysis and Steric Effects in Metal Chelates *(Buckingham* and *Sargeson)*	6	219

	VOL.	PAGE
Conformational Analysis and Torsion Angles *(Bucourt)*	8	159
Conformational Barriers and Interconversion Pathways in Some Small Ring Molecules *(Malloy, Bauman* and *Carreira)*	11	97
Conformational Changes, Determination of Associated Energy by Ultrasonic Absorption and Vibrational Spectroscopy *(Wyn-Jones* and *Pethrick)*	5	205
Conformational Changes by Rotation about sp^2-sp^3 Carbon-Carbon Single Bonds *(Karabatsos* and *Fenoglio)*	5	167
Conformational Energies, Table of *(Hirsch)*	1	199
Conformational Interconversion Mechanisms, Multi-step *(Dale)*	9	199
Conformations of 5-Membered Rings *(Fuchs)*	10	1
Conjugated Cyclohexenones, Kinetic 1,2 Addition of Anions to, Steric Course of *(Toromanoff)*	2	157
Crystal Structures of Steroids *(Duax, Weeks* and *Rohrer)*	9	271
Cyclobutane and Heterocyclic Analogs, Stereochemistry of *(Moriarty)*	8	271
Cyclohexyl Radicals, and Vinylic, The Stereochemistry of *(Simamura)*	4	1
Double Bonds, Fast Isomerization about *(Kalinowski* and *Kessler)*	7	295
Electronic Structure and Stereochemistry of Simple Carbonium Ions, *(Buss, Schleyer* and *Allen)*	7	253
Electrophilic Additions to Olefins and Acetylenes, Stereochemistry of *(Fahey)*	3	237
Enzymatic Reactions, Stereochemistry of, by Use of Hydrogen Isotopes *(Arigoni* and *Eliel)*	4	127
1,2-Epoxides, Stereochemical Aspects of the Synthesis of *(Berti)*	7	93
EPR, in Stereochemistry of Nitroxides *(Janzen)*	6	177
Five-Membered Rings, Conformations of *(Fuchs)*	10	1
Foundations of Classical Stereochemistry *(Mason)*	9	1
Geometry and Conformational Properties of Some Five- and Six-Membered Heterocyclic Compounds Containing Oxygen or Sulfur *(Romers, Altona, Buys* and *Havinga)*	4	39
Hassel, O. and Barton, D. H. R. - Fundamental Contributions to Conformational Analysis *(Hassel, Barton)*	6	1
Helix Models, of Optical Activity *(Brewster)*	2	1
Heterocyclic Compounds, Five- and Six-Membered, Containing Oxygen or Sulfur, Geometry and Conformational Properties of *(Romers, Altona, Buys* and *Havinga)*	4	39
Heterocyclic Four-Membered Rings, Stereochemistry of *(Moriarty)*	8	271
Heterotopism *(Mislow* and *Raban)*	1	1
Hydrogen-Bonded Compounds, Intramolecular, in Dilute Solution, Conformational Analysis of, by Infrared Spectroscopy *(Aaron)*	11	1
Hydrogen Isotopes at Noncyclic Positions, Chirality Due to the Presence of *(Arigoni* and *Eliel)*	4	127

	VOL.	PAGE
Infrared Spectroscopy, Conformational Analysis of Intramolecular Hydrogen-Bonded Compounds in Dilute Solution by *(Aaron)*	11	1
Intramolecular Hydrogen-Bonded Compounds, in Dilute Solution, Conformational Analysis of, by Infrared Spectroscopy *(Aaron)*	11	1
Intramolecular Rate Processes *(Binsch)*	3	97
Inversion, Atomic, Pyramidal *(Lambert)*	6	19
Isomerization, Fast, About Double Bonds *(Kalinowski* and *Kessler)*	7	295
Ketones, Cyclic and Bicyclic, Reduction of, by Complex Metal Hydrides *(Boone* and *Ashby)*	11	53
Lanthanide-induced Shift Technique - Applications in Conformational Analysis *(Hofer)*	9	111
Lanthanide Shift Reagents, Chiral *(Sullivan)*	10	287
Mass Spectrometry and the Stereochemistry of Organic Molecules *(Green)*	9	35
Metal Chelates, Conformational Analysis and Steric Effects in *(Buckingham* and *Sargeson)*	6	219
Metal Hydrides, Complex, Reduction of Cyclic and Bicyclic Ketones by *(Boone* and *Ashby)*	11	53
Metallocenes, Stereochemistry of *(Schlögl)*	1	39
Metal Nitrosyls, Structures of *(Feltham* and *Enemark)*	12	155
Molecular Mechanics Calculations - Application to Organic Chemistry *(Osawa* and *Musso)*	13	117
Monolayers, Chiral, at the Air-Water Interface *(Stewart* and *Arnett)*	13	195
Multi-step Conformational Interconversion Mechanisms *(Dale)*	9	199
Nitroxides, Stereochemistry of *(Janzen)*	6	177
Non-Chair Conformations of Six-Membered Rings *(Kellie and Riddell)*	8	225
Nuclear Magnetic Resonance, Chiral Solvating Agents in *(Pirkle* and *Hoover)*	13	263
Nuclear Magnetic Resonance, ^{13}C, Stereochemical Aspects of *(Wilson* and *Stothers)*	8	1
Nuclear Magnetic Resonance, for Study of Intra-Molecular Rate Processes *(Binsch)*	3	97
Nuclear Overhauser Effect, Some Chemical Applications of *(Bell* and *Saunders)*	7	1
Olefins, Stereochemistry of Carbene Additions to *(Closs)*	3	193
Olefins, Stereochemistry of Electrophilic Additions to *(Fahey)*	3	237
Optical Activity, Helix Models of *(Brewster)*	2	1
Optical Circular Dichroism, Recent Applications in Organic Chemistry *(Crabbé)*	1	93
Optical Purity, Modern Methods for the Determination of *(Raban* and *Mislow)*	2	199
Optical Rotatory Dispersion, Recent Applications in Organic Chemistry *(Crabbé)*	1	93
Organosulfur Compounds, Chiral *(Mikolajczyk* and *Drabowicz)*	13	333

	VOL.	PAGE
Overhauser Effect, Nuclear, Some Chemical Applications of *(Bell* and *Saunders)*	7	1
Phosphorus Chemistry, Stereochemical Aspects of *(Gallagher* and *Jenkins)*	3	1
Phosphorus-containing Cyclohexanes, Stereochemical Aspects of *(Maryanoff, Hutchins* and *Maryanoff)*	11	186
Piperidines, Quaternization Stereochemistry of *(McKenna)*	5	275
Planar and Axially Dissymmetric Molecules, Absolute Configuration of *(Krow)*	5	31
Polymer Stereochemistry, Concepts of *(Goodman)*	2	73
Polypeptide Stereochemistry *(Goodman, Verdini, Choi* and *Masuda)*	5	69
Pyramidal Atomic Inversion *(Lambert)*	6	19
Quaternization of Piperidines, Stereochemistry of *(McKenna)*	5	75
Radicals, Cyclohexyl and Vinylic, The Stereochemistry of *(Simamura)*	4	1
Reduction, of Cyclic and Bicyclic Ketones by Complex Metal Hydrides *(Boone* and *Ashby)*	11	53
Resolving-Agents and Resolutions in Organic Chemistry *(Wilen)*	6	107
Rotational Isomerism about sp^2-sp^3 Carbon-Carbon Single Bonds *(Karabatsos* and *Fenoglio)*	5	167
Small Ring Molecules, Conformational Barriers and Interconversion Pathways in Some *(Malloy, Bauman* and *Carreira)*	11	97
Stereochemical Aspects of ^{13}C Nmr Spectroscopy *(Wilson* and *Stothers)*	8	1
Stereochemical Aspects of Phosphorus-containing Cyclohexanes *(Maryanoff, Hutchins* and *Maryanoff)*	11	186
Stereochemical Nomenclature and Notation in Inorganic Chemistry *(Sloan)*	12	1
Stereochemistry, Classical, The Foundations of *(Mason)*	9	1
Stereochemistry, Dynamic, A Mathematical Theory of *(Ugi* and *Ruch)*	4	99
Stereochemistry of Chelate Complexes *(Saito)*	10	95
Stereochemistry of Cyclobutane and Heterocyclic Analogs *(Moriarty)*	8	271
Stereochemistry of Germanium and Tin Compounds *(Gielen)*	12	217
Stereochemistry of Nitroxides *(Janzen)*	6	177
Stereochemistry of Organic Molecules, and Mass Spectrometry *(Green)*	9	35
Stereochemistry of Reactions of Transition Metal-Carbon Sigma Bonds *(Flood)*	12	37
Stereochemistry of Transition Metal Carbonyl Clusters *(Johnson* and *Benfield)*	12	253
Stereoisomeric Relationships, of Grups in Molecules *(Mislow* and *Raban)*	1	1
Stereoselective Aldol Condensations *(Evans, Nelson* and *Taber)*	13	1
Steroids, Crystal Structures of *(Duax, Weeks* and *Rohrer)*	9	271
Structures, Crystal, of Steroids *(Duax, Weeks* and *Rohrer)*	9	271

	VOL.	PAGE
Torsion Angle Concept in Conformational Analysis *(Bucourt)*	8	159
Ultrasonic Absorption and Vibrational Spectroscopy, Use of, to Determine the Energies Associated with Conformational Changes *(Wyn-Jones* and *Pethrick)*	5	205
Vibrational Spectroscopy and Ultrasonic Absorption, Use of, to Determine the Energies Associated with Conformational Changes *(Wyn-Jones* and *Pethrick)*	5	205
Vinylic Radicals, and Cyclohexyl, The Stereochemistry of *(Simamura)*	4	1
Wittig Reaction, Stereochemistry of *(Schlosser)*	5	1